Development of Photoinduced Minisci Alkylation

Chia-Yu Huang

Thesis submitted to McGill University

in partial fulfillment of the requirement for the degree of

Doctor of Philosophy

Department of Chemistry

McGill University, Montréal

October 2022

Abstract

Chia-Yu Huang *Supervisor: Prof. Dr. Chao-Jun Li*

McGill University

This thesis focuses on developing photoinduced alkyl radical generation methods which advance the knowledge in Minisci alkylation, a fundamentally important organic chemical transformation.

Chapter 1 briefly introduces the background of photochemistry in organic synthesis, photoinduced alkyl radical generation, and Minisci reaction.

Chapter 2 to 4 depict my photoinduced Minisci alkylation projects. The first two projects are cross-dehydrogenative Minisci alkylations, in which hydrogen atom transfer plays the key alkyl radical formation step. Using diacetyl as a sustainable and traceless reagent (Chapter 2) or chlorine radical as a powerful oxy radical surrogate (Chapter 3), alkyl radical could be generated from naturally abundant alkyl C-H bonds under environmentally friendly conditions. On the other hand, my last project is oxidative Minisci alkylation, which utilizes single-electron transfer to form the alkyl radical from easily accessible alkyltrifluoroborate salt (Chapter 4). While this protocol solves the regioselectivity and other issues in the previous cross-dehydrogenative coupling designs, some quinoline-based photocatalysts have been explored. All these chapters include reaction design, optimizations, substrate scope, and mechanistic studies.

Finally, chapter 5 gives future perspectives on the developed methodologies in this thesis, and chapter 6 summarizes their contributions to fundamental knowledge.

Résumé

Chia Yu Huang *Superviseur : Prof. Dr. Chao-Jun Li*

université McGill

Cette thèse porte sur le développement de méthodes de génération de radicaux alkyles photoinduits faisant progresser les connaissances sur l'alkylation de type Minisci, une transformation chimique organique de grande importance fondamentale.

Le chapitre 1 présente brièvement le contexte de la photochimie dans le cadre de la synthèse organique, la génération de radicaux alkyle photoinduits et la réaction de Minisci.

Les chapitres 2 à 4 décrivent mes projets d'alkylation de Minisci photoinduite. Les deux premiers projets sont des alkylations de Minisci à déshydrogénation croisée, dans lesquelles le transfert d'atomes d'hydrogène joue un rôle clé dans la formation des radicaux alkylés. En utilisant le diacétyle comme réactif durable et sans trace (chapitre 2), ou bien le radical chlore comme puissant substitut au radical oxy (chapitre 3), les radicaux alkylés peuvent être générés à partir de liaisons alkyles C-H naturellement abondantes tout en utilisant des conditions respectueuses de l'environnement. D'autre part, mon dernier projet est l'alkylation de Minisci de type oxydatif, qui utilise le transfert d'un seul électron pour former le radical alkyle à partir d'un sel d'alkyltrifluoroborate facilement accessible (chapitre 4). Alors que ce protocole résout la régiosélectivité ainsi que d'autres problèmes présents lors des conceptions de couplage déshydrogénatif croisé précédentes, certains photocatalyseurs à base de quinoléine ont aussi été explorés. Tous ces chapitres incluent également les conceptions de réaction, les optimisations, les étendues

réactionnelles, ainsi que les études mécanistiques.

Enfin, le chapitre 5 donne les futures perspectives concernant les méthodologies développées dans cette thèse, et le chapitre 6 résumera leurs apports aux connaissances fondamentales.

“I am a slow walker, but I never walk backward.”

- Abraham Lincoln

for my dear parents, Shu-Jen Chen, Ruey-Lin Huang, and Jiunn-Chia Huang

Acknowledgments

First and foremost, to my supervisor Prof. Chao-Jun Li, I sincerely thank you for your instruction and support during my Ph.D. study. Your philosophy and enthusiasm for scientific research have demonstrated how a distinguished chemist should be. I will remember and follow what you taught me in my future chemistry career.

I want to thank my review committee, Prof. Youla Tsantrizos and Prof. Masad J. Damha, for their constructive advice during my review times. To Prof. Bruce Arndtsen, James Gleason, and my supervisor Prof. Chao-Jun Li, thank you for giving me high-quality and informative graduate courses. To our administrative and departmental staff, Ms. Chantal Marotte, Mr. Mike Daoust, Dr. Robin Stein, Dr. Nadim, Saadé, and Dr. Alexander Wahba, thank you for the assistance on administration, teaching assistance and spectroscopy analysis.

I am grateful to be a member of the Li group and meet a group of excellent chemists, Prof. Dr. Wenbo Liu, Dr. Zihang Qiu, Dr. Siting Ni, Dr. Chenchen Li, Dr. Sosthène Ung, and others. They were unselfish and willing to share their knowledge and chemicals with other labmates. To our research associate Dr. Inna Perepichka, thank you for keeping our lab organized. To Mr. Hyotaik (Harry) Kang, I feel lucky we joined the Li group simultaneously so we could study and work together.

To our former labmate and my research collaborator Dr. Jianbin Li, thank you for sharing research ideas, technical knowledge, writing and presentation skills with me throughout my study. It was also a precious time to be your roommate, and I will always remember those food orderings, Friday movies, and stupid jokes.

I also want to thank other research groups and members in the department for their generosity in sharing chemicals and instruments, especially Ms. Ying-Hsuan Liu and Mr. Ehsan Hamzehpoor from the Perepichka group, Mr. Ifenna I. Mbaezue from the Tsantrizo group, Mr. Chunling (Blue) Lan from Auclair group, Dr. Haiyang Huang from Lumb group,

and Ms. Cuihan Zhou from Arndtsen group, who spent their time preparing chemicals for me. To my previous supervisor at National Taiwan Normal University, Prof. Ching-Fa Yao, thank you for tutoring and supporting my undergraduate and graduate research for more than six years. I appreciate you treated me as your own child and gave me countless pieces of life advice. To our previous postdocs at National Taiwan Normal University, Dr. Chun-Wei Kuo and Dr. Kavala Veerababu, thank you for supervising my research projects and teaching me how to be a good researcher. To my teachers at National Taiwan Normal University, especially Prof. Ching-Fa Yao, Prof. Hsyueh-Liang Wu, and Prof. Wenwei Lin, thank you for your comprehensive and interesting chemistry courses.

To my previous chemistry teacher at Yangming High School, Mr. 黃國益, thank you for showing me the beauty of chemistry and encouraging me. Without your encouragement to gain a deeper insight into the chemistry subject, I probably would not have become a chemist.

To Ouro Kronii, Miori Celesta, Rosuuri, Yoclesh, Yuria of Ailurus, and many other VTubers, thank you for accompanying me during the most stressful research period. I hope you will entertain more people and fulfill your dreams in the near future.

To my dear parents, Ruey-Lin Huang and Shu-Jen Chen, thank you for giving me unconditional love and supporting me all the time so I can pursue my dreams without hesitation. To my beloved younger brother Jiunn-Chia Huang, thank you for taking care of our family members even when we are far from each other. I am proud to be your brother.

Contributions of authors

A portion of content in the review papers I contributed were included in chapters 1 and 2:

(1) En Route to Intermolecular Cross-Dehydrogenative Coupling (CDC) Reactions. **C.-Y. Huang**[+], H. Kang[+], J. Li, C.-J. Li*, *J. Org. Chem.* **2019**, *84*, 12705-12721. ([+]contribute equally)

The manuscript was prepared by me and revised by Mr. Hyotaik Kang, Dr. Jianbin Li, and Prof. Chao-Jun Li.

(2) Cross-dehydrogenative coupling of unactivated alkanes. J. Li, **C.-Y. Huang**, C.-J. Li*, *Trends Chem.* **2022**, *4*, 479-494.

(3) Photocatalytic C(sp^3) radical generation via C-H, C-C, and C-X bond cleavage. **C.-Y. Huang**[+], J. Li[+], C.-J. Li*, *Chem. Sci.* **2022**, *13*, 5465-5504. ([+]contribute equally)

The manuscript was prepared by me and revised by Dr. Jianbin Li and Prof. Chao-Jun Li.

The following published research papers will be discussed in chapters 2 to 4 in the order shown below:

(4) Diacetyl as A "Traceless" Visible Light Photosensitizer in Metal-Free Cross-Dehydrogenative Coupling Reactions. **C.-Y. Huang**[+], J. Li[+], W. Liu, C.-J. Li*, *Chem. Sci.* **2019**, *10*, 5018-5024. ([+]contribute equally)

All the experiments, including optimizations, scope, and mechanistic studies, were carried

out by me with guidance from Dr. Jianbin Li, Dr. Wenbo Liu, and Prof. Dr. Chao-Jun Li. The manuscript was prepared by me and revised by Dr. Jianbin Li and Prof. Dr. Chao-Jun Li.

(5) A Cross-Dehydrogenative C(sp^3)-H Heteroarylation via Photo-Induced Catalytic Chlorine Radical Generation. **C.-Y. Huang**[+], J. Li[+], C.-J. Li*, *Nat. Commun.* **2021**, *12*, 4010. ([+]contribute equally)

All the experiments, including optimizations, scope, and mechanistic studies, were carried out by me with guidance from Dr. Jianbin Li and Prof. Dr. Chao-Jun Li. The manuscript was prepared by me and revised by Dr. Jianbin Li and Prof. Dr. Chao-Jun Li.

(6) Development of a Quinolinium/Cobaloxime Dual Photocatalytic System for Oxidative C-C Cross-Couplings via H_2 Release. J. Li[+], **C.-Y. Huang**[+], J.-T. Han, C.-J. Li*, *ACS Cat.* **2021**, *11*, 14148-14158. ([+]contribute equally)

The reaction optimizations and scope were carried out by me with guidance from Dr. Jianbin Li and Prof. Dr. Chao-Jun Li. The electrochemical experiments were performed by Dr. Jianbin Li. The photophysical studies were performed by me and Dr. Jianbin Li, and the DFT calculation of the photocatalyst in the manuscript was performed by Mr. Jing-Tan Han. The manuscript was prepared by Dr. Jianbin Li and revised by me and Prof. Dr. Chao-Jun Li.

Table of Contents

Abstract 1
Résumé 2
Acknowledgments 6
Contributions of authors 8
List of Abbreviations 12
List of Tables 13
List of Figures 13
List of Schemes 14
Chapter 1 Photochemistry, alkyl radical, and heteroarene functionalization 17
1.1 Organic photochemistry 17
1.2 Photoinduced alkyl radical generation 22
1.2.1 Alkyl radical 22
1.2.2 Unimolecular homolytic cleavage 24
1.2.3 Bimolecular homolytic substitution (S_H2) 27
1.2.4 Single-electron transfer (SET) 42
1.2.5 Radical cascade 65
1.3 Heteroarene C-C bond formation 68
1.3.1 Heteroarene 68
1.3.2 Nucleophilic attack 70
1.3.3 Heteroarene oxidation 71
1.3.4 Radical addition 74
1.3.5 C-H metalation 76
1.4 Conclusions and outlook 78
1.5 References 79
Chapter 2 Diacetyl-mediated cross-dehydrogenative Minisci alkylation 94
2.1 Introduction 94
2.2 Reaction design 96
2.3 Results and discussion 98
2.4 Mechanistic studies 107
2.5 Conclusions and outlook 111
2.6 Author contributions 112
2.7 Experimental section 113
2.8 Characterization data for compounds 115

2.9 References....146
Chapter 3 Chloride-catalyzed cross-dehydrogenative Minisci alkylation....152
3.1 Introduction....152
3.2 Reaction design....155
3.3 Results and discussion....156
3.4 Mechanistic studies....161
3.5 Conclusions and outlook....165
3.6 Author contributions....166
3.7 Experimental section....167
3.8 Characterization data for compounds....169
3.9 References....209
Chapter 4 Quinoline-catalyzed Minisci alkylation with alkyltrifluoroborate....216
4.1 Introduction....216
4.2 Reaction design....217
4.3 Results and discussion....220
4.4 Mechanistic studies....223
4.5 Synthetic applications....230
4.6 Conclusions and outlook....233
4.7 Author contributions....233
4.8 Experimental section....234
4.8.1 General procedures....234
4.8.2 Electrochemical measurements....245
4.8.3 Quantum yield measurement....246
4.9 Characterization data for compounds....247
4.10 References....277
Chapter 5 Future perspective for the methodologies developed in this thesis....284
Chapter 6 Conrtibutions to fundamental knowledge....286
Appendix....288
Appendix 1: NMR spectra for new compounds in chapter 2....288
Appendix 2: NMR spectra for new compounds in chapter 3....328
Appendix 3: NMR spectra for new compounds in chapter 4....359

List of Abbreviations

Ac	acetyl	LG	leaving group
Ar	aryl	LMCT	ligand to metal charge transfer
BDE	bond dissociation energy	LUMO	lowest unoccupied molecular orbital
BHT	2,6-di-*tert*-butyl-4-methylphenol	MeTHF	2-methyltetrahydrofuran
Boc	*tert*-butyloxycarbonyl	NHS	*N*-hydroxysuccinimide
^{s}Bu	*sec*-butyl	OA	oxidative addition
CDC	cross-dehydrogenative-coupling	PCET	proton-coupled electron transfer
CFL	compact fluorescent lamp	Phth	phthalimidyl
CMD	concerted metalation-deprotonation	PMP	*p*-methoxyphenyl
Cy	cyclohexyl	ppy	2-phenylpyridinyl
DCE	1,2-dichloroethane	^{i}Pr	*iso*-propyl
DMA	*N,N*-dimethylacetamide	py	pyridine
DME	dimethoxyethane	QN	quinoline
DMF	*N,N*-dimethylformamide	RE	reductive elimination
dmgH	dimethylglyoxime	R•	Alkyl radical
DMPO	5,5-dimethyl-1-pyrroline-*N*-oxide	SCE	standard calomel electrode
DPQN	2,4-diphenylquinoline	SET	single-electron transfer
DTBP	di-*tert*-butyl peroxide	SOMO	singly occupied molecular orbital
dtbpy	4,4'-di-*tert*-butyl-2,2'-dipyridyl	TBADT	tetrabutylammonium decatungstate
E^{red}	reduction potential	TBHP	*tert*-butyl hydrogen peroxide
ET	energy transfer	TCD	thermal conductivity detector
FG	functional group	TEMPO	(2,2,6,6-tetramethylpiperidin-1-yl)oxyl
GC	gas chromatography	Tf	trifluoromethylsulfonyl
HAT	hydrogen atom transfer	TFA	trifluoroacetic acid
hν	photon	THP	tetrahydropyran
HOMO	highest occupied molecular orbital	THF	tetrahydrofuran
IC	internal conversion	UV	ultraviolet
ISC	intersystem crossing	XAT	halogen atom transfer
KIE	kinetic isotope effect		

List of Tables

Table 2.1 Optimization for the coupling of 2-phenylquinoline and THF. 99
Table 2.2 Optimization for the coupling of 4-methylquinoline and cyclohexane. 105
Table 3.1 Optimizations for the coupling of 2-phenylquinoline and cyclohexane. 156
Table 4.1 Evaluation of the quinoline-base photocatalyst. 218

List of Figures

Figure 1.1 Jablonski diagram 18
Figure 1.2 Energy diagram of thermal and photochemical isomerization of stilbene. 19
Figure 1.3 Dexter energy transfer. 20
Figure 1.4 Photoinduced single-electron transfer. 21
Figure 1.5. Applications of photochemistry in organic synthesis. 22
Figure 1.6 General strategies in photochemical R• formation. 23
Figure 1.7 Common BDE of C(sp^3)-H and heteroatom-H. 28
Figure 1.8 Some heteroaryl compounds. 69
Figure 1.9 Heteroaryl C-C formation strategies. 69
Figure 1.10 C-C bond formation via heteroarene oxidation. 72
Figure 1.11 Different types of Minisci reactions. 75
Figure 1.12 C-H metalation of heteroarens. 77
Figure 1.13 Research interest in this thesis. 79
Figure 2.1 R• generations through C-C, C-X and C-H bond cleavage. 94
Figure 2.2 Representative methods for generating HAT agents in Minisci alkylations 95
Figure 2.3 Diacetyl as a peroxide/persulfate surrogate. 97
Figure 2.4 Demonstration of impurity removal. 100
Figure 2.5 Purified isotope mixtures of 3a and 3a-d_7 from the KIE experiment. 109
Figure 2.6 The 40 W CFL reaction setup. 113
Figure 2.7 Gram-scale synthesis of heteroarene 3a. 115
Figure 3.1 Common BDE of C(sp^3)-H and heteroatom-H. 152
Figure 3.2 Chloride-to-chlorine radical strategy in HAT reactions. 153
Figure 3.3 Proposed dehydrogenative alkylation reaction. 155
Figure 3.4 Substrate scope of alkane. 158
Figure 3.5 Substrate scope of heteroarene. 160
Figure 3.6 The general reaction setup. 167
Figure 3.7 Gram-scale synthesis of heteroarene 7b. 169
Figure 4.1 CV of 20 mM $DPQN^{2,4\text{-di-OMe}}$ and $DPQN^{2,4\text{-di-OMe}}$-H^+. 225

Figure 4.2 Stacked UV-vis and fluorescence spectra of DPQN$^{2,4\text{-di-OMe}}$-H$^+$. 225
Figure 4.3 Transient absorption decay of DPQN$^{2,4\text{-di-OMe}}$-H$^+$ at 375 nm. 227
Figure 4.4 Light on/off experiment of the standard reaction. 227
Figure 4.5 Polymer recycling test. 245

List of Schemes

Scheme 1.1 Photoinduced C=C and C-I cleavage. 19
Scheme 1.2 Transition metal-free Sonogashira coupling. 24
Scheme 1.3 Boracene-based alkyl borate as the alkyl radical source. 25
Scheme 1.4. Photocatalytic R-S bond formation/homolysis for R• generation. 26
Scheme 1.5 Representative S_H2-enabled R• generation. 27
Scheme 1.6. Phosphate-enabled C(sp^3)-H azidation. 29
Scheme 1.7. Employing alcohols as HAT agents. 30
Scheme 1.8. TBADT/cobaloxime-catalyzed CDC of alkanes and alkenes. 31
Scheme 1.9. Ketone-enabled C(sp^3)-H formylation. 33
Scheme 1.10. Quinuclidine as HAT agent for α-C(sp^3)-H activation of alcohol. 34
Scheme 1.11. Thiol-catalyzed dehydrative heteroarene alkylation with alcohol. 35
Scheme 1.12. Chlorine radical-enabled C(sp^3)-H activations. 37
Scheme 1.13 Bromine radical-enabled CDC. 38
Scheme 1.14. Vinyl radical-mediated ATRC reaction. 39
Scheme 1.15. Silyl radical-mediated XAT for alkyl fluoride synthesis. 40
Scheme 1.16. Giese addition with alkyl halide via amine-mediated XAT. 42
Scheme 1.17 Reduction potentials of representative molecules 43
Scheme 1.18 R• formation from carboxylic acids. 45
Scheme 1.19 R• formation from redox-active esters. 46
Scheme 1.20 Iminyl radical-induced ring-opening/halogenation. 47
Scheme 1.21 Iminyl radical-induced ring-opening/three-component coupling. 48
Scheme 1.22 Aromatization-induced R• extrusion from 4-alkyl DHP. 49
Scheme 1.23 Aromatization-induced R• extrusion from 2-alkyl dihydrobenzothiazoles. 50
Scheme 1.24 Halolactonization of unsaturated fatty carboxylic acid. 51
Scheme 1.25. R• generation from β-scission of alcohol derivative. 53
Scheme 1.26. Ketone as R• source for Minisci alkylation. 54
Scheme 1.27. R• generation via oxonium reduction. 55
Scheme 1.28. R• generation via C-N cleavage of Katritzsky salt. 56
Scheme 1.29. R• generation via C-N cleavage of quaternary nitrogen salt 57
Scheme 1.30. Reductive C=N cleavage of iminium salt. 58

Scheme 1.31. Reductive cleavage of alkyl sulfonium salt. 59
Scheme 1.32. R• from sulfinate or sulfinamide. 61
Scheme 1.33. Employing alkyl bromide for enantioselective radical-radical coupling. 62
Scheme 1.34. Utilizing alkyl trifluoroborate for radical coupling reactions. 63
Scheme 1.35. Oxidative R-Si cleavage of alkyl silicate for conjugate addition. 64
Scheme 1.36 Dearomative cyclization of alkenyl *N*-arylsulfonamides. 66
Scheme 1.37 Radical addition to [1.1.1]propellane. 68
Scheme 1.38 C3-Acylation and alkylamination of indole. 70
Scheme 1.39 Alkylation and formylation of benzothiophene. 71
Scheme 1.40 Homo- and cross-coupling of thiophene. 73
Scheme 1.41 Cyanation of heteroarenes. 73
Scheme 1.42 Minisci's heteroarene alkylations. 74
Scheme 1.43 General mechanism of Minisci's alkylations of 4-methylquinoline. 75
Scheme 1.44 Trifluoromethylation of heteroarenes. 76
Scheme 1.45 Regioselective C-H functionalization of *N*-pyrimidyl indole. 77
Scheme 2.1 Preliminary studies of diacetyl-enabled CDC reaction 98
Scheme 2.2 Coupling of heteroarenes with THF. 101
Scheme 2.3 Unsuccessful substrates. 102
Scheme 2.4 Coupling of 2-phenylquinoline with ethers. 103
Scheme 2.5 Modified protocol for ether scope 104
Scheme 2.6 Coupling of heteroarenes with unactivated alkanes. 106
Scheme 2.7 Mechanistic studies regarding diacetyl as a hydrogen atom abstractor 108
Scheme 2.8 Plausible pathways to generate the *tert*-butyl oxy radical. 109
Scheme 2.9 Side-product analysis of DTBP-assisted reaction. 110
Scheme 2.10 Plausible reaction mechanisms. 111
Scheme 3.1 Designed dehydrogenative alkylation mechanism. 155
Scheme 3.2 Gram-scale synthesis of 7b. 159
Scheme 3.3 Mechanistic studies (1). 162
Scheme 3.4 Mechanistic studies (2). 163
Scheme 3.5, UV-vis and fluorescence spectra of 4-methylquinoline (lepidine), with and without acid. 164
Scheme 4.1 Evaluation of other photocatalysts. 219
Scheme 4.2 Gram-scale synthesis of $DPQN^{2,4\text{-di-}OMe}$. 219
Scheme 4.3 Substrate scope of alkyl trifluoroborate. 220
Scheme 4.4 Substrate scope of heteroarene. 221
Scheme 4.5 Substrate scope of notable heteroarene. 222

Scheme 4.6 Photophysical properties of [QN]s. 224
Scheme 4.7. Radical pathway investigations. 228
Scheme 4.8 Proposed reaction mechanism. 229
Scheme 4.9 Synthesis of polymer-supported photocatalyst and its recycling test. 230
Scheme 4.10 [QN]/[Co] dual catalysis for oxidative (hetero)arene alkylations. 231
Scheme 4.11 [QN]/[Co] dual catalysis for oxidative alkene difunctionalizations. 232

Chapter 1 Photochemistry, alkyl radical, and heteroarene functionalization

This chapter presents the background of photochemistry in organic chemistry, representative photoinduced alkyl radical generation methods, and heteroarenes functionalizations, which are related to my research projects in the following chapters.

1.1 Organic photochemistry

Photochemistry is a specific research field studying the action of light on chemical reactions. As early as 1886, Italian chemists Ciamician and Silber have studied the conversion of quinone to quinol by light and the action of light on nitrobenzene in alcoholic solution.[1] In 1912, Ciamician individually published a perspective, *The Photochemistry of the Future*, to highlight the advantages of using solar energy to alleviate the usage of fossil fuels in industry and other potential applications in the future, which made photochemistry a major branch of chemistry.[2]

There are several definitions for photochemistry. For instance, in Well's *Introduction to Molecular Photochemistry*, photochemistry is to study chemical behaviors and physical processes of molecules that have absorbed ultraviolet or visible light;[3] on the other hand, in Turro's *Modern Molecular Photochemistry*, it was considered studying those of electronically excited molecules.[4] In fact, since electrically excited states are normally achieved when molecules absorb ultraviolet or visible light, these descriptions are not contradictory.

One could use the Jablonski diagram to explain the photoexcitation of molecules (or atoms) (**Figure 1.1**). When the photon energy reaches the energy gap between two orbitals of a ground state (S_0) molecule, the photon ($h\nu$) can be absorbed. The molecule is then excited to higher energy singlet states (S_1, S_2, S_3…) by elevating one of its electrons to a higher orbital level.

These excited states possessing two unpaired electrons are usually unstable and transient. They can undergo radiationless internal conversion (IC) to lower states, normally S_1 or S_0 accompanying fluorescence emission. Alternatively, a singlet state substrate could experience a radiationless intersystem crossing (ISC) and turn into its triplet excited state (T), in which two unpaired electrons have parallel spins. According to Hund's rule of maximum multiplicity, triplet excited states have higher multiplicity states and are more stable; at the same time, the spin state transition from triplet to singlet (or reverse) is formally forbidden by the selection rule. Therefore, triplet state substrates usually have longer lifetimes than the same level singlet states. However, triplet states could still return to the S_0 via ISC or phosphorescence emission.

Figure 1.1 Jablonski diagram

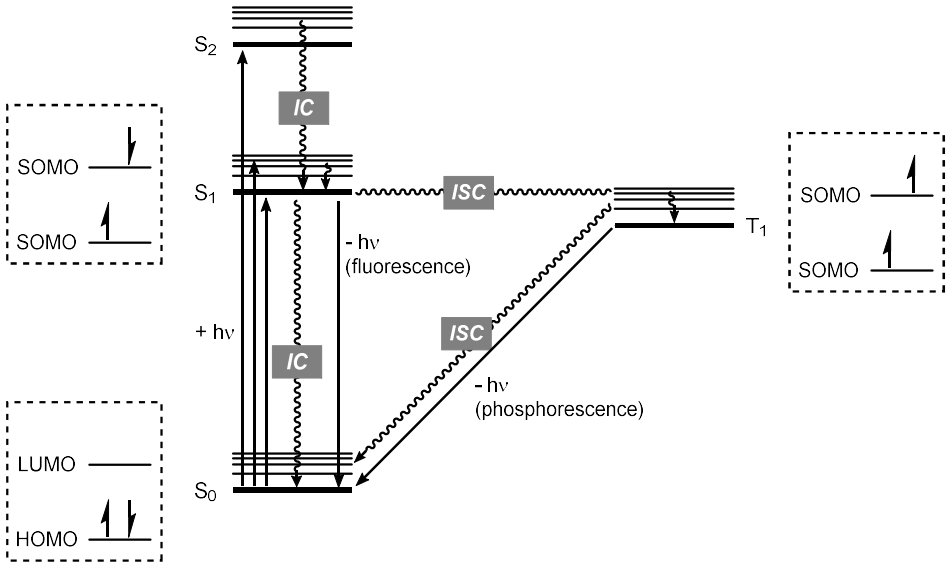

In organic photochemistry, the photoexcited molecules are used for substrate transformations. Because these molecules are usually located in high-energy positions in energy diagrams, they show distinct mechanistic pathways from conventional thermochemistry. Taking the isomerization of stilbene as an example, high temperature is

usually a requirement to overcome the energy barrier for breaking the C=C bond and accomplish the *trans* to *cis* isomerization, while thermolysis of the stilbenes would retard the reaction (**Figure 1.2**).[5-6] In contrast, by photoexciting *trans*-stilbene to its excited state, the isomerization could be accomplished under ultraviolet light irradiation at ambient temperature.

Figure 1.2 Energy diagram of thermal and photochemical isomerization of stilbene.

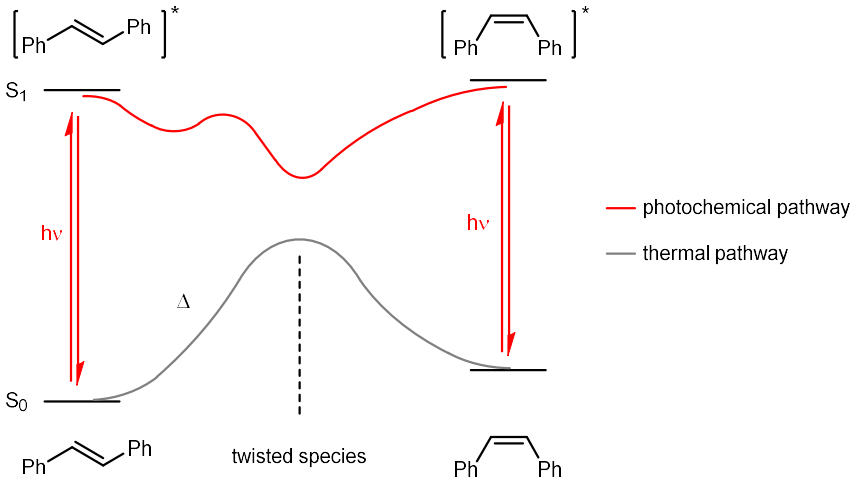

Scheme 1.1 Photoinduced C=C and C-I cleavage.[9-10]

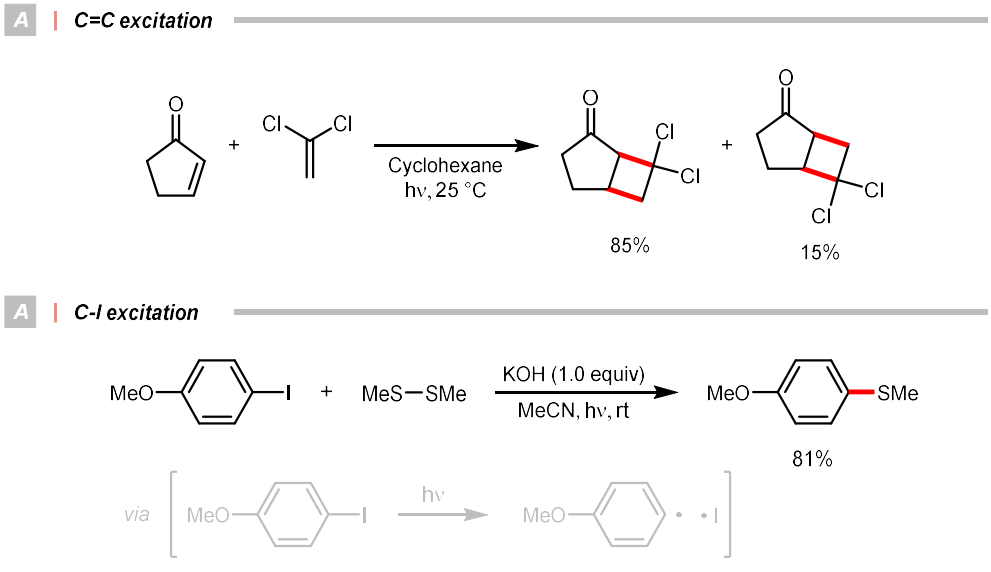

The application of photochemistry in organic synthesis is versatile and not limited to photoexcitation-induced bond isomerization. The [2+2] cycloaddition of an excited state alkene with another alkene species still represents the most powerful method to synthesize cyclobutane (**Scheme 1.1A**).[7] When a weak carbon-heteroatom or heteroatom-heteroatom bond is being excited instead, it could efficiently generate a radical pair for the ensuing reactions without a radical initiator or heating (**Scheme 1.1B**).[8]

Instead of experiencing bond cleavages, a photoexcited molecule could also transfer its energy to other ground-state species, exciting them and returning to the ground state. In this case, a photoexcitable molecule could be employed to facilitate the activation of non-excitable substrates. According to Dexter's theory, the simultaneous intermolecular exchange of excited- and ground-state electrons is responsible for such an energy transfer (ET) process (**Figure 1.3**).[11]

Figure 1.3 Dexter energy transfer.

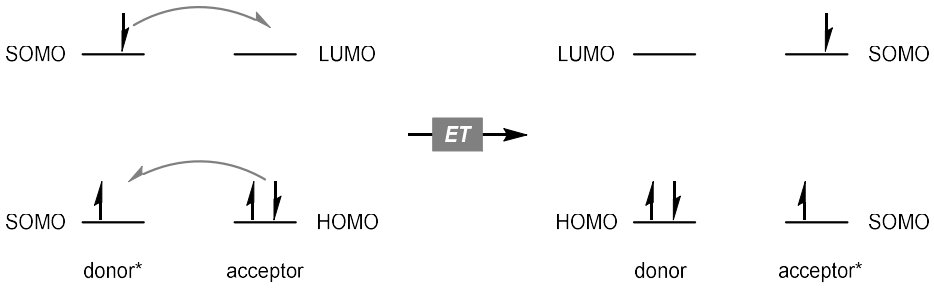

Overcoming energy barriers is not the only intriguing feature of organic photochemistry. In a photoexcited molecule, both the highest occupied molecular orbital (HOMO) and the lowest unoccupied molecular orbital (LUMO) become singly occupied molecular orbitals (SOMOs). The lower SOMO could receive an electron from an electron donor, while the higher SOMO could donate an electron to an electron acceptor, depending on their orbital lyings

(**Figure 1.4**).[12] Therefore, photoinduced single-electron transfer (SET) reactions are also viable in synthetic applications.

Figure 1.4 Photoinduced single-electron transfer.

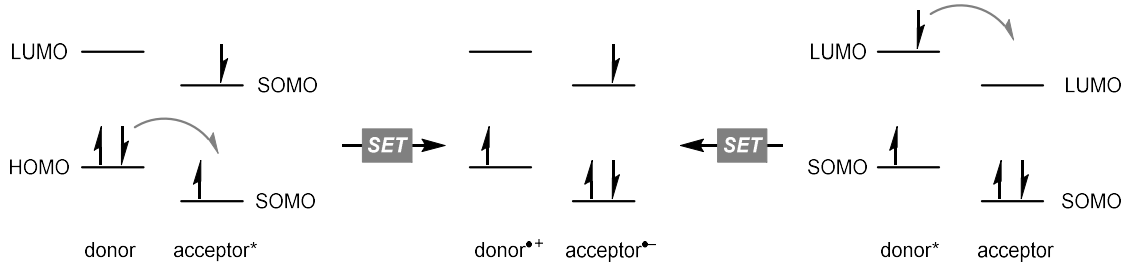

Nowadays, chemists care more than just product formation; with the rising consciousness of green chemistry, synthetic chemists also aim for high atom, step, and energy economies, utilize naturally abundant feedstocks and bypass hazardous or non-regenerable reagents while developing novel synthetic protocols. In this context, photochemistry provides a new option because photons are considered unlimited and traceless energy sources. Due to this environmentally friendly feature, it is not surprising that photochemistry is now of great research interest to the synthetic chemistry society. Its application could be frequently seen in the industry, pharmacochemistry, and key steps in synthesizing of complex molecules and macromolecules.[13] It is also notable that apart from the direct photoexcitation of substrates, the renaissance of photocatalysis stimulated the exploration of photosensitizable molecules that serve as energy transfer[7] or photoredox catalysts[14] under ultraviolet A (UVA, ~315-380 nm) or visible light (~380-750 nm) irradiations, making reaction processes more controllable and suitable for UV light-sensitive substrates (**Figure 1.5**).

Figure 1.5. Applications of photochemistry in organic synthesis.

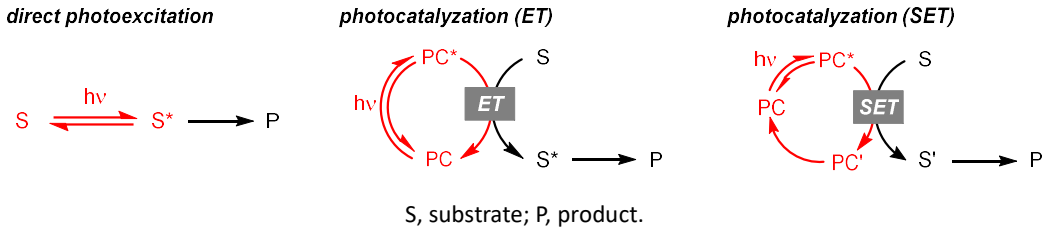

S, substrate; P, product.

1.2 Photoinduced alkyl radical generation

1.2.1 Alkyl radical

The alkyl radical (R•) represents one of the fundamental organic species in synthetic chemistry and is highly enabling in various settings. R• can be derived from feed-stock chemicals such as alkane, alkene, alcohol, amine, aldehyde, ketone, carboxylic acid and their derivatives, making it a versatile option for different synthetic purposes. Besides, it features complimentary reactivities to other alkyl intermediates (e.g., carbocation, carbanion, and carbene), providing flexible synthetic routes to build up the C(sp^3)-rich scaffold and complexity.

Historically, R• was rarely involved in reaction designs since it was often produced via energy-intensive or user-unfriendly pathways. In these cases, R• was less controllable, leading to non-productive quenching or other undesired side reactions. For instance, the thermolysis of peroxides or persulfates to form oxy radicals at high temperatures exemplified one common practice of delivering R• via activating aliphatic C-H bonds or carboxyl groups. Utilizing toxic metals such as organotin reagents to fragment alkyl (pseudo)halides was another routine method for R• generation.

Gratifyingly, photochemistry has provided distinct mechanistic pathways to bypass these thermal-chemical drawbacks. For instance, direct photoexcitation of radical precursors in early photochemistry represented a clean and straightforward strategy to generate radical

pairs, implemented in many R• formations under mild reaction temperature; however, high-energy photons were usually required. Alternatively, using photocatalysis to liberate R• catalytically, usually under visible light, could effectively manage a low concentration of radical species and minimize counterproductive radical accumulations. More importantly, photocatalysts are tunable in terms of redox potential and excited-state energy, hence, suitable for multiple synthetic cases, and the resulting R• was well orchestrated by the catalysts in the system, which could elicit reactivities that were unattainable by conventional means, e.g., enantioselective alkylation, radical-radical cross-coupling and photoredox/transition metal dual catalysis.

This section reviews the recent advances in photochemical R• generation from mechanistic perspectives.[15-19] They were categorized into four types based on the key steps during R• generation, which are (a) unimolecular homolytic cleavage, (b) bimolecular homolytic substitution (S_H2), (c) single-electron transfer (SET), and (d) radical cascade (**Figure 1.6**). In this survey, factors that govern each R• generation mode could be discussed and exemplified.

Figure 1.6 General strategies in photochemical R• formation.

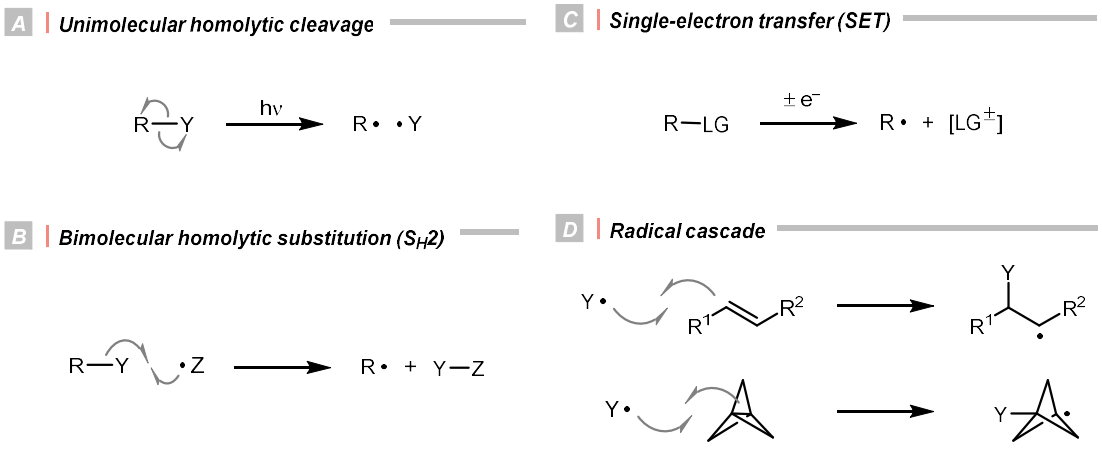

LG, leaving group.

1.2.2 Unimolecular homolytic cleavage

Unimolecular homolysis of an R-Y bond is one way to form R• for alkylation reactions under photoexcitation. Such a process relies on the dissociation of weak chemical bonds; alkyl iodides and ultraviolet (UV) light were usually applied in early studies. Nevertheless, some tactics have been developed and allowed unimolecular cleavage of new alkyl derivatives under visible light these years.

Alkyl iodides are photosensitive and relatively accessible compounds that undergo homocleavage and generate R•. In 2015, Li et al reported a transition metal-free Sonogashira coupling of alkyl iodides and phenylacetylenes in water (**Scheme 1.2**).[20] Mechanistically, the alkyl iodide was homolyzed under UV light irradiation to generate an alkyl radical and an iodine atom, which reacted with alkyne to produce α-iodo-β-alkyl styrene. NaO^{t}Bu base and moderate heating were required for efficient E2 elimination of hydrogen iodide.

Scheme 1.2 Transition metal-free Sonogashira coupling.

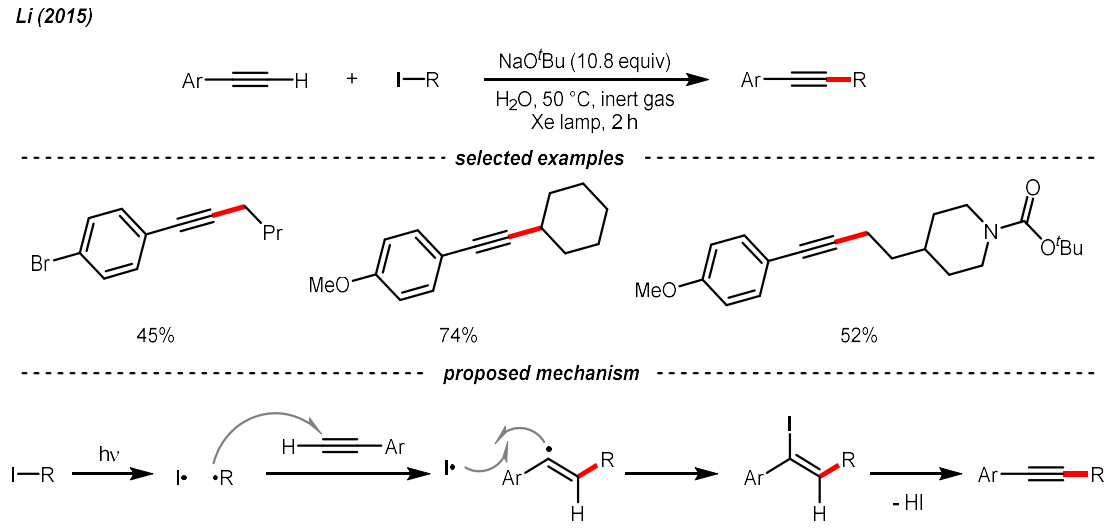

In many cases, alkyl borates engender R• through single-electron oxidation. By tuning a borate structure to shift its photochemical absorption, it could be photoexcited upon and

induce bond homolysis. In this regard, A visible light-induced C-B cleavage of boracene-based alkyl borate was recently conceived by the team of Sumida, Hosoya, and Ohmiya.[21] The alkyl borate synthesized from alkyl lithium and boracene has light absorption above 400 nm; therefore, it could be excited at 440 nm and generate R• through C-B cleavage. Various R•-based transformations such as Giese addition, heteroarylation, dimerization, Suzuki-Miyaura coupling, and alkene difunctionalization were demonstrated compatible with this system, with or without a transition metal catalyst (**Scheme 1.3**).

Scheme 1.3 Boracene-based alkyl borate as the alkyl radical source.

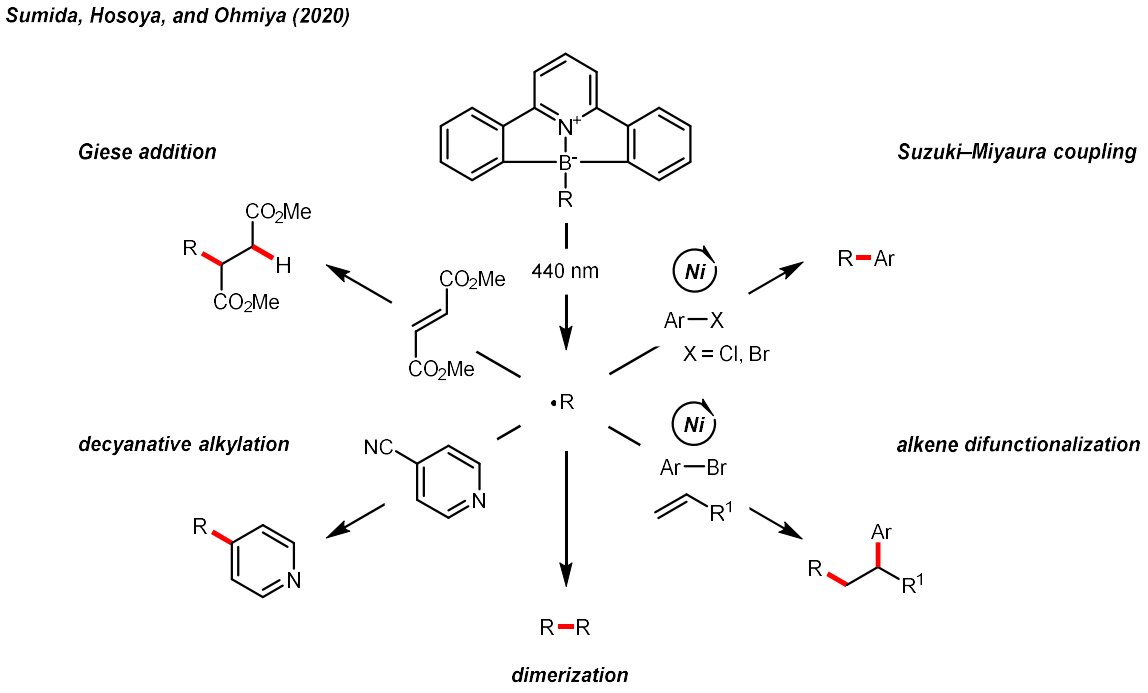

Even though these photochemical alkylations via homolytic cleavage of weak C-X bonds precedented, radical dimerization, disproportionation and other off-target processes were frequently involved due to the global excitation of reaction components, leading to narrow substrate scope and less controllable radical process. Gratifyingly, this type of R• generation could be significantly improved with a photochemical trigger.[7]

Scheme 1.4. Photocatalytic R-S bond formation/homolysis for R• generation.

Melchiorre (2019)

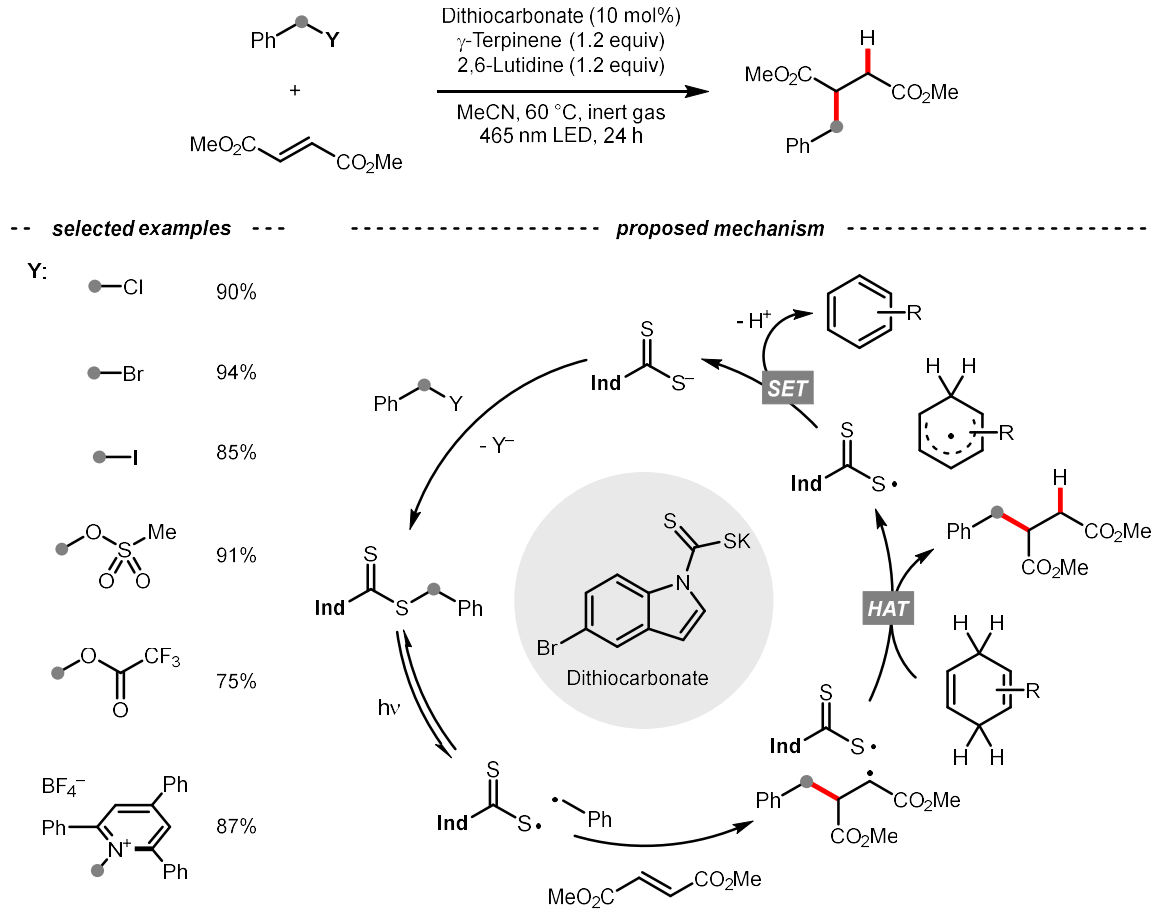

In 2019, the group of Melchiorre designed an indole-based dithiocarbamate organocatalyst to tackle this challenge (**Scheme 1.4**).[22] The nucleophilic attack of the dithiocarbamate to alkyl halides/pseudohalides could form the visible light-absorbing radical precursors, which could undergo R-S homolysis to afford a thiyl radical and the desired R•. With a substoichiometric quantity of dithiocarbamate as a photochemical trigger, the σ-bond homolysis to give R• becomes much more efficient and controllable. To this end, R• could be smoothly engaged in the conjugate addition with electron-deficient alkenes (Giese addition), wherein the γ-terpinene was added as the terminal reductant, serving as

the terminal reductant of the product hydrogen atom source and for catalyst turnover. It was noteworthy that the side reactions with thiyl radical were inconsequential since the so-formed adduct could be subjected to the light-enabled homolysis again and liberate the thiyl radical for its catalytic cycle.

1.2.3 Bimolecular homolytic substitution (S_H2)

Unlike unimolecular homolysis, bimolecular homolytic substitution (S_H2) involves generating an R• from molecule R-Y using an atom transfer agent Z•. Given the polarized transition state (TS) [R···Y···Z] • that leads to R-Y bond cleavage and Y-Z bond formation, two crucial factors, polar effect and bond-dissociation energy (BDE), should be considered in such an intermolecular process (**Scheme 1.5**).[23-24]

Matching the philicity of the R• precursor (R-Y) and the S_H2 species (Z•) is the primary concern for the feasibility and kinetics of an S_H2 process. Guided by this polarity-matching model, more efficient R-Y and Z• could be designed to facilitate the R• generation via lower-lying TS. More importantly, it allows the prediction of regioselectivity in the presence of multiple atom abstraction sites. BDE is another important parameter since the stronger Y-Z bond than the R-Y bond could provide the thermodynamic driving force to this atom transfer event and effectively prevent its backward reaction.

Scheme 1.5 Representative S_H2-enabled R• generation.

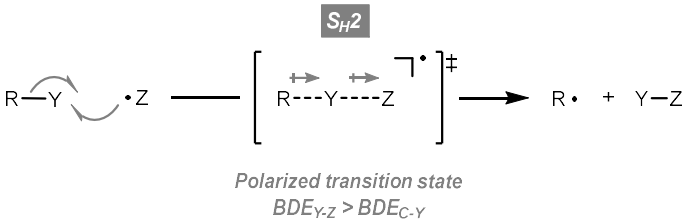

Although numerous examples are presented in the literature, the current mainstay uses the easily accessible alkanes (Y = H) and alkyl halides (Y = halide) as the R• sources. Therefore,

the corresponding hydrogen and halogen atom transfer strategies (HAT and XAT) will be discussed.

1.2.5.1 Hydrogen atom transfer (HAT). Hydrogen atom transfer is a general method to activate the R-H bond and generate R•. Due to the slightly hydridic nature of C(sp^3)-H bonds and their high bond dissociation energy (BDEs ~ 85 to 105 kcal/mol, **Figure 1.7**),[25-26] an electrophilic hydrogen atom abstractor is required, which is typically some electronegative-element-based radical (Z•) with a robust H-Z bond. However, considering the instabilities of electrophilic radicals, enabling their generation remains a common challenge in the HAT process and encourages numerous efforts in HAT reagent and reaction design.

Figure 1.7 Common BDE of C(sp^3)-H and heteroatom-H.

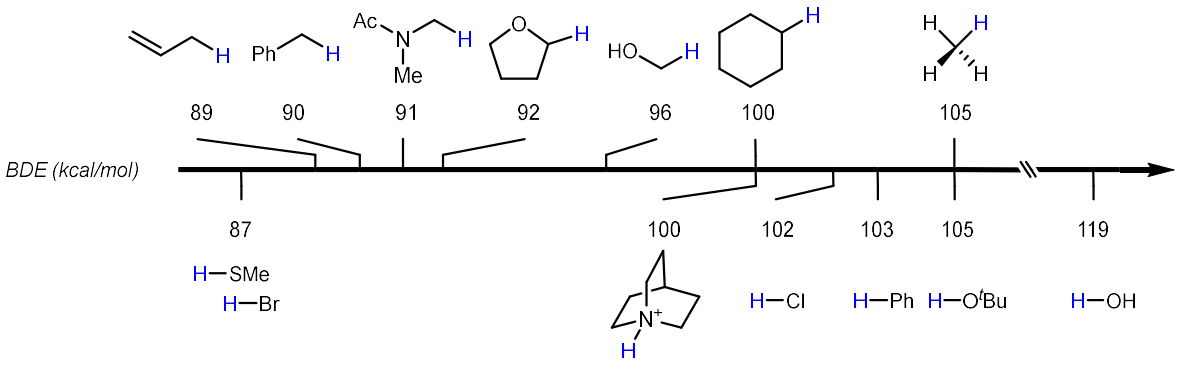

Oxy radical-based HAT. In light of the high electronegativity of oxygen and the strong bonding of O-H, oxy radicals are potent hydrogen atom abstractors. Moreover, as oxygenated compounds are readily accessible, many of them could be used or engineered as oxy radical precursors. Among them, molecular oxygen (O_2), peroxide and persulfate exemplified some classic options of oxy radical sources, demonstrating their versatile HAT reactions with R-H bonds under photochemical conditions.[27-28] Other than these choices, using alcohols and alkoxides to photochemically generate oxy radicals have gained popularity.

Organophotoredox catalysts, e.g., acridinium, feature strong visible light absorption and broad redox windows. In 2018, the collaboration between Nicewicz's and Alexanian's group showed that under visible light, the strongly oxidizing acridinium photocatalyst could catalyze the azidation of the non-activated C(sp^3)-H bond using K_3PO_4 as the HAT agent (**Scheme 1.6**).[29] Taking advantage of the photoexcited acridinium [Mes-Acr^+-Ph]*, K_3PO_4 was directly turned into the phosphate radical and afforded the R• via HAT with R-H. Aside from azidation, other reactions, including fluorination, chlorination, bromination, trifluoromethylation, and alkylation, were successful with the corresponding functionalizing reagents to trap the R•.

Scheme 1.6. Phosphate-enabled C(sp^3)-H azidation.

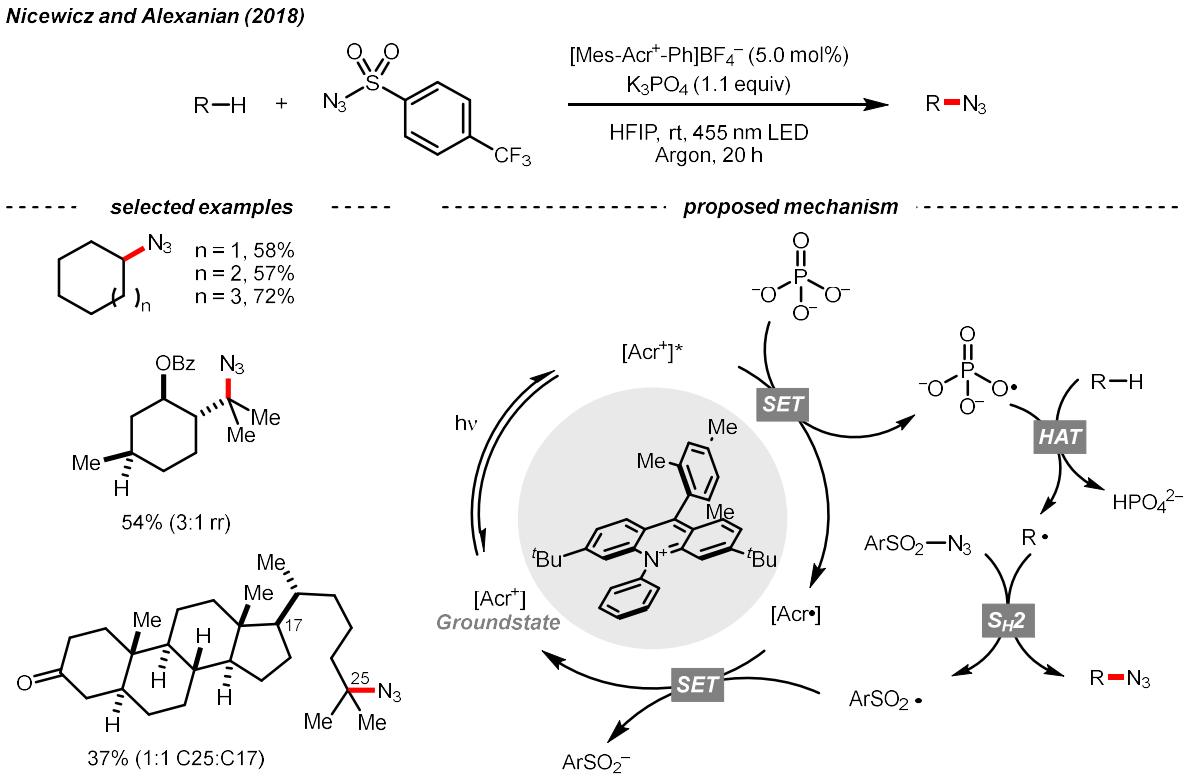

Scheme 1.7. Employing alcohols as HAT agents.

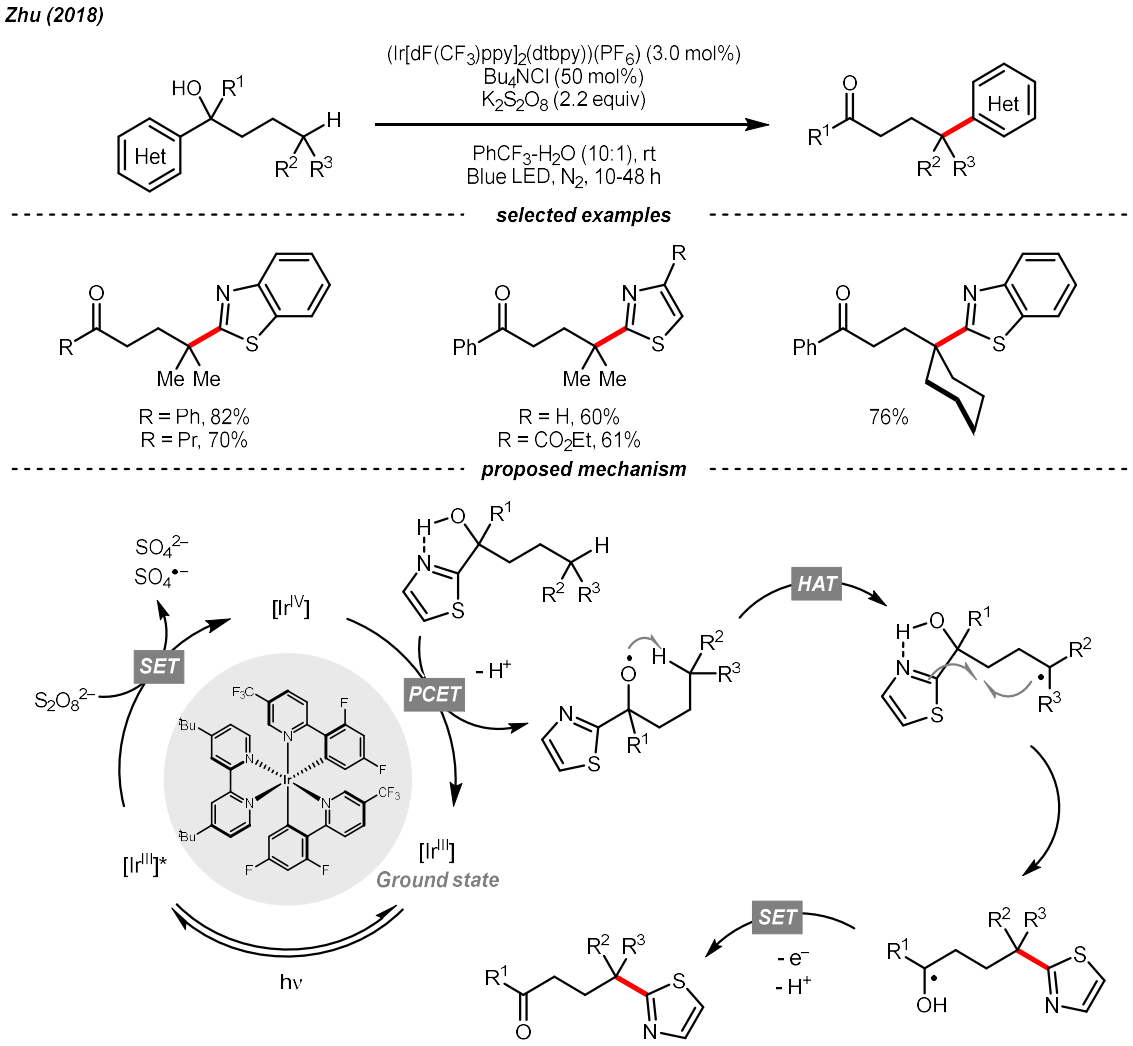

Recently, alcohols were also shown as interesting organic precursors of oxy radicals, and various strategies were developed to tackle the challenging single-electron oxidation of alcohols. In 2018, Zhu's group documented a photocatalyzed remote C(sp^3)-H heteroarylation reaction (**Scheme 1.7**).[30] With $K_2S_2O_8$ as the terminal oxidant, α-heteroaryl tertiary alcohols were converted to γ-heteroaryl ketones through sequential HAT/migratory arylation. An intramolecular proton-coupled electron transfer (PCET) might be operative to overcome the high oxidation barrier of the -OH group, which was oxidized by the Ir(IV)

species with the assistance of the internal heteroaromatic base. 1,5-Hydrogen atom transfer (1,5-HAT) ensued to give the long-chain R• and triggered the heteroarene transfer. The ketyl radical resulting from the migration was then oxidized to the ketone product. In addition to this work, migratory C(sp^3)-H cyanation, alkenylation and alkynylation were achieved by replacing heteroaromatic moiety under similar reaction conditions.[31-34]

Scheme 1.8. TBADT/cobaloxime-catalyzed CDC of alkanes and alkenes.

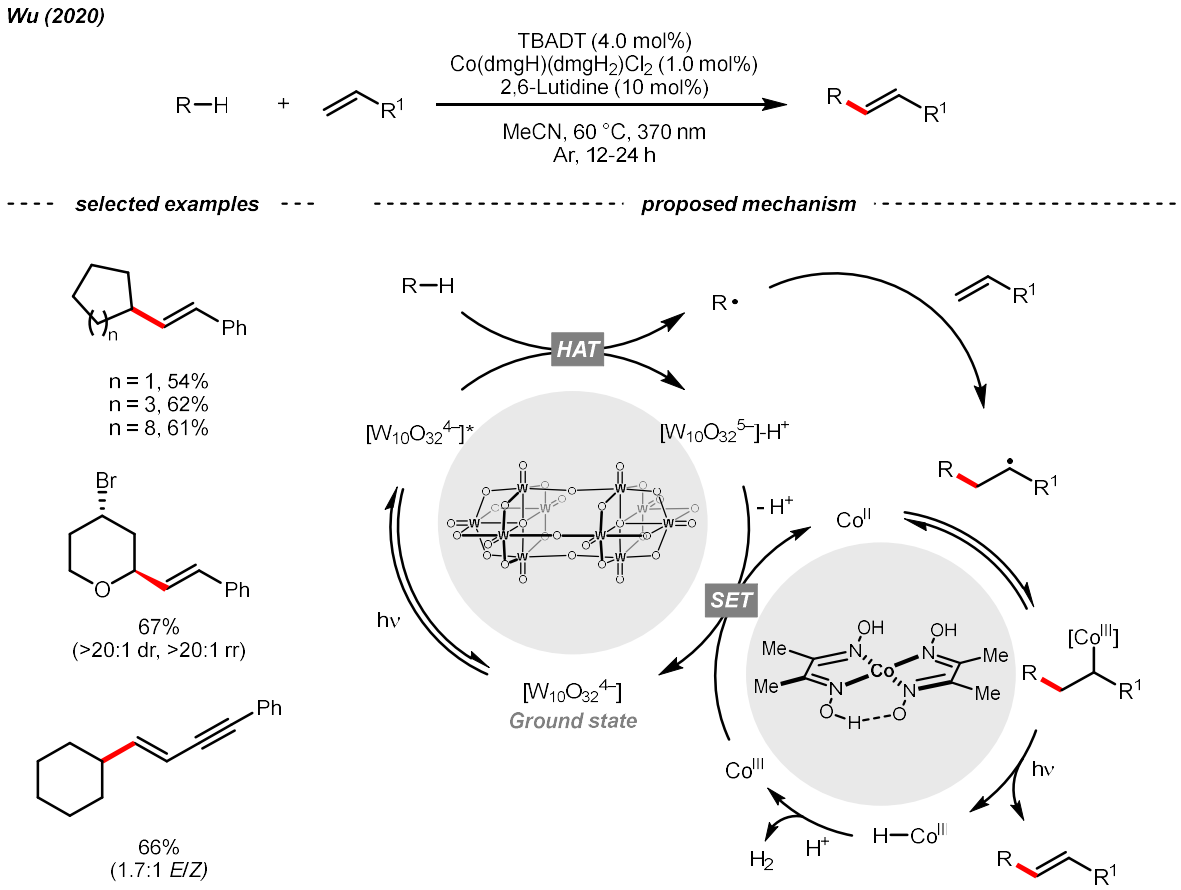

Tetrabutylammonium decatungstate (TBADT), a high-order inorganic oxide, could host a formal oxy radical on its periphery under near-ultraviolet (UVA) light irradiation. Capitalizing on this property, Wu et al designed a cross-dehydrogenative coupling between

alkanes and alkenes by merging tungsten and cobalt catalysis (**Scheme 1.8**).[35] In this dual catalysis system, tungsten was responsible for R• generation via HAT, while cobalt was proposed to turn over such a net oxidative coupling via H_2 evolution. Specifically, HAT occurred between the photoexcited decatungstate $[W_{10}O_{32}^{4-}]^*$ and alkane, affording an R• and $[W_{10}O_{32}]^{5-}$-H^+. While R• underwent the Giese addition toward the alkenyl C=C bond and produced an R'•, $[W_{10}O_{32}]^{5-}$-H^+ reduced the Co(III) into Co(II). Binding of Co(II) and R'• followed by β-hydride elimination furnished the alkylated alkene product with a high E/Z ratio and a Co(III)-H. Later, the cobaloxime cycle was closed by quenching the Co(III)-H with proton and releasing H_2.

Organic photosensitizers could display oxy radical characters under light irradiation. Ketone is a representative in this class, considering the long history of Norrish-type II chemistry. In 2018, Kamijo's group reported a photo-irradiated formal C(sp^3)-H formylation reaction using phenyl(pyridin-4-yl)methanone (4Bzpy) as the HAT agent and benzenesulfonylmethanal *O*-benzyloxime as the R• acceptor. Simple hydrolysis of the aldoxime product will deliver the aliphatic aldehydes product (**Scheme 1.9**).[36] A broad scope of C(sp^3)-H substrates, including ethers, thioethers, carbamates, and simple cyclic alkanes, was formylated in moderate to excellent product yields under mild photochemical conditions. Notably, although 1.0 equiv of 4Bzpy was used in this redox-neutral reaction, some extent of turnover could be observed as 20 mol% of perfluorobenzophenone can produce the cyclooctyl formaldehyde product in 50% yield. This result implied that the extra 4Bzpy might accelerate the product formation, and the current protocol could potentially be catalytic after further optimizations.

Scheme 1.9. Ketone-enabled C(sp^3)-H formylation.

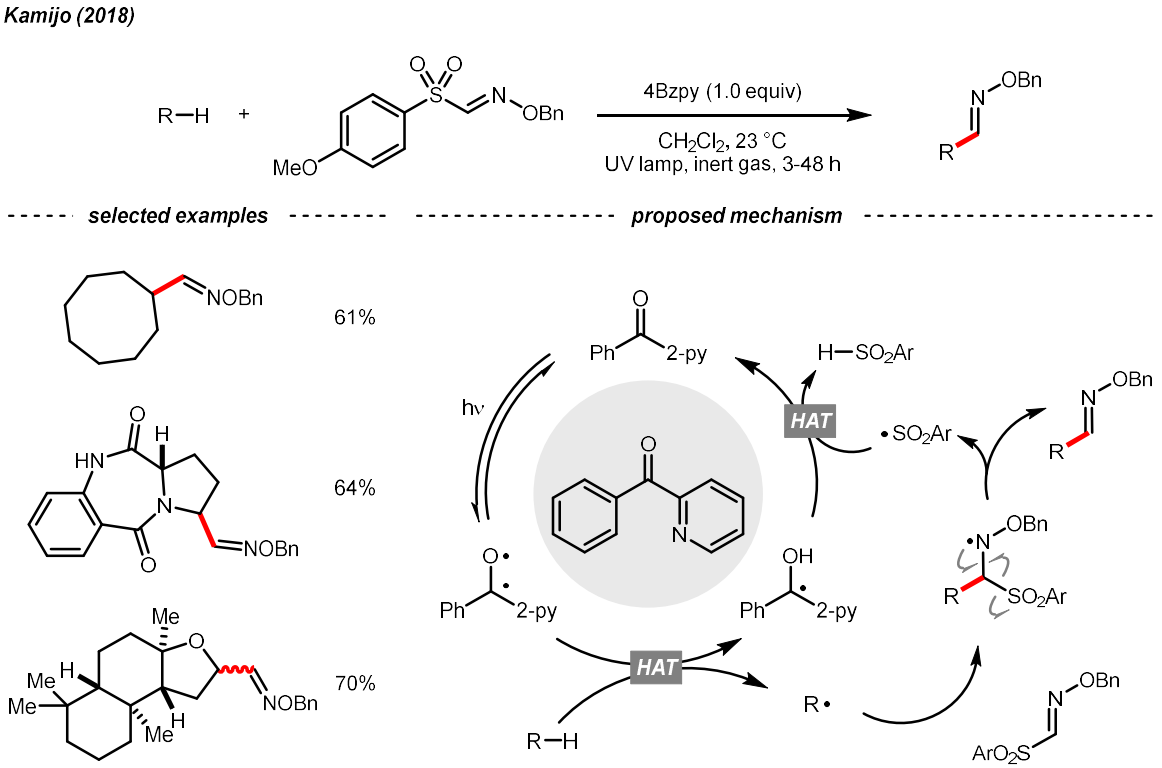

Nitrogen-centered radical-based HAT. Adjacent to oxygen, nitrogen is also a highly electronegative element. Early examples of nitrogen-centered radical (NCR) could be traced back to the Hofmann–Löffler–Freytag (HLF) reaction, which was an intramolecular NCR-mediated HAT reaction.[37-38] Although nitrogen is less electronegative than oxygen, NCRs could fine-tune their steric and electronic properties by varying the *N*-substituents.

In 2015, MacMillan et al reported an iridium/quinuclidine/phosphate triple-catalyzed photoredox reaction between alcoholic α-C(sp^3)-H bonds and electron-poor alkenes (**Scheme 1.10**).[26] In the tentative mechanism, the active NCR was generated from the oxidation of quinuclidine by the photoexcited iridium polypyridyl photocatalyst (Ir[dF(CF$_3$)ppy]$_2$(dtbpy))(PF$_6$), which produced the R• selectively at the alcoholic α-position. The unique regioselectivity might stem from hydrogen bonding between alcoholic O-H and

phosphate, which weakens the α-C(sp^3)-H bond of alcohol. Such an interaction would allow the selective alkylation with strong C(sp^3)-H bonds in the presence of weaker ones such as allylic, benzylic, α-ethereal and α-carbonyl C(sp^3)-H bonds.

Scheme 1.10. Quinuclidine as HAT agent for α-C(sp^3)-H activation of alcohol.

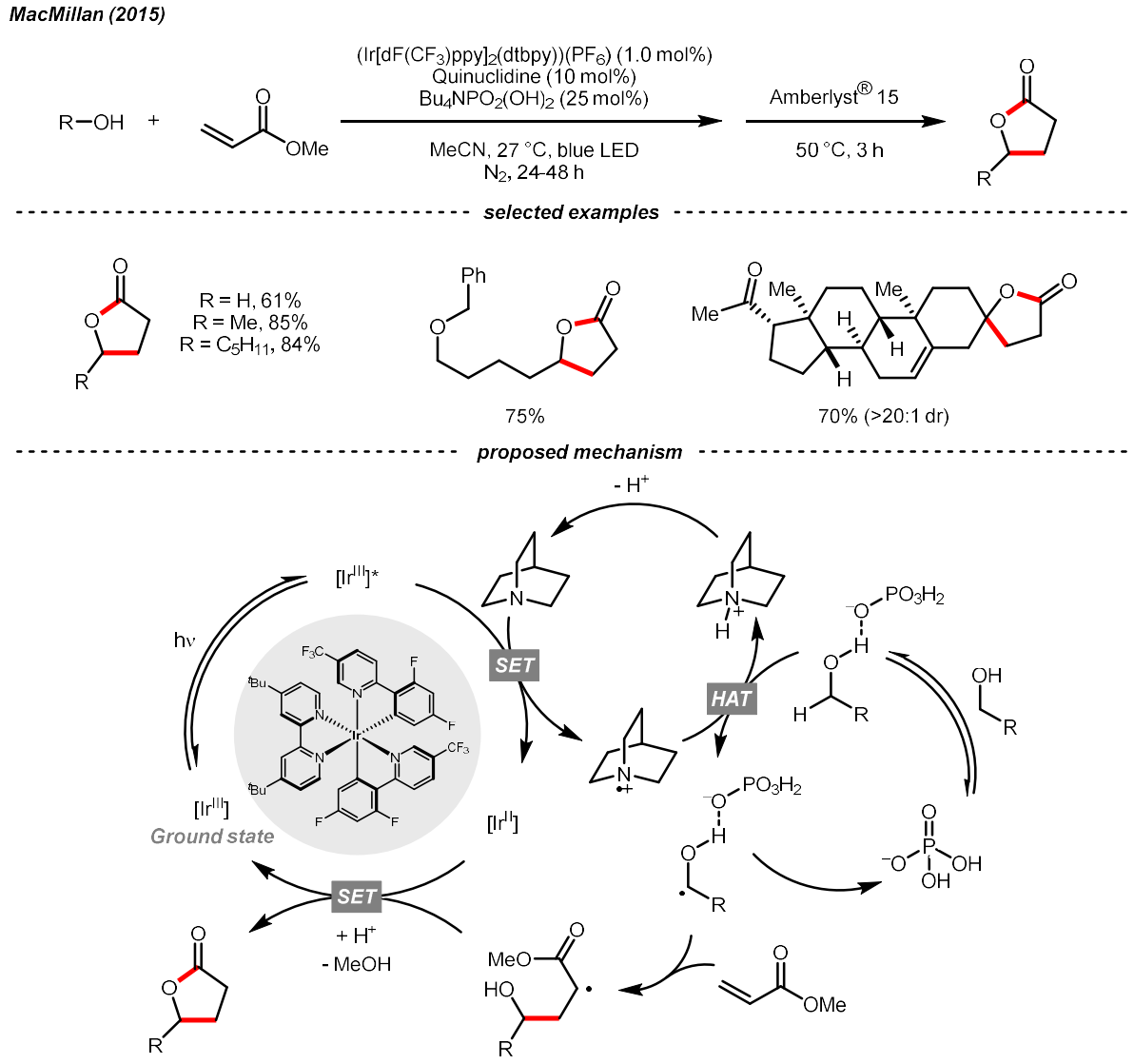

Thiyl radical-based HAT. Moving downward in the chalcogen column, *S*-centered (thiyl) radical, despite being less electrophilic than oxy radical, could also perform HAT with some

C(sp^3)-H bonds. In general, thiyl radical could be generated easier because of the more polarizable and less electronegative sulfur center.

Scheme 1.11. Thiol-catalyzed dehydrative heteroarene alkylation with alcohol.

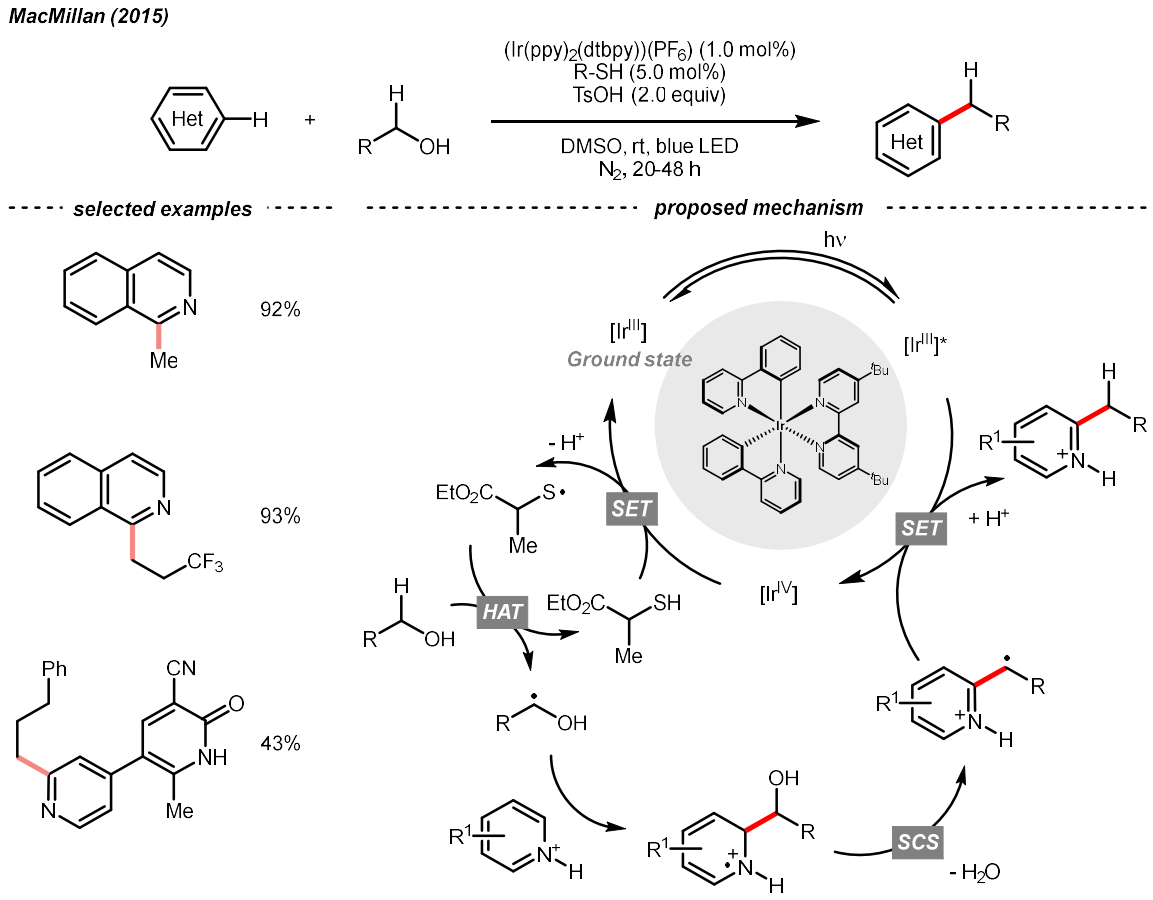

Like the oxy radical, thiyl radicals can be formed from thiols and thiobenzoates.[39-40] By merging a thiol catalyst and iridium photocatalyst, the group of MacMillan reported a dehydrative Minisci alkylation reaction using alcohols as the alkyl sources (**Scheme 1.11**).[39] Mechanistically, the essential thiyl radical came from the SET between $[(Ir(ppy)_2(dtbpy))_2]^{2+}$ and thiol catalyst. Then, the thiyl radical abstracted the hydrogen atom from alcoholic α-C(sp^3)-H thanks to the polar effect; otherwise, such transformation would be

thermodynamically unfavorable (BDE_{S-H} for thiol ~ 87 kcal/mol; BDE_{C-H} for MeOH = 96 kcal/mol). The nucleophilic addition of R• to the protonated heteroarene, following spin-center shift (SCS)-induced dehydration and some proton/electron shuttle steps would give the alkylated Minisci product. Notably, the successful application of methanol represented a breakthrough in the field of methylation.

Halogen atom-enabled HAT. The application of halogen atom (X•) in organic synthesis could date back to more than 150 years ago, when Regnault discovered that dichloromethane could be formed by exposing chloromethane and chloroform to sunlight.[41] While the Cl•-involved process remains a common practice for alkyl chloride synthesis, many novel C(sp^3)-H functionalization reactions have been established by embedding the Cl•-mediated HAT in photocatalysis.

Chlorides (Cl^-) salts represent a sustainable source of Cl• for laboratory synthesis. However, oxidation of Cl^- to Cl• ($E_{1/2}^{red}$ = +2.03 V vs SCE in MeCN) mandates strong oxidants,[42] and controlling the reactivity of Cl• remains challenging. In 2018, Barriault and his group reported an elegant solution to solve these two problems and realized an (Ir[dF(CF_3)ppy]$_2$(dtbpy))Cl-catalyzed Giese reaction with alkanes (**Scheme 1.12**).[43] Mechanistically, a radical process with Cl• and R• was proposed. The former was produced from the SET between excited Ir(III) and chloride under gentle heating conditions since the Cl^- oxidation was unfavorable in this case ($E_{1/2}^{red}$ Ir*(III)/Ir(II) = +1.21 V vs SCE in MeCN). The latter was derived from the HAT between Cl• and alkanes and was subjected to the Giese pathway. Interestingly, the reactivity of Cl• could be tamed at low concentration with pyridine as the solvent, wherein it exhibited enhanced selectivity toward tertiary C(sp^3)-H bonds than others in cyclopentyl methyl ether.

Scheme 1.12. Chlorine radical-enabled C(sp³)-H activations.

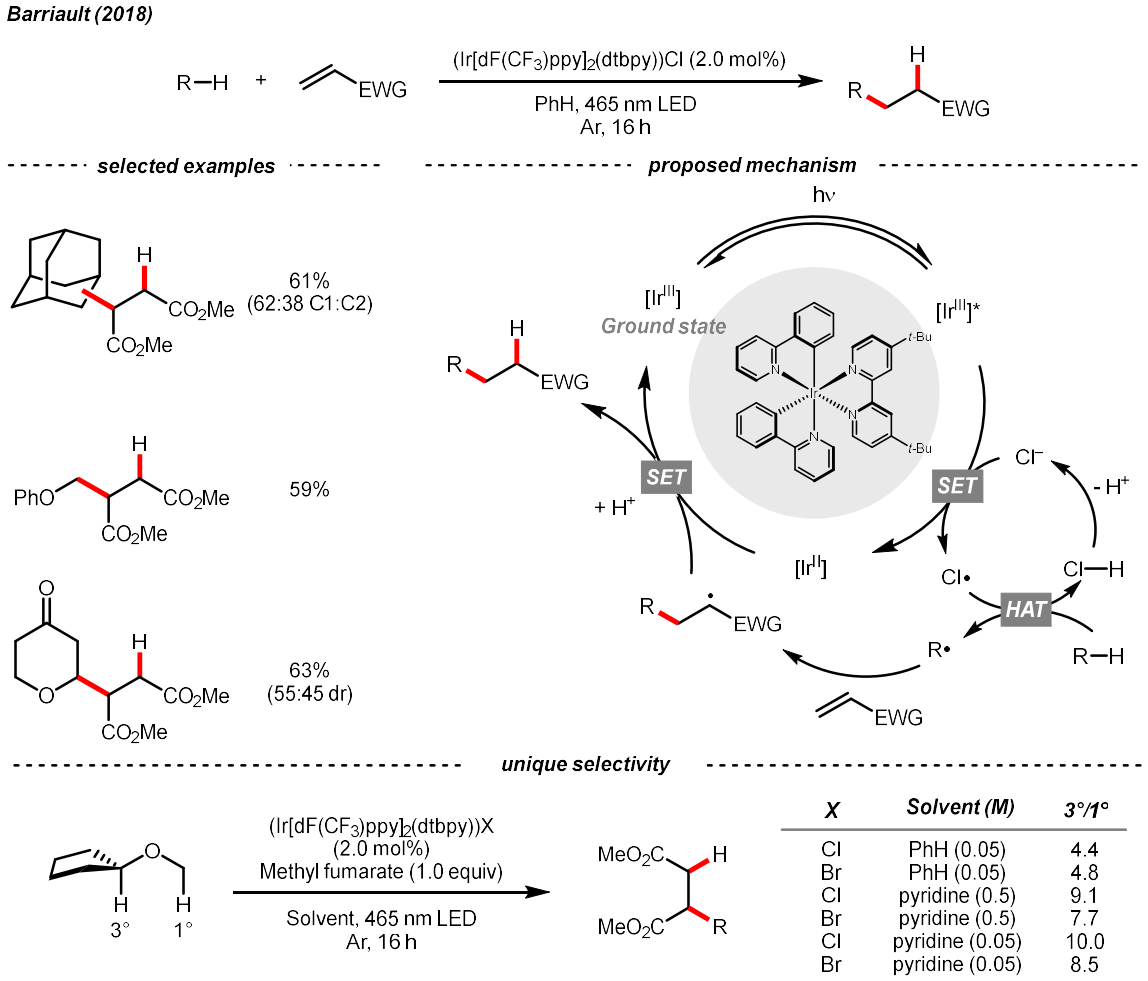

X	Solvent (M)	3°/1°
Cl	PhH (0.05)	4.4
Br	PhH (0.05)	4.8
Cl	pyridine (0.5)	9.1
Br	pyridine (0.5)	7.7
Cl	pyridine (0.05)	10.0
Br	pyridine (0.05)	8.5

Compared to Cl^-, bromide (Br^-) has a lower reduction potential ($E_{1/2}^{red}$ = +1.60 V vs SCE in MeCN), weaker hydrogen-halide bond (BDE for H-Br = 87 kcal/mol) and less electronegativity; therefore, bromine radical (Br•) is theoretically a more selective HAT agent that is easier to obtain.[44] Based on these properties, Ishida and Murakami et al utilized the nickel/iridium dual metallophotocatalytic system for the CDC between toluene derivatives and benzaldehydes (**Scheme 1.13**).[45] The direct Br^--to-Ir*(III) electron transfer of the in situ formed [Ir(ppy)$_2$(dtbpy)]Br led to the Br• formation. Impressively, by fine-tuning the molar ratio of toluenes and aldehydes, the yield of cross-coupling products could be optimized.

Scheme 1.13 Bromine radical-enabled CDC.

Ishida & Murakami (2020)

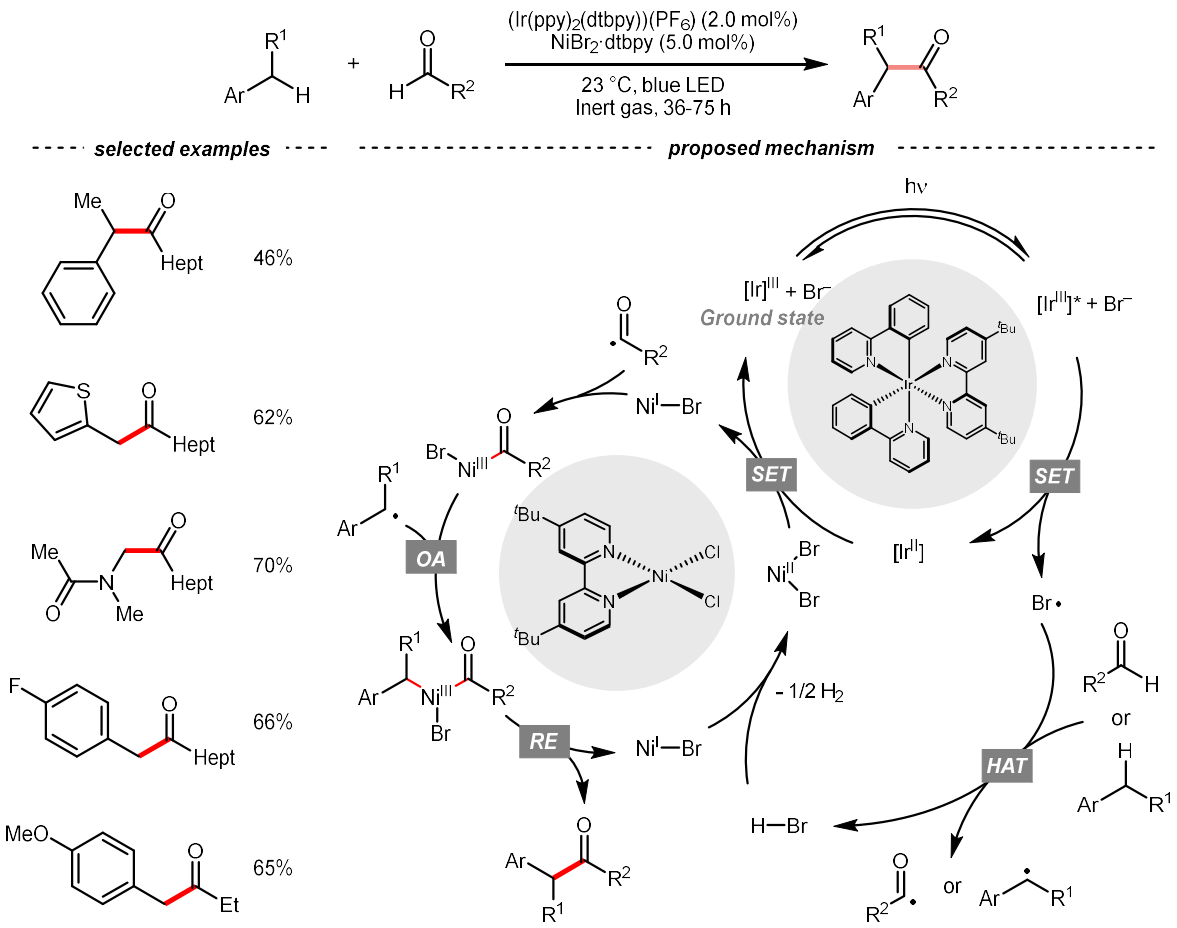

Carbon-centered radical-based HAT. Unlike heteroatom-based radicals, most non-functionalized *C*-centered radicals are nucleophilic. Since the components on both sides of the HAT equation are very similar in terms of the C-H bond strength and *C*-centered radical polarity, low kinetics of the HAT step, premature coupling process and other side reactions are major concerns of this protocol. It also explained its rare application in the intermolecular process. However, *C*-centered radical-mediated HAT enjoyed rapid development in recent years owing to the renaissance of photocatalysis. Along this line, Gevorgyan, Reiser, Zhu and other research groups have devoted themselves to advancing HAT chemistry with *C*-centered hydrogen abstractors in transition metal-catalyzed or metal-free reactions.[46-48]

Scheme 1.14. Vinyl radical-mediated ATRC reaction.

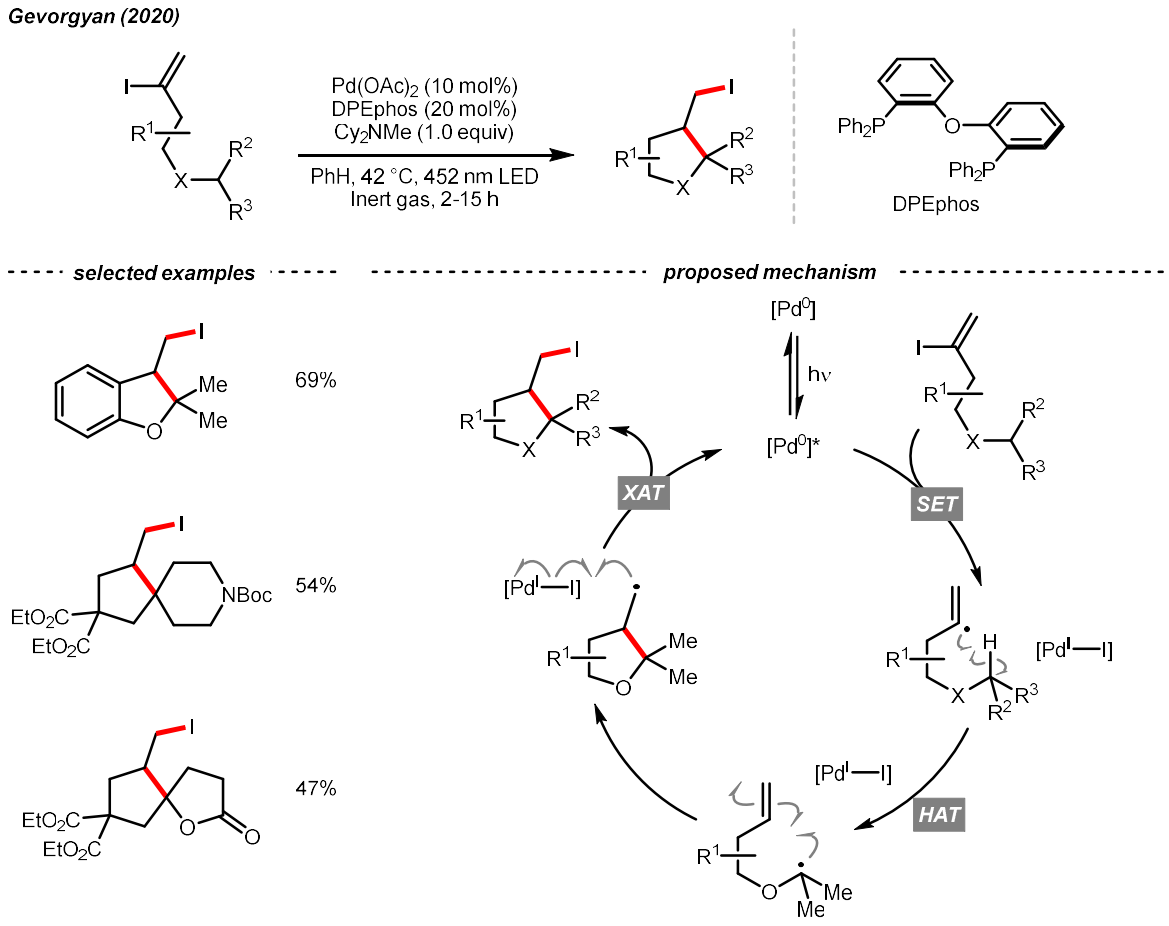

In 2020, Gevorgyan's group described a photo-induced intramolecular atom-transfer radical cyclization (ATRC) reaction of vinyl iodides to synthesize 3-iodomethyl dihydrobenzofurans under palladium photocatalysis (**Scheme 1.14**).[49] An unprecedented hybrid vinyl/Pd(I) radical pair intermediate was proposed as a consequence of SET between the photoexcited Pd(0) catalyst and vinyl iodide. A 1,5-HAT process between the vinyl radical and tertiary C(sp^3)-H bonds then proceeded, generating an R• for the iodocyclization.

Halogen atom transfer (XAT). The XAT resembles HAT, which has demonstrated its synthetic utility for decades. Historically, XAT was enabled by some nucleophilic radicals (e.g.,

tin, chromium, silyl, and aryl radicals) that can abstract halogen atoms from alkyl halides and give R•.[50-53] With the surging development of photocatalysis, these XAT radicals could be generated efficiently under mild conditions, especially those non-metallic ones, which significantly broaden the application of such an R•-generating strategy.[54]

Scheme 1.15. Silyl radical-mediated XAT for alkyl fluoride synthesis.

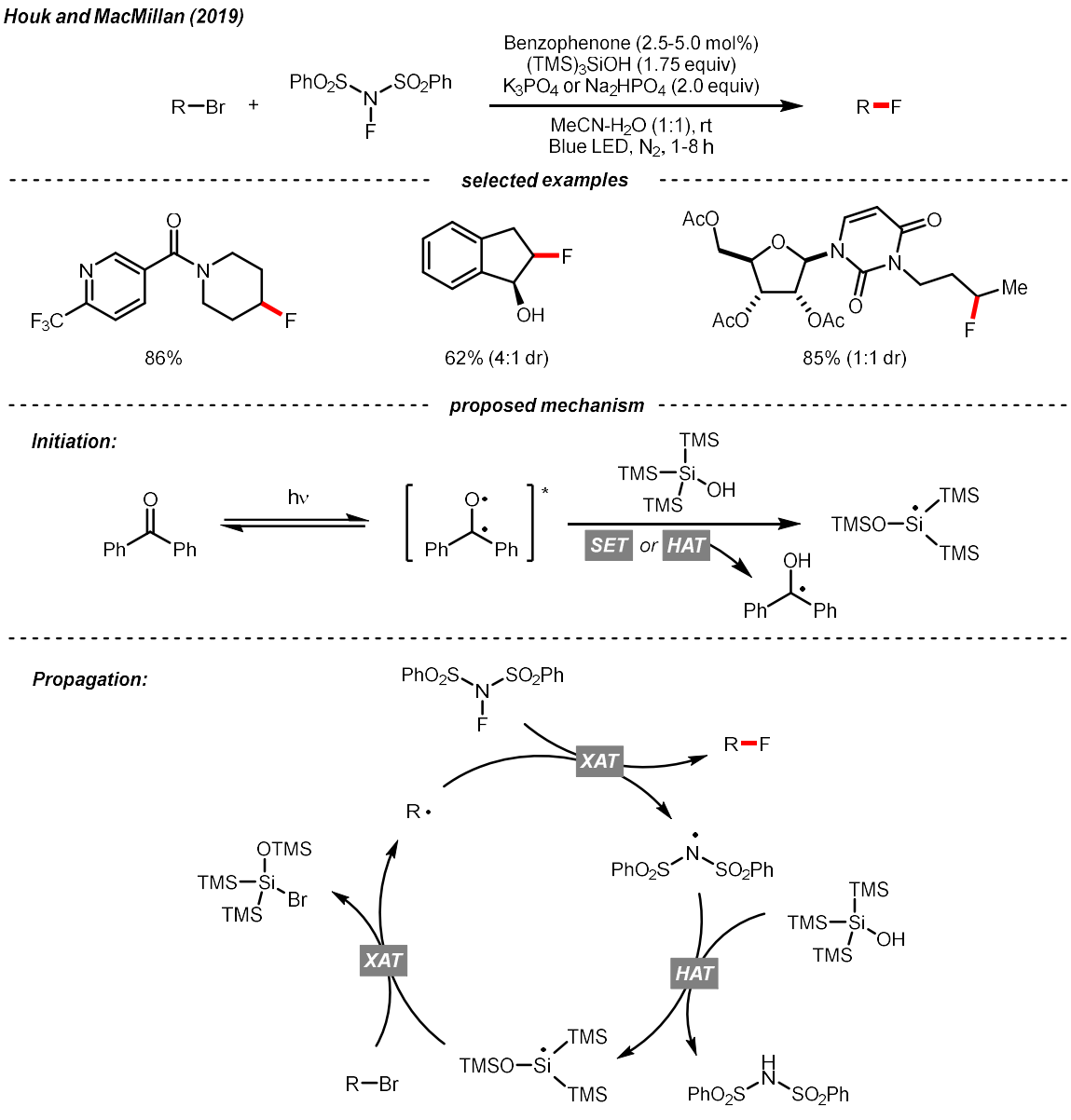

In this context, MacMillan and Houk's team developed a photo-induced reductive fluorination reaction of alkyl bromide via the XAT process (**Scheme 1.15**).[55] Based on the supersilanol-mediated bromine atom transfer strategy developed in MacMillan's laboratory,[56-58] this reaction was optimized with catalytic benzophenone and stoichiometric quantity of silyl radical source, tris(trimethylsilyl)silanol $(TMS)_3SiOH$) and electrophilic fluorinating reagent, *N*-fluorobenzenesulfonimide (NFSI). Initially, under blue LED irradiation, the excited benzophenone catalyzed the generation of silyl radical (Si•), in which the supersilanol might experience a HAT or SET process followed by the Brook rearrangement. Then, the Si• was subjected to the XAT with the alkyl bromide to give R•. The R• was fluorinated by NFSI to produce an alkyl fluoride and an NCR (sulfonamido radical), which could regenerate the Si• and propagate the radical chain process.

In addition to Si•, using *C*-centered radicals for XAT with alkyl halides was recently demonstrated by Juliá, Leonori and their co-workers. In this contribution, a $C(sp^3)$-$C(sp^3)$ bond formation reaction between alkyl halides and alkenes was disclosed, which was catalyzed by an organophotoredox catalyst 1,2,3,5-tetrakis(carbazol-9-yl)-4,6-dicyanobenzene (4CzIPN) under visible light irradiation (**Scheme 1.16**).[59] Initially, an α-amino radical resulted from the single-electron oxidation of tertiary amine by excited 4CzIPN. The key XAT benefited from the strong nucleophilicity of α-aminoalkyl radicals, which stabilized the polar XAT transition state and facilitated the R• generation. Then, the R• followed the typical reaction pathway of Giese-type radical addition to alkenes. A judicious choice of XAT reagent is essential in this design since the XAT byproduct, α-iodoamine, could degrade into an iminium iodide, therefore, combating the back halogen atom transfer.

Scheme 1.16. Giese addition with alkyl halide via amine-mediated XAT.

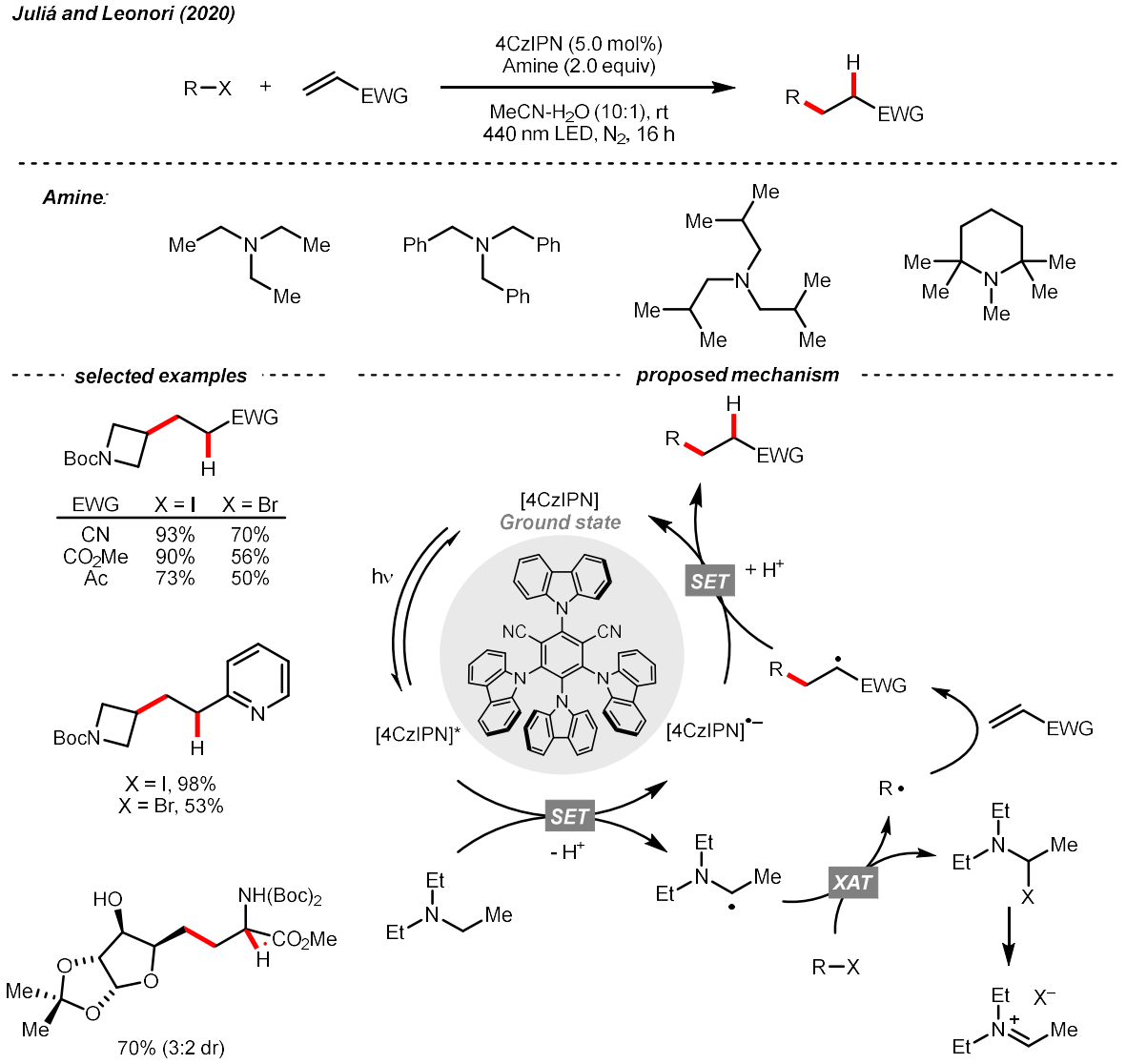

1.2.4 Single-electron transfer (SET)

Implementing SET on redox-active species R-Y to fragment either the radical species (in neutral, cationic or anionic forms) is a general strategy to generate R• in the realm of photocatalysis. Given that an extremely broad scope of chemicals could serve as R• precursors under the photoredox manifold, SET represents a highly advantageous and widely applicable strategy for the R• generation.

Scheme 1.17 Reduction potentials of representative molecules

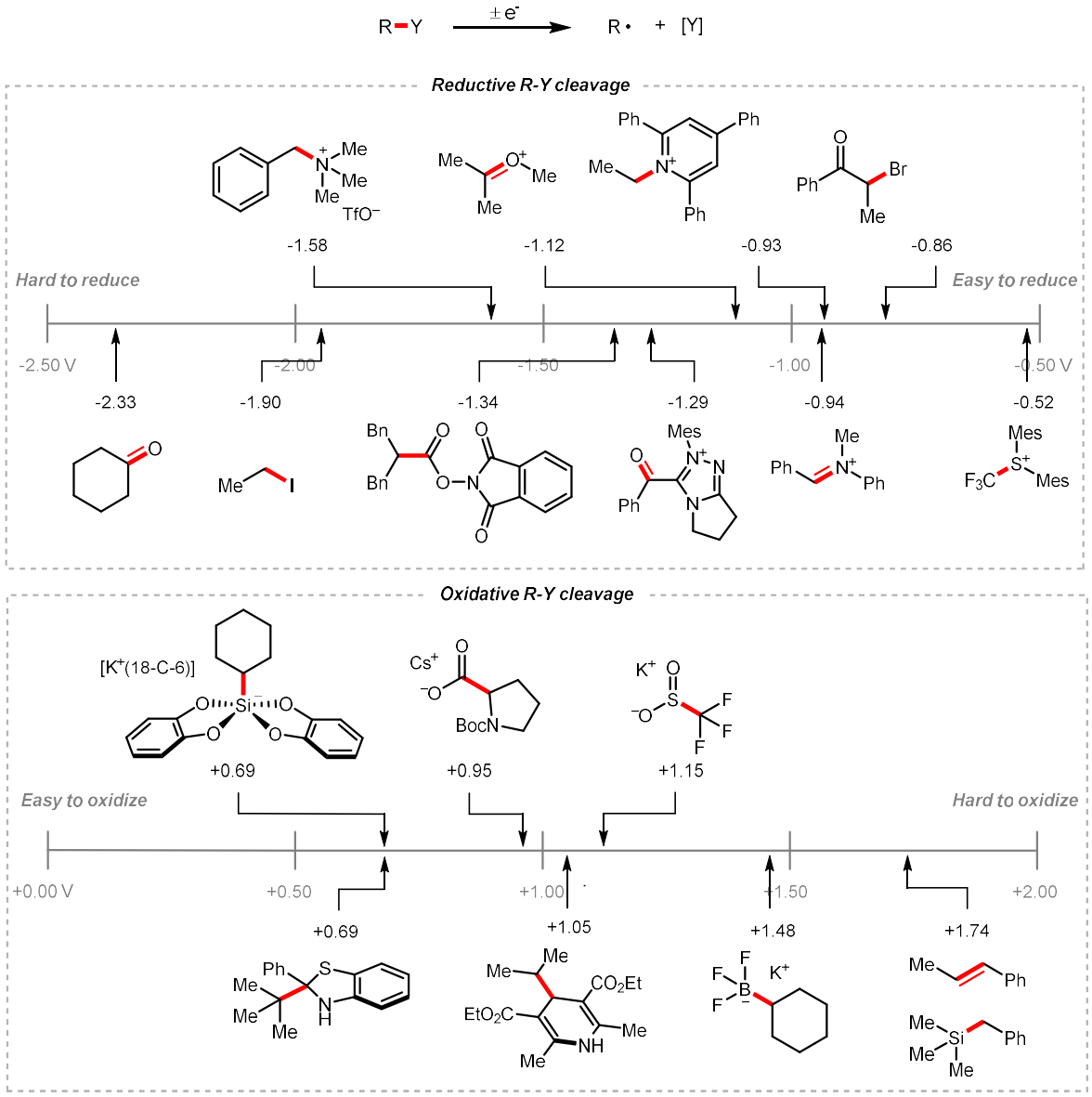

SET could be divided into single-electron oxidation and reduction depending on the nature of the redox-active R• precursor. Redox potential is the primary parameter for judging the feasibility of this electron-transfer process, which relates to its thermodynamic driving force. Therefore, orchestrating the redox couple in photochemistry could facilitate the R• generation and minimize off-target routes such as over-oxidation/reduction and back-

electron transfer. However, other factors could also matter, such as the release of ring strain, rearomatization, gas evolution and substrate pre-assembly, especially for those potential-mismatch cases.

So far, various photochemistry systems and a library of redox-active R• precursors have been documented. As listed in **Scheme 1.17**, some R• precursors are categorized based on their redox behaviors during the SET for either oxidation or reduction. The key bonds broken (R-Y) for the R• generation, along with their reduction potentials, are also highlighted.

R-C cleavage. C-C bonds are common units in organic molecules, partially explaining the highest diversity of R• precursors that involve C-C cleavage during SET to form R•.

Alkyl carboxylic acids are abundant and stable R• sources.[60] Although CO_2 extrusion offers the enthalpic advantage to elicit R• from carboxylic acids, high temperatures and strong oxidants, and sometimes the presence of transition metals, were often required in traditional methods to promote oxidative decarboxylation. However, recent advancements in photocatalysis allow decarboxylative R• generation to procced under mild conditions.[61]

In 2014, Doyle, MacMillan and their co-workers reported the seminal work of metallophotoredox catalysis by combining photoredox catalysis with nickel catalysis for decarboxylative arylation of α-amino acids with aryl halides,[62] which revolutionized the conventional design of transition metal-catalyzed cross-couplings.[63, 19] Later in 2016, the team of Fu and MacMillan updated this dual catalysis protocol to an asymmetric version using a chiral bisoxazoline ligand (**Scheme 1.18**).[64] In this metallophotoredox mechanism, single-electron oxidation of the carboxylate with the excited Ir(III) photocatalyst generated a carboxyl radical, which decomposed into an R• via CO_2 release. Meanwhile, the chiral aryl nickel(II) bromide generated from the oxidative addition of Ni(0) to aryl bromide can trap the R•, which was followed by the reductive elimination to afford the α-arylated amines in moderate to good yields with good to excellent enantioselectivities.

Scheme 1.18 R• formation from carboxylic acids.

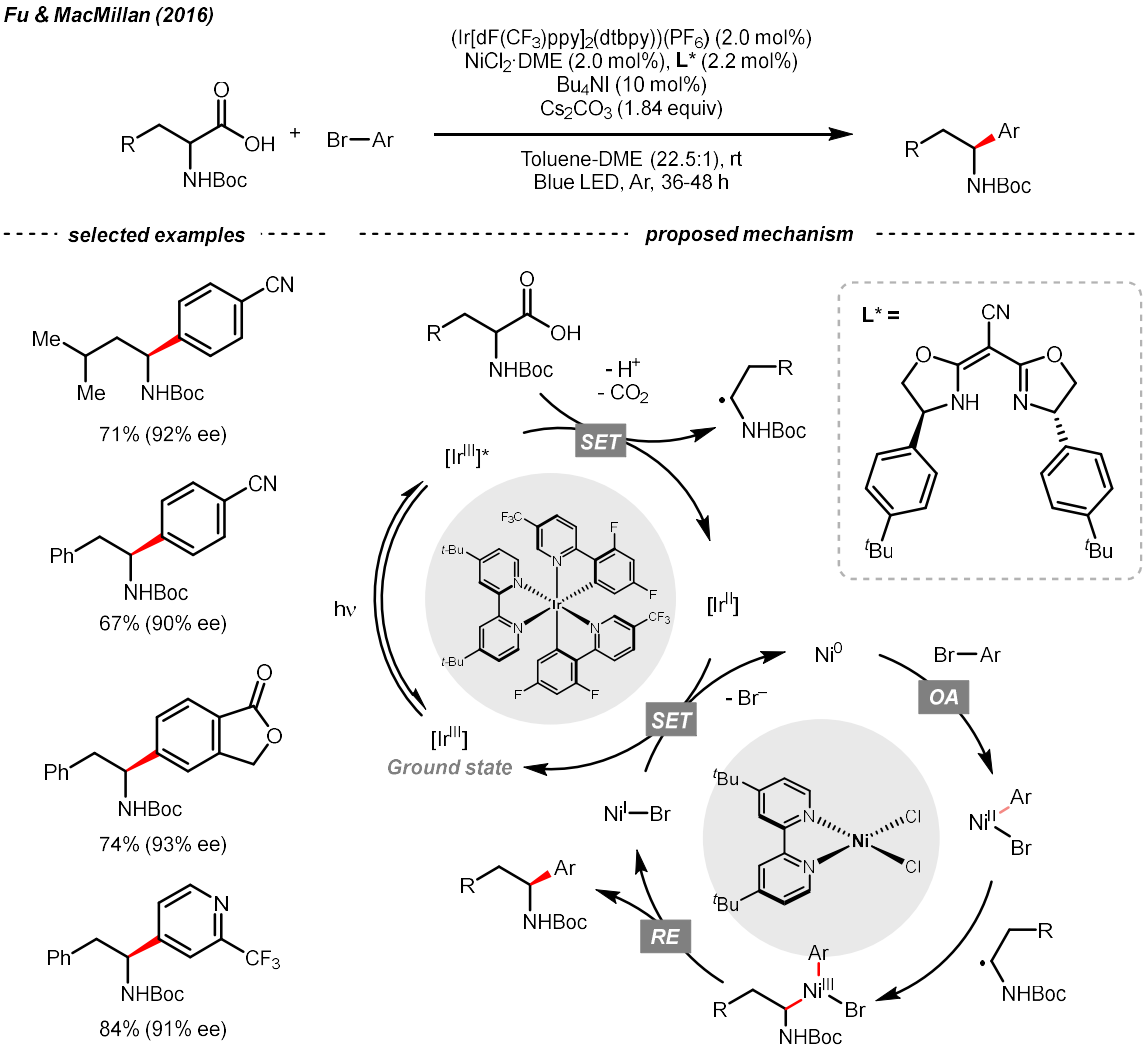

Pioneered by Okada, and later by Baran, Glorius and others, converting the carboxylic acid into the *N*-(acyloxy)phthalimide, so-called redox-active ester (RAE), could reverse the redox properties of carboxylic acid to favor a reductive decarboxylation.[65-71] One recent photocatalytic example was Liao's report of decarboxylative thiolation of *N*-(acyloxy)phthalimides utilizing Na_2-eosin Y in the presence of sulfur donor and amine reductant (**Scheme 1.19**).[72]

Scheme 1.19 R• formation from redox-active esters.

Liao (2020)

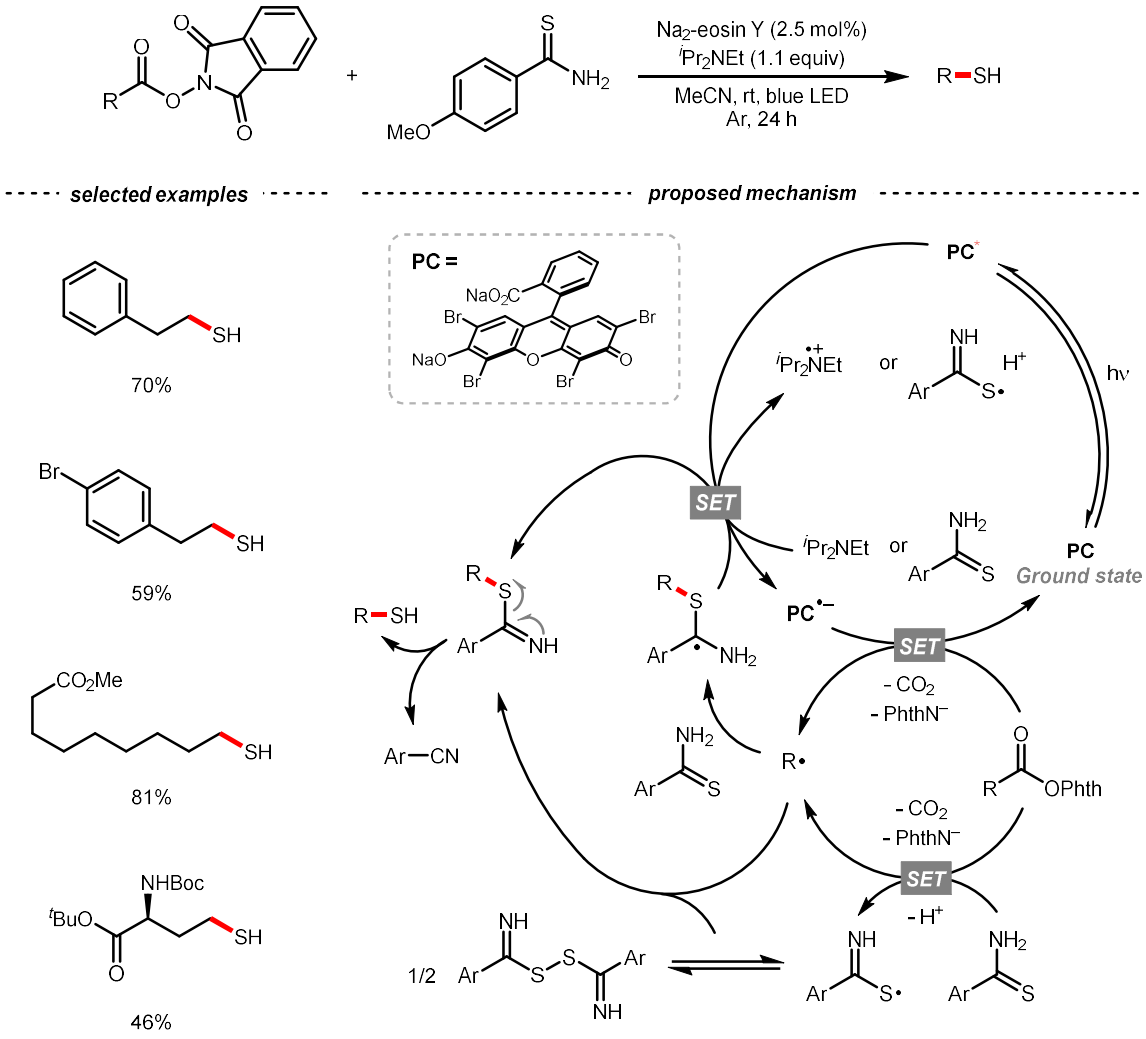

Mindful of the sensitivity of thiol products toward oxidative conditions, reductive generation of R• from photocatalytic decarboxylation could effectively avoid the undesired oxidation and complement the oxidative synthesis pathway. Under the photoreduction conditions, RAE underwent a SET/fragmentation sequence to release CO_2 and phthalimide and give the R•, which was thiolated subsequently.

Scheme 1.20 Iminyl radical-induced ring-opening/halogenation.

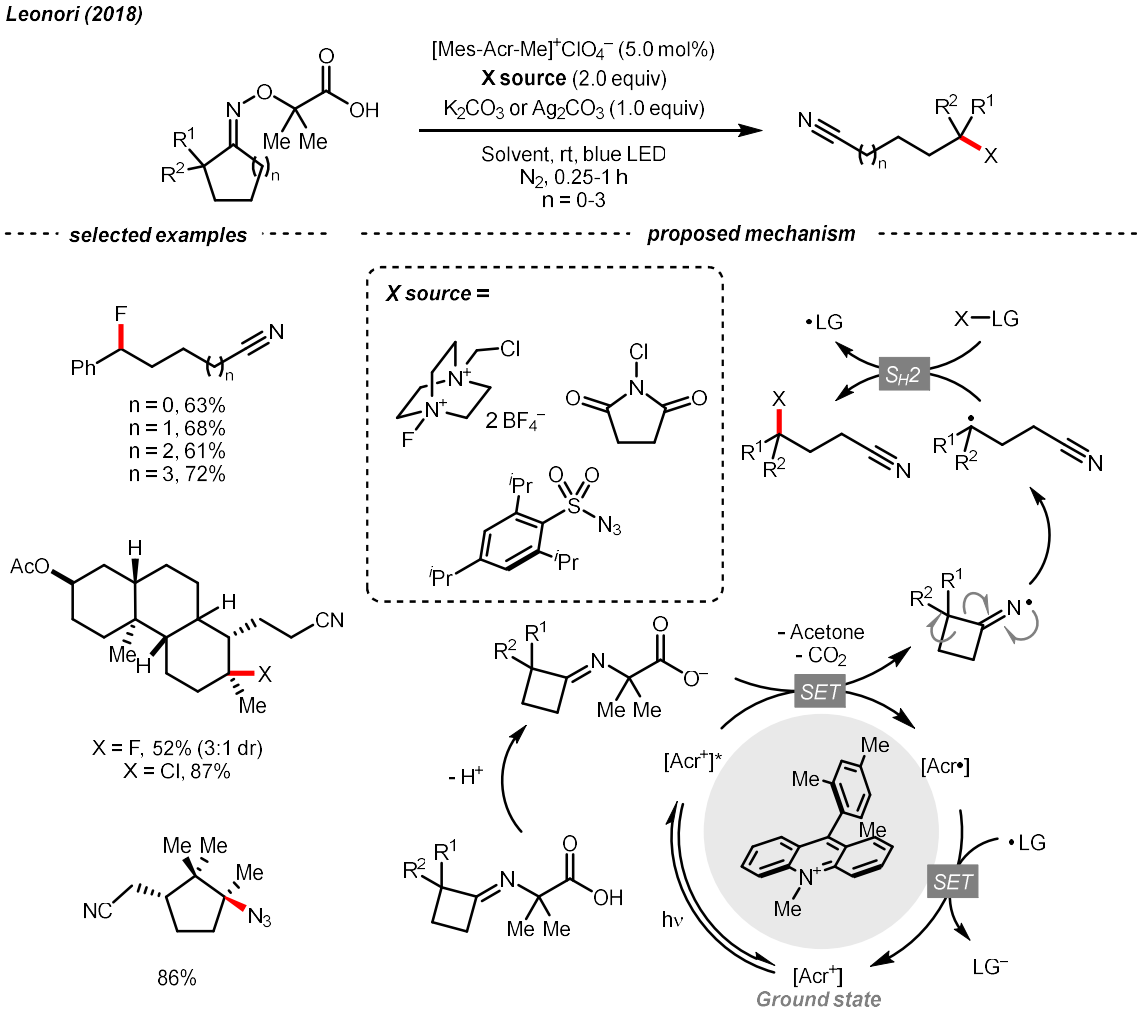

NCR resulting from SET could enable R• generation via C-C cleavage. Especially, ring-opening of cyclic iminyl radical intermediates, which are commonly derived from oxime derivatives, are useful in synthesizing alkyl nitriles. In 2018, Leonori's group showcased a photoredox synthesis of remotely functionalized alkyl nitriles using *O*-alkylated oximes derived from carboxylic acid (**Scheme 1.20**).[73] With the equimolar carbonate base, the carboxylate was oxidized by the acridinium photocatalyst (Fukuzumi's catalyst). Following CO_2 and acetone extrusion, the cyclic iminyl radical quickly fragmented into the R• with a terminal nitrile group for the subsequent fluorination, chlorination, or azidation. Ring-

opening of four-membered rings was facile, while the unstrained five to seven-membered ones required two α-methyl or one α-phenyl substituent to facilitate C-C cleavages by generating more stable R•. By intercepting the cyanated R• with nickel catalysis, radical ring-opening-arylation, -vinylation and -alkylation cascades were achieved by the same group with corresponding carbon electrophiles.

Scheme 1.21 Iminyl radical-induced ring-opening/three-component coupling.

Xiao (2018)

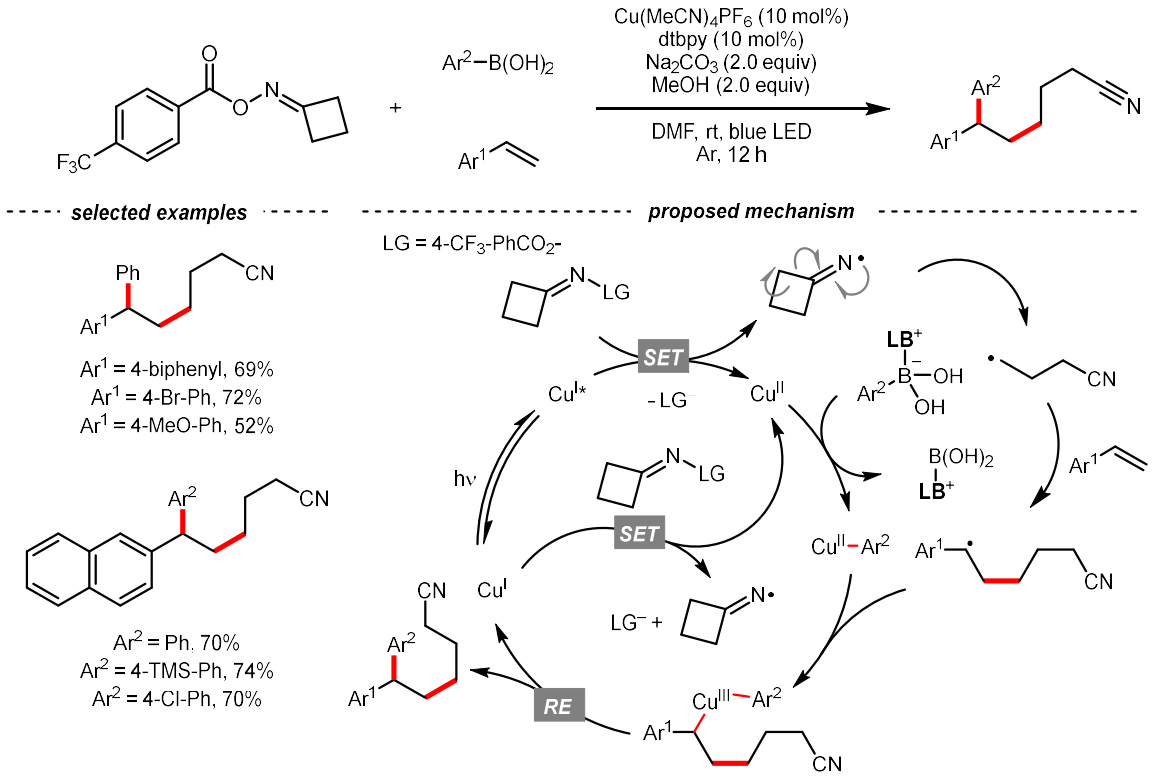

LB, Lewis base.

Reductive SET of engineered oximes could also furnish the same iminyl radicals for R• generation. In the same year, Xiao et al exemplified a visible-light-induced copper-catalyzed styrene difunctionalization reaction with oxime esters and aryl boronic acids (**Scheme 1.21**).[74] In their proposed mechanism, the excited copper(I) reduced the O-benzoyl oxime ester and triggered its N-O cleavage and β-scission. Meanwhile, copper(II) exchanged its

ligand with boronic acid to form an aryl Cu(II) species. The generated R• was trapped by the styrene and subsequently by the aryl copper(II) intermediate, which gave the 1,2-difunctionalized alkane after a facile Cu(III) reductive elimination and closed the copper catalytic cycle.

Scheme 1.22 Aromatization-induced R• extrusion from 4-alkyl DHP.

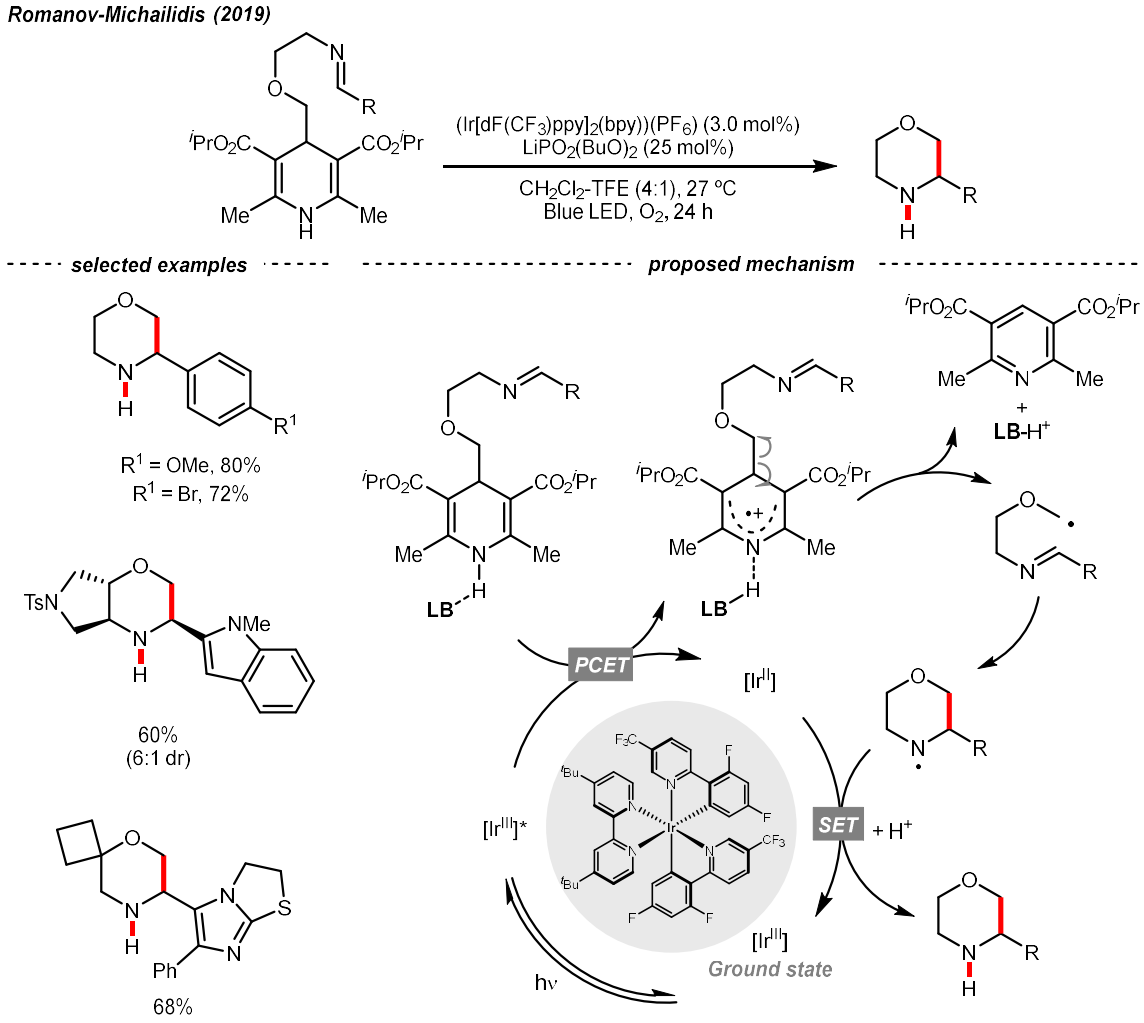

Aza-cyclohexadienyl radical is a special amino radical that mostly stems from the oxidative SET with dihydropyridines (DHPs). Bearing a strong tendency toward rearomatization via C-C cleavage at its para-position, 4-alkylated DHPs are viable R• sources. Taking a C4-

iminoalkylated Hantzsch ester as the starting material, Romanov-Michailidis et al elaborated the synthesis of several 3-aryl morpholines via R• cyclization (**Scheme 1.22**).[75] Mechanistically, PECT between the (Ir[dF(CF3)ppy]2(bpy))(PF6) and a Lewis base (LB) was believed to be a key step in their O2-mediated cyclization protocol. Ring-closure of the R• with its imine tail and the subsequent reductive quenching will give the morpholine as the desired product. Interestingly, pioneered by Melchiorre's group, several photocatalyst-free alkylation protocols with direct excitation of Hantzsch esters to engender R• were documented.[76-77]

Scheme 1.23 Aromatization-induced R• extrusion from 2-alkyl dihydrobenzothiazoles.

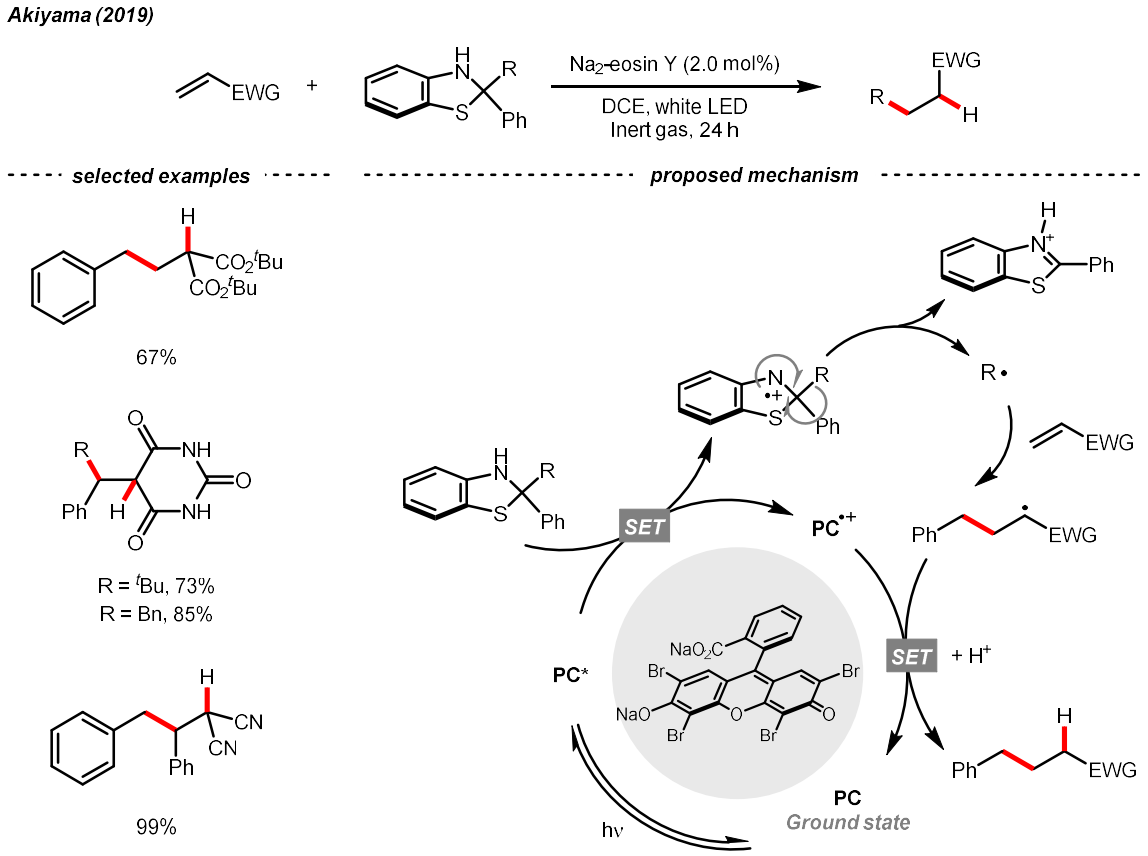

Aside from DHPs, other heterocycles and carbocycles could implement the rearomative C-

C cleavage to give the R•. For instance, Akiyama's group used C2-alkylated 2-phenyl dihydrobenzothiazoles for photo-induced radical alkylation with electron-deficient alkene as the acceptor and Na2-eosin Y as the photocatalyst (**Scheme 1.23**).[78]

Scheme 1.24 Halolactonization of unsaturated fatty carboxylic acid.

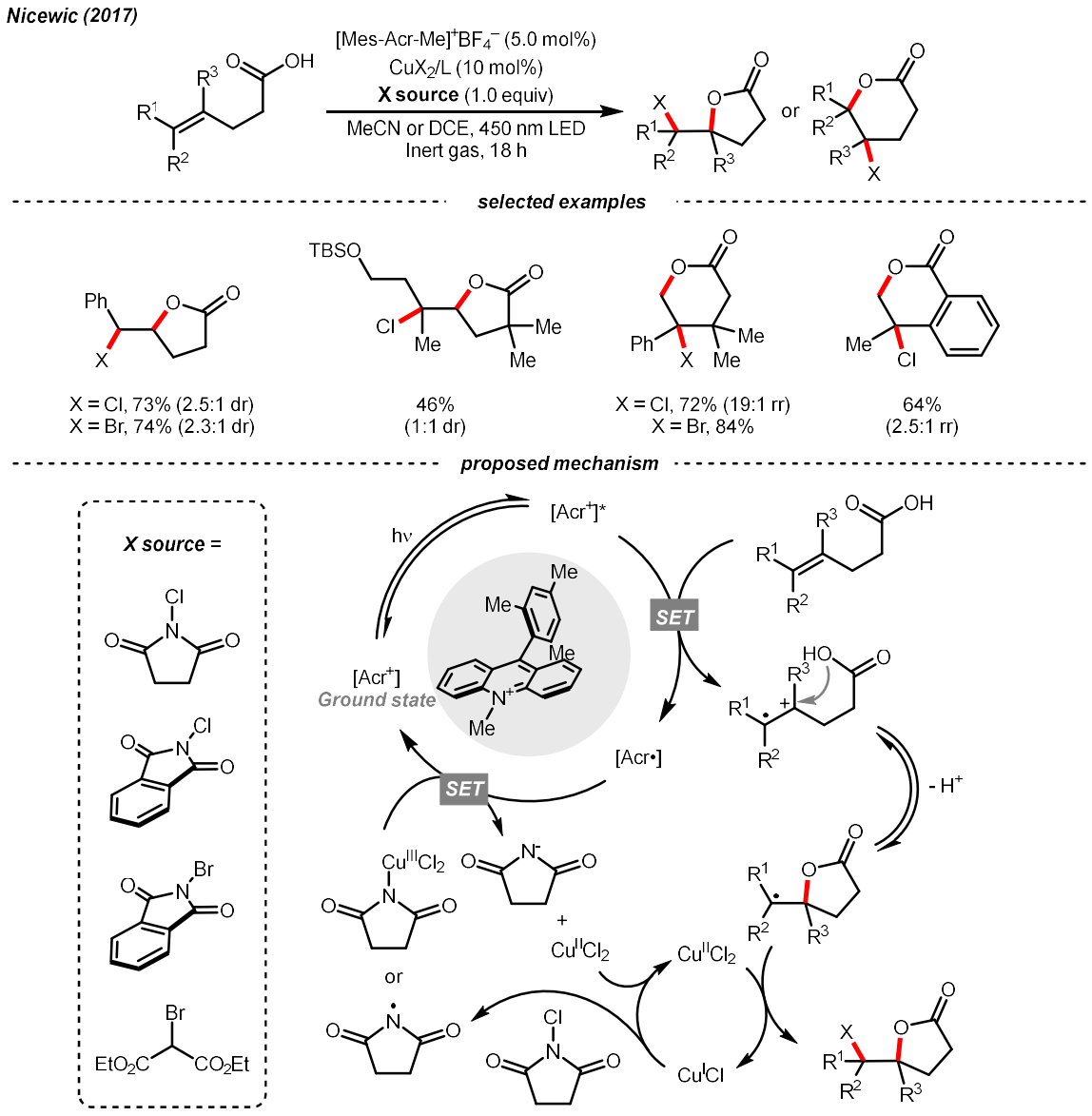

Other than cleaving C-C σ-bond, breaking C-C π-bonds under the SET mechanism could engender the R•, and more technically, the R• ion. Single-electron oxidation of a C=C bond

gives a C-C radical cation, simultaneously serving as an R• source and an electrophile for alkene difunctionalizations. Under this reaction paradigm, Nicewicz and his co-workers disclosed their seminal discovery on photocatalyzed intramolecular hydroetherification of alkenols in 2012.[79] Later, several intra- and intermolecular alkene hydrofunctionalizations followed.[80-82] In 2017, they advanced this protocol by merging Cu(II) catalyst and electrophilic halogen sources for halolactonization of unsaturated fatty carboxylic acids (**Scheme 1.24**).[83] The strongly oxidizing [Mes-Acr$^+$-Me]ClO_4^- played a pivotal role in this alkene radical cation chemistry since the reduction potential of alkenes was often beyond the reach of many common photocatalysts.

R-O cleavage. C-O cleavage exemplified a typical reaction outcome of SET to generate R• from alcohol and its derivatives. Encouraged by the well-known Barton-McCombie deoxygenation with xanthate and its later generations,[84] recent reports revealed various complementary reaction conditions using photocatalysis.

In 2015, the groups of Overman and MacMillan collaboratively unveiled a photocatalytic Giese-type approach to construct quaternary carbon centers using oxalates as the alcohol activating groups (**Scheme 1.25**).[85] In this redox-neutral fragment coupling, reductive quenching of the Ir*(III) by tertiary alcohol-derived caesium oxalate was conceived as feasible. The R• obtained from two C-O cleavages was added toward electron-deprived alkene, furnishing the alkylated product through electron and proton transfer with the rest of the photocatalytic cycle. The double decarboxylation of secondary alkali metal oxalates was less efficient, slightly limiting the scope of applicable alcohols. However, such an oxalate-based approach opened chemical space for various radical transformations soon after, as the same group published a metallophotoredox cross-coupling reaction with the oxalate salts.[86] It is worth noting that under the SET manifold, many other smart approaches have been devised to cleave the alcohol C-O bonds, for example, the phosphoranyl radical-mediated

benzyl alcohol deoxygenation.[87]

Scheme 1.25. R• generation from β-scission of alcohol derivative.

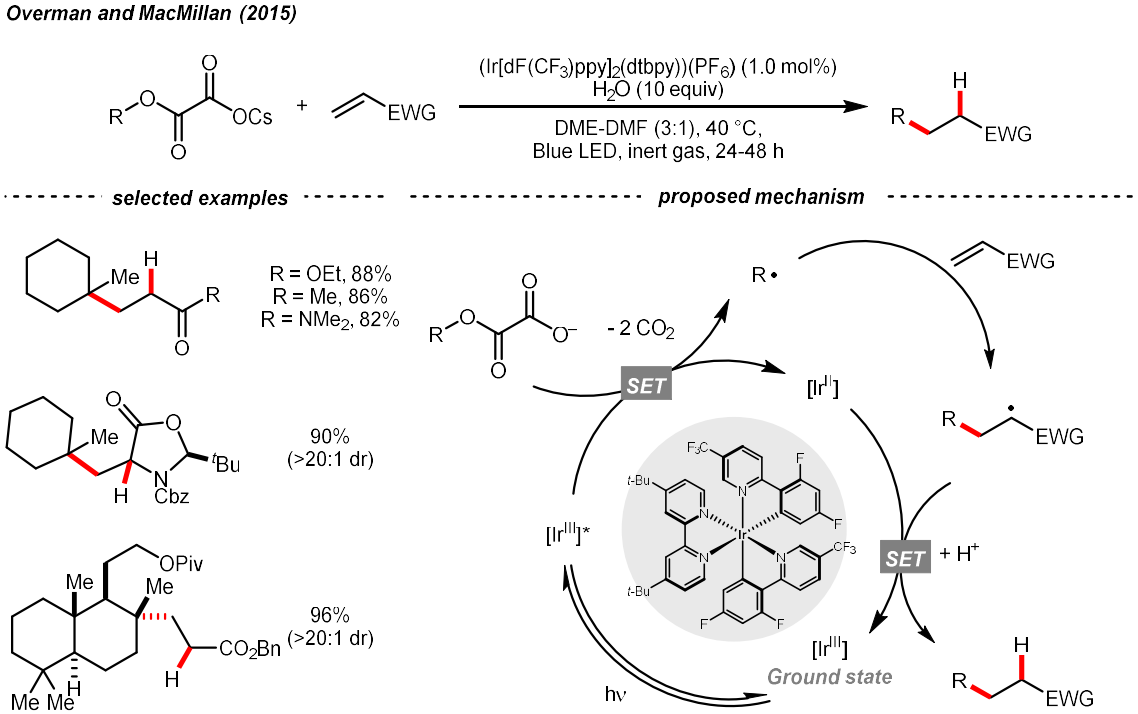

With photoredox catalysis, C=O could also serve as the R• precursor via SET-enabled C-O cleavage. Combining $[Ir(ppy)_2(dtbbpy)]PF_6$, tris(trimethylsilyl)silane (TTMSS), and trifluoroacetic acid (TFA), Wang's group realized a photocatalyzed deoxygenative hydroheteroarylation of ketone (**Scheme 1.26**).[88] A stepwise C-O cleavage mechanism involving ketyl radical (R•) was proposed. Hypothetically, the protonated ketone obtained an electron via a PCET mechanism, which derived from the photoreduction of Ir*(III) by TTMSS. The nucleophilic ketyl radical was added to the protonated heteroarene, which gave an α-aminoradical after proton transfer. Driven by the rearomatization, an SCS process proceeded with the removal of H_2O, providing the alkylated heteroarene via the HAT with solvent. Concurrently, Huang's group reported a similar deoxygenative Minisci alkylation with

aldehydes, which was proposed as a photocatalytic Br•-mediated process.[89]

Scheme 1.26. Ketone as R• source for Minisci alkylation.

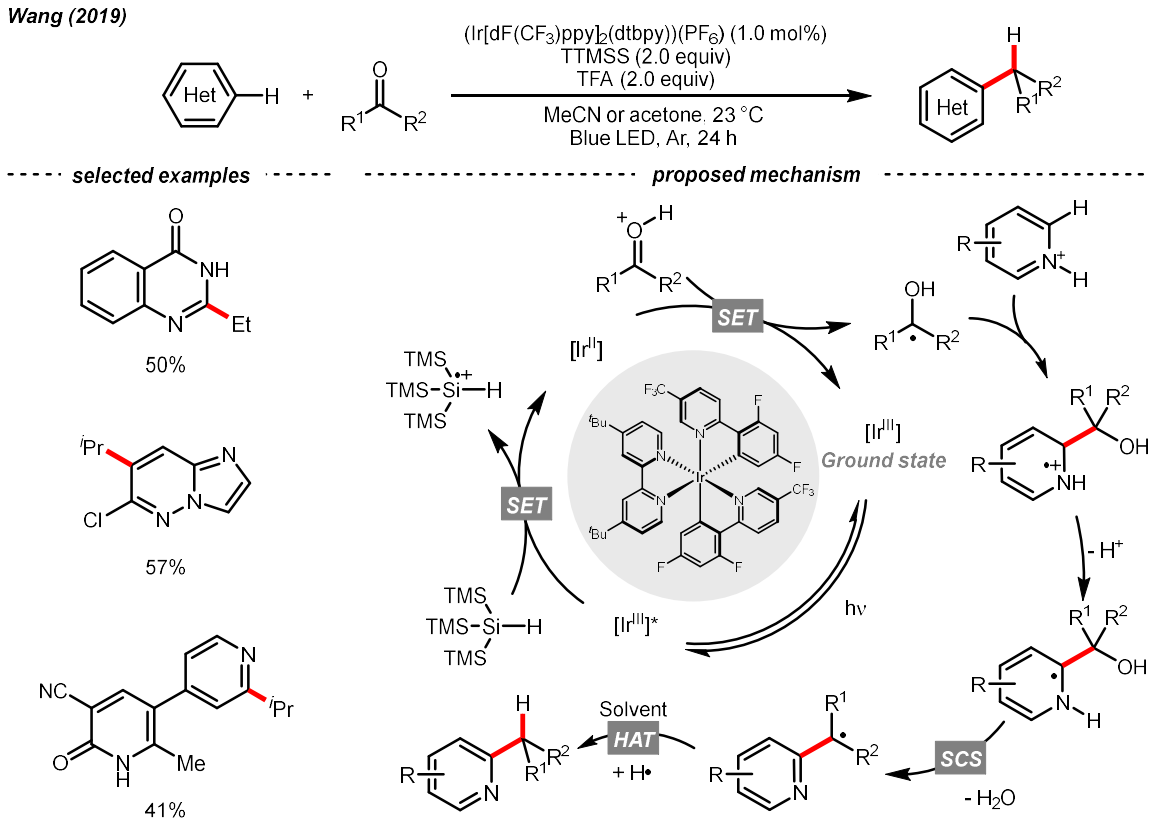

TTMSS, tris(trimethylsilyl)silane.

Also, in 2020, Dixon et al utilized alkyl enol ethers under acidic conditions and generated oxonium tautomers in situ as activated carbonyl and R• precursor (**Scheme 1.27**).[90] In this work, the oxonium ion was reduced by the Ir(II) derived from the SET between excited Ir(III) photocatalyst and 4-phenyl Hantzsch ester, forming an α-ethereal radical (R•). Adding such an R• to the conjugated alkenes followed by HAT with the Hantzsch ester brought the α-tertiary dialkyl ethers as desired products.

Scheme 1.27. R• generation via oxonium reduction.

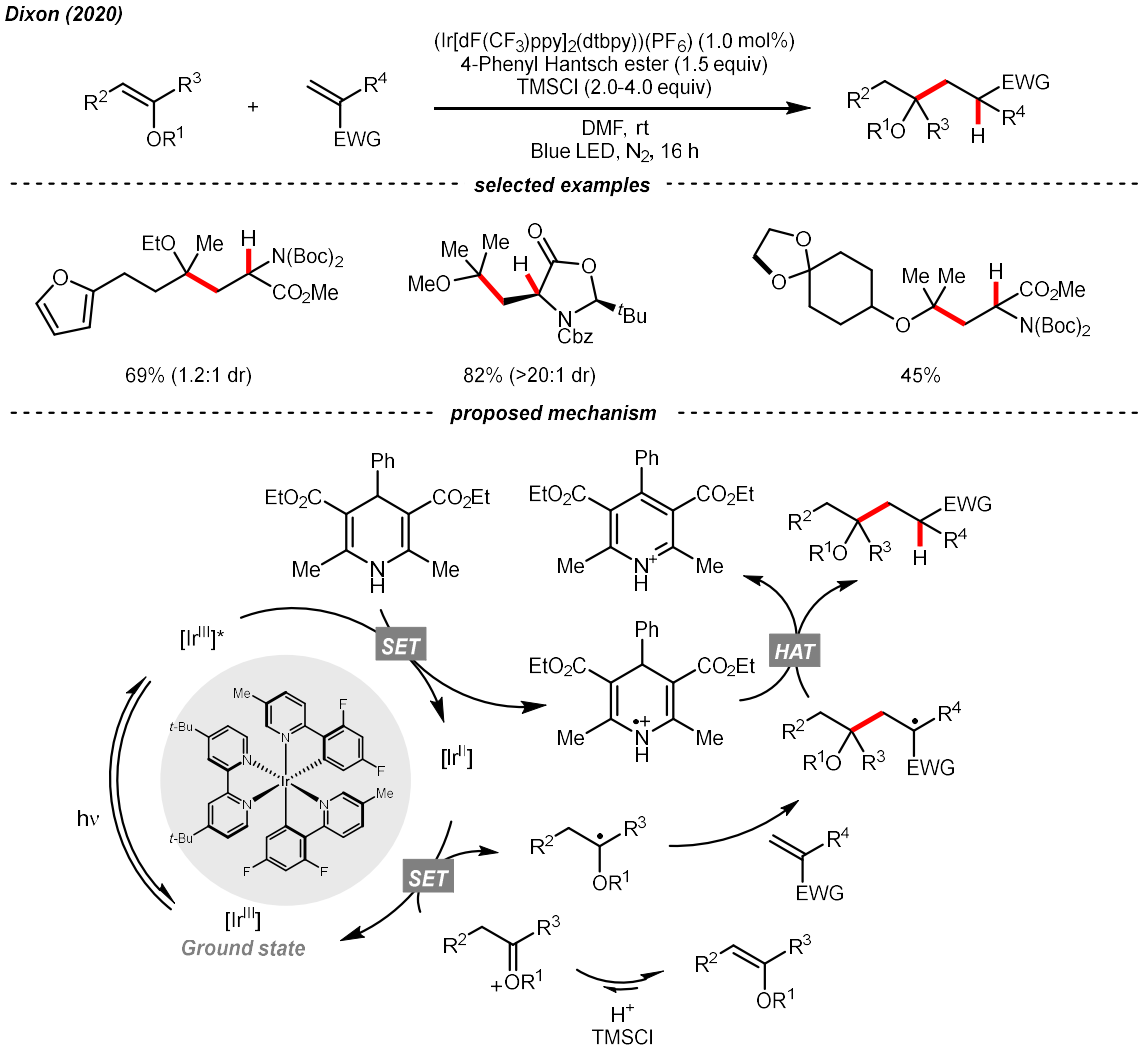

C-N cleavage. While photocatalytic radical C-N bond formation is of tremendous interest in academic and industrial settings, C-N bond cleavage typifies an equally important direction, which played an indispensable role in R• generation strategies within the SET manifold.

Quaternary ammonium or pyridinium salts, featuring highly polarized C-N bonds because of the cationic nitrogen, are widely used in radical alkylations via single-electron reduction. In 2017, Glorius et al described a novel Minisci alkylation reaction with Katritzsky salts (R-

TPP) under iridium photocatalysis (**Scheme 1.28**).[91] Mechanistically, the electron-deficient pyridinium accepted an electron from the excited Ir(III) and formed a dihydropyridine radical, whose C-N fragmentation will engender the R• for addition to the neutral heteroarene. Notably, Brønsted acids, typical additives in Minisci alkylation conditions, were absent in Glorius's case. Moreover, electron-rich heteroarenes were accommodated in this photocatalytic approach, in which various proteinogenic amino acids were masked as R• sources via radical deamination.

Scheme 1.28. R• generation via C-N cleavage of Katritzsky salt.

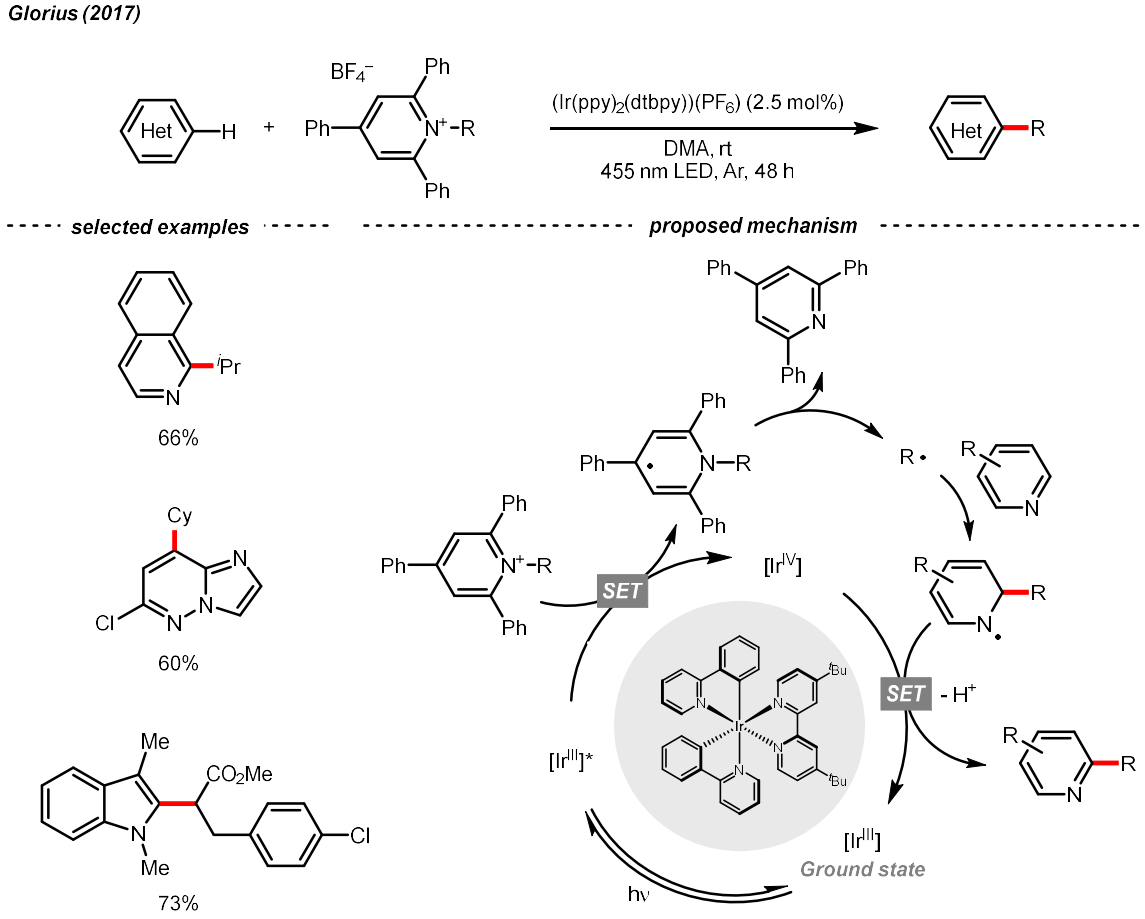

For the Katritzsky salt-based method above, the pyridinium-forming process is limited to

the condensation with less hindered primary amines.[92-94] In contrast, quarternary ammonium salts could originate from nearly all types of amines via exhaustive alkylation, typically with methyl iodide or triflate. Using these bench-stable R• sources, Yu's group achieved the photocatalyzed reductive cross-electrophile coupling reactions with alkyl ammonium salts and benzaldehydes or CO_2 (**Scheme 1.29**).[95]

Scheme 1.29. R• generation via C-N cleavage of quaternary nitrogen salt

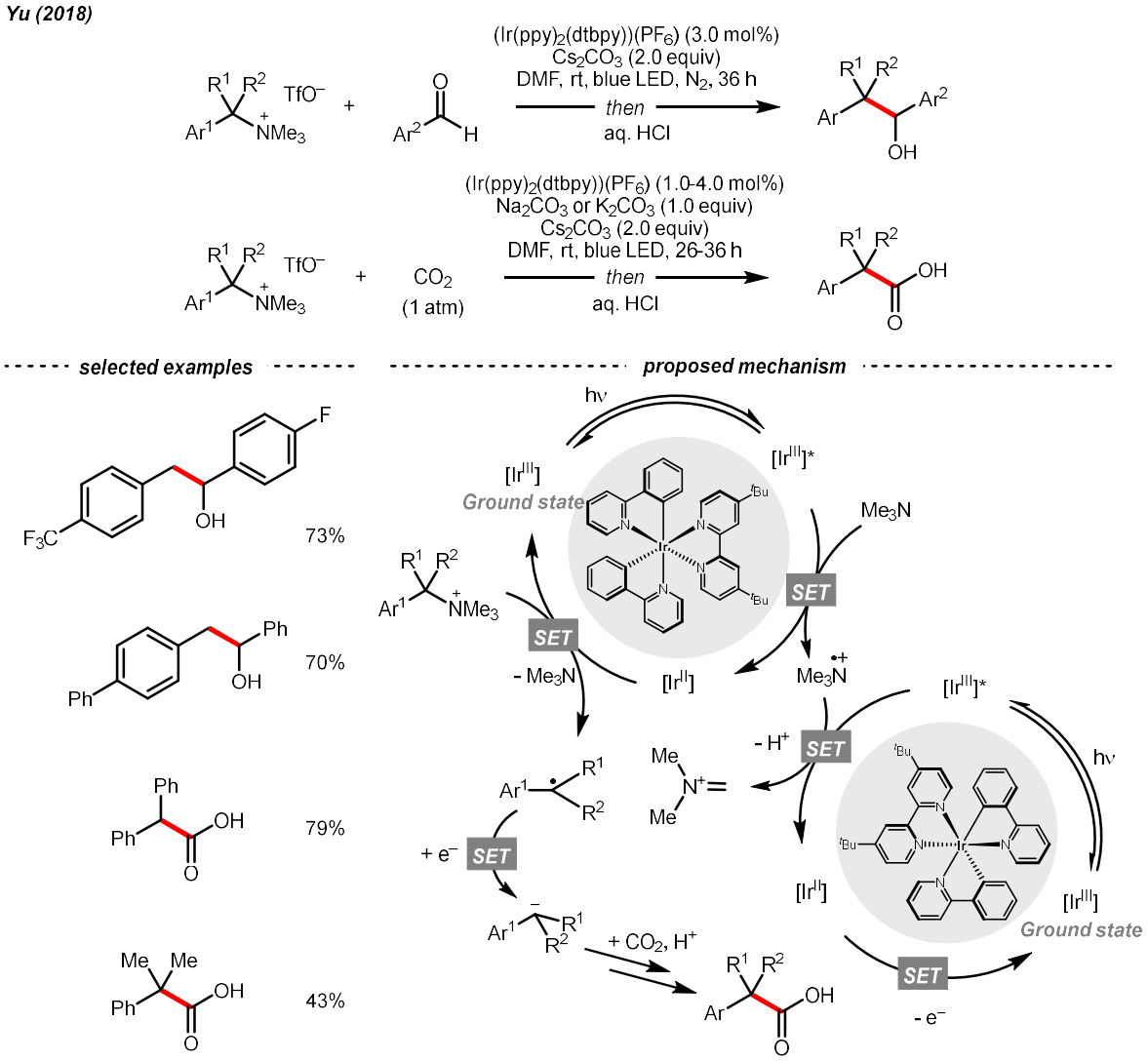

Resembling the Katritzsky salts, a single-electron reduction of the ammonium salt with

the in situ generated Ir(II) could break the C-N bond and produce the R•. The NMe_3 released from ammonium decomposition served as a reductant to reduce Ir(III) and regenerate the Ir(II), which further reduced R• into a carbanion to react with benzaldehyde or CO_2, giving benzyl alcohols and carboxylic acids, respectively.

Scheme 1.30. Reductive C=N cleavage of iminium salt.

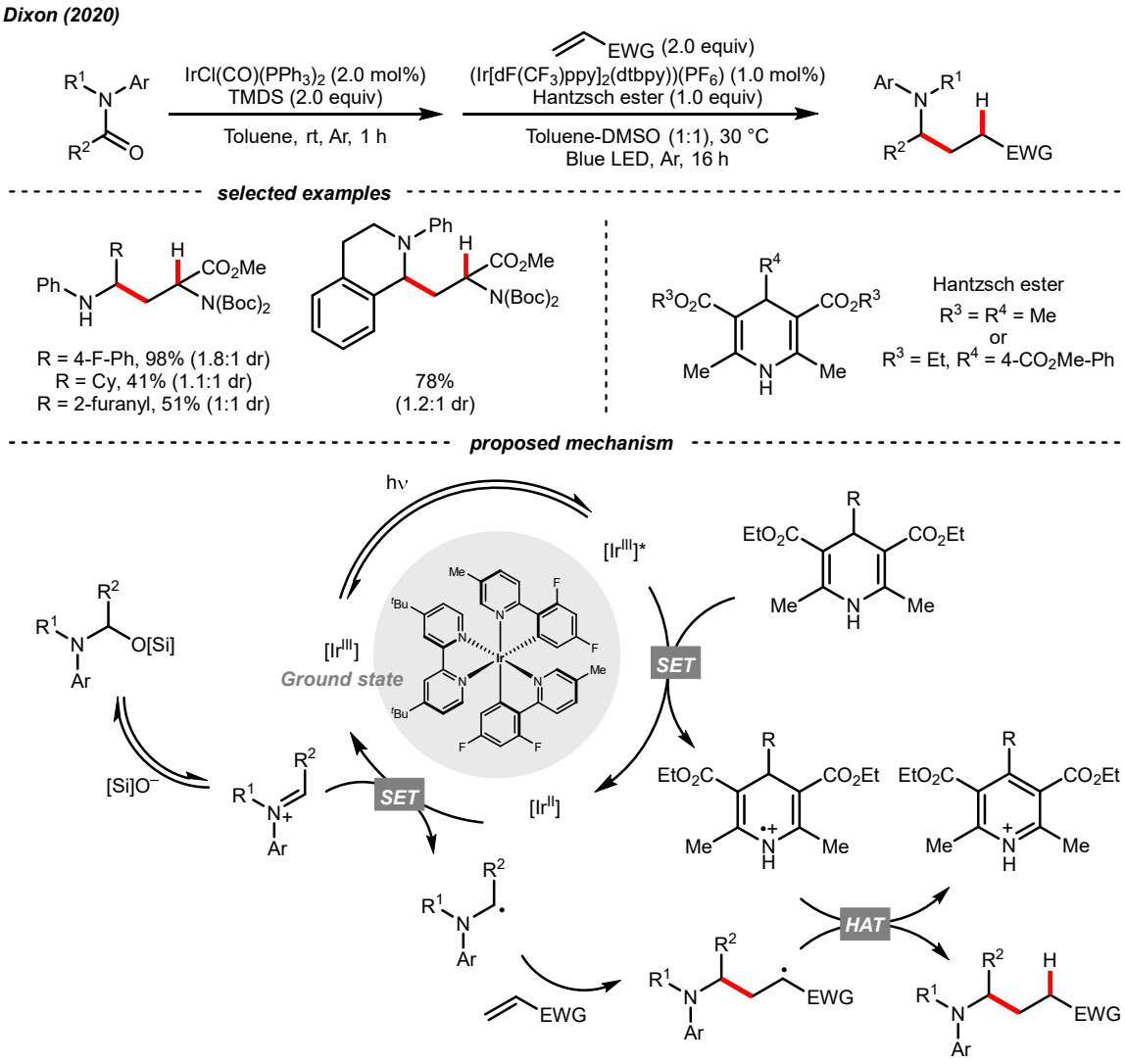

Instead of breaking the C-N σ-bond, cleaving the π-bond in C=N-containing compounds

could afford R•. In the case of iminiums, the group of Duarte and Dixon in 2020 detailed a deoxygenative alkylation reaction of tertiary amides, with iminium ions as the key intermediates to generate α-amino radicals for Giese addition (**Scheme 1.30**).[96] In the first step, hydrosilylation of the amide to furnish an iminium was executed with 1,1,3,3-tetramethyl disiloxane (TMDS) and Vaska's catalyst ($IrCl(CO)(PPh_3)_2$). Then, the iminium was subject to the reductive coupling with iridium photocatalyst, Hantzsch ester and Michael acceptors under photo-irradiation, which shares a similar mechanism to the developed enol ether alkylations (**Scheme 1.27**).[90]

Scheme 1.31. Reductive cleavage of alkyl sulfonium salt.

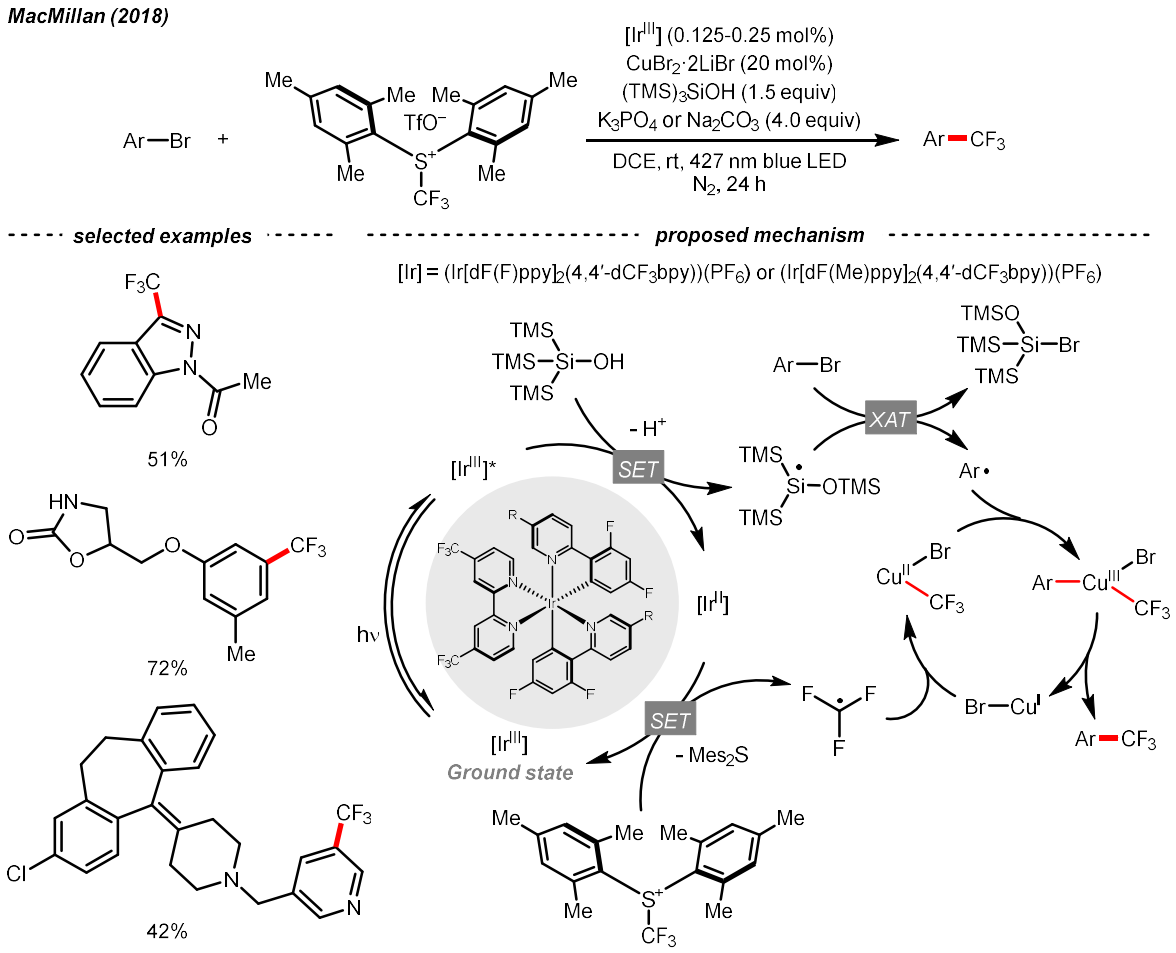

R-S cleavage. Due to the flexible oxidation state of sulfur, various S-based radical alkylating reagents were developed, accompanied by their own photoredox systems. Alkyl sulfonium salt can be easily synthesized from alkyl halides, thiols and alcohols.[97-101] Upon receiving an electron, such a trivalent species undergoes R-S cleavage to release an R• and a thioether. In 2018, MacMillan et al disclosed a Cu(II)/Ir(III) dual photocatalytic system to couple aryl bromides and trifluoromethylsulfonium salt in the presence of a supersilanol (**Scheme 1.31**).[102]

The photoredox cycle began with the generation of Si• via SET. Similar to their reductive fluorination reaction with aliphatic bromide (**Scheme 1.15**) yet, in this case, the aryl bromide was subjected to Si•-mediated XAT, giving the aryl radical (Ar•). On the other hand, the interaction between modified Umemoto's reagent, dimesityl(trifluoromethyl)sulfonium, and Ir(II) gave CF_3• radical through reductive C-S cleavage. On the copper side, the interception of CF_3• by Cu(I) preceded the Ar• trapping, and the facile Cu(III) reductive elimination rendered the trifluorotoluenes as desired products. The same tactic could apply to alkyl bromides, as shown in their later report.[103]

Sulfinate is also an S-containing radical alkylating reagent that undergoes oxidative decomposition to give R• with SO_2 evolution. In 2021, an application of perfluoroalkyl sulfinates ($NaSO_2R_f$) in migratory alkene difunctionalizations with intramolecular heteroaryl groups was presented by the research team of Tang, Wang, and Cai (**Scheme 1.32**).[104] Using potassium-modified carbon nitride (CN-K) as a recyclable photosensitive material, the electron-hole pair generated under light irradiation and ambient atmosphere could oxidize $NaSO_2R_f$ into a perfluoroalkyl radical (R_f•). The R_f• addition to the olefin tail of the heteroarylmethanol triggered the heteroaryl group migration, which furnished the terminally perfluoroalkylated ketone as the expected product after losing an electron. Interestingly, formyl and benzyl oxime ether groups can undergo the same type of functional

group translocation.

Scheme 1.32. R• from sulfinate or sulfinamide.

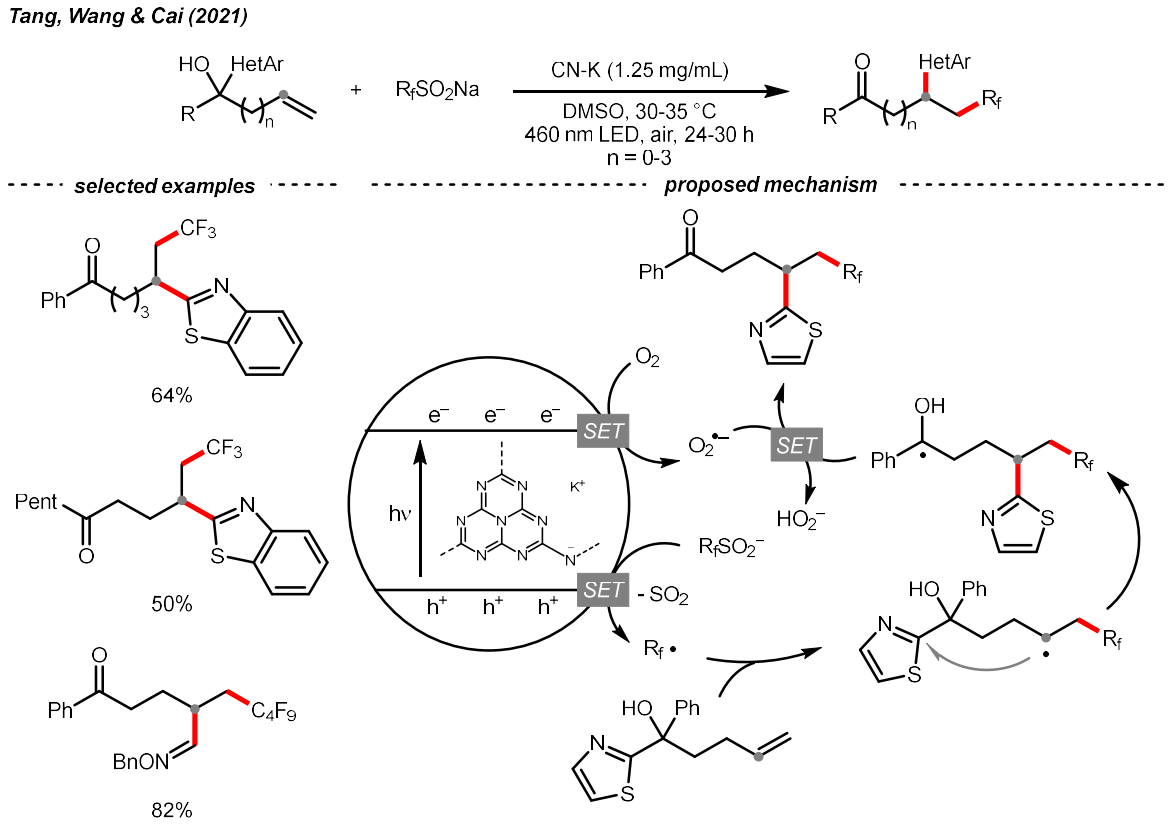

R-X cleavage. Alkyl halides are one of the earliest employed R• precursors that are still widely used in modern synthesis because of their structural diversity and commercial availability. Among them, iodides and bromides, which possess relatively weak C-X bonds, are more popular choices, although some advanced techniques allow the R• generation with chlorides and fluorides.

The rapid progress of photoredox chemistry endows alkyl halides with new activation modes, among which SET represents the mostly seen ways to streamline the generation of R•.[105] In 2018, Jiang et al disclosed an enantioselective cross-coupling between α-

bromoketones and α-amino acids with the aid of chiral phosphoric acid (SPINOL-CPA) and dicyanopyrazine-derived chromophore (DPZ) under visible light irradiation (**Scheme 1.33**).[106] The photoexcited DPZ functioned as an electron transfer catalyst, which mediated the generation of two electronically distinct R• from the alkyl bromide and carboxylic acid via reductive and oxidative SET, respectively. The CPA then managed the radical-radical cross-coupling with these two R• in an enantioselective fashion, synthesizing numerous β-amino ketones in good to excellent enantioselectivities.

Scheme 1.33. Employing alkyl bromide for enantioselective radical-radical coupling.

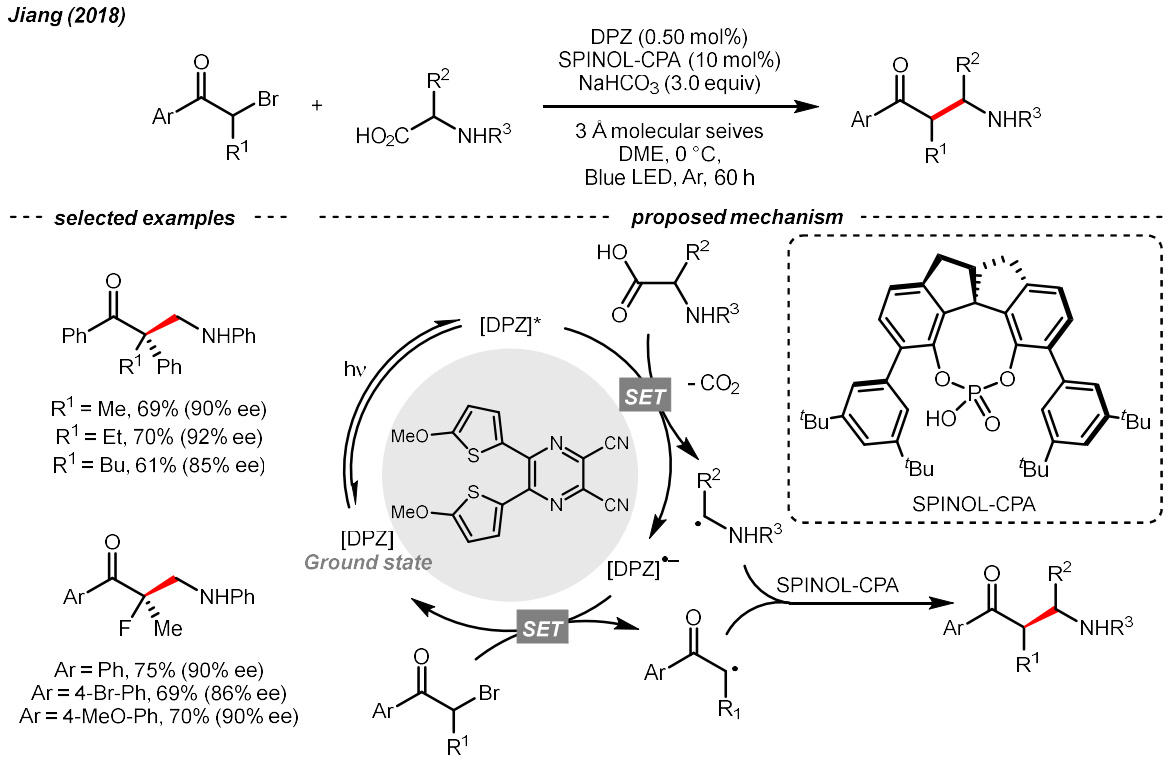

R-B cleavage. Like the alkyl halides, boronic acid and its derivatives are highly enabling R• precursors, which feature opposite electronic demand during the SET with photoredox catalysts. Among them, potassium trifluoroborate, which was intensively studied by Molander's group, is a common option due to its high stability and easily accessible redox

potential.[107-114]

By merging photocatalysis and nickel catalysis, the challenging C(sp^2)-C(sp^3) Suzuki-Miyaura coupling with aryl bromides and benzyltrifluoroborates was realized by Molander's group in 2014 (**Scheme 1.34**).[115] Soon after, secondary,[116] tertiary[117] trifluoroborates and other variants are shown as effective in their later publications. The SET between Ir*(III) and trifluoroborate and the trapping of corresponding R• by Ar-Ni(II) to promote the product-forming reductive elimination were two common mechanistic traits for all these dual catalyzed cross-couplings. Unlike the conventional two-electron transmetalation pathways in which alkyl nucleophiles were often problematic organometallic partners, such a SET scenario with alkyl trifluoroborates grants a unique and complementary reactivity.

Scheme 1.34. Utilizing alkyl trifluoroborate for radical coupling reactions.

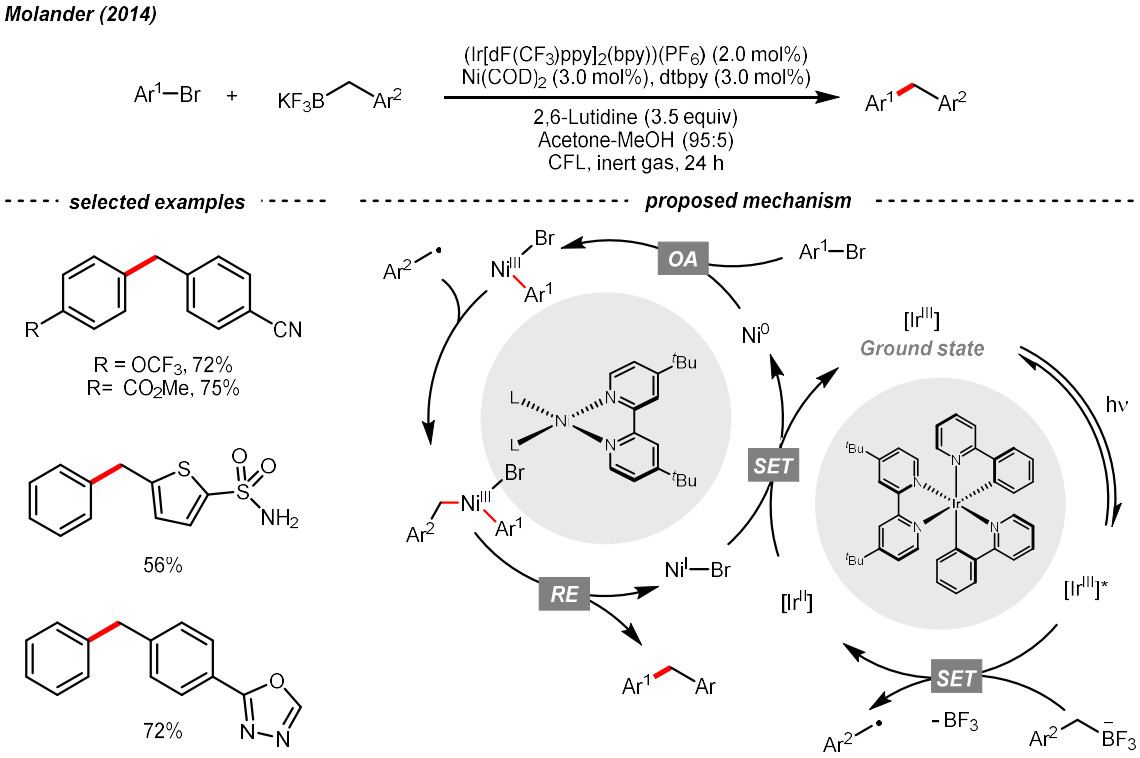

R-Si cleavage. Analogous to boronic acids, silane and other silica-based compounds are

other organometallic reagents that effect the R• generation by C-Si bond scission under mildly photoredox conditions.

Scheme 1.35. Oxidative R-Si cleavage of alkyl silicate for conjugate addition.

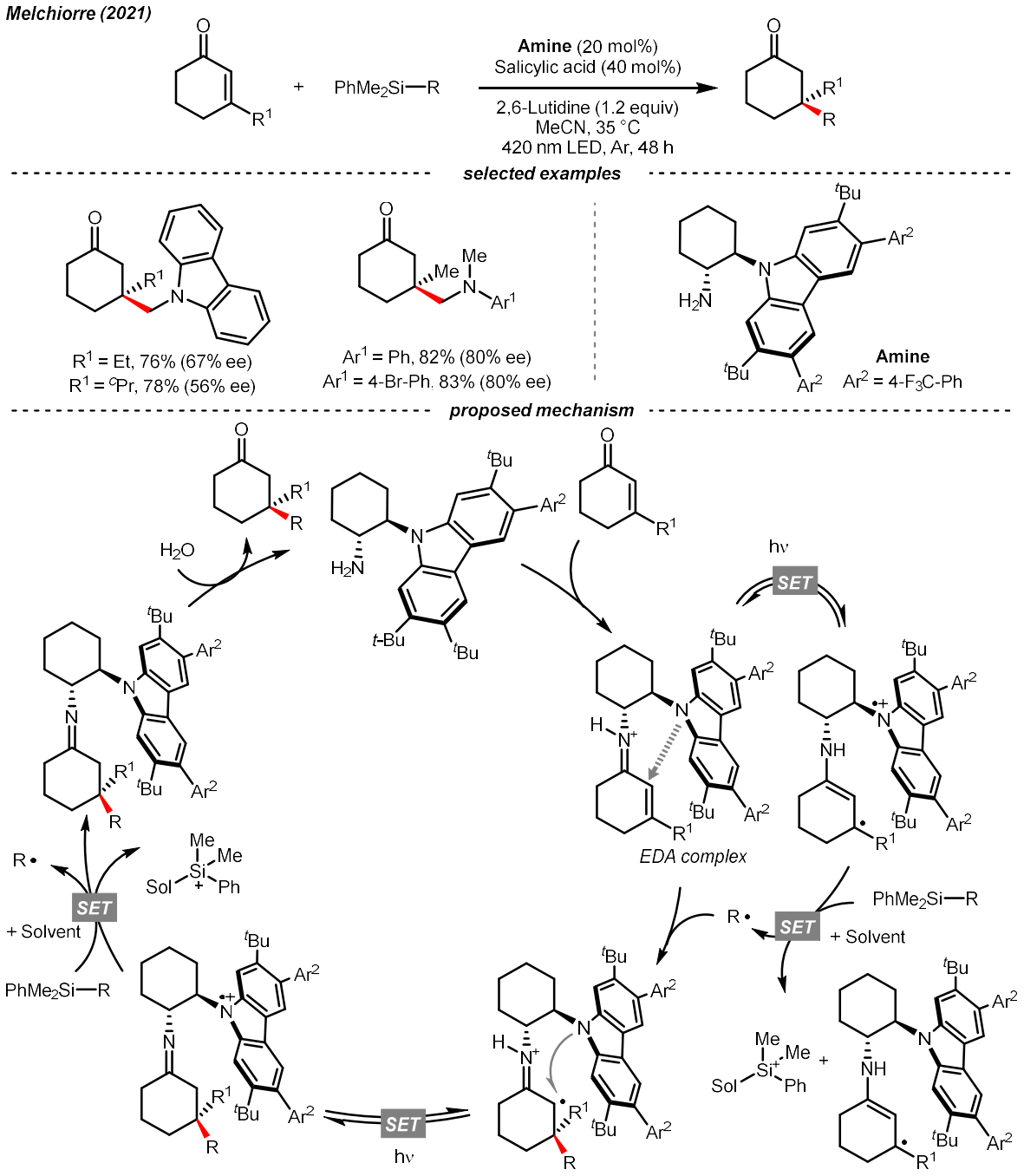

One recent application of alkylsilane in asymmetric addition to α,β-unsaturated ketones was demonstrated by Melchiorre's laboratory (**Scheme 1.35**).[118] Combining the iminium-catalyzed photooxidation[119] and electron-donor acceptor (EDA) complex chemistry established in his group,[120] a chiral carbazole-tethered amine organocatalyst was developed. The iminium EDA intermediate formed by condensing the amine catalyst and conjugated ketone substrate absorbed visible light and enabled an intramolecular-electron transfer to create a long-lived carbazole radical. Silanes within this redox window, typically those α-nitrogenated, were applicable R• precursors, which would undergo an oxidative fragmentation to break the C-Si bonds. Importantly, the MeCN coordination could facilitate the desilylation by forming a $[MeCN\text{-}SiR_3]^+$ complex and inhibiting back-electron transfer.

The carbazole handle was bifunctional; guided by such a bulky shield, R• would attack the conjugated iminium preferentially at the less hindered face, giving an α-iminyl radical. On the other hand, the electron-rich carbazole could be an electron sink; therefore, another intramolecular SET engendered a new carbazole radical cation, which triggered a radical chain mechanism. Subsequent hydrolysis of the β-functionalized imine led to product formation and catalyst regeneration.

1.2.5 Radical cascade

Radical addition to the unsaturated π-bond in alkene and the strained σ-bond in propellane could increase the structure and functional complexity of the radical species. In some cases, such a radical translocation process could expedite the new radical generation since the radical adducts are usually more stable. Furthermore, radical philicity reversal is also a common purpose by introducing these primary radical acceptors, which could be highly useful in organic synthesis and polymer chemistry.

Scheme 1.36 Dearomative cyclization of alkenyl *N*-arylsulfonamides.

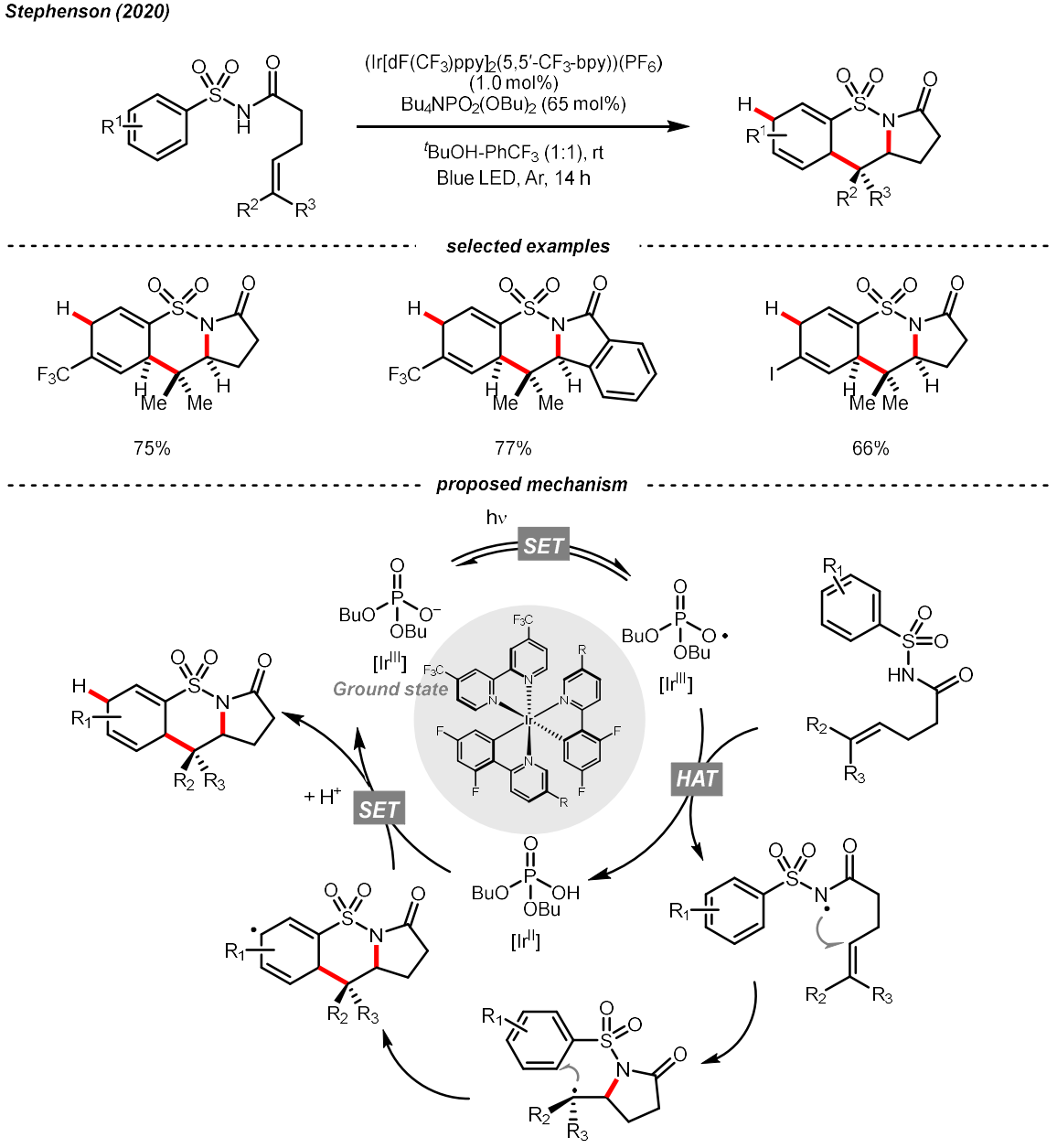

Addition to an alkene. The addition of R• to electronically matched double bonds is commonly seen in alkene difunctionalizations, some of which have been overviewed in previous examples.[121-122] Instead, adding heteroatomic radicals to the olefins and merging

the new R• in different radical cascade reactions will be exemplified below.

As an intramolecular example, Stephenson's laboratory reported a photo-induced dearomative cyclization of alkenyl *N*-arylsulfonamides with (Ir[dF(CF_3)ppy]$_2$(5,5′-CF_3-bpy))(PF_6) and a HAT agent $Bu_4NPO_2(OBu)_2$ (**Scheme 1.36**).[123]

At first, a ground-state Ir(III) and dibutyl phosphate aggregation, as proposed by Alexanian and Knowles (**Scheme 1.6**), was suspected of enabling the NCR generation. Nonetheless, careful spectroscopic studies suggested the MS-PCET and deprotonation/oxidation mechanism to generate the NCR were less likely in this case. Instead, after light-induced SET between the Ir(III) and phosphate, an oxy radical departed and performed the HAT with the sulfonamido N-H. NCR addition to the terminal alkene formed an R•, which then performed an intramolecular radical cyclization to the pendent arene. Subsequent SET/protonation steps of the cyclohexadienyl radical delivered the dearomatized product.

Addition to propellane. Radical addition to [1.1.1]propellane was recently demonstrated as an enabling synthetic route to access disubstituted [1.1.1]propellane (BCP),[124-129] which represents a high-value three-dimensional bioisostere for phenyl, alkynyl, and *tert*-butyl groups in drug designs.[130-131] It also provides a mechanistic pathway different from the two-electron nucleophilic[131] and electrophilic activation[132] of [1.1.1]propellane.

Driven by its great utility, MacMillan's group reported a difunctionalization reaction of [1.1.1]propellane by merging copper catalysis and iridium photocatalysis (**Scheme 1.37**).[129] In their tentative mechanism, the excited Ir(III) photocatalyst reduced the iodonium dicarboxylate, alkyl bromide, or sulfonothioate via SET to generate a C- or S-centered radicals, respectively, which could combine with [1.1.1]propellane to give a bicyclo[1.1.1]pentyl radical (R•) through strain release. By leveraging copper catalysis, the R• was then coupled with various nucleophiles such as electron-rich arenes, anilines, and sulfonamides, offering

1,3-disubstituted BCPs through the facile R-Cu(III)-Nu reductive elimination.

Scheme 1.37 Radical addition to [1.1.1]propellane.

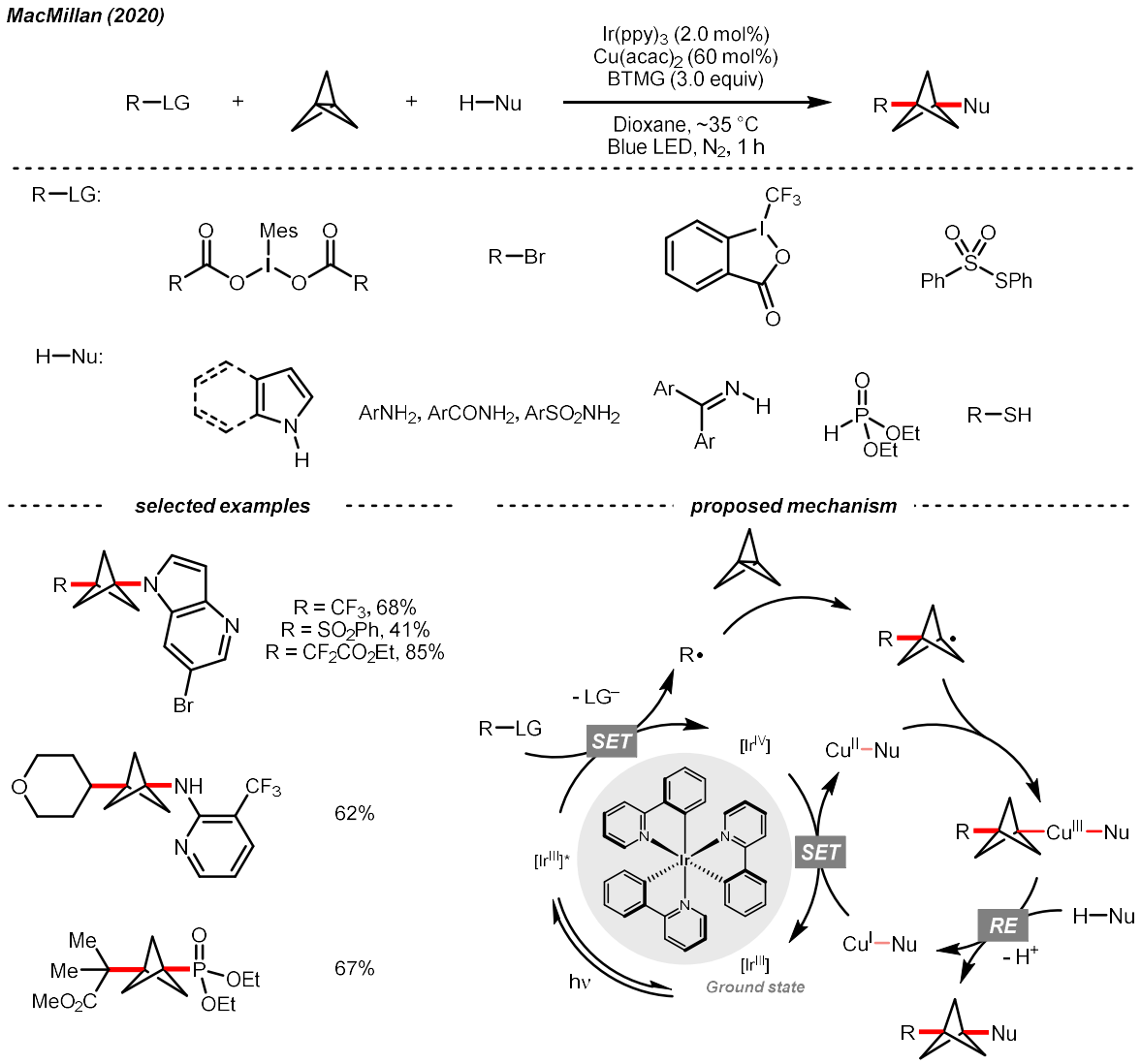

1.3 Heteroarene C-C bond formation

1.3.1 Heteroarene

Heteroarenes are ubiquitous and indispensable in our daily life. For instance, L-tryptophane is an indole-derived amino acid essential for the biosynthesis of proteins in the human body.[133] Caffeine, the most-consumed psychoactive drug worldwide, is a pyrimidinedione-

fused imidazole that can be found in coffee and tea.[134] Methylene blue was first synthesized in 1876 as a thiazine drug; it is also a common organic dye.[135] Fasudil is an isoquinoline-based vasodilator that has been exploited to treat cerebral vasospasm.[136] Quinine, a natural quinoline derivative isolated from cinchona trees, has been used to treat malaria since the eighteenth century (**Figure 1.8**).[137]

Figure 1.8 Some heteroaryl compounds.

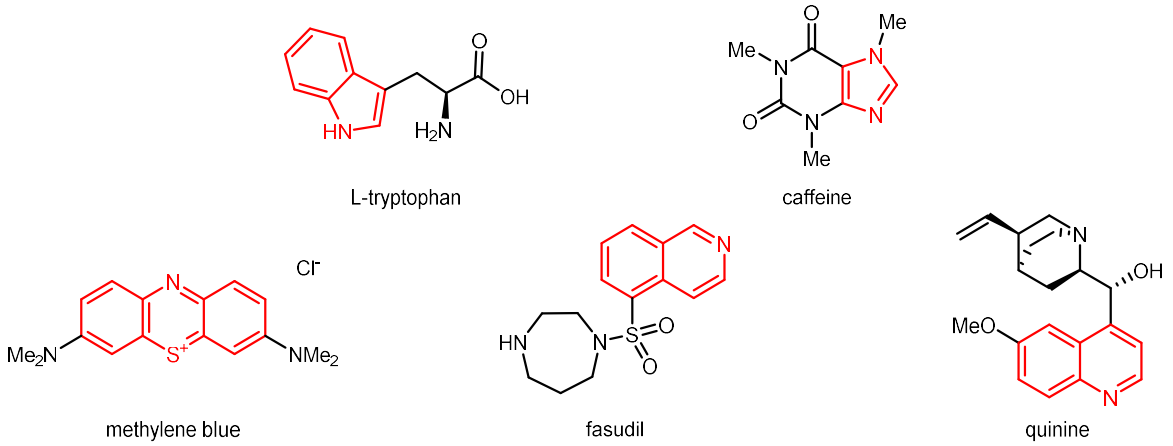

Figure 1.9 Heteroaryl C-C formation strategies.

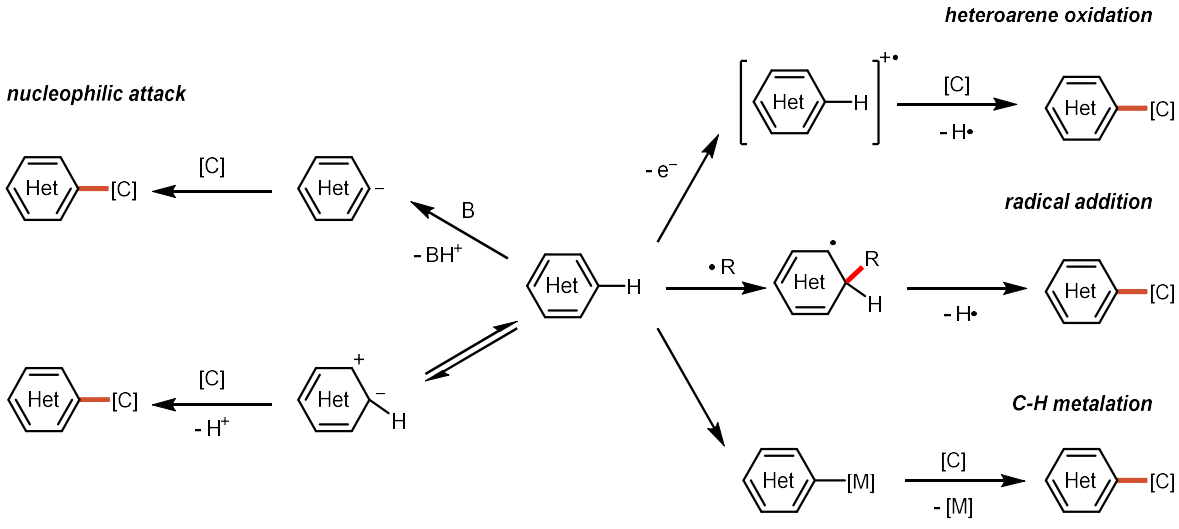

B, base; [M], metal.

Due to the versatile structures and applications of heteroarenes in agrochemistry, pharmacochemistry and industry, synthetic chemists have established several systematical C-H functionalization tactics to fastly increase the complexity of heteroarenes. In this context, C-C bond formation is of the greatest research interest because carbon skeletons are the central framework of most organic substances. Considering the existing heteroarene C-C formations from C-H bonds, they could be categorized into four types, which are (a) nucleophilic attack, (b) heteroarene oxidation, (c) radical addition, and (d) C-H metalation (**Figure 1.9**).

1.3.2 Nucleophilic attack

An electron-rich heteroarene such as indole, imidazole, and benzofuran could perform electrophilic aromatic substitution (S_EAr) to electrophiles, for example, acyl chloride, imine and aldehyde, to build up C-C bonds. This strategy takes advantage of the intrinsic resonance of heteroarenes; therefore, no external reagent is required to activate the heteroarenes, and their regioselectivities are predictable.

Scheme 1.38 C3-Acylation and alkylamination of indole.[138-139]

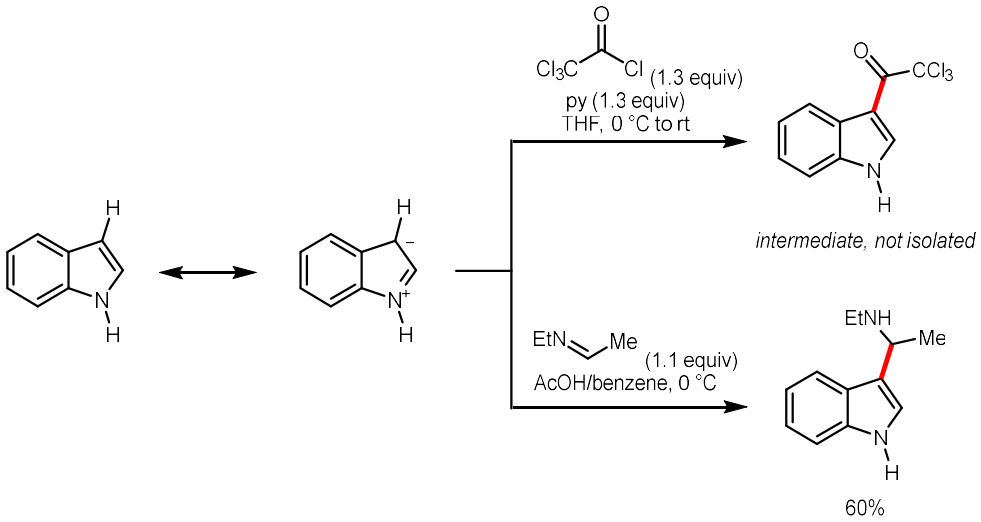

For instance, Indole is known for its C3 nucleophilicity. It could react with trichloroacetyl chloride and pyridine to form 3-trichloroacetylated indole, in which alcohols could substitute the trichloromethyl group to furnish esters (**Scheme 1.38**). On the other hand, indole could also nucleophilically attack imines under acidic conditions to give indolated alkyl amines.

Alternatively, acidic C-H bonds on heteroarenes, usually adjacent to the heteroatoms, could be deprotonated by strong bases. This strategy is generally operated in one-pot multistep synthesis since organolithium or Grignard reagent deprotonation of a heteroarene is required before an electrophile is introduced (**Scheme 1.39**). However, it is still recognized as a facile C-C formation method commonly applied in regioselective alkylation and formylation, especially in large-scale feedstock syntheses.

Scheme 1.39 Alkylation and formylation of benzothiophene.[140-141]

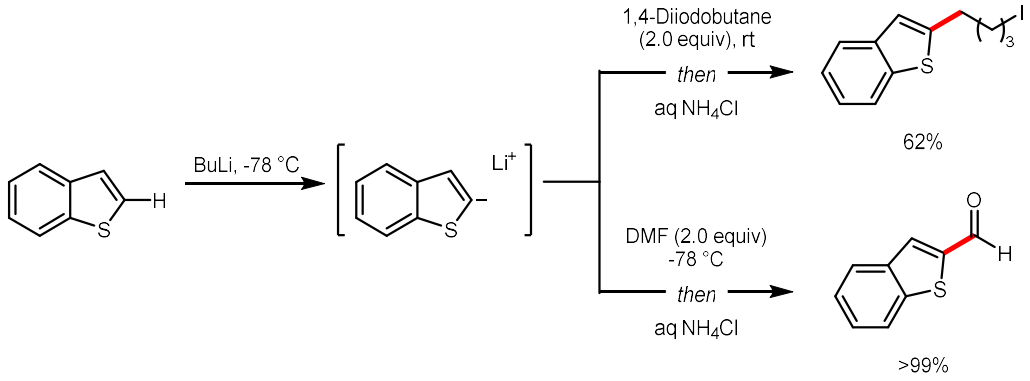

1.3.3 Heteroarene oxidation

Although electron-rich heteroarenes are electronically mismatched with carbon nucleophiles, they could lose an electron and become radical cations, which are good electrophiles instead.[142] In the developed methods, heteroarene oxidation has been achieved with chemical oxidants hypervalent iodines and transition metal salts, photoredox or high-valent metal catalysts, or electrochemical oxidation. Usually, homocoupling and intramolecular coupling are demonstrated to guarantee a good yield of the desired product;

nevertheless, by controlling the reactivity between two coupling partners or introducing a higher equivalent of one nucleophile, an appreciable amount of cross-(hetero)arylation or cyanation product could be furnished (**Figure 1.10**).

Figure 1.10 C-C bond formation via heteroarene oxidation.

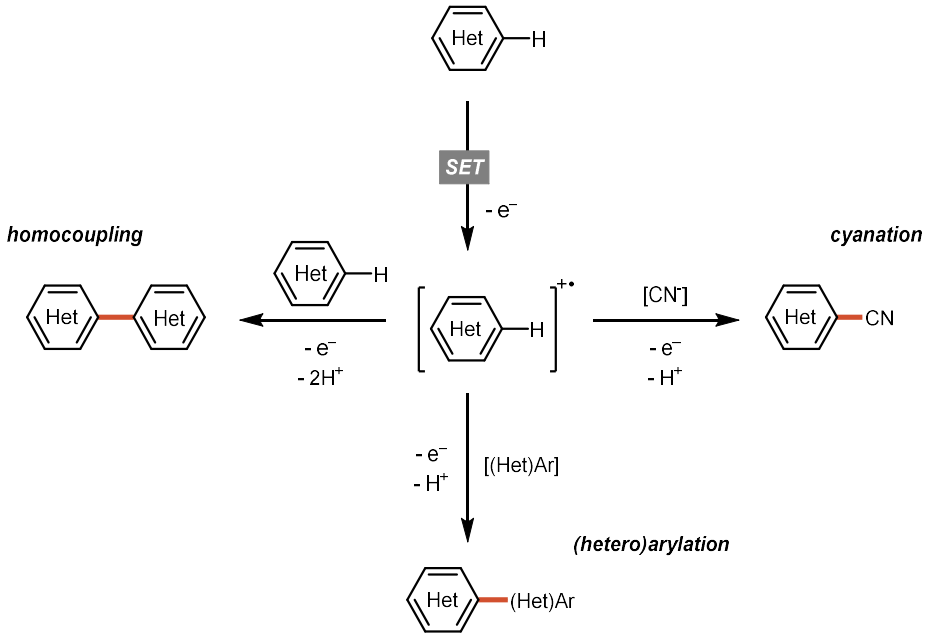

Taking the C2 functionalization of thiophenes as an example, the group of Kita exploited Koser's Reagent (hydroxy(tosyloxy)iodobenzene, HTIB) as the oxidant to homocouple a series of thiophene derivatives under simple and metal-free conditions (**Scheme 1.40**).[143] In the demonstration of the short-step synthesis of oligoaryl, the dimer of 3,4-dimethoxythiophene was further subjected to 3 equiv of pentamethylbenzene in the presence of (bis(trifluoroacetoxy)iodo)benzene (PIFA) oxidant to give a 2-arylated bithiophene product.

Scheme 1.40 Homo- and cross-coupling of thiophene.

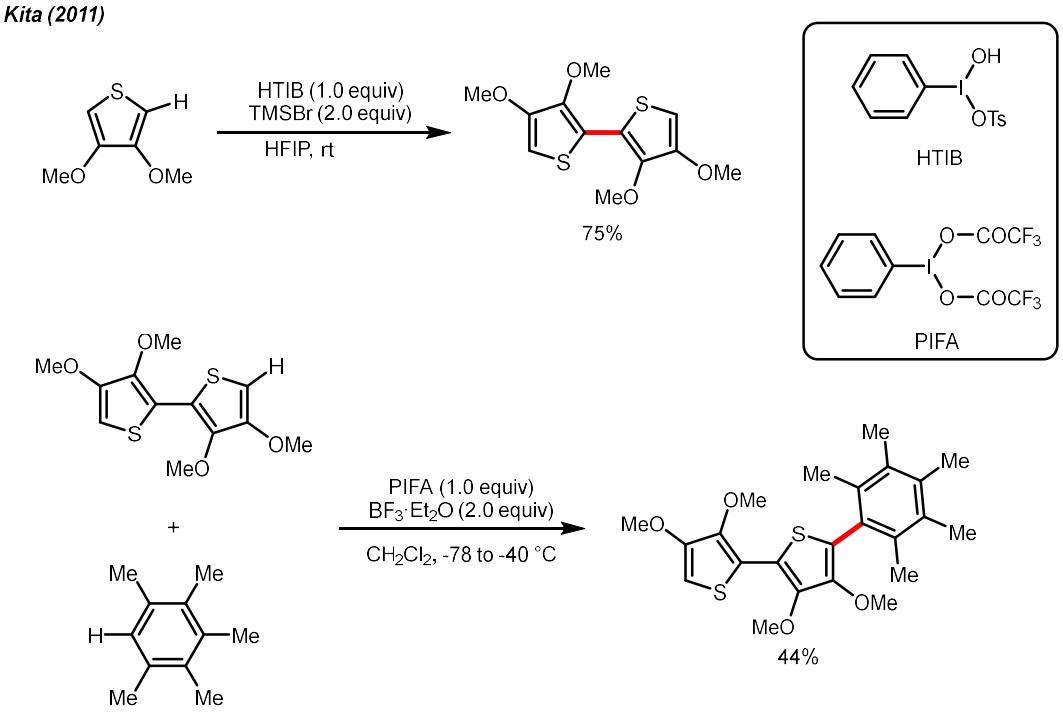

The same group also reported the metal-free cyanation of different heteroaryl compounds using trimethylsilyl cyanide (TMSCN) as the cyano source (**Scheme 1.41**).[144] Similar to the cross-coupling conditions of thiophene yet replacing electron-rich arene with cyanide, various thiophene, benzothiophene, and indole could be functionalized at their C2 position.

Scheme 1.41 Cyanation of heteroarenes.

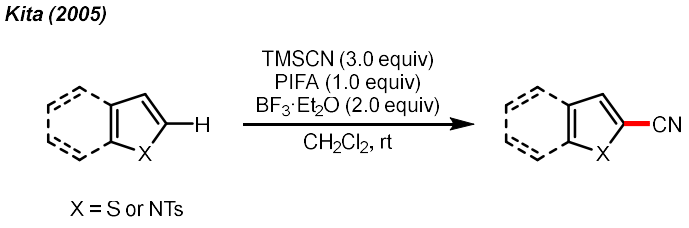

1.3.4 Radical addition

In 1968, Francesco Minisci utilized alkyl hydrogen peroxide and oxaziridine as the alkyl sources to functionalize nitrogen-containing heteroarenes, with an iron catalyst to decompose peroxide/oxaziridine under acidic reaction conditions.[145] Later, Minisci and his team reported a series of heteroarene alkylations using aliphatic acids, alkyl iodide, and alkanes (**Scheme 1.42**).[146-148]

Scheme 1.42 Minisci's heteroarene alkylations.

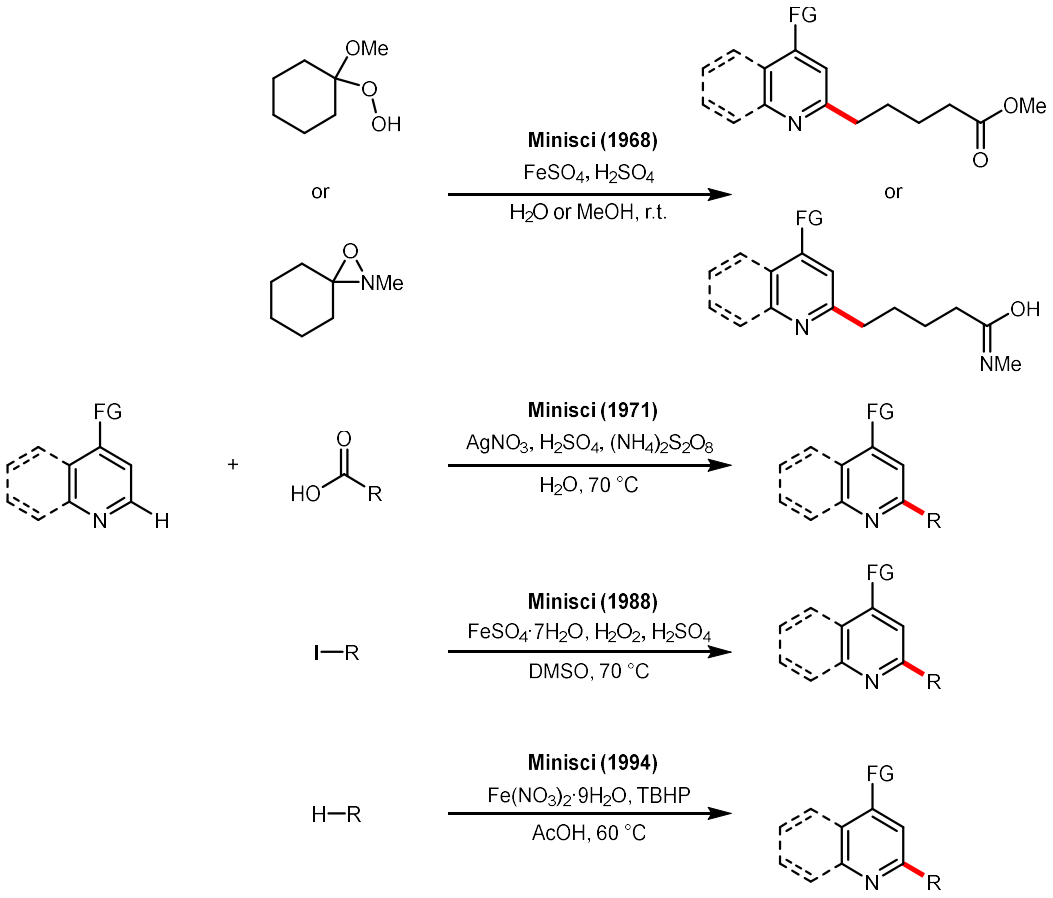

Considering their reaction mechanisms, an R• was formed in situ from its precursor (**Scheme 1.43**). A heteroarene, usually a nitrogen-containing one such as pyridine, quinoline,

and isoquinoline, was protonated to become more electrophilic, facilitating the alkyl radical addition. The alkylated heteroarene could be obtained after formally removing a hydrogen atom.

Scheme 1.43 General mechanism of Minisci's alkylations of 4-methylquinoline.

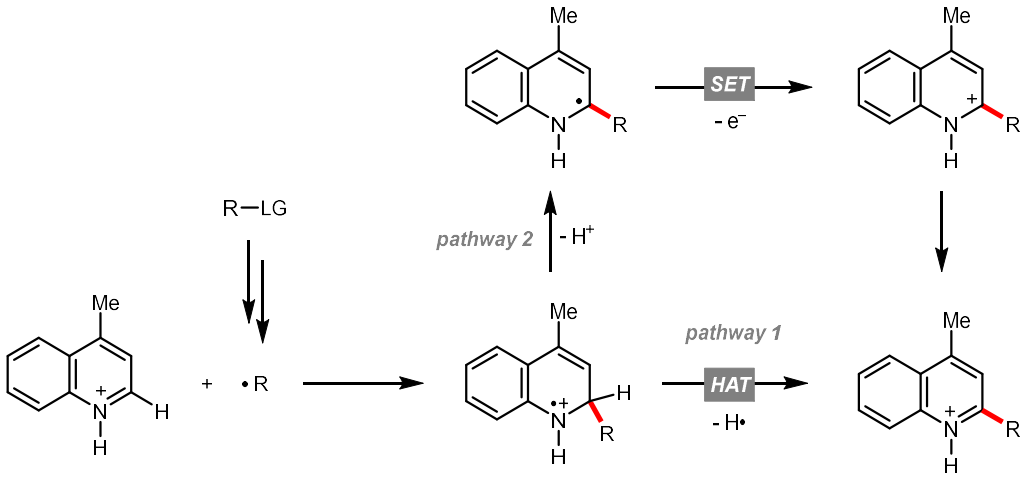

Figure 1.11 Different types of Minisci reactions.

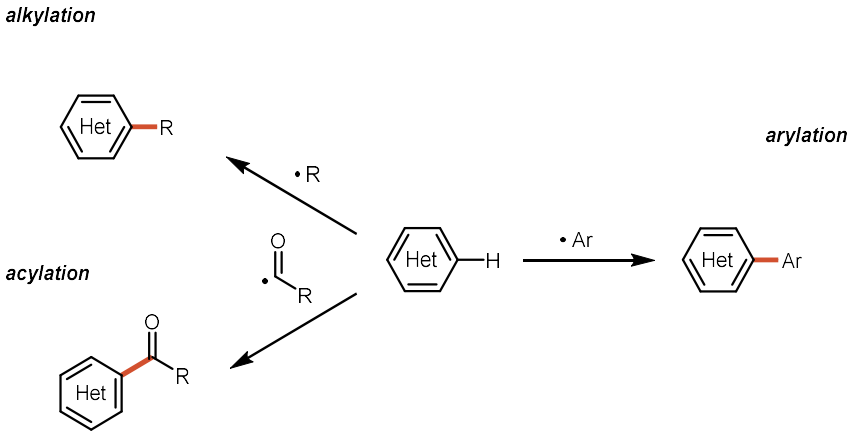

Unlike the abovementioned heteroarene functionalizations, this free radical-involved reaction shows distinct reactivities and selectivity toward electron-deficient heteroarenes, which is nowadays termed Minisci alkylation.[149-150] Due to its mechanistic simplicity and the

variety of heteroarenes, most of the alkyl radical sources are compatible in this prototype, making it a powerful tool not only to increase the complexity of heteroarenes but to demonstrate different means of alkyl radical generations. It is also noticeable that many research groups also disclosed other *C*-centered radicals, such as acyl and aryl radicals, to fulfil other Minisci-type reactions (**Figure 1.11**).

While most *C*-centered radicals are nucleophilic, perfluoroalkyl radicals are electrophilic; therefore, they could be subjected to electron-rich heteroarene alkylations. A recent example from Li and his team exemplified the trifluoromethylation of heteroarene using α-methyl-α-trifluoromethylsulfone phenyl methyl ketones under UV light (**Scheme 1.44**). By photolyzing the ketone's C-S bond followed by SO_2 extrusion, many electron-rich heteroarenes were trifluoromethylated under such catalyst-free redox-neutral reaction conditions.

Scheme 1.44 Trifluoromethylation of heteroarenes.

Li (2017)

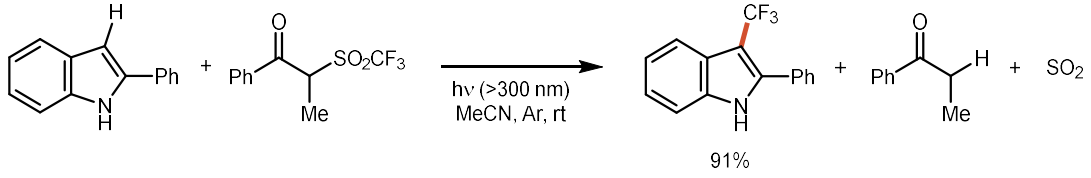

1.3.5 C-H metalation

Transition metal-mediated or -catalyzed C-H activation is a powerful method to activate divergent C-H bonds, including heteroaryl ones.[151-152] In aid of a transition metal species, the activation of a heteroaryl C-H bond under strongly basic or oxidative conditions could be bypassed through mechanisms such as oxidative addition (OA) or concerted metalation-deprotonation (CMD) under mild conditions (**Figure 1.12**). Since the reactivity of the engendered metallated heteroarene is tunable based on the employed transition metal/ligand, additives, and temperature, various coupling partners (i.e., organometallic

salts, organo (pseudo)halides, hydrocarbons) are applicable under oxidative or redox-neutral conditions, making it an important research field in heteroarene chemistry.

Figure 1.12 C-H metalation of heteroarens.

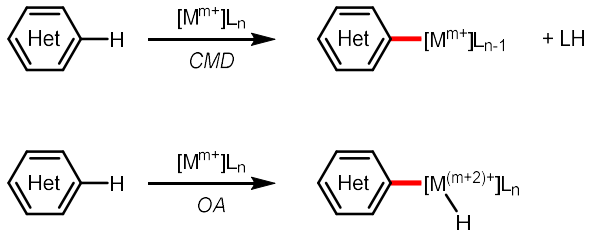

OA, oxidative addition; CMD, concerted metalation-deprotonation

Scheme 1.45 Regioselective C-H functionalization of *N*-pyrimidyl indole.

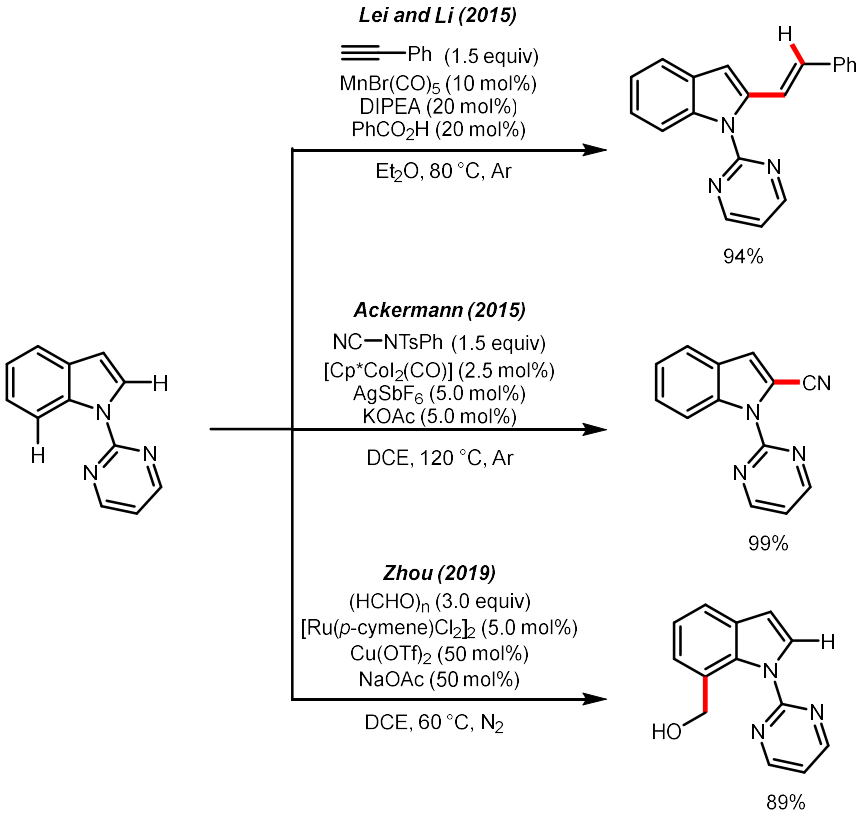

One intriguing feature of metallic C-H activation is its controllable regioselectivity. For instance, by installing a pyrimidyl group on indole's N1 position, the team of Lei and Li reported a C2 hydroalkenylation with phenylacetylene and manganese catalyst.[153] The group of Ackermann also used tosylphenylcyanamide as a cyanation reagent to achieve C2 cyanation with a cobalt catalyst.[154] In contrast, Zhao et al combined ruthenium catalyst and polyformaldehyde to functionalize C7 position of indole, affording 7-hydroxymethylated indole as the product (**Scheme 1.45**).[155]

1.4 Conclusions and outlook

We have explained the fundamental concept and mechanisms of organic photochemistry, including the three general ways photons participate in organic chemistry: (a) direct photoexcitation, (b) photocatalyzed energy transfer, and (c) photoinduced single-electron transfer. We also reviewed the photoinduced alkyl radical generations and their application in organic chemistry, in which the alkyl radical formation could be categorized into four mechanisms: (a) unimolecular homolytic cleavage, (b) bimolecular homolytic substitution, (c) single-electron transfer, and (d) radical cascade.

In the following chapters, we aim to contribute some photoinduced alkyl radical generation methods to the chemical society using two common radical precursors, alkane and trifluoroborate salt; two alkyl radical generation techniques, hydrogen atom transfer (unimolecular homolytic cleavage) and single-electron transfer, were employed. Instead of using mainstream protocols, we sought other efficient and sustainable alkyl radical generation using novel reagents (photoexcited diacetyl) and catalysts (chlorine radical and quinoline-based photocatalysts). Considering that heteroarenes have versatile utility, the generated alkyl radical was subjected to the functionalization of electron-deficient heteroarenes, namely, Minisci alkylation (**Figure 1.13**). The reaction designs, substrate

scopes, and mechanistic studies are included and will be discussed in the following chapters.

Figure 1.13 Research interest in this thesis.

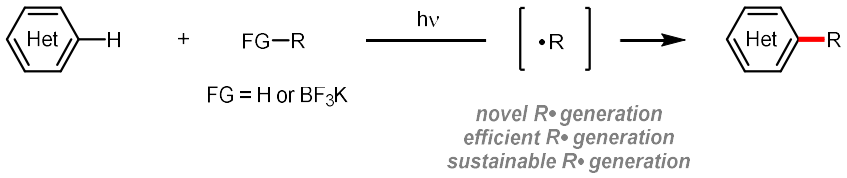

1.5 References

1. R. Nasini *et al.* Obituary Notices: John Young Buchanan, 1844–1925; Giacomo Luigi Ciamician, 1857–1922; Samuel Henry Davies, 1870–1925; William Henry Deering, 1848–1925; Francis Robert Japp, 1848–1925; Francis Jones, 1845–1925; Edmund Knecht, 1861–1925; William Robert Lang. *J. Chem. Soc.* **1926**, *129*, 993-1050.

2. G. Ciamician. The Photochemistry of the Future. *Science* **1912**, *36*, 385-394.

3. C. H. J. Wells. *Introduction to Molecular Photochemistry*. Chapman and Hall, London, **1972**.

4. N. J. Turro. *Modern Molecular Photochemistry*. University Science Books, Sausalito, **1991**.

5. M. Calvin & H. W. Alter. Substituted Stilbenes. II. Thermal Isomerization. *J. Chem. Phys.* **1951**, *19*, 768-770.

6. D. C. Todd *et al.* Fluorescence Upconversion Study of *cis*-Stilbene Isomerization. *J. Chem. Phys.* **1990**, *93*, 8658-8668.

7. Q.-Q. Zhou, Y.-Q. Zou, L.-Q. Lu & W.-J. Xiao. Visible-Light-Induced Organic Photochemical Reactions through Energy-Transfer Pathways. *Angew. Chem. Int. Ed.* **2019**, *58*, 1586-1604.

8. Y. Sumida & H. Ohmiya. Direct Excitation Strategy for Radical Generation in Organic Synthesis. *Chem. Soc. Rev.* **2021**, *50*, 6320-6332.

9. D. Cao, P. Pan, C.-J. Li & H. Zeng. Photo-Induced Transition-Metal and Photosensitizer Free Cross-Coupling of Aryl Halides with Disulfides. *Green Synth. Catal* **2021**, *2*, 303-306.

10. R. O. Loutfy & P. D. Mayo. Primary Bond Formation in the Addition of Cyclopentenone to Chloroethylenes. *Can. J. Chem.* **1972**, *50*, 3465-3471.

11. F. Strieth-Kalthoff *et al.* Energy Transfer Catalysis Mediated by Visible Light: Principles, Applications, Directions. *Chem. Soc. Rev.* **2018**, *47*, 7190-7202.

12. N. Hoffmann. Efficient Photochemical Electron Transfer Sensitization of Homogeneous Organic Reactions. *J. Photochem. Photobiol. C: Photochem. Rev.* **2008**, *9*, 43-60.

13. A. B. Beeler. Introduction: Photochemistry in Organic Synthesis. *Chem. Rev.* **2016**, *116*, 9629-9630.

14. T. Bortolato, S. Cuadros, G. Simionato & L. Dell'Amico. The Advent and Development of Organophotoredox Catalysis. *Chem. Commun.* **2022**, *58*, 1263-1283.

15. L. Capaldo, D. Ravelli & M. Fagnoni. Direct Photocatalyzed Hydrogen Atom Transfer (HAT) for Aliphatic C-H Bonds Elaboration. *Chem. Rev.* **2022**, *122*, 1875-1924.

16. S. Crespi & M. Fagnoni. Generation of Alkyl Radicals: From the Tyranny of Tin to the Photon Democracy. *Chem. Rev.* **2020**, *120*, 9790-9833.

17. A. L. Gant Kanegusuku & J. L. Roizen. Recent Advances in Photoredox-Mediated Radical Conjugate Addition Reactions: An Expanding Toolkit for the Giese Reaction. *Angew. Chem. Int. Ed.* **2021**, *60*, 21116-21149.

18. J. K. Matsui, S. B. Lang, D. R. Heitz & G. A. Molander. Photoredox-Mediated Routes to Radicals: The Value of Catalytic Radical Generation in Synthetic Methods Development. *ACS Catal.* **2017**, *7*, 2563-2575.

19. C. Zhu, H. Yue, L. Chu & M. Rueping. Recent Advances in Photoredox and Nickel Dual-Catalyzed Cascade Reactions: Pushing the Boundaries of Complexity. *Chem. Sci.* **2020**, *11*, 4051-4064.

20. W. Liu, L. Li & C. J. Li. Empowering a Transition-Metal-Free Coupling between Alkyne and Alkyl Iodide with Light in Water. *Nat. Commun.* **2015**, *6*, 6526.

21. Y. Sato *et al.* Generation of Alkyl Radical through Direct Excitation of Boracene-Based Alkylborate. *J. Am. Chem. Soc.* **2020**, *142*, 9938-9943.

22. B. Schweitzer-Chaput, M. A. Horwitz, E. De Pedro Beato & P. Melchiorre. Photochemical Generation of Radicals from Alkyl Electrophiles Using a Nucleophilic Organic Catalyst. *Nat. Chem.* **2019**, *11*, 129-135.

23. M. Salamone & M. Bietti. Tuning Reactivity and Selectivity in Hydrogen Atom Transfer from Aliphatic C-H Bonds to Alkoxyl Radicals: Role of Structural and Medium Effects. *Acc. Chem. Res.* **2015**, *48*, 2895-2903.

24. J. M. Tedder. Which Factors Determine the Reactivity and Regioselectivity of Free Radical Substitution and Addition Reactions? *Angew. Chem. Int. Ed.* **1982**, *21*, 401-410.

25. S. J. Blanksby & G. B. Ellison. Bond Dissociation Energies of Organic Molecules. *Acc. Chem. Res.* **2003**, *36*, 255-263.

26. J. L. Jeffrey, J. A. Terrett & D. W. MacMillan. O-H Hydrogen Bonding Promotes H-Atom Transfer from α C-H Bonds for C-Alkylation of Alcohols. *Science* **2015**, *349*, 1532-1536.

27. M. Bhakat, P. Biswas, J. Dey & J. Guin. Heteroarylation of Ethers, Amides, and Alcohols with Light and O_2. *Org. Lett.* **2021**, *23*, 6886-6890.

28. G.-X. Li *et al.* Photoredox-Mediated Minisci C-H Alkylation of *N*-Heteroarenes Using Boronic Acids and Hypervalent Iodine. *Chem. Sci.* **2016**, *7*, 6407-6412.

29. K. A. Margrey, W. L. Czaplyski, D. A. Nicewicz & E. J. Alexanian. A General Strategy for Aliphatic C-H Functionalization Enabled by Organic Photoredox Catalysis. *J. Am. Chem. Soc.* **2018**, *140*, 4213-4217.

30. X. Wu *et al.* Tertiary-Alcohol-Directed Functionalization of Remote C(sp^3)-H Bonds by Sequential Hydrogen Atom and Heteroaryl Migrations. *Angew. Chem. Int. Ed.* **2018**, *57*, 1640-1644.

31. X. Tang & A. Studer. Alkene 1,2-Difunctionalization by Radical Alkenyl Migration. *Angew. Chem. Int. Ed.* **2018**, *57*, 814-817.

32. X. Tang & A. Studer. α-Perfluoroalkyl-β-alkynylation of Alkenes via Radical Alkynyl Migration. *Chem. Sci.* **2017**, *8*, 6888-6892.

33. M. Wang, L. Huan & C. Zhu. Cyanohydrin-Mediated Cyanation of Remote Unactivated C(sp^3)-H Bonds. *Org. Lett.* **2019**, *21*, 821-825.

34. X. Wu & C. Zhu. Radical-Mediated Remote Functional Group Migration. *Acc. Chem. Res.* **2020**, *53*, 1620-1636.

35. H. Cao *et al.* Photoinduced Site-Selective Alkenylation of Alkanes and Aldehydes with Aryl Alkenes. *Nat. Commun.* **2020**, *11*, 1956.

36. S. Kamijo *et al.* Photo-Induced Substitutive Introduction of the Aldoxime Functional Group to Carbon Chains: A Formal Formylation of Non-Acidic C(sp^3)-H Bonds. *Angew. Chem. Int. Ed.* **2016**, *55*, 9695-9699.

37. H. Chen & S. Yu. Remote C-C Bond Formation via Visible Light Photoredox-Catalyzed Intramolecular Hydrogen Atom Transfer. *Org. Biomol. Chem.* **2020**, *18*, 4519-4532.

38. X. Wu & C. Zhu. Radical Functionalization of Remote C(sp^3)-H Bonds Mediated by Unprotected Alcohols and Amides. *J. Chin. Chem. Soc.* **2020**, *2*, 813-828.

39. J. Jin & D. W. C. MacMillan. Alcohols as Alkylating Agents in Heteroarene C-H Functionalization. *Nature* **2015**, *525*, 87-90.

40. Y. Shen, I. Funez-Ardoiz, F. Schoenebeck & T. Rovis. Site-Selective α-C-H Functionalization of Trialkylamines via Reversible Hydrogen Atom Transfer Catalysis. *J. Am. Chem. Soc.* **2021**, *143*, 18952-18959.

41. V. Regnault. Ueber Die Wirkung Des Chlors Auf Den Chlorwasserstoffäther Des Alkohols Und Des Holzgeistes, So Wie Über Mehrere Puncte Der Aethertheorie. *J. Prakt. Chem.* **1840**, *19*, 193-218.

42. B. J. Shields & A. G. Doyle. Direct C(sp^3)-H Cross Coupling Enabled by Catalytic Generation of Chlorine Radicals. *J. Am. Chem. Soc.* **2016**, *138*, 12719-12722.

43. S. Rohe, A. O. Morris, T. McCallum & L. Barriault. Hydrogen Atom Transfer Reactions via Photoredox Catalyzed Chlorine Atom Generation. *Angew. Chem. Int. Ed.* **2018**, *57*, 15664-15669.

44. L. Troian-Gautier *et al.* Halide Photoredox Chemistry. *Chem. Rev.* **2019**, *119*, 4628-4683.

45. T. Kawasaki, N. Ishida & M. Murakami. Dehydrogenative Coupling of Benzylic and Aldehydic C-H Bonds. *J. Am. Chem. Soc.* **2020**, *142*, 3366-3370.

46. P. Chuentragool, D. Kurandina & V. Gevorgyan. Catalysis with Palladium Complexes Photoexcited by Visible Light. *Angew. Chem. Int. Ed.* **2019**, *58*, 11586-11598.

47. D. Nagib, L. Stateman & K. Nakafuku. Remote C-H Functionalization via Selective Hydrogen Atom Transfer. *Synthesis* **2018**, *50*, 1569-1586.

48. S. Sarkar, K. P. S. Cheung & V. Gevorgyan. C-H Functionalization Reactions Enabled by Hydrogen Atom Transfer to Carbon-Centered Radicals. *Chem. Sci.* **2020**, *11*, 12974-12993.

49. M. Ratushnyy, M. Parasram, Y. Wang & V. Gevorgyan. Palladium-Catalyzed Atom-Transfer Radical Cyclization at Remote Unactivated C(sp^3)-H Sites: Hydrogen-Atom Transfer of Hybrid Vinyl Palladium Radical Intermediates. *Angew. Chem. Int. Ed.* **2018**, *57*, 2712-2715.

50. C. Chatgilialoglu. Organosilanes as Radical-Based Reducing Agents in Synthesis. *Acc. Chem. Res.* **1992**, *25*, 188-194.

51. F. Minisci *et al.* Polar Effects in Free-Radical Reactions. Rate Constants in Phenylation and New Methods of Selective Alkylation of Heteroaromatic Bases. *J. Org. Chem.* **2002**, *51*, 4411-4416.

52. W. H. Tamblyn, E. A. Vogler & J. K. Kochi. Polar Effect in Alkyl Radical Reactions. Carbon Kinetic Isotope Effects in Halogen Atom Transfer to Tin(III) and Chromium(II). *J. Org. Chem.* **1980**, *45*, 3912-3915.

53. E. Tatunashvili & C. S. P. McErlean. Generation and Reaction of Alkyl Radicals in Open Reaction Vessels. *Org. Biomol. Chem.* **2020**, *18*, 7818-7821.

54. F. Juliá, T. Constantin & D. Leonori. Applications of Halogen-Atom Transfer (XAT) for the Generation of Carbon Radicals in Synthetic Photochemistry and Photocatalysis. *Chem. Rev.* **2022**, *122*, 2292-2352.

55. G. H. Lovett *et al.* Open-Shell Fluorination of Alkyl Bromides: Unexpected Selectivity in a Silyl Radical-Mediated Chain Process. *J. Am. Chem. Soc.* **2019**, *141*, 20031-20036.

56. V. Bacauanu *et al.* Metallaphotoredox Difluoromethylation of Aryl Bromides. *Angew. Chem. Int. Ed.* **2018**, *57*, 12543-12548.

57. T. Q. Chen & D. W. C. MacMillan. A Metallaphotoredox Strategy for the Cross-Electrophile Coupling of α-Chloro Carbonyls with Aryl Halides. *Angew. Chem. Int. Ed.* **2019**, *58*, 14584-14588.

58. P. Zhang, C. C. Le & D. W. C. MacMillan. Silyl Radical Activation of Alkyl Halides in Metallaphotoredox Catalysis: A Unique Pathway for Cross-Electrophile Coupling. *J. Am. Chem. Soc.* **2016**, *138*, 8084-8087.

59. T. Constantin *et al.* Aminoalkyl Radicals as Halogen-Atom Transfer Agents for Activation of Alkyl and Aryl Halides. *Science* **2020**, *367*, 1021-1026.

60. J. Schwarz & B. König. Decarboxylative Reactions with and without Light-A Comparison. *Green Chem.* **2018**, *20*, 323-361.

61. J. Xuan, Z. G. Zhang & W. J. Xiao. Visible-Light-Induced Decarboxylative Functionalization of Carboxylic Acids and Their Derivatives. *Angew. Chem. Int. Ed.* **2015**, *54*, 15632-15641.

62. Z. Zuo *et al.* Merging Photoredox with Nickel Catalysis: Coupling of α-Carboxyl sp^3-Carbons with Aryl Halides. *Science* **2014**, *345*, 437-440.

63. K. L. Skubi, T. R. Blum & T. P. Yoon. Dual Catalysis Strategies in Photochemical Synthesis. *Chem. Rev.* **2016**, *116*, 10035-10074.

64. Z. Zuo *et al.* Enantioselective Decarboxylative Arylation of α-Amino Acids via the Merger of Photoredox and Nickel Catalysis. *J. Am. Chem. Soc.* **2016**, *138*, 1832-1835.

65. L. Candish, M. Teders & F. Glorius. Transition-Metal-Free, Visible-Light-Enabled Decarboxylative Borylation of Aryl *N*-Hydroxyphthalimide Esters. *J. Am. Chem. Soc.* **2017**, *139*, 7440-7443.

66. J. T. Edwards *et al.* Decarboxylative Alkenylation. *Nature* **2017**, *545*, 213-218.

67. A. Fawcett *et al.* Photoinduced Decarboxylative Borylation of Carboxylic Acids. *Science* **2017**, *357*, 283-286.

68. M.-C. Fu *et al.* Photocatalytic Decarboxylative Alkylations Mediated by Triphenylphosphine and Sodium Iodide. *Science* **2019**, *363*, 1429-1434.

69. K. Okada *et al.* Photosensitized Decarboxylative Michael Addition through *N*-(Acyloxy)phthalimides via an Electron-Transfer Mechanism. *J. Am. Chem. Soc.* **1991**, *113*, 9401-9402.

70. J. M. Smith *et al.* Decarboxylative Alkynylation. *Angew. Chem. Int. Ed.* **2017**, *56*, 11906-11910.

71. J. Wang *et al.* Cu-Catalyzed Decarboxylative Borylation. *ACS Catal.* **2018**, *8*, 9537-9542.

72. T. Cao *et al.* Decarboxylative Thiolation of Redox-Active Esters to Free Thiols and Further Diversification. *Nat. Commun.* **2020**, *11*, 5340.

73. E. M. Dauncey *et al.* Photoinduced Remote Functionalisations by Iminyl Radical Promoted C-C and C-H Bond Cleavage Cascades. *Angew. Chem. Int. Ed.* **2018**, *57*, 744-748.

74. X. Y. Yu *et al.* Copper-Catalyzed Radical Cross-Coupling of Redox-Active Oxime Esters, Styrenes, and Boronic Acids. *Angew. Chem. Int. Ed.* **2018**, *57*, 15505-15509.

75. N. B. Bissonnette, J. M. Ellis, L. G. Hamann & F. Romanov-Michailidis. Expedient Access to Saturated Nitrogen Heterocycles by Photoredox Cyclization of Imino-Tethered Dihydropyridines. *Chem. Sci.* **2019**, *10*, 9591-9596.

76. E. Gandolfo, X. Tang, S. Raha Roy & P. Melchiorre. Photochemical Asymmetric Nickel-Catalyzed Acyl Cross-Coupling. *Angew. Chem. Int. Ed.* **2019**, *58*, 16854-16858.

77. T. Van Leeuwen, L. Buzzetti, L. A. Perego & P. Melchiorre. A Redox-Active Nickel Complex That Acts as an Electron Mediator in Photochemical Giese Reactions. *Angew. Chem. Int. Ed.* **2019**, *58*, 4953-4957.

78. T. Uchikura *et al.* Benzothiazolines as Radical Transfer Reagents: Hydroalkylation and Hydroacylation of Alkenes by Radical Generation under Photoirradiation Conditions. *Chem. Commun.* **2019**, *55*, 11171-11174.

79. D. S. Hamilton & D. A. Nicewicz. Direct Catalytic Anti-Markovnikov Hydroetherification of Alkenols. *J. Am. Chem. Soc.* **2012**, *134*, 18577-18580.

80. T. M. Nguyen, N. Manohar & D. A. Nicewicz. Anti-Markovnikov Hydroamination of Alkenes Catalyzed by a Two-Component Organic Photoredox System: Direct Access to Phenethylamine Derivatives. *Angew. Chem. Int. Ed.* **2014**, *53*, 6198-6201.

81. T. M. Nguyen & D. A. Nicewicz. Anti-Markovnikov Hydroamination of Alkenes Catalyzed by an Organic Photoredox System. *J. Am. Chem. Soc.* **2013**, *135*, 9588-9591.

82. A. J. Perkowski & D. A. Nicewicz. Direct Catalytic Anti-Markovnikov Addition of Carboxylic Acids to Alkenes. *J. Am. Chem. Soc.* **2013**, *135*, 10334-10337.

83. J. D. Griffin, C. L. Cavanaugh & D. A. Nicewicz. Reversing the Regioselectivity of Halofunctionalization Reactions through Cooperative Photoredox and Copper Catalysis. *Angew. Chem. Int. Ed.* **2017**, *56*, 2097-2100.

84. L. Chenneberg & C. Ollivier. Tin-Free Alternatives to the Barton-Mccombie Deoxygenation of Alcohols to Alkanes Involving Reductive Electron Transfer. *Chimia (Aarau)* **2016**, *70*, 67-76.

85. C. C. Nawrat *et al.* Oxalates as Activating Groups for Alcohols in Visible Light Photoredox Catalysis: Formation of Quaternary Centers by Redox-Neutral Fragment Coupling. *J. Am. Chem. Soc.* **2015**, *137*, 11270-11273.

86. L. Chu, J. M. Lipshultz & D. W. C. MacMillan. Merging Photoredox and Nickel Catalysis: The Direct Synthesis of Ketones by the Decarboxylative Arylation of α-Oxo Acids. *Angew. Chem. Int. Ed.* **2015**, *54*, 7929-7933.

87. E. E. Stache, A. B. Ertel, T. Rovis & A. G. Doyle. Generation of Phosphoranyl Radicals via Photoredox Catalysis Enables Voltage-Independent Activation of Strong C-O Bonds. *ACS Catal.* **2018**, *8*, 11134-11139.

88. J. Dong *et al.* Ketones and Aldehydes as Alkyl Radical Equivalents for C-H Functionalization of Heteroarenes. *Sci. Adv.* **2019**, *5*, eaax9955.

89. Z. Wang *et al.* Bromide-Promoted Visible-Light-Induced Reductive Minisci Reaction with Aldehydes. *ACS Catal.* **2020**, *10*, 154-159.

90. J. A. Leitch, T. Rossolini, T. Rogova & D. J. Dixon. α-Tertiary Dialkyl Ether Synthesis via Reductive Photocatalytic α-Functionalization of Alkyl Enol Ethers. *ACS Catal.* **2020**, *10*, 11430-11437.

91. F. J. R. Klauck, M. J. James & F. Glorius. Deaminative Strategy for the Visible-Light-Mediated Generation of Alkyl Radicals. *Angew. Chem. Int. Ed.* **2017**, *56*, 12336-12339.

92. J. T. M. Correia *et al.* Photoinduced Deaminative Strategies: Katritzky Salts as Alkyl Radical Precursors. *Chem. Commun.* **2020**, *56*, 503-514.

93. S. L. Rössler *et al.* Pyridinium Salts as Redox-Active Functional Group Transfer Reagents. *Angew. Chem. Int. Ed.* **2020**, *59*, 9264-9280.

94. J. Wu, L. He, A. Noble & V. K. Aggarwal. Photoinduced Deaminative Borylation of Alkylamines. *J. Am. Chem. Soc.* **2018**, *140*, 10700-10704.

95. L. L. Liao *et al.* Visible-Light-Driven External-Reductant-Free Cross-Electrophile Couplings of Tetraalkyl Ammonium Salts. *J. Am. Chem. Soc.* **2018**, *140*, 17338-17342.

96. T. Rogova *et al.* Reverse Polarity Reductive Functionalization of Tertiary Amides via a Dual Iridium-Catalyzed Hydrosilylation and Single Electron Transfer Strategy. *ACS Catal.* **2020**, *10*, 11438-11447.

97. C. Chen *et al.* Generation of Non-Stabilized Alkyl Radicals from Thianthrenium Salts for C-B and C-C Bond Formation. *Nat. Commun.* **2021**, *12*, 4526.

98. J. Gao, J. Feng & D. Du. Shining Light on C-S Bonds: Recent Advances in C-C Bond Formation Reactions via C-S Bond Cleavage under Photoredox Catalysis. *Chem. Asian J.* **2020**, *15*, 3637-3659.

99. H. Jia *et al.* Trifluoromethyl Thianthrenium Triflate: A Readily Available Trifluoromethylating Reagent with Formal CF_3^+, $CF_3^\bullet$, and CF_3^- Reactivity. *J. Am. Chem. Soc.* **2021**, *143*, 7623-7628.

100. Á. Péter, G. J. P. Perry & D. J. Procter. Radical C-C Bond Formation Using Sulfonium Salts and Light. *Adv. Synth. Catal.* **2020**, *362*, 2135-2142.

101. X. Zhu *et al.* Alkylsulfonium Salts for the Photochemical Desulphurizative Functionalization of Heteroarenes. *Org. Chem. Front.* **2022**, *9*, 347-355.

102. C. Le *et al.* A Radical Approach to the Copper Oxidative Addition Problem: Trifluoromethylation of Bromoarenes. *Science* **2018**, *360*, 1010-1014.

103. D. J. P. Kornfilt & D. W. C. MacMillan. Copper-Catalyzed Trifluoromethylation of Alkyl Bromides. *J. Am. Chem. Soc.* **2019**, *141*, 6853-6858.

104. Y. He *et al.* Semi-Heterogeneous Photocatalytic Fluoroalkylation-Distal Functionalization of Unactivated Alkenes with R_fSO_2Na under Air Atmosphere. *Green Chem.* **2021**, *23*, 9577-9582.

105. S. Ye, T. Xiang, X. Li & J. Wu. Metal-Catalyzed Radical-Type Transformation of Unactivated Alkyl Halides with C-C Bond Formation under Photoinduced Conditions. *Org. Chem. Front.* **2019**, *6*, 2183-2199.

106. J. Li *et al.* Formal Enantioconvergent Substitution of Alkyl Halides via Catalytic Asymmetric Photoredox Radical Coupling. *Nat. Commun.* **2018**, *9*, 2445.

107. M. El Khatib, R. A. M. Serafim & G. A. Molander. α-Arylation/Heteroarylation of Chiral α-Aminomethyltrifluoroborates by Synergistic Iridium Photoredox/Nickel Cross-Coupling Catalysis. *Angew. Chem. Int. Ed.* **2016**, *55*, 254-258.

108. J. K. Matsui, D. N. Primer & G. A. Molander. Metal-Free C-H Alkylation of Heteroarenes with Alkyltrifluoroborates: A General Protocol for 1°, 2° and 3° Alkylation. *Chem. Sci.* **2017**, *8*, 3512-3522.

109. G. A. Molander, V. Colombel & V. A. Braz. Direct Alkylation of Heteroaryls Using Potassium Alkyl- and Alkoxymethyltrifluoroborates. *Org. Lett.* **2011**, *13*, 1852-1855.

110. G. A. Molander & N. Ellis. Organotrifluoroborates: Protected Boronic Acids That Expand the Versatility of the Suzuki Coupling Reaction. *Acc. Chem. Res.* **2007**, *40*, 275-286.

111. M. Presset *et al.* Synthesis and Minisci Reactions of Organotrifluoroborato Building Blocks. *J. Org. Chem.* **2013**, *78*, 4615-4619.

112. D. N. Primer & G. A. Molander. Enabling the Cross-Coupling of Tertiary Organoboron Nucleophiles through Radical-Mediated Alkyl Transfer. *J. Am. Chem. Soc.* **2017**, *139*, 9847-9850.

113. J. C. Tellis *et al.* Single-Electron Transmetalation via Photoredox/Nickel Dual Catalysis: Unlocking a New Paradigm for sp^3-sp^2 Cross-Coupling. *Acc. Chem. Res.* **2016**, *49*, 1429-1439.

114. Y. Yamashita, J. C. Tellis & G. A. Molander. Protecting Group-Free, Selective Cross-Coupling of Alkyltrifluoroborates with Borylated Aryl Bromides via Photoredox/Nickel Dual Catalysis. *Proc. Natl. Acad. Sci. U.S.A.* **2015**, *112*, 12026-12029.

115. J. C. Tellis, D. N. Primer & G. A. Molander. Single-Electron Transmetalation in Organoboron Cross-Coupling by Photoredox/Nickel Dual Catalysis. *Science* **2014**, *4345*, 433-436.

116. D. N. Primer, I. Karakaya, J. C. Tellis & G. A. Molander. Single-Electron Transmetalation: An Enabling Technology for Secondary Alkylboron Cross-Coupling. *J. Am. Chem. Soc.* **2015**, *137*, 2195-2198.

117. D. N. Primer & G. A. Molander. Enabling the Cross-Coupling of Tertiary Organoboron Nucleophiles through Radical-Mediated Alkyl Transfer. *J. Am. Chem. Soc.* **2017**, *139*, 9847-9850.

118. Z.-Y. Cao, T. Ghosh & P. Melchiorre. Enantioselective Radical Conjugate Additions Driven by a Photoactive Intramolecular Iminium-Ion-Based EDA Complex. *Nat. Commun.* **2018**, *9*, 3274.

119. M. Silvi *et al.* Visible-Light Excitation of Iminium Ions Enables the Enantioselective Catalytic β-Alkylation of Enals. *Nat. Chem.* **2017**, *9*, 868-873.

120. G. E. M. Crisenza, D. Mazzarella & P. Melchiorre. Synthetic Methods Driven by the Photoactivity of Electron Donor-Acceptor Complexes. *J. Am. Chem. Soc.* **2020**, *142*, 5461-5476.

121. H. Jiang & A. Studer. Intermolecular Radical Carboamination of Alkenes. *Chem. Soc. Rev.* **2020**, *49*, 1790-1811.

122. W.-J. Xiao, F.-D. Lu, G.-F. He & L.-Q. Lu. Metallaphotoredox Catalysis for Multicomponent Coupling Reactions. *Green Chem.* **2021**, *23*, 5379-5393.

123. R. C. McAtee, E. A. Noten & C. R. J. Stephenson. Arene Dearomatization through a Catalytic *N*-Centered Radical Cascade Reaction. *Nat. Commun.* **2020**, *11*, 2528.

124. J. Kanazawa, K. Maeda & M. Uchiyama. Radical Multicomponent Carboamination of [1.1.1]Propellane. *J. Am. Chem. Soc.* **2017**, *139*, 17791-17794.

125. M. Kondo *et al.* Silaboration of [1.1.1]Propellane: A Storable Feedstock for Bicyclo[1.1.1]pentane Derivatives. *Angew. Chem. Int. Ed.* **2020**, *59*, 1970-1974.

126. J. Nugent *et al.* A General Route to Bicyclo[1.1.1]pentanes through Photoredox Catalysis. *ACS Catal.* **2019**, *9*, 9568-9574.

127. M. Ociepa, A. J. Wierzba, J. Turkowska & D. Gryko. Polarity-Reversal Strategy for the Functionalization of Electrophilic Strained Molecules via Light-Driven Cobalt Catalysis. *J. Am. Chem. Soc.* **2020**, *142*, 5355-5361.

128. S. K. Rout *et al.* A Radical Exchange Process: Synthesis of Bicyclo[1.1.1]pentane Derivatives of Xanthates. *Chem. Commun.* **2019**, *55*, 14976-14979.

129. X. Zhang *et al.* Copper-Mediated Synthesis of Drug-Like Bicyclopentanes. *Nature* **2020**, *580*, 220-226.

130. J. Kanazawa & M. Uchiyama. Recent Advances in the Synthetic Chemistry of Bicyclo[1.1.1]pentane. *Synlett* **2019**, *30*, 1-11.

131. J. Turkowska, J. Durka & D. Gryko. Strain Release-an Old Tool for New Transformations. *Chem. Commun.* **2020**, *56*, 5718-5734.

132. S. Livesley *et al.* Electrophilic Activation of [1.1.1]Propellane for the Synthesis of Nitrogen-Substituted Bicyclo[1.1.1]pentanes. *Angew. Chem. Int. Ed.* **2021**, *61*, e202111291.

133. R. J. Wurtman *et al.* Effects of Normal Meals Rich in Carbohydrates or Proteins on Plasma Tryptophan and Tyrosine Ratios. *Am. J. Clin. Nutr.* **2003**, *77*, 128-132.

134. A. Nehlig, J.-L. Daval & G. Debry. Caffeine and the Central Nervous System: Mechanisms of Action, Biochemical, Metabolic and Psychostimulant Effects. *Brain Res. Rev.* **1992**, *17*, 139-170.

135. P. J. Hanzlik. Methylene Blue as Antidote for Cyanide Poisoning *J. Am. Med. Assoc.* **1933**, *100*, 357.

136. S. A. Doggrell. Rho-Kinase Inhibitors Show Promise in Pulmonary Hypertension. *Expert Opin. Investig. Drugs* **2005**, *14*, 1157-1159.

137. H. Reyburn, G. Mtove, I. Hendriksen & L. V. Seidlein. Oral Quinine for the Treatment of Uncomplicated Malaria. *Brit. Med. J.* **2009**, *339*, b2066.

138. T. Abe & K. Yamada. Amination/Cyclization Cascade by Acid-Catalyzed Activation of Indolenine for the One-Pot Synthesis of Phaitanthrin E. *Org. Lett.* **2016**, *18*, 6504-6507.

139. H. R. Snyder & D. S. Matteson. The Synthesis of the 2-Amino-3-(3-indolyl)-butyric Acids (β-Methyltryptophans). *J. Am. Chem. Soc.* **1957**, *79*, 2217-2221.

140. A. Modak, E. N. Pinter & S. P. Cook. Copper-Catalyzed, *N*-Directed Csp^3-H Trifluoromethylthiolation ($-SCF_3$) and Trifluoromethylselenation ($-SeCF_3$). *J. Am. Chem. Soc.* **2019**, *141*, 18405-18410.

141. Z.-F. Xiao *et al.* Zinc Iodide-Mediated Direct Synthesis of 2,3-Dihydroisoxazoles from Alkynes and Nitrones. *Adv. Synth. Catal.* **2016**, *358*, 1859-1863.

142. H.-L. Cui. Recent Progress in (Hetero)arene Cation Radical-Based Heteroarene Modification. *Org. Biomol. Chem.* **2020**, *18*, 2975-2990.

143. K. Morimoto *et al.* Metal-Free Oxidative Coupling Reactions via Σ-Iodonium Intermediates: The Efficient Synthesis of Bithiophenes Using Hypervalent Iodine Reagents. *Eur. J. Org. Chem.* **2011**, *2011*, 6326-6334.

144. T. Dohi *et al.* Novel and Direct Oxidative Cyanation Reactions of Heteroaromatic Compounds Mediated by a Hypervalent Iodine(III) Reagent. *Org. Lett.* **2005**, *7*, 537-540.

145. F. Minisci *et al.* Nucleophilic Character of Alkyl Radicals: New Syntheses by Alkyl Radicals Generated in Redox Processes. *Tetrahedron Lett.* **1968**, *9*, 5609-5612.

146. F. Fontana, F. Minisci & E. Vismara. New General and Convenient Sources of Alkyl Radicals, Useful for Selective Syntheses. *Tetrahedron Lett.* **1988**, *29*, 1975-1978.

147. F. Minisci *et al.* Nucleophilic Character of Alkyl Radicals-VI. *Tetrahedron* **1971**, *27*, 3575-3579.

148. F. Minisci & F. Fontana. Mechanism of the Gif-Barton Type Alkane Functionalization by Halide and Pseudohalide Ions. *Tetrahedron Lett.* **1994**, *35*, 1427-1430.

149. J. Dong, Y. Liu & Q. Wang. Recent Advances in Visible-Light-Mediated Minisci Reactions. *Chin. J. Org. Chem.* **2021**, *41*, 3771-3791.

150. R. S. J. Proctor & R. J. Phipps. Recent Advances in Minisci-Type Reactions. *Angew. Chem. Int. Ed.* **2019**, *58*, 13666-13699.

151. A. Bera, L. M. Kabadwal, S. Bera & D. Banerjee. Recent Advances on Non-Precious Metal-Catalyzed C-H Functionalization of *N*-Heteroarenes. *Chem. Commun.* **2022**, *58*, 10-28.

152. S. Jeong & J. M. Joo. Transition-Metal-Catalyzed Divergent C-H Functionalization of Five-Membered Heteroarenes. *Acc. Chem. Res.* **2021**, *54*, 4518-4529.

153. L. Shi *et al.* Manganese Catalyzed C-H Functionalization of Indoles with Alkynes to Synthesize Bis/Trisubstituted Indolylalkenes and Carbazoles: The Acid Is the Key to Control Selectivity. *Chem. Commun.* **2015**, *51*, 7136-7139.

154. J. Li & L. Ackermann. Cobalt-Catalyzed C-H Cyanation of Arenes and Heteroarenes. *Angew. Chem. Int. Ed.* **2015**, *54*, 3635-3638.

155. Y. Chen *et al.* Ru(II)-Catalyzed Regioselective C-7 Hydroxymethylation of Indolines with Formaldehyde. *Tetrahedron Lett.* **2019**, *60*, 1481-1486.

Chapter 2 Diacetyl-mediated cross-dehydrogenative Minisci alkylation

This chapter utilizes diacetyl as an abundant and innocuous photosensitized reagent for metal-free cross-dehydrogenative Minisci alkylations. Two diacetyl-involved coupling methods were developed, and their respective mechanistic pathways were studied.[1]

2.1 Introduction

Heteroarenes are important skeletons in pharmaceutical and agricultural uses, as well as small molecule studies. The functionalization of these molecules, especially at the late stage to create diversity and increase complexity, is a long-lasting topic.[2-3]

The Minisci alkylation represents a powerful reaction to construct C(sp^2)-C(sp^3) bonds between electron-deficient heteroarenes and electron-rich alkyl radicals (R•), which is complementary to the Friedel-Crafts alkylation of electron-rich arenes. Over the past few decades, many efforts have been devoted to developing novel Minisci alkylations, predominantly focusing on the R• generation in more efficient and sustainable ways (**Figure 2.1**).

Figure 2.1 R• generations through C-C, C-X and C-H bond cleavage.

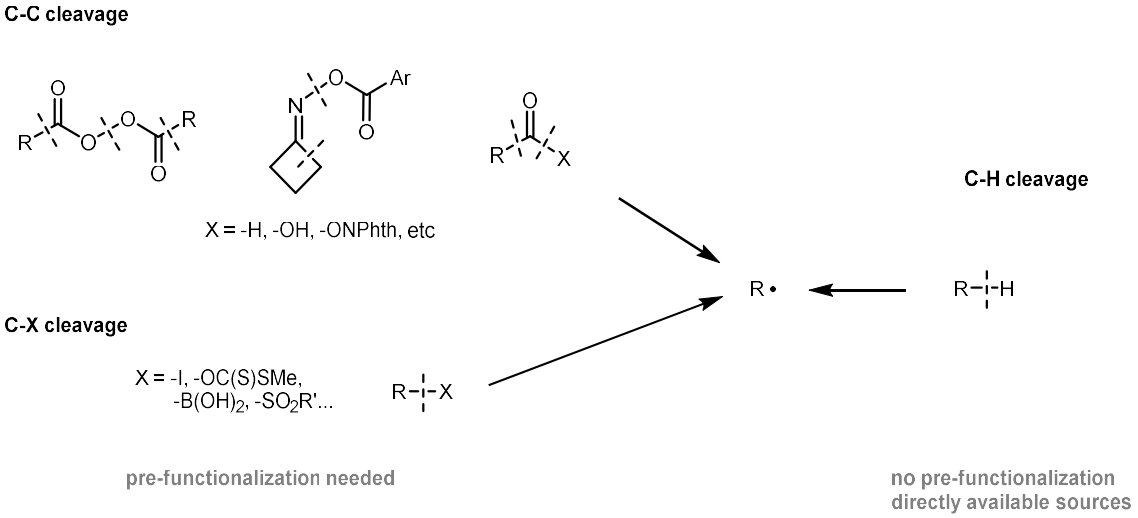

Although R• can be generated through carbon-heteroatom bond cleavage of alkyl iodide,[4] boronic acid[5-6] and others,[7-10] or carbon-carbon bond cleavage of aldehyde,[11] acid derivatives,[12] and oxime esters,[13-16] pre-synthesis of the R• precursors is required. Alternatively, the direct R• generation from alkanes is the most desirable because alkyl structures are naturally abundant, and formal removal of H_2 through cross-dehydrogenative-coupling (CDC) between the alkanes and arenes gives the greatest atom and step economy.[17-19]

Figure 2.2 Representative methods for generating HAT agents in Minisci alkylations

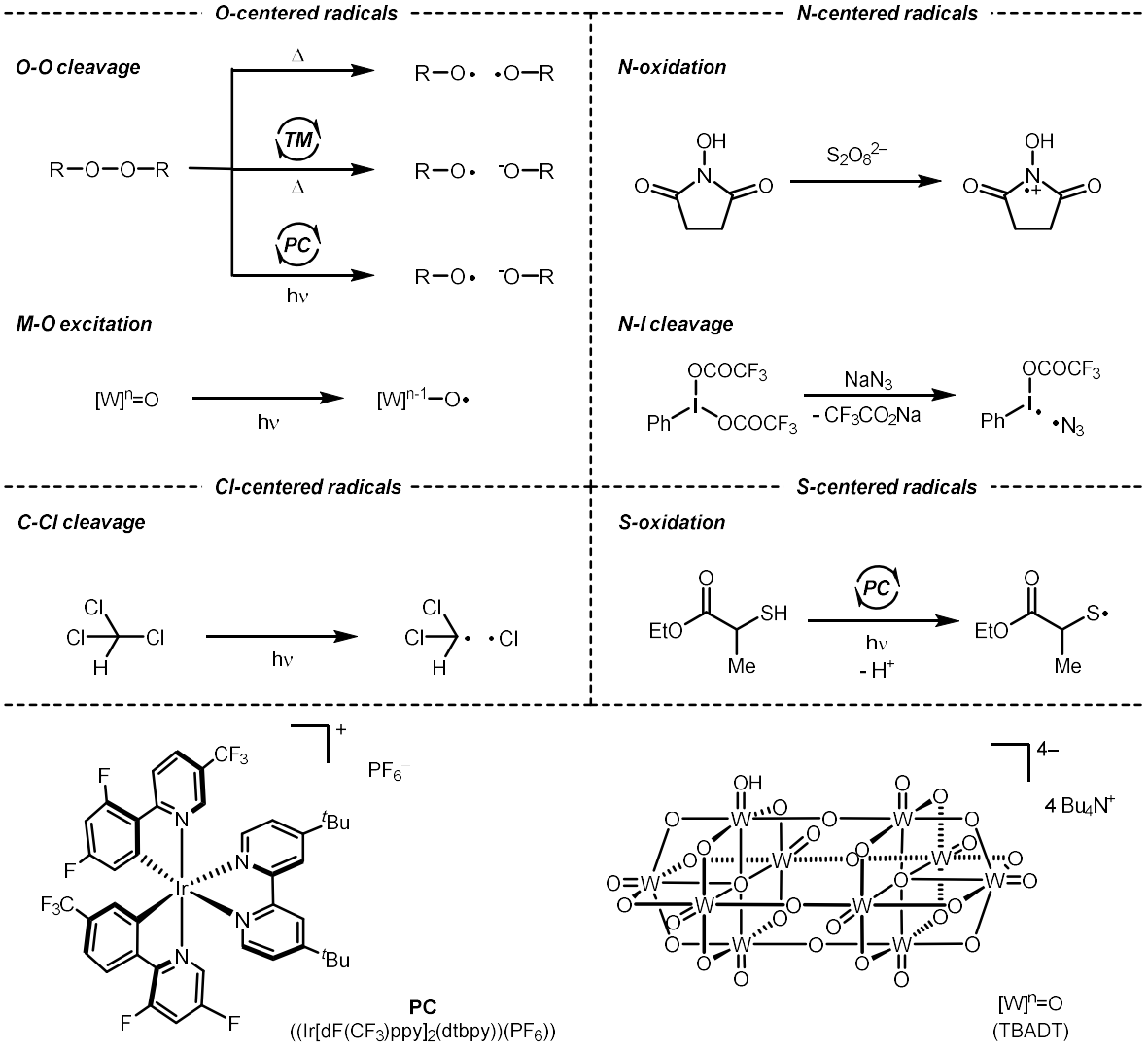

The key to cross-dehydrogenative Minisci alkylation is the activation of inert C(sp^3)-H bonds, among which the most general and simple way was via hydrogen atom transfer (HAT). Thereby, an efficient HAT agent is a requisite in the reaction design (**Figure 2.2**). Most of the strategies used *O*-centered radicals, routinely generated from peroxides or persulfates, to perform the hydrogen atom abstraction from alkanes. Traditional methods relied on thermo-cleavage of the O-O bonds; however, high reaction temperatures might deteriorate the reaction selectivity and functional group tolerance, and heating the explosive peroxides could cause safety concerns and limit the reaction scale.[20-23] To solve these issues, visible light-mediated CDC with iridium photocatalyst at room temperature was introduced by MacMillan.[24] Alternatively, Ravelli and Ryu's team employed solar light to activate decatungstate photocatalyst as the HAT agent, with persulfate being added to regenerate the photocatalyst.[25] Other than oxy radical-based oxidant, hydrogen atom abstractors such as *N*-centered radical cations from *N*-hydroxysuccinimide (NHS)[26-27] and azide,[28] thiyl radicals from thiols,[29] and chlorine radical from dichloromethane,[30] were also feasible under milder photo reaction conditions.

Although several facile cross-dehydrogenative Minisci alkylation strategies have been developed, it would still be desirable to conduct such reactions under mild conditions without costly photocatalysts and special light sources. On the other hand, since a stoichiometric amount of the oxidant is required for net oxidative reactions, removing excessive oxidant and its byproducts during work-up needs tedious and costly laboratory processes. With these in mind, we sought an innocuous and easily removable organic HAT agent.

2.2 Reaction design

Triplet state ketones and peroxides/persulfates share similar redox reactivities to a certain

degree. For example, Baran's group has designed a series of sulfinate salts for the C-H functionalization of heteroarenes mediated by peroxide.[8-9] Later, our group reported a photoinduced C(sp^2)-H trifluoromethylation with CF_3SO_2Na enabled by excited acetone or diacetyl (2,3-butanedione) as the transient single-electron oxidants (**Figure 2.3A**).[31] Inspired by the persulfate-based bimolecular homolytic substitution (S_H2) reaction of organoboranes,[32-33] we demonstrated that alkyl/aryl trifluoroborates could be converted to alkyl/aryl radicals through S_H2 by diacetyl under visible light irradiation (**Figure 2.3B**).[34] Based on these works, we hypothesized that triplet state ketones could substitute peroxides/persulfates in other *C*-centered radical generation processes, such as HAT. Indeed, ketones have been used in some HAT processes;[35-39] however, such application in cross-dehydrogenative coupling remained underexplored.

Figure 2.3 Diacetyl as a peroxide/persulfate surrogate.

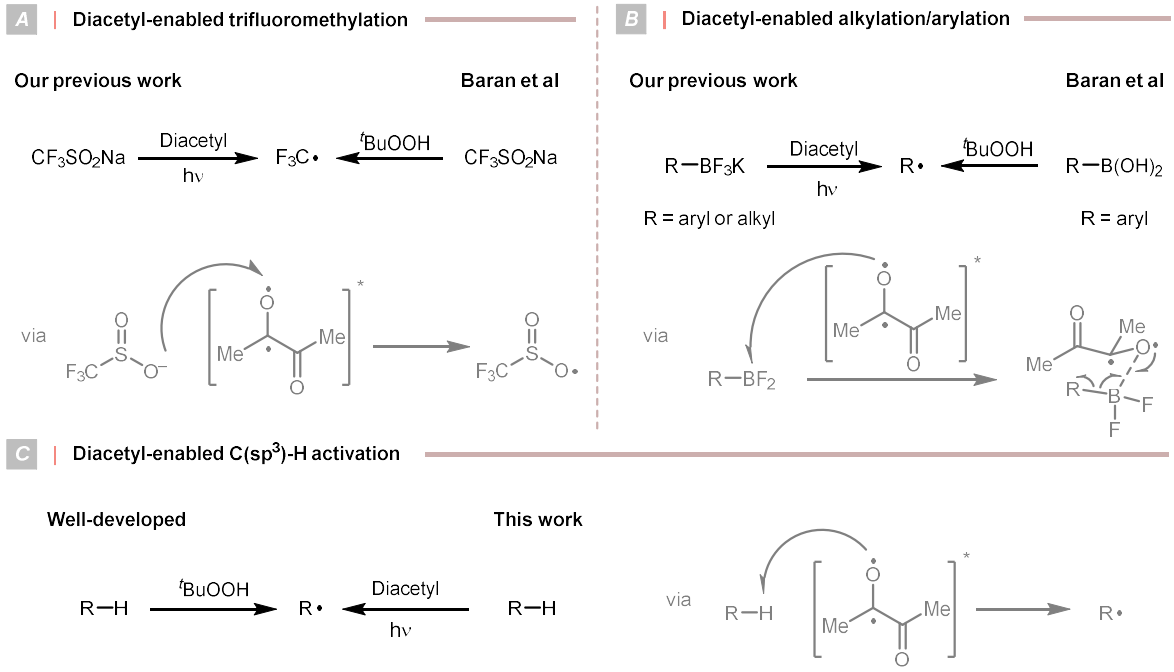

As a stoichiometric amount of oxidant is required for the dehydrogenative process, removing excessive oxidant and its byproducts needs a tedious and costly laboratory

endeavor. Diacetyl is the smallest visible light-sensitive ketone (380-460 nm),[31] which can be a traceless photosensitizer due to its high volatility and solubility in water (200 g/L at 20 °C). The reduced product of diacetyl, acetoin, is miscible with water (1 kg/L at 20 °C). Considering these, byproducts derived from diacetyl could be removed by aqueous work-up and reduced pressure. Furthermore, diacetyl is readily available and non-toxic. These advantages make diacetyl an ideal candidate in the cross-dehydrogenative system. Combining the literature reports and our previous experience, we hypothesized that diacetyl could serve as a HAT agent in cross-dehydrogenative Minisci alkylation due to its diradical character at its excited state (**Figure 2.3C**), and the success of this reaction would be a milestone in the exploration of ketone-enabled Minisci reactions and advance the development of greener cross-coupling reactions.

2.3 Results and discussion

In the preliminary studies, 2-phenylquinoline (**1a**) and tetrahydrofuran (THF, **2a**) were selected as the model coupling substrates. The corresponding alkylated product **3a** was detected by GC-MS under visible light irradiation using a 40 W compact fluorescent lamp (CFL, ~400-700 nm) as the light source.

Scheme 2.1 Preliminary studies of diacetyl-enabled CDC reaction

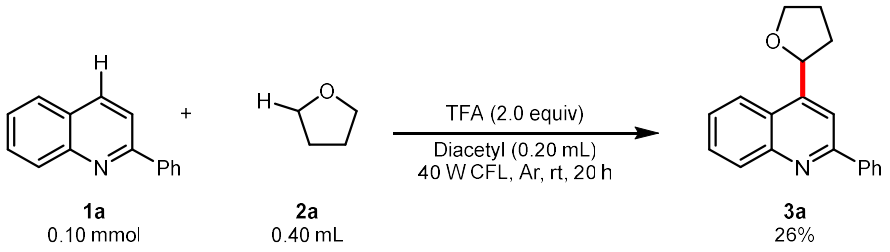

1a 0.10 mmol **2a** 0.40 mL **3a** 26%

We then started the optimization of this reaction. As given in **Table 2.1**, trifluoroacetic acid (TFA) was essential for the transformation, while acetic (AcOH) and triflic acid (TfOH)

were not effective proton sources (Table 1, entries 2 and 3). Different loadings of THF and diacetyl were investigated; the combination of 0.20 mL of THF and 0.20 mL of diacetyl gave the highest yield (entry 4). The reaction was promoted to completion by prolonging the reaction time to 36 h (entry 7). Finally, the control experiments showed that the light and diacetyl are indispensable for the reaction, while an inert atmosphere protects the reaction from oxygen interferences and assures a good yield (entries 8, 9 and 10).

Table 2.1 Optimization for the coupling of 2-phenylquinoline and THF.

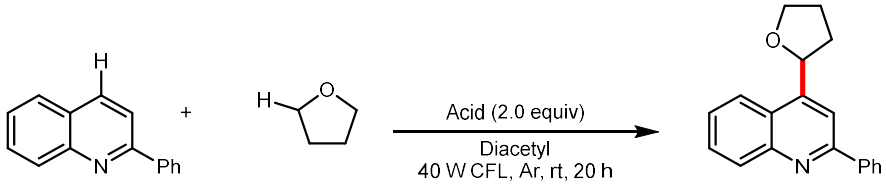

1a 0.10 mmol | **2a** 0.40 mL | **3a** 26%

Entry[a]	**2a** (mL)	Diacetyl (mL)	Acid	Conversion (%)	Yield (%)[b]
1[c]	0.40	0.20	TFA	74	71
2	0.40	0.20	AcOH	<1	-
3	0.40	0.20	TfOH	<1	-
4	0.20	0.20	TFA	90	88
5	0.20	0.10	TFA	56	55
6	0.10	0.10	TFA	60	53
7[c]	0.20	0.20	TFA	100	90 (86)
8[d]	0.20	0.20	TFA	80	64
9	0.40	-	TFA	<1	-
10[e]	0.20	0.20	TFA	<1	-

[a]Reaction conditions: **1a** (0.10 mmol**,** 1.0 equiv), **2a**, and acid (0.20 mmol, 2.0 equiv) in diacetyl under a 40W CFL irradiation at room temperature under argon for 20 h unless otherwise noted. [b]Yields were determined by ^{1}H NMR using mesitylene as the internal standard. The yield in parenthesis was the isolated one. [c]The reaction was run for 36 h. [d]The reaction was run under air. [e]The reaction was run at 70 °C in the dark.

Notably, most of the byproducts in this reaction could be removed simply by aqueous workup and reduced pressure without chromatography purification, as demonstrated by comparing NMR spectra in NMR spectra of (a) the pure **2a**, (b) the crude **3a** after basification, (c) the crude **3a** after basification, extraction, and concentration, and (d) the pure **3a** (**Figure 2.4**).

Figure 2.4 Demonstration of impurity removal.

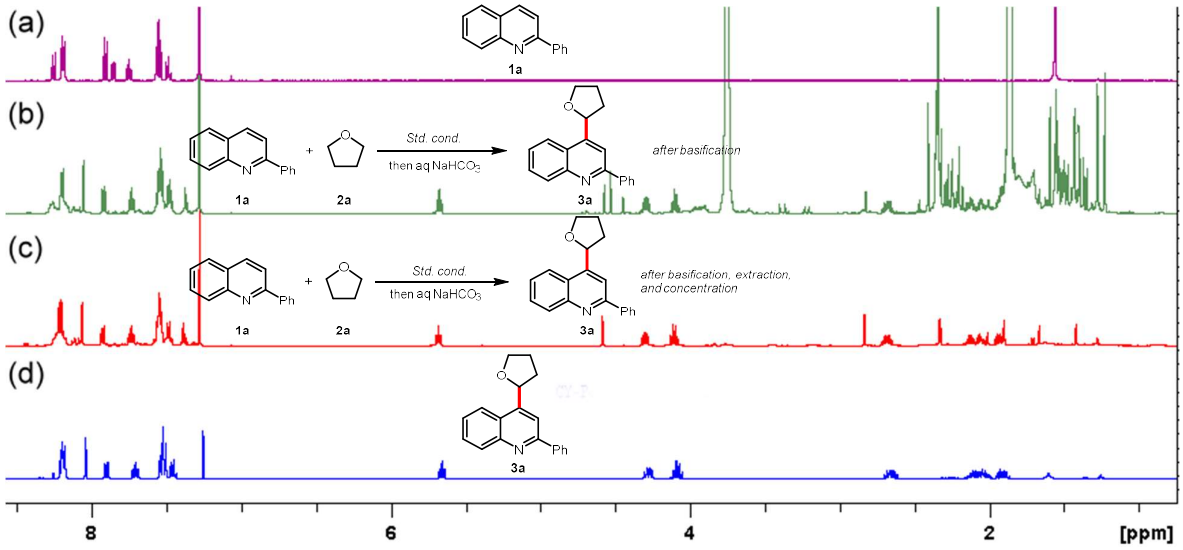

NMR spectra of (a) the pure **2a**, (b) the crude **3a** after basification, (c) the crude **3a** after basification, extraction, and concentration, and (d) the pure **3a**.

With the optimized conditions in hand, we tested the generality of this method (**Scheme 2.2**). By coupling various heteroarenes with THF (**2a**), the reaction tolerated diverse functional groups such as halo (**4a** to **6a**, **14a**, and **24a**), acetyl (**9a**), cyano (**17a**), alkoxy (**11a** and **14a**) and alkyl groups (**13a** and **14a**). Most substrates provided moderate to excellent yields of the corresponding products without significant yield bias between C2- and C4-alkylations (**3a** and **18a**, **16a** and **20a**). Substrates with steric effect (**19a**) or strong electron-donating group (**11a**), which might obstruct the radical addition, were provided in moderate yields. The 3-substituted quinoline selectively gave the C4-alkylated product **17a**. The C4-alkylated quinoline **15a** was obtained as the major product when unsubstituted quinoline was used, showing that the quinolinium C4 position might be more active in this method. Furthermore, pharmaceutically valuable molecules such as quinine (**26a**) and fasudil (**27a**) or complex menthol and L-alanine derivatives (**28a** and **29a**) were functionalizable. To show the potential applications in industrial and pharmaceutical uses, we demonstrated a gram-

scale reaction with 2-phenylquinoline (**1a**), in which 89% yield of the product (**3a**) was obtained.

Scheme 2.2 Coupling of heteroarenes with THF.

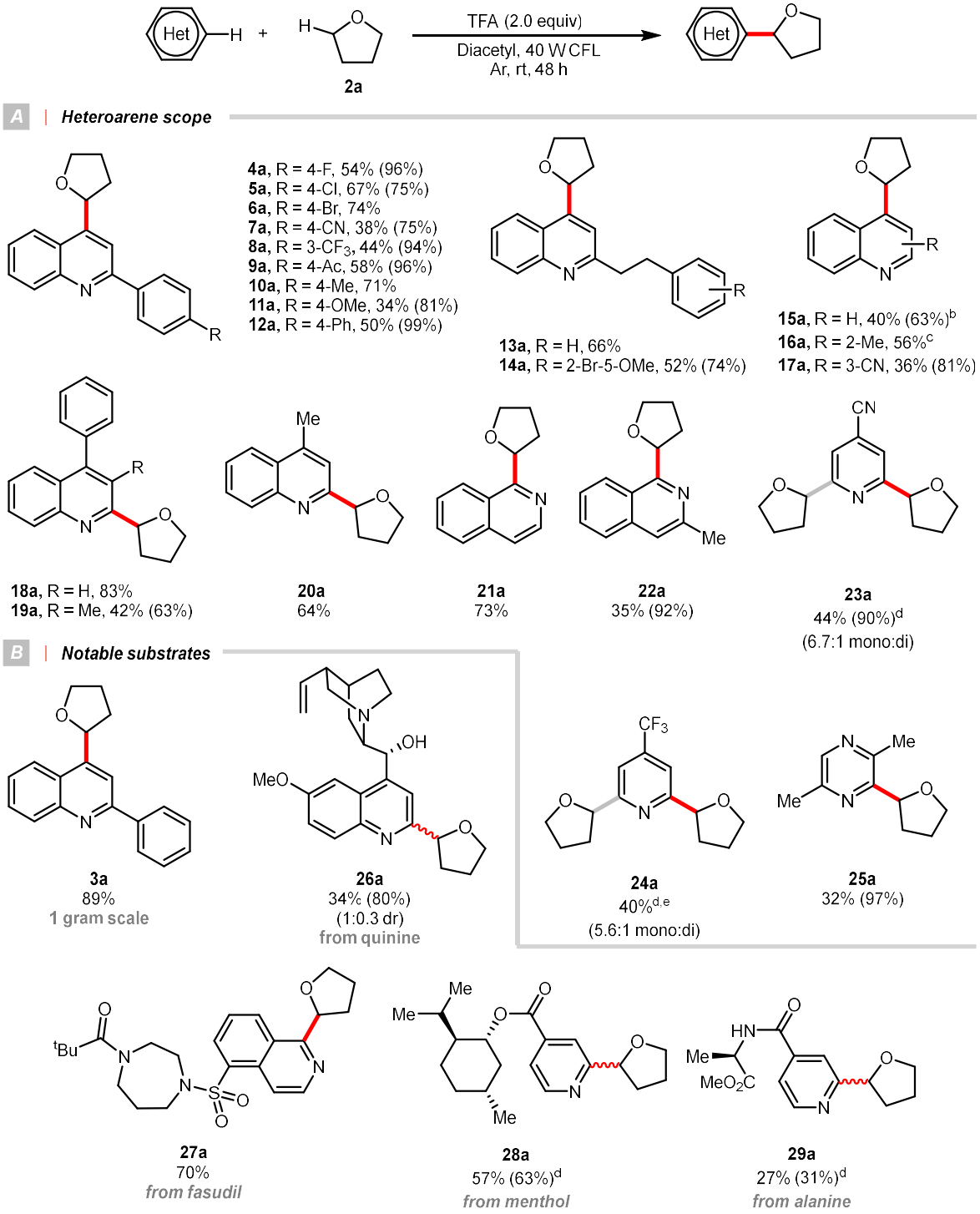

[a]Reaction conditions: heteroarene (0.10 mmol, 1.0 equiv), **2a** (0.20 mL), and TFA (0.20 mmol, 2.0 equiv) in diacetyl (0.20 mL) under a 40 W CFL irradiation at room temperature under argon for 48 h unless otherwise noted. Yields were the isolated ones, and the ones in parentheses were based on recovered starting materials. [b]0.1 mL of diacetyl and 0.20 mL of MeCN were added. [c]The reaction was run for 36 h. [d]20 equiv of TFA was added. [e]^{1}H NMR yield. [f]0.30 mL THF.

Other heterocycles such as isoquinolines (**21a** and **22a**), pyridines (**23a** and **24a**), and pyrazine (**25a**) were functionalized smoothly with this protocol. However, the reaction failed with heterocycles such as benzothiazole, benzoxazole and quinoxaline and gave poor NMR yields (**Scheme 1.23**).

Scheme 2.3 Unsuccessful substrates.

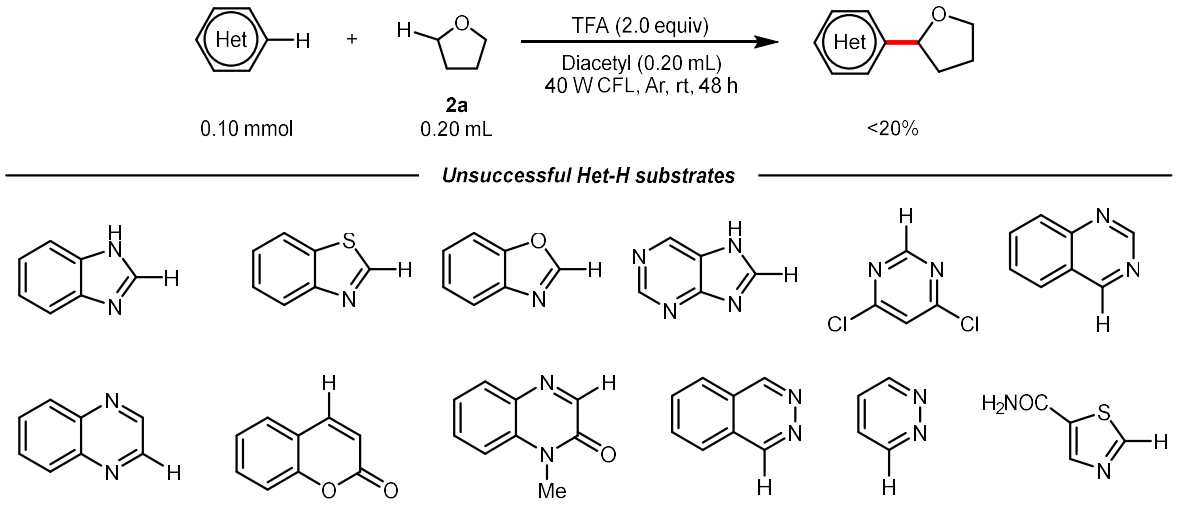

We further investigated the reactions of 2-phenylquinoline (**1a**) with other ether derivatives (**Scheme 2.4**). Diethyl ether gave an excellent yield of the alkylated product **30a**. Reaction with 2-methyl tetrahydrofuran and benzyl ethyl ether also provided the desired products **31a** and **32a**, in which the reactions occurred selectively on the less hindered α-carbon. Surprisingly, ethers such as 1,2-dimethoxyethane (DME), tetrahydropyran, and dioxane yielded only 11% to 18% of the corresponding products **33a**, **34a**, and **35a**.

Scheme 2.4 Coupling of 2-phenylquinoline with ethers.

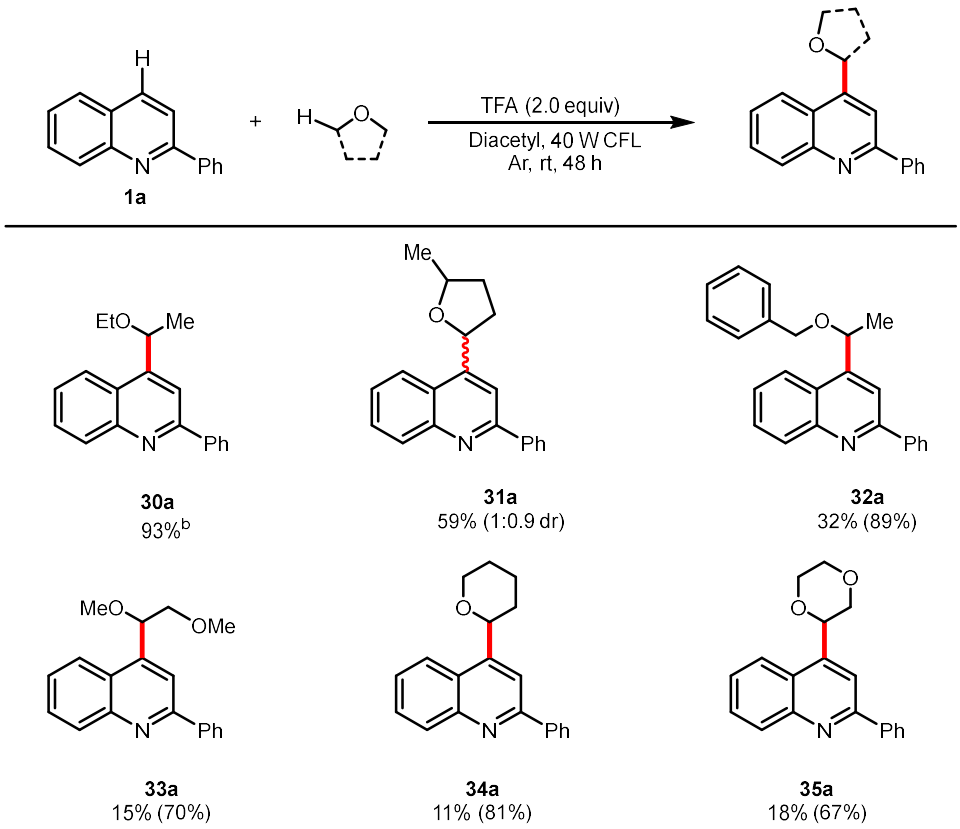

[a]Reaction conditions: **1a** (0.10 mmol, 1.0 equiv), ether (0.20 mL), and TFA (0.20 mmol, 2.0 equiv) in diacetyl (0.20 mL) under a 40 W CFL irradiation at room temperature under argon for 48 h unless otherwise noted. Yields were the isolated ones, and the ones in parentheses were based on recovered starting materials. [b]0.30 mL of ether.

According to the literature,[40-41] the bond dissociation energies of these ethers are slightly higher, roughly 2 to 4 kcal/mol, than the THF. Unlike traditionally oxyradicals, we postulated that the diactyl diradical could be stabalized through resonance, which makes it a milder and more selective oxidant toward C-H species. This resulted in low efficiency in oxidizing stronger C-H bonds; as a result, a stronger oxidant is necessary. It is known that triplet state photosensitizers can serve as energy transferrers to facilitate alkene isomerization,[42-43] cycloaddition,[44-47] metallic reductive elimination[48-50] and homolytic bond cleavage.[51-53] Theoretically, the triplet state energy of diacetyl, about 55 to 57 kcal/mol,[54] would be enough

to induce the homolysis of peroxide O-O bonds (BDE generally lower than 50 kcal/mol[55-56]). Considering that di-*tert*-butyl peroxide (DTBP) has a low O-O bond-dissociation energy (38 kcal/mol) and the byproduct *tert*-butanol is easily removable, 2.0 equiv of DTBP was chosen to be added to the reaction system. The reactions proceeded smoothly under room temperature and reached completion after 20 h to give good yields of the products **33a** to **35a**.

Scheme 2.5 Modified protocol for ether scope.

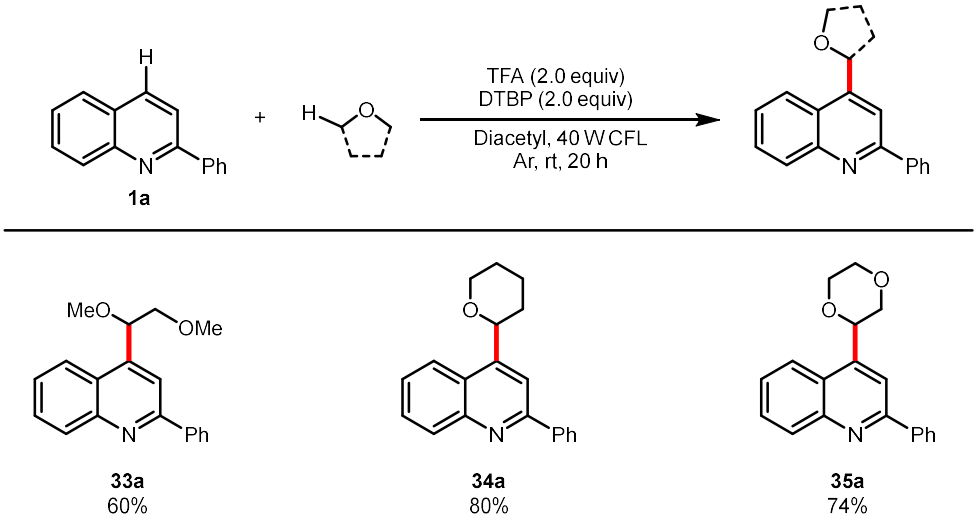

[a]Reaction conditions: **1a** (0.10 mmol, 1.0 equiv), ether (0.20 mL), TFA (0.20 mmol, 2.0 equiv), and DTBP (0.20 mmol, 2.0 equiv) in diacetyl (0.20 mL) under a 40 W CFL irradiation at room temperature under argon for 20 h. Yields were the isolated ones.

When diacetyl was used to cleave the strong C-H bond of cyclohexane (**36a**), it was not surprising that only a trace amount of cyclohexyl adduct **37a** was observed (**Table 2.2**, entry 1). Further optimizations were carried out with DTBP as the oxidant, and 84% of **37a** could be obtained with MeCN as the cosolvent (entries 2 to 11). To exclude the possible thermolysis of peroxide at room temperature, a control experiment was conducted at 4 °C, and the same yield could be obtained by prolonging the reaction time to 24 h (entry 3). On the contrary, no

reaction occurred in the absence of light, even when the reaction was heated to 70 °C (entry 4). These control experiments supported the energy transfer- rather than thermo-induced peroxide cleavage. To be noticed, the efficiency of this energy transfer pathway at low temperatures might provide a synthetic option for thermosensitive substrates.

Table 2.2 Optimization for the coupling of 4-methylquinoline and cyclohexane.

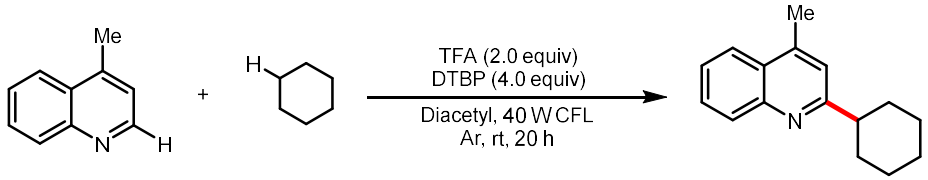

35a 0.10 mmol | **36a** | **37a**

Entry[a]	**36a** (mL)	Diacetyl (mL)	Cosolvent	Conversion (%)	Yield (%)[b]
1[c]	0.20	0.20	-	17	6
2	0.20	0.20	-	80	54
3	0.10	0.20	-	84	56
4	0.20	0.10	-	86	48
5	0.10	0.10	-	91	57
6	0.10	0.10	MeOH	65	35
7	0.10	0.10	DCM	77	56
8	0.10	0.10	AcOH	100	82
9	0.10	0.10	acetone	100	80
10	0.10	0.10	EtOAc	100	83
11	0.10	0.10	MeCN	100	87 (84)
12[d]	0.10	0.10	MeCN	90	78
13[e]	0.10	0.10	MeCN	100	86
14[f]	0.40	0.10	-	<5	0

[a]Reaction conditions: **35a** (0.10 mmol, 1.0 equiv), **36a**, TFA (0.20 mmol, 2.0 equiv), and DTBP (0.40 mmol, 4.0 equiv) in diacetyl and cosolvent under light irradiation at room temperature under argon for 20 h unless otherwise noted. [b]Yields were determined by ^{1}H NMR using mesitylene as the internal standard. The yield in parenthesis was the isolated one. [c]No DTBP. [d]2.0 equiv of DTBP was added. [e]The reaction was conducted at 4 °C for 24 h. [f]The reaction was heated to 70 °C in the dark.

Scheme 2.6 Coupling of heteroarenes with unactivated alkanes.

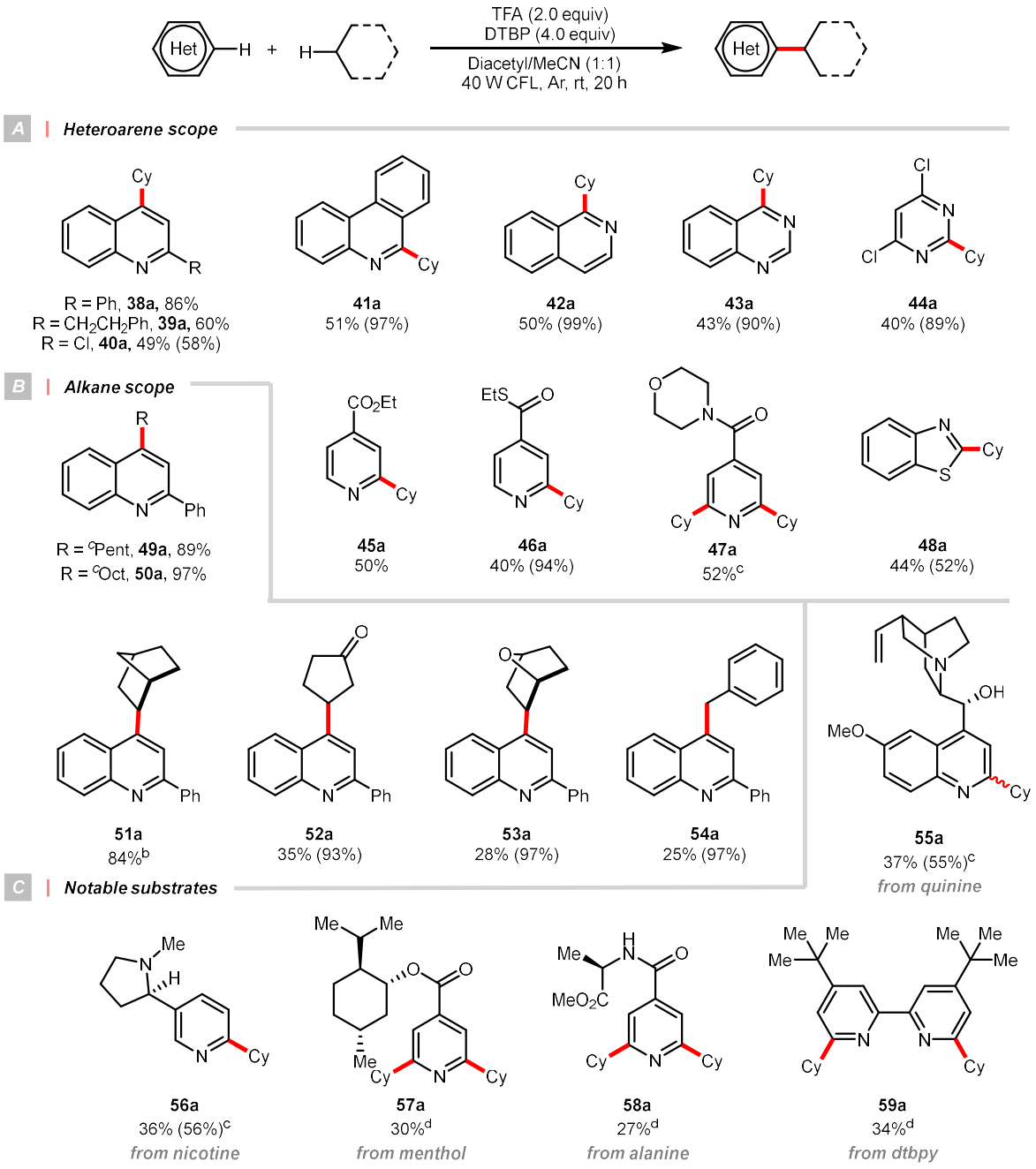

[a]Reaction conditions: heteroarene (0.10 mmol, 1.0 equiv), alkane (0.1 mL), TFA (0.20 mmol, 2.0 equiv), DTBP (0.40 mmol, 4.0 equiv), and diacetyl (0.1 mL) in MeCN (0.20 mL) under a 40 W CFL irradiation at room temperature under argon for 20 h unless otherwise noted. Yields were the isolated ones, and the ones in parentheses were based on recovered starting materials. [b]5.0 equiv of alkane was added. [c]3.0 equiv of TFA was added. [d]0.20 mL of alkane, 8.0 equiv of DTBP, 0.20 mL of diacetyl, and 0.4 mL of MeCN were added.

The scope of this modified protocol was then examined (**Scheme 2.6**). Heterocycles including phenanthridine, isoquinoline, quinazoline, pyrimidine, and benzothiazole were functionalized smoothly and gave moderate yields of the corresponding products (**38a** to **48a**). Other simple alkylated products were obtained by replacing cyclohexane with cyclopentane and cyclooctane, giving excellent yields of heterocycle derivatives **49a** and **50a**. Reaction with bridged hydrocarbon norbornane gave an excellent yield of the alkylated product **51a**; reactions with cyclopentanone, 7-oxabicyclo[2.2.1]heptane and toluene gave poor to moderate yields of the corresponding products **52a**, **53a**, and **54a**. Notable substrates, for example, quinine (**55a**), nicotine (**56a**), menthol and L-alanine derivatives (**57a** and **58a**), could be functionalized, albeit with lower yields. The method was also useful for modifying heterocyclic ligands, such as 4,4'-di-*tert*-butyl-2,2'-dipyridyl, (dtbpy) and gave the dialkylated product **59a**.

2.4 Mechanistic studies

Mechanistic studies were performed to consolidate that diacetyl could be a hydrogen atom abstractor for ethereal α-C-H (**Scheme 2.7**). When radical quencher such as 2,2,6,6-tetramethyl-1-piperidinyloxyl (TEMPO) or 2,6-di-*tert*-butyl-4-methylphenol (BHT) was added to the model reaction, product formation was significantly suppressed, implying that a radical pathway was involved (**Scheme 2.7A**). A ring-closing experiment was carried out between radical acceptor **60a** and THF; an appreciable amount of the alkylated adduct **61a** was isolated, confirming the formation of the THF radical (**Scheme 2.7B**). A prominent primary isotope effect was observed in the KIE experiments (k_H/k_D = 4, **Figure 2.5**), indicating that the α-C-H homocleavage of THF should be the rate-determining step in this reaction (**Scheme 2.7C**).[57] It should be noted that no H/D scrambling was observed from the reaction with THF-d_8. To rule out the acyl radical-involved HAT pathway,[58] we replaced

diacetyl with its analogue, benzil (**62a**), to perform the coupling of **1a** and **2a**; 75% of the alkylated quinoline **3a** was obtained, accompanying 33% of vicinal diol **63a**, 12% of benzoin (**64a**), and a trace amount of benzaldehyde (**65a**) (**Scheme 2.7D**). This result suggested the direct HAT with excited diketone played an indispensable role in the R• generation.

Scheme 2.7 Mechanistic studies regarding diacetyl as a hydrogen atom abstractor

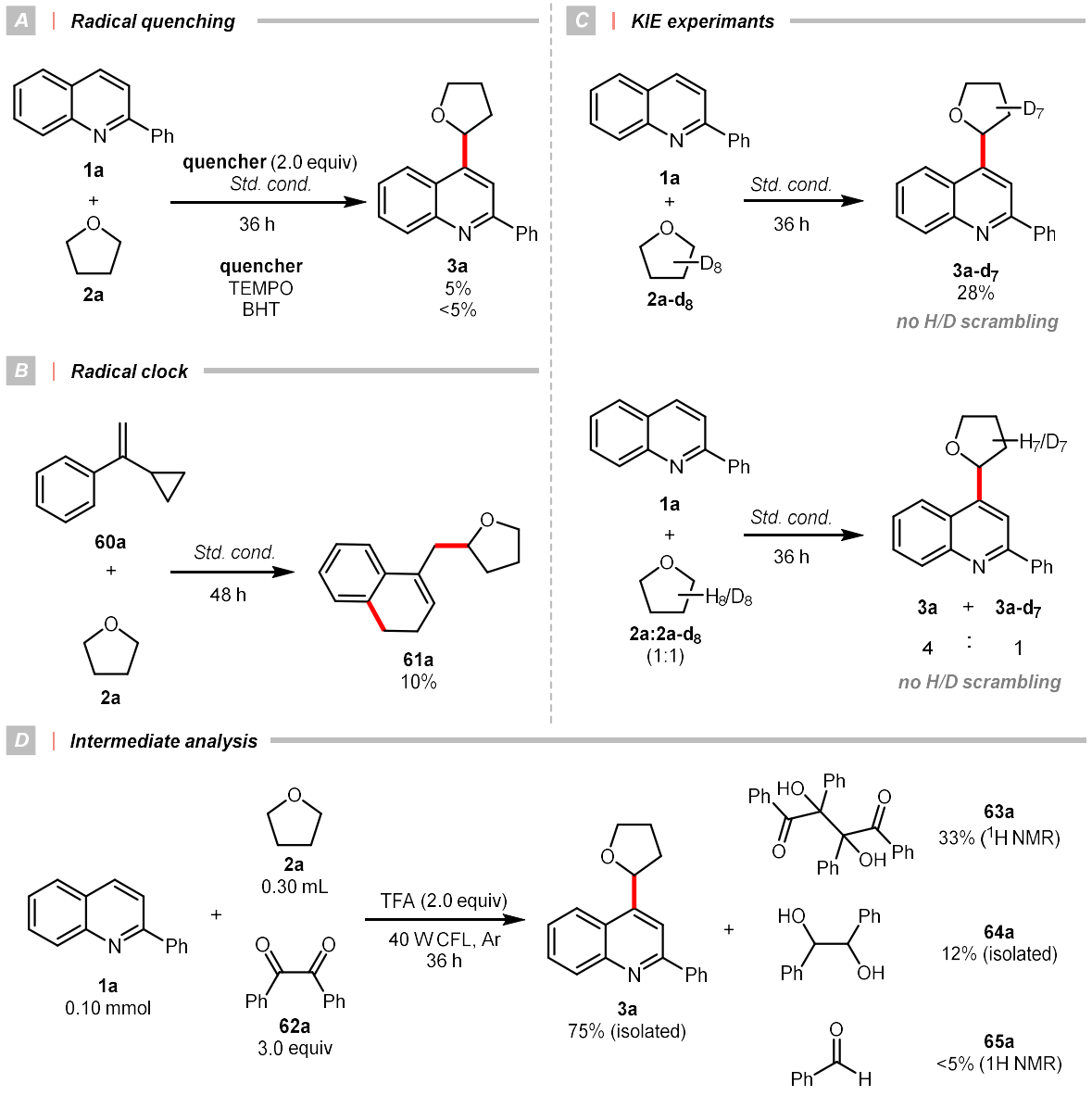

Figure 2.5 Purified isotope mixtures of 3a and 3a-d$_7$ from the KIE experiment.

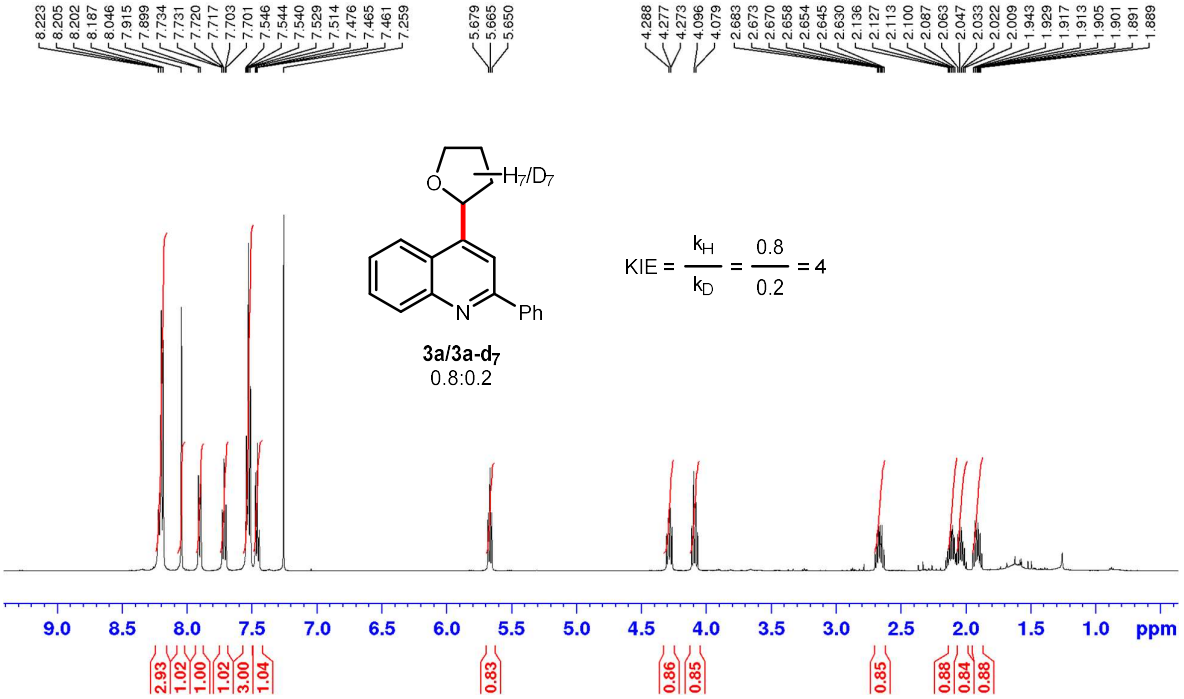

Scheme 2.8 Plausible pathways to generate the *tert*-butyl oxy radical.

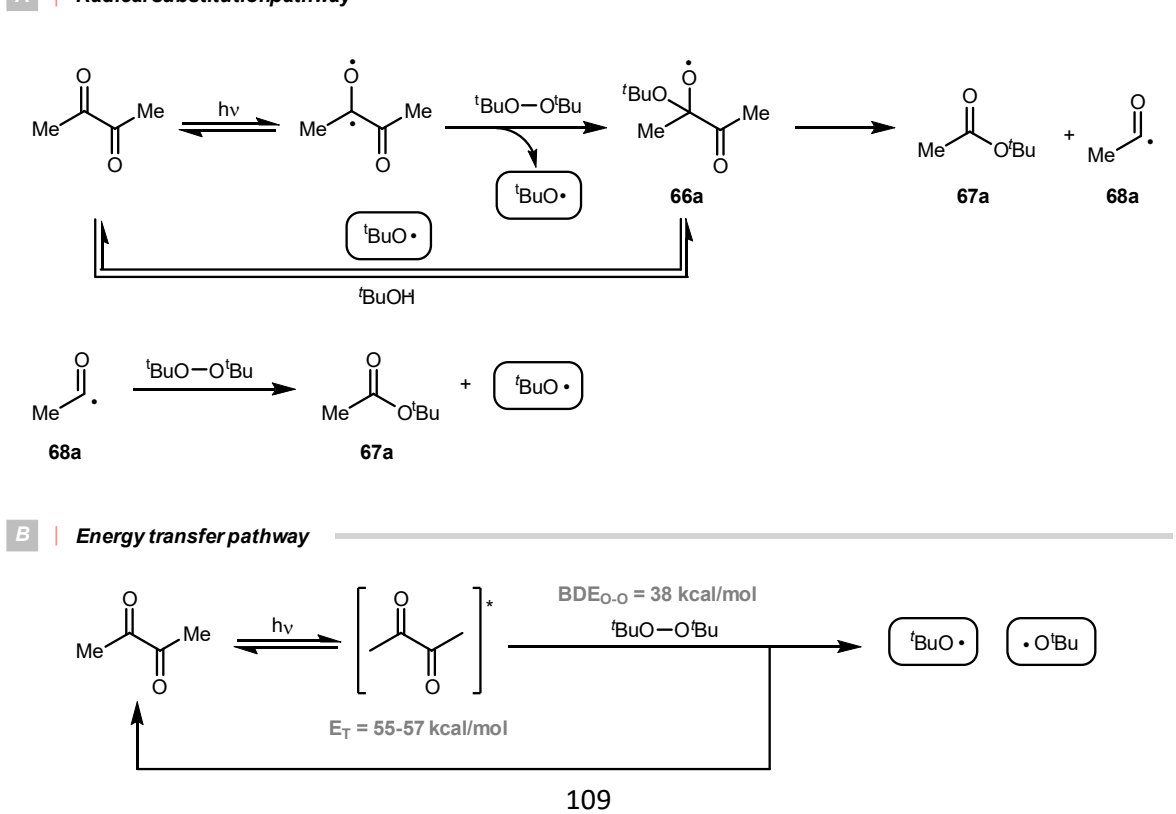

On the other hand, to elucidate the mechanism of DTBP-assisted alkylation, two attempted interactions between diacetyl and DTBP that generated the *tert*-butyl oxy radical were proposed. In **Scheme 2.8A**, the excited diacetyl could undergo hemolytic substitution on DTBP to release an equivalent of *tert*-butyl oxy radical and an oxy intermediate **66a**, which could decompose into *tert*-butyl acetate (**67a**) and acetyl radical (**68a**). Although the acetyl radical is not a good hydrogen atom abstractor, it could further react with another equivalent of DTBP to generate *tert*-butyl oxy radical. Alternatively, the excited state diacetyl could be an energy transfer agent and transfer its energy to DTBP, inducing the O-O homolysis ($BDE_{O\text{-}O}$ = 38 kcal/mol) (**Scheme 2.8B**).

There was no simple method to eliminate the energy transfer pathway. Therefore, we tested the radical substitution pathway by analyzing the amount of *tert*-butyl acetate (**67a**) generated from the reaction. Following the general procedure, the reaction between 2-phenylquinoline (**1a**) and DME was run for 12 h and analyzed by GC-MS (**Scheme 2.9**). 41% of the quinoline **31a** was obtained, with only trace amounts of *tert*-butyl acetate (**67a**) and the ether derivative **69a** were observed. Although the radical substitution pathway could not be excluded, these experimental results suggested that diacetyl-enabled energy transfer might be responsible for the DTBP homolysis.

Scheme 2.9 Side-product analysis of DTBP-assisted reaction.

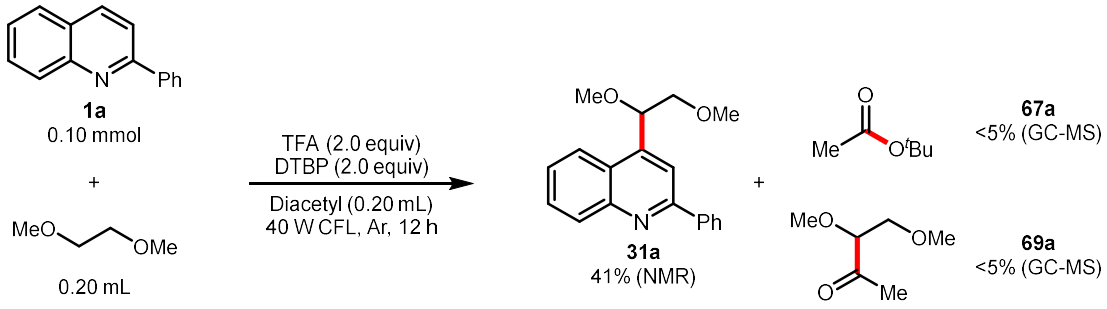

Based on the mechanistic investigations presented above, a plausible mechanism for the diacetyl-enabled cross-dehydrogenative Minisci alkylation was proposed. First, the photoexcited diacetyl abstracted a hydrogen atom from a C(sp^3)-H to generate an R• for heteroarene coupling (**Scheme 2.10**, right). Then, the protonated ketyl radical **70a** underwent tautomerization to form an enol radical **71a** and perform the second HAT, rearomatized the alkyl adduct **72a** and gave the product. On the other hand, when DTBP was added (**Scheme 2.10**, left), the photoexcited diacetyl became an energy transfer agent, which transferred its energy to DTBP and induced the homocleavage of DTBP to generate *tert*-butyl oxy radicals to dominate the HAT process.

Scheme 2.10 Plausible reaction mechanisms.

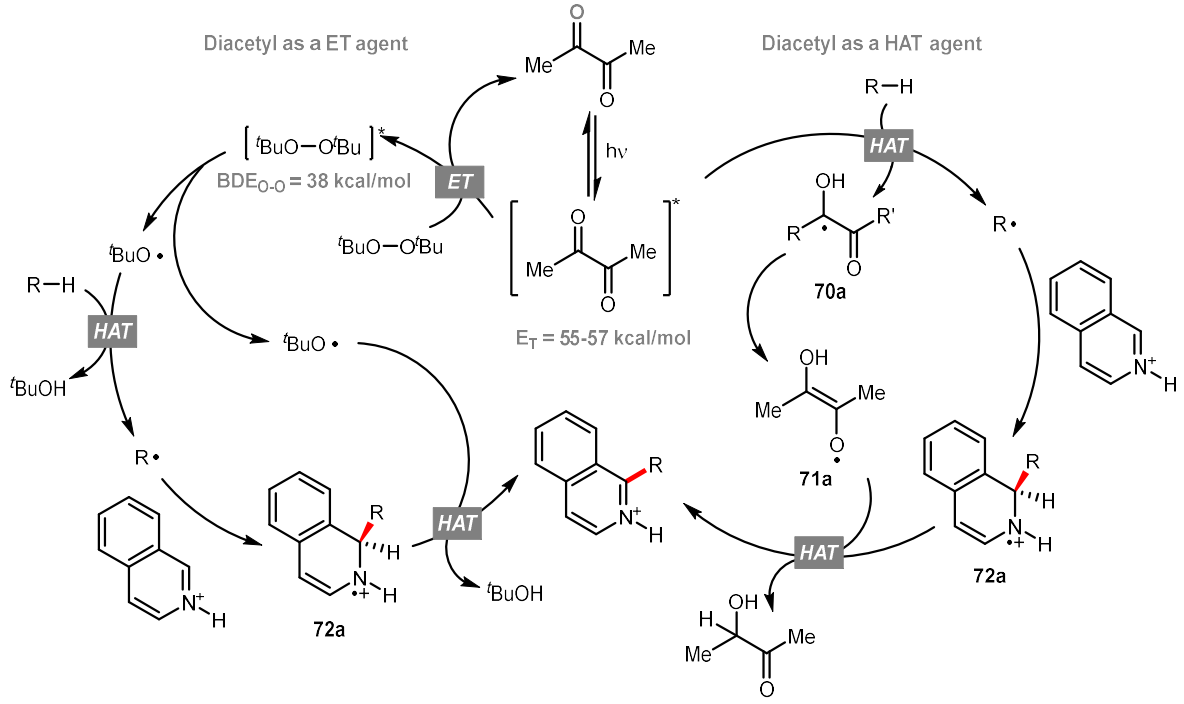

2.5 Conclusions and outlook

In summary, the first ketone-enabled cross-dehydrogenative Minisci alkylation using diacetyl as a traceless and sustainable photosensitive reagent has been developed. This approach

utilized the excited diacetyl as either a hydrogen atom transfer or energy transfer agent to couple heterocycles and alkanes under mild conditions. Control experiments and mechanistic studies suggested the involvement of radical processes.

Although this method has some limitations regarding the HAT ability of diacetyl, which could be told from the low conversion efficiency with some alkane and heteroarene substrates, the addition of DTBP into such mild reaction conditions provided a safe but enabling protocol toward broader substrate scope. It was worth noting that following this work, the group of Phipps demonstrated an elegant enantioselective cross-dehydrogenative Minisci alkylation between heteroarenes and amides utilizing diacetyl as the key HAT agent.[59] We believed more related works using diacetyl as a sustainable reagent would be carried out, and further studies would help us gain insight into the HAT ability of diacetyl and other potential traceless diketone photosensitizers.

2.6 Author contributions

Prof. Chao-Jun Li designed the project. I carried out all the experiments in this chapter with guidance from Prof. Chao-Jun Li, Dr. Wenbo Liu, and Dr. Jianbin Li. The manuscript was prepared by me and revised by Dr. Jianbin Li, Dr. Wenbo Liu, and Prof. Chao-Jun Li. All the authors approved the publication of this work.

2.7 Experimental section

Figure 2.6 The 40 W CFL reaction setup.

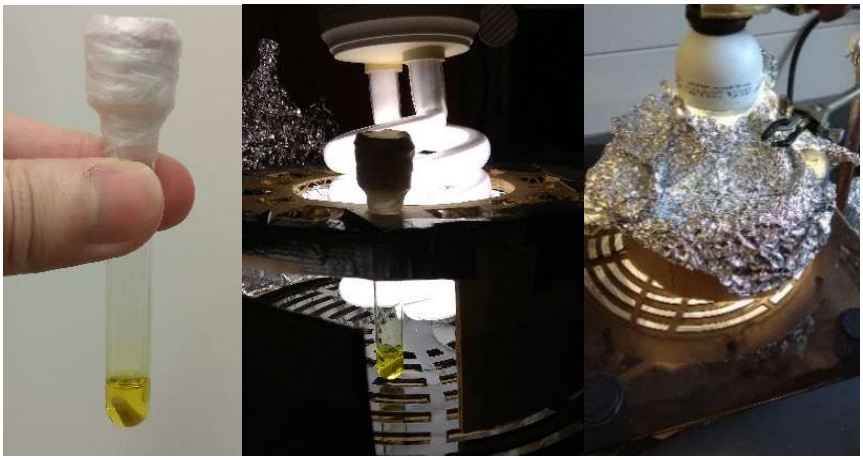

General procedure A. The following procedure applies to all the coupling of heteroarenes and ethers unless otherwise noted. To a glass tube (Fisherbrand Disposable Culture Tubes 10 mm × 75 mm) equipped with a Teflon-coated magnetic stirring bar were added heteroarene (0.10 mmol, 1.0 equiv), ether (0.20 mL), TFA (15.3 μL, 0.20 mmol, 2.0 equiv), and diacetyl (0.20 mL). The tube was sealed with a rubber septum, degassed by three freeze-pump-thaw cycles and back-filled with argon. The reaction mixture was then stirred at room temperature under a 40 W CFL irradiation. After 36-48 h, the reaction mixture was basified with sat $NaHCO_3$, extracted with EtOAc, filtered through a short pad of $MgSO_4$, and concentrated to afford the crude product. The product was isolated with preparative thin-layer chromatography.

General procedure B. The following procedure applies to all the coupling of heteroarenes and ethers that were inefficient with general procedure A. To a glass tube (Fisherbrand Disposable Culture Tubes 10 mm × 75 mm) equipped with a Teflon-coated magnetic stirring

bar were added heteroarene (0.10 mmol, 1.0 equiv), ether (0.20 mL), TFA (15.3 μL, 0.20 mmol, 2.0 equiv), DTBP (36.6 μL, 0.20 mmol, 2.0 equiv), and diacetyl (0.20 mL). The tube was sealed with a rubber septum, degassed by three freeze-pump-thaw cycles and back-filled with argon. The reaction mixture was then stirred at room temperature under a 40 W CFL irradiation. After 20 h, the reaction mixture was basified with sat $NaHCO_3$, extracted with EtOAc, filtered through a short pad of $MgSO_4$, and concentrated to afford the crude product. The product was isolated with preparative thin-layer chromatography.

General procedure C. The following procedure applies to all the coupling of heteroarenes and unactivated alkanes. To a glass tube (Fisherbrand Disposable Culture Tubes 10 mm × 75 mm) equipped with a Teflon-coated magnetic stirring bar were added heteroarene (0.10 mmol, 1.0 equiv), alkane (0.1 mL), TFA (15.3 μL, 0.20 mmol, 2.0 equiv), DTBP (73 μL, 0.40 mmol, 4.0 equiv), diacetyl (0.1 mL), and MeCN (0.20 mL). The tube was sealed with a rubber septum, degassed by three freeze-pump-thaw cycles and back-filled with argon. The reaction mixture was then stirred at room temperature under a 40 W CFL irradiation. After 20 h, the reaction mixture was basified with sat $NaHCO_3$, extracted with EtOAc, filtered through a short pad of $MgSO_4$, and concentrated to afford the crude product. The product was isolated with preparative thin-layer chromatography.

Gram-scale synthesis of 3a. To a 50 mL round bottom flask equipped with a Teflon-coated magnetic stirring bar were added heteroarene **1a** (1.0 g, 47.8 mmol, 1.0 equiv), THF **2a** (9.6 mL) and diacetyl (9.6 mL). The reaction mixture was sealed with a rubber septum and purged with argon for 30 min before TFA (0.73 mL, 95.6 mmol, 2.0 equiv) was injected via a syringe. The reaction mixture was then stirred at room temperature under two 40 W CFL irradiations. After 120 h, the reaction mixture was basified with sat $NaHCO_3$, extracted with EtOAc, washed

with water, dried over $MgSO_4$, and concentrated to afford the crude product. The isolated product was obtained by column chromatography.

Figure 2.7 Gram-scale synthesis of heteroarene 3a.

2.8 Characterization data for compounds

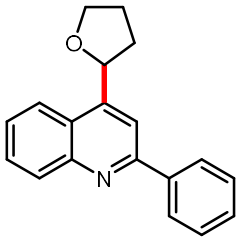

2-phenyl-4-(tetrahydrofuran-2-yl)quinoline (3a). Following the general procedure A. Isolated with Hex/DCM/EtOAc (1:1:0.05) on preparative thin-layer chromatography. Colorless oil (23.7 mg, 86%). **^{1}H NMR** (500 MHz, $CDCl_3$) δ 8.23-8.16 (m, 3H), 8.05 (s, 1H), 7.91 (d, *J* = 8.4 Hz, 1H), 7.74-7.68 (m, 1H), 7.56-7.49 (m, 3H), 7.49-7.42 (m, 1H), 5.56 (*J* = 7.1 Hz, 1H), 4.31-4.25 (m, 1H), 4.14-4.05 (m, 1H), 2.72-2.61 (m, 1H), 2.18-1.98 (m, 2H), 1.96-1.85 (m, 1H). **^{13}C NMR** (126 MHz, $CDCl_3$) δ 157.6, 150.1, 148.6, 140.2, 130.8, 129.4, 129.3, 129.0, 127.9, 126.2, 124.8, 123.2, 114.5, 69.3, 34.2, 26.1. **GC-MS** (EI, m/z) for $C_{15}H_{17}NO$ Calcd: 275.1, found: 275.2. Spectra data are consistent with the reported literature.[60]

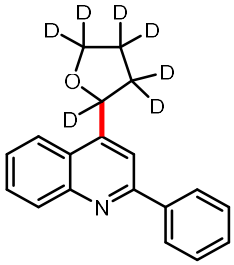

2-phenyl-4-(heptadeuterotetrafuran-2-yl)quinoline (3a-d$_7$). Following the general procedure A. Isolated with Hex/DCM/EtOAc (1:1:0.05) on preparative thin-layer chromatography. Colorless oil (7.9 mg, 28%). **^{1}H NMR** (500 MHz, $CDCl_3$) δ 8.24-8.16 (m, 3H), 8.05 (s, 1H), 7.90 (d, *J* = 8.4 Hz, 1H), 7.74-7.69 (m, 1H), 7.56-7.50 (m, 3H), 7.49-7.44 (m, 1H). **^{13}C NMR** (126 MHz, $CDCl_3$) δ 157.6, 130.8, 129.5, 129.3, 129.0, 127.9, 126.3, 124.8, 123.2, 114.6. **HRMS** Calcd for $C_{19}H_{11}D_7NO$ [M+H$^+$]: 283.1822, found: 283.1831. The compound was not reported.

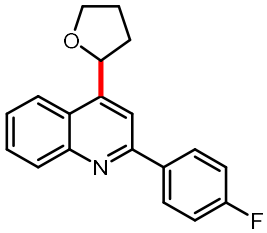

2-(4-fluorophenyl)-4-(tetrahydrofuran-2-yl)quinoline (4a). Following the general procedure A. Isolated with Hex/DCM/EtOAc (1:1:0.05) on preparative thin-layer chromatography. Colorless oil (15.9 mg, 54%). **^{1}H NMR** (500 MHz, $CDCl_3$) δ 8.23-8.15 (m, 3H), 8.00 (s, 1H), 7.90 (d, *J* = 8.4 Hz, 1H), 7.75-7.69 (m, 1H), 7.56-7.51 (m, 1H), 7.23-7.17 (m, 2H), 5.65 (t, *J* = 7.1 Hz, 1H), 4.31-4.25 (m, 1H), 4.09 (q, *J* = 7.5 Hz, 1H), 2.71-2.63 (m, 1H), 2.17-1.98 (m, 2H), 1.94-1.85 (m, 1H). **^{13}C NMR** (126 MHz, $CDCl_3$) δ 164.0 (d, *J* = 249 Hz), 156.5, 150.4, 148.5, 136.2, 130.7, 129.8, 129.7, 129.5, 126.3, 124.6, 123.2, 115.9 (d, *J* = 22 Hz), 114.1, 69.3, 34.2, 26.2. **HRMS** Calcd for $C_{19}H_{27}FNO$ [M+H$^+$]: 294.1289, found: 294.1283. The compound

was not reported.

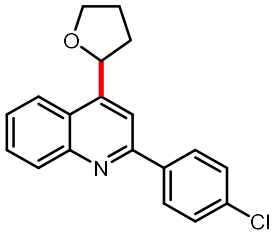

2-(4-chlorophenyl)-4-(tetrahydrofuran-2-yl)quinoline (5a). Following the general procedure A. Isolated with Hex/DCM/EtOAc (1:1:0.05) on preparative thin-layer chromatography. Colorless oil (20.7 mg, 67%). **^{1}H NMR** (500 MHz, $CDCl_3$) δ 8.21-8.13 (m, 3H), 8.01 (s, 1H), 7.90 (d, *J* = 8.4 Hz, 1H), 7.74-7.69 (m, 1H), 7.56-7.51 (m, 1H), 7.49 (d, *J* = 8.7 Hz, 2H), 5.65 (t, *J* = 7.1 Hz, 1H), 4.32-4.23 (m, 1H), 4.08 (q, *J* = 7.5 Hz, 1H), 2.771-2.63 (m, 1H), 2.17-1.99 (m, 2H), 1.94-1.84 (m, 1H). **^{13}C NMR** (126 MHz, $CDCl_3$) δ 156.2, 150.4, 148.5, 138.5, 135.7, 130.7, 129.5, 129.1, 126.5, 124.8, 123.2, 114.0, 77.2, 69.3, 34.2, 26.2. **HRMS** Calcd for $C_{19}H_{17}ClNO$ [M+H$^+$]: 310.0993, found: 310.0990. The compound was not reported.

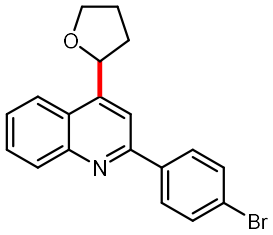

2-(4-bromophenyl)-4-(tetrahydrofuran-2-yl)quinoline (6a). Following the general procedure A. Isolated with Hex/DCM/EtOAc (1:1:0.05) on preparative thin-layer chromatography. Colorless oil (26.1 mg, 74%). **^{1}H NMR** (500 MHz, $CDCl_3$) δ 8.19 (d, *J* = 8.4 Hz, 1H), 8.09 (d, *J* = 8.6 Hz, 2H), 8.01 (s, 1H), 7.90 (d, *J* = 8.4 Hz, 1H), 7.75-7.70 (m, 1H), 7.65 (d, *J* = 8.6 Hz, 2H), 7.57-7.51 (m, 1H), 5.65 (t, *J* = 7.2 Hz, 1H), 4.31-4.42 (m, 1H), 4.09 (q, *J* = 7.5 Hz, 1H), 2.71-2.63 (m, 1H), 2.17-1.98 (m, 2H), 1.93-1.85 (m, 1H). **^{13}C NMR** (126 MHz, $CDCl_3$)

δ 156.3, 150.5, 148.5, 138.9, 132.1, 130.7, 129.5, 129.4, 126.5, 124.8, 124.1, 123.3, 114.0, 69.2, 34.3, 26.3. **HRMS** Calcd for $C_{19}H_{17}BrNO$ [M+H$^+$]: 354.0488, found: 354.0486. The compound was not reported.

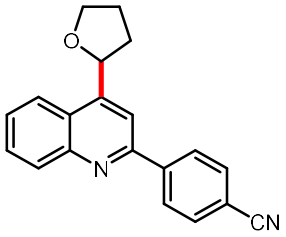

4-(4-(tetrahydrofuran-2-yl)quinolin-2-yl)benzonitrile (7a). Following the general procedure A. Isolated with Hex/DCM/EtOAc (1:1:0.2) on preparative thin-layer chromatography. Colorless solid (11.4 mg, 38%). **^{1}H NMR** (500 MHz, $CDCl_3$) δ 8.33 (d, *J* = 8.5 Hz, 2H), 8.20 (d, *J* = 8.2 Hz, 1H), 8.06 (s, 1H), 7.92 (d, *J* = 7.8 Hz, 1H), 7.81 (d, *J* = 8.5 Hz, 2H), 7.78-7.73 (m, 1H), 7.61-7.56 (m, 1H), 5.65 (t, *J* = 7.3 Hz, 1H), 4.32-4.28 (m, 1H), 4.09 (q, *J* = 7.5 Hz, 1H), 2.74-2.64 (m, 1H), 2.18-2.00 (m, 2H), 1.92-1.84 (m, 1H). **^{13}C NMR** (126 MHz, $CDCl_3$) δ 155.0, 150.8, 148.3, 144.0, 132.5, 130.8, 129.6, 128.2, 126.9, 124.9, 123.1, 118.9, 113.9, 112.7, 76.9, 69.0, 34.1, 26.1. **HRMS** Calcd for $C_{20}H_{17}N_2O$ [M+H$^+$]: 301.1335, found: 301.1330. The compound was not reported.

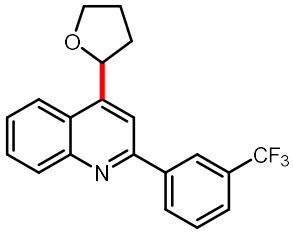

4-(tetrahydrofuran-2-yl)-2-(3-(trifluoromethyl)phenyl)quinoline (8a). Following the general procedure A. Isolated with Hex/DCM/EtOAc (1:1:0.05) on preparative thin-layer chromatography. Colorless oil (15.1 mg, 44%). **^{1}H NMR** (500 MHz, $CDCl_3$) δ 8.49 (s, 1H), 8.39

(d, *J* = 7.8 Hz, 1H), 8.22 (d, *J* = 8.4 Hz, 1H), 8.06 (s, 1H), 7.92 (d, *J* = 8.4 Hz, 1H), 7.77-7.70 (m, 2H), 7.67-7.62 (m, 1H), 7.59-7.55 (m, 1H), 5.67 (t, *J* = 7.2 Hz, 1H), 4.34-4.28 (m, 1H), 4.10 (q, *J* = 7.5 Hz, 1H), 2.73-2.64 (m, 1H), 2.18-2.01 (m, 2H), 1.95-1.86 (m, 1H). **^{13}C NMR** (126 MHz, $CDCl_3$) δ 155.8, 150.8, 149.0, 140.8, 131.4 (q, *J* = 32 Hz), 131.0, 130.6, 129.6, 129.4, 126.7, 126.0 (q, *J* = 4 Hz), 124.9, 124.7 (q, *J* = 4 Hz), 124.4 (q, *J* = 272 Hz), 123.3, 114.1, 69.3, 34.3, 26.3. **HRMS** Calcd for$C_{20}H_{17}F_3NO$ [M+H$^+$]: 344.1257, found: 344.1256. The compound was not reported.

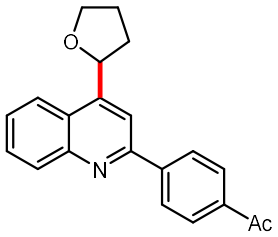

1-(4-(4-(tetrahydrofuran-2-yl)quinolin-2-yl)phenyl)ethanone (9a). Following the general procedure A. Isolated with Hex/DCM/EtOAc (1:1:0.2) on preparative thin-layer chromatography. Colorless oil (12.1 mg, 38%). **^{1}H NMR** (500 MHz, $CDCl_3$) δ 8.31 (d, *J* = 8.5 Hz, 2H), 8.22 (d, *J* = 8.4 Hz, 1H), 8.11 (d, *J* = 8.5 Hz, 2H), 8.09 (s, 1H), 7.92 (d, *J* = 7.7 Hz, 1H), 7.77-7.72 (m, 1H), 7.59-7.54 (m, 1H), 5.67 (t, *J* = 7.2 Hz, 1H), 4.32-4.67 (m, 1H), 4.10 (q, *J* = 7.5 Hz, 1H), 2.73-2.64 (m, 4H), 2.18-2.00 (m, 2H), 1.95-1.86 (m, 1H). **^{13}C NMR** (126 MHz, $CDCl_3$) δ 198.2, 156.2, 150.6, 148.6, 144.3, 137.6, 130.9, 129.6, 129.0, 128.0, 126.8, 125.0, 123.3, 114.5, 69.3, 34.3, 27.0, 26.3. **HRMS** Calcd for $C_{21}H_{20}NO_2$ [M+H$^+$]: 318.1489, found: 318.1484. The compound was not reported.

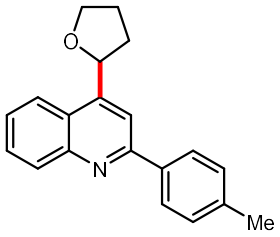

4-(tetrahydrofuran-2-yl)-2-(p-tolyl)quinoline (10a). Following the general procedure A. Isolated with Hex/DCM/EtOAc (1:1:0.05) on preparative thin-layer chromatography. Colorless oil (20.6 mg, 71%). **^{1}H NMR** (500 MHz, $CDCl_3$) δ 8.19 (d, *J* = 8.4 Hz, 1H), 8.10 (d, *J* = 8.2 Hz, 2H), 8.02 (s, 1H), 7.89 (d, *J* = 8.3 Hz, 1H), 7.73-7.68 (m, 1H), 7.54-7.49 (m, 1H), 7.33 (d, *J* = 8.2 Hz, 2H), 5.65 (t, *J* = 7.1 Hz, 1H), 4.31-4.25 (m, 1H), 4.08 (q, *J* = 7.5 Hz, 1H), 2.70-2.60 (m, 1H), 2.44 (s, 3H), 2.16-1.98 (m, 2H), 1.96-1.86 (m, 1H). **^{13}C NMR** (126 MHz, $CDCl_3$) δ 157.5, 150.0, 148.6, 139.5, 137.3, 130.7, 129.7, 129.3, 127.7, 126.1, 124.7, 123.2, 114.4, 69.3, 34.2, 26.2, 21.6. **HRMS** Calcd for $C_{20}H_{20}NO$ [M+H$^+$]: 290.1539, found: 290.1541. The compound was not reported.

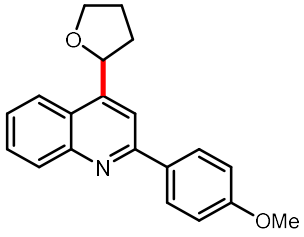

2-(4-methoxyphenyl)-4-(tetrahydrofuran-2-yl)quinoline (11a). Following the general procedure A. Isolated with Hex/DCM/EtOAc (1:1:0.05) on preparative thin-layer chromatography. Yellow oil (10.4 mg, 34%). **^{1}H NMR** (500 MHz, $CDCl_3$) δ 8.24-8.17 (m, 3H), 8.03 (s, 1H), 7.90 (d, *J* = 8.4 Hz, 1H), 7.74-7.69 (m, 1H), 7.56-7.50 (m, 1H), 7.07 (d, *J* = 8.9 Hz, 2H), 5.67 (t, *J* = 7.1 Hz, 1H), 4.33-4.27 (m, 1H), 4.11 (q, *J* = 7.5 Hz, 1H), 3.9 (s, 3H), 2.73-2.63 (m, 1H), 2.18-2.01 (m, 2H), 1.96-1.88 (m, 1H). **^{13}C NMR** (126 MHz, $CDCl_3$) δ 161.1, 157.1, 130.4, 129.4, 129.3, 126.0, 124.5, 123.2, 114.4, 114.1, 69.3, 55.6, 34.2, 26.2. **HRMS** Calcd for

$C_{20}H_{20}NO_2$ [M+H$^+$]: 306.1489, found: 306.1481. The compound was not reported.

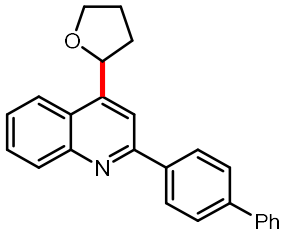

2-([1,1'-biphenyl]-4-yl)-4-(tetrahydrofuran-2-yl)quinoline (12a). Following the general procedure A. Isolated with Hex/DCM/EtOAc (1:1:0.05) on preparative thin-layer chromatography. Colorless gum (17.6 mg, 50%). **^{1}H NMR** (500 MHz, $CDCl_3$) δ 8.29 (d, *J* = 8.5 Hz, 2H), 8.23 (d, *J* = 8.4 Hz, 1H), 8.10 (s, 1H), 7.92 (d, *J* = 8.4 Hz, 1H), 7.77 (d, *J* = 8.5 Hz, 2H), 7.75-7.71 (m, 1H), 7.71-7.67 (m, 2H), 7.57-7.52 (m, 1H), 7.50-7.46 (m, 2H), 7.41-7.36 (m, 1H), 5.68 (t, *J* = 7.1 Hz, 1H), 4.33-4.27 (m, 1H), 4.10 (q, J = 7.5 Hz, 1H), 2.72-2.63 (m, 1H), 2.17-2.00 (m, 2H), 1.97-1.88 (m, 1H). **^{13}C NMR** (126 MHz, $CDCl_3$) δ 157.1, 150.2, 148.6, 142.2, 140.9, 139.0, 130.8, 129.4, 129.0, 128.3, 127.8, 127.7, 127.4, 126.3, 124.8, 123.2, 114.4, 69.3, 34.2, 26.2. **HRMS** Calcd for $C_{25}H_{22}NO$ [M+H$^+$]: 352.1696, found: 352.1690. The compound was not reported.

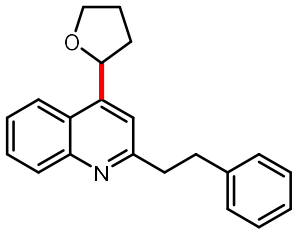

2-phenethyl-4-(tetrahydrofuran-2-yl)quinoline (13a). Following the general procedure A. Isolated with Hex/DCM/EtOAc (1:1:0.2) on preparative thin-layer chromatography. Colorless oil (20.1 mg, 66%). **^{1}H NMR** (500 MHz, $CDCl_3$) δ 8.10 (d, *J* = 8.5 Hz, 1H), 7.86 (d, *J* = 8.4 Hz, 1H), 7.72-7.65 (m, 1H), 7.53-7.47 (m, 1H), 7.37 (s, 1H), 7.31-7.24 (m, 4H), 7.21-7.16

(m, 1H), 5.58 (t, *J* = 7.1 Hz, 1H), 4.19-4.11 (m, 1H), 4.02 (q, *J* = 7.5 Hz, 1H), 3.32-3.26 (m, 2H), 3.22-3.09 (m, 2H), 2.64-2.55 (m, 1H), 2.11-2.00 (m, 1H), 2.00-1.90 (m, 1H), 1.86-1.76 (m, 1H). **^{13}C NMR** (126 MHz, $CDCl_3$) δ 162.1, 149.5, 148.3, 141.8, 129.9, 129.1, 128.8, 128.6, 126.1, 125.8, 124.4, 123.2, 117.0, 77.0, 69.2, 41.4, 36.2, 34.1, 26.1. **HRMS** Calcd for $C_{21}H_{22}NO$ [M+H$^+$]: 304.1696, found: 304.1683. The compound was not reported.

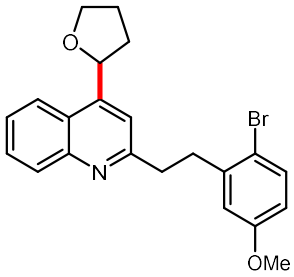

2-(2-bromo-5-methoxyphenethyl)-4-(tetrahydrofuran-2-yl)quinoline (14a). Following the general procedure A. Isolated with Hex/DCM/EtOAc (1:1:0.2) on preparative thin-layer chromatography. Colorless oil (21.4 mg, 52%). **^{1}H NMR** (500 MHz, $CDCl_3$) δ 8.10 (d, *J* = 8.5 Hz, 1H), 7.86 (d, *J* = 8.4 Hz, 1H), 7.70-7.66 (m, 1H), 7.53-7.47 (m, 1H), 7.42 (d, *J* = 8.7 Hz, 1H), 7.39 (s, 1H), 6.79 (d, *J* = 3.0 Hz, 1H), 6.63 (dd, *J* = 8.7, 3.0 Hz, 1H), 5.58 (t, *J* = 7.1 Hz, 1H), 4.19-4.13 (m, 1H), 4.03 (q, *J* = 7.5 Hz, 1H), 3.69 (s, 3H), 3.31-3.17 (m, 4H), 2.63-2.55 (m, 1H), 2.11-1.91 (m, 2H), 1.86-1.78 (m, 1H). **^{13}C NMR** (126 MHz, $CDCl_3$) δ 161.7, 159.1, 149.6, 148.2, 142.0, 133.4, 129.9, 129.1, 125.8, 124.4, 123.3, 117.0, 116.1, 115.1, 114.0, 77.0, 69.2, 55.5, 39.4, 36.6, 34.1, 26.1. **HRMS** Calcd for $C_{22}H_{23}BrNO_2$ [M+H$^+$]: 412.0907, found: 412.0924. The compound was not reported.

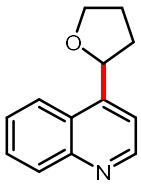

4-(tetrahydrofuran-2-yl)quinoline (15a). Following the general procedure A using 0.1 mL of diacetyl and 0.20 mL of MeCN. Isolated with Hex/EtOAc (5:2) on preparative thin-layer chromatography. Colorless oil (8.0 mg, 40%). **^{1}H NMR** (500 MHz, $CDCl_3$) δ 8.92 (d, *J* = 4.5 Hz, 1H), 8.17 (d, *J* = 8.1 Hz, 1H), 7.95 (d, *J* = 8.5 Hz, 1H), 7.77-7.71 (m, 1H), 7.61-7.56 (m, 2H), 5.65 (t, *J* = 7.1 Hz, 1H), 4.29-4.22 (m, 1H), 4.12-4.04 (m, 1H), 2.70-2.60 (m, 1H), 2.17-1.98 (m, 2H), 1.94-1.85 (m, 1H). **^{13}C NMR** (126 MHz, $CDCl_3$) δ 150.7, 149.7, 148.3, 130.5, 129.2, 126.6, 125.8, 123.4, 116.7, 69.2, 34.2, 26.2. **GC-MS** (EI, m/z) for $C_{13}H_{13}NO$ Calcd: 199.1, found: 199.1. Spectra data are consistent with the reported literature.[61]

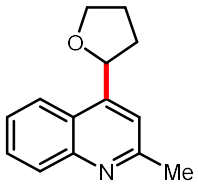

2-methyl-4-(tetrahydrofuran-2-yl)quinoline (16a). Following the general procedure A. Isolated with Hex/DCM/EtOAc (1:1:0.2) on preparative thin-layer chromatography. Colorless oil (11.1 mg, 52%). **^{1}H NMR** (500 MHz, $CDCl_3$) δ 8.04 (d, *J* = 8.4 Hz, 1H), 7.84 (d, *J* = 8.4 Hz, 1H), 7.70-7.63 (m, 1H), 7.52-7.45 (m, 1H), 7.44 (s, 1H), 5.58 (t, *J* = 7.1 Hz, 1H), 4.27-4.20 (m, 1H), 4.04 (q, *J* = 7.5 Hz, 1H), 2.74 (s, 3H), 2.67-2.55 (m, 1H), 2.15-1.95 (m, 2H), 1.90-1.80 (m, 1H). **^{13}C NMR** (126 MHz, $CDCl_3$) δ 159.1, 149.2, 148.0, 129.5, 128.9, 125.5, 123.9, 123, 117.2, 69.0, 33.9, 26.0, 25.6. **GC-MS** (EI, m/z) for $C_{14}H_{15}NO$ Calcd: 213.1, found: 213.1. Spectra data are consistent with the reported literature.[23]

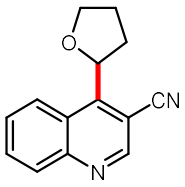

4-(tetrahydrofuran-2-yl)quinoline-3-carbonitrile **(17a).** Following the general procedure A. Isolated with Hex/DCM/EtOAc (1:1:0.25) on preparative thin-layer chromatography. Colorless solid (8.1 mg, 36%). **^{1}H NMR** (500 MHz, $CDCl_3$) δ 9.02 (s, 1H), 8.18 (d, *J* = 8.5 Hz, 1H), 8.12 (d, *J* = 8.3 Hz, 1H), 7.88-7.83 (m, 1H), 7.69-7.64 (m, 1H), 5.81 (t, *J* = 7.6 Hz, 1H), 4.51-4.45 (m, 1H), 4.15-4.07 (m, 1H), 2.68-2.60 (m, 1H), 2.25-2.15 (m, 2H), 2.03-1.56 (m, 1H). **^{13}C NMR** (126 MHz, $CDCl_3$) δ 155.7, 152.0, 148.8, 132.2, 130.9, 128.3, 124.5, 124.0, 117.4, 104.0, 69.8, 35.3, 26.9. **HRMS** Calcd for $C_{14}H_{12}N_2NaO$ [M+Na$^+$]: 247.0842, found: 247.0840. The compound was not reported.

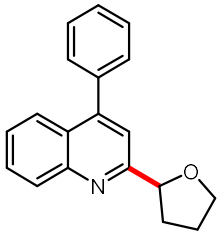

4-phenyl-2-(tetrahydrofuran-2-yl)quinoline (18a). Following the general procedure A. Isolated with Hex/DCM/EtOAc (1:1:0.1) on preparative thin-layer chromatography. Colorless oil (22.9 mg, 83%). **^{1}H NMR** (500 MHz, $CDCl_3$) δ 8.13 (d, *J* = 8.4 Hz, 1H), 7.89 (d, *J* = 8.4 Hz, 1H), 7.73-7.67 (m, 1H), 7.57-7.44 (m, 7H), 5.22 (t, *J* = 7.1 Hz, 1H), 4.19-4.13 (m, 1H), 4.07-4.00 (m, 1H), 2.60-2.51 (m, 1H), 2.18-2.00 (m, 3H). **^{13}C NMR** (126 MHz, $CDCl_3$) δ 163.3, 149.4, 148.2, 138.6, 129.8, 129.5, 128.7, 128.5, 126.3, 126.2, 126.0, 118.4, 82.3, 69.5, 33.7, 26.2. **HRMS** Calcd for $C_{19}H_{18}NO$ [M+H$^+$]: 276.1383, found: 276.1384. The compound was not reported.

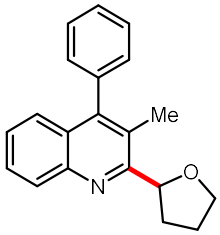

3-methyl-4-phenyl-2-(tetrahydrofuran-2-yl)quinoline (19a). Following the general procedure A. Isolated with Hex/DCM/EtOAc (1:1:0.1) on preparative thin-layer chromatography. Colorless oil (12.2 mg, 42%). **^{1}H NMR** (500 MHz, $CDCl_3$) δ 8.12 (d, *J* = 8.4 Hz, 1H), 7.63-7.57 (m, 1H), 7.55-7.49 (m, 2H), 7.49-7.44 (m, 1H), 7.37-7.28 (m, 2H), 7.26-7.21 (m, 2H), 5.39 (t, *J* = 7.0 Hz, 1H), 4.22 (q, *J* = 7.3 Hz, 1H), 4.05-3.97 (m, 1H), 2.60-2.51 (m, 1H), 2.38-2.30 (m, 1H), 2.28 (s, 3H), 2.27-2.18 (m, 1H), 2.14-2.03 (m, 1H). **^{13}C NMR** (126 MHz, $CDCl_3$) δ 159.8, 147.5, 145.9, 137.9, 129.8, 129.6, 129.6, 128.8, 128.7, 128.2, 127.9, 127.5, 127.0, 126.2, 126.1, 79.9, 69.1, 30.3, 26.3, 16.3. **HRMS** Calcd for $C_{20}H_{20}NO$ [M+H$^+$]: 290.1539, found: 290.1542. The compound was not reported.

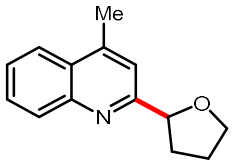

4-methyl-2-(tetrahydrofuran-2-yl)quinoline (20a). Following the general procedure A. Isolated with Hex/DCM/EtOAc (1:1:0.2) on preparative thin-layer chromatography. Colorless oil (13.6 mg, 64%). **^{1}H NMR** (500 MHz, $CDCl_3$) δ 8.05 (d, *J* = 8.4 Hz, 1H), 7.97 (d, *J* = 8.4 Hz, 1H), 7.71-7.65 (m, 1H), 7.55-7.49 (m, 1H), 7.44 (s, 1H), 5.13 (t, *J* = 7.0 Hz, 1H), 4.21-4.14 (m, 1H), 4.07-4.00 (m, 1H), 2.71 (s, 3H), 2.55-2.47 (m, 1H), 2.11-1.99 (m, 3H). **^{13}C NMR** (126 MHz, $CDCl_3$) δ 163.3, 147.6, 145.1, 129.8, 129.3, 127.7, 126.0, 123.9, 118.8, 82.3, 69.5, 33.5, 26.2, 19.1. **GC-MS** (EI, m/z) for $C_{14}H_{15}NO$ Calcd: 213.1, found: 213.1. Spectra data are consistent with the reported literature.[62]

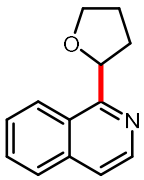

1-(tetrahydrofuran-2-yl)isoquinoline (21a). Following the general procedure A. Isolated with Hex/DCM/EtOAc (1:1:0.2) on preparative thin-layer chromatography. Colorless oil (14.5 mg, 73%). **^{1}H NMR** (500 MHz, $CDCl_3$) δ 8.50 (d, *J* = 5.7 Hz, 1H), 8.34 (d, *J* = 8.5 Hz, 1H), 7.83 (d, *J* = 8.1 Hz, 1H), 7.71-7.65 (m, 1H), 7.64-7.56 (m, 2H), 5.72 (t, *J* = 7.1 Hz, 1H), 4.19 (q, *J* = 7.3 Hz, 1H), 4.08-4.00 (m, 1H), 2.58-2.47 (m, 1H), 2.46-2.36 (m, 1H), 2.23-2.06 (m, 2H). **^{13}C NMR** (126 MHz, $CDCl_3$) δ 159.8, 141.8, 136.7, 130.0, 127.5, 127.3, 126.8, 125.5, 120.7, 79.3, 69.2, 31.0, 26.4. **GC-MS** (EI, m/z) for $C_{13}H_{13}NO$ Calcd: 199.1, found: 199.1. Spectra data are consistent with the reported literature.[62]

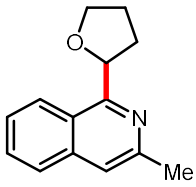

3-methyl-1-(tetrahydrofuran-2-yl)isoquinoline (22a). Following the general procedure A. Isolated with Hex/DCM/EtOAc (1:1:0.2) on preparative thin-layer chromatography. Colorless oil (7.5 mg, 35%). **^{1}H NMR** (500 MHz, $CDCl_3$) δ 8.31 (d, *J* = 8.5 Hz, 1H), 7.72 (d, *J* = 8.3 Hz, 1H), 7.63-7.58 (m, 1H), 7.53-7.48 (m, 1H), 7.40 (s, 1H), 5.65 (t, *J* = 7.2 Hz, 1H), 4.23-4.17 (m, 1H), 4.05-3.99 (m, 1H), 2.68 (s, 3H), 2.59-2.51 (m, 1H), 2.41-2.32 (m, 1H), 2.23-2.05 (m, 2H). **^{13}C NMR** (126 MHz, $CDCl_3$) δ 159.1, 150.4, 137.6, 129.8, 126.9, 126.2, 125.5, 124.9, 118.6, 80.0, 69.1, 30.9, 26.3, 24.6. **GC-MS** (EI, m/z) for $C_{14}H_{15}NO$ Calcd: 213.1, found: 213.0. Spectra data are consistent with the reported literature.[26]

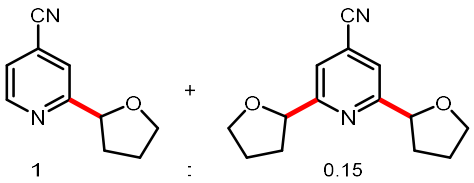

2-(tetrahydrofuran-2-yl)isonicotinonitrile (23a) and 2,6-bis(tetrahydrofuran-2-ylisonicotinonitrile (23a'). Following the general procedure A using 20 equiv of TFA. Isolated with preparative thin-layer chromatography with Hex/DCM/EtOAc (1:1:0.2) on preparative thin-layer chromatography. Colorless oil (8.3 mg, 44%, mono:di = 1:0.15). **^{1}H NMR** (500 MHz, $CDCl_3$) δ 8.71 (d, *J* = 4.9 Hz, 1H), 7.72 (s, 1H), 7.56 (s, 0.3 H), 7.39 (dd, *J* = 4.9, 1.3 Hz, 1H), 5.08-4.99 (m, 1H+0.3 H), 4.15-4.06 (m, 1H+0.3H), 4.03-3.95 (m, 1H+0.3H), 2.51-2.41 (m, 1H+0.3H), 2.05-1.89 (m, 3H+0.9H). **^{13}C NMR** (126 MHz, $CDCl_3$) δ 165.5, 164.7, 150.1, 123.6, 121.8, 121.4, 121.1, 119.9, 117.4, 117.0, 80.9, 80.9, 69.5, 69.5, 33.3, 33.2, 25.9, 25.8. **GC-MS** (EI, m/z) for $C_{10}H_{10}N_2O$ Calcd: 174.1, found: 174.1; for $C_{14}H_{16}N_2O_2$ Calcd: 244.1, found: 244.2. Spectra data are consistent with the reported literature.[26]

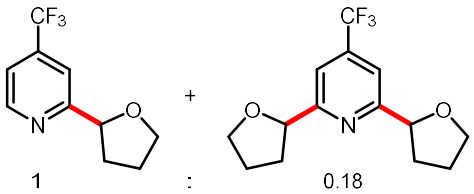

2-(tetrahydrofuran-2-yl)-4-(trifluoromethyl)pyridine (24a) and 2,6-bis(tetrahydrofuran-2-yl)-4-(trifluoromethyl)pyridine (24a'). Following the general procedure A using 20 equiv of TFA. Isolated with preparative thin-layer chromatography with Hex/EtOAc (5:1). Colorless oil (9.1 mg, 40%, mono:di = 1:0.18). **^{1}H NMR** (500 MHz, $CDCl_3$) δ 8.72 (s, 1H), 7.71 (s, 1H), 7.54 (s, 0.36H), 7.39 (d, *J* = 4.6 Hz, 1H), 5.12-5.03 (m, 1H+0.36H), 4.17-4.09 (m, 1H+0.36H), 4.04-3.96 (m, 1H+0.36H), 2.53-2.41 (m, 1H+0.36H), 2.06-1.90 (m, 3H+1.08H). **^{13}C NMR** (126 MHz, $CDCl_3$) δ 165.2, 164.6, 150.1, 138.9 (q, *J* = 34 Hz), 123 (q, *J* =

273 Hz), 117.9, 115.8, 114.0, 114.0, 81.3, 81.1, 69.5, 33.5, 33.3, 26.0, 25.9. **HRMS** Calcd for $C_{10}H_{10}F_3NONa$ [M+Na$^+$]: 240.0607, found: 240.0597. **HRMS** Calcd for $C_{14}H_{16}F_3NONa$ [M+Na$^+$]: 310.1025, found: 310.1015. The compound was not reported.

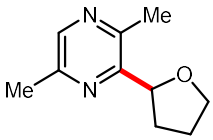

2,5-dimethyl-3-(tetrahydrofuran-2-yl)pyrazine (25a). Following the general procedure A. Isolated with Hex/EtOAc (5:2) on preparative thin-layer chromatography. Colorless oil (5.7 mg, 32%). **^{1}H NMR** (500 MHz, $CDCl_3$) δ 8.22 (s, 1H), 5.11 (t, *J* = 7.1 Hz, 1H), 4.15-4.08 (m, 1H), 3.97-3.91 (m, 1H), 2.59 (s, 3H), 2.51 (s, 3H), 2.27-2.21 (m, 2H), 2.19-2.10 (m, 1H), 2.10-1.98 (m, 1H). **^{13}C NMR** (126 MHz, $CDCl_3$) δ 153.1, 150.4, 148.9, 142.2, 78.6, 69.2, 30.5, 26.4, 21.4, 21.2. **HRMS** Calcd for $C_{10}H_{14}N_2NaO$ [M+Na$^+$]: 201.0998, found: 201.0990. The compound was not reported.

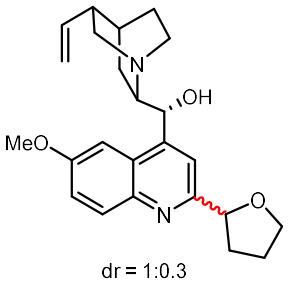

(1*R*)-(6-methoxy-2-(tetrahydrofuran-2-yl)quinolin-4-yl)((2*S*,4*S*,5*R*)-5-vinylquinuclidin-2-yl)methanol (26a). Following the general procedure A. Isolated with Hex/DCM/EtOAc/MeOH (1:1:0.25:0.25) on preparative thin-layer chromatography. Colorless solid (13.4 mg, 34%, dr = 1:0.3). **^{1}H NMR** (500 MHz, $CDCl_3$) δ 7.88 (d, *J* = 9.2 Hz, 1H+0.3H), 7.76 (s, 0.3H), 7.74 (s, 1H), 7.25-7.20 (m, 1H+0.3H), 7.13 (d, *J* = 2.5 Hz, 0.3H), 7.05 (d, *J* = 2.6 Hz, 1H), 6.02 (s, 1H), 5.99 (s, 0.3H), 5.66-5.53 (m, 1H+0.3H), 5.10-5.04 (m, 1H+0.3H),

5.02-4.94 (m, 2H+0.6H), 4.20-4.13 (m, 1H+0.3H), 4.04-3.94 (m, 2H+0.6H), 3.87 (s, 0.9H), 3.82 (s, 3H), 3.39-3.30 (m, 1H+0.3H), 3.29-3.20 (m, 1H+0.3H), 2.97-2.87 (m, 2H+0.6H), 2.55-2.40 (m, 2H+0.6H), 2.07-1.93 (m, 6H+1.8H), 1.72-1.63 (m, 1H+0.3H), 1.40-1.32 (m, 1H+0.3H), 1.29-1.20 (m, 1H+0.3H). **^{13}C NMR** (126 MHz, $CDCl_3$) δ 163.4, 163.1, 160.3, 160.1, 158.3, 158.1, 146.0, 143.7, 139.0, 131.5, 131.5, 125.1, 122.2, 122.1, 116.5, 115.8, 115.6, 100.3, 82.5, 82.3, 69.4, 69.3, 60.2, 60.1, 56.1, 56.0, 55.6, 43.8, 43.7, 38.3, 33.6, 33.3, 29.9, 27.6, 27.4, 26.2, 26.2, 25.6, 19.4. **HRMS** Calcd for $C_{24}H_{31}N_2O_3$ [M+H$^+$]: 395.2329, found: 395.2324. The compound was not reported.

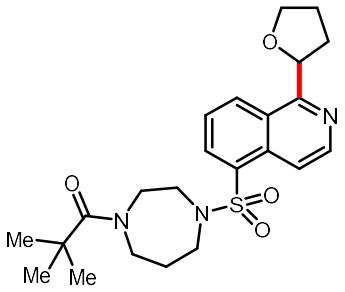

2,2-dimethyl-1-(4-((1-(tetrahydrofuran-2-yl)isoquinolin-5-yl)sulfonyl)azepan-1-yl)propan-1-one (27a). Following the general procedure A. Isolated with Hex/ EtOAc (1:2) on preparative thin-layer chromatography. Pale yellow oil (31.1 mg, 70%). **^{1}H NMR** (500 MHz, $CDCl_3$) δ 8.66 (d, *J* = 8.5 Hz, 1H), 8.62 (d, *J* = 6.1 Hz, 1H), 8.34 (d, *J* = 6.1 Hz, 1H), 8.32 (d, *J* = 7.2 Hz, 1H), 7.69-7.63 (m, 1H), 5.69 (t, *J* = 7.0 Hz, 1H), 4.15-4.07 (m, 1H), 4.05-3.99 (m, 1H), 3.74-3.68 (m, 2H), 3.66 (t, *J* = 6.3 Hz, 2H), 3.45 (t, *J* = 5.2 Hz, 2H), 3.43-3.36 (m, 2H), 2.67-2.58 (m, 1H), 2.42-2.32 (m, 1H), 2.22-2.07 (m, 2H), 2.00-1.93 (m, 2H), 1.22 (s, 9H). **^{13}C NMR** (126 MHz, $CDCl_3$) δ 177.5, 160.6, 143.6, 134.9, 133.0, 132.6, 131.6, 127.7, 125.7, 117.3, 79.5, 69.3, 50.4, 47.6, 39.2, 30.4, 28.7, 26.3. **HRMS** Calcd for $C_{23}H_{32}N_3O_4S$ [M+H$^+$]: 446.2108, found: 446.2094. The compound was not reported.

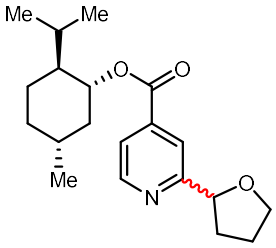

(1*R*,2*S*,5*R*)-2-isopropyl-5-methylcyclohexyl-2-(tetrahydrofuran-2-yl)isonicotinate (28a). Following the general procedure A using 20 equiv of TFA. Isolated with Hex/ EtOAc (5:1) on preparative thin-layer chromatography. Colorless oil (18.9 mg, 57%). **^{1}H NMR** (500 MHz, $CDCl_3$) δ 9.13 (s, 1H), 8.28-8.24 (m, 1H), 7.53 (dd, *J* = 8.2, 0.6 Hz, 1H), 5.07 (t, *J* = 6.4 Hz, 1H), 4.94 (td, *J* = 10.8, 4.4 Hz, 1H), 4.14-4.07 (m, 1H), 4.02-3.97 (m, 1H), 2.50-2.41 (m, 1H), 2.16-2.08 (m, 1H), 2.04-1.88 (m, 4H), 1.78-1.50 (m, 5H), 1.17-1.06 (m, 2H), 0.95-0.89 (m, 6H), 0.79 (d, *J* = 7.0 Hz, 3H). **^{13}C NMR** (126 MHz, $CDCl_3$) δ 167.7, 167.7, 165.1, 150.6, 150.5, 137.9, 137.9, 125.2, 119.4, 119.4, 81.4, 75.5, 69.4, 47.4, 41.1, 34.4, 33.3, 31.7, 26.8, 26.8, 25.9, 25.9, 23.9, 23.8, 22.2, 20.9, 16.8, 16.7. **HRMS** Calcd for $C_{20}H_{29}NNaO_3$ [M+Na$^+$]: 354.2040, found: 354.2044. The compound was not reported.

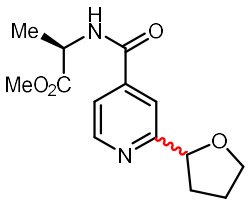

(*R*)-methyl-2-(2-(tetrahydrofuran-2-yl)isonicotinamido)propanoate (29a). Following the general procedure A using 20 equiv of TFA. Isolated with Hex/EtOAc (1:2) on preparative thin-layer chromatography. Colorless oil (7.5 mg, 27%). **^{1}H NMR** (500 MHz, $CDCl_3$) δ 8.67 (d, *J* = 5.0 Hz, 1H), 7.75 (s, 1H), 7.57-7.52 (m, 1H), 6.82 (s, 1H), 5.09-5.04 (m, 1H), 4.84-4.75 (m, 1H), 4.18-4.10 (m, 1H), 4.03-3.97 (m, 1H), 3.81 (d, *J* = 1.7 Hz, 3H), 2.51-2.42 (m, 1H), 2.07-1.92 (m, 3H), 1.54 (dd, *J* = 7.2, 1.5 Hz, 3H). **^{13}C NMR** (126 MHz, $CDCl_3$) δ 173.5, 173.5, 165.4,

165.3, 164.6, 150.2, 150.2, 142.0, 141.9, 119.9, 119.8, 116.9, 116.8, 81.3, 81.3, 69.4, 69.4, 52.9, 48.9, 48.8, 33.4, 33.3, 26.0, 18.7, 18.7. **HRMS** Calcd for $C_{14}H_{18}N_2NaO_4$ [M+Na$^+$]: 301.1159, found: 301.1159. The compound was not reported.

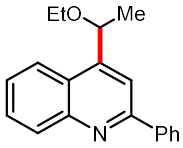

4-(1-ethoxyethyl)-2-phenylquinoline (30a). Following the general procedure A using 0.30 mL of ether. Isolated with Hex/DCM/EtOAc (1:1:0.05) on preparative thin-layer chromatography. Colorless oil (25.8 mg, 93%). **^{1}H NMR** (500 MHz, $CDCl_3$) δ 8.25-8.17 (m, 3H), 8.11 (d, *J* = 9.1 Hz, 1H), 8.00 (s, 1H), 7.74-7.69 (m, 1H), 7.57-7.51 (m, 3H), 7.50-7.44 (m, 1H), 5.20 (q, *J* = 6.5 Hz, 1H), 3.55-3.48 (m, 2H), 1.65 (d, *J* = 6.6 Hz, 3H), 1.28 (t, *J* = 7.0 Hz, 3H). **^{13}C NMR** (126 MHz, $CDCl_3$) δ 157.6, 150.6, 148.9, 140.0, 130.9, 129.5, 129.4, 129.0, 127.8, 126.3, 125.3, 123.1, 115.6, 74.8, 65.0, 23.7, 15.7. **GC-MS** (EI, m/z) for $C_{19}H_{19}NO$ Calcd: 277.1, found: 277.2. Spectra data are consistent with the reported literature.[62]

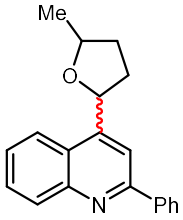

4-(5-methyltetrahydrofuran-2-yl)-2-phenylquinoline (31a). Following the general procedure A. Isolated with Hex/DCM/EtOAc (1:1:0.05) on preparative thin-layer chromatography. Colorless oil (17.1 mg, 59%, dr = 1:0.9). **^{1}H NMR** (500 MHz, $CDCl_3$) δ 8.23-8.16 (m, 3H+2.7H), 8.14 (s, 0.9H), 8.05 (s, 1H), 7.92-7.87 (m, 1H+0.9H), 7.74-7.68 (m, 1H+0.9H), 7.56-7.50 (m, 3H+2.7H), 7.49-7.43 (m, 1+0.9H), 5.81 (t, *J* = 7.3 Hz, 1H), 5.66 (t, *J* = 7.1 Hz, 0.9H), 4.57-4.49 (m, 1H), 4.36-4.29 (m, 0.9H), 2.80-2.72 (m, 1H), 2.70-2.62 (m, 0.9H),

2.22-2.12 (m, 1H+0.9H), 1.99-1.88 (m, 1H+0.9H), 1.81-1.71 (m, 1H), 1.66-1.57 (m, 0.9H), 1.52 (d, *J* = 6.1 Hz, 2.7H), 1.44 (d, *J* = 6.1 Hz, 3H). **^{13}C NMR** (126 MHz, $CDCl_3$) δ 157.7, 157.6, 150.6, 150.3, 148.7, 148.6, 140.3, 130.8, 130.8, 129.4, 129.3, 129.3, 129.2, 129.0, 129.0, 127.9, 127.8, 127.7, 126.2, 126.2, 124.7, 123.3, 123.2, 114.9, 114.3, 76.7, 76.5, 34.9, 34.4, 34.1, 33.2, 21.6, 21.2. **HRMS** Calcd for $C_{20}H_{20}NO$ [M+H$^+$]: 290.1539, found: 290.1536. The compound was not reported.

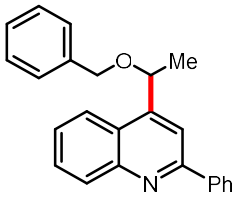

4-(1-(benzyloxy)ethyl)-2-phenylquinoline (32a). Following the general procedure A. Isolated with Hex/EtOAc (20:1) on preparative thin-layer chromatography. Colorless solid (10.9 mg, 32%). **^{1}H NMR** (500 MHz, $CDCl_3$) δ 8.26 (d, *J* = 8.4 Hz, 1H), 8.21 (d, *J* = 7.2 Hz, 2H), 8.11 (d, *J* = 8.4 Hz, 1H), 8.09 (s, 1H), 7.79-7.73 (m, 1H), 7.59-7.53 (m, 3H), 7.52-7.47 (m, 1H), 7.42-7.31 (m, 5H), 5.32 (q, *J* = 6.6 Hz, 1H), 4.64 (d, *J* = 11.9 Hz, 1H), 4.47 (d, *J* = 11.9 Hz, 1H), 1.71 (d, *J* = 6.6 Hz, 3H). **^{13}C NMR** (126 MHz, $CDCl_3$) δ 157.6, 150.1, 148.9, 138.9, 138.3, 130.9, 129.6, 129.5, 129.0, 128.7, 128.0, 127.8, 126.4, 125.2, 123.1, 115.9, 74.4, 71.3, 23.7. **HRMS** Calcd for $C_{24}H_{22}NO$ [M+H$^+$]: 340.1696, found: 340.1683. The compound was not reported.

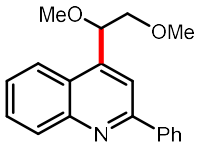

4-(1,2-dimethoxyethyl)-2-phenylquinoline (33a). Following the general procedure B. Isolated with Hex/DCM/EtOAc (1:1:0.05) on preparative thin-layer chromatography. Colorless oil (17.6 mg, 60%). **^{1}H NMR** (500 MHz, $CDCl_3$) δ 8.28-8.20 (m, 3H), 8.13 (d, *J* = 7.8

Hz, 1H), 8.04 (s, 1H), 7.79-7.74 (m, 1H), 7.62-7.54 (m, 3H), 7.53-7.48 (m, 1H), 5.25 (dd, *J* = 7.8, 3.0 Hz, 1H), 3.79-3.74 (m, 1H), 3.72-3.67 (m, 1H), 3.47 (s, 3H), 3.47 (s, 3H). **^{13}C NMR** (126 MHz, $CDCl_3$) δ 157.4, 148.8, 145.0, 139.7, 131.0, 129.7, 129.6, 129.1, 127.8, 126.7, 125.6, 122.8, 116.9, 80.3, 76.7, 59.6, 58.0. **HRMS** Calcd for $C_{19}H_{20}NO_2$ [M+H$^+$]: 294.1489, found: 294.1483. The compound was not reported.

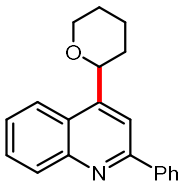

2-phenyl-4-(tetrahydro-2*H*-pyran-2-yl)quinoline (34a). Following the general procedure B. Isolated with Hex/DCM/EtOAc (1:1:0.05) on preparative thin-layer chromatography. Colorless oil (23.1 mg, 80%). **^{1}H NMR** (500 MHz, $CDCl_3$) δ 8.23-8.18 (m, 3H), 8.06 (s, 1H), 7.98 (d, *J* = 7.9 Hz, 1H), 7.73-7.67 (m, 1H), 7.55-7.49 (m, 3H), 7.48-7.43 (m, 1H), 5.09 (dd, *J* = 11.2, 1.8 Hz, 1H), 4.33-4.27 (m, 1H), 3.83-3.75 (m, 1H), 2.15-2.07 (m, 1H), 2.06-1.97 (m, 1H), 1.89-1.77 (m, 2H), 1.73-1.61 (m, 2H). **^{13}C NMR** (126 MHz, $CDCl_3$) δ 157.6, 149.4, 148.6, 140.1, 130.8, 129.4, 129.3, 128.9, 127.9, 126.2, 124.5, 123, 115.6, 76.6, 69.5, 34.0, 26.2, 24.3. **GC-MS** (EI, m/z) for $C_{20}H_{19}NO$ Calcd: 289.1, found: 289.2. Spectra data are consistent with the reported literature.[63]

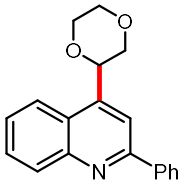

4-(1,4-dioxan-2-yl)-2-phenylquinoline (35a). Following the general procedure B. Isolated with Hex/DCM/EtOAc (1:1:0.05) on preparative thin-layer chromatography. Colorless solid

(21.5 mg, 74%). **^{1}H NMR** (500 MHz, $CDCl_3$) δ 8.24-8.17 (m, 3H), 8.10 (s, 1H), 8.01 (d, *J* = 8.3 Hz, 1H), 7.74-7.70 (m, 1H), 7.58-7.50 (m, 3H), 7.49-7.44 (m, 1H), 5.43 (dd, *J* = 9.9, 2.4 Hz, 1H), 4.18 (dd, *J* = 11.9, 2.6 Hz, 1H), 4.14-4.05 (m, 2H), 3.95-3.88 (m, 1H), 3.88-3.80 (m, 1H), 3.55-3.47 (m, 1H). **^{13}C NMR** (126 MHz, $CDCl_3$) δ 157.6, 148.5, 144.3, 139.8, 131.0, 129.6, 129.6, 129.0, 127.8, 126.7, 124.4, 122.5, 116.4, 74.6, 72.3, 67.6, 66.9. **GC-MS** (EI, m/z) for $C_{19}H_{17}NO_2$ Calcd: 291.1, found: 291.1. Spectra data are consistent with the reported literature.[62]

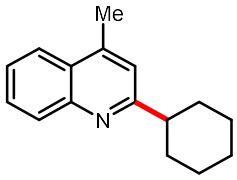

2-cyclohexyl-4-methylquinoline (37a). Following the general procedure C. Isolated with Hex/EtOAc (20:1) on preparative thin-layer chromatography. Colorless oil (18.9 mg, 84%). **^{1}H NMR** (500 MHz, $CDCl_3$) δ 8.05 (d, *J* = 8.4 Hz, 1H), 7.94 (d, *J* = 8.3 Hz, 1H), 7.69-7.63 (m, 1H), 7.52-7.46 (m, 1H), 7.17 (s, 1H), 2.92-2.83 (m, 1H), 2.68 (s, 3H), 2.05-1.98 (m, 2H), 1.93-1.85 (m, 2H), 1.83-1.75 (m, 1H), 1.68-1.56 (m, 2H), 1.53-1.41 (m, 2H), 1.39-1.27 (m, 1H). **^{13}C NMR** (126 MHz, $CDCl_3$) δ 166.7, 147.8, 144.4, 129.7, 129.1, 127.2, 125.6, 123.8, 120.4, 47.8, 33.0, 26.8, 26.3, 19.0. **GC-MS** (EI, m/z) for $C_{16}H_{19}N$ Calcd: 225.2, found: 225.1. Spectra data are consistent with the reported literature.[60]

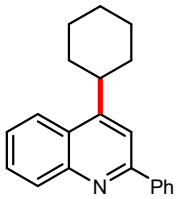

4-cyclohexyl-2-phenylquinoline (38a). Following the general procedure C. Isolated with Hex/EtOAc (20:1) on preparative thin-layer chromatography. Colorless solid (24.7 mg, 86%). **^{1}H NMR** (500 MHz, $CDCl_3$) δ 8.20 (d, *J* = 8.4 Hz, 1H), 8.18-8.13 (m, 2H), 8.10 (d, *J* = 8.4 Hz, 1H),

7.76 (m, 1H), 7.73-7.68 (m, 1H), 7.56-7.51 (m, 3H), 7.49-7.44 (m, 1H), 3.43-3.33 (m, 1H), 2.12-2.06 (m, 2H), 2.01-1.93 (m, 2H), 1.92-1.85 (m, 1H), 1.69-1.53 (m, 4H), 1.44-1.33 (m, 1H). **^{13}C NMR** (126 MHz, $CDCl_3$) δ 157.5, 154.2, 148.8, 140.5, 130.9, 129.3, 129.2, 129.0, 127.8, 126.1, 123, 115.7, 39.3, 33.9, 27.2, 26.5. **GC-MS** (EI, m/z) for $C_{21}H_{21}N$ Calcd: 287.2, found: 287.2. Spectra data are consistent with the reported literature.[60]

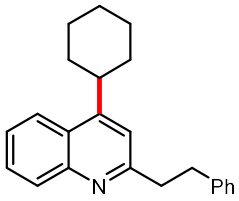

4-cyclohexyl-2-phenethylquinoline (39a). Following the general procedure C. Isolated with Hex/EtOAc (5:1) on preparative thin-layer chromatography. Colorless oil (19.0 mg, 60%). **^{1}H NMR** (500 MHz, $CDCl_3$) δ 8.09 (d, *J* = 8.4 Hz, 1H), 8.05 (d, *J* = 8.4 Hz, 1H), 7.70-7.65 (m, 1H), 7.53-7.48 (m, 1H), 7.32-7.23 (m, 4H), 7.23-7.18 (m, 1H), 7.05 (s, 1H), 3.32-3.23 (m, 3H), 3.19-3.13 (m, 2H), 2.00-1.89 (m, 4H), 1.89-1.82 (m, 1H), 1.60-1.41 (4H), 1.38-1.28 (m, 1H). **^{13}C NMR** (126 MHz, $CDCl_3$) δ 161.8, 153.5, 148.5, 141.9, 130.0, 128.9, 128.8, 128.6, 126.1, 125.7, 125.6, 123.1, 118.2, 41.4, 39.0, 36.3, 33.7, 27.1, 26.5. **HRMS** Calcd for $C_{23}H_{26}N$ [$M+H^+$]: 316.2060, found: 316.2069. The compound was not reported.

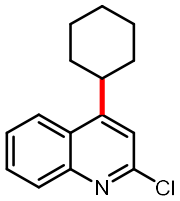

2-chloro-4-cyclohexylquinoline (40a). Following the general procedure C. Isolated with Hex/EtOAc (20:1) on preparative thin-layer chromatography. Colorless oil (12.0 mg, 49%). **^{1}H NMR** (500 MHz, $CDCl_3$) δ 8.06-8.00 (m, 1H), 7.72-7.66 (m, 1H), 7.58-7.53 (m, 1H), 7.26 (s,

1H), 3.33-3.25 (m, 1H), 2.04-1.90 (m, 4H), 1.89-1.82 (m, 1H), 1.59-1.46 (m, 4H), 1.39-1.28 (m, 1H). **^{13}C NMR** (126 MHz, $CDCl_3$) δ 157.1, 151.3, 148.4, 130.1, 129.7, 126.7, 125.8, 123.3, 118.9, 39.3, 33.6, 27.0, 26.3. **GC-MS** (EI, m/z) for $C_{15}H_{16}ClN$ Calcd: 245.1, found: 245.1. Spectra data are consistent with the reported literature.[60]

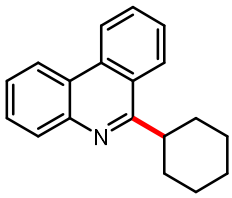

6-cyclohexylphenanthridine (41a). Following the general procedure C. Isolated with Hex/EtOAc (10:1) on preparative thin-layer chromatography. Colorless oil (13.3 mg, 51%). **^{1}H NMR** (500 MHz, $CDCl_3$) δ 8.68 (d, *J* = 8.2 Hz, 1H), 8.56 (d, *J* = 7.5 Hz, 1H), 8.34 (d, *J* = 8.3 Hz, 1H), 8.16 (d, *J* = 8.1 Hz, 1H), 7.87-7.81 (m, 1H), 7.76-7.68 (m, 2H), 7.66-7.60 (m, 1H), 3.69-3.59 (m, 1H), 2.15-2.07 (m, 2H), 2.04-1.91 (m, 4H), 1.92-1.83 (m, 1H), 1.67-1.54 (m, 2H), 1.52-1.41 (m, 1H). **^{13}C NMR** (126 MHz, $CDCl_3$) δ 165.5, 144.1, 133.2, 130.1, 130.1, 128.6, 127.3, 126.3, 125.8, 124.9, 123.5, 122.8, 122.0, 42.2, 32.5, 27.1, 26.5. **GC-MS** (EI, m/z) for $C_{19}H_{19}N$ Calcd: 261.2, found: 261.1. Spectra data are consistent with the reported literature.[13]

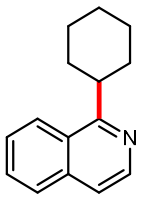

1-cyclohexylisoquinoline (42a). Following the general procedure C. Isolated with Hex/DCM/EtOAc (1:1:0.05) on preparative thin-layer chromatography. Colorless oil (10.6 mg, 50%). **^{1}H NMR** (500 MHz, $CDCl_3$) δ 8.48 (d, *J* = 5.7 Hz, 1H), 8.23 (d, *J* = 8.5 Hz, 1H), 7.81 (d, *J* = 8.1 Hz, 1H), 7.68-7.63 (m, 1H), 7.61-7.55 (m, 1H), 7.48 (d, *J* = 5.7 Hz, 1H), 3.60-3.52 (m, 1H),

2.02-1.90 (m, 4H), 1.89-1.77 (m, 3H), 1.59-1.48 (m, 2H), 1.45-1.34 (m, 1H). **^{13}C NMR** (126 MHz, $CDCl_3$) δ 165.9, 142.1, 136.6, 129.8, 127.8, 127.0, 126.5, 125.0, 119.1, 41.7, 32.8, 27.1, 26.5. **GC-MS** (EI, m/z) for $C_{15}H_{17}N$ Calcd: 211.1, found: 211.2. Spectra data are consistent with the reported literature.[60]

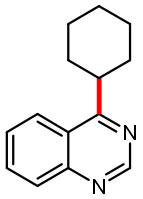

4-cyclohexylquinazoline (43a). Following the general procedure C. Isolated with Hex/DCM/EtOAc (1:1:0.2) on preparative thin-layer chromatography. Colorless oil (9.1 mg, 43%). **^{1}H NMR** (500 MHz, $CDCl_3$) δ 9.25 (s, 1H), 8.19 (d, *J* = 8.2 Hz, 1H), 8.04 (d, *J* = 8.4 Hz, 1H), 7.90-7.81 (m, 1H), 7.67-7.60 (m, 1H), 3.61-3.52 (m, 1H), 2.01-1.90 (m, 4H), 1.88-1.76 (m, 3H), 1.60-1.46 (m, 2H), 1.44-1.33 (m, 1H). **^{13}C NMR** (126 MHz, $CDCl_3$) δ 175.3, 155.0, 150.3, 133.5, 129.6, 127.5, 124.4, 123.5, 41.5, 32.2, 26.7, 26.2. **GC-MS** (EI, m/z) for $C_{14}H_{16}N_2$ Calcd: 212.1, found: 212.2. Spectra data are consistent with the reported literature.[13]

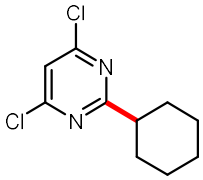

4,6-dichloro-2-cyclohexylpyrimidine (44a). Following the general procedure C. Isolated with Hex/EtOAc (10:1) on preparative thin-layer chromatography. Colorless oil (9.2 mg, 40%). **^{1}H NMR** (500 MHz, $CDCl_3$) δ 7.22 (s, 1H), 2.89-2.79 (m, 1H), 2.20-1.94 (m, 2H), 1.89-1.81 (m, 2H), 1.77-1.69 (m, 1H), 1.66-1.56 (m, 2H), 1.45-1.22 (m, 3H). **^{13}C NMR** (126 MHz, $CDCl_3$) δ 176.7, 161.9, 118.6, 47.4, 31.7, 26.1, 25.9. **HRMS** Calcd for $C_{10}H_{13}N_2Cl_2$ [M+H$^+$]:

231.0450, found: 231.0456. The compound was not reported.

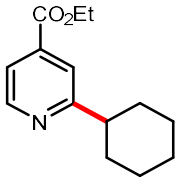

ethyl 2-cyclohexylisonicotinate (45a). Following the general procedure C. Isolated with Hex/EtOAc (5:1) on preparative thin-layer chromatography. Colorless oil (11.7 mg, 50%). **^{1}H NMR** (500 MHz, $CDCl_3$) δ 8.69 (d, *J* = 5.0 Hz, 1H), 7.74 (s, 1H), 7.67 (d, *J* = 5.0 Hz, 1H), 4.43 (q, *J* = 7.1 Hz, 2H), 2.85-2.77 (m, 1H), 2.02-1.95 (m, 2H), 1.94-1.86 (m, 2H), 1.83-1.75 (m, 1H), 1.64-1.53 (m, 2H), 1.51-1.39 (m, 5H), 1.37-1.26 (m, 1H). **^{13}C NMR** (126 MHz, $CDCl_3$) δ 167.9, 165.8, 150.0, 138.3, 120.6, 120.4, 61.9, 46.8, 33.0, 26.7, 26.2, 14.4. **HRMS** Calcd for $C_{14}H_{20}O_2N$ [M+H$^+$]: 234.1489, found: 234.1496. The compound was not reported.

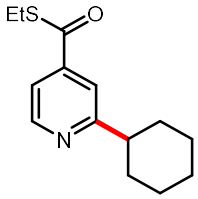

ethyl 2-cyclohexylpyridine-4-carbothioate (46a). Following the general procedure C. Isolated with Hex/EtOAc (10:1) on preparative thin-layer chromatography. Colorless oil (10 mg, 40%). **^{1}H NMR** (500 MHz, $CDCl_3$) δ 8.67 (d, *J* = 5.1 Hz, 1H), 7.59 (s, 1H), 7.54 (d, *J* = 5.1 Hz, 1H), 3.10 (q, *J* = 7.4 Hz, 2H), 2.82-2.74 (m, 1H), 2.00-1.93 (m, 2H), 1.91-1.83 (m, 2H), 179-1.72 (m, 1H), 1.60-1.49 (m, 2H), 1.48-1.23 (m, 6H). **^{13}C NMR** (126 MHz, $CDCl_3$) δ 192.1, 168.2, 150.2, 144.1, 118.0, 117.9, 46.8, 33.0, 26.7, 26.2, 23.9, 14.8. **HRMS** Calcd for $C_{14}H_{20}ONS$ [M+H$^+$]: 250.1260, found: 250.1267. The compound was not reported.

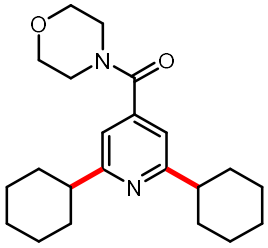

(2,6-dicyclohexylpyridin-4-yl)(morpholino)methanone (47a). Following the general procedure C using 8 equiv of DTBP, 0.20 mL of diacetyl, and 0.4 mL of MeCN. Isolated with Hex/DCM/EtOAc (1:1:0.2) on preparative thin-layer chromatography. Colorless solid (18.6 mg, 52%). **^{1}H NMR** (500 MHz, $CDCl_3$) δ 6.92 (s, 2H), 3.78 (s, 4H), 3.62 (s, 2H), 3.37 (s, 2H), 2.74-2.65 (m, 2H), 1.99-1.91 (m, 4H), 1.88-1.80 (m, 4H), 1.78-1.69 (m, 2H), 1.53-1.33 (m, 8H), 1.32-1.20 (m, 2H). **^{13}C NMR** (126 MHz, $CDCl_3$) δ 169.3, 166.7, 143.2, 115.4, 67.0, 48.1, 46.8, 42.5, 33.1, 26.7, 26.2. **HRMS** Calcd for $C_{22}H_{33}O_2N_2$ [M+H$^+$]: 357.2537, found: 357.2542. The compound was not reported.

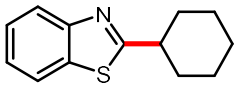

2-cyclohexylbenzo[*d*]thiazole (48a). Following the general procedure C. Isolated with Hex/EtOAc (20:1) on preparative thin-layer chromatography. Colorless oil (9.5 mg, 44%). **^{1}H NMR** (500 MHz, $CDCl_3$) δ 7.97 (d, *J* = 8.1 Hz, 1H), 7.84 (d, *J* = 8.1 Hz, 1H), 7.46-7.42 (m, 1H), 7.35-7.31 (m, 1H), 3.15-3.07 (m, 1H), 2.25-2.16 (m, 2H), 1.92-1.85 (m, 2H), 1.81-1.74 (m, 1H), 1.70-1.59 (m, 2H), 1.51-1.39 (m, 2H), 1.38-1.27 (m, 1H). **^{13}C NMR** (126 MHz, $CDCl_3$) δ 177.8, 153.3, 134.8, 126.0, 124.7, 122.8, 121.8, 43.7, 33.6, 26.3, 26.0. **GC-MS** (EI, m/z) for $C_{13}H_{15}NS$ Calcd: 217.1, found: 217.1. Spectra data are consistent with the reported literature.[60]

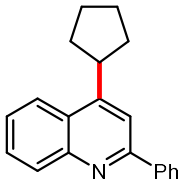

4-cyclopentyl-2-phenylquinoline (49a). Following the general procedure C. Isolated with Hex/EtOAc (20:1) on preparative thin-layer chromatography. Colorless oil (24.4 mg, 89%). **^{1}H NMR** (500 MHz, $CDCl_3$) δ 8.20 (d, *J* = 8.2 Hz, 1H), 8.16-8.10 (m, 3H), 7.78 (s, 1H), 7.74-7.68 (m, 1H), 7.56-7.51 (m, 3H), 7.49-7.44 (m, 1H), 3.88-3.79 (m, 1H), 2.32-2.21 (m, 2H), 1.98-1.79 (m, 6H). **^{13}C NMR** (126 MHz, $CDCl_3$) δ 157.5, 153.0, 148.7, 140.5, 130.7, 129.3, 129.2, 129.0, 127.8, 127.0, 126.0, 123.8, 115.4, 41.0, 33.6, 25.7. **HRMS** Calcd for $C_{20}H_{20}N$ [M+H$^+$]: 274.1590, found: 274.1596. The compound was not reported.

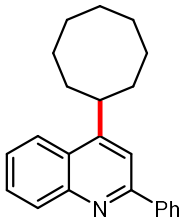

4-cyclooctyl-2-phenylquinoline (50a). Following the general procedure C. Isolated with Hex/EtOAc (20:1) on preparative thin-layer chromatography. Colorless oil (30.7 mg, 97%). **^{1}H NMR** (500 MHz, $CDCl_3$) δ 8.20 (d, *J* = 8.4 Hz, 1H), 8.17-8.13 (m, 2H), 8.10 (d, *J* = 8.4 Hz, 1H), 7.75 (s, 1H), 7.73-7.68 (m, 1H), 7.57-7.51 (m, 3H), 7.49-7.44 (m, 1H), 3.69-3.61 (m, 1H), 2.06-1.66 (m, 14H). **^{13}C NMR** (126 MHz, $CDCl_3$) δ 157.4, 156.6, 148.9, 140.4, 130.9, 129.3, 129.2, 129.0, 127.8, 126.1, 125.8, 123.2, 116.4, 33.9, 27.0, 26.8, 26.4. **HRMS** Calcd for $C_{23}H_{26}N$ [M+H$^+$]: 316.2060, found: 316.2070. The compound was not reported.

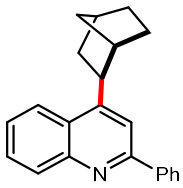

4-((2S)-bicyclo[2.2.1]heptan-2-yl)-2-phenylquinoline (51a). Following the general procedure C. Isolated with Hex/EtOAc (30:1) on preparative thin-layer chromatography.

Colorless oil (25.2 mg, 84%). **^{1}H NMR** (500 MHz, $CDCl_3$) δ 8.19 (d, *J* = 8.4 Hz, 1H), 8.16-8.13 (m, 2H), 8.06 (d, *J* = 7.8 Hz, 1H), 7.75 (s, 1H), 7.73-7.68 (m, 1H), 7.57-7.51 (m, 3H), 7.49-7.45 (m, 1H), 3.42 (dd, *J* = 9.0, 5.5 Hz, 1H), 2.68 (d, *J* = 3.8 Hz, 1H), 2.47-2.43 (m, 1H), 2.08-2.01 (m, 1H), 1.82-1.65 (m, 4H), 1.60-1.53 (m, 1H), 1.49-1.41 (m, 1H), 1.40-1.36 (m, 1H). **^{13}C NMR** (126 MHz, $CDCl_3$) δ 157.4, 153.5, 148.8, 140.6, 130.7, 129.3, 129.2, 129.0, 127.8, 126.7, 126.0, 124.1, 115.1, 43.2, 41.5, 39.4, 37.2, 36.9, 30.5, 29.3. **HRMS** Calcd for $C_{22}H_{22}N$ [M+H$^+$]: 300.1747, found: 300.1756. The compound was not reported.

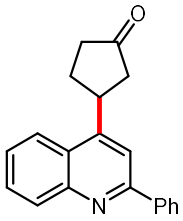

3-(2-phenylquinolin-4-yl)cyclopentanone (52a). Following the general procedure C. Isolated with Hex/EtOAc (5:2) on preparative thin-layer chromatography. Colorless oil (10.1 mg, 35%). **^{1}H NMR** (500 MHz, $CDCl_3$) δ 8.30-8.02 (s, 1H), 8.13 (d, *J* = 7.3 Hz, 2H), 8.08 (d, *J* = 8.4 Hz, 1H), 7.79-7.72 (m, 2H), 7.62-7.57 (m, 1H), 7.57-7.51 (m, 2H), 7.50-7.45 (m, 1H), 4.30-4.21 (m, 1H), 2.87 (dd, *J* = 18.4, 7.4 Hz, 1H), 2.67-2.41 (m, 4H), 2.32-2.21 (m, 1H). **^{13}C NMR** (126 MHz, $CDCl_3$) δ 217.2, 157.5, 149.2, 148.8, 139.7, 131.0, 129.7, 129.7, 129.1, 127.8, 126.7, 126.2, 122.9, 115.1, 45.1, 38.3, 37.6, 29.9. **HRMS** Calcd for $C_{20}H_{18}NO$ [M+H$^+$]: 288.1383, found: 288.1380. The compound was not reported.

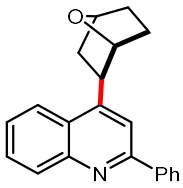

4-(7-oxabicyclo[2.2.1]heptan-2-yl)-2-phenylquinoline (53a). Following the general procedure C. Isolated with Hex/EtOAc (20:1) on preparative thin-layer chromatography.

Colorless oil (8.5 mg, 28%). **^{1}H NMR** (500 MHz, $CDCl_3$) δ 8.21-8.14 (m, 3H), 8.04 (d, *J* = 8.3 Hz, 1H), 8.00 (s, 1H), 7.74-7.68 (m, 1H), 7.57-7.49 (m, 3H), 7.48-7.42 (m, 1H), 4.85-4.80 (m, 2H), 3.72 (dd, *J* = 9.1, 4.8 Hz, 1H), 2.32-2.24 (m, 1H), 1.98-1.85 (m, 3H), 1.82-1.76 (m, 1H), 1.74-1.67 (m, 1H). **^{13}C NMR** (126 MHz, $CDCl_3$) δ 157.7, 152.1, 148.7, 140.2, 130.9, 129.4, 129.3, 128.9, 127.9, 126.2, 126.1, 123, 116.1, 81.1, 76.8, 43.5, 41.1, 30.6, 30.0. **HRMS** Calcd for $C_{21}H_{20}ON$ [M+H$^+$]: 302.1539, found: 302.1548. The compound was not reported.

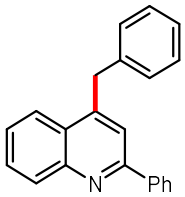

4-benzyl-2-phenylquinoline (54a). Following the general procedure C. Isolated with Hex/EtOAc (20:1) on preparative thin-layer chromatography. Colorless oil (7.4 mg, 25%). **^{1}H NMR** (500 MHz, $CDCl_3$) δ 8.20 (d, *J* = 8.4 Hz, 1H), 8.11 (d, *J* = 7.1 Hz, 2H), 8.03 (d, *J* = 8.4 Hz, 1H), 7.74-7.68 (m, 1H), 7.65 (s, 1H), 7.53-7.48 (m, 3H), 7.47-7.42 (m, 1H), 7.34-7.28 (m, 2H), 7.27-7.22 (m, 3H), 4.51 (s, 2H). **^{13}C NMR** (126 MHz, $CDCl_3$) δ 157.4, 148.7, 147.3, 139.9, 139.0, 130.6, 129.6, 129.5, 129.1, 129.0, 129.0, 127.8, 126.8, 126.8, 126.5, 124.0, 120.1, 38.8. **HRMS** Calcd for $C_{22}H_{18}N$ [M+H$^+$]: 296.1434, found: 296.1440. The compound was not reported.

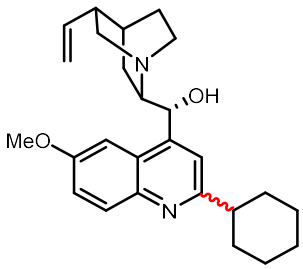

(1*R*)-(2-cyclohexyl-6-methoxyquinolin-4-yl)((2*S*,4*S*,5*R*)-5-vinylquinuclidin-2-yl)methanol (55a). Following the general procedure C using 3.0 equiv of TFA. Isolated with

Hex/EtOAc/MeOH (3:2:1) on preparative thin-layer chromatography. Colorless solid (15.1 mg, 37%). **^{1}H NMR** (500 MHz, $CDCl_3$) δ 7.79 (d, *J* = 9.2 Hz, 1H), 7.54 (s, 1H), 7.11 (dd, *J* = 9.2, 2.6 Hz, 1H), 6.91 (d, *J* = 2.6 Hz, 1H), 6.24 (s, 1H), 5.61-5.49 (m, 1H), 5.02 (dd, *J* = 14.0, 3.8 Hz, 2H), 4.40-4.28 (m, 1H), 3.72 (s 3H), 3.53-3.43 (m, 1H), 3.31 (t, *J* = 9.0 Hz, 1H), 3.16-2.98 (m, 2H), 2.89-2.79 (m, 1H), 2.69-2.60 (m, 1H), 2.27-1.22 (m, 16H). **^{13}C NMR** (126 MHz, $CDCl_3$) δ 163.8, 157.9, 144.2, 143.7, 137.6, 131.3, 124.0, 122.0, 117.5, 117.1, 99.5, 66.7, 60.4, 55.9, 54.9, 47.5, 44.0, 37.6, 33.1, 33.0, 27.2, 26.8, 26.8, 26.3, 24.6, 18.3. **HRMS** Calcd for $C_{26}H_{35}O_2N_2$ [M+H$^+$]: 407.2693, found: 407.2700. The compound was not reported.

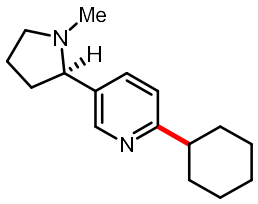

(*R*)-2-cyclohexyl-5-(1-methylpyrrolidin-2-yl)pyridine (56a). Following the general procedure C using 3.0 equiv of TFA. Isolated with Hex/DCM/EtOAc/MeOH (1:1:2.5:0.5) on preparative thin-layer chromatography. Yellow oil (8.8 mg, 36%). **^{1}H NMR** (500 MHz, $CDCl_3$) δ 8.41 (d, *J* = 2.1 Hz, 1H), 7.63 (dd, *J* = 8.0, 2.1 Hz, 1H), 7.13 (d, *J* = 8.0 Hz, 1H), 3.25 (t, *J* = 8.2 Hz, 1H), 3.07 (t, *J* = 8.2 Hz, 1H), 2.73-2.64 (m, 1H), 2.36-2.25 (m, 1H), 2.22-2.12 (m, 4H), 2.00-1.90 (m, 2H), 1.89-1.80 (m, 2H), 1.80-1.69 (2H), 1.56-1.35 (m, 5H), 1.34-1.24 (m, 2H). **^{13}C NMR** (126 MHz, $CDCl_3$) δ 165.8, 149.0, 135.5, 121.2, 69.0, 57.2, 46.5, 40.6, 35.1, 33.2, 26.8, 26.3, 22.7. **GC-MS** (EI, m/z) for $C_{16}H_{24}N_2$ Calcd: 244.2, found: 244.1. Spectra data are consistent with the reported literature.[64]

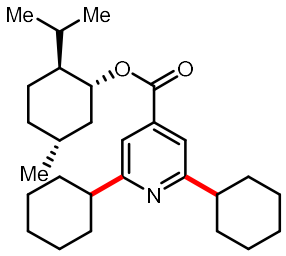

(1*R*,2*S*,5*R*)-2-isopropyl-5-methylcyclohexyl-2,6-dicyclohexylisonicotinate (57a). Following the general procedure C using 8 equiv of DTBP, 0.20 mL of diacetyl, and 0.4 mL of MECN. Isolated with Hex/EtOAc (30:1) on preparative thin-layer chromatography. Colorless solid (12.8 mg, 30%). **^{1}H NMR** (500 MHz, $CDCl_3$) δ 7.48 (s, 2H), 5.00-4.91 (m, 1H), 2.79-2.70 (m, 2H), 2.12-2.05 (m, 1H), 2.00-1.81 (m, 9H), 1.79-1.70 (m, 4H), 1.62-1.37 (m, 10H), 1.35-1.24 (m, 2H), 1.18-1.08 (m, 2H), 0.96-0.89 (m, 7H), 0.80 (d, *J* = 7.0 Hz, 3H). **^{13}C NMR** (126 MHz, $CDCl_3$) δ 166.9, 165.8, 138.8, 117.4, 75.6, 47.3, 46.8, 41.1, 34.5, 33.1, 31.7, 26.8, 26.7, 26.3, 23.9, 22.2, 20.9, 16.8. **HRMS** Calcd for $C_{28}H_{44}O_2N$ [M+H$^+$]: 426.3367, found: 426.3372. The compound was not reported.

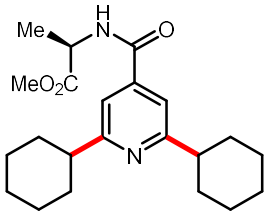

(*R*)-methyl-2-(2,6-dicyclohexylisonicotinamido)propanoate (58a). Following the general procedure C using 8 equiv of DTBP, 0.20 mL of diacetyl, and 0.4 mL of MeCN. Isolated with Hex/EtOAc (5:2) on preparative thin-layer chromatography. Colorless solid (10.1 mg, 27%). **^{1}H NMR** (500 MHz, $CDCl_3$) δ 7.26 (s, 2H), 6.76 (d, *J* = 7.1 Hz, 1H), 4.79 (quint, 1H), 3.80 (s, 3H), 2.77-2.68 (m, 2H), 1.98-1.91 (m, 4H), 1.88-1.80 (m, 4H), 1.78-1.71 (m, 2H), 1.57-1.36 (m, 11H), 1.34-1.22 (m, 2H). **^{13}C NMR** (126 MHz, $CDCl_3$) δ 173.7, 167.1, 166.3, 142.0, 115.3, 52.9, 48.7, 46.9, 33.1, 26.7, 26.3, 18.8. **HRMS** Calcd for $C_{22}H_{33}O_3N_2$ [M+H$^+$]: 373.2486, found:

373.2490. The compound was not reported.

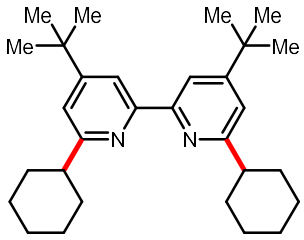

4,4'-di-tert-butyl-6,6'-dicyclohexyl-2,2'-bipyridine (59a). Following the general procedure C using 8 equiv of DTBP, 0.20 mL of diacetyl, and 0.4 mL of MeCN. Isolated with Hex/EtOAc (30:1) on preparative thin-layer chromatography. Colorless solid (14.7 mg, 34%). **^{1}H NMR** (500 MHz, $CDCl_3$) δ 8.20 (d, *J* = 1.5 Hz, 2H), 7.11 (d, *J* = 1.5 Hz, 2H), 2.81-2.70 (m, 2H), 2.07-1.96 (m, 4H), 1.93-1.83 (m, 4H), 1.81-1.73 (m, 2H), 1.68-1.55 (m, 4H), 1.53-1.20 (m, 24H). **^{13}C NMR** (126 MHz, $CDCl_3$) δ 165.8, 160.8, 156.5, 117.7, 116.1, 46.9, 35.1, 33.3, 31.0, 26.9, 26.5. **HRMS** Calcd for $C_{30}H_{45}N_2$ [M+H$^+$]: 433.3577, found: 433.3584. The compound was not reported.

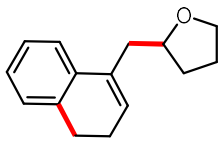

2-((3,4-dihydronaphthalen-1-yl)methyl)tetrahydrofuran (61a). Colorless oil. **^{1}H NMR** (500 MHz, $CDCl_3$) δ 7.32-7.27 (m, 1H), 7.22-7.16 (m, 2H), 5.95 (t, *J* = 4.5 Hz, 1H), 4.13-4.05 (m, 1H), 3.95-3.88 (m, 1H), 3.77-3.69 (m, 1H), 2.89-2.81 (m, 1H), 2.79-2.69 (m, 2H), 2.53-2.46 (m, 1H), 2.29-2.21 (m, 2H), 1.99-1.80 (m, 4H). **^{13}C NMR** (126 MHz, $CDCl_3$) δ 136.9, 135.0, 133.9, 127.8, 126.9, 126.9, 126.5, 122.9, 77.9, 68.1, 39.2, 31.6, 28.6, 25.8, 23.4. **HRMS** Calcd for $C_{15}H_{19}O$ [M+H$^+$]: 215.1430, found: 215.1436. The compound was not reported.

2.9 References

1. C.-Y. Huang, J. Li, W. Liu & C.-J. Li. Diacetyl as a "Traceless" Visible Light Photosensitizer in Metal-Free Cross-Dehydrogenative Coupling Reactions. *Chem. Sci.* **2019**, *10*, 5018-5024.

2. R. S. J. Proctor, H. J. Davis & R. J. Phipps. Catalytic Enantioselective Minisci-Type Addition to Heteroarenes. *Science* **2018**, *360*, 419-422.

3. J. Wu, Y. Liu, C. Lu & Q. Shen. Palladium-Catalyzed Difluoromethylthiolation of Heteroaryl Bromides, Iodides, Triflates and Aryl Iodides. *Chem. Sci.* **2016**, *7*, 3757-3762.

4. F. Fontana, F. Minisci & E. Vismara. New General and Convenient Sources of Alkyl Radicals, Useful for Selective Syntheses. *Tetrahedron Lett.* **1988**, *29*, 1975-1978.

5. G.-X. Li *et al.* Photoredox-Mediated Minisci C-H Alkylation of *N*-Heteroarenes Using Boronic Acids and Hypervalent Iodine. *Chem. Sci.* **2016**, *7*, 6407-6412.

6. L. Zhang & Z.-Q. Liu. Molecular Oxygen-Mediated Minisci-Type Radical Alkylation of Heteroarenes with Boronic Acids. *Org. Lett.* **2017**, *19*, 6594-6597.

7. F. Coppa *et al.* A Novel Radical Reaction of Alkyl Xantates Useful for the Selective Substitution of Heteroaromatic Bases. *Tetrahedron Lett.* **1992**, *33*, 687-690.

8. Y. Fujiwara *et al.* A New Reagent for Direct Difluoromethylation. *J. Am. Chem. Soc.* **2012**, *134*, 1494-1497.

9. Y. Ji *et al.* Innate C-H Trifluoromethylation of Heterocycles. *Proc. Natl. Acad. Sci. U.S.A.* **2011**, *108*, 14411-14415.

10. P. Liu, W. Liu & C.-J. Li. Catalyst-Free and Redox-Neutral Innate Trifluoromethylation and Alkylation of Aromatics Enabled by Light. *J. Am. Chem. Soc.* **2017**, *139*, 14315-14321.

11. R.-J. Tang, L. Kang & L. Yang. Metal-Free Oxidative Decarbonylative Coupling of Aliphatic Aldehydes with Azaarenes: Successful Minisci-Type Alkylation of Various Heterocycles. *Adv. Synth. Catal.* **2015**, *357*, 2055-2060.

12. W.-M. Cheng, R. Shang, M.-C. Fu & Y. Fu. Photoredox-Catalysed Decarboxylative Alkylation of *N*-Heteroarenes with *N*-(Acyloxy)phthalimides. *Chem. Eur. J.* **2017**, *23*, 2537-2541.

13. R. A. Garza-Sanchez, A. Tlahuext-Aca, G. Tavakoli & F. Glorius. Visible Light-Mediated Direct Decarboxylative C-H Functionalization of Heteroarenes. *ACS Catal.* **2017**, *7*, 4057-4061.

14. L. Yang *et al.* Direct C-H Cyanoalkylation of Quinoxalin-2(1*H*)-ones via Radical C-C Bond Cleavage. *Org. Lett.* **2018**, *20*, 1034-1037.

15. X. Y. Yu *et al.* A Visible-Light-Driven Iminyl Radical-Mediated C-C Single Bond Cleavage/Radical Addition Cascade of Oxime Esters. *Angew. Chem. Int. Ed.* **2018**, *57*, 738-743.

16. B. Zhao & Z. Shi. Copper-Catalyzed Intermolecular Heck-Like Coupling of Cyclobutanone Oximes Initiated by Selective C-C Bond Cleavage. *Angew. Chem. Int. Ed.* **2017**, *56*, 12727-12731.

17. S. A. Girard, T. Knauber & C.-J. Li. The Cross-Dehydrogenative Coupling of C(sp^3)-H Bonds: A Versatile Strategy for C-C Bond Formations. *Angew. Chem. Int. Ed.* **2014**, *53*, 74-100.

18. C.-J. Li. Cross-Dehydrogenative Coupling (Cdc): Exploring C-C Bond Formations Beyond Functional Group Transformations. *Acc. Chem. Res.* **2009**, *42*, 335-344.

19. H. Yi *et al.* Recent Advances in Radical C-H Activation/Radical Cross-Coupling. *Chem Rev.* **2017**, *117*, 9016-9085.

20. G. Deng & C.-J. Li. $Sc(OTf)_3$-Catalyzed Direct Alkylation of Quinolines and Pyridines with Alkanes. *Org. Lett.* **2009**, *11*, 1171-1174.

21. C. Giordano, F. Minisci, E. Vismara & S. Levi. A General, Selective, and Convenient Procedure of Homolytic Formylation of Heteroaromatic Bases. *J. Org. Chem.* **1986**, *51*, 536-537.

22. X. Li, H.-Y. Wang & Z.-J. Shi. Transition-Metal-Free Cross-Dehydrogenative Alkylation of Pyridines under Neutral Conditions. *New J. Chem.* **2013**, *37*, 1704-1706.

23. N. Okugawa, K. Moriyama & H. Togo. Introduction of Ether Groups onto Electron-Deficient Nitrogen-Containing Heteroaromatics Using Radical Chemistry under Transition-Metal-Free Conditions. *Eur. J. Org. Chem.* **2015**, *2015*, 4973-4981.

24. J. Jin & D. W. C. Macmillan. Direct α-Arylation of Ethers through the Combination of Photoredox-Mediated C-H Functionalization and the Minisci Reaction. *Angew. Chem. Int. Ed.* **2015**, *54*, 1565-1569.

25. M. C. Quattrini *et al.* Versatile Cross-Dehydrogenative Coupling of Heteroaromatics and Hydrogen Donors via Decatungstate Photocatalysis. *Chem. Commun.* **2017**, *53*, 2335-2338.

26. S. Liu, A. Liu, Y. Zhang & W. Wang. Direct Cα-Heteroarylation of Structurally Diverse Ethers via a Mild *N*-Hydroxysuccinimide Mediated Cross-Dehydrogenative Coupling Reaction. *Chem. Sci.* **2017**, *8*, 4044-4050.

27. L. Niu *et al.* Visible Light-Induced Direct α C-H Functionalization of Alcohols. *Nat. Commun.* **2019**, *10*, 467.

28. A. P. Antonchick & L. Burgmann. Direct Selective Oxidative Cross-Coupling of Simple Alkanes with Heteroarenes. *Angew. Chem. Int. Ed.* **2013**, *52*, 3267-3271.

29. J. Jin & D. W. C. MacMillan. Alcohols as Alkylating Agents in Heteroarene C-H Functionalization. *Nature* **2015**, *525*, 87-90.

30. W. Liu, X. Yang, Z.-Z. Zhou & C.-J. Li. Simple and Clean Photo-Induced Methylation of Heteroarenes with Meoh. *Chem* **2017**, *2*, 688-702.

31. L. Li *et al.* Simple and Clean Photoinduced Aromatic Trifluoromethylation Reaction. *J. Am. Chem. Soc.* **2016**, *138*, 5809-5812.

32. J. W. Lockner, D. D. Dixon, R. Risgaard & P. S. Baran. Practical Radical Cyclizations with Arylboronic Acids and Trifluoroborates. *Org. Lett.* **2011**, *13*, 5628-5631.

33. I. B. Seiple *et al.* Direct C-H Arylation of Electron-Deficient Heterocycles with Arylboronic Acids. *J. Am. Chem. Soc.* **2010**, *132*, 13194-13196.

34. W. Liu, P. Liu, L. Lv & C.-J. Li. Metal-Free and Redox-Neutral Conversion of Organotrifluoroborates into Radicals Enabled by Visible Light. *Angew. Chem. Int. Ed.* **2018**, *57*, 13499-13503.

35. A. M. Cardarelli, M. Fagnoni, M. Mella & A. Albini. Hydrocarbon Activation. Synthesis of β-Cycloalkyl (Di)nitriles through Photosensitized Conjugate Radical Addition. *J. Org. Chem.* **2001**, *66*, 7320-7327.

36. H. A. J. Carless & S. Mwesigye-Kibende. Intramolecular Hydrogen Abstraction in Ketone Photochemistry: The First Examples of ζ-Hydrogen Abstraction. *J. Chem. Soc., Chem. Commun.* **1987**, 1673-1674.

37. S. Kamijo, T. Hoshikawa & M. Inoue. Photochemically Induced Radical Transformation of C(sp^3)-H Bonds to C(sp^3)-CN Bonds. *Org. Lett.* **2011**, *13*, 5928-5931.

38. C. Walling & M. J. Gibian. Hydrogen Abstraction Reactions by the Triplet States of Ketones. *J. Am. Chem. Soc.* **1965**, *87*, 3361-3364.

39. J.-B. Xia, C. Zhu & C. Chen. Visible Light-Promoted Metal-Free C-H Activation: Diarylketone-Catalyzed Selective Benzylic Mono- and Difluorination. *J. Am. Chem. Soc.* **2013**, *135*, 17494-17500.

40. E. T. Denisov & I. B. Afanas'ev *Oxidation and Antioxidants in Organic Chemistry and Biology*. Taylor & Francis Group, Boca Raton, **2005**, pp 281-298.

41. H. Matsubara, S. Suzuki & S. Hirano. An Ab Initio and DFT Study of the Autoxidation of THF and THP. *Org. Biomol. Chem.* **2015**, *13*, 4686-4692.

42. R. Gilmour & J. Metternich. Photocatalytic $E \rightarrow Z$ Isomerization of Alkenes. *Synlett* **2016**, *27*, 2541-2552.

43. K. Singh, S. J. Staig & J. D. Weaver. Facile Synthesis of *Z*-Alkenes via Uphill Catalysis. *J. Am. Chem. Soc.* **2014**, *136*, 5275-5278.

44. Z. Lu & T. P. Yoon. Visible Light Photocatalysis of [2+2] Styrene Cycloadditions by Energy Transfer. *Angew. Chem. Int. Ed.* **2012**, *51*, 10329-10332.

45. N. Münster *et al.* Visible Light Photocatalysis of 6π Heterocyclization. *Angew. Chem. Int. Ed.* **2017**, *56*, 9468-9472.

46. P. Sharma, B. Lygo, W. Lewis & J. E. Moses. Biomimetic Synthesis and Structural Reassignment of the Tridachiahydropyrones. *J. Am. Chem. Soc.* **2009**, *131*, 5966-5972.

47. J. Zhao *et al.* Intramolecular Crossed [2+2] Photocycloaddition through Visible Light-Induced Energy Transfer. *J. Am. Chem. Soc.* **2017**, *139*, 9807-9810.

48. D. R. Heitz, J. C. Tellis & G. A. Molander. Photochemical Nickel-Catalyzed C-H Arylation: Synthetic Scope and Mechanistic Investigations. *J. Am. Chem. Soc.* **2016**, *138*, 12715-12718.

49. Y. Shen, Y. Gu & R. Martin. sp^3 C-H Arylation and Alkylation Enabled by the Synergy of Triplet Excited Ketones and Nickel Catalysts. *J. Am. Chem. Soc.* **2018**, *140*, 12200-12209.

50. E. R. Welin *et al.* Photosensitized, Energy Transfer-Mediated Organometallic Catalysis through Electronically Excited Nickel(II). *Science* **2017**, *355*, 380-385.

51. E. Arceo, E. Montroni & P. Melchiorre. Photo-Organocatalysis of Atom-Transfer Radical Additions to Alkenes. *Angew. Chem. Int. Ed.* **2014**, *53*, 12064-12068.

52. E. P. Farney & T. P. Yoon. Visible-Light Sensitization of Vinyl Azides by Transition-Metal Photocatalysis. *Angew. Chem. Int. Ed.* **2014**, *53*, 793-797.

53. M. Teders *et al.* The Energy-Transfer-Enabled Biocompatible Disulfide-Ene Reaction. *Nat. Chem.* **2018**, *10*, 981-988.

54. T. H. Fife & L. H. Brod. General Acid Catalysis and the pH-Independent Hydrolysis of 2-(*p*-Nitrophenoxy) Tetrahydropyran. *J. Am. Chem. Soc.* **1970**, *92*, 1681-1684.

55. F. Agapito, B. J. Costa Cabral & J. A. Martinho Simões. Oxygen-Oxygen Bond Dissociation Enthalpies of Di-*tert*-Butyl Peroxide and Di-trifluoromethyl Peroxide. *J. Mol. Struct.: THEOCHEM* **2005**, *729*, 223-227.

56. S. L. Khursan, D. A. Mikhailov, A. A. Gusmanov & I. M. Borisov. Bond Dissociation Energies of Organic Peroxide Compounds. *Russ. J. Phys. Chem. A* **2001**, *75*, 724-732.

57. Y. Zhu & Y. Wei. Copper Catalyzed Direct Alkenylation of Simple Alkanes with Styrenes. *Chem. Sci.* **2014**, *5*, 2379-2382.

58. L. Zhang *et al.* The Combination of Benzaldehyde and Nickel-Catalyzed Photoredox C(sp^3)-H Alkylation/Arylation. *Angew. Chem. Int. Ed.* **2019**, *58*, 1823-1827.

59. R. S. J. Proctor, P. Chuentragool, A. C. Colgan & R. J. Phipps. Hydrogen Atom Transfer-Driven Enantioselective Minisci Reaction of Amides. *J. Am. Chem. Soc.* **2021**, *143*, 4928-4934.

60. J. Wang, G.-X. Li, G. He & G. Chen. Photoredox-Mediated Minisci Alkylation of *N*-Heteroarenes Using Carboxylic Acids and Hypervalent Iodine. *Asian J. Org. Chem.* **2018**, *7*, 1307-1310.

61. T. Caronna *et al.* Sunlight-Induced Reactions of Some Heterocyclic Bases with Ethers in the Presence of TiO_2. *J. Photochem. Photobiol.* **2005**, *171*, 237-242.

62. L. Barriault, T. McCallum, L.-A. Jouanno & A. Cannillo. Persulfate-Enabled Direct C-H Alkylation of Heteroarenes with Unactivated Ethers. *Synlett* **2016**, *27*, 1282-1286.

63. J. Jin & D. W. C. MacMillan. Direct α-Arylation of Ethers through the Combination of Photoredox-Mediated C-H Functionalization and the Minisci Reaction. *Angew. Chem. Int. Ed.* **2015**, *54*, 1565-1569.

64. Á. Gutiérrez-Bonet, C. Remeur, J. K. Matsui & G. A. Molander. Late-Stage C-H Alkylation of Heterocycles and 1,4-Quinones via Oxidative Homolysis of 1,4-Dihydropyridines. *J. Am. Chem. Soc.* **2017**, *139*, 12251-12258.

Chapter 3 Chloride-catalyzed cross-dehydrogenative Minisci alkylation

In the previous chapter, we revealed two simple and green diacetyl-enabled dehydrogenative Minisci alkylation methods to couple C(sp^3)-H. To develop a more enabling protocol to activate strong C(sp^3)-H bonds under oxidant-free conditions, this chapter conceives a photoinduced and oxidant-free dehydrogenative Minisci alkylation using chlorine radical as the HAT agent and cobaloxime catalyst for catalytic turnover. [1]

3.1 Introduction

The alkyl radical (R•), one of the most fundamental intermediates in organic synthesis, constitutes an important approach to rapid molecular construction. Its generation from functionalized precursors such as aliphatic carboxylic acids, boronic reagents, halides, and others has been well-established and broadly applied as efficient paradigms in routine synthesis.[2-13] Of equal importance, direct R• generation from the readily available non-functionalized alkanes represents a more straightforward and sustainable method.[14]

Figure 3.1 Common BDE of C(sp^3)-H and heteroatom-H.

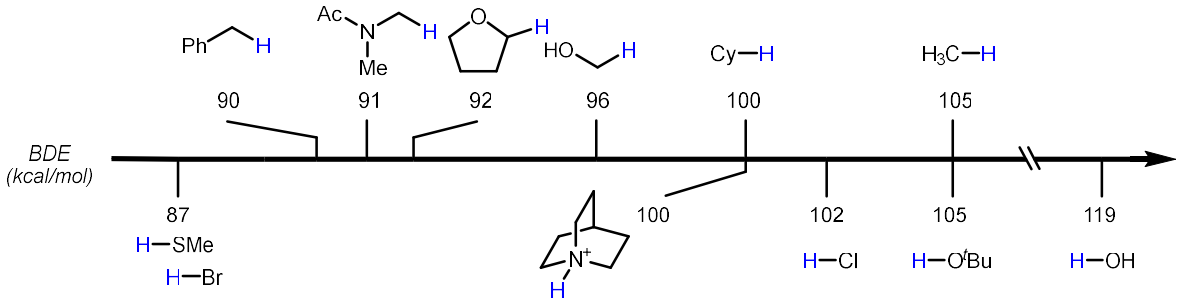

However, due to the high bond dissociation energies (BDEs),[15-16] current strategies involving the homolysis of strong C(sp^3)-H bonds mostly rely on the hydrogen atom transfer (HAT) with electrophilic heteroatom radicals. For instance, bromo-,[17-19] nitrogen-,[16, 20] or oxygen-centered radicals[21-22, 20, 23] (**Figure 3.1**). In this context, robust redox catalysts or

strongly oxidizing reagents are required, whereas precise control over the site selectivity among ubiquitous C(sp^3)-H bonds in a molecule with broad substrate scope imposes grand challenges.

Chlorine radical (Cl•) is an efficient HAT agent that could cleave various C(sp^3)-H bonds. Using chloride (Cl^-) in Cl• generation benefits organic syntheses because it is innocuous and abundant in diverse salt forms. Nevertheless, the unfavorable chloride-to-chlorine oxidation (E° = 1.36 V vs NHE)[24] and untamed reactivity of Cl• compared with other halide analogues[25, 18, 26-27, 19] make chlorine radical-promoted alkylation rarely explored. In this endeavor, few strategies have been disclosed for the efficient usage of Cl•, including (a) the direct single-electron transfer (SET) from Cl^- to photocatalyst under photothermal conditions;[28-31] (b) the ligand-to-metal charge transfer (LMCT), which has been employed for the coupling of alkanes and organohalides by metallophotoredox catalysis;[32-37] (c) the photolysis of in situ generated Cl_2 via electrooxidation of HCl;[38] (d) the bimolecular homolytic substitution (S_H2) between chloroborate and an oxy radical for the alkane borylation.[39] These pioneering examples demonstrate the potential of Cl^- to realize the HAT process via Cl• intermediate (**Figure 3.2**).

Figure 3.2 Chloride-to-chlorine radical strategy in HAT reactions.

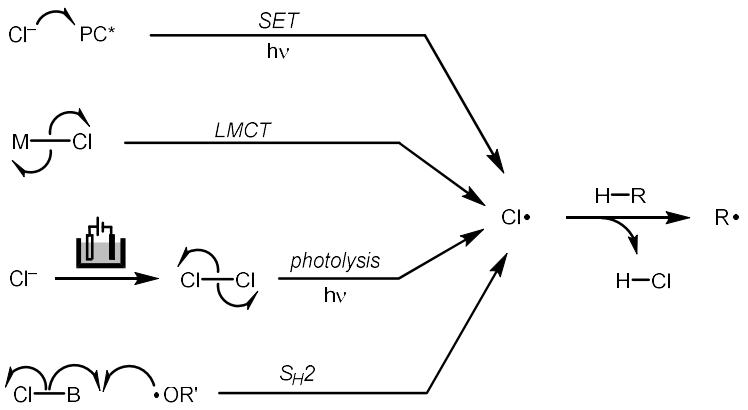

The Minisci alkylation involves the coupling between heteroarenes and nucleophilic alkyl radicals. Given the diversity of heteroarenes and their countless applications in material science, agrochemicals, and the pharmaceutical industry, the Minisci alkylation plays a pivotal role in synthetic chemistry. Since the key of the Minisci alkylation is the R• generation, it prompted us to consider the possibility of merging the chlorine radical-mediated R• generation manifold with the Minisci alkylation, which could allow the heteroarene diversification simply through the coupling with widely available C(sp^3)-H feedstocks.[40] Furthermore, an H_2-evolving Minisci alkylation is more desirable for its highest step- and atom-economy.[41-42] Owing to the strong aliphatic C-H bonds and the net oxidative nature, excessive alkane (normally as solvent) and oxidant loadings, high temperature, or precious catalysts are not uncommon. Therefore, a catalytic cross-dehydrogenative Minisci alkylation without stoichiometric chemical oxidants is long-sought-after.[40] Our group has a long-term interest in the arene functionalization facilitated by the excited aromatics under catalyst-free conditions.[43-48] Recently, we also documented a simple and clean Minisci alkylation reaction via formal dehydrative coupling of heteroarenes with alcohols. Taking advantage of the superior redox properties of the excited heteroarenes, metallophotoredox catalysts could be strategically avoided.[49]

Based on these literature precedents,[50-51] we envisioned that heteroarene itself could be an intrinsic photosensitizer, allowing efficient Cl^- oxidation in the Minisci reaction. This work presents a dehydrogenative Minisci alkylation using catalytic Cl^- under photochemical conditions (**Figure 3.3**). Owing to the strong hydrogen atom affinity of Cl•, a wide range of C(sp^3)-H bonds could be heteroarylated with good functional group tolerance and substrate diversity. Notably, with the strategic introduction of the cobaloxime catalyst, we formulated a chemical oxidant-free heteroarene alkylation protocol by releasing H_2.

Figure 3.3 Proposed dehydrogenative alkylation reaction.

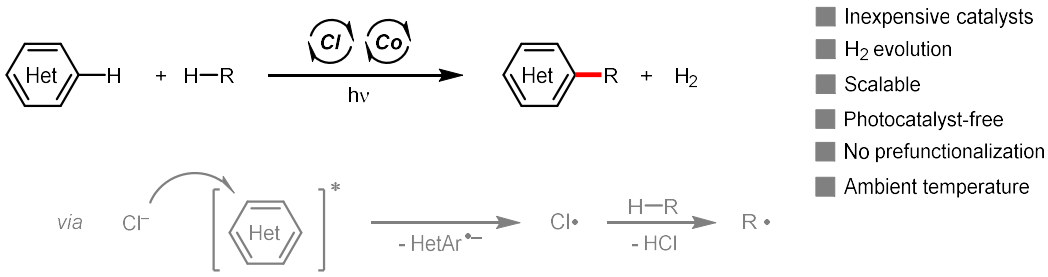

3.2 Reaction design

The proposed dehydrogenative alkylation pathway is depicted in **Scheme 3.1**. It was hypothesized that the excited heteroarenes could oxidize the Cl^- under irradiation to generate the Cl• for aliphatic C-H abstraction from an alkane. Adding the so-formed R• to another equivalent of heteroarene followed by hydrogen atom removal would give the desired alkylated heteroarene. Meanwhile, to efficiently quench the generated heteroaryl radical intermediate, a readily accessible cobaloxime catalyst $[Co(dmgH)_2(py)]Cl$ was introduced to the system[52-56] not only to prevent the over-reduction of this intermediate but also to serve as an H_2 evolution catalyst.

Scheme 3.1 Designed dehydrogenative alkylation mechanism.

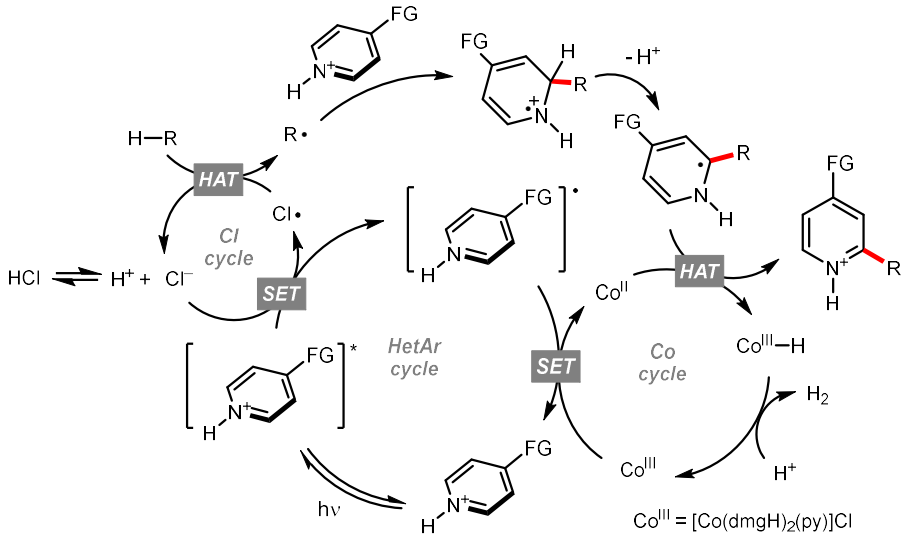

3.3 Results and discussion

In our initial evaluation, 2-phenylquinoline (**1b**) and cyclohexane (**2b**) were chosen as model substrates with trifluoroacetic acid (TFA), Bu_4NCl, and cobaloxime $[Co(dmgH)_2(py)]Cl$ in $CHCl_3$. Delightfully, the desired coupling product **3b** could be obtained in good conversion and product yield. After considerable efforts, the optimal reaction conditions yielded 80% of **3b** when 20 mol% Bu_4NCl, 5.0 mol% $[Co(dmgH)_2(py)]Cl$, and 3.0 equiv of TFA were used in $CHCl_3$ under photo-irradiation (>280 nm) for 20 h (**Table 3.1**, entry 1). During the optimizations, three key reaction components, including Bu_4NCl, $[Co(dmgH)_2(py)]Cl$, and $CHCl_3$,[49] were identified, all of which could potentially serve as the Cl• sources. The reaction could proceed smoothly in the presence of any of these chlorides; otherwise, no reaction occurred (entries 2 to 8). Importantly, the cobaloxime catalyst could improve the reaction productivity by minimizing the over-reduction of quinoline to tetrahydroquinoline or other off-target decomposition reactivities. A significant solvent effect was observed in this transformation. In the chlorinated solvent $CHCl_3$, heteroarene **1b** was alkylated efficiently without side reaction detected; however, when other solvents were used, poor selectivity and side product formations were often observed (e.g., in entry 4, 10% tetrahydroquinoline was obtained). The reaction was partially suppressed by oxygen (entry 9), and poor transformations were observed using low-energy photons or in the dark (entries 10 to 12).

Table 3.1 Optimizations for the coupling of 2-phenylquinoline and cyclohexane.

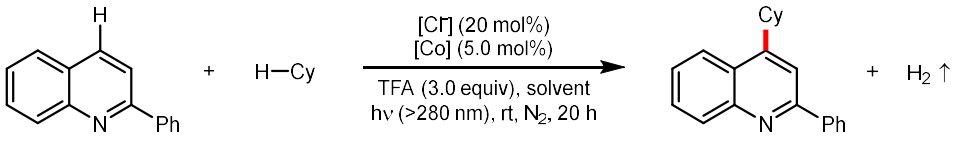

1b **2b** **3b**

Entry[a]	[Cl⁻]	[Co]	Solvent	Conversion (%)	Yield (%)
1	Bu_4NCl	$[Co(dmgH)_2(py)]Cl$	$CHCl_3$	84	80
2	-	$[Co(dmgH)_2(py)]Cl$	$CHCl_3$	56	56
3	Bu_4NCl	-	$CHCl_3$	83	65
4	Bu_4NCl	$[Co(dmgH)_2(py)]Cl$	MeCN	100	70

5	-	$[Co(dmgH)_2(py)]Cl$	MeCN	64	46
6	Bu_4NCl	$Co(dmgBF_2)_2$	MeCN	78	69
7	-	$Co(dmgBF_2)_2$	$CHCl_3$	60	58
8	-	$Co(dmgBF_2)_2$	MeCN	3	0
9[b]	Bu_4NCl	$[Co(dmgH)_2(py)]Cl$	$CHCl_3$	48	41
10[c]	Bu_4NCl	$[Co(dmgH)_2(py)]Cl$	$CHCl_3$	53	52
11[d]	Bu_4NCl	$[Co(dmgH)_2(py)]Cl$	$CHCl_3$	3	3
12[e]	Bu_4NCl	$[Co(dmgH)_2(py)]Cl$	$CHCl_3$	1	0

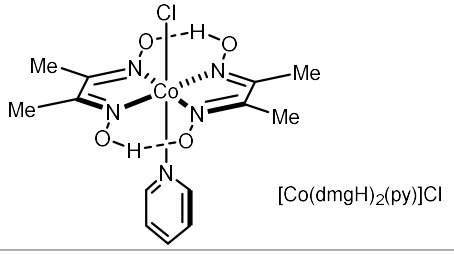

$[Co(dmgH)_2(py)]Cl$

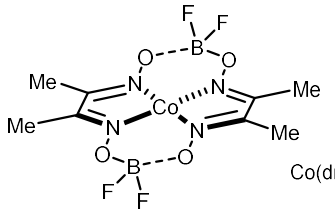

$Co(dmgBF_2)_2$

[a]Reaction conditions: **1b** (0.20 mmol, 1.0 equiv), **2b** (0.60 mL), $[Cl^-]$ (40 μmol, 20 mol%), [Co] (10 μmol, 5.0 mol%), and TFA (0.60 mmol, 3.0 equiv) in solvent (1.5 mL) and irradiated by >280 nm light at room temperature under nitrogen for 20 h. Yields were determined by ^1H NMR using CH_2Br_2 as the internal standard. [b]The reaction was conducted under air. [c]The reaction was irradiated by >345 nm light. [d]The reaction was irradiated by >395 nm light. [e]The reaction was run in the dark.

After obtaining the optimal reaction conditions, we approached the substrate scope to different C(sp^3)-H species using 2-phenylquinoline (**1b**) as the coupling partner (**Figure 3.4**). Simple cyclic alkanes containing five to twelve carbons afforded the corresponding alkylated heteroarenes **3b** to **7b** in moderate to good yields, and so did bridged alkanes norbornane and adamantane (**8b** and **9b**). Carbonyl compound cyclopentanone was functionalized at the β-position and afforded the desired product **10b**. Benzylic C-H abstractions of methylbenzene derivatives also provided benzylated heteroarenes (**11b** to **14b**).[57] It was not surprising that ethylated quinoline **15b** was produced as the major product with diethyl ether (Et_2O) as the alkane source;[49] and the similar C-O cleavage was observed with 1,2-dimethoxyethane (DME) to give the deethoxylated products **16b**; gratifyingly, the non-cleaved ethereal compounds **17b** and **18b** could be obtained by decreasing the acid amount to 1.2 to 2.0 equiv.[38] However, the C-O cleavage was still inevitable with tetrahydrofuran (THF) and methanol (**19b** to **22b**). Reactions with tetrahydropyran (THP) and its analogues

proceeded smoothly and gave good yields of the products **23b** to **26b**. α-C(sp^3)-H functionalization of amine derivatives, for example, amides, sulfonamide and phosphoramide, were all successful (**27b** to **33b**). Interestingly, the HAT of the *N*-methyl group of *N*,*N*-dimethylformamide (DMF) is more favorable than the formyl one and the alkylated heteroarene **29b** was obtained as the major product.

Figure 3.4 Substrate scope of alkane.

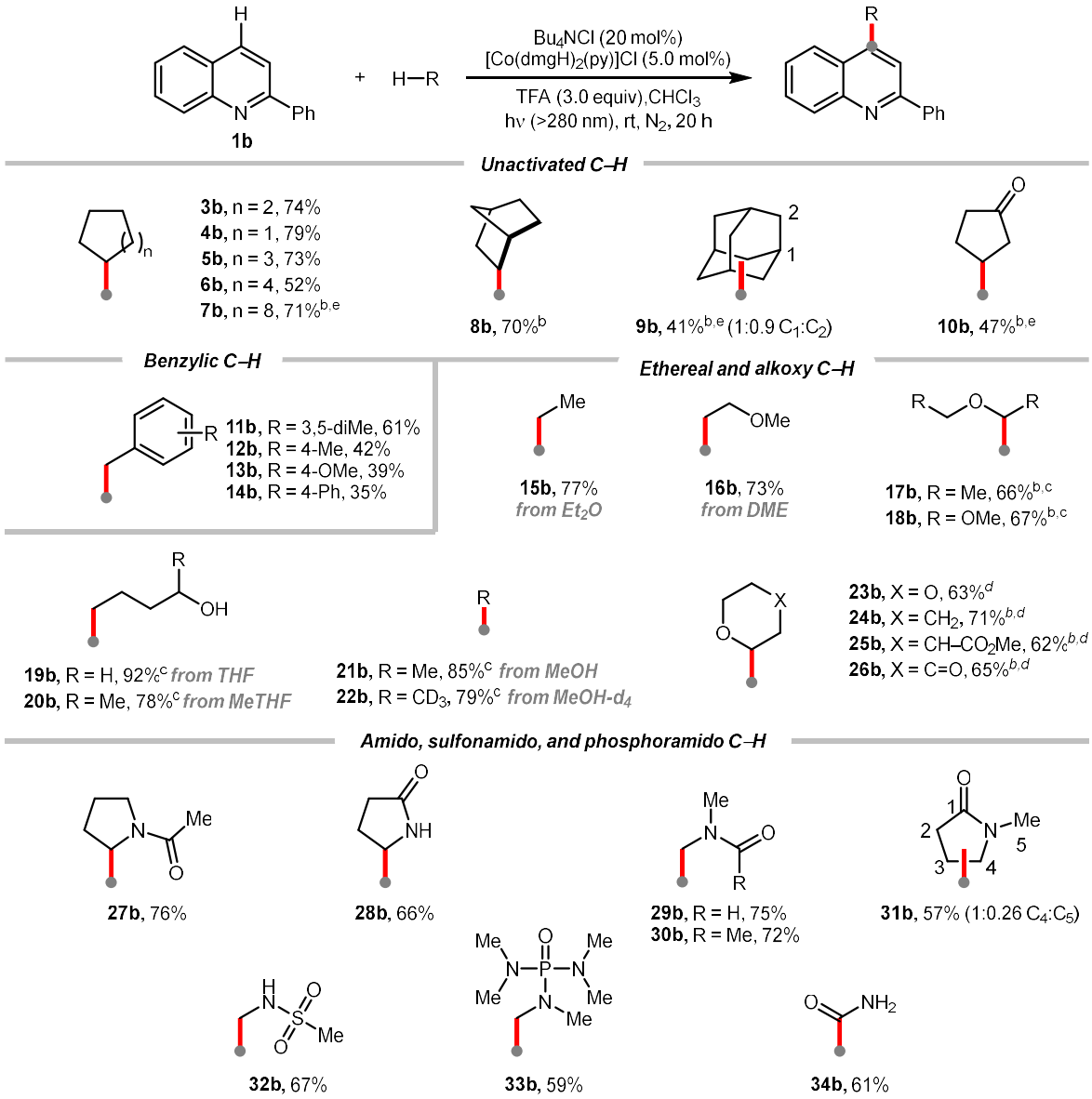

[a]Reaction conditions: **1b** (0.20 mmol, 1.0 equiv), alkane (0.60 mL for liquid, or 10 equiv for solid), Bu_4NCl (40 μmol, 20 mol%), $[Co(dmgH)_2(py)]Cl$ (10 μmol, 5.0 mol%), and TFA (0.60 mmol, 3.0 equiv) in $CHCl_3$ (1.5 mL) and irradiated by >280 nm light at room temperature under nitrogen for 20 h, unless otherwise specified, and the yields were isolated ones.. [b]The reaction was run for 36 h. [c]1.2 equiv of TFA was used. [d]2.0 equiv of TFA was used. [e]The reaction was heated to 55-60 °C. MeTHF, 2-methyltetrahydrofuran; DME, 1,2-dimethoxyethane.

Few alkane substrates, for instance, cyclododecane, adamantane and cyclopentane, were inert at ambient temperature, and a slight temperature increase to 55 to 60 °C was helpful for their transformations (**7b**, **9b**, and **10b**). The unique regioselectivity of Cl• could be displayed from some substrates. For example, the HAT on adamantane is slightly favorable on the tertiary C-H bond in comparison to the secondary one (**9b**), yet 2-methyltetrahydrofuran (MeTHF) only afforded the secondary carbon-functionalized product (**20b**); functionalization of the *N*-methylpyrrolidinone (NMP) primarily occurred at the secondary C4 position rather the primary C5 one (**31b**). Other than alkyl substrates, the amidation of heteroarene was also viable with formamide, which furnished the amido product **34b**.

Noticeably, the potential application of this reaction was briefly demonstrated by a challenging gram-scale reaction of heteroarene **1b** with 3.0 equiv of cyclododecane, and delightfully the desired product **7b** could be obtained in 54% isolated yield (**Scheme 3.2**).

Scheme 3.2 Gram-scale synthesis of 7b.

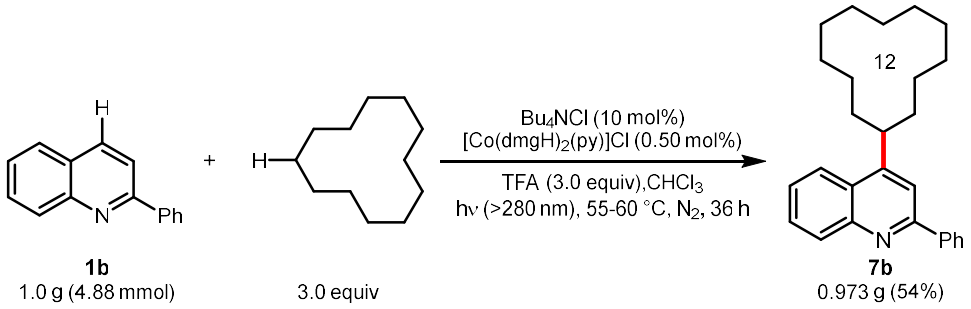

Figure 3.5 Substrate scope of heteroarene.

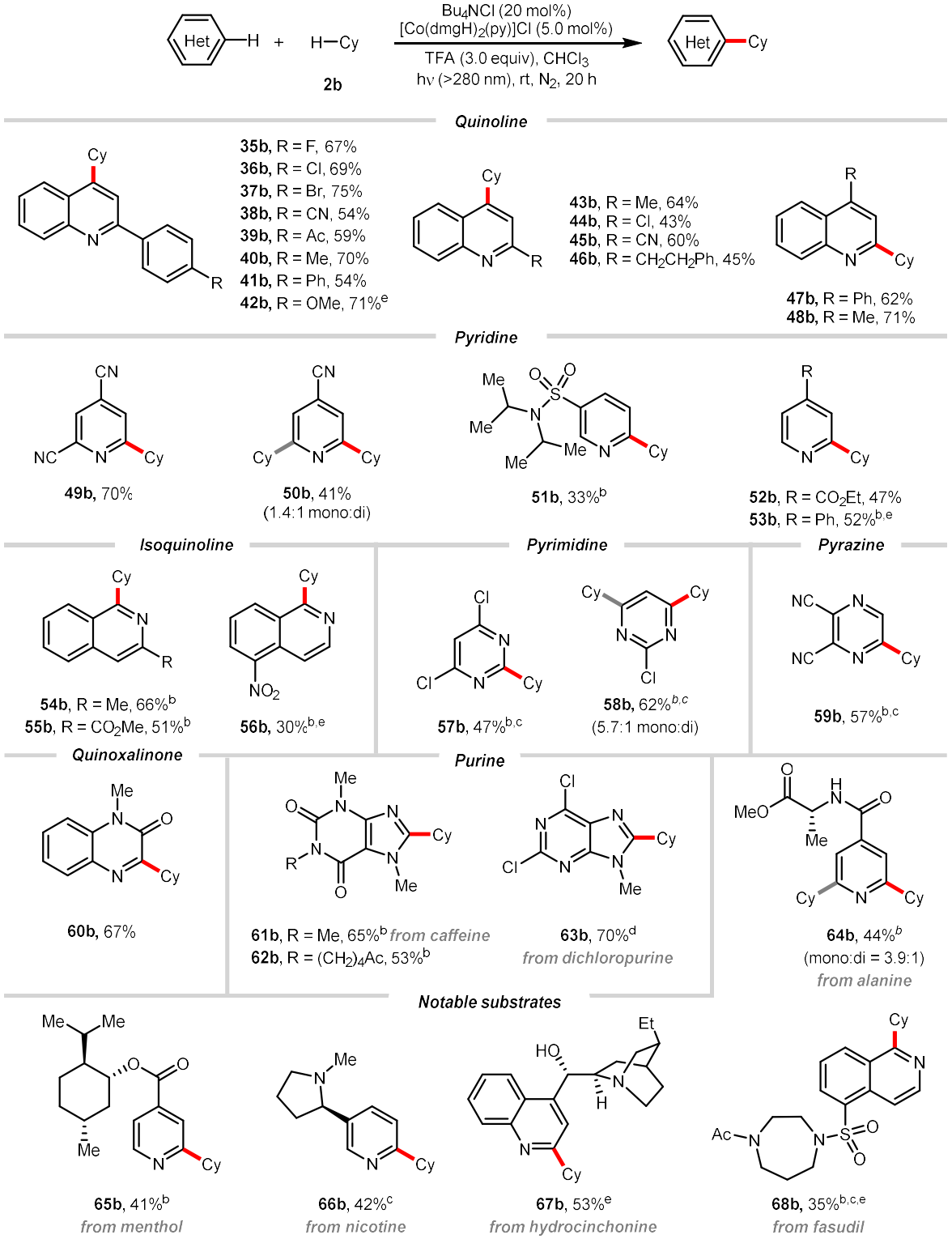

[a]Reaction conditions: heteroarene (0.20 mmol, 1.0 equiv), **2b** (0.60 mL), Bu_4NCl (40 μmol, 20 mol%), $[Co(dmgH)_2(py)]Cl$ (10 μmol, 5.0 mol%), and TFA (0.60 mmol, 3.0 equiv) in $CHCl_3$ (1.5 mL) and irradiated by

>280 nm light at room temperature under nitrogen for 20 h, unless otherwise specified, and the yields were isolated ones. [b]The reaction was run for 36 h. [c]4.0 equiv of TFA was used. [d]5.0 equiv of TFA was used. [e]The reaction was heated to 55-60 °C.

Further substrate and functional group tolerance were examined by coupling various heterocycles with cyclohexane (**2b**). Satisfyingly, many substituents such as halides, cyano, acetyl, ester, amino, nitro, and sulfonamide are compatible with our method, as shown in **Figure 3.5**. Quinoline, pyridine, and isoquinoline moieties afforded the corresponding alkylated products with up to 75% yield (**35b** to **56b**); other heterocycles like pyrimidine (**57b** and **58b**), pyrazine (**59b**), quinoxalinone (**60b**), and purine (**61b** to **63b**) were also proven to be feasible. Complex heterocycles bearing different aliphatic C(sp^3)-H bonds were examined, including alanine and menthol-derived pyridines (**64b** and **65b**), and nicotine (**66b**) were successfully turned into the desired products with moderate yields. Alkylation of hydrocinchonine, a common chiral ligand candidate in synthetic chemistry, gave an appreciable yield of the product (**67b**) with its hydroxy group preserved. After protecting its amino group, fasudil, a potent Rho-kinase inhibitor and vasodilator, also provided the desired product (**68b**).

3.4 Mechanistic studies

A series of experiments were conducted to gain insight into this transformation. We found radical quenchers, 2,2,6,6-tetramethylpiperidine 1-oxyl (TEMPO) and 3,5-di-*tert*-4-butylhydroxytoluene (BHT), significantly suppressed the product formation. Noticeably, the radical adduct **69b** was detected by GC-MS in the case of TEMPO, indicating an R•-involved mechanistic scenario (**Scheme 3.3A**). A radical trapping experiment also evidenced the involvement of R• by subjecting the alkene **70b** to our alkane arylation reaction with heteroarene **1b** and Bu_4NCl (**Scheme 3.3B**) in which a cycloalkylated product **71b** was

isolated. All these results supported the presence of R• in the plausible mechanism.

Scheme 3.3 Mechanistic studies (1).

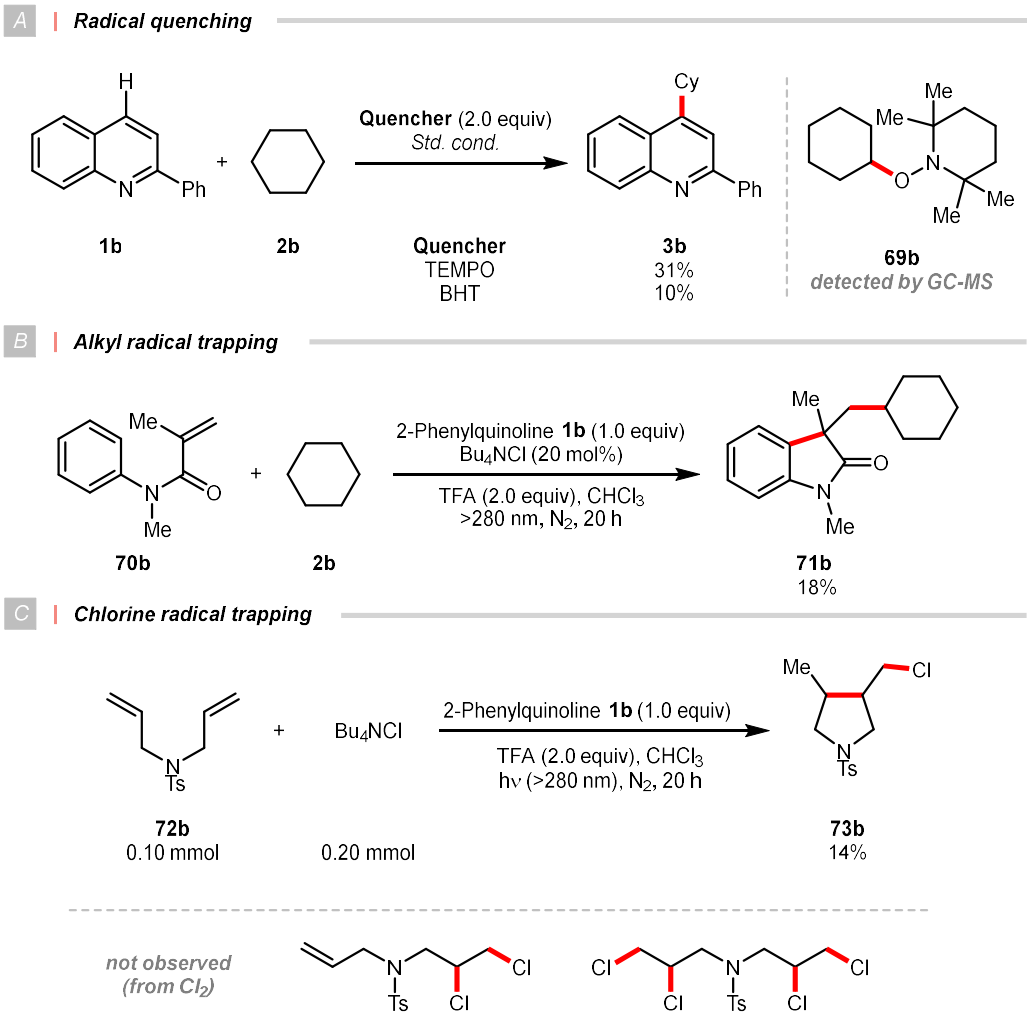

To probe more details of the chlorine species, a diallyl sulfonamide **72b** was submitted to the alkylation reaction of **1b** with a stoichiometric amount of Bu_4NCl. As expected, a cyclochlorinated compound **73b** was isolated, suggesting the formation of Cl• in our case (**Scheme 3.3C**). According to some literature,[58, 38] Cl_2 might not be an active intermediate in our system as the characteristic alkenyl dichlorination products were not observed. On the

contrary, no cyclochlorination occurred when the same diallyl compound **72b** was irradiated with Bu_4NCl and cobaloxime catalyst in the absence of heteroarene and chlorinated solvent, indicating that the LMCT-induced Cl• generation by the cobaloxime catalyst might not be operative in this reaction.

Scheme 3.4 Mechanistic studies (2).

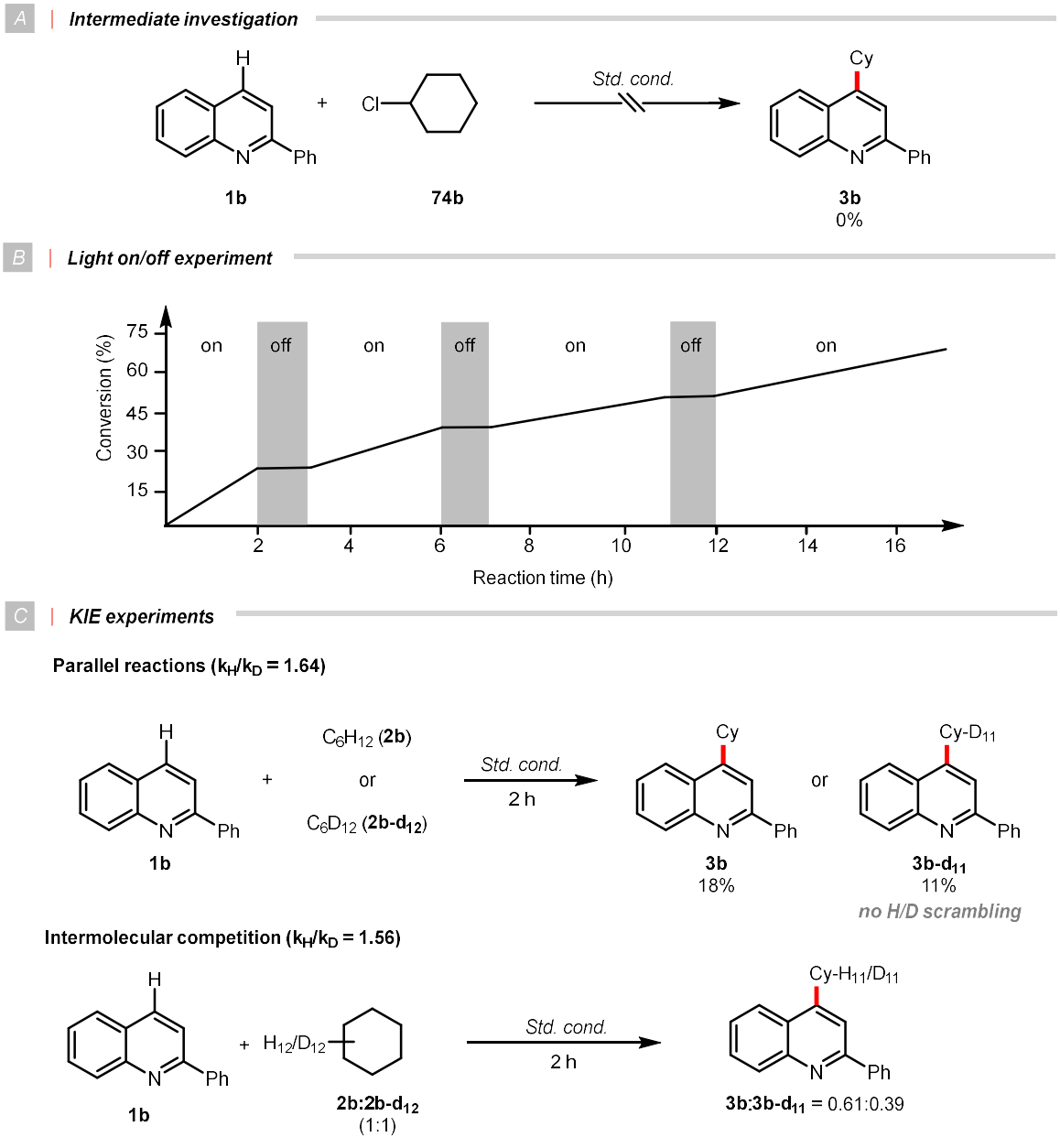

D | ***H_2 detection***

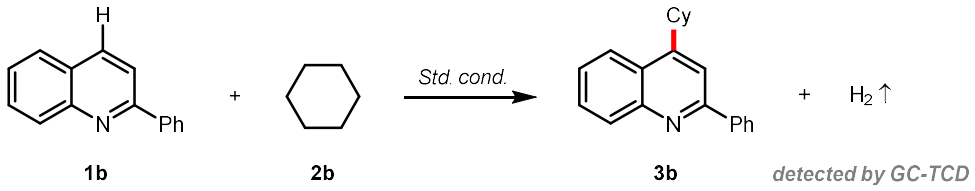

Scheme 3.5, UV-vis spectra and fluorescence quenching of 4-methylquinoline (lepidine), with and without acid.

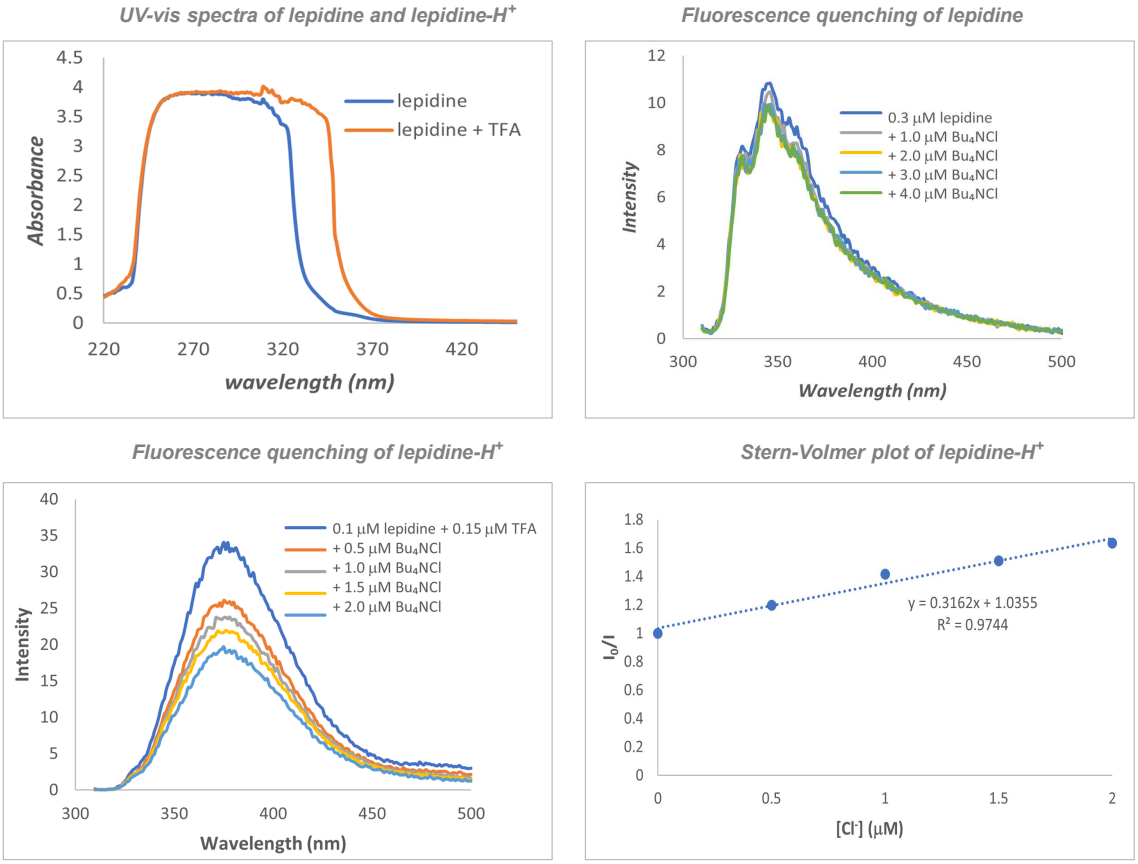

Upper left: UV-vis spectra of 50 mM lepidine and lepidine-TFA (1:1) in $CHCl_3$. Upper right: fluorescence quenching of 0.3 μM lepidine with Bu_4NCl in $CHCl_3$. Bottom left: fluorescence quenching of 0.10 μM lepidine-H^+ with Bu_4NCl in $CHCl_3$. Bottom right: Stern-Volmer plot of 0.10 μM lepidine-H^+ with Bu_4NCl in $CHCl_3$.

No reaction was observed when cyclohexane (**2b**) was replaced with cyclohexyl chloride (**74b**), indicating that **74b** was not an active intermediate in generating the cyclohexyl radical

through C-Cl bond cleavage (**Scheme 3.4A**). The light on-and-off experiment showed that continuous irradiation was essential for product formation (**Scheme 3.4B**). Besides, both parallel and competing kinetic isotope effects were examined, giving k_H/k_D = 1.64 and 1.56, respectively, which suggested that the alkyl C-H cleavage might not be the rate-determining step (**Scheme 3.4C**).[9]

Moreover, the H_2 evolution was confirmed by the GC-TCD analysis (**Scheme 3.4D**). From the UV-vis spectra and fluorescence quenching experiments, strong interaction between excited lepidine and Cl^- was observed only in the presence of an acid, emphasizing the indispensable role of TFA in protonating the heteroarene for Cl^- oxidation (**Scheme 3.5**). All these experiments surmised radical generation (R• and Cl•) and H_2 evolution reaction pathways.

3.5 Conclusions and outlook

We have developed a new approach toward photoinduced dehydrogenative Minisci alkylation, which couples a wide range of heterocycles with strong aliphatic C-H bonds. At the same time, the merger of catalytic Cl• generation and hydrogen evolution granted simple and chemical oxidant-free reaction conditions. Mechanistic studies supported the direct Cl• generation via the SET between Cl^- and excited heteroarene. As a powerful platform, complex molecules bearing diverse C(sp^3)-H patterns and functional groups were feasible for alkylations, and a large-scale synthesis was demonstrated with low alkane loading.

As a logical extension based on the current mechanistic framework, this coupling reaction should be realized under visible light irradiation with the catalytic introduction of a more conjugated heteroarene. Indeed, 43% of the alkylated heteroarene **3b** could be furnished with 5.0 mol% of 2,4-diphenylquinoline as the photocatalyst.[51]

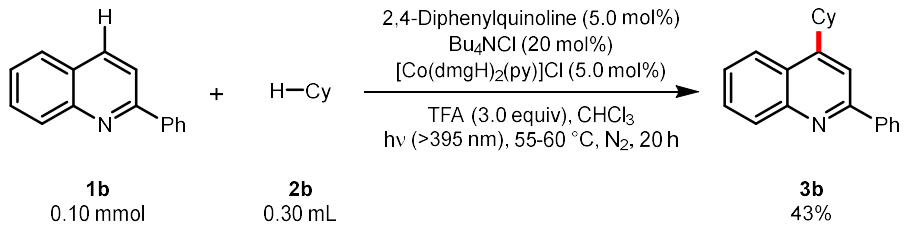

1b
0.10 mmol

2b
0.30 mL

3b
43%

We believed these encouraging results could enlighten more visible light-promoted Cl• generation strategies for coupling reactions, advance the excited arene chemistry, and inspire future cross-dehydrogenative coupling designs.

3.6 Author contributions

Prof. Chao-Jun Li and Dr. Jianbin Li designed the project. I carried out all the experiments in this chapter with guidance from Prof. Chao-Jun Li and Dr. Jianbin Li. The manuscript was prepared by me and revised by Prof. Chao-Jun Li and Dr. Jianbin Li. All the authors approved the publication of this work.

3.7 Experimental section

Figure 3.6 The general reaction setup.

With cooling water to maintain at room temperature, or heating with a hotplate to reach 55-60 °C. The light source is 3.0 to 5.0 cm away from the water bath, with a 280 nm optical filter to block wavelengths below.

General procedure A (coupling with liquid alkane). To a 10 mL pyrex microwave tube equipped with a Teflon-coated magnetic stirring bar were added heteroarene (0.20 mmol, 1.0 equiv) and $[Co(dmgH)_2(py)]Cl$ (4.0 mg, 10 μmol, 5.0 mol%). The tube was sealed with a rubber septum, evacuated and backfilled with argon three times before liquid alkane (0.60 mL) was injected. To the mixture were then sequentially added Bu_4NCl (11.1 mg, 40 μmol, 20 mol%), $CHCl_3$ (1.5 mL), and TFA (46 μL, 0.60 mmol, 3.0 equiv) in the glovebox and the tube was again sealed with an aluminum cap with a septum, which was then taken out from the glovebox and stirred at room temperature under a 300 W Xe lamp (with a 280 nm filter) irradiation. After 20-36 h, the reaction mixture was basified with sat $NaHCO_3$, extracted with EtOAc, filtered through a short pad of $MgSO_4$, and concentrated to afford the crude product. The product was isolated with preparative thin-layer chromatography.

General procedure B (coupling with solid alkane). To a 10 mL pyrex microwave tube equipped with a Teflon-coated magnetic stirring bar were added heteroarene (0.20 mmol, 1.0 equiv), solid alkane (2.0 mmol, 10 equiv), and $[Co(dmgH)_2(py)]Cl$ (4.0 mg, 10 μmol, 5.0 mol%). The tube was sealed with a rubber septum, evacuated and backfilled with argon three times. To the mixture were then sequentially added Bu_4NCl (11.1 mg, 40 μmol, 20 mol%), $CHCl_3$ (1.5 mL), and TFA (46 μL, 0.60 mmol, 3.0 equiv) in the glovebox and the tube was again sealed with an aluminum cap with a septum, which was then taken out from the glovebox and stirred at room temperature under a 300 W Xe lamp (with a 280 nm filter) irradiation. After 20-36 h, the reaction mixture was basified with sat $NaHCO_3$, extracted with EtOAc, filtered through a short pad of $MgSO_4$, and concentrated to afford the crude product. The product was isolated with preparative thin-layer chromatography.

Gram scale synthesis of 7b. To a 25 mL Schlenk tube equipped with a Teflon-coated magnetic stirring bar were added heteroarene **1b** (1.0 g, 4.9 mmol, 1.0 equiv), cyclododecane (2.5 g, 14.6 mmol, 3.0 equiv), and $[Co(dmgH)_2(py)]Cl$ (9.7 mg, 24.1 μmol, 0.5 mol%). The tube was evacuated and backfilled with argon three times. To the mixture were then sequentially added Bu_4NCl (136 mg, 0.98 mmol, 10 mol%), $CHCl_3$ (8.0 mL), and TFA (1.1 mL, 14.6 mmol, 3.0 equiv) in the glovebox, and then sealed with a screw cap. The reaction tube was taken out from the glovebox and stirred at 55-60 °C under irradiation of a 300 W Xe lamp (with a 280 nm filter). After 72 h, the reaction mixture was basified with sat $NaHCO_3$ (aq), extracted with EtOAc, dried over $MgSO_4$, and concentrated to afford the crude product. The product was isolated by column chromatography using EtOAc/Hexane (0-3%) to afford a pale-yellow solid (0.975 g, 54%).

Figure 3.7 Gram-scale synthesis of heteroarene 7b.

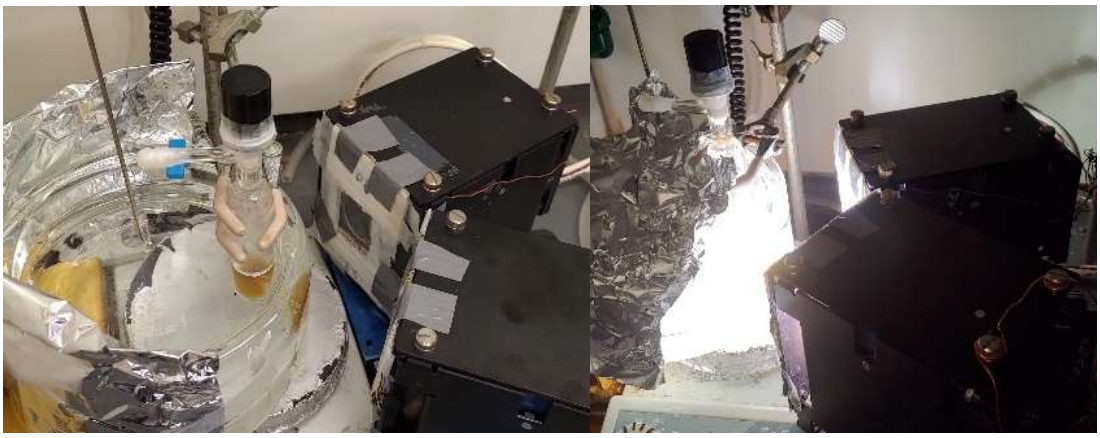

3.8 Characterization data for compounds

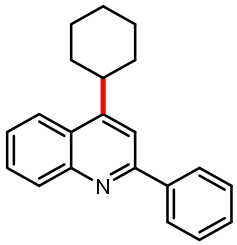

4-cyclohexyl-2-phenylquinoline (3b). Following the general procedure A, the product was isolated with Hex/EtOAc (10:1) on preparative thin-layer chromatography. white solid (42.5 mg, 74%). **^{1}H NMR** (500 MHz, $CDCl_3$) δ 8.21 (d, *J* = 8.4 Hz, 1H), 8.18 - 8. 15 (m, 2H), 8.12 (d, *J* = 8.4 Hz, 1H), 7.78 (s, 1H), 7.75 - 7.70 (m, 1H), 7.58 - 7.52 (m, 3H), 7.50 - 7.45 (m, 1H), 3.46 - 3.35 (m, 1H), 2.15 - 2.07 (m, 2H), 2.02 - 1.95 (m, 2H), 1.94 - 1.87 (m, 1H), 1.73 - 1.55 (m, 4H), 1.47 - 1.35 (m, 1H). **^{13}C NMR** (125 MHz, $CDCl_3$) δ 157.4, 153.9, 148.6, 140.3, 130.7, 129.1, 129.0, 128.8, 127.6, 125.9, 122.9, 115.5, 39.1, 33.7, 27.0, 26.4. **GC-MS** (EI, m/z) for $C_{21}H_{21}N$ Calcd: 287.2, found: 287.1. Spectra data are consistent with the reported literature.[38]

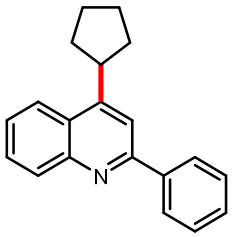

4-cyclopentyl-2-phenylquinoline (4b). Following the general procedure A, the product was isolated with Hex/EtOAc (10:1) on preparative thin-layer chromatography. Colorless oil (43.2 mg, 79%). **^{1}H NMR** (500 MHz, $CDCl_3$) δ 8.22 (d, *J* = 7.1 Hz, 1H), 8.19 - 8.13 (m, 3H), 7.81 (s, 1H), 7.76 - 7.70 (m, 1H), 7.58 - 7.52 (m, 3H), 7.51 - 7.46 (m, 1H), 3.90 - 3.80 (m, 1H), 2.35 - 2.23 (m, 2H), 2.01 - 1.80 (m, 6H). **^{13}C NMR** (125 MHz, $CDCl_3$) δ 157.3, 152.8, 148.6, 140.3, 130.6, 129.1, 129.0, 128.8, 127.6, 126.8, 125.8, 123.6, 115.2, 40.8, 33.4, 25.5. **GC-MS** (EI, m/z) for $C_{20}H_{19}N$ Calcd: 273.2, found: 273.1. Spectra data are consistent with the reported literature.[38]

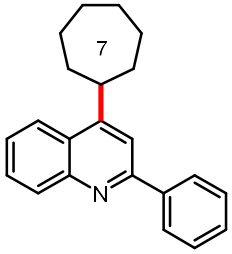

4-cycloheptyl-2-phenylquinoline (5b). Following the general procedure A, the product was isolated with Hex/EtOAc (10:1) on preparative thin-layer chromatography. Colorless oil (44.0 mg, 73%). **^{1}H NMR** (500 MHz, $CDCl_3$) δ 8.22 (d, *J* = 8.4 Hz, 1H), 8.19 - 8.15 (m, 2H), 8.11 (dd, *J* = 8.6, 1.4 Hz, 1H), 7.79 (s, 1H), 7.75 - 7.70 (m, 1H), 7.59 - 7.52 (m, 3H), 7.51 - 7.46 (m, 1H), 3.61 - 3.52 (m, 1H), 2.19 - 2.10 (m, 2H), 2.00 - 1.79 (m, 6H), 1.79 - 1.67 (m, 4H). **^{13}C NMR** (125 MHz, $CDCl_3$) δ 157.3, 155.9, 148.6, 140.3, 130.7, 129.1, 129.0, 128.8, 127.6, 125.9, 125.6, 123, 115.8, 40.8, 35.9, 27.9, 27.6. **GC-MS** (EI, m/z) for $C_{22}H_{23}N$ Calcd: 301.2, found: 301.1. Spectra data are consistent with the reported literature.[38]

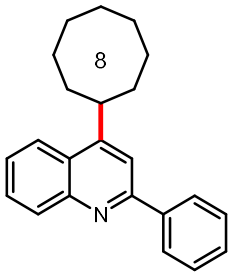

4-cyclooctyl-2-phenylquinoline (6b). Following the general procedure A, the product was isolated with Hex/EtOAc (10:1) on preparative thin-layer chromatography. Colorless oil (32.8 mg, 52%). **^{1}H NMR** (500 MHz, $CDCl_3$) δ 8.22 (d, *J* = 8.8 Hz, 1H), 8.20 - 8.14 (m, 2H), 8.12 (d, *J* = 8.7 Hz, 1H), 7.78 (s, 1H), 7.75 - 7.68 (m, 1H), 7.60 - 7.51 (m, 3H), 7.51 - 7.45 (m, 1H), 3.74 - 3.61 (m, 1H), 2.10 - 1.96 (m, 4H), 1.95 - 1.85 (m, 2H), 1.85 - 1.73 (m, 8H). **^{13}C NMR** (125 MHz, $CDCl_3$) δ 157.3, 156.4, 148.7, 140.3, 130.8, 129.1, 129.0, 128.8, 127.6, 125.9, 125.6, 123.1, 116.3, 33.8, 26.9, 26.6, 26.2. **GC-MS** (EI, m/z) for $C_{23}H_{25}N$ Calcd: 315.2, found: 315.2. Spectra data are consistent with the reported literature.[38]

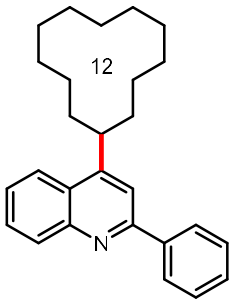

4-cyclododecyl-2-phenylquinoline (7b). Following the general procedure B, the reaction was run at 55-60 °C for 36 h,the product was isolated with Hex/EtOAc (10:1) on preparative thin-layer chromatography. white solid (52.8 mg, 71%). **^{1}H NMR** (500 MHz, $CDCl_3$) δ 8.24 (d, *J* = 8.4 Hz, 1H), 8.22 - 8.12 (m, 3H), 7.79 (s, 1H), 7.77 - 7.70 (m, 1H), 7.61 - 7.54 (m, 3H), 7.53 - 7.47 (m, 1H), 3.80 - 3.66 (m, 1H), 2.06 - 1.95 (m, 2H), 1.83 - 1.73 (m, 2H), 1.65 - 1.38 (m, 16H), 1.38 - 1.26 (m, 2H). **^{13}C NMR** (125 MHz, $CDCl_3$) δ 157.1, 153.9, 148.7, 140.3, 130.8,

129.1, 129.0, 128.8, 127.7, 126.6, 126.0, 122.9, 116.7, 34.6, 30.2, 24.1, 23.6, 23.5, 22.6. **GC-MS** (EI, m/z) for $C_{27}H_{33}N$ Calcd: 371.3.2, found: 371.3. Spectra data are consistent with the reported literature.[38]

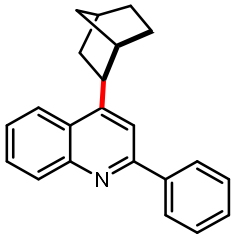

4-bicyclo[2.2.1]heptan-2-yl)-2-phenylquinoline (8b). Following the general procedure B, the reaction was run for 36 h, and the product was isolated with Hex/EtOAc (10:1) on preparative thin-layer chromatography. Colorless oil (41.9 mg, 70%). **^{1}H NMR** (500 MHz, $CDCl_3$) δ 8.21 (d, *J* = 8.5 Hz, 1H), 8.18 - 8.14 (m, 2H), 8.09 (d, *J* = 8.4 Hz, 1H), 7.77 (s, 1H), 7.75 - 7.69 (m, 1H), 7.59 - 7.52 (m, 3H), 7.52 - 7.46 (m, 1H), 3.48 - 3.41 (m, 1H), 2.70 (d, *J* = 4.1 Hz, 1H), 2.52 - 2.43 (m, 1H), 2.12 - 2.03 (m, 1H), 1.85 - 1.66 (m, 4H), 1.63 - 1.54 (m, 1H), 1.51 - 1.44 (m, 1H), 1.43 - 1.37 (m, 1H). **^{13}C NMR** (125 MHz, $CDCl_3$) δ 157.2, 153.3, 148.7, 140.4, 130.5, 129.1, 129.0, 128.8, 127.7, 126.5, 125.8, 123.9, 114.9, 43.0, 41.3, 39.3, 37.0, 36.7, 30.3, 29.1. **GC-MS** (EI, m/z) for $C_{22}H_{21}N$ Calcd: 299.2, found: 299.1. Spectra data are consistent with the reported literature.[38]

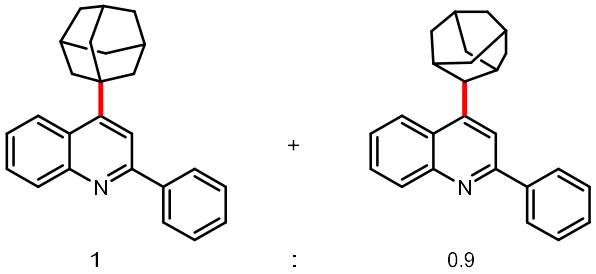

(4-adamantan-1-yl)-2-phenylquinoline (9b) and 4-adamantan-2-yl)-2-

phenylquinoline (9b'), 1:0.9 congeners. Following the general procedure B, the reaction was run at 55-60 °C for 36 h, and the product was isolated with Hex/EtOAc (10:1) on preparative thin-layer chromatography. Colorless oil (27.8 mg, 41%). **^{1}H NMR** (500 MHz, $CDCl_3$) δ 8.62 (d, *J* = 8.7 Hz, 1H), 8.26 - 8.12 (m, 3H+2.7H), 8.03 (s, 0.9H), 7.94 (d, *J* = 8.4 Hz, 0.9H), 7.80 (s, 1H), 7.71 - 7.63 (m, 1H+0.9H), 7.58 - 7.43 (m, 3H+2.7H), 3.79 (s, 0.9H), 2.50 (s, 1.8H), 2.40 - 2.34 (m, 6H), 2.28 - 1.69 (m, 9H+10.8H). **^{13}C NMR** (125 MHz, $CDCl_3$) δ ^{13}C NMR (125 MHz, $CDCl_3$) δ 157.2, 156.9, 156.0, 151.8, 149.8, 148.8, 140.4, 131.7, 130.9, 129.1, 129.1, 128.8, 128.8, 128.8, 128.2, 127.6, 127.6, 126.5, 126.1, 125.8, 125.7, 124.6, 123.8, 117.4, 116.4, 45.5, 42.3, 40.1, 38.9, 37.8, 37.0, 33.0, 32.7, 29.1, 28.3, 27.7. **HRMS** ($M+H^+$) for $C_{25}H_{26}N$ Calcd: 340.2060, found: 340.2054. The compound was not reported.

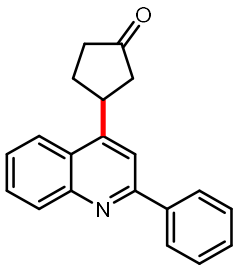

3-(2-phenylquinolin-4-yl)cyclopentan-1-one (10b). Following the general procedure A, the reaction was run at 55-60 °C for 36 h, and the product was isolated with Hex/EtOAc (5:2) on preparative thin-layer chromatography. Colorless oil (27.0 mg, 47%). **^{1}H NMR** (500 MHz, $CDCl_3$) δ 8.25 (d, *J* = 8.7 Hz, 1H), 8.18 - 8.13 (m, 2H), 8.10 (d, *J* = 7.8 Hz, 1H), 7.81 - 7.74 (m, 2H), 7.64 - 7.59 (m, 1H), 7.59 - 7.53 (m, 2H), 7.53 - 7.47 (m, 1H), 4.33 - 4.23 (m, 1H), 2.94 - 2.85 (m, 1H), 2.70 - 2.53 (m, 3H), 2.53 - 2.43 (m, 1H), 2.34 - 2.23 (m, 1H). **^{13}C NMR** (125 MHz, $CDCl_3$) δ 217.1, 157.3, 149.1, 148.7, 139.7, 130.9, 129.5, 129.5, 128.9, 127.6, 126.5, 126.0, 122.8, 114.9, 45.0, 38.1, 37.4, 29.8. **GC-MS** (EI, m/z) for $C_{20}H_{17}NO$ Calcd: 287.1, found: 287.0. Spectra data are consistent with the reported literature.[59]

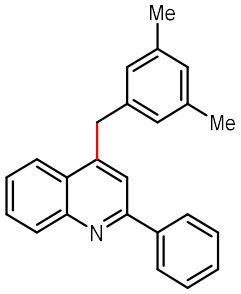

4-(3,5-dimethylbenzyl)-2-phenylquinoline (11b). Following the general procedure A, the product was isolated with Hex/EtOAc (10:1) on preparative thin-layer chromatography. Colorless oil (39.5 mg, 61%). **^{1}H NMR** (500 MHz, $CDCl_3$) δ 8.23 (d, *J* = 7.2 Hz, 1H), 8.19 - 8.14 (m, 2H), 8.06 (d, *J* = 7.8 Hz, 1H), 7.76 - 7.69 (m, 2H), 7.57 - 7.46 (m, 4H), 6.91 (s, 1H), 6.88 (s, 2H), 4.45 (s, 2H), 2.30 (s, 6H). **^{13}C NMR** (125 MHz, $CDCl_3$) δ 157.2, 148.6, 147.3, 139.8, 138.7, 138.3, 130.4, 129.3, 129.3, 128.8, 128.3, 127.6, 126.7, 126.7, 126.3, 123.9, 120.0, 38.5, 21.3. **GC-MS** (EI, m/z) for $C_{24}H_{21}N$ Calcd: 323.2, found: 323.1. Spectra data are consistent with the reported literature.[38]

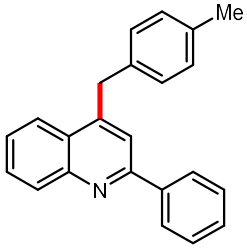

4-(4-methylbenzyl)-2-phenylquinoline (12b). Following the general procedure A, the product was isolated with Hex/EtOAc (10:1) on preparative thin-layer chromatography. Colorless oil (26.0 mg, 42%). **^{1}H NMR** (500 MHz, $CDCl_3$) δ 8.21 (d, *J* = 8.2 Hz, 1H), 8.15 - 8.11 (m, 2H), 8.05 (d, *J* = 9.0 Hz, 1H), 7.75 - 7.70 (m, 1H), 7.68 (s, 1H), 7.56 - 7.50 (m, 3H), 7.49 - 7.44 (m, 1H), 7.28 (s, 1H), 7.19 - 7.11 (m, 4H), 4.49 (s, 2H), 2.35 (s, 3H). **^{13}C NMR** (125 MHz, $CDCl_3$) δ 157.2, 148.6, 147.3, 139.8, 136.2, 135.7, 130.5, 129.4, 129.3, 129.2, 128.8, 128.7,

127.6, 126.6, 126.3, 123.8, 119.9, 38.2, 21.1. **GC-MS** (EI, m/z) for $C_{23}H_{19}N$ Calcd: 309.2, found: 309.1. Spectra data are consistent with the reported literature.[38]

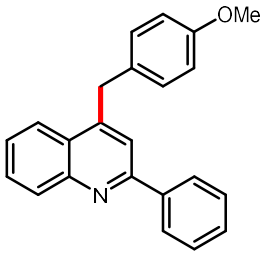

4-(4-methoxybenzyl)-2-phenylquinoline (13b). Following the general procedure A, the product was isolated with Hex/EtOAc (10:1) on preparative thin-layer chromatography. Yellow solid (25.4 mg, 39%). **^{1}H NMR** (500 MHz, $CDCl_3$) δ 8.22 (d, *J* = 7.9 Hz, 1H), 8.16 - 8.10 (m, 2H), 8.06 (dd, *J* = 8.4, 1.4 Hz, 1H), 7.77 - 7.70 (m, 1H), 7.65 (s, 1H), 7.56 - 7.50 (m, 3H), 7.50 - 7.44 (m, 1H), 7.19 (d, *J* = 8.6 Hz, 2H), 6.88 (d, *J* = 8.7 Hz, 2H), 4.47 (s, 2H), 3.82 (s, 3H). **^{13}C NMR** (125 MHz, $CDCl_3$) δ 158.3, 157.2, 148.6, 147.5, 139.8, 130.7, 130.5, 129.9, 129.3, 129.3, 128.8, 127.6, 126.6, 126.3, 123.7, 119.7, 114.2, 55.3, 37.7. **HRMS** ($M+H^+$) for $C_{23}H_{20}NO$ Calcd: 326.1539, found: 326.1543. The compound was not reported.

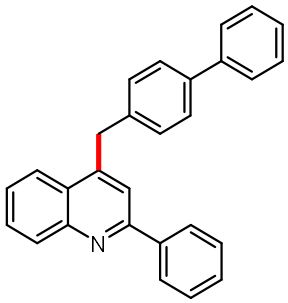

4-([1,1'-biphenyl]-4-ylmethyl)-2-phenylquinoline (14b). Following the general procedure B, the product was isolated with Hex/EtOAc (10:1) on preparative thin-layer chromatography. Yellow solid (26.0 mg, 35%). **^{1}H NMR** (500 MHz, $CDCl_3$) δ 8.25 (d, *J* = 8.0 Hz, 1H), 8.18 - 8.14 (m, 2H), 8.09 (d, *J* = 7.7, 1H), 7.78 - 7.72 (m, 2H), 7.64 - 7.51 (m, 7H), 7.51 -

7.42 (m, 3H), 7.40 - 7.31 (m, 3H), 4.57 (s, 2H). **^{13}C NMR** (125 MHz, $CDCl_3$) δ 157.2, 148.6, 146.9, 140.7, 139.8, 139.6, 137.9, 130.5, 129.4, 129.3, 129.3, 128.8, 128.8, 127.6, 127.5, 127.3, 127.0, 126.6, 126.4, 123.8, 120.0, 38.2. **HRMS** ($M+H^+$) for $C_{28}H_{22}N$ Calcd: 372.1747, found: 372.1745. The compound was not reported.

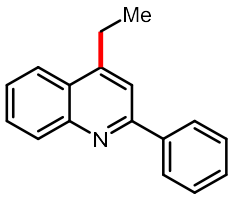

4-ethyl-2-phenylquinoline (15b). Following the general procedure A, the product was isolated with Hex/EtOAc (10:1) on preparative thin-layer chromatography. Colorless oil (35.9 mg, 77%). **^{1}H NMR** (500 MHz, $CDCl_3$) δ 8.24 - 8.16 (m, 3H), 8.07 (dd, *J* = 8.3, 1.3 Hz, 1H), 7.78 - 7.70 (m, 2H), 7.59 - 7.52 (m, 3H), 7.52 - 7.46 (m, 1H), 3.21 (q, *J* = 0.8 Hz, 2H), 1.48 (t, *J* = 7.6 Hz, 3H). **^{13}C NMR** (125 MHz, $CDCl_3$) δ 157.3, 150.5, 148.4, 140.1, 130.5, 129.2, 129.2, 128.8, 127.6, 126.4, 126.0, 123.3, 117.8, 25.4, 14.3. **GC-MS** (EI, m/z) for $C_{17}H_{15}N$ Calcd: 233.1, found: 233.1. Spectra data are consistent with the reported literature.[60]

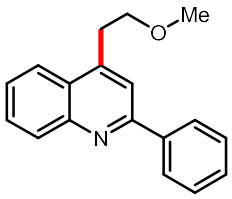

4-(2-methoxyethyl)-2-phenylquinoline (16b). Following the general procedure A, the product was isolated with Hex/EtOAc (10:1) on preparative thin-layer chromatography. Colorless oil (38.4 mg, 73%). **^{1}H NMR** (500 MHz, $CDCl_3$) δ 8.23 - 8.16 (m, 3H), 8.08 (d, *J* = 8.4 Hz, 1H), 7.80 (s, 1H), 7.77 - 7.71 (m, 1H), 7.60 - 7.53 (m, 3H), 7.51 - 7.46 (m, 1H), 3.84 (t, *J* = 7.0 Hz, 2H), 3.45 (t, *J* = 7.0 Hz, 2H), 3.43 (s, 3H). **^{13}C NMR** (125 MHz, $CDCl_3$) δ 157.1, 148.5,

145.4, 139.8, 130.6, 129.3, 129.2, 128.8, 127.6, 126.7, 126.2, 123.3, 119.5, 72.1, 58.9, 32.8. **HRMS** ($M+H^+$) for $C_{18}H_{18}NO$ Calcd: 264.1383, found: 264.1371. The compound was not reported.

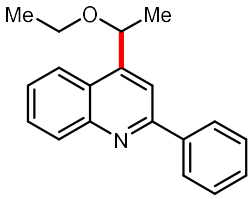

4-(1-ethoxyethyl)-2-phenylquinoline (17b). Following the general procedure A, the reaction was run with 1.2 equiv of TFA for 36 h, and the product was isolated with Hex/EtOAc (10:1) on preparative thin-layer chromatography. Colorless oil (33.6 mg, 66%). **^{1}H NMR** (500 MHz, $CDCl_3$) δ 8.27 - 8.19 (m, 3H), 8.13 (d, *J* = 8.4 Hz, 1H), 8.03 (s, 1H), 7.77 - 7.72 (m, 1H), 7.59 - 7.54 (m, 3H), 7.52 - 7.47 (m, 1H), 5.22 (q, *J* = 6.6 Hz, 1H), 3.58 - 3.49 (m, 2H), 1.67 (d, *J* = 6.6 Hz, 3H), 1.31 (t, *J* = 7.0 Hz, 3H). **^{13}C NMR** (125 MHz, $CDCl_3$) δ 157.4, 150.3, 148.7, 139.8, 130.7, 129.3, 129.2, 128.8, 127.6, 126.1, 125.1, 122.9, 115.4, 74.6, 64.8, 23.5, 15.6. **GC-MS** (EI, m/z) for $C_{19}H_{19}NO$ Calcd: 277.1, found: 277.1. Spectra data are consistent with the reported literature.[38]

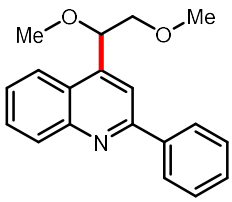

4-(1,2-dimethoxyethyl)-2-phenylquinoline (18b). Following the general procedure A, the reaction was run with 1.2 equiv of TFA for 36 h, and the product was isolated with Hex/EtOAc (10:1) on preparative thin-layer chromatography. Colorless oil (39.3 mg, 67%). **^{1}H NMR** (500 MHz, $CDCl_3$) δ 8.28 - 8.21 (m, 3H), 8.13 (d, *J* = 6.7 Hz, 1H), 8.04 (s, 1H), 7.79 -

7.74 (m, 1H), 7.62 - 7.54 (m, 3H), 7.53 - 7.47 (m, 1H), 5.25 (dd, *J* = 7.7, 3.0 Hz, 1H), 3.79 - 3.67 (m, 2H), 3.47 (s, 6H). **^{13}C NMR** (125 MHz, $CDCl_3$) δ 157.2, 148.7, 144.8, 139.6, 130.8, 129.5, 129.4, 128.9, 127.6, 126.5, 125.4, 122.6, 116.7, 80.1, 76.5, 59.4, 57.8. **GC-MS** (EI, m/z) for $C_{19}H_{19}NO_2$ Calcd: 293.1, found: 293.1. Spectra data are consistent with the reported literature.[38]

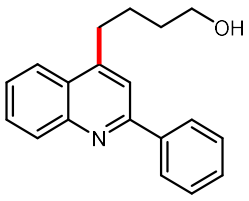

4-(2-phenylquinolin-4-yl)butan-1-ol (19b). Following the general procedure A, the reaction was run with 1.2 equiv of TFA, and the product was isolated with Hex/EtOAc (5:3) on preparative thin-layer chromatography. Colorless oil (51.0 mg, 92%). **^{1}H NMR** (500 MHz, $CDCl_3$) δ 8.22 (d, *J* = 8.4 Hz, 1H), 8.16 - 8.12 (m, 2H), 8.06 - 8.00 (m, 1H), 7.75 - 7.67 (m, 2H), 7.57 - 7.51 (m, 3H), 7.50 - 7.44 (m, 1H), 3.75 - 3.62 (m, 2H), 3.20 - 3.08 (m, 2H), 2.04 - 1.84 (m, 3H), 1.77 - 1.67 (m, 2H). **^{13}C NMR** (125 MHz, $CDCl_3$) δ 157.2, 148.9, 148.5, 139.9, 130.4, 129.3, 129.2, 128.8, 127.6, 126.5, 126.1, 123.4, 118.8, 62.4, 32.6, 32.2, 26.3. **GC-MS** (EI, m/z) for $C_{19}H_{19}N$ Calcd: 277.1, found: 277.1. Spectra data are consistent with the reported literature.[38]

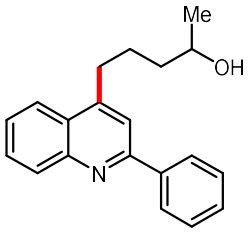

5-(2-phenylquinolin-4-yl)pentan-2-ol (20b). Following the general procedure A, the reaction was run with 2.0 equiv of TFA, and the product was isolated with Hex/EtOAc (5:2) on preparative thin-layer chromatography. Colorless oil (45.5 mg, 78%). **^{1}H NMR** (500 MHz, $CDCl_3$) δ 8.22 (d, *J* = 8.4 Hz, 1H), 8.18 - 8.13 (m, 2H), 8.06 - 8.02 (m, 1H), 7.75 - 7.70 (m, 2H), 7.57 - 7.51 (m, 3H), 7.50 - 7.45 (m, 1H), 3.92 - 3.81 (m, 1H), 3.21 - 3.07 (m, 2H), 2.00 - 1.70 (m, 3H), 1.68 - 1.54 (m, 2H), 1.22 (d, *J* = 6.1 Hz, 3H). **^{13}C NMR** (125 MHz, $CDCl_3$) δ 157.1, 148.9, 148.5, 139.9, 130.5, 129.3, 129.2, 128.8, 127.6, 126.5, 126.1, 123.4, 118.8, 67.8, 39.1, 32.4, 26.3, 23.7. **HRMS** ($M+H^+$) for $C_{20}H_{22}NO$ Calcd: 292.1696, found: 292.1682. The compound was not reported.

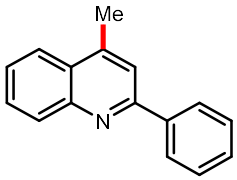

4-methyl-2-phenylquinoline (21b). Following the general procedure A, the reaction was run with 1.2 equiv of TFA, and the product was isolated with Hex/EtOAc (10:1) on preparative thin-layer chromatography. Colorless oil (37.3 mg, 85%). **^{1}H NMR** (500 MHz, $CDCl_3$) δ 8.23 - 8.16 (m, 3H), 8.03 (d, *J* = 7.1 Hz, 1H), 7.77 - 7.72 (m, 2H), 7.60 - 7.53 (m, 3H), 7.51 - 7.46 (m, 1H), 2.80 (s, 3H). **^{13}C NMR** (125 MHz, $CDCl_3$) δ 157.1, 148.2, 144.8, 139.9, 130.3, 129.3, 129.2, 128.8, 127.6, 127.3, 126.0, 123.6, 119.8, 19.0. **GC-MS** (EI, m/z) for $C_{16}H_{13}N$ Calcd: 219.1, found: 219.1. Spectra data are consistent with the reported literature.[51]

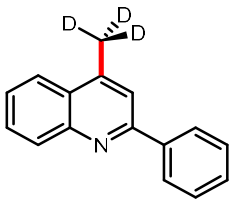

4-(methyl-d_3)-2-phenylquinoline (22b). Following the general procedure A, the product was isolated with Hex/EtOAc (10:1) on preparative thin-layer chromatography. Colorless oil (35.1 mg, 79%). **^{1}H NMR** (500 MHz, $CDCl_3$) δ 8.23 - 8.15 (m, 3H), 8.02 (dd, *J* = 8.4, 1.4 Hz, 1H), 7.78 - 7.71 (m, 2H), 7.60 - 7.51 (m, 3H), 7.51 - 7.45, (m, 1H). **^{13}C NMR** (125 MHz, $CDCl_3$) δ 157.1, 148.2, 144.7, 139.9, 130.3, 129.3, 129.2, 128.8, 127.6, 127.3, 126.0, 123.6, 119.8. HRMS ($M+Na^+$) for $C_{16}H_{10}D_3NNa$ Calcd: 245.1129, found: 245.1125. The compound was not reported.

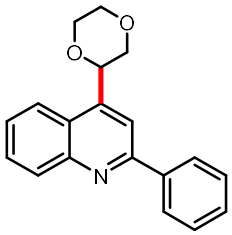

4-(1,4-dioxan-2-yl)-2-phenylquinoline (23b). Following the general procedure A, the reaction was run with 2.0 equiv of TFA, and the product was isolated with Hex/EtOAc (5:1) on preparative thin-layer chromatography. white solid (36.7 mg, 63%). **^{1}H NMR** (500 MHz, $CDCl_3$) δ 8.26 - 8.21 (m, 3H), 8.13 (s, 1H), 8.03 (d, *J* = 8.4 Hz, 1H), 7.78 - 7.73 (m, 1H), 7.60 - 7.53 (m, 3H), 7.52 - 7.47 (m, 1H), 5.45 (dd, *J* = 9.9, 2.0 Hz, 1H), 4.21 (dd, *J* = 11.9, 2.7 Hz, 1H), 4.17 - 4.08 (m, 2H), 3.96 - 3.91 (m, 1H), 3.90 - 3.83 (m, 1H), 3.54 (dd, *J* = 11.9, 9.9 Hz, 1H). **^{13}C NMR** (125 MHz, $CDCl_3$) δ 157.4, 148.3, 144.1, 139.6, 130.8, 129.4, 129.4, 128.8, 127.6, 126.5, 124.2, 122.3, 116.2, 74.4, 72.1, 67.4, 66.7. **GC-MS** (EI, m/z) for $C_{19}H_{17}NO_2$ Calcd: 291.1, found: 291.1. Spectra data are consistent with the reported literature.[38]

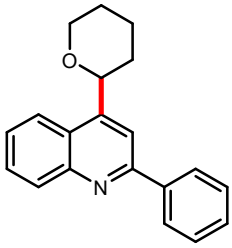

2-phenyl-4-(tetrahydro-2*H*-pyran-2-yl)quinoline (24b). Following the general procedure A, the reaction was run with 2.0 equiv of TFA for 36 h, and the product was isolated with Hex/EtOAc (5:1) on preparative thin-layer chromatography. Colorless oil (41.1 mg, 71%). **^{1}H NMR** (500 MHz, $CDCl_3$) δ 8.26 - 8.19 (m, 3H), 8.09 (s, 1H), 8.01 (d, *J* = 10.1 Hz, 1H), 7.76 - 7.70 (m, 1H), 7.58 - 7.51 (m, 3H), 7.51 - 7.45 (m, 1H), 5.12 (dd, *J* = 11.2, 2.1 Hz, 1H), 4.35 - 4.27 (m, 1H), 3.85 - 3.76 (m, 1H), 2.18 - 2.11 (m, 1H), 2.09 - 2.01 (m, 1H), 1.92 - 1.79 (m, 2H), 1.76 - 1.64 (m, 2H). **^{13}C NMR** (125 MHz, $CDCl_3$) δ 157.5, 149.2, 148.5, 139.9, 130.7, 129.2, 129.1, 128.7, 127.7, 126.0, 124.3, 122.9, 115.4, 76.4, 69.3, 33.8, 26.0, 24.1. **GC-MS** (EI, m/z) for $C_{20}H_{19}NO$ Calcd: 289.1, found: 289.1. Spectra data are consistent with the reported literature.[38]

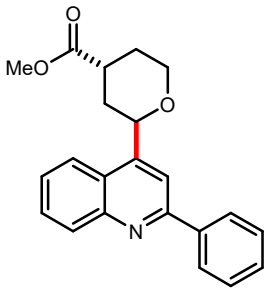

methyl 2-(*trans*-2-phenylquinolin-4-yl)tetrahydro-2*H*-pyran-4-carboxylate (25b). Following the general procedure A, the reaction was run with 2.0 equiv of TFA for 36 h, and the product was isolated with Hex/EtOAc (5:1) on preparative thin-layer chromatography. white solid (43.1 mg, 62%). **^{1}H NMR** (500 MHz, $CDCl_3$) δ 8.25 - 8.20 (m, 3H), 8.17 (d, *J* = 10.1 Hz, 1H), 8.10 (s, 1H), 7.76 - 7.71 (m, 1H), 7.62 - 7.57 (m, 1H), 7.57 - 7.52 (m, 2H), 7.50 - 7.45

(m, 1H), 5.41 (d, *J* = 13.7 Hz, 1H), 4.22 (dd, *J* = 12.1, 4.7 Hz, 1H), 3.93 - 3.81 (m, 4H), 3.08 - 2.99 (m, 1H), 2.67 - 2.58 (m, 1H), 2.25 - 2.07 (m, 2H), 1.83 - 1.73 (m, 1H). **^{13}C NMR** (125 MHz, $CDCl_3$) δ 175.0, 157.4, 149.0, 148.4, 139.9, 130.6, 129.2, 129.2, 128.7, 127.7, 126.3, 124.2, 122.9, 114.9, 72.9, 65.9, 52.1, 37.5, 34.6, 27.4. **GC-MS** (EI, m/z) for $C_{22}H_{21}NO_3$ Calcd: 347.2, found: 347.1. Spectra data are consistent with the reported literature.[38]

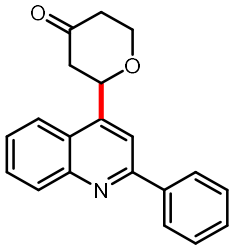

2-(2-phenylquinolin-4-yl)tetrahydro-4*H*-pyran-4-one (26b). Following the general procedure **A, the** reaction was run with 2.0 equiv of TFA for 36 h, and the product was isolated with Hex/EtOAc (5:2) on preparative thin-layer chromatography. white solid (39.4 mg, 65%). **^{1}H NMR** (500 MHz, $CDCl_3$) δ 8.27 - 8.21 (m, 3H), 8.15 (s, 1H), 7.93 (d, *J* = 8.4 Hz, 1H), 7.78 - 7.73 (m, 1H), 7.60 - 7.54 (m, 3H), 7.52 - 7.47 (m, 1H), 5.44 (dd, *J* = 11.4, 2.7 Hz, 1H), 4.60 (ddd, *J* = 11.7, 7.5, 1.5 Hz, 1H), 4.04 (td, *J* = 12.0, 2.9 Hz, 1H), 2.96 (dt, *J* = 14.7, 2.4 Hz, 1H), 2.91 - 2.82 (m, 1H), 2.76 - 2.68 (m, 1H), 2.61 - 2.55 (m, 1H). **^{13}C NMR** (125 MHz, $CDCl_3$) δ 205.4, 157.4, 148.6, 146.3, 139.6, 130.9, 129.5, 129.5, 128.9, 127.6, 126.6, 123.6, 122.3, 115.2, 76.0, 67.0, 49.3, 42.2. **HRMS** ($M+H^+$) for $C_{20}H_{18}NO_2$ Calcd: 304.1332, found: 304.1331. The compound was not reported.

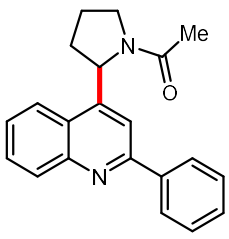

1-(2-(2-phenylquinolin-4-yl)pyrrolidin-1-yl)ethan-1-one, 1:0.65 rotamers (27b). Following the general procedure A, the product was isolated with Hex/EtOAc (1:3) on preparative thin-layer chromatography. Yellow oil (48.1 mg, 76%). **^{1}H NMR** (500 MHz, $CDCl_3$) δ 8.27 (d, *J* = 8.4 Hz, 1H), 8.22 (d, *J* = 7.9 Hz, 0.65H), 8.17 - 8.10 (m, 2H), 8.12 - 8.05 (m, 1.3H), 8.03 (d, *J* = 9.7 Hz, 0.65H), 8.00 (d, *J* = 8.3 Hz, 1H), 7.83 - 7.77 (m, 1H), 7.75 - 7.70 (m, 0.65H), 7.65 - 7.60 (m, 2H), 7.57 - 7.45 (m, 3H+3.25H), 6.00 (d, *J* = 9.4 Hz, 0.65H), 5.72 (d, *J* = 7.4 Hz, 1H), 4.01 - 3.90 (m, 1H+0.65H), 3.84 - 3.70 (m, 1H+0.65H), 2.72 - 2.61 (m, 1H), 2.55 - 2.47 (m, 0.65H), 2.28 (s, 1.95H), 2.19 - 1.97 (m, 3H+1.95H), 1.92 (s, 3H). **^{13}C NMR** (125 MHz, $CDCl_3$) δ 170.2, 169.5, 157.3, 157.2, 148.8, 148.8, 148.4, 148.3, 140.2, 139.3, 131.0, 130.6, 129.7, 129.7, 129.3, 129.2, 129.0, 128.8, 127.7, 127.7, 126.7, 126.2, 124.7, 124.2, 123.2, 122.3, 114.8, 114.4, 58.9, 57.3, 48.6, 47.0, 34.5, 32.7, 24.0, 22.8, 22.5, 22.2. **GC-MS** (EI, m/z) for $C_{21}H_{20}N_2O$ Calcd: 316.2, found: 316.1. Spectra data are consistent with the reported literature.[38]

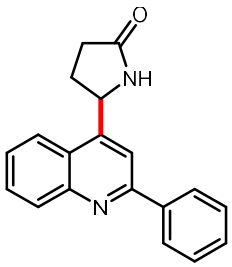

5-(2-phenylquinolin-4-yl)pyrrolidin-2-one (28b). Following the general procedure A, the product was isolated with Hex/EtOAc/MeOH (2:1:0.5) on preparative thin-layer chromatography. white solid (38.1 mg, 66%). **^{1}H NMR** (500 MHz, $CDCl_3$) δ 8.27 (d, *J* = 6.9 Hz, 1H), 8.14 - 8.08 (m, 2H), 7.88 (d, *J* = 8.4 Hz, 1H), 7.84 (s, 1H), 7.81 - 7.75 (m, 1H), 7.62 - 7.56 (m, 1H), 7.52 - 7.43 (m, 3H), 6.85 (s, 1H), 5.50 (dd, *J* = 8.6, 5.3 Hz, 1H), 2.94 - 2.83 (m, 1H), 2.49 (t, *J* = 8.1 Hz, 2H), 2.11 - 2.01 (m, 1H). **^{13}C NMR** (125 MHz, $CDCl_3$) δ 178.8, 157.3, 148.6, 148.5, 139.3, 130.9, 129.7, 129.6, 128.9, 127.6, 126.7, 124.2, 122.1, 113.6, 53.9, 29.7, 29.6.

HRMS (M+Na$^+$) for $C_{19}H_{16}N_2NaO$ Calcd: 311.1155, found: 311.1158. The compound was not reported.

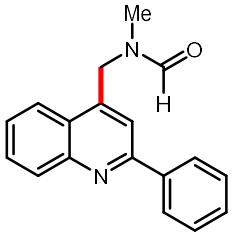

***N*-methyl-*N*-((2-phenylquinolin-4-yl)methyl)formamide, 1:0.5 rotamers (29b).** Following the general procedure A, the product was isolated with Hex/EtOAc/MeOH (1:1:0.2) on preparative thin-layer chromatography. Yellow oil (41.5 mg, 75%). **^{1}H NMR** (500 MHz, $CDCl_3$) δ 8.43 (s, 0.5H), 8.30 - 8.19 (m, 2H+0.5H), 8.21 - 8.14 (m, 2H+1H), 8.09 (d, *J* = 8.7 Hz, 1H), 7.92 (d, *J* = 8.4 Hz, 0.5H), 7.83 - 7.72 (m, 2H+0.5H), 7.66 (s, 0.5H), 7.63 - 7.53 (m, 3H+1.5H), 7.52 - 7.48 (m, 1H+0.5H), 5.07 (s, 2H), 4.98 (s, 1H), 2.99 (s, 1.5H), 2.91 (s, 3H). **^{13}C NMR** (125 MHz, $CDCl_3$) δ 163.4, 162.6, 157.3, 157.0, 148.6, 148.5, 141.9, 141.7, 139.4, 139.1, 130.9, 130.5, 130.0, 129.9, 129.7, 129.5, 129.0, 128.9, 127.6, 127.6, 126.9, 126.9, 125.6, 125.1, 123.2, 121.8, 118.9, 116.7, 50.1, 45.2, 34.4, 30.5. **HRMS** (M+H$^+$) for $C_{18}H_{17}N_2O$ Calcd: 277.1335, found: 277.1330. The compound was not reported.

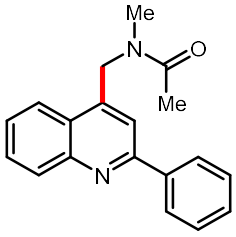

***N*-methyl-*N*-((2-phenylquinolin-4-yl)methyl)acetamide, 1:0.5 rotamers (30b).** Following the general procedure A, the product was isolated with Hex/EtOAc (1:1) on preparative thin-layer chromatography. Yellow oil (41.8 mg, 72%). **^{1}H NMR** (500 MHz, $CDCl_3$)

δ 8.28 (d, *J* = 10.2 Hz, 0.5H), 8.23 (d, *J* = 10.4 Hz, 1H), 8.19 - 8.12 (m, 2H+1H), 8.09 (d, *J* = 6.4 Hz, 1H), 7.90 (d, *J* = 8.2 Hz, 0.5H), 7.84 - 7.79 (m, 0.5H), 7.79 - 7.74 (m, 1H), 7.70 (s, 1H), 7.65 - 7.54 (m, 3H+2H), 7.53 - 7.49 (m, 1H+0.5H), 5.17 (s, 2H), 5.10 (s, 1H), 3.17 (s, 1.5H), 3.00 (s, 3H), 2.27 (s, 3H), 2.18 (s, 1.5H). **^{13}C NMR** (125 MHz, $CDCl_3$) δ 171.5, 170.8, 157.6, 157.1, 148.6, 148.4, 143.1, 142.4, 139.6, 139.2, 130.9, 130.5, 129.9, 129.7, 129.7, 129.4, 129.0, 128.9, 127.6, 127.6, 126.8, 126.8, 125.8, 124.9, 123.3, 121.6, 118.5, 114.7, 51.5, 47.9, 35.7, 34.7, 21.9, 21.3. **HRMS** ($M+Na^+$) for $C_{19}H_{18}N_2NaO$ Calcd: 313.1311, found: 313.1299. The compound was not reported.

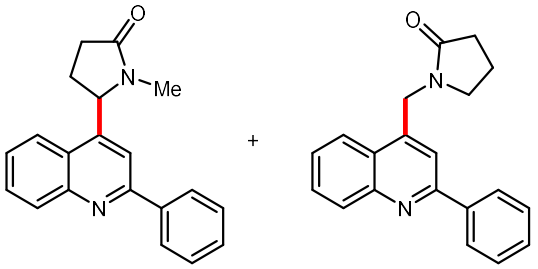

1-methyl-5-(2-phenylquinolin-4-yl)pyrrolidin-2-one (31b) and 1-((2-phenylquinolin-4-yl)methyl)pyrrolidin-2-one (31b'), 1:0.26 congeners. Following the general procedureA, the product was isolated with Hex/EtOAc/MeOH (2:1:0.4) on preparative thin-layer chromatography. Yellow oil (34.5 mg, 57%). ^{1}H NMR (500 MHz, $CDCl_3$) δ 8.28 (d, *J* = 8.4 Hz, 1H), 8.23 (d, J = 8.4 Hz, 0.26H), 8.19 - 8.13 (m, 2H+0.52H), 7.96 (d, *J* = 8.5 Hz, 1H), 7.82 - 7.74 (m, 1H+0.52H), 7.65 - 7.53 (m, 4H+0.78H), 7.53 - 7.46 (m, 1H+0.52H), 5.41 (s, 1H), 4.99 (s, 0.52H), 3.28 (t, *J* = 7.0 Hz, 0.52H), 2.95 (s, 3H), 2.82 - 2.71 (m, 1H), 2.65 - 2.48 (m, 2H+0.52H), 2.09 - 1.94 (m, 1H+0.52H). ^{13}C NMR (125 MHz, $CDCl_3$) δ 176.0, 174.9, 157.4, 157.0, 149.0, 148.6, 146.7, 142.4, 139.4, 139.2, 131.0, 130.5, 129.9, 129.8, 129.7, 129.5, 129.0, 128.9, 128.9, 127.6, 127.5, 127.0, 126.8, 125.7, 124.7, 123.4, 122.0, 119.1, 113.9, 60.0, 46.8,

44.2, 30.8, 29.5, 29.1, 27.2, 17.8. HRMS (M+H$^+$) for $C_{20}H_{18}N_2NaO$ Calcd: 325.1311, found: 325.1309. The compound was not reported.

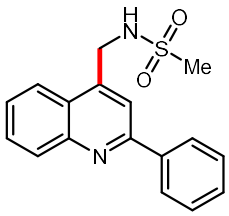

***N*-((2-phenylquinolin-4-yl)methyl)methanesulfonamide (32b).** Following the general procedure A, the product was isolated with Hex/EtOAc/MeOH (2:1:0.1) on preparative thin-layer chromatography. Yellow solid (41.9 mg, 67%). **^{1}H NMR** (500 MHz, $CDCl_3$) δ 8.23 (d, *J* = 9.2 Hz, 1H), 8.16 - 8.12 (m, 2H), 7.97 (d, *J* = 7.7 Hz, 1H), 7.88 (s, 1H), 7.79 - 7.74 (m, 1H), 7.62 - 7.57 (m, 1H), 7.56 - 7.47 (m, 3H), 5.09 (t, *J* = 6.2 Hz, 1H), 4.82 (d, *J* = 0.9 Hz, 2H), 2.99 (s, 3H). **^{13}C NMR** (125 MHz, $CDCl_3$) δ 157.1, 148.4, 142.3, 139.1, 130.7, 129.9, 129.7, 128.9, 127.5, 127.0, 124.9, 122.4, 117.8, 44.1, 41.2. **GC-MS** (EI, m/z) for $C_{17}H_{16}N_2O_2S$ Calcd: 312.1, found: 312.0. Spectra data are consistent with the reported literature.[38]

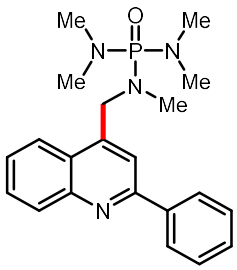

***N*,*N*',*N*',*N*'',*N*''-pentamethyl-*N*-((2-phenylquinolin-4-yl)methyl)phosphoramide (33b).** Following the general procedure A, the product was isolated with Hex/EtOAc/MeOH (1:1:0.5) on preparative thin-layer chromatography. Yellow oil (45.1 mg, 59%). **^{1}H NMR** (500 MHz, $CDCl_3$) δ 8.28 (d, *J* = 8.3 Hz, 1H), 8.23 - 8.19 (m, 3H), 7.99 (s, 1H), 7.75 - 7.70 (m, 1H), 7.58 - 7.52 (m, 3H), 7.50 - 7.45 (m, 1H), 4.74 (d, *J* = 8.0 Hz, 2H), 2.70 (d, *J* = 9.5 Hz, 12H),

2.67 (d, *J* = 9.0 Hz, 3H). **^{13}C NMR** (125 MHz, $CDCl_3$) δ 157.0, 148.6, 144.5, 139.7, 130.4, 129.5, 129.4, 128.9, 127.5, 126.3, 126.0, 123.3, 117.9, 50.4, 50.4, 36.9, 36.9, 34.9, 34.8. **^{31}P NMR** (203 MHz, $CDCl_3$) δ 25.2 (s, 1P). **GC-MS** (EI, m/z) for $C_{21}H_{27}N_4OP$ Calcd: 382.2, found: 382.2. Spectra data are consistent with the reported literature.[38]

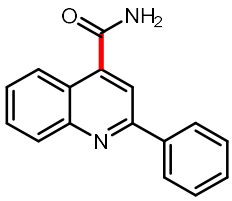

2-phenylquinoline-4-carboxamide (34b). Following the general procedure A, the product was isolated with Hex/EtOAc/MeOH (1:1:0.5) on preparative thin-layer chromatography. white solid (30.3 mg, 61%). **^{1}H NMR** (500 MHz, $CDCl_3$) δ 8.28 (d, *J* = 10.1 Hz, 1H), 8.22 (d, *J* = 8.4 Hz, 1H), 8.18 - 8.15 (m, 2H), 7.98 (s, 1H), 7.81 - 7.76 (m, 1H), 7.63 - 7.58 (m, 1H), 7.58 - 7.48 (m, 3H), 6.22 (s, 2H). **^{13}C NMR** (125 MHz, $CDCl_3$) δ 169.4, 156.8, 148.8, 141.7, 138.7, 130.3, 130.2, 129.8, 129.0, 127.5, 127.5, 124.9, 123.1, 116.6. **GC-MS** (EI, m/z) for $C_{16}H_{12}N_2O$ Calcd: 248.1, found: 248.1. Spectra data are consistent with the reported literature.[61]

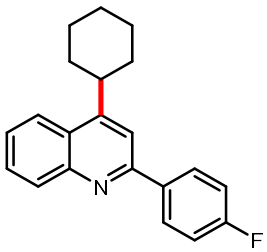

4-cyclohexyl-2-(4-fluorophenyl)quinoline (35b). Following the general procedure A, the product was isolated with Hex/EtOAc (10:1) on preparative thin-layer chromatography. white solid (40.9 mg, 67%). **^{1}H NMR** (500 MHz, $CDCl_3$) δ 8.21 - 8.15 (m, 3H), 8.11 (d, *J* = 8.5 Hz, 1H), 7.75 - 7.70 (m, 2H), 7.58 - 7.53 (m, 1H), 7.26 - 7.21 (m, 2H), 3.45 - 3.35 (m, 1H), 2.14

- 2.08 (m, 2H), 2.02 - 1.96 (m, 2H), 1.94 - 1.87 (m, 1H), 1.70 - 1.55 (m, 4H), 1.46 - 1.34 (m, 1H). **^{13}C NMR** (125 MHz, $CDCl_3$) δ 163.7 (d, *J* = 249 Hz), 156.2, 154.1, 148.6, 136.4 (d, *J* = 3 Hz), 130.6, 129.3 (d, *J* = 33 Hz), 129.1, 126.0, 125.8, 122.9, 115.7 (d, *J* = 22 Hz), 115.1, 39.1, 33.7, 27.0, 26.3. **^{19}F NMR** (470 MHz, $CDCl_3$) δ -112.86 - -112.94 (m, 1F). **HRMS** ($M+H^+$) for $C_{21}H_{21}FN$ Calcd: 306.1653, found: 306.1644. The compound was not reported.

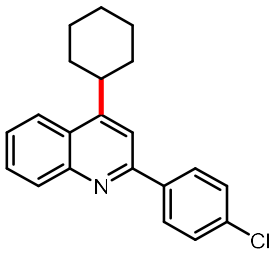

2-(4-chlorophenyl)-4-cyclohexylquinoline (36b). Following the general procedure A, the product was isolated with Hex/EtOAc (10:1) on preparative thin-layer chromatography. white solid (44.4 mg, 69%). **^{1}H NMR** (500 MHz, $CDCl_3$) δ 8.19 (dd, *J* = 8.4, 1.3 Hz, 1H), 8.16 - 8.09 (m, 3H), 7.76 - 7.70 (m, 2H), 7.60 - 7.55 (m, 1H), 7.55 - 7.48 (m, 2H), 3.44 - 3.35 (m, 1H), 2.16 - 2.07 (m, 2H), 2.03 - 1.96 (m, 2H), 1.95 - 1.87 (m, 1H), 1.70 - 1.54 (m, 4H), 1.46 - 1.35 (m, 1H). **^{13}C NMR** (125 MHz, $CDCl_3$) δ 156.0, 154.2, 148.6, 138.7, 135.3, 130.7, 129.2, 128.9, 128.9, 126.1, 125.9, 122.9, 115.0, 39.2, 33.7, 27.0, 26.3. **HRMS** ($M+H^+$) for $C_{21}H_{21}ClN$ Calcd: 322.1357, found: 322.1351. The compound was not reported.

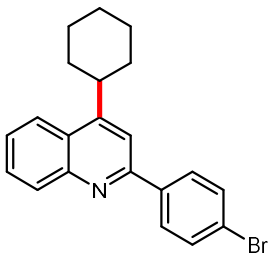

2-(4-bromophenyl)-4-cyclohexylquinoline (37b). Following the general procedure A, the product was isolated with Hex/EtOAc (10:1) on preparative thin-layer chromatography.

white solid (54.9 mg, 75%). **^{1}H NMR** (500 MHz, $CDCl_3$) δ 8.19 (d, *J* = 8.4 Hz, 1H), 8.11 (d, *J* = 6.9 Hz, 1H), 8.09 - 8.04 (m, 2H), 7.76 - 7.70 (m, 2H), 7.70 - 7.64 (m, 2H), 7.59 - 7.54 (m, 1H), 3.44 - 3.36 (m, 1H), 2.15 - 2.06 (m, 2H), 2.02 - 1.95 (m, 2H), 1.95 - 1.87 (m, 1H), 1.71 - 1.55 (m, 4H), 1.46 - 1.36 (m, 1H). **^{13}C NMR** (125 MHz, $CDCl_3$) δ 156.0, 154.3, 148.6, 139.1, 131.9, 130.7, 129.2, 129.2, 126.1, 126.0, 123.7, 122.9, 115.0, 39.2, 33.7, 27.0, 26.3. **HRMS** ($M+H^+$) for $C_{21}H_{21}BrN$ Calcd: 366.0852, found: 366.0836. The compound was not reported.

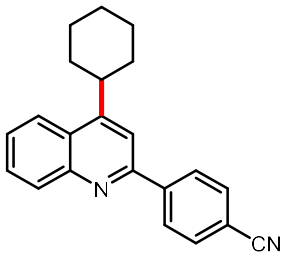

4-(4-cyclohexylquinolin-2-yl)benzonitrile (38b). Following the general procedure A, the product was isolated with Hex/EtOAc (5:1) on preparative thin-layer chromatography. white solid (33.7 mg, 54%). **^{1}H NMR** (500 MHz, $CDCl_3$) δ 8.31 (d, *J* = 8.7 Hz, 2H), 8.21 (d, *J* = 8.4 Hz, 1H), 8.14 (d, *J* = 8.5 Hz, 1H), 7.83 (d, *J* = 8.0 Hz, 2H), 7.79 - 7.73 (m, 2H), 7.64 - 7.58 (m, 1H), 3.47 - 3.37 (m, 1H), 2.15 - 2.07 (m, 2H), 2.04 - 1.96 (m, 2H), 1.96 - 1.87 (m, 1H), 1.71 - 1.54 (m, 4H), 1.47 - 1.38 (m, 1H). **^{13}C NMR** (125 MHz, $CDCl_3$) δ 154.9, 154.8, 148.6, 144.3, 132.6, 130.9, 129.5, 128.1, 126.7, 126.2, 123, 118.9, 115.1, 112.5, 39.2, 33.7, 26.9, 26.3. **HRMS** ($M+H^+$) for $C_{22}H_{21}N_2$ Calcd: 313.1699, found: 313.1689. The compound was not reported.

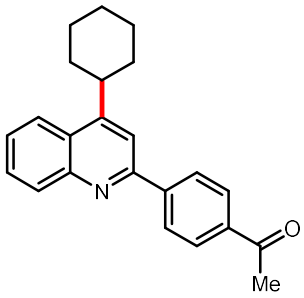

1-(4-(4-cyclohexylquinolin-2-yl)phenyl)ethan-1-one (39b). Following the general procedure A, the product was isolated with Hex/EtOAc (5:2) on preparative thin-layer chromatography. white solid (38.9 mg, 59%). **^{1}H NMR** (500 MHz, $CDCl_3$) δ 8.27 (d, *J* = 8.4 Hz, 2H), 8.21 (d, *J* = 6.6 Hz, 1H), 8.15 - 8.10 (m, 3H), 7.80 (s, 1H), 7.76 - 7.71 (m, 1H), 7.61 - 7.56 (m, 1H), 3.46 - 3.37 (m, 1H), 2.69 (s, 3H), 2.14 - 2.06 (m, 2H), 2.02 - 1.94 (m, 2H), 1.94 - 1.86 (m, 1H), 1.71 - 1.55 (m, 4H), 1.46 - 1.36 (m, 1H). **^{13}C NMR** (125 MHz, $CDCl_3$) δ 198.0, 155.9, 154.4, 148.6, 144.5, 137.2, 130.8, 129.3, 128.8, 127.8, 126.4, 126.2, 122.9, 115.4, 39.2, 33.7, 27.0, 26.8, 26.3. **HRMS** ($M+H^+$) for $C_{23}H_{24}NO$ Calcd: 330.1852, found: 330.1841. The compound was not reported.

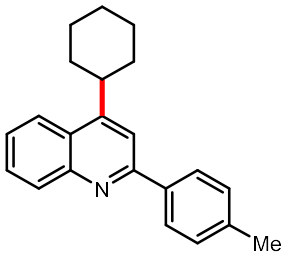

4-cyclohexyl-2-(*p*-tolyl)quinoline (40b). Following the general procedure A, the product was isolated with Hex/EtOAc (10:1) on preparative thin-layer chromatography. Colorless oil (42.2 mg, 70%). **^{1}H NMR** (500 MHz, $CDCl_3$) δ 8.21 (d, *J* = 8.4 Hz, 1H), 8.13 - 8.06 (m, 3H), 7.77 (s, 1H), 7.74 - 7.68 (m, 1H), 7.57 - 7.52 (m, 1H), 7.36 (d, *J* = 8.0 Hz, 2H), 3.45 - 3.34 (m, 1H), 2.47 (s, 3H), 2.15 - 2.07 (m, 2H), 2.03 - 1.95 (m, 2H), 1.94 - 1.86 (m, 1H), 1.70 - 1.55 (m, 4H), 1.45 - 1.35 (m, 1H). **^{13}C NMR** (125 MHz, $CDCl_3$) δ 157.3, 153.8, 148.6, 139.2, 137.5, 130.6,

129.5, 128.9, 127.5, 125.8, 125.7, 122.8, 115.3, 39.1, 33.7, 27.0, 26.4, 21.4. **HRMS** ($M+H^+$) for $C_{22}H_{24}N$ Calcd: 302.1903, found: 302.1892. The compound was not reported.

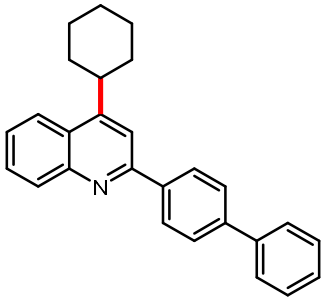

2-([1,1'-biphenyl]-4-yl)-4-cyclohexylquinoline (41b). Following the general procedure A, the product was isolated with Hex/EtOAc (10:1) on preparative thin-layer chromatography. white solid (39.3 mg, 54%). **^{1}H NMR** (500 MHz, $CDCl_3$) δ 8.28 (d, *J* = 6.7 Hz, 2H), 8.25 (d, *J* = 10.1 Hz, 1H), 8.13 (d, *J* = 8.5 Hz, 1H), 7.84 (s, 1H), 7.80 (d, *J* = 8.5 Hz, 2H), 7.77 - 7.69 (m, 3H), 7.60 - 7.55 (m, 1H), 7.54 - 7.49 (m, 2H), 7.44 - 7.39 (m, 1H), 3.47 - 3.37 (m, 1H), 2.17 - 2.10 (m, 2H), 2.03 - 1.97 (m, 2H), 1.97 - 1.88 (m, 1H), 1.75 - 1.57 (m, 4H), 1.48 - 1.37 (m, 1H). **^{13}C NMR** (125 MHz, $CDCl_3$) δ 156.9, 154.0, 148.7, 141.9, 140.7, 139.2, 130.7, 129.1, 128.9, 128.0, 127.6, 127.5, 127.2, 126.0, 125.9, 122.9, 115.4, 39.2, 33.7, 27.0, 26.4. **HRMS** ($M+H^+$) for $C_{27}H_{26}N$ Calcd: 364.2060, found: 364.2049. The compound was not reported.

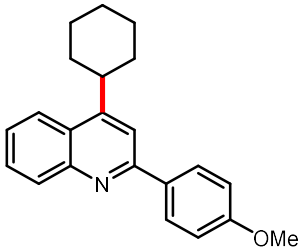

4-cyclohexyl-2-(4-methoxyphenyl)quinoline (42b). Following the general procedure A, the reaction was run at 55-60 °C, and the product was isolated with Hex/EtOAc (10:1) on preparative thin-layer chromatography. white solid (45.1 mg, 71%). **^{1}H NMR** (500 MHz,

$CDCl_3$) δ 8.20 - 8.12 (m, 3H), 8.09 (d, *J* = 8.4 Hz, 1H), 7.74 (s, 1H), 7.72 - 7.68 (m, 1H), 7.56 - 7.50 (m, 1H), 7.07 (d, *J* = 8.8 Hz, 2H), 3.92 (s, 3H), 3.42 - 3.34 (m, 1H), 2.14 - 2.07 (m, 2H), 2.02 - 1.95 (m, 2H), 1.94 - 1.86 (m, 1H), 1.71 - 1.54 (m, 4H), 1.47 - 1.35 (m, 1H). **^{13}C NMR** (125 MHz, $CDCl_3$) δ 160.7, 156.9, 153.7, 148.6, 132.9, 130.5, 128.9, 128.9, 125.6, 125.5, 122.8, 115.0, 114.2, 55.4, 39.1, 33.7, 27.0, 26.4. **HRMS** ($M+H^+$) for $C_{22}H_{24}NO$ Calcd: 318.1852, found: 318.1850. The compound was not reported.

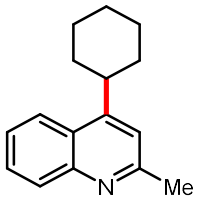

4-cyclohexyl-2-methylquinoline (43b). Following the general procedure A, the product was isolated with Hex/EtOAc (10:1) on preparative thin-layer chromatography. Colorless oil (28.8 mg, 64%). **^{1}H NMR** (500 MHz, $CDCl_3$) δ 8.06 (d, *J* = 8.5 Hz, 2H), 7.70 - 7.65 (m, 1H), 7.54 - 7.48 (m, 1H), 7.19 (s, 1H), 3.37 - 3.27 (m, 1H), 2.74 (s, 3H), 2.07 - 1.99 (m, 2H), 1.99 - 1.91 (m, 2H), 1.91 - 1.85 (m, 1H), 1.62 - 1.50 (m, 4H), 1.42 - 1.32 (m, 1H). **^{13}C NMR** (125 MHz, $CDCl_3$) δ 158.8, 153.4, 148.1, 129.5, 128.8, 125.3, 125.2, 122.8, 118.3, 38.8, 33.6, 27.0, 26.3, 25.5. **GC-MS** (EI, m/z) for $C_{16}H_{19}N$ Calcd: 225.2, found: 225.1. Spectra data are consistent with the reported literature.[62]

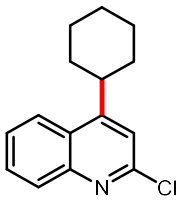

2-chloro-4-cyclohexylquinoline (44b). Following the general procedure A, the product was isolated with Hex/EtOAc (10:1) on preparative thin-layer chromatography. white solid

(21.1 mg, 43%). **^{1}H NMR** (500 MHz, $CDCl_3$) δ 8.08 - 8.02 (m, 2H), 7.75 - 7.68 (m, 1H), 7.61 - 7.56 (m, 1H), 7.28 (s, 1H), 3.36 - 3.27 (m, 1H), 2.08 - 1.92 (m, 4H), 1.92 - 1.83 (m, 1H), 1.61 - 1.49 (m 4H), 1.42 - 1.31 (m, 1H). **^{13}C NMR** (125 MHz, $CDCl_3$) δ 156.9, 151.1, 148.2, 130.0, 129.5, 126.5, 125.6, 123.2, 118.7, 39.1, 33.4, 26.8, 26.2. **GC-MS** (EI, m/z) for $C_{15}H_{16}ClN$ Calcd: 245.1, 247.1, found: 245.1, 247.0. Spectra data are consistent with the reported literature.[63]

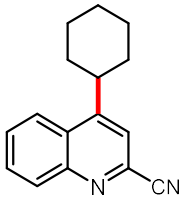

4-cyclohexylquinoline-2-carbonitrile (45b). Following the general procedure A, the product was isolated with Hex/EtOAc (10:1) on preparative thin-layer chromatography. Yellow solid (28.4 mg, 60%). **^{1}H NMR** (500 MHz, $CDCl_3$) δ 8.19 (dd, *J* = 8.6, 1.3 Hz, 1H), 8.16 (dd, *J* = 8.6, 1.3 Hz, 1H), 7.85 - 7.80 (m, 1H), 7.75 - 7.70 (m, 1H), 7.60 (s, 1H), 3.44 - 3.32 (m, 1H), 2.08 - 1.93 (m, 4H), 1.93 - 1.84 (m, 1H), 1.65 - 1.52 (m, 4H), 1.44 - 1.33 (m, 1H). **^{13}C NMR** (125 MHz, $CDCl_3$) δ 155.7, 148.4, 133.8, 131.0, 130.5, 129.0, 127.5, 123.1, 120.0, 118.0, 39.1, 33.5, 26.7, 26.1. **GC-MS** (EI, m/z) for $C_{16}H_{15}N_2$ Calcd: 236.1, found: 236.1. Spectra data are consistent with the reported literature.[63]

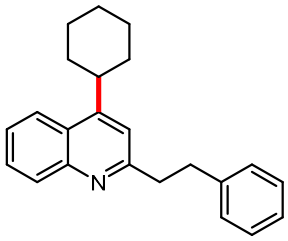

4-cyclohexyl-2-phenethylquinoline (46b). Following the general procedure A, the product was isolated with Hex/EtOAc (7:1) on preparative thin-layer chromatography.

Yellow oil (28.4 mg, 45%). **^{1}H NMR** (500 MHz, $CDCl_3$) δ 8.11 (d, *J* = 8.5 Hz, 1H), 8.07 (d, *J* = 6.9 Hz, 1H), 7.72 - 7.66 (m, 1H), 7.56 - 7.49 (m, 1H), 7.33 - 7.20 (m, 6H), 3.34 - 3.24 (m, 3H), 3.21 - 3.12 (m, 2H), 2.01 - 1.90 (m, 4H), 1.90 - 1.83 (m, 1H), 1.63 - 1.42 (m, 4H), 1.41 - 1.30 (m, 1H). **^{13}C NMR** (125 MHz, $CDCl_3$) δ 161.6, 153.3, 148.3, 141.7, 129.8, 128.7, 128.6, 128.4, 126.0, 125.5, 125.4, 122.9, 118.0, 41.3, 38.8, 36.1, 33.5, 26.9, 26.3. **HRMS** ($M+H^+$) for $C_{23}H_{26}N$ Calcd: 316.2060, found: 316.2057. The compound was not reported.

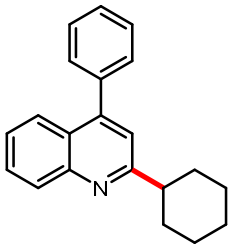

2-cyclohexyl-4-phenylquinoline (47b). Following the general procedure A, the product was isolated with Hex/EtOAc (5:1) on preparative thin-layer chromatography. Colorless oil (35.6 mg, 62%). **^{1}H NMR** (500 MHz, $CDCl_3$) δ 8.14 (d, *J* = 7.0 Hz, 1H), 7.89 (dd, *J* = 8.4, 1.4 Hz, 1H), 7.73 - 7.68 (m, 1H), 7.57 - 7.49 (m, 5H), 7.47 - 7.43 (m, 1H), 7.29 (s, 1H), 2.99 (tt, *J* = 12.0, 3.4 Hz, 1H), 2.14 - 2.06 (m, 2H), 1.96 - 1.89 (m, 2H), 1.86 - 1.78 (m, 1H), 1.75 - 1.63 (m, 2H), 1.56 - 1.45 (m, 2H), 1.41 - 1.30 (m, 1H). **^{13}C NMR** (125 MHz, $CDCl_3$) δ 166.4, 148.6, 148.3, 138.6, 129.6, 129.4, 129.1, 128.5, 128.3, 125.7, 125.6, 125.5, 119.9, 47.7, 32.9, 26.6, 26.1. **GC-MS** (EI, m/z) for $C_{21}H_{21}N$ Calcd: 287.2, found: 287.1. Spectra data are consistent with the reported literature.[64]

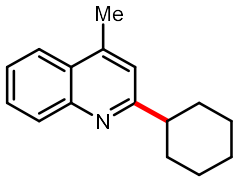

2-cyclohexyl-4-methylquinoline (48b). Following the general procedure A, the product was isolated with Hex/EtOAc (10:1) on preparative thin-layer chromatography. Colorless oil (32.0 mg, 71%). **^{1}H NMR** (500 MHz, $CDCl_3$) δ 8.07 (dd, *J* = 8.4, 1.3 Hz, 1H), 7.96 (dd, *J* = 8.3, 1.4 Hz, 1H), 7.71 - 7.65 (m, 1H), 7.54 - 7.47 (m, 1H), 7.19 (s, 1H), 2.90 (tt, *J* = 12.1, 3.4 Hz, 1H), 2.70 (s, 3H), 2.07 - 2.00 (m, 2H), 1.95 - 1.87 (m, 2H), 1.85 - 1.78 (m, 1H), 1.70 - 1.60 (m, 2H), 1.55 - 1.43 (m, 2H), 1.43 - 1.31 (m, 1H). **^{13}C NMR** (125 MHz, $CDCl_3$) δ 166.5, 147.7, 144.2, 129.5, 128.9, 127.1, 125.4, 123.6, 120.3, 47.6, 32.9, 26.6, 26.2, 18.9. **GC-MS** (EI, m/z) for $C_{16}H_{19}N$ Calcd: 225.2, found: 225.2. Spectra data are consistent with the reported literature.[65]

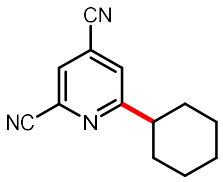

6-cyclohexylpyridine-2,4-dicarbonitrile (49b). Following the general procedure A, the product was isolated with Hex/EtOAc (10:1) on preparative thin-layer chromatography. Yellow oil (29.6 mg, 70%). **^{1}H NMR** (500 MHz, $CDCl_3$) δ 8.84 (s, 1H), 7.86 (d, *J* = 0.8 Hz, 1H), 3.04 (tt, *J* = 12.1, 3.1 Hz, 1H), 2.01 - 1.92 (m, 4H), 1.91 - 1.83 (m, 1H), 1.65 - 1.45 (m, 4H), 1.39 - 1.28 (m, 1H). **^{13}C NMR** (125 MHz, $CDCl_3$) δ 151.0, 148.6, 132.1, 129.9, 121.0, 115.8, 114.1, 41.8, 32.9, 26.2, 25.4. **HRMS** ($M+Na^+$) for $C_{13}H_{13}N_3Na$ Calcd: 234.1002, found: 234.0995. The compound was not reported.

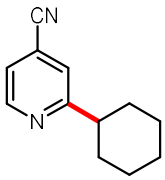

2-cyclohexylisonicotinonitrile (50b). Following the general procedure A, the product was isolated with Hex/EtOAc (10:1) on preparative thin-layer chromatography. Yellow oil (8.9

mg, 24%). **^{1}H NMR** (500 MHz, $CDCl_3$) δ 8.72 (d, *J* = 5.0 Hz, 1H), 7.40 (s, 1H), 7.35 (dd, *J* = 4.9, 1.5 Hz, 1H), 2.78 (tt, *J* = 11.9, 3.4 Hz, 1H), 2.01 - 1.94 (m, 2H), 1.93 - 1.83 (m, 2H), 1.83 - 1.74 (m, 1H), 1.60 - 1.37 (m, 4H), 1.36 - 1.24 (m, 2H). **^{13}C NMR** (125 MHz, $CDCl_3$) δ 168.2, 150.1, 122.9, 122.4, 120.6, 116.9, 46.4, 32.6, 26.3, 25.9. **GC-MS** (EI, m/z) for $C_{12}H_{14}N_2$ Calcd: 186.1, found: 186.1. Spectra data are consistent with the reported literature.[66]

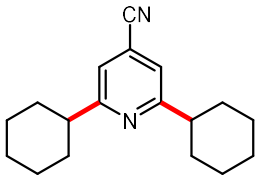

2,6-dicyclohexylisonicotinonitrile (50b'). Following the general procedure A, the product was isolated with Hex/EtOAc (10:1) on preparative thin-layer chromatography. Yellow oil (9.1 mg, 17%). **^{1}H NMR** (500 MHz, $CDCl_3$) δ 7.18 (s, 1H), 2.74 (tt, *J* = 11.7, 3.4 Hz, 1H), 2.01 - 1.93 (m, 2H), 1.92 - 1.84 (m, 2H), 1.82 - 1.75 (m, 1H), 1.56 - 1.38 (m, 4H), 1.36 - 1.26 (m, 1H). **^{13}C NMR** (125 MHz, $CDCl_3$) δ 167.2, 120.6, 119.6, 117.6, 46.4, 32.7, 26.4, 26.0. **GC-MS** (EI, m/z) for $C_{18}H_{24}N_2$ Calcd: 268.2, found: 268.1. Spectra data are consistent with the reported literature.[63]

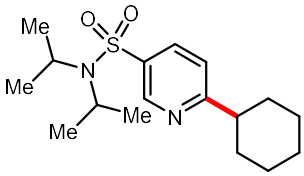

6-cyclohexyl-*N*,*N*-diisopropylpyridine-3-sulfonamide (51b). Following the general procedure A, the reaction was run for 36 h, and the product was isolated with Hex/EtOAc (2:1) on preparative thin-layer chromatography. white solid (21.4 mg, 33%). **^{1}H NMR** (500 MHz, $CDCl_3$) δ 8.99 (d, *J* = 1.5 Hz, 1H), 8.05 (dd, *J* = 8.3, 2.4 Hz, 1H), 7.27 (d, *J* = 8.3 Hz, 1H), 3.74 (p, *J* = 6.8 Hz, 2H), 2.79 (tt, *J* = 11.9, 3.4 Hz, 1H), 2.00 - 1.93 (m, 2H), 1.92 - 1.85 (m, 2H),

1.82 - 1.75 (m, 1H), 1.60 - 1.49 (m, 2H), 1.49 - 1.25 (m, 15H). **^{13}C NMR** (125 MHz, $CDCl_3$) δ 170.2, 147.6, 136.4, 135.1, 120.8, 48.8, 46.6, 32.7, 26.4, 25.9, 22.0. **HRMS** ($M+Na^+$) for $C_{17}H_{28}N_2NaO_2S$ Calcd: 347.1764, found: 347.1755. The compound was not reported.

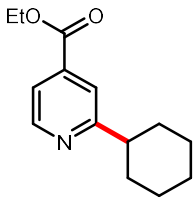

ethyl 2-cyclohexylisonicotinate (52b). Following the general procedure A, the product was isolated with Hex/EtOAc (5:1) on preparative thin-layer chromatography. Colorless oil (21.9 mg, 47%). **^{1}H NMR** (500 MHz, $CDCl_3$) δ 8.68 (d, *J* = 5.0 Hz, 1H), 7.73 (s, 1H), 7.66 (dd, *J* = 5.1, 1.6 Hz, 1H), 4.43 (q, *J* = 7.1 Hz, 2H), 2.81 (tt, *J* = 12.0, 3.4 Hz, 1H), 2.03 - 1.93 (m, 2H), 1.93 - 1.82 (m, 2H), 1.82 - 1.73 (m, 1H), 1.62 - 1.53 (m, 2H), 1.49 - 1.39 (m, 5H), 1.37 - 1.27 (m, 1H). **^{13}C NMR** (125 MHz, $CDCl_3$) δ 167.7, 165.6, 149.8, 138.0, 120.3, 120.2, 61.7, 46.6, 32.8, 26.5, 26.0, 14.2. **GC-MS** (EI, m/z) for $C_{14}H_{19}NO_2$ Calcd: 233.1, found: 233.1. Spectra data are consistent with the reported literature.[59]

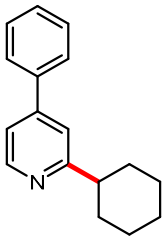

2-cyclohexyl-4-phenylpyridine (53b). Following the general procedure A, the reaction was run at 55-60 °C for 36 h, and the product was isolated with Hex/EtOAc (5:2) on preparative thin-layer chromatography. Colorless oil (24.7 mg, 52%). **^{1}H NMR** (500 MHz, $CDCl_3$) δ 8.60 (dd, *J* = 5.2, 0.8 Hz, 1H), 7.68 - 7.63 (m, 2H), 7.53 - 7.48 (m, 2H), 7.48 - 7.43 (m,

1H), 7.48 - 7.43 (m, 1H), 7.40 - 7.38 (m, 1H), 2.80 (tt, *J* = 12.0, 3.4 Hz, 1H), 2.06 - 1.99 (m, 2H), 1.94 - 1.88 (m, 2H), 1.83 - 1.76 (m, 1H), 1.66 - 1.57 (m, 2H), 1.52 - 1.41 (m, 2H), 1.39 - 1.28 (m, 1H). **^{13}C NMR** (125 MHz, $CDCl_3$) δ 167.0, 149.5, 148.9, 138.8, 129.0, 128.8, 127.1, 119.2, 119.1, 46.7, 33.0, 26.6, 26.1. **GC-MS** (EI, m/z) for $C_{17}H_{19}N$ Calcd: 237.2, found: 237.1. Spectra data are consistent with the reported literature.[63]

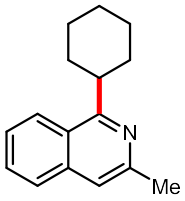

1-cyclohexyl-3-methylisoquinoline (54b). Following the general procedure A, the reaction was run for 36 h, and the product was isolated with Hex/EtOAc (10:1) on preparative thin-layer chromatography. Colorless oil (29.7 mg, 66%). **^{1}H NMR** (500 MHz, $CDCl_3$) δ 8.19 (d, *J* = 8.4 Hz, 1H), 7.73 (d, *J* = 7.8 Hz, 1H), 7.63 - 7.57 (m, 1H), 7.54 - 7.47 (m, 1H), 7.32 (s, 1H), 3.55 (tt, *J* = 11.5, 3.3 Hz, 1H), 2.68 (s, 3H), 2.01 - 1.77 (m, 7H), 1.62 - 1.50 (m, 2H), 1.48 - 1.37 (m, 1H). **^{13}C NMR** (125 MHz, $CDCl_3$) δ 165.0, 150.5, 137.1, 129.3, 126.9, 125.6, 124.7, 124.3, 116.6, 41.6, 32.5, 26.9, 26.2, 24.5. **GC-MS** (EI, m/z) for $C_{16}H_{19}N$ Calcd: 225.2, found: 225.1. Spectra data are consistent with the reported literature.[67]

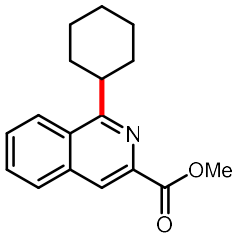

methyl 1-cyclohexylisoquinoline-3-carboxylate (55b). Following the general procedure A, the reaction was run for 36 h, and the product was isolated with Hex/EtOAc (5:1) on

preparative thin-layer chromatography. white solid (27.5 mg, 51%). **^{1}H NMR** (500 MHz, $CDCl_3$) δ 8.42 (s, 1H), 8.32 - 8.28 (m, 1H), 7.99 - 7.94 (m, 1H), 7.78 - 7.69 (m, 2H), 4.05 (s, 3H), 3.59 (tt, *J* = 11.1, 3.8 Hz, 1H), 2.06 - 1.92 (m, 6H), 1.86 - 1.79 (m, 1H), 1.63 - 1.51 (m, 2H), 1.50 - 1.39 (m, 1H). **^{13}C NMR** (125 MHz, $CDCl_3$) δ 166.9, 166.1, 140.7, 136.0, 130.1, 129.1, 129.0, 127.8, 125.0, 122.4, 52.7, 42.1, 32.2, 26.8, 26.1. **GC-MS** (EI, m/z) for $C_{17}H_{19}NO_2$ Calcd: 269.1, found: 269.1. Spectra data are consistent with the reported literature.[63]

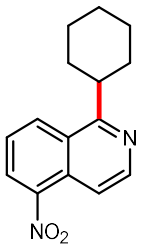

1-cyclohexyl-5-nitroisoquinoline (56b). Following the general procedure A, the reaction was run at 55-60 °C for 36 h, and the product was isolated with Hex/EtOAc (1:1) on preparative thin-layer chromatography. Yellow oil (15.4 mg, 30%). **^{1}H NMR** (500 MHz, $CDCl_3$) δ 8.71 (d, *J* = 6.1 Hz, 1H), 8.60 (dd, *J* = 8.5, 0.8 Hz, 1H), 8.45 (dd, *J* = 7.7, 1.1 Hz, 1H), 8.24 (dd, *J* = 6.1, 1.0 Hz, 1H), 7.74 - 7.68 (m, 1H), 3.60 (tt, *J* = 11.6, 3.2 Hz, 1H), 2.04 - 1.94 (m, 4H), 1.93 - 1.81 (m, 3H), 1.60 - 1.50 (m, 2H), 1.47 - 1.36 (m, 1H). **^{13}C NMR** (125 MHz, $CDCl_3$) δ 166.5, 146.1, 145.3, 131.4, 128.9, 127.2, 126.9, 125.1, 113.4, 42.2, 32.7, 26.8, 26.1. **GC-MS** (EI, m/z) for $C_{15}H_{16}N_2O_2$ Calcd: 256.1, found: 256.1. Spectra data are consistent with the reported literature.[66]

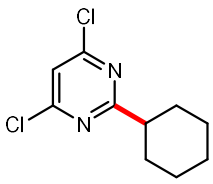

4,6-dichloro-2-cyclohexylpyrimidine (57b). Following the general procedure A, the reaction was run with 4.0 equiv of TFA for 36 h, and the product was isolated with Hex/EtOAc (10:1) on preparative thin-layer chromatography. Colorless oil (21.7 mg, 47%). **^{1}H NMR** (500 MHz, $CDCl_3$) δ 7.24 (s, 1H), 2.87 (tt, *J* = 11.8, 3.5 Hz, 1H), 2.03 - 1.98 (m, 2H), 1.89 - 1.85 (m, 2H), 1.78 - 1.73 (m, 1H), 1.68 - 1.57 (m, 2H), 1.46 - 1.25 (m, 3H). **^{13}C NMR** (125 MHz, $CDCl_3$) δ 176.5, 161.7, 118.5, 47.2, 31.5, 25.9, 25.7. **GC-MS** (EI, m/z) for $C_{10}H_{12}Cl_2N_2$ Calcd: 230.0, 232.0, found: 230.0, 232.0. Spectra data are consistent with the reported literature.[59]

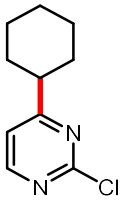

2-chloro-4-cyclohexylpyrimidine (58b). Following the general procedure A, the reaction was run with 4.0 equiv of TFA for 36 h, the product was isolated with Hex/EtOAc (10:1) on preparative thin-layer chromatography. Colorless oil (20.8 mg, 53%). **^{1}H NMR** (500 MHz, $CDCl_3$) δ 8.51 (d, *J* = 5.1 Hz, 1H), 7.13 (d, *J* = 5.1 Hz, 1H), 2.69 (tt, *J* = 11.9, 3.4 Hz, 1H), 2.01 - 1.94 (m, 2H), 1.93 - 1.85 (m, 2H), 1.81 - 1.74 (m, 1H), 1.57 - 1.46 (m, 2H), 1.46 - 1.35 (m, 2H), 1.34 - 1.23 (m, 1H). **^{13}C NMR** (125 MHz, $CDCl_3$) δ 178.6, 161.2, 159.3, 117.0, 45.9, 31.9, 26.0, 25.7. **GC-MS** (EI, m/z) for $C_{10}H_{13}ClN_2$ Calcd: 196.1, 198.1, found: 196.1, 198.1. Spectra data are consistent with the reported literature.[68]

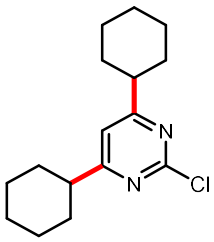

2-chloro-4,6-dicyclohexylpyrimidine (58b'). Following the general procedure A, the reaction was run with 4.0 equiv of TFA for 36 h, and the product was isolated with Hex/EtOAc (10:1) on preparative thin-layer chromatography. Colorless oil (5 mg, 9%). **^{1}H NMR** (500 MHz, $CDCl_3$) δ 6.94 (s, 1H), 2.70 - 2.60 (m, 2H), 2.00 - 1.92 (m, 4H), 1.92 - 1.83 (m, 4H), 1.80 - 1.73 (m, 2H), 1.56 - 1.46 (m, 4H), 1.46 - 1.35 (m, 4H), 1.35 - 1.24 (m, 2H). **^{13}C NMR** (125 MHz, $CDCl_3$) δ 178.2, 160.7, 114.0, 45.9, 32.0, 26.1, 25.7. **GC-MS** (EI, m/z) for $C_{16}H_{23}ClN_2$ Calcd: 278.2, 280.2, found: 278.1, 280.1. Spectra data are consistent with the reported literature.[63]

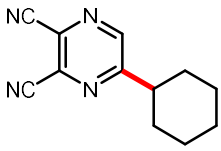

5-cyclohexylpyrazine-2,3-dicarbonitrile (59b). Following the general procedure A, the reaction was run with 4.0 equiv of TFA for 36 h, and the product was isolated with Hex/EtOAc (1:1) on preparative thin-layer chromatography. brown oil (24.2 mg, 57%). **^{1}H NMR** (500 MHz, $CDCl_3$) δ 8.76 (s, 1H), 2.94 (tt, *J* = 11.9, 3.3 Hz, 1H), 2.01 - 1.90 (m, 4H), 1.86 - 1.80 (m, 1H), 1.68 - 1.58 (m, 2H), 1.52 - 1.40 (m, 2H), 1.39 - 1.31 (m, 1H). **^{13}C NMR** (125 MHz, $CDCl_3$) δ 165.7, 146.4, 133.1, 131.0, 113.1, 113.1, 44.3, 31.9, 25.9, 25.4. **HRMS** ($M+Na^+$) for $C_{12}H_{12}N_4Na$ Calcd: 235.0954, found: 235.0943. The compound was not reported.

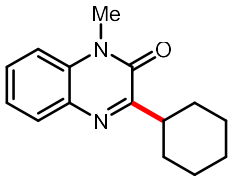

3-cyclohexyl-1-methylquinoxalin-2(1*H*)-one (60b). Following the general procedure A, the product was isolated with Hex/EtOAc (5:1) on preparative thin-layer chromatography. white solid (32.5 mg, 67%). **^{1}H NMR** (500 MHz, $CDCl_3$) δ 7.86 (dd, *J* = 8.1, 1.5 Hz, 1H), 7.56 - 7.50 (m, 1H), 7.37 - 7.32 (m, 1H), 7.32 - 7.29 (m, 1H), 3.72 (s, 3H), 3.36 (tt, *J* = 11.6, 3.3 Hz, 1H), 2.02 - 1.94 (m, 2H), 1.92 - 1.86 (m, 2H), 1.82 - 1.76 (m, 1H), 1.65 - 1.55 (m, 2H), 1.55 - 1.43 (m, 2H), 1.39 - 1.27 (m, 1H). **^{13}C NMR** (125 MHz, $CDCl_3$) δ 164.3, 154.6, 132.9, 132.9, 129.8, 129.4, 123.4, 113.5, 40.8, 30.5, 29.1, 26.3, 26.2. **GC-MS** (EI, m/z) for $C_{15}H_{18}N_2O$ Calcd: 242.1, found: 242.1. Spectra data are consistent with the reported literature.[69]

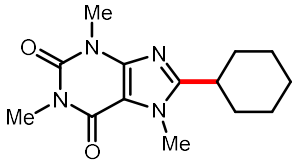

8-cyclohexyl-1,3,7-trimethyl-3,7-dihydro-1*H*-purine-2,6-dione (61b). Following the general procedure A, the reaction was run with 4.0 equiv of TFA, and the product was isolated with Hex/EtOAc (1:1) on preparative thin-layer chromatography. white solid (35.9 mg, 65%). **^{1}H NMR** (500 MHz, $CDCl_3$) δ 3.94 (s, 3H), 3.58 (s, 3H), 3.40 (s, 3H), 2.72 (tt, *J* = 11.6, 3.5 Hz, 1H), 1.93 - 1.83 (m, 4H), 1.80 - 1.66 (m, 3H), 1.45 - 1.29 (m, 3H). **^{13}C NMR** (125 MHz, $CDCl_3$) δ 158.0, 155.5, 151.8, 148.1, 107.0, 35.8, 31.4, 30.9, 29.7, 27.8, 26.0, 25.6. **GC-MS** (EI, m/z) for $C_{14}H_{20}N4O2$ Calcd: 276.2, found: 276.1. Spectra data are consistent with the reported literature.[70]

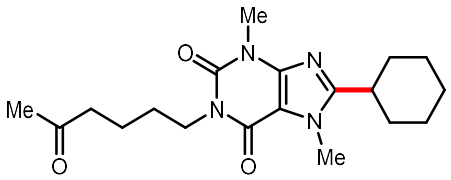

8-cyclohexyl-7-methyl-1-(4-oxopentyl)-3,7-dihydro-1*H*-purine-2,6-dione (62b). Following the general procedure A, the reaction was run with 4.0 equiv of TFA, and the product was isolated with Hex/EtOAc (1:1) on preparative thin-layer chromatography. white solid (38.2 mg, 53%). **^{1}H NMR** (500 MHz, $CDCl_3$) δ 4.01 (t, *J* = 7.0 Hz, 2H), 3.93 (s, 3H), 3.57 (s, 3H), 2.72 (tt, *J* = 11.6, 3.4 Hz, 1H), 2.51 (t, *J* = 7.1 Hz, 2H), 2.15 (s, 3H), 1.94 - 1.84 (m, 4H), 1.81 - 1.61 (m, 6H), 1.45 - 1.32 (m, 3H). **^{13}C NMR** (125 MHz, $CDCl_3$) δ 208.8, 158.0, 155.3, 151.5, 148.2, 107.0, 43.3, 40.6, 35.8, 31.4, 30.9, 29.9, 29.7, 27.5, 26.0, 25.6, 21.0. **HRMS** ($M+Na^+$) for $C_{19}H_{28}N_4NaO_3$ Calcd: 383.2054, found: 383.2042. The compound was not reported.

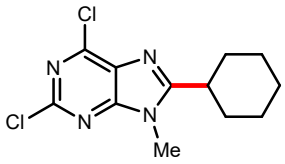

2,6-dichloro-8-cyclohexyl-9-methyl-9*H*-purine (63b). Following the general procedure A, the reaction was run with 5.0 equivof TFA, and the product was isolated with Hex/EtOAc (1:1) on preparative thin-layer chromatography. white solid (39.9 mg, 70%). **^{1}H NMR** (500 MHz, $CDCl_3$) δ 3.83 (s, 3H), 2.90 (tt, *J* = 11.8, 3.5 Hz, 1H), 2.05 - 1.91 (m, 4H), 1.90 - 1.76 (m, 3H), 1.51 - 1.34 (m, 3H). **^{13}C NMR** (125 MHz, $CDCl_3$) δ 163.1, 154.7, 151.7, 149.5, 130.2, 36.9, 30.8, 29.2, 25.9, 25.5. **GC-MS** (EI, m/z) for $C_{12}H_{14}Cl_2N_4$ Calcd: 284.1, 286.1, found: 284.0, 286.0. Spectra data are consistent with the reported literature.[64]

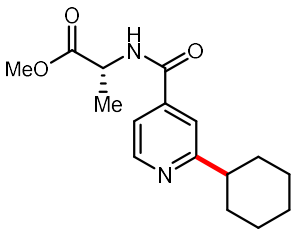

(*R*)-methyl-2-(2-cyclohexylisonicotinamido)propanoate (64b). Following the general procedure A, the reaction was run for 36 h, and the product was isolated with Hex/EtOAc (1:1) on preparative thin-layer chromatography. white oil (20.3 mg, 35%). **^{1}H NMR** (500 MHz, $CDCl_3$) δ 8.66 (d, *J* = 5.8 Hz, 1H), 7.52 (s, 1H), 7.42 (dd, *J* = 5.1, 1.7 Hz, 1H), 6.88 (d, *J* = 9.5 Hz, 1H), 4.81 (p, *J* = 7.2 Hz, 1H), 3.82 (s, 3H), 2.78 (tt, *J* = 12.0, 3.5 Hz, 1H), 2.00 - 1.93 (m, 2H), 1.92 - 1.84 (m, 2H), 1.81 - 1.74 (m, 1H), 1.62 - 1.51 (m, 5H), 1.49 - 1.38 (m, 2H), 1.36 - 1.24 (m, 1H). **^{13}C NMR** (125 MHz, $CDCl_3$) δ 173.4, 167.9, 165.4, 149.8, 141.4, 118.5, 118.1, 52.7, 48.6, 46.6, 32.8, 26.5, 26.0, 18.5. **HRMS** ($M+Na^+$) for $C_{16}H_{22}N_2NaO_3$ Calcd: 313.1523, found: 313.1514. The compound was not reported.

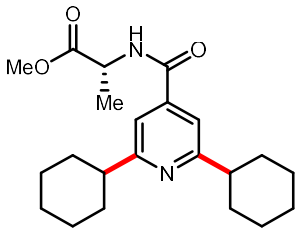

(*R*)-methyl-2-(2,6-dicyclohexylisonicotinamido)propanoate (64b'). Following the general procedure A, the reaction was run for 36 h, and the product was isolated with Hex/EtOAc (5:2) on preparative thin-layer chromatography. white solid (6.7 mg, 9%). **^{1}H NMR** (500 MHz, $CDCl_3$) δ 7.28 (s, 2H), 6.80 (d, *J* = 6.8 Hz, 1H), 4.81 (p, *J* = 7.2 Hz, 1H), 3.82 (s, 3H), 2.75 (tt, *J* = 11.8, 3.4 Hz, 2H), 1.99 - 1.94 (m, 4H), 1.89 - 1.84 (m, 4H), 1.79 - 1.73 (m, 2H), 1.59 - 1.48 (m, 7H), 1.48 - 1.37 (m, 4H), 1.36 - 1.23 (m, 2H). **^{13}C NMR** (125 MHz, $CDCl_3$) δ 173.5, 166.9, 166.2, 141.8, 115.1, 52.7, 48.5, 46.7, 32.9, 26.5, 26.1, 18.6. **GC-MS** (EI, m/z) for

$C_{22}H_{32}N_2O_3$ Calcd: 372.2, found: 372.2. Spectra data are consistent with the reported literature.[59]

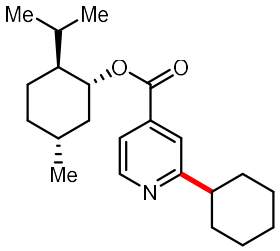

(1*R*,2*S*,5*R*)-2-isopropyl-5-methylcyclohexyl 2-cyclohexylisonicotinate (65b). Following the general procedure A, the reaction was run for 36 h, and the product was isolated with Hex/EtOAc (10:1) on preparative thin-layer chromatography. Colorless oil (28.2 mg, 41%). **^{1}H NMR** (500 MHz, $CDCl_3$) δ 8.68 (dd, *J* = 5.0, 0.9 Hz, 1H), 7.72 (s, 1H), 7.66 (dd, *J* = 5.1, 1.6 Hz, 1H), 4.98 (td, *J* = 10.9, 4.4 Hz, 1H), 2.81 (tt, *J* = 11.9, 3.4 Hz, 1H), 2.15 - 2.09 (m, 1H), 2.01 - 1.86 (m, 5H), 1.82 - 1.72 (m, 3H), 1.64 - 1.53 (m, 4H), 1.51 - 1.39 (m, 2H), 1.37 - 1.27 (m, 1H), 1.21 - 1.10 (m, 2H), 1.00 - 0.90 (m, 7H), 0.82 (d, *J* = 6.9 Hz, 3H). **^{13}C NMR** (125 MHz, $CDCl_3$) δ 167.6, 165.1, 149.8, 138.4, 120.4, 120.2, 75.8, 47.2, 46.6, 40.8, 34.2, 32.8, 32.8, 31.5, 26.6, 26.5, 26.0, 23.6, 22.0, 20.7, 16.5. **HRMS** ($M+H^+$) for $C_{22}H_{34}NO_2$ Calcd: 344.2584, found: 344.2571. The compound was not reported.

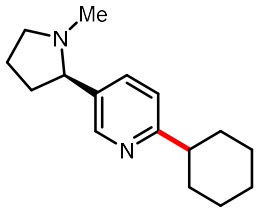

(*R*)-2-cyclohexyl-5-(1-methylpyrrolidin-2-yl)pyridine (66b). Following the general procedure A, the reaction was run with 4.0 equiv of TFA, and the product was isolated with Hex/EtOAc/MeOH (2:1:0.5) on preparative thin-layer chromatography. Yellow oil (20.5 mg,

42%). **^{1}H NMR** (500 MHz, $CDCl_3$) δ 8.43 (d, *J* = 1.8 Hz, 1H), 7.64 (dd, *J* = 8.1, 2.3 Hz, 1H), 7.14 (d, *J* = 8.0 Hz, 1H), 3.26 (t, *J* = 9.6 Hz, 1H), 3.07 (t, *J* = 8.3 Hz, 1H), 2.71 (tt, *J* = 11.9, 3.4 Hz, 1H), 2.34 - 2.26 (m, 1H), 2.23 - 2.14 (m, 4H), 2.02 - 1.93 (m, 2H), 1.90 - 1.71 (m, 5H), 1.58 - 1.24 (m, 6H). **^{13}C NMR** (125 MHz, $CDCl_3$) δ 165.5, 148.8, 135.2, 120.9, 68.7, 57.1, 46.3, 40.4, 35.0, 33.0, 33.0, 26.6, 26.1, 22.6. **GC-MS** (EI, m/z) for $C_{16}H_{24}N_2$ Calcd: 244.2, found: 244.1. Spectra data are consistent with the reported literature.[59]

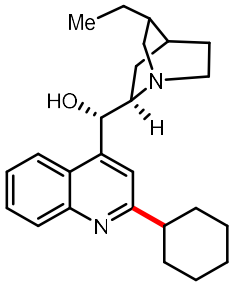

(*S*)-(2-cyclohexylquinolin-4-yl)((1*S*,2*S*,4*S*,5*R*)-5-ethylquinuclidin-2-yl)methanol (67b). Following the general procedure A, the reaction was run at 55-60 °C, and the product was isolated with Hex/EtOAc/MeOH (1:1:1) on preparative thin-layer chromatography. white solid (40.1 mg, 53%). **^{1}H NMR** (500 MHz, $CDCl_3$) δ 8.05 (d, *J* = 7.0 Hz, 1H), 7.77 (d, *J* = 9.8 Hz, 1H), 7.65 - 7.57 (m, 2H), 7.35 - 7.30 (m, 1H), 6.06 (s, 1H), 3.62 (d, *J* = 8.6 Hz, 1H), 3.24 - 3.06 (m, 3H), 3.00 - 2.84 (m, 2H), 2.18 - 2.05 (m, 1H), 2.02 - 1.94 (m, 2H), 1.93 - 1.85 (m, 2H), 1.85 - 1.75 (m, 2H), 1.70 - 1.25 (m, 11H), 1.04 - 0.96 (m, 1H), 0.92 (t, *J* = 7.2 Hz, 3H). **^{13}C NMR** (125 MHz, $CDCl_3$) δ 166.6, 147.8, 147.0, 129.9, 128.9, 126.0, 123.8, 122.1, 117.0, 68.9, 60.3, 50.8, 49.7, 47.7, 36.3, 32.8, 32.7, 26.5, 26.0, 25.8, 25.4, 24.7, 19.1, 11.8. **HRMS** ($M+H^+$) for $C_{25}H_{35}N_2O$ Calcd: 379.2744, found: 379.2731. The compound was not reported.

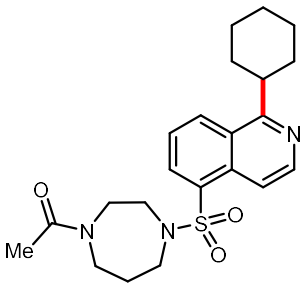

1-(4-((1-cyclohexylisoquinolin-5-yl)sulfonyl)-1,4-diazepan-1-yl)ethan-1-one, undefined ratio of conformational isomers (68b). Following the general procedure A, the reaction was run with 4.0 equiv of TFA at 55-60 °C for 36 h, and the product was isolated with Hex/EtOAc/MeOH (1:1:0.5) on preparative thin-layer chromatography. white solid (29.1 mg, 35%). **^{1}H NMR** (500 MHz, $CDCl_3$) δ 8.66 - 8.62 (m, 1H), 8.54 - 8.48 (m, 1H), 8.35 - 8.28 (m, 1H), 8.23 (d, *J* = 6.0 Hz, 1H), 7.70 - 7.64 (m, 1H), 3.76 - 3.76 (m, 1H), 3.70 - 3.55 (m, 4H), 3.56 - 3.49 (m, 1H), 3.49 - 3.38 (m, 3H), 2.09 - 2.05 (m, 3H), 2.05 - 1.91 (m, 6H), 1.91 - 1.79 (m, 3H), 1.62 - 1.48 (m, 2H), 1.48 - 1.33 (m, 1H). **^{13}C NMR** (125 MHz, $CDCl_3$) δ 170.2, 170.0, 166.8, 166.8, 144.1, 144.0, 134.7, 132.4, 132.4, 132.2, 130.6, 130.6, 126.9, 125.2, 115.2, 115.2, 50.9, 50.1, 49.2, 48.3, 48.0, 47.6, 46.8, 44.4, 42.1, 42.1, 32.7, 28.9, 27.6, 26.8, 26.1, 21.6, 21.1 (excessive peaks came from the conformational behavior of both amide and sulfonamide groups.). **GC-MS** (EI, m/z) for $C_{22}H_{29}N_3S_3$ Calcd: 415.2, found: 415.1. Spectra data are consistent with the reported literature.[3]

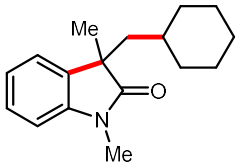

3-(cyclohexylmethyl)-1,3-dimethylindolin-2-one (71b). Colorless oil. **^{1}H NMR** (500 MHz, $CDCl_3$) δ 7.31 - 7.26 (m, 1H), 7.18 (d, *J* = 6.0 Hz, 1H), 7.10 - 7.05 (m, 1H), 6.87 (d, *J* = 7.7 Hz, 1H), 3.24 (s, 3H), 1.95 (dd, *J* = 14.1, 7.0 Hz, 1H), 1.75 (dd, *J* = 14.0, 5.2 Hz, 1H), 1.57 - 1.45 (m,

3H), 1.39 - 1.31 (m, 4H), 1.26 - 1.19 (m, 1H), 1.05 - 0.91 (m, 4H), 0.89 - 0.71 (m, 2H). **^{13}C NMR** (125 MHz, $CDCl_3$) δ 181.2, 143.1, 134.4, 127.5, 122.7, 122.3, 108.0, 47.9, 45.4, 34.7, 34.5, 33.5, 26.2, 26.2, 26.1, 26.0. **GC-MS** (EI, m/z) for $C_{17}H_{23}NO$ Calcd: 257.2, found: 257.1. Spectra data are consistent with the reported literature.[71]

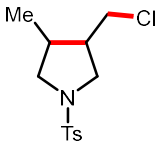

3-(chloromethyl)-4-methyl-1-tosylpyrrolidine, 1:0.5 diastereomers (73b). Yellow oil. **^{1}H NMR** (500 MHz, $CDCl_3$) δ 7.77 - 7.68 (m, 2H+1H), 7.40 - 7.30 (m, 2H+1H), 3.57 - 3.39 (m, 3H+1.5H), 3.34 (dd, *J* = 11.1, 7.5 Hz, 0.5H), 3.25 - 3.11 (m, 2H+0.5H), 3.04 (dd, *J* = 9.8, 4.9 Hz, 1H), 2.83 (dd, *J* = 9.8, 8.0 Hz, 0.5H), 2.48 - 2.28 (m, 3H+3.5H), 2.04 - 1.94 (m, 1H), 0.98 (d, *J* = 6.4 Hz, 1.5H), 0.86 (d, *J* = 6.9 Hz, 3H). **^{13}C NMR** (125 MHz, $CDCl_3$) δ 143.6, 143.5, 133.8, 133.4, 129.7, 127.6, 127.5, 54.8, 54.4, 51.3, 50.1, 47.8, 44.9, 44.4, 42.7, 36.4, 34.9, 21.6, 16.7, 12.8. **GC-MS** (EI, m/z) for $C_{22}H_{29}N_3S_3$ Calcd: 287.1, 289.1, found: 287.0, 289.0. Spectra data are consistent with the reported literature.[72]

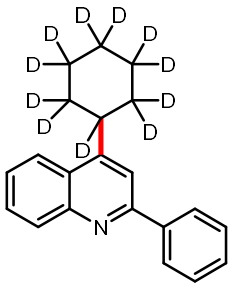

4-(cyclohexyl-*d*$_{11}$)-2-phenylquinoline (3b-*d*$_{11}$). White solid. **^{1}H NMR** (500 MHz, $CDCl_3$) δ 8.22 (dd, *J* = 8.4, 1.3 Hz, 1H), 8.17 - 8.15 (m, 2H), 8.13 - 8.09 (m, 1H), 7.78 (s, 1H), 7.75 - 7.70 (m, 1H), 7.59 - 7.52 (m, 3H), 7.51 - 7.46 (m, 1H). **^{13}C NMR** (125 MHz, $CDCl_3$) δ 157.4, 154.0,

148.6, 140.3, 130.7, 129.1, 129.0, 128.8, 127.6, 125.9, 125.9, 122.9, 115.5. **HRMS** ($M+H^+$) for $C_{12}H_{11}D_{11}N$ Calcd: 299.2437, found: 299.2426. The compound was not reported.

3.9 References

1. C.-Y. Huang, J. Li & C.-J. Li. A Cross-Dehydrogenative C(sp^3)-H Heteroarylation via Photo-Induced Catalytic Chlorine Radical Generation. *Nat. Commun.* **2021**, *12*, 4010.

2. L. Buzzetti, A. Prieto, S. R. Roy & P. Melchiorre. Radical-Based C-C Bond-Forming Processes Enabled by the Photoexcitation of 4-Alkyl-1,4-dihydropyridines. *Angew. Chem. Int. Ed.* **2017**, *56*, 15039-15043.

3. R. A. Garza-Sanchez, A. Tlahuext-Aca, G. Tavakoli & F. Glorius. Visible Light-Mediated Direct Decarboxylative C-H Functionalization of Heteroarenes. *ACS Catal.* **2017**, *7*, 4057-4061.

4. P. Liu, W. Liu & C.-J. Li. Catalyst-Free and Redox-Neutral Innate Trifluoromethylation and Alkylation of Aromatics Enabled by Light. *J. Am. Chem. Soc.* **2017**, *139*, 14315-14321.

5. W. Liu, P. Liu, L. Lv & C.-J. Li. Metal-Free and Redox-Neutral Conversion of Organotrifluoroborates into Radicals Enabled by Visible Light. *Angew. Chem. Int. Ed.* **2018**, *57*, 13499-13503.

6. R. S. J. Proctor, H. J. Davis & R. J. Phipps. Catalytic Enantioselective Minisci-Type Addition to Heteroarenes. *Science* **2018**, *360*, 419-422.

7. M. Silvi *et al.* Visible-Light Excitation of Iminium Ions Enables the Enantioselective Catalytic β-Alkylation of Enals. *Nat. Chem.* **2017**, *9*, 868-873.

8. D. Spinnato *et al.* A Photochemical Organocatalytic Strategy for the α-Alkylation of Ketones by Using Radicals. *Angew. Chem. Int. Ed.* **2020**, *59*, 9485-9490.

9. Z. Wang *et al.* Bromide-Promoted Visible-Light-Induced Reductive Minisci Reaction with Aldehydes. *ACS Catal.* **2020**, *10*, 154-159.

10. X.-Y. Yu *et al.* A Visible-Light-Driven Iminyl Radical-Mediated C-C Single Bond Cleavage/Radical Addition Cascade of Oxime Esters. *Angew. Chem. Int. Ed.* **2018**, *57*, 738-743.

11. D. Zheng & A. Studer. Asymmetric Synthesis of Heterocyclic γ-Amino-Acid and Diamine Derivatives by Three-Component Radical Cascade Reactions. *Angew. Chem. Int. Ed.* **2019**, *131*, 15950-15954.

12. Z. Zuo *et al.* Merging Photoredox with Nickel Catalysis: Coupling of Alpha-Carboxyl sp^3-Carbons with Aryl Halides. *Science* **2014**, *345*, 437-440.

13. Z. Zuo & D. W. MacMillan. Decarboxylative Arylation of α-Amino Acids via Photoredox Catalysis: A One-Step Conversion of Biomass to Drug Pharmacophore. *J. Am. Chem. Soc.* **2014**, *136*, 5257-5260.

14. H. Yi *et al.* Recent Advances in Radical C-H Activation/Radical Cross-Coupling. *Chem Rev.* **2017**, *117*, 9016-9085.

15. S. J. Blanksby & G. B. Ellison. Bond Dissociation Energies of Organic Molecules. *Acc. Chem. Res.* **2003**, *36*, 255-263.

16. J. L. Jeffrey, J. A. Terrett & D. W. MacMillan. O-H Hydrogen Bonding Promotes H-Atom Transfer from α C-H Bonds for C-Alkylation of Alcohols. *Science* **2015**, *349*, 1532-1536.

17. N. Ishida *et al.* Carboxylation of Benzylic and Aliphatic C-H Bonds with CO_2 Induced by Light/Ketone/Nickel. *J. Am. Chem. Soc.* **2019**, *141*, 19611-19615.

18. T. Kawasaki, N. Ishida & M. Murakami. Dehydrogenative Coupling of Benzylic and Aldehydic C-H Bonds. *J. Am. Chem. Soc.* **2020**, *142*, 3366-3370.

19. Z. Wang *et al.* LiBr-Promoted Photoredox Minisci-Type Alkylations of Quinolines with Ethers. *Adv. Synth. Catal.* **2019**, *361*, 5643-5647.

20. M. H. Shaw *et al.* Native Functionality in Triple Catalytic Cross-Coupling: sp^3 C-H Bonds as Latent Nucleophiles. *Science* **2016**, *352*, 1304-1308.

21. A. Hu, J.-J. Guo, H. Pan & Z. Zuo. Selective Functionalization of Methane, Ethane, and Higher Alkanes by Cerium Photocatalysis. *Science* **2018**, *361*, 668-672.

22. P. J. Sarver *et al.* The Merger of Decatungstate and Copper Catalysis to Enable Aliphatic C(sp^3)-H Trifluoromethylation. *Nat. Commun.* **2020**, *12*, 459-467.

23. Y. Shen, Y. Gu & R. Martin. sp^3 *C*- Arylation and Alkylation Enabled by the Synergy of Triplet Excited Ketones and Nickel Catalysts. *J. Am. Chem. Soc.* **2018**, *140*, 12200-12209.

24. J. Du, Z. Chen, C. Chen & T. J. Meyer. A Half-Reaction Alternative to Water Oxidation: Chloride Oxidation to Chlorine Catalyzed by Silver Ion. *J. Am. Chem. Soc.* **2015**, *137*, 3193-3196.

25. D. R. Heitz, J. C. Tellis & G. A. Molander. Photochemical Nickel-Catalyzed C-H Arylation: Synthetic Scope and Mechanistic Investigations. *J. Am. Chem. Soc.* **2016**, *138*, 12715-12718.

26. T. Kawasaki, N. Ishida & M. Murakami. Photoinduced Specific Acylation of Phenolic Hydroxy Groups with Aldehydes. *Angew. Chem. Int. Ed.* **2020**, *59*, 18267-18271.

27. L. Niu *et al.* Visible Light-Induced Direct Alpha C-H Functionalization of Alcohols. *Nat. Commun.* **2019**, *10*, 467.

28. H.-P. Deng, Q. Zhou & J. Wu. Microtubing-Reactor-Assisted Aliphatic C-H Functionalization with HCl as a Hydrogen-Atom-Transfer Catalyst Precursor in Conjunction with an Organic Photoredox Catalyst. *Angew. Chem. Int. Ed.* **2018**, *57*, 12661-12665.

29. K. Ohkubo, A. Fujimoto & S. Fukuzumi. Metal-Free Oxygenation of Cyclohexane with Oxygen Catalyzed by 9-Mesityl-10-methylacridinium and Hydrogen Chloride under Visible Light Irradiation. *Chem. Commun.* **2011**, *47*, 8515-8517.

30. K. Ohkubo, K. Mizushima & S. Fukuzumi. Oxygenation and Chlorination of Aromatic Hydrocarbons with Hydrochloric Acid Photosensitized by 9-Mesityl-10-methylacridinium under Visible Light Irradiation. *Res. Chem. Intermed.* **2013**, *39*, 205-220.

31. S. Rohe, A. O. Morris, T. McCallum & L. Barriault. Hydrogen Atom Transfer Reactions via Photoredox Catalyzed Chlorine Atom Generation. *Angew. Chem. Int. Ed.* **2018**, *57*, 15664-15669.

32. L. K. G. Ackerman, J. I. Martinez Alvarado & A. G. Doyle. Direct C-C Bond Formation from Alkanes Using Ni-Photoredox Catalysis. *J. Am. Chem. Soc.* **2018**, *140*, 14059-14063.

33. H.-P. Deng *et al.* Photoinduced Nickel-Catalyzed Chemo- and Regioselective Hydroalkylation of Internal Alkynes with Ether and Amide α-Hetero C(sp^3)-H Bonds. *J. Am. Chem. Soc.* **2017**, *139*, 13579-13584.

34. P. Lian *et al.* Visible-Light-Induced Vicinal Dichlorination of Alkenes through LMCT Excitation of $CuCl_2$. *Angew. Chem. Int. Ed.* **2020**, *59*, 23603-23608.

35. M. K. Nielsen *et al.* Mild, Redox-Neutral Formylation of Aryl Chlorides through the Photocatalytic Generation of Chlorine Radicals. *Angew. Chem. Int. Ed.* **2017**, *56*, 7191-7194.

36. B. J. Shields & A. G. Doyle. Direct C(sp^3)-H Cross Coupling Enabled by Catalytic Generation of Chlorine Radicals. *J. Am. Chem. Soc.* **2016**, *138*, 12719-12722.

37. S. M. Treacy & T. Rovis. Copper Catalyzed C(sp^3)-H Bond Alkylation via Photoinduced Ligand-to-Metal Charge Transfer. *J. Am. Chem. Soc.* **2021**, *143*, 2729-2735.

38. P. Xu, P.-Y. Chen & H.-C. Xu. Scalable Photoelectrochemical Dehydrogenative Cross-Coupling of Heteroarenes with Aliphatic C-H Bonds. *Angew. Chem. Int. Ed.* **2020**, *59*, 14275-14280.

39. C. Shu, A. Noble & V. K. Aggarwal. Metal-Free Photoinduced C(sp^3)-H Borylation of Alkanes. *Nature* **2020**, *586*, 714-719.

40. R. S. J. Proctor & R. J. Phipps. Recent Advances in Minisci-Type Reactions. *Angew. Chem. Int. Ed.* **2019**, *58*, 13666-13699.

41. S. A. Girard, T. Knauber & C.-J. Li. The Cross-Dehydrogenative Coupling of C(sp^3)-H Bonds: A Versatile Strategy for C-C Bond Formations. *Angew. Chem. Int. Ed.* **2014**, *53*, 74-100.

42. C.-J. Li. Cross-Dehydrogenative Coupling (CDC): Exploring C-C Bond Formations Beyond Functional Group Transformations. *Acc. Chem. Res.* **2009**, *42*, 335-344.

43. L. Li *et al.* Photo-Induced Iodination of Aryl Halides under Very Mild Conditions. *Nat. Protoc.* **2016**, *11*, 1948-1954.

44. L. Li *et al.* Photo-Induced Metal-Catalyst-Free Aromatic Finkelstein Reaction. *J. Am. Chem. Soc.* **2015**, *137*, 8328-8231.

45. L. Li *et al.* Simple and Clean Photoinduced Aromatic Trifluoromethylation Reaction. *J. Am. Chem. Soc.* **2016**, *138*, 5809-5812.

46. W. Liu, J. Li, C.-Y. Huang & C.-J. Li. Aromatic Chemistry in the Excited State: Facilitating Metal-Free Substitutions and Cross-Couplings. *Angew. Chem. Int. Ed.* **2020**, *59*, 1786-1796.

47. W. Liu, J. Li, P. Querard & C.-J. Li. Transition-Metal-Free C-C, C-O, and C-N Cross-Couplings Enabled by Light. *J. Am. Chem. Soc.* **2019**, *141*, 6755-6764.

48. W. Liu, X. Yang, Y. Gao & C.-J. Li. Simple and Efficient Generation of Aryl Radicals from Aryl Triflates: Synthesis of Aryl Boronates and Aryl Iodides at Room Temperature. *J. Am. Chem. Soc.* **2017**, *139*, 8621-8627.

49. W. Liu, X. Yang, Z.-Z. Zhou & C.-J. Li. Simple and Clean Photo-Induced Methylation of Heteroarenes with MeOH. *Chem* **2017**, *2*, 688-702.

50. P. S. Mariano. Electron-Transfer Mechanisms in Photochemical Transformations of Iminium Salts. *Acc. Chem. Res.* **1983**, *16*, 130-137.

51. T. McCallum *et al.* The Photochemical Alkylation and Reduction of Heteroarenes. *Chem. Sci.* **2017**, *8*, 7412-7418.

52. H. Cao *et al.* Photoinduced Site-Selective Alkenylation of Alkanes and Aldehydes with Aryl Alkenes. *Nat. Commun.* **2020**, *11*, 1956.

53. J. B. McManus, J. D. Griffin, A. R. White & D. A. Nicewicz. Homobenzylic Oxygenation Enabled by Dual Organic Photoredox and Cobalt Catalysis. *J. Am. Chem. Soc.* **2020**, *142*, 10325-10330.

54. S. U. Dighe *et al.* A Photochemical Dehydrogenative Strategy for Aniline Synthesis. *Nature* **2020**, *584*, 75-81.

55. H. Yi *et al.* Photocatalytic Dehydrogenative Cross-Coupling of Alkenes with Alcohols or Azoles without External Oxidant. *Angew. Chem. Int. Ed.* **2017**, *56*, 1120-1124.

56. H. Zhao & D. Leonori. Minimization of Back-Electron Transfer Enables the Elusive sp^3 C-H Functionalization of Secondary Anilines. *Angew. Chem. Int. Ed.* **2021**, *60*, 7669-7674.

57. S. K. Kariofillis & A. G. Doyle. Synthetic and Mechanistic Implications of Chlorine Photoelimination in Nickel/Photoredox C(sp^3)-H Cross-Coupling. *Acc. Chem. Res.* **2021**, *54*, 988-1000.

58. N. Fu, G. S. Sauer & S. Lin. Electrocatalytic Radical Dichlorination of Alkenes with Nucleophilic Chlorine Sources. *J. Am. Chem. Soc.* **2017**, *139*, 15548-15553.

59. C.-Y. Huang, J. Li, W. Liu & C.-J. Li. Diacetyl as a "Traceless" Visible Light Photosensitizer in Metal-Free Cross-Dehydrogenative Coupling Reactions. *Chem. Sci.* **2019**, *10*, 5018-5024.

60. T. Xu *et al.* Pd-Catalyzed Tandem Reaction of 2-Aminostyryl Nitriles with Arylboronic Acids: Synthesis of 2-Arylquinolines. *J. Org. Chem.* **2019**, *84*, 13604-13614.

61. A. Ramaraju *et al.* Cu-Catalyzed Coupling of *O*-Acyl Oximes with Isatins: Domino Rearrangement Strategy for Direct Access to Quinoline-4-carboxamides by C-N Bond Cleavage. *Eur. J. Org. Chem.* **2018**, *2018*, 2963-2971.

62. G. Ikarashi, T. Morofuji & N. Kano. Terminal-Oxidant-Free Photocatalytic C-H Alkylations of Heteroarenes with Alkylsilicates as Alkyl Radical Precursors. *Chem. Commun.* **2020**, *56*, 10006-10009.

63. X. Shao, X. Wu, S. Wu & C. Zhu. Metal-Free Radical-Mediated C(sp^3)-H Heteroarylation of Alkanes. *Org. Lett.* **2020**, *22*, 7450-7454.

64. H. Zhao & J. Jin. Visible Light-Promoted Aliphatic C-H Arylation Using Selectfluor as a Hydrogen Atom Transfer Reagent. *Org. Lett.* **2019**, *21*, 6179-6184.

65. M.-C. Fu *et al.* Photocatalytic Decarboxylative Alkylations Mediated by Triphenylphosphine and Sodium Iodide. *Science* **2019**, *363*, 1429-1434.

66. J. Zhou *et al.* Copper-Catalyzed Versatile C(sp^3)-H Arylation: Synthetic Scope and Regioselectivity Investigations. *Org. Chem. Front.* **2019**, *6*, 1594-1598.

67. D. R. Sutherland, M. Veguillas, C. L. Oates & A.-L. Lee. Metal-, Photocatalyst-, and Light-Free, Late-Stage C-H Alkylation of Heteroarenes and 1,4-Quinones Using Carboxylic Acids. *Org. Lett.* **2018**, *20*, 6863-6867.

68. I. B. Perry *et al.* Direct Arylation of Strong Aliphatic C-H Bonds. *Nature* **2018**, *560*, 70-75.

69. X.-K. He *et al.* Bi-OAc-Accelerated C3-H Alkylation of Quinoxalin-2(1*H*)-ones under Visible-Light Irradiation. *Org. Lett.* **2020**, *22*, 5984-5989.

70. A. P. Antonchick & L. Burgmann. Direct Selective Oxidative Cross-Coupling of Simple Alkanes with Heteroarenes. *Angew. Chem. Int. Ed.* **2013**, *52*, 3267-3271.

71. A. Ling, L. Zhang, R. X. Tan & Z.-Q. Liu. Molecular Oxygen-Promoted General and Site-Specific Alkylation with Organoboronic Acid. *J. Org. Chem.* **2018**, *83*, 14489-14497.

72. T. Taniguchi, N. Goto, A. Nishibata & H. Ishibashi. Iron-Catalyzed Redox Radical Cyclizations of 1,6-Dienes and Enynes. *Org. Lett.* **2010**, *12*, 112-115.

Chapter 4 Quinoline-catalyzed Minisci alkylation with alkyltrifluoroborate

In the previous chapter, we have developed a photocatalyst- and chemical oxidant-free dehydrogenative Minisci alkylation utilizing a chloride/cobaloxime dual catalytic platform under ultraviolet light irradiation. By exploring a quinoline-based photocatalyst **DPQN$^{2,4\text{-di-OMe}}$**, a chemical oxidant-free oxidative Minisci alkylation using alkyltrifluoroborates as alkyl radical (R•) sources under visible light irradiation will be presented in this chapter.[1]

4.1 Introduction

The catalytic proficiency of photocatalysts to effect *C*-centered radical generation has revolutionized how chemists conceive and elicit novel reactivities.[2-8] In this context, the advent of polypyridyl metallocomplexes of iridium and ruthenium enlightened a wide range of photochemical approaches to forge C-C bonds.[9-12, 3, 13, 4, 14, 5-7, 15-16, 8, 17] Concerning their high costs and potential toxicity, more sustainable organic dyes and some well-tailored organic-based photocatalysts were introduced. Unfortunately, organic dyes often suffer narrow redox windows and poor solubility.[18] Many commercialized organophotocatalysts are structurally sophisticated, therefore, necessitating prolonged and inconvenient synthesis.[14]

We have strategized a light-enabled cross-dehydrogenative Minisci alkylation between heteroarenes and alkanes, which comprised the SET between excited heteroaromatics and chloride salt to generate chlorine radical (Cl·) and the Cl·-assisted hydrogen atom abstraction (HAT) to confer R• as the key mechanistic scenarios.[1] Despite its pronounced reactivities toward inert C-H substrates and granting numerous alkylated heteroarenes, such a design still suffered inherent drawbacks. During the SET event, energetic ultraviolet photons (>280 nm) were demanded for global excitation of the heteroaromatic reactants, inevitably limiting the scope due to the off-target substrate decomposition and excluding examples that showed unmatched absorption patterns. Also, because of the untamed reactivity of Cl·, excessive or manipulated C-H coupling partners were often required to combat the site selectivity issue.[19]

Mindful of these concerns, we reasoned that developing cost-effective organophotocatalysts and simplifying the reaction pathway could solve these problems in Minisci alkylation. More importantly, the new conditions might serve as templates for other related oxidative cross-couplings with minimum modification.

4.2 Reaction design

Conjugated heteroaromatic motifs, especially N-heterocycles, are frequently seen in photocatalytic chromophores. Indeed, isolated heteroarenes, for instance, quinolines, have been capitalized as single-electron oxidants that could oxidize some intractable reactants under photochemical conditions,[20-22] albeit requiring energetic ultraviolet photons and restricting the reaction scope only in quinoline functionalization.

For the new organophotocatalyst design, we hypothesized that engineering the C2 and C4 positions of quinoline skeletons with π-extended substituents could be advantageous, moving its absorption to the visible light region and simultaneously blocking their radicophilic sites.[23] By inspecting some representative photocatalysts (e.g., Fukuzumi's and Nicewicz's catalysts), cationic nitrogen centers appear to be common traits. As such, we expected that simple protonation of our quinoline photocatalyst could exert an equal effect. If successful, such a convenient and tunable activation mode would considerably simplify photocatalyst synthesis since the exocyclic *N*-substituents of the above-noted counterparts were tethered via nucleophilic displacement or metal-catalyzed cross-couplings. Moreover, it could be envisaged that pairing this modified quinoline photocatalyst and a prolific radical precursor with reasonably low reduction potential could further polish the current protocols for oxidative Minisci alkylation. To this end, potassium alkyltrifluoroborates (R-BF_3K), which were widely accessible, structurally diverse, and shelf-stable,[24-31, 16, 32-33] could be ideal candidates for evaluating our organophotocatalyst design.

To establish proof of concept, slightly excessive potassium cyclohexyltrifluoroborate (**2c**, Cy-BF_3K, E^{red} = +1.5 V vs SCE) was opted to alkylate lepidine (**1c**) in the presence of trifluoroacetic acid (TFA), cobaloxime [$Co(dmgH)_2(py)$]Cl and various entrants of quinoline photocatalysts in dioxane under visible light irradiation (**Table 4.1**). Delightfully, 2,4-diphenylquinoline (**DPQN**) afforded the cyclohexylated product **3c** in a 25% yield (entry 1). Encouraged by this result, a library of **DPQN** derivatives was quickly constructed with anilines, benzaldehydes and phenylacetylenes as building blocks to assess the substitution effect of **DPQN**.

Mindful of the instrumental role of cationization in enhancing photocatalytic performance,[2, 34-35, 22, 36-37] electron-donating groups might be beneficial. Furthermore, locating the electron-releasing substituents on **DPQN** could structurally correlate with

the donor-acceptor patterns of acridiniums. Unsurprisingly, the yield of **3c** dropped when an electron-withdrawing trifluoromethyl group resided on the DPQN parent structure (entry 2). On the contrary, the productivity was significantly elevated when using methylated and methoxylated DPQNs (entries 3 to 6). On the electronic ground, methyl and methoxy groups could also combat the susceptibility of catalysts towards radical attack, therefore conferring stability against their deactivation.[38-39] This might rationalize **DPQN$^{2,4\text{-di-OMe}}$** ranked the most robust and efficient photocatalysts in this series, giving a good yield of the cyclohexylation product even at 0.025 mol% loading, albeit with a longer reaction time (72 h). Removal of either aryl handle from **DPQN** completely suppressed the reaction, presumably due to the unmatched photoabsorptive profiles or the non-productive consumption of radical intermediates (entries 7 to 10). Control experiments showed that photocatalyst, cobalt, acid, light and inert atmosphere were all vital for this photoinduced oxidative cross-coupling reaction. Notably, among some commercial photocatalysts evaluated, $[Ru(bpy)_3](PF_6)_2$, Eosin Y, Rose bengal, and Rhodamine brought poor results of the Minisci alkylation (<25%), while Nicewicz's catalyst and $(Ir[dF(CF_3)ppy]_2(dtbpy))(PF_6)$ gave comparable results (**Scheme 4.1**).

Table 4.1 Evaluation of the quinoline-base photocatalyst.

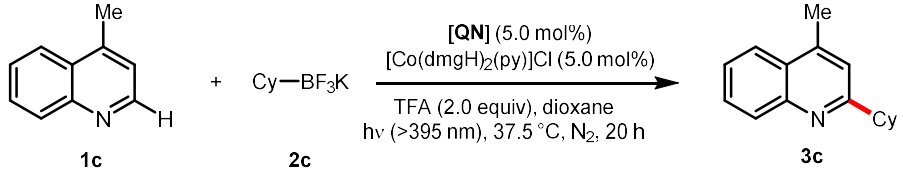

1c 2c 3c

Entry[a]	[QN]	R	R'	Yield (%)	Entry[a]	[QN]	R	R'	Yield (%)
1	**DPQN**	Ph	Ph	25	6[b]	**DPQN$^{2,4\text{-di-OMe}}$**	4-OMe-Ph	4-OMe-Ph	96
2	**DPQN$^{2\text{-CF}_3}$**	4-CF_3-Ph	Ph	19	7	**QN$^{2\text{-Ph}}$**	Ph	H	0
3	**DPQN$^{2\text{-Me}}$**	4-Me-Ph	Ph	65	8	**QN$^{4\text{-Ph}}$**	H	Ph	0
4	**DPQN$^{2\text{-OMe}}$**	4-OMe-Ph	Ph	79	9	**QN$^{2\text{-Ph-4-Me}}$**	Ph	Me	0
5	**DPQN$^{4\text{-OMe}}$**	Ph	4-OMe-Ph	86	10	**QN$^{2\text{-Me-4-Ph}}$**	Me	Ph	0

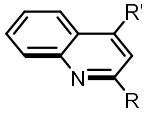

[QN]

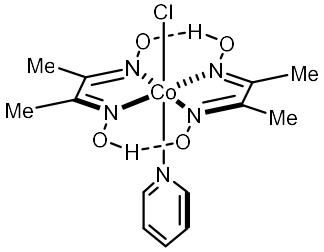

$[Co(dmgH)_2(py)]Cl$

[a]Reaction conditions: **1c** (0.10 mmol, 1.0 equiv), **2c** (0,15 mmol, 1.5 equiv), [**QN**] (5.0 μmol, 5.0 mol%), $[Co(dmgH)_2(py)]Cl$ (5.0 μmol, 5.0 mol%), TFA (0.20 mmol, 2.0 equiv) in dioxane (1.5 mL) under nitrogen at 37.5 °C and irradiated by >395 nm light for 20 hours. Yields were determined by ^1H NMR using CH_2Br_2 as the internal standard [b] Trace or no product was formed without [**QN**], [Co], TFA, or light, or under air atmosphere. [c]With 0.025 mol% [**QN**] for 72-hour irradiation. **[QN]**, quinoline photocatalyst; dmgH, dimethylglyoxime; py, pyridine; TFA, trifluoroacetic acid; hν, photon.

Scheme 4.1 Evaluation of other photocatalysts.

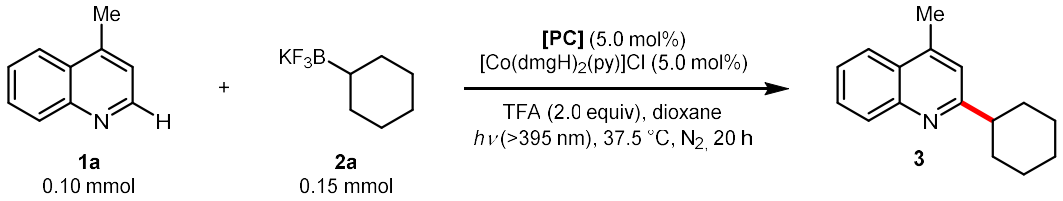

PC:

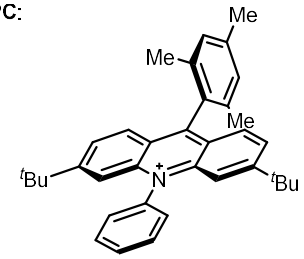

[di-*t*-Bu-Mes-Acr-Ph]$^+$ (87%)

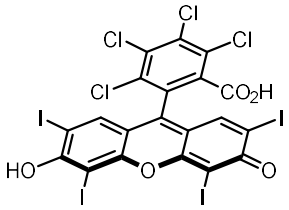

Rose bengal (0%)

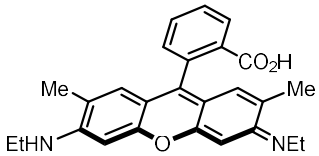

Rhodamine 6G (0%)

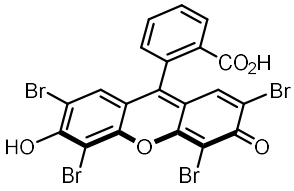

Eosin Y (25%)

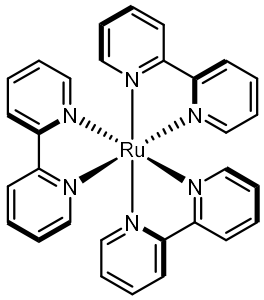

(Ru(bpy)$_3$)(PF$_6$)$_2$ (0%)

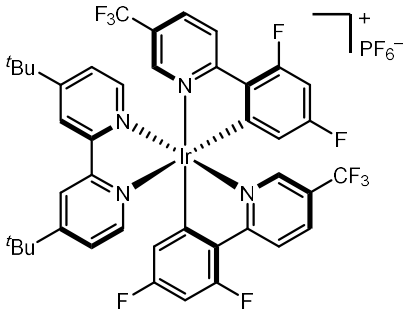

(Ir[dF(CF$_3$)ppy]$_2$(dtbpy))(PF$_6$) (96%)

Therefore, 1.0 equiv heteroarene, 1.5 equiv alkyltrifluoroborate, 5.0 mol% **DPQN$^{2,4\text{-di-OMe}}$**, 5.0 mol% [Co(dmgH)$_2$(py)]Cl and 2.0 equiv TFA in dioxane under argon with visible light irradiation (>395 nm) marked our optimal conditions. Notably, **DPQN$^{2,4\text{-di-OMe}}$** could be easily prepared in a multigram scale (**Scheme 4.2**).

Scheme 4.2 Gram-scale synthesis of DPQN$^{2,4\text{-di-OMe}}$.

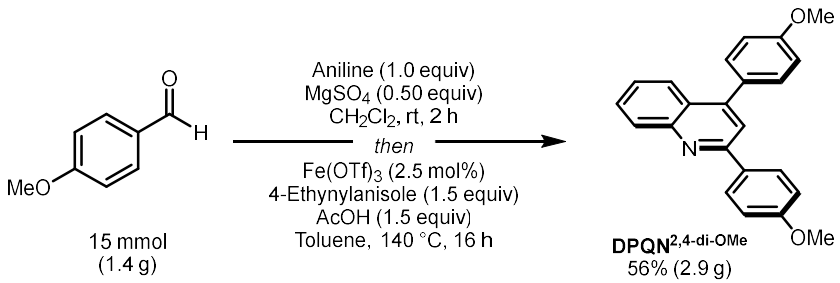

4.3 Results and discussion

Armed with the optimal conditions, we sought to apply this [**QN**]/[Co] dual-catalyzed protocol to the alkylation of lepidine **1c** with various alkyltrifluoroborates (**Scheme 4.3**). To our delight, a broad spectrum of alkyltrifluoroborates, including 1°, 2° and 3° ones, were proven viable in this transformation. Simple alkyl groups such as the isopropyl, sec-butyl, n-pentyl, and tert-butyl could be installed, providing the elaborated lepidines smoothly (**4c** to **7c**), so as the four to six-membered cyclic substituents (**8c** and **9c**). The bridged reagents like 1-adamantyl and 2-norbonyl ones were heteroarylated successfully, which afforded the target products **10c** and **11c** in good to excellent yields. Functionalized alkyltrifluoroborates bearing ester, ketone, ethereal, carbamoyl, benzyloxy, allyloxy, and propargyloxy groups were also compatible, giving alkylated lepidines in satisfactory yields (**12c** to **22c**).

Scheme 4.3 Substrate scope of alkyl trifluoroborate.

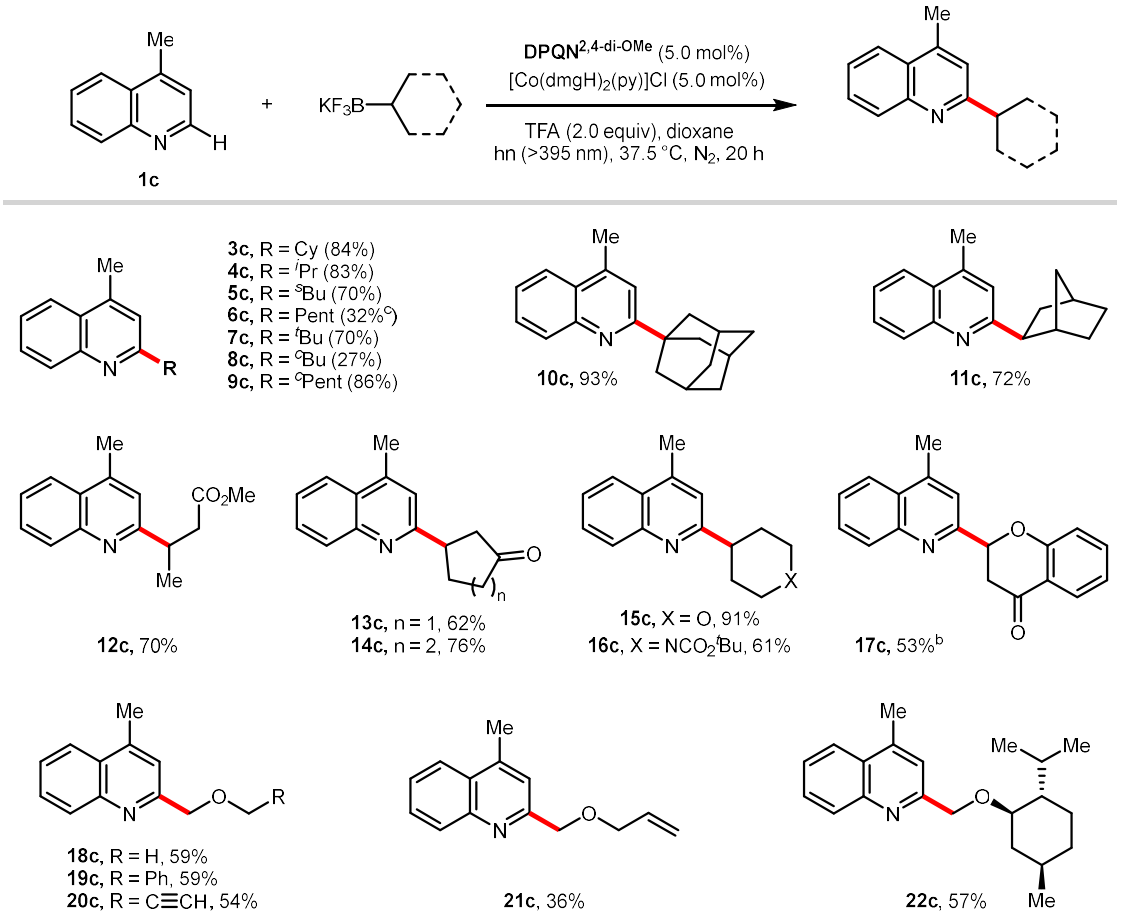

[a]Reaction conditions: **1c** (0.10 mmol, 1.0 equiv), alkyl trifluoroborate (0,15 mmol, 1.5 equiv), **DPQN**$^{2,4\text{-di-OMe}}$

(5.0 μmol, 5.0 mol%), [Co(dmgH)$_2$(py)]Cl (5.0 μmol, 5.0 mol%), TFA (0.20 mmol, 2.0 equiv) in dioxane (1.5 mL) under nitrogen at 37.5 °C and irradiated by >395 nm light for 20 hours. Yields were the isolated ones. [b]3.0 equiv alkyl trifluoroborate. [c]EtOAc as the solvent. Cy, cyclohexyl; ^{i}Pr, isopropyl; ^{s}Bu, *sec*-butyl; Pent, pentyl; ^{t}Bu, *tert*-butyl; ^{c}Bu, cyclobutyl; ^{c}Pent, cyclopentyl; **DPQN$^{2,4\text{-di-OMe}}$**, 2,4-bis(4-methoxyphenyl)quinoline; dmgH, dimethylglyoxime; py, pyridine; TFA, trifluoroacetic acid; hν, photon.

Scheme 4.4 Substrate scope of heteroarene.

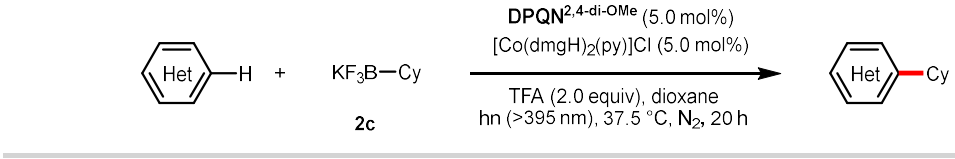

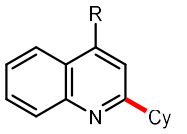

23c, R = Ph, (80%)
24c, R = CN, (56%[b])

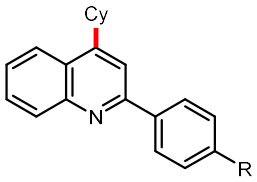

25c, R = H (66%)
26c, R = F (53%)
27c, R = Br (74%)
28c, R = Ac (43%[b])

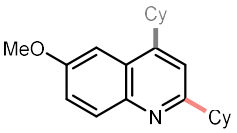

29c, 43%[c,e,f]
(10:1 mono:di)

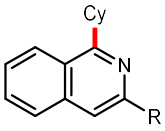

30c, R = H (62%, 6.2:1 C1:C3)
31c, R = Me (70%)
32c, R = CO_2Me (65%)

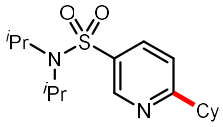

33c, 41%[b,e]

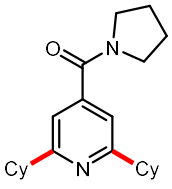

34c, 32%[b,e]

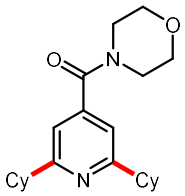

35c, 42%[b,e]

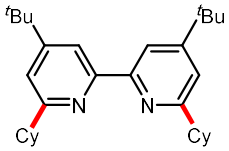

36c, 28%[c,d]

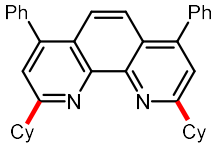

37c, 45%[c,d,g]

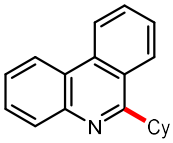

38c, 96%

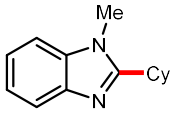

39c, 57%[b]

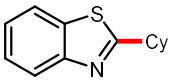

40c, 60%[b]

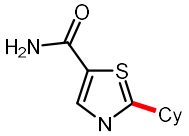

41c, 45%[b]

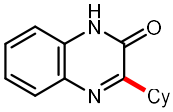

42c, 58%[b,e]

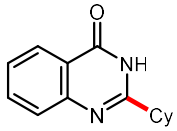

43c, 73%[b]

[a]Reaction conditions: **1c** (0.10 mmol, 1.0 equiv), alkyl trifluoroborate (0,15 mmol, 1.5 equiv), **DPQN$^{2,4\text{-di-OMe}}$** (5.0 μmol, 5.0 mol%), [Co(dmgH)$_2$(py)]Cl (5.0 μmol, 5.0 mol%), TFA (0.20 mmol, 2.0 equiv) in dioxane (1.5 mL) under nitrogen at 37.5 °C and irradiated by >395 nm light for 20 hours. Yields were the isolated ones. [b]3.0 equiv alkyl trifluoroborate. [c]4.0 equiv alkyl trifluoroborate. [d]3.0 equiv TFA. [e]EtOAc as the solvent. . [f]Run for 40 h. [g]NMR yield. Cy, cyclohexyl; ^{i}Pr, isopropyl; ^{t}Bu, *tert*-butyl; **DPQN$^{2,4\text{-di-OMe}}$**, 2,4-bis(4-methoxyphenyl)quinoline; dmgH, dimethylglyoxime; py, pyridine; TFA, trifluoroacetic acid; hν, photon.

Further scope examination was conducted with different heteroaromatic pharmacophores with cyclohexyltrifluoroborate (**2c**) as the coupling partner (**Scheme 4.4**). A variety of substituents on heterocycles like cyano, halo, ketone, alkoxy, ester, sulfonamido, amino, amido groups and others were well tolerated in this reaction (**23c** to **52c**). Besides quinoline compounds, elaboration of isoquinoline, pyridine, bipyridine, phenanthroline, phenanthridine, benzimidazole, benzothiazole, thiazole, quinoxalinone and quinazolinone were shown to be effective (**30c** to **43c**).

Scheme 4.5 Substrate scope of notable heteroarene.

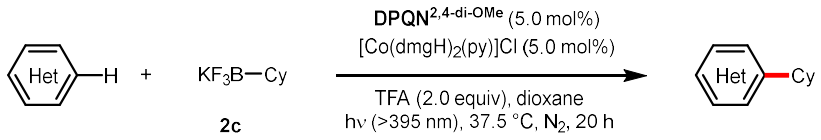

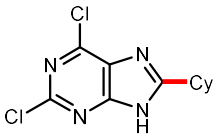

44c, 64%[b,d]
from purine

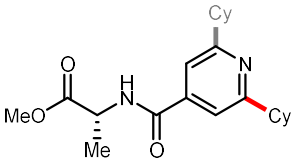

45c, 40%[d]
(1:1 mono:di)
from alanine

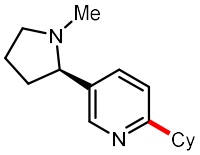

46c, 44%[b]
from nicotine

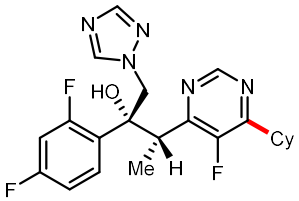

47c, 39%[b,d]
from voriconazole

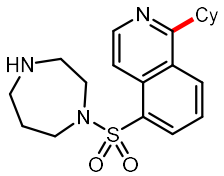

48c, 65%[b,d]
from fasudil

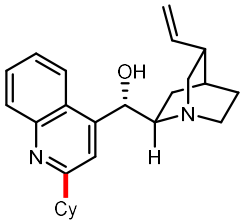

49c, 44%
from cinchonine

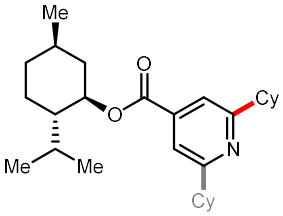

50c, 50%[d]
(1:1 mono:di)
from menthol

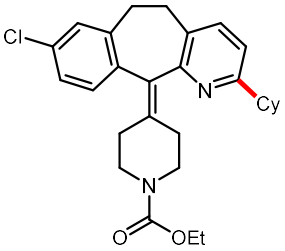

51c, 46%[b,d]
from loratadine

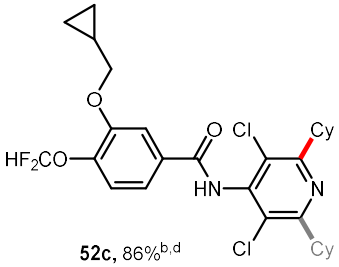

52c, 86%[b,d]
(2:1 mono:di)
from roflumilast

[a]Reaction conditions: **1c** (0.10 mmol, 1.0 equiv), alkyl trifluoroborate (0,15 mmol, 1.5 equiv), **DPQN$^{2,4\text{-di-OMe}}$** (5.0 μmol, 5.0 mol%), $[Co(dmgH)_2(py)]Cl$ (5.0 μmol, 5.0 mol%), TFA (0.20 mmol, 2.0 equiv) in dioxane (1.5 mL) under nitrogen at 37.5 °C and irradiated by >395 nm light for 20 hours. Yields were the isolated ones. [b]3.0 equiv alkyl trifluoroborate. [c]4.0 equiv alkyl trifluoroborate. [d]3.0 equiv TFA. Cy, cyclohexyl; **DPQN$^{2,4\text{-di-OMe}}$**, 2,4-bis(4-methoxyphenyl)quinoline; dmgH, dimethylglyoxime; py, pyridine; TFA, trifluoroacetic acid;

hν, photon.

To showcase the robustness of this protocol, the alkylation of substrates with high molecular complexity was evaluated (**Scheme 4.5**). Encouragingly, cyclohexylation of dichloropurine provided the expected product **44c** in moderate yield. Couplings of pyridines consisting of alanine, pyrrolidine, and menthol moieties proceeded efficiently (**45c**, **46c**, and **50c**). It was worth mentioning that more structurally complex pyridine derivatives could also be applied in our current protocol. For example, loratadine and roflumilast, registered for allergy medications and phosphodiesterase-4 (PED-4) inhibition, respectively, could be transformed into desirable products with their carbamate or carbamate amide group remaining untouched (**51c** and **52c**). Other bioactive examples, including the antifungal agent voriconazole and the marketed isoquinoline-based vasodilator, fasudil, could be utilized directly without functional group protection (**47c** and **48c**). We were pleased to see that cinchonine, which is quinoline-cored and bears both hydroxyl and amino groups, could be easily modified by our protocol (**49c**).

4.4 Mechanistic studies

To rationalize the advantageous effect of methoxy substituents on the protonated **DPQN$^{2,4\text{-di-OMe}}$**-H$^+$ and further elucidate our proposed "proton activation" concept, the electronically neutral and deficient variants (**DPQN** and **DPQN$^{2\text{-CF}_3}$**), as well as the non-protonated **DPQN$^{2,4\text{-di-OMe}}$**, were selected as representative catalysts for more investigations. Interestingly, the stronger visible light absorption of protonated **DPQN$^{2,4\text{-di-OMe}}$** could be directly visualized under ambient conditions as its neutral form and the other two in acidic media were basically colorless (**Scheme 4.6A**, upper). Such differences were even more obvious under 390 nm LED light irradiation since proton-activated **DPQN$^{2,4\text{-di-OMe}}$** gave a much brighter luminescence (**Scheme 4.6A**, lower). With this observation in mind, the absorptivity (**Scheme 4.6B**) and fluorescence (**Scheme 4.6C**) of these **DPQN**s were measured. Unsurprisingly, protonated **DPQN$^{2,4\text{-di-OMe}}$** outweighed the other three in both measurements, which agreed with its markedly higher Stern-Volmer quenching efficiency by the cyclohexyltrifluoroborate (**Scheme 4.6D**). These results emphasized the significance of electron-releasing substituents on the diarylquinoline framework and the presence of an acid, which synergistically augmented the photoproductivity of **DPQN$^{2,4\text{-di-OMe}}$**.

Scheme 4.6 Photophysical properties of [QN]s.

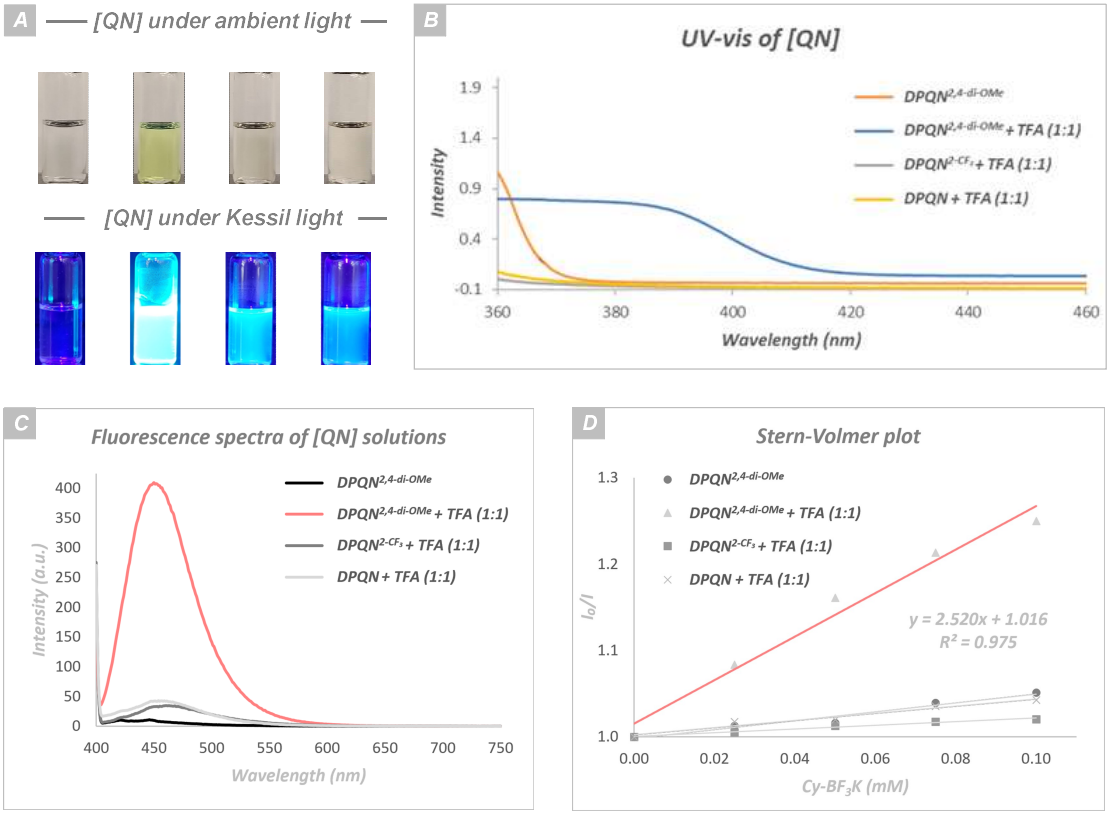

A, from left to right, 10 μM dioxane solutions of **DPQN$^{2,4\text{-di-OMe}}$**, **DPQN$^{2,4\text{-di-OMe}}$-H$^+$**, **DPQN-H$^+$**, and **DPQN$^{2\text{-CF3}}$-H$^+$**, under ambient light (upper) or 390 nm light irradiation (lower). B, UV-vis of 2.5 mM [**QN**] dioxane solutions. C, fluorescence spectra of 0.50 mM [**QN**] dioxane solutions. D, Stern-Volmer plots of 0.50 mM [**QN**] dioxane solutions with a varied amount of $CyBF_3K$, irradiated at 395 nm.

Our optimal photocatalyst **DPQN$^{2,4\text{-di-OMe}}$** was further characterized by several spectroscopic techniques to collect some of its photophysical parameters.[40] In the cyclic voltammogram (CV) measurements, the working electrode was made of glassy carbon, and a Pt wire was used as the counter electrode to complete the electrochemical setup. A scan rate of 20 mV/s was used for all experiments. All the potentials were noted with respect to the Ag/AgCl electrode unless otherwise specified. The reduction potential referenced to the standard calomel electrode (SCE) could be calculated by subtracting 0.039 V from the E(Ag/AgCl). It followed that

$$E(SCE) = E(Ag/AgCl) - 0.039\ V$$

The plots were shown in (**Figure 4.1**), which showed that the redox process of neutral **DPQN$^{2,4\text{-di-OMe}}$** was electrochemically reversible ($E_{1/2}$([QN]/[**QN$^{\bullet-}$**]) = -0.95 V vs SCE), while it was irreversibly reduced in the presence of TFA ($E_{p/2}$([**QN-H^{+}**]/[QN-**H$^{\bullet}$**] = -0.81 V vs SCE). Such changes complied with some exploratory findings that the ground-state species could be more prone to reduction upon protonation and partially justified the requirement of acid in our system.[41, 22, 36-37]

Figure 4.1 CV of 20 mM DPQN$^{2,4\text{-di-OMe}}$ and DPQN$^{2,4\text{-di-OMe}}$-H^{+}.

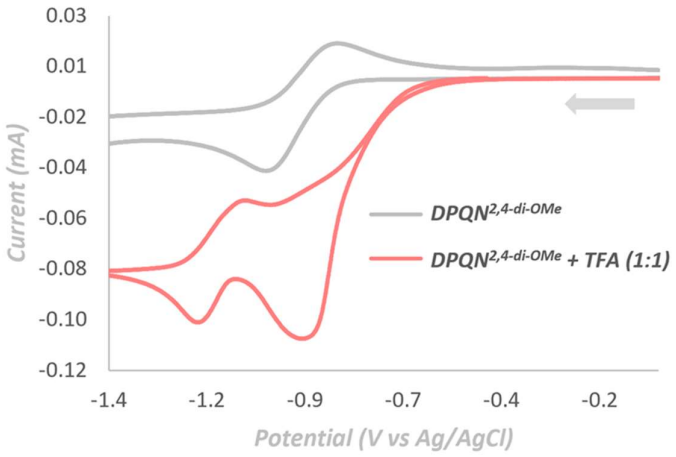

QN photoredox catalyst	*Free base*		*Protonated form*	
	E_p (V)	$E_{1/2}$ (V)	E_p (V)	$E_{p/2}$ (V)
DPQN$^{2,4\text{-di-OMe}}$	-1.00	-0.91	-0.91	-0.81

E_p, peak potential; $E_{1/2}$, half-wave potential (for reversible peaks, the average of anodic and cathodic peak potentials); $E_{p/2}$, half peak potential (half-maximum current).

Figure 4.2 Stacked UV-vis and fluorescence spectra of DPQN$^{2,4\text{-di-OMe}}$-H^{+}.

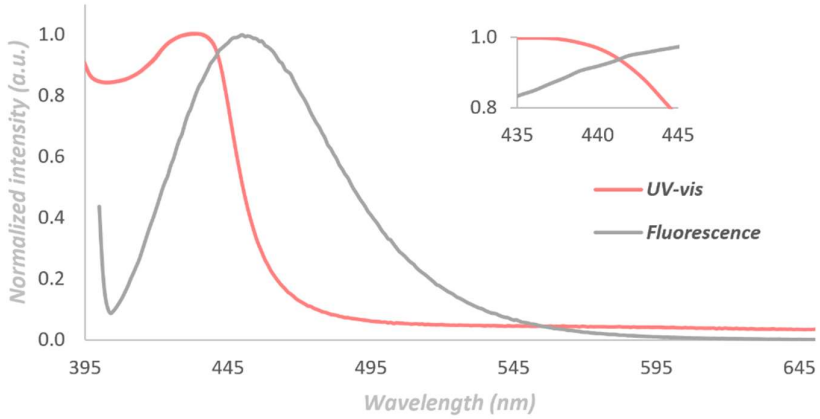

Normalized UV-vis spectrum of 1.25 mM **DPQN$^{2,4\text{-di-OMe}}$-H^{+}** dioxane solution and fluorescence spectra of

0.50 mM **DPQN$^{2,4\text{-di-OMe}}$-H^{+}** dioxane solution (at 395 nm).

Ultraviolet-visible (UV-vis) and fluorescence spectra demonstrated that the positively charged **DPQN$^{2,4\text{-di-OMe}}$** absorbed strongly above 395 nm and emitted mostly at around 455 nm, with the intersection at 428 nm (**Figure 4.2**).

The excited-state redox potential $E_{1/2}$ (PC*/PC^{-}) was estimated by the following equation:

$$E_{1/2}\,(\mathrm{PC^*/PC^-}) = E_{0\text{-}0} + E_{1/2}\,(\mathrm{PC/PC^-})$$

where $E_{1/2}$ (PC/PC^{-}) was the ground state redox potential; $E_{0\text{-}0}$ was the energy difference between 0th vibrational states of the ground state and excited state, which can be approximated by the intersection point between the normalized absorption and emission spectra.[42-43]

For a simpler symbolization, it should be noted that all the calculations and discussion in this section were based on the TFA-protonated **DPQN$^{2,4\text{-di-OMe}}$** (1:1), which meant that the ground state photoredox catalyst (PC) was +1 charged and PC$^{\cdot}$ was neutral. All the potentials were reduction potentials, which were noted with respect to the Ag/AgCl electrode unless otherwise specified. The potential referenced to SCE could be calculated by subtracting 0.039 V from the E(Ag/AgCl), following that E(SCE) = E(Ag/AgCl) - 0.039 V.[44]

Since **DPQN$^{2,4\text{-di-OMe}}$** gave irreversible peaks in cyclic voltammogram (Figure S12), $E_{p/2}$ (PC/PC^{-}) was used for its ground state redox potential, $E_{1/2}$ (PC/PC^{-}), which was determined to be -0.81 V.

For the excitation energy, $E_{0\text{-}0}$, since the wavelength of the cross point in absorption and emission spectra was 441 nm, it could be translated into $E_{0\text{-}0}$ = 2.81 eV. Therefore,

$$E_{1/2}\,(\mathrm{PC^*/PC^-}) = E_{0\text{-}0} + E_{1/2}\,(\mathrm{PC/PC^-}) = 2.81\ \mathrm{V} - 0.81\ \mathrm{V} = +\,2.00\ \mathrm{V\ vs\ Ag/AgCl}$$

and,

$$E_{1/2}\,(\mathrm{PC^*/PC^{\cdot}}) = 2.00\ \mathrm{V} - 0.039\ \mathrm{V} = +\,1.96\ \mathrm{V\ vs\ SCE}$$

With such an extensive oxidation window, photoinduced electron transfer with alkyltrifluoroborates was assured, as evidenced by the Stern-Volmer plot (K_{SV} = 2.5 mM^{-1}, **Scheme 4.6D**). Furthermore, simple calculations of the fluorescence lifetime of the **DPQN$^{2,4\text{-di-OMe}}$-H^{+}** also gave the singlet excited state lifetime τ = 2.07$\pm$ 0.01 ns (**Figure 4.3**). These results resemble some acridinium photocatalysts (Fukuzumi's Mes-Acr^{+}-Me catalyst, $E_{1/2}$ (PC^*/PC^-) = +1.94 V vs SCE, τ ~6 ns; Nicewicz's Mes-Acr^{+}-Ph catalyst, $E_{1/2}$ (PC^*/PC^-) = +1.88 V vs SCE, τ ~1.5 ns), which are powerful for photochemical oxidation processes.[45, 14]

Figure 4.3 Transient absorption decay of DPQN$^{2,4\text{-di-OMe}}$-H^{+} at 375 nm.

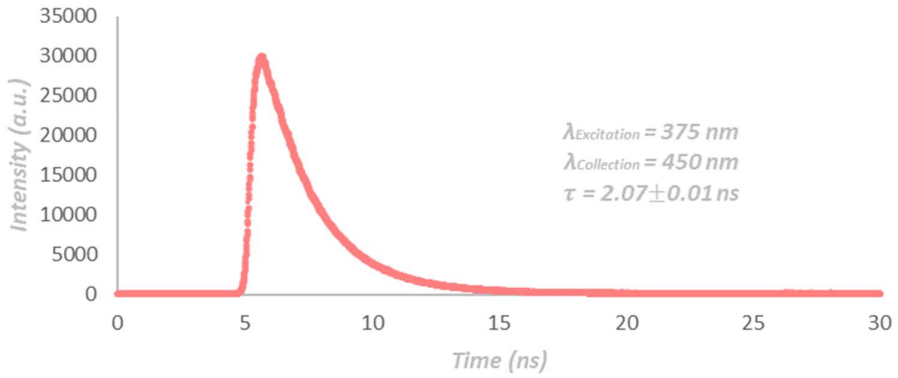

Next, we focused on gaining insight into the overall reaction process. Light on-and-off experiments indicated that continuous light irradiation was indispensable for the reaction since an inconsequential increase in product yield persisted in the dark (**Figure 4.4**). In light of the quantum yield (Φ = 14.5%), a chain process was less likely in our system (see experiment section for calculation details).

Figure 4.4 Light on/off experiment of the standard reaction.

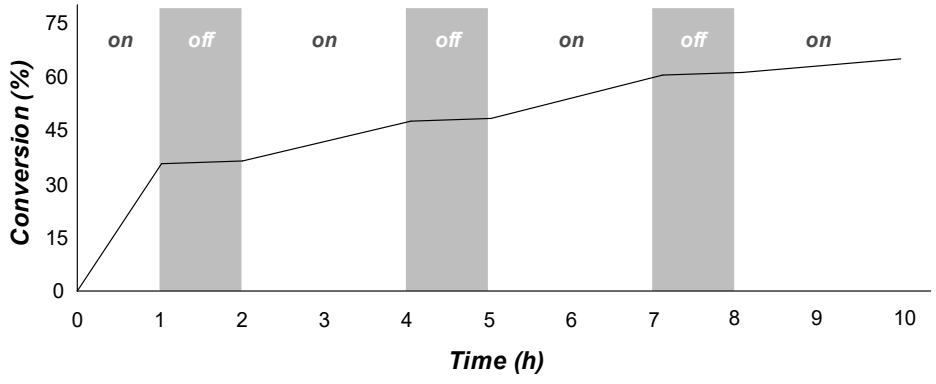

Scheme 4.7. Radical pathway investigations.

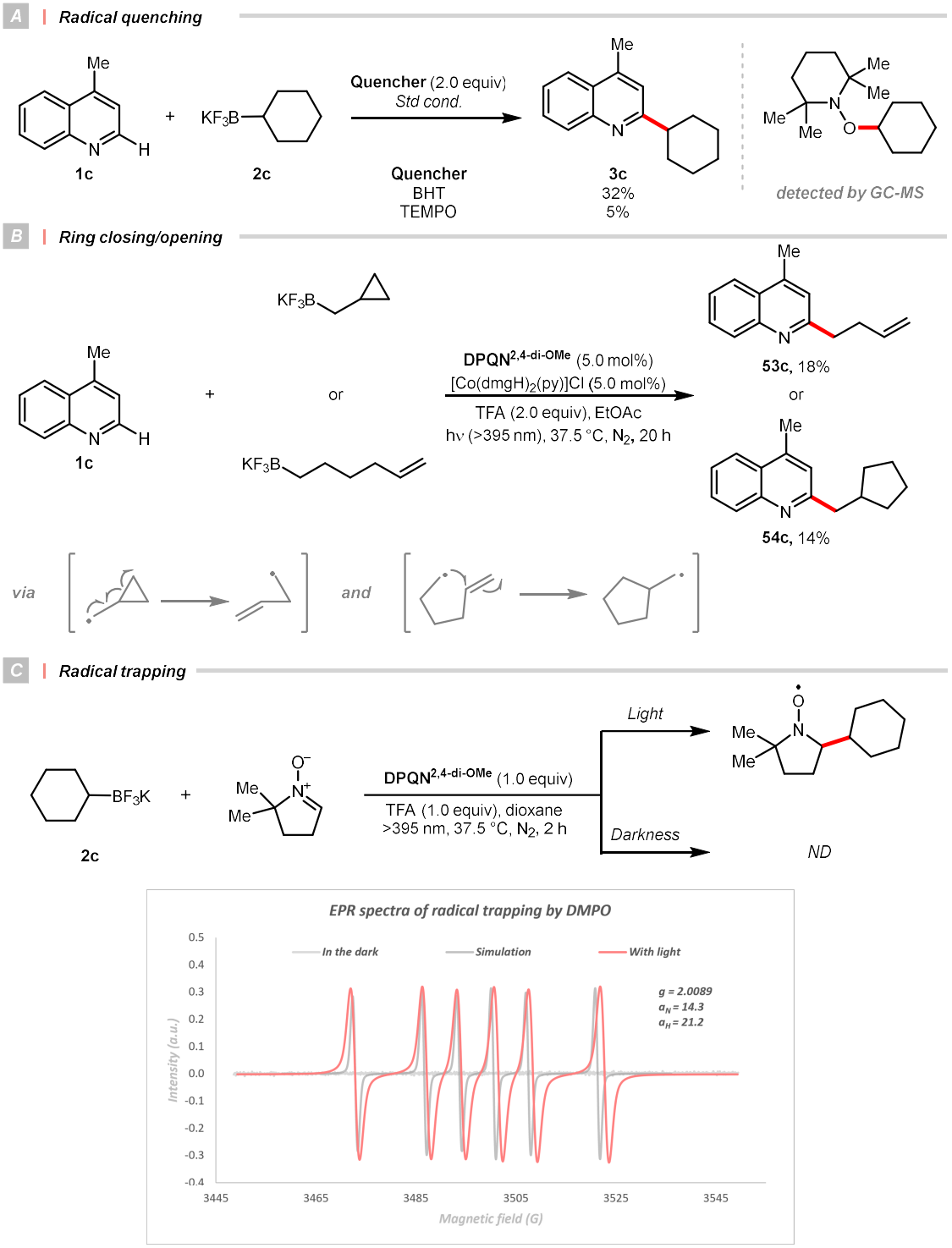

When radical quenchers, 3,5-di-*tert*-4-butylhydroxytoluene (BHT) and 2,2,6,6-tetramethylpiperidine 1-oxyl (TEMPO), were present, the desired reactivities were mostly inhibited, and the cyclohexyl-added TEMPO was detected in the latter case, which

suggested the involvement of R• in our reaction (**Scheme 4.7**). Also, radical-clock reagents, including (cyclopropylmethy)trifluoroborate and 5-hexenyltrifluoroborate, were subjected to our standard conditions. As expected, the ring-opening and -closing products were isolated successfully (**53c** and **54c**), again signaling the presence of radical intermediacy. Furthermore, electron paramagnetic resonance (EPR) provided direct evidence for the existence of open-shell species. Under light irradiation, the cyclohexyl radical was trapped by 5,5-dimethyl-1-pyrroline-*N*-oxide (DMPO), whose EPR spectrum was fully consistent with the literature and our simulation, while such a response was silenced in the dark. Lastly, H_2 evolution was confirmed by gas chromatography-thermal conductivity detector (GC-TCD), which was in accordance with our acceptorless oxidative coupling design.

Scheme 4.8 Proposed reaction mechanism.

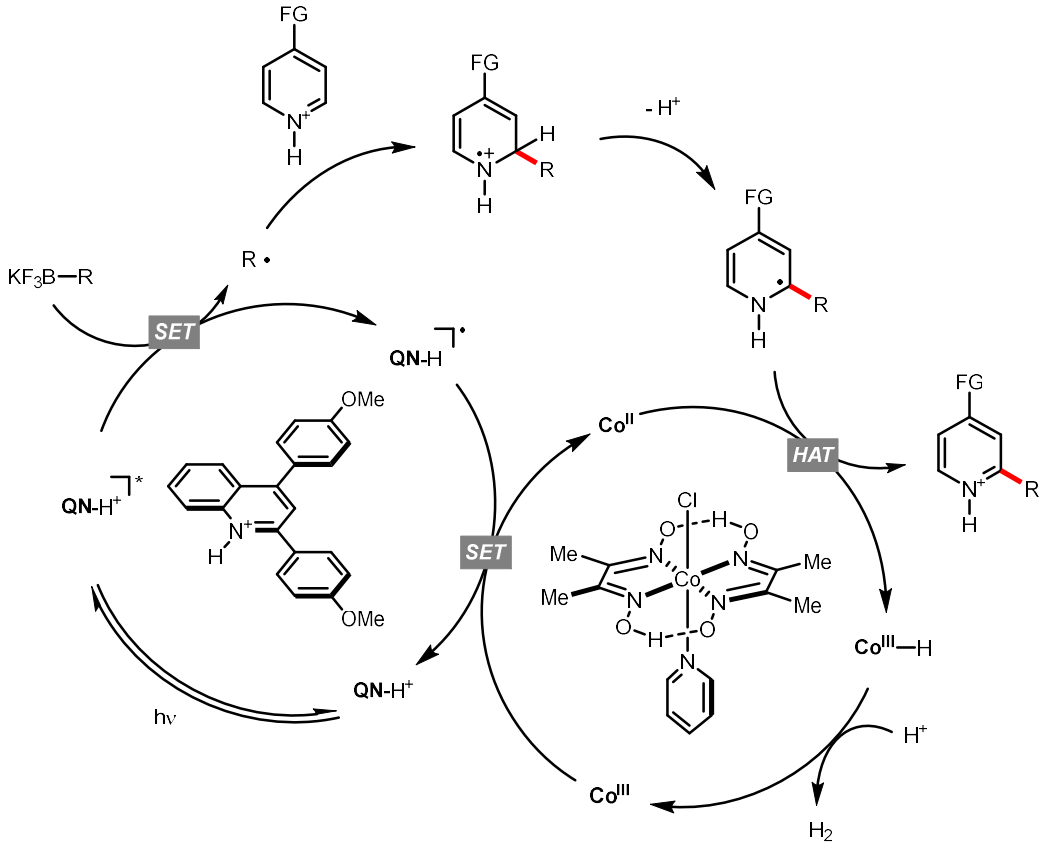

Taken together, a tentative reaction mechanism was proposed and shown in **Scheme 4.8**. Driven by the visible light irradiation, the excited diarylquinoline [**QN**-H$^+$]* underwent a reductive quenching by the alkyltrifluoroborate, generating two radical

intermediates, R• and heteroaryl radical [**QN**-H]•. While the R• attacked the protonated heteroarene followed by deprotonation to give an α-amino radical species, the [**QN**-H]• ($E_{p/2}$([**QN**-H$^+$]/[**QN**- H]• = -0.81 V vs SCE) reduced the cobaloxime Co^{III} into Co^{II} ($E^{red}(Co^{III}/Co^{II})$ = -0.16 V vs SCE)[46] via SET and regenerated the active catalyst [**QN**-H$^+$]. Concurrently, formal HAT occurred between the α-amino radical species and Co^{II}, which delivered Co^{III}-H and the desired alkylated product after rearomatization. The Co^{III}-H then reduced the H$^+$ and closed the catalytic cycle via releasing H_2.

4.5 Synthetic applications

The facile access of different **DPQN** congeners, which were easily immobilized on the commercially available amino-modified polystyrene (PS) beads via amide coupling, allowed the convenient preparation of solid-supported organophotocatalysts (**Scheme 4.9A**). Robustness tests showed that the **DPQN$^{2,4\text{-di-OR}}$@PS** in only 0.50 mol% loading could be re-used for oxidative Minisci alkylation five times after simple filtration (**Scheme 4.9B**).

Scheme 4.9 Synthesis of polymer-supported photocatalyst and its recycling test.

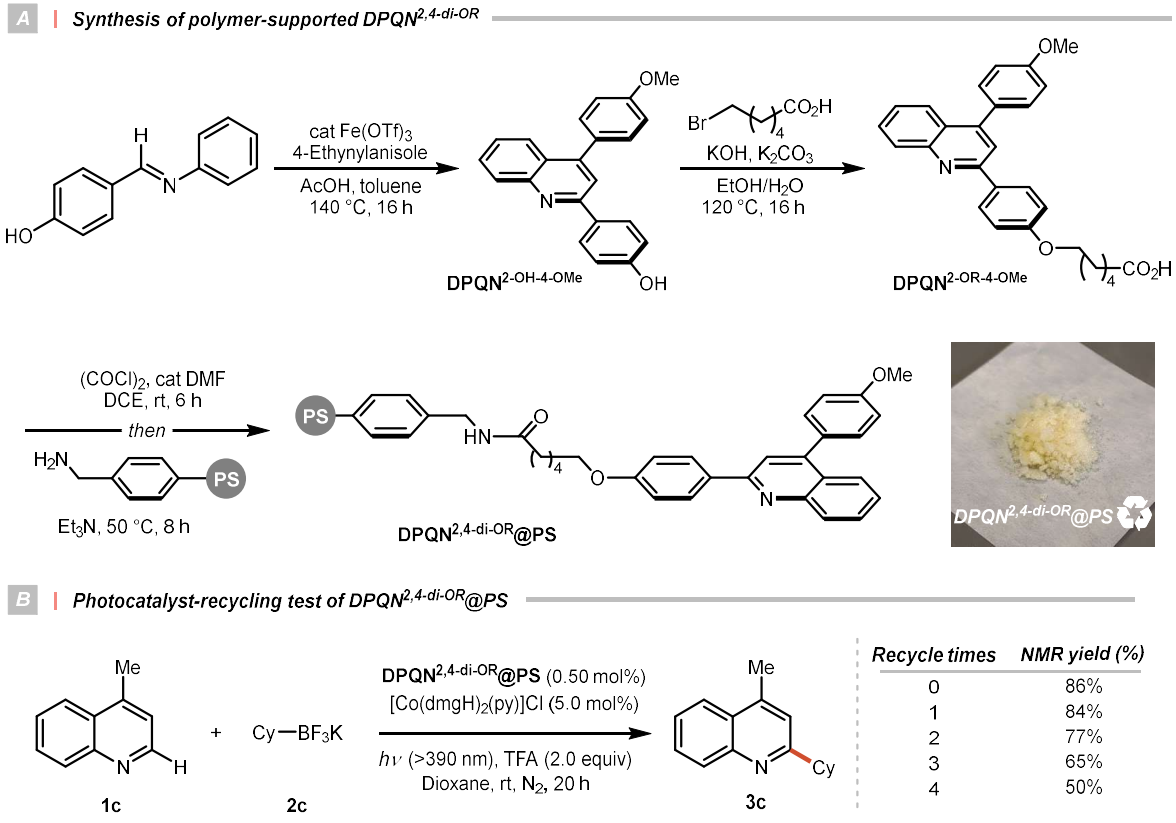

Scheme 4.10 [QN]/[Co] dual catalysis for oxidative (hetero)arene alkylations.

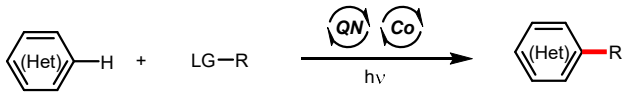

Entry	LG—R	Product	Entry	LG—R	Product
1	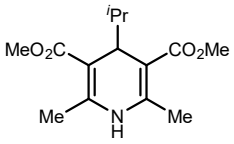	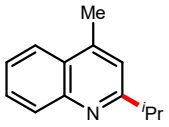 **4c**, 84%	5	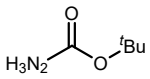	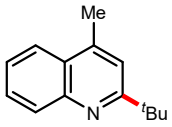 **7c**, 44%
2	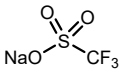	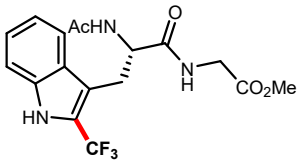 **55c**, 45%	6	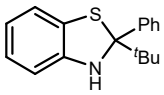	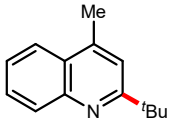 **7c**, 77%
3	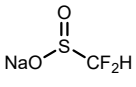	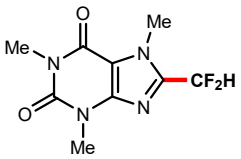 **56c**, 42%	7	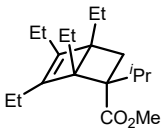	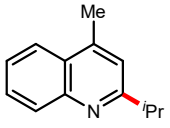 **4c**, 66%
4	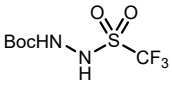	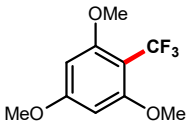 **57c**, 60%	8	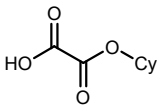	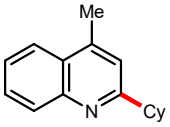 **3c**, 39%

See experimental section for details. Cy, cyclohexyl; ^{i}Pr, *iso*-propyl; ^{t}Bu, *tert*-butyl; Boc, *tert*-butyloxycarbonyl.

Motivated by the successful attempts above, the photosynthetic versatility and generality of the **DPQN$^{2,4\text{-di-OMe}}$**-based oxidative coupling platform were further explored by harnessing its oxidatively initiated reactivities with more radical alkylating reagents (**Scheme 4.10**). In terms of radical donors, C4-alkylated Hantzsch esters showed comparable productivity in heteroaromatic C-H substitution in place of the R-BF_3K (entry 1).[41, 47] Most of the established (fluoro)alkylation methods using sulfinate-derived radicals were operated with oxidants.[48-58] Through our dual catalytic platform, (fluoro)alkylated products, including the high-value trifluoromethylated dipeptide **55c**

and difluoromethylated caffeine **56c**, could now be obtained in an H_2-releasing manner (entries 2 and 3).[59, 57] Inspired by the elegant difluoromethylating reagent developed by Xu's group,[60] an analogous reagent (TfNHNHBoc) was exploited to expedite the trifluoromethyl radical, which was captured by 1,3,5-trimethoxybenzene to afford **57c** (entry 4). Interestingly, when the non-protected Boc-hydrazide was applied directly, the *tert*-butylated product **7c** was obtained (entry 5). Our quinoline/cobalt co-catalyzed system could also accommodate other attractive alkylating reagents, which liberated the desired radicals driven by either restoring aromaticity[61-62] or extruding CO_2[63-64] (entries 6 to 8).

Scheme 4.11 [QN]/[Co] dual catalysis for oxidative alkene difunctionalizations.

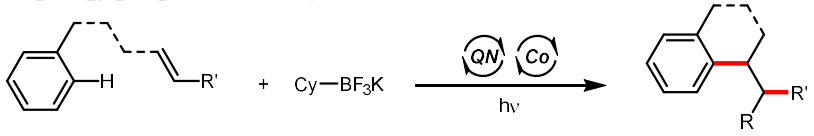

Entry	Substrate	Product	Entry	Substrate	Product
1	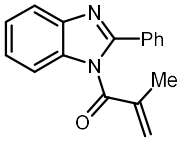	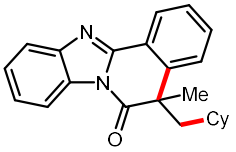 **58c**, 68%	4	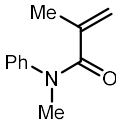	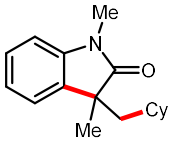 **61c**, 54%
2	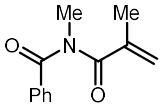	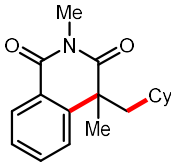 **59c**, 59%	5	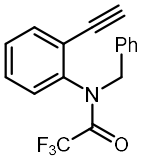	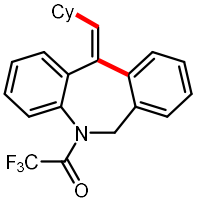 **62c**, 45%
3	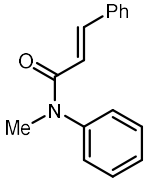	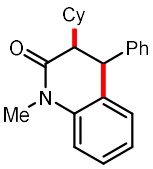 **60c**, 49%			

See experimental section for details. Cy, cyclohexyl.

Of equal importance, other types of **DPQN**$^{2,4\text{-di-OMe}}$-catalyzed photoreactions were investigated with Cy-BF_3K and suitable radical acceptors with unsaturated bondings (**Scheme 4.11**). Giese-type addition of cyclohexyl radical (Cy·) to electron-poor C=C double bond was found amenable, which could trigger a cascade radical addition to the pendent benzene ring and accomplish the tandem alkene dicarbofunctionalization.

Accordingly, the synthesis of several fused heterocycles (**58c** to **61c**) was succeeded under our optimal conditions (entries 1 to 4). Similarly, alkyne could behave as the SOMOphile, furnishing the polycyclic arene **62c** smoothly by our photochemical manifold (entry 5). To be noticed, stoichiometric chemical oxidants were unnecessary for balancing the redox status in all cases of oxidative couplings above. Collectively, they illustrated the tremendous synthetic potential of **DPQN$^{2,4\text{-di-OMe}}$** in future photochemistry development.

4.6 Conclusions and outlook

A highly promising photoredox catalyst based on diarylquinoline, **DPQN$^{2,4\text{-di-OMe}}$**, which was uniquely enabling in some oxidatively initiated chemistry, was successfully synthesized via a three-component coupling of the corresponding aldehyde, alkyne and amine. As preliminary trials, we established a visible light-mediated oxidative Minisci alkylation between heteroarene and numerous carbon radical precursors in a catalytic combination of **DPQN$^{2,4\text{-di-OMe}}$** and cobaloxime. This productive partnership could also empower a set of photoredox reactions for C-C bond formation without chemical oxidants, wherein other radical acceptors intercepted R• for different synthetic purposes.

The chemical space of the **DPQN** photocatalyst series was still largely underutilized, and the exploration of the photochemical possibilities of **DPQN$^{2,4\text{-di-OMe}}$** remained in its infancy. Considering these encouraging preliminary results, we envisioned that **DPQN$^{2,4\text{-di-OMe}}$**, with its simplicity and versatility, holds vast promise to catalyze more appealing photoreactions and inspire future efforts in the synthetic community on its exciting chemistry. Moreover, its unique "proton activation" could have implications for researching synthetically useful photoredox catalysts.

4.7 Author contributions

Prof. Chao-Jun Li, Dr. Jianbin Li, and I designed the project. I carried out the reaction optimizations and substrate scope; Dr. Jianbin Li performed the electrochemical experiments; both Dr. Jianbin Li and I carried out the photophysical property studies of the photocatalysts; the DFT calculation of the photocatalyst in the manuscript was performed by Mr. Jing-Tan Han. The manuscript was prepared by me and Dr. Jianbin Li, and revised by Prof. Chao-Jun Li. All the authors approved the publication of this work.

4.8 Experimental section

4.8.1 General procedures

Synthesis of the photocatalyst DPQN$^{2,4\text{-di-OMe}}$

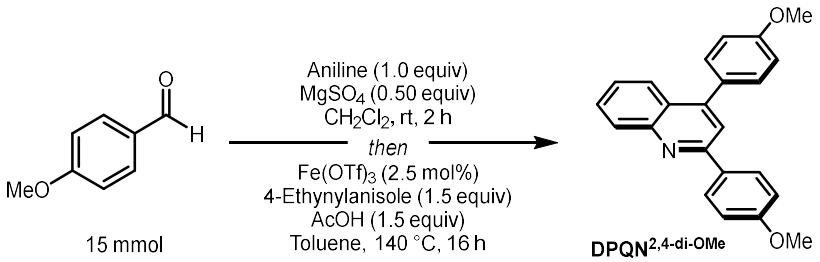

The following procedure was modified from the reported literature.[65] To a 10 mL glass tube equipped with a Teflon-coated magnetic stirring bar were added *p*-anisaldehyde (2.0 g, 15 mmol, 1.0 equiv), aniline (1.4 g, 15 mmol, 1.0 equiv), and anhydrous $MgSO_4$ (0.90 g, 7.5 mmol, 0.50 equiv). Then, CH_2Cl_2 (5.0 mL) was added to the reaction mixture, which was stirred at room temperature. After 2 h, the $MgSO_4$ was filtered and washed with CH_2Cl_2, and the filtrate was concentrated in a 50 mL glass tube to dryness to afford the crude imine, which was directly used without further purification.

To the crude imine were sequentially added 4-ethynylanisole (2.9 mL, 22.5 mmol, 1.5 equiv), $Fe(OTf)_3$ (188.6 mg, 375 μmol, 2.5 mol%), toluene (15.0 mL), and AcOH (1.3 mL, 22.5 mmol, 1.5 equiv). The reaction mixture was gradually heated from 90 °C to 140 °C. After being stirred at 140 °C for 16 h, the insolubles were filtered with a short celite pad and washed with EtOAc. The organic layer was basified with sat $NaHCO_3$ (aq), dried over anhydrous $MgSO_4$ and concentrated. The residue was then purified by column chromatography (Hex:EtOAc = 20:1 to 5:1) and recrystallized with pentane/Et_2O to afford the pure **DPQN$^{2,4\text{-di-OMe}}$** (2.92 g, 57%).

Synthesis of the immobilized photocatalyst DPQN$^{2,4\text{-di-OR}}$@PS

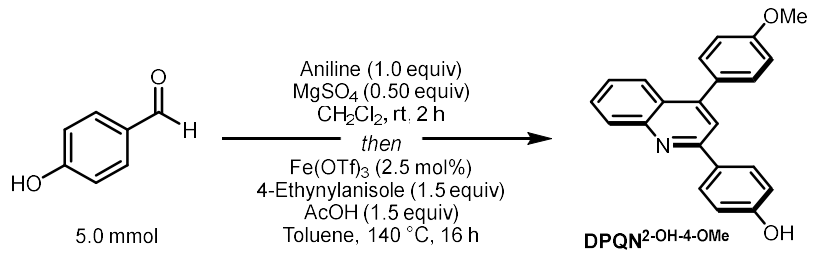

Step 1: To a 10 mL glass tube equipped with a Teflon-coated magnetic stirring bar were added *p*-hydroxybenzaldehyde (610.6 mg, 5.0 mmol, 1.0 equiv), aniline (465.7 mg, 5.0

mmol, 1.0 equiv), and anhydrous $MgSO_4$ (300.9 mg, 2.5 mmol, 0.50 equiv). Then, CH_2Cl_2 (5.0 mL) was added to the reaction mixture, which was stirred at room temperature. After 2 h, the $MgSO_4$ was filtered and washed with CH_2Cl_2, and the filtrate was concentrated in a 20 mL glass tube to dryness to afford the crude imine, which was directly used without further purification.

To the crude imine were sequentially added 4-ethynylanisole (1.3 mL, 10 mmol, 2.0 equiv), $Fe(OTf)_3$ (62.9 mg, 375 μmol, 2.5 mol%), toluene (5.0 mL) and AcOH (428.9 mL, 0.75 mmol, 1.5 equiv). The reaction mixture was gradually heated from 90 °C to 140 °C. After being stirred at 140 °C for 16 h, the insolubles were filtered with a short celite pad and washed with EtOAc. The filtrate was basified with sat $NaHCO_3$ (aq) and extracted with EtOAc. The organic layer was dried over anhydrous $MgSO_4$ and concentrated. The residue was then purified by column chromatography (Hex:EtOAc = 10:1 to 5:3) and recrystallized with pentane/Et_2O to afford the pure **DPQN$^{2\text{-OH-4-OMe}}$** (0.41 g, 25%).

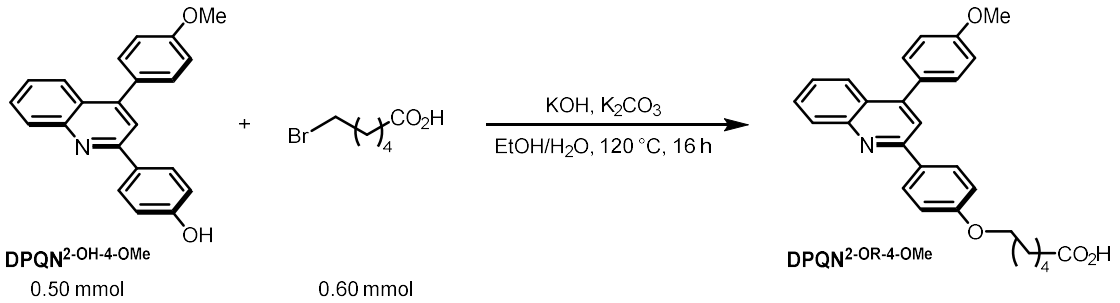

Step 2: To a 10 mL pyrex microwave tube equipped with a Teflon-coated magnetic stirring bar were added **DPQN$^{2\text{-OH-4-OMe}}$** (163.7 mg, 0.50 mmol, 1.0 equiv), 6-bromohexanoic acid (84 μL, 0.60 mmol, 1.2 equiv), 10 wt% KOH (1.25 mL), sat K_2CO_3 (0.50 mL), and EtOH (1.5 mL). After being stirred at 120 °C for 16 h, the reaction mixture was acidified with 18 wt% HCl to pH 5.0 to 6.0 and extracted with EtOAc. The organic layer was dried over anhydrous $MgSO_4$ and concentrated. The residue was then purified by column chromatography (Hex:EtOAc = 10:1 to 5:3) and recrystallized with pentane/Et_2O to afford the pure **DPQN$^{2\text{-OR-4-OMe}}$** (66.3 mg, 30%).

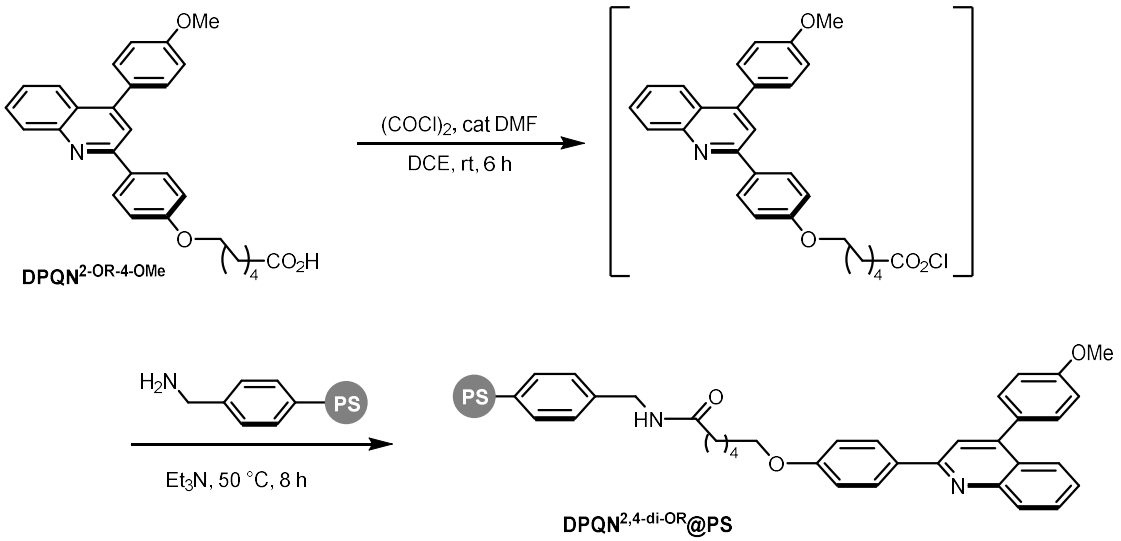

Step 3: The following procedure was modified from the reported literature.[66] To a 10 mL glass tube equipped with a Teflon-coated magnetic stirring bar were added **DPQN$^{2\text{-OR-4-OMe}}$** (44.1 mg, 0.10 mmol, 1.0 equiv) and DCE (5.0 mL), which was followed by the dropwise addition of oxalyl chloride (16 μL, 0.20 mmol, 2.0 equiv) and a drop DMF. After being stirred for 6 h, to the reaction mixture were added (aminomethyl)polystyrene (250 mg, Sigma Aldrich, purchase ID:515620) and Et_3N (0.70 mL, 0.50 mmol). After being stirred at 50 °C for 8 h, the reaction was quenched by benzoyl chloride (87 μL, 0.75 mmol, 7.5 equiv) and Et_3N (292 μL, 0.75 mmol, 7.5 equiv) and kept stirring at 50 °C. After 2 h, the insoluble beads were washed with MeOH, water, acetone, and CH_2Cl_2. After drying at 60 °C for 3 h, pale yellow **DPQN$^{2,4\text{-di-OR}}$@PS** beads were obtained (408.1 mg). The filtrate was concentrated and taken for ^{1}H NMR analysis using CH_2Br_2 as the internal standard, which showed that 69% of the starting **DPQN$^{2\text{-OR-4-OMe}}$** was recovered.

The increased weight of PS beads after the reaction (250 mg vs 408.1 mg) comes from 1) installation of **DPQN$^{2\text{-OR-4-OMe}}$**; 2) the benzoyl protecting groups of the amine residues on the surface. We assumed that the non-recovered **DPQN$^{2\text{-OR-4-OMe}}$** (31%, 0.031 mmol) were all on the PS beads. Therefore, the loading of **DPQN$^{2\text{-OR-4-OMe}}$** on **DPQN$^{2,4\text{-di-OR}}$@PS** is

$$0.031 \text{ mmol}/408.1 \text{ mg} = 7.6 \cdot 10^{-5} \text{ mmol/mg}.$$

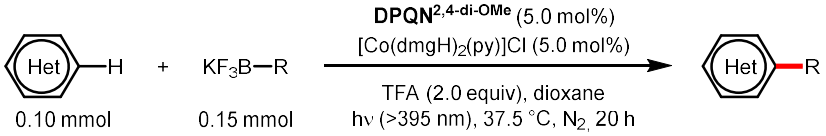

General procedure A (coupling with trifluoroborate). The following procedure applies to all the coupling of heteroarenes and alkyltrifluoroborates unless otherwise noted. To a 10 mL pyrex microwave tube equipped with a Teflon-coated magnetic stirring bar were added heteroarene (0.10 mmol, 1.0 equiv), potassium alkyltrifluoroborate (0.15 mmol, 1.5 equiv), **DPQN$^{2,4\text{-di-OMe}}$** (1.7 mg, 5.0 μmol, 5.0 mol%) and [Co(dmgH)$_2$(py)]Cl (2.0 mg, 5.0 μmol, 5.0 mol%). The tube was sealed with a rubber septum, evacuated and backfilled with argon three times before dioxane (1.5 mL) was injected. To the mixture was then added TFA (15.3 μL, 0.20 mmol, 2.0 equiv) in the glovebox, and the tube was sealed again by an aluminum cap with a septum, which was taken out from the glovebox and stirred at 37.5 °C under a 300 W Xe lamp (with a 395 nm filter) irradiation. After 20 h, the reaction mixture was basified with sat NaHCO$_3$ (aq), extracted with EtOAc, filtered through a short pad of MgSO$_4$, and concentrated to afford the crude product. The product was isolated with preparative thin-layer chromatography.

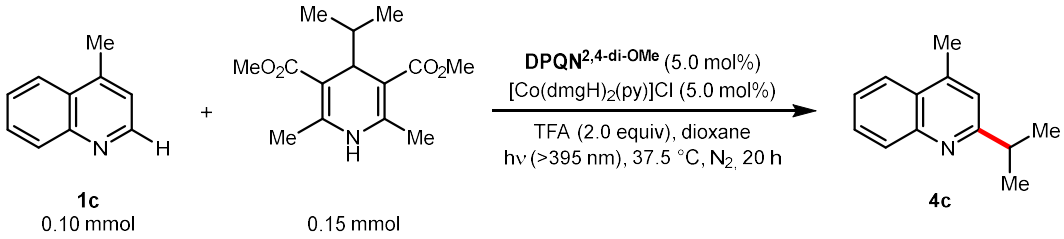

General procedure B (coupling with dihydropyridine). The following procedure applies to all the coupling of heteroarenes and 4-alkyldihydropyridines unless otherwise noted. To a 10 mL pyrex microwave tube equipped with a Teflon-coated magnetic stirring bar were added heteroarene **1c** (13.3 μL, 0.10 mmol, 1.0 equiv), 4-alkyldihydropyridine (40.1 mg, 0.15 mmol, 1.5 equiv), **DPQN$^{2,4\text{-di-OMe}}$** (1.7 mg, 5.0 μmol, 5.0 mol%) and [Co(dmgH)$_2$(py)]Cl (2.0 mg, 5.0 μmol, 5.0 mol%). The tube was sealed with a rubber septum, evacuated and backfilled with argon three times before dioxane (1.5 mL) was injected. To the mixture was then added TFA (15.3 μL, 0.20 mmol, 2.0 equiv) in the glovebox, and the tube was sealed again by an aluminum cap with a septum, which was taken out from the glovebox and stirred at 37.5 °C under a 300 W Xe lamp (with a 395 nm filter) irradiation. After 20 h, the reaction mixture was basified with sat NaHCO$_3$ (aq),

extracted with EtOAc, filtered through a short pad of $MgSO_4$, and concentrated to afford the crude product. The product was isolated with preparative thin-layer chromatography.

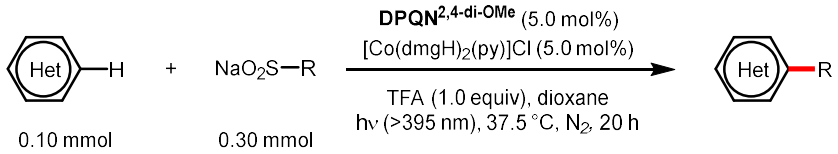

General procedure C (coupling with sulfinate). The following procedure applies to all the coupling of heteroarenes and alkylsulfinates unless otherwise noted. To a 10 mL pyrex microwave tube equipped with a Teflon-coated magnetic stirring bar were added heteroarene (0.10 mmol, 1.0 equiv), sodium alkylsulfinates (0.30 mmol, 3.0 equiv), **DPQN$^{2,4\text{-di-OMe}}$** (1.7 mg, 5.0 μmol, 5.0 mol%) and $[Co(dmgH)_2(py)]Cl$ (2.0 mg, 5.0 μmol, 5.0 mol%). The tube was sealed with a rubber septum, evacuated and backfilled with argon three times before dioxane (1.5 mL) was injected. To the mixture was then added TFA (7.7 μL, 0.10 mmol, 1.0 equiv) in the glovebox, and the tube was sealed again by an aluminum cap with a septum, which was taken out from the glovebox and stirred at 37.5 °C under a 300 W Xe lamp (with a 395 nm filter) irradiation. After 20 h, the reaction mixture was basified with sat $NaHCO_3$ (aq), extracted with EtOAc, filtered through a short pad of $MgSO_4$, and concentrated to afford the crude product. The product was isolated with preparative thin-layer chromatography.

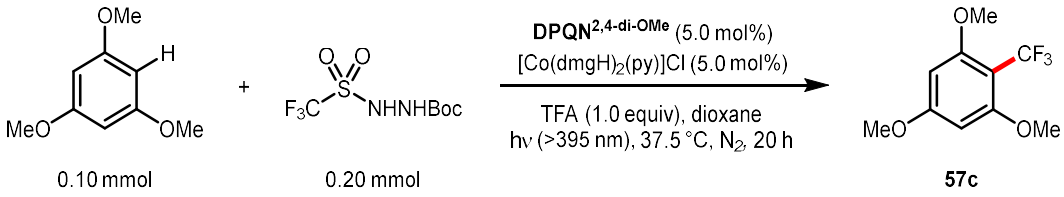

General procedure D (coupling with Tf-hydrazide). To a 10 mL pyrex microwave tube equipped with a Teflon-coated magnetic stirring bar were added 1,3,5-trimethoxybenzene (16.8 mg, 0.10 mmol, 1.0 equiv), $CF_3SO_2NHNHBoc$ (52.8 mg, 0.20 mmol, 2.0 equiv), **DPQN$^{2,4\text{-di-OMe}}$** (1.7 mg, 5.0 μmol, 5.0 mol%) and $[Co(dmgH)_2(py)]Cl$ (2.0 mg, 5.0 μmol, 5.0 mol%). The tube was sealed with a rubber septum, evacuated and backfilled with argon three times before dioxane (1.5 mL) was injected. To the mixture was then added TFA (7.7 μL, 0.10 mmol, 1.0 equiv) in the glovebox, and the tube was sealed again by an aluminum cap with a septum, which was taken out from the glovebox and stirred at 37.5 °C under a 300 W Xe lamp (with a 395 nm filter) irradiation. After 20

h, the reaction mixture was basified with sat $NaHCO_3$ (aq), extracted with EtOAc, filtered through a short pad of $MgSO_4$, and concentrated to afford the crude product. The product was isolated with preparative thin-layer chromatography.

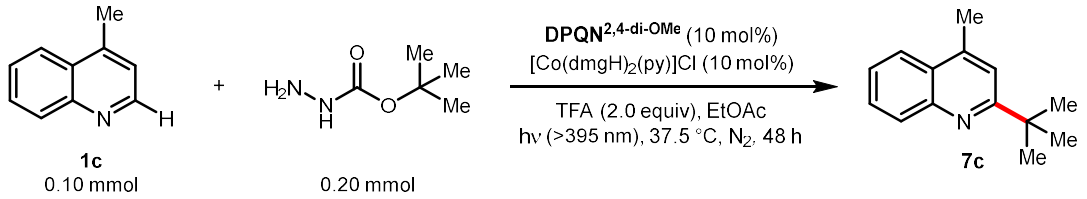

General procedure E (coupling with Boc-hydrazide). To a 10 mL pyrex microwave tube equipped with a Teflon-coated magnetic stirring bar were added heteroarene (**1a**, 13.3 μL, 0.10 mmol, 1.0 equiv), Boc-hydrazide (26.4 mg, 0.20 mmol, 2.0 equiv), **DPQN$^{2,4\text{-di-OMe}}$** (3.4 mg, 10 μmol, 10 mol%) and $[Co(dmgH)_2(py)]Cl$ (4.0 mg, 10 μmol, 10 mol%). The tube was sealed with a rubber septum, evacuated and backfilled with argon three times before EtOAc (1.5 mL) was injected. To the mixture was then added TFA (15.3 μL, 0.20 mmol, 2.0 equiv) in the glovebox, and the tube was sealed again by an aluminum cap with a septum, which was taken out from the glovebox and stirred at 37.5 °C under a 300 W Xe lamp (with a 395 nm filter) irradiation. After 48 h, the reaction mixture was basified with sat $NaHCO_3$ (aq), extracted with EtOAc, filtered through a short pad of $MgSO_4$, and concentrated to afford the crude product. The product was isolated with preparative thin-layer chromatography.

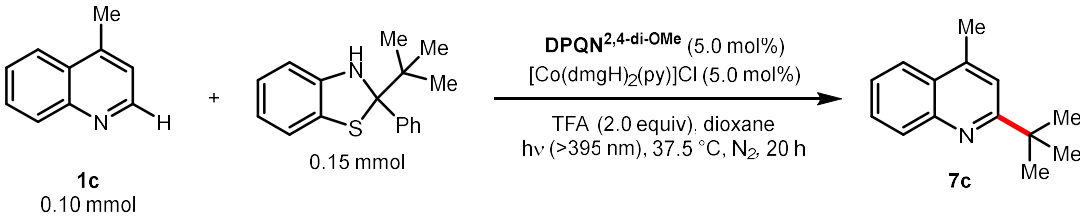

General procedure F (coupling with dihydrobenzothiazole). To a 10 mL pyrex microwave tube equipped with a Teflon-coated magnetic stirring bar were added heteroarene (**1a**, 13.3 μL, 0.10 mmol, 1.0 equiv), 2-(*tert*-butyl)-2-phenyl-2,3-dihydrobenzothiazole (40.4 mg, 0.15 mmol, 1.5 equiv), **DPQN$^{2,4\text{-di-OMe}}$** (1.7 mg, 5.0 μmol, 5.0 mol%) and $[Co(dmgH)_2(py)]Cl$ (2.0 mg, 5.0 μmol, 5.0 mol%). The tube was sealed with a rubber septum, evacuated and backfilled with argon three times before dioxane (1.5 mL) was injected. To the mixture was then added TFA (15.3 μL, 0.20 mmol, 2.0 equiv) in the

glovebox, and the tube was sealed again by an aluminum cap with a septum, which was taken out from the glovebox and stirred at 37.5 °C under a 300 W Xe lamp (with a 395 nm filter) irradiation. After 20 h, the reaction mixture was basified with sat $NaHCO_3$ (aq), extracted with EtOAc, filtered through a short pad of $MgSO_4$, and concentrated to afford the crude product. The product was isolated with preparative thin-layer chromatography.

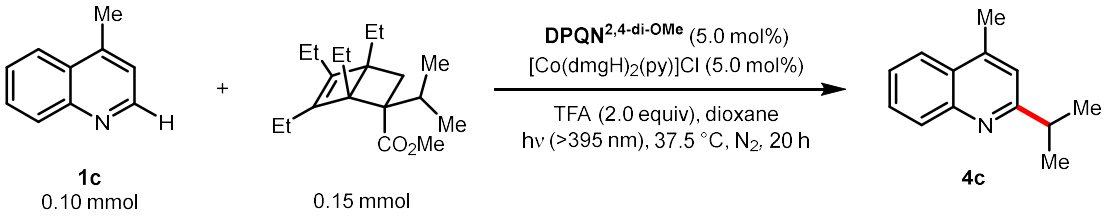

General procedure G (coupling with bicyclo[2.2.0]hexene). To a 10 mL pyrex microwave tube equipped with a Teflon-coated magnetic stirring bar were added heteroarene (**1a**, 13.3 µL, 0.10 mmol, 1.0 equiv), methyl 1,4,5,6-tetraethyl-2-isopropylbicyclo[2.2.0]hex-5-ene-2-carboxylate (43.9 mg, 0.15 mmol, 1.5 equiv), **DPQN$^{2,4\text{-di-OMe}}$** (1.7 mg, 5.0 µmol, 5.0 mol%) and $[Co(dmgH)_2(py)]Cl$ (2.0 mg, 5.0 µmol, 5.0 mol%). The tube was sealed with a rubber septum, evacuated and backfilled with argon three times before dioxane (1.5 mL) was injected. To the mixture was then added TFA (15.3 µL, 0.20 mmol, 2.0 equiv) in the glovebox and sealed with an aluminum cap with a septum, which was then taken out from the glovebox and stirred at 37.5 °C under a 300 W Xe lamp (with a 395 nm filter) irradiation. After 20 h, the reaction mixture was basified with sat $NaHCO_3$ (aq), extracted with EtOAc, filtered through a short pad of $MgSO_4$, and concentrated to afford the crude product. The product was isolated with preparative thin-layer chromatography.

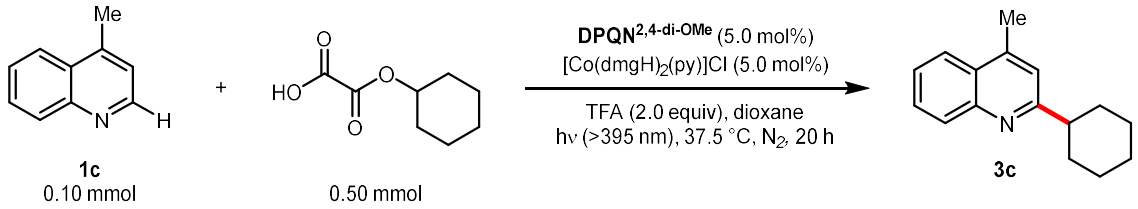

General procedure H (coupling with oxalic acid). To a 10 mL pyrex microwave tube equipped with a Teflon-coated magnetic stirring bar were added heteroarene (**1a**, 13.3 µL, 0.10 mmol 1.0 equiv), cyclohexyl oxalic acid (86.1 mg, 0.50 mmol, 5.0 equiv), **DPQN$^{2,4\text{-di-OMe}}$** (1.7 mg, 5.0 µmol, 5.0 mol%) and $[Co(dmgH)_2(py)]Cl$ (2.0 mg, 5.0 µmol, 5.0 mol%).

The tube was sealed with a rubber septum, evacuated and backfilled with argon three times before dioxane (1.5 mL) was injected. To the mixture was then added TFA (15.3 μL, 0.20 mmol, 2.0 equiv) in the glovebox, and the tube was sealed again by an aluminum cap with a septum, which was taken out from the glovebox and stirred at 37.5 °C under a 300 W Xe lamp (with a 395 nm filter) irradiation. After 20 h, the reaction mixture was basified with sat $NaHCO_3$ (aq), extracted with EtOAc, filtered through a short pad of $MgSO_4$, and concentrated to afford the crude product. The product was isolated with preparative thin-layer chromatography.

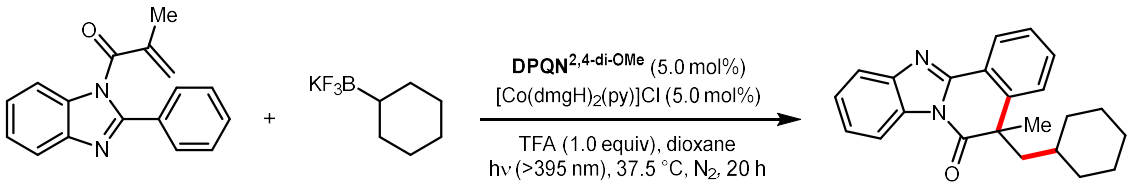

0.10 mmol

2c
0.30 mmol

58c

General procedure I (coupling with methacrylamide). To a 10 mL pyrex microwave tube equipped with a Teflon-coated magnetic stirring bar were added 2-methyl-1-(2-phenyl-1*H*-benzoimidazol-1-yl)prop-2-en-1-one (26.2 mg, 0.10 mmol, 1.0 equiv), potassium cyclohexyltrifluoroborate (**2a,** 57 mg, 0.30 mmol, 3.0 equiv), **DPQN$^{2,4\text{-di-OMe}}$** (1.7 mg, 5.0 μmol, 5.0 mol%) and $[Co(dmgH)_2(py)]Cl$ (2.0 mg, 5.0 μmol, 5.0 mol%). The tube was sealed with a rubber septum, evacuated and backfilled with argon three times before dioxane (1.5 mL) was injected. To the mixture was then added TFA (7.7 μL, 0.10 mmol, 1.0 equiv) in the glovebox, and the tube was sealed again by an aluminum cap with a septum, which was taken out from the glovebox and stirred at 37.5 °C under a 300 W Xe lamp (with a 395 nm filter) irradiation. After 20 h, the reaction mixture was basified with sat $NaHCO_3$ (aq), extracted with EtOAc, filtered through a short pad of $MgSO_4$, and concentrated to afford the crude product. The product was isolated with preparative thin-layer chromatography.

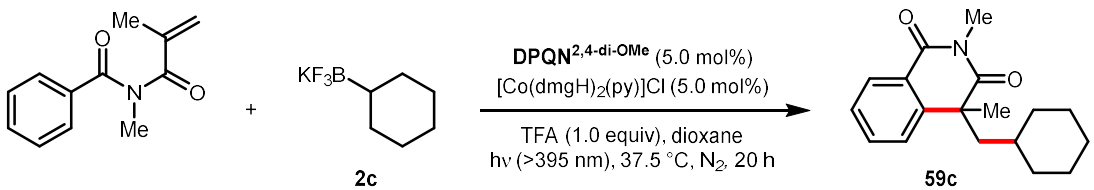

0.10 mmol

2c
0.30 mmol

59c

General procedure J (coupling with methacrylamide). To a 10 mL pyrex microwave tube equipped with a Teflon-coated magnetic stirring bar were added *N*-methacryloyl-*N*-methylbenzamide (20.3 mg, 0.10 mmol, 1.0 equiv), potassium cyclohexyltrifluoroborate (**2a**, 57 mg, 0.30 mmol, 3.0 equiv), **DPQN$^{2,4\text{-di-OMe}}$** (1.7 mg, 5.0 μmol, 5.0 mol%) and [Co(dmgH)$_2$(py)]Cl (2.0 mg, 5.0 μmol, 5.0 mol%). The tube was sealed with a rubber septum, evacuated and backfilled with argon three times before dioxane (1.5 mL) was injected. To the mixture was then added TFA (7.7 μL, 0.10 mmol, 1.0 equiv) in the glovebox, and the tube was sealed again by an aluminum cap with a septum, which was taken out from the glovebox and stirred at 37.5 °C under a 300 W Xe lamp (with a 395 nm filter) irradiation. After 20 h, the reaction mixture was basified with sat NaHCO$_3$ (aq), extracted with EtOAc, filtered through a short pad of MgSO$_4$, and concentrated to afford the crude product. The product was isolated with preparative thin-layer chromatography.

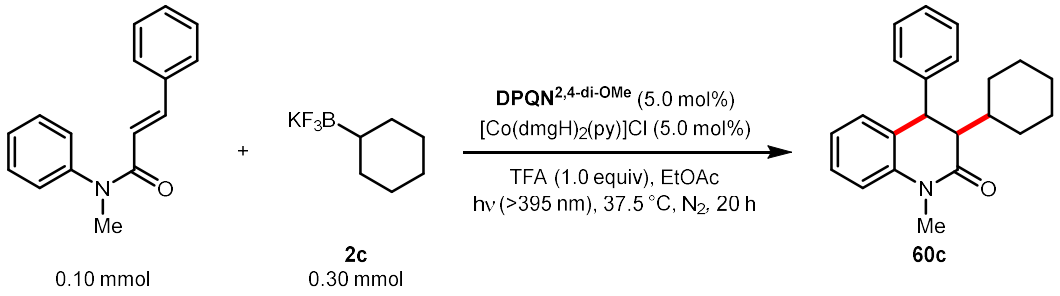

General procedure K (coupling with cinnamamide). To a 10 mL pyrex microwave tube equipped with a Teflon-coated magnetic stirring bar were added *N*-methyl-*N*-phenylcinnamamide (23.7 mg, 0.10 mmol, 1.0 equiv), potassium cyclohexyltrifluoroborate (**2a**, 57 mg, 0.30 mmol, 3.0 equiv), **DPQN$^{2,4\text{-di-OMe}}$** (1.7 mg, 5.0 μmol, 5.0 mol%) and [Co(dmgH)$_2$(py)]Cl (2.0 mg, 5.0 μmol, 5.0 mol%). The tube was sealed with a rubber septum, evacuated and backfilled with argon three times before EtOAc (1.5 mL) was injected. To the mixture was then added TFA (7.7 μL, 0.10 mmol, 1.0 equiv) in the glovebox, and the tube was sealed again by an aluminum cap with a septum, which was taken out from the glovebox and stirred at 37.5 °C under a 300 W Xe lamp (with a 395 nm filter) irradiation. After 20 h, the reaction mixture was basified with sat NaHCO$_3$ (aq), extracted with EtOAc, filtered through a short pad of MgSO$_4$, and concentrated to afford the crude product. The product was isolated with preparative thin-layer chromatography.

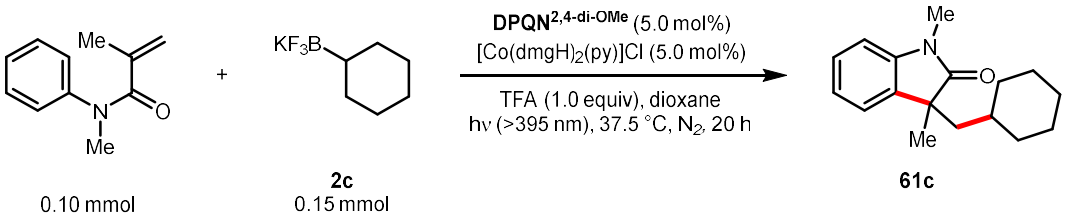

General procedure L (coupling with methacrylamide). To a 10 mL pyrex microwave tube equipped with a Teflon-coated magnetic stirring bar were added *N*-methyl-*N*-phenylmethacrylamide (17.5 mg, 0.10 mmol, 1.0 equiv), potassium cyclohexyltrifluoroborate **2a** (28.5 mg, 0.15 mmol, 1.5 equiv), **DPQN$^{2,4\text{-di-OMe}}$** (1.7 mg, 5.0 μmol, 5.0 mol%) and [Co(dmgH)$_2$(py)]Cl (2.0 mg, 5.0 μmol, 5.0 mol%). The tube was sealed with a rubber septum, evacuated and backfilled with argon three times before dioxane (1.5 mL) was injected. To the mixture was then added TFA (7.7 μL, 0.10 mmol, 1.0 equiv) in the glovebox, and the tube was sealed again by an aluminum cap with a septum, which was taken out from the glovebox and stirred at 37.5 °C under a 300 W Xe lamp (with a 395 nm filter) irradiation. After 20 h, the reaction mixture was basified with sat $NaHCO_3$ (aq), extracted with EtOAc, filtered through a short pad of $MgSO_4$, and concentrated to afford the crude product. The product was isolated with preparative thin-layer chromatography.

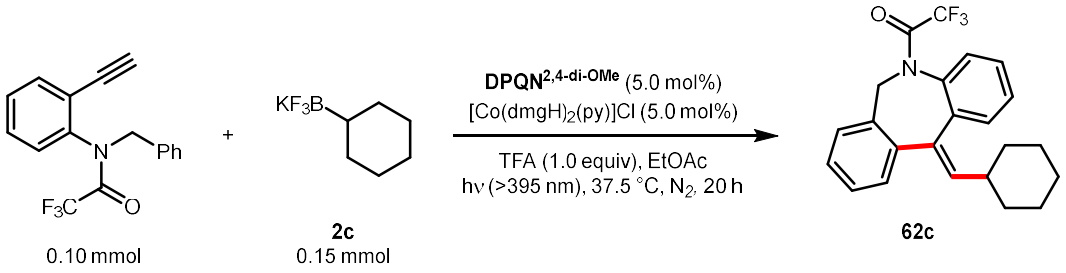

General procedure M (coupling with alkyne). To a 10 mL pyrex microwave tube equipped with a Teflon-coated magnetic stirring bar were added *N*-benzyl-*N*-(2-ethynylphenyl)-2,2,2-trifluoroacetamide (30.3 mg, 0.10 mmol, 1.0 equiv), potassium cyclohexyltrifluoroborate (**2a**, 28.5 mg, 0.15 mmol, 1.5 equiv), **DPQN$^{2,4\text{-di-OMe}}$** (1.7 mg, 5.0 μmol, 5.0 mol%) and [Co(dmgH)$_2$(py)]Cl (2.0 mg, 5.0 μmol, 5.0 mol%). The tube was sealed with a rubber septum, evacuated and backfilled with argon three times before EtOAc (1.5 mL) was injected. To the mixture was then added TFA (7.7μL, 0.10 mmol, 1.0 equiv) in the glovebox, and the tube was sealed again by an aluminum cap with a septum, which was taken out from the glovebox and stirred at 37.5 °C under a 300 W Xe lamp

(with a 395 nm filter) irradiation. After 20 h, the reaction mixture was basified with sat $NaHCO_3$ (aq), extracted with EtOAc, filtered through a short pad of $MgSO_4$, and concentrated to afford the crude product. The product was isolated with preparative thin-layer chromatography.

Recycling test of polymer DPQN$^{2,4\text{-di-OR}}$@PS

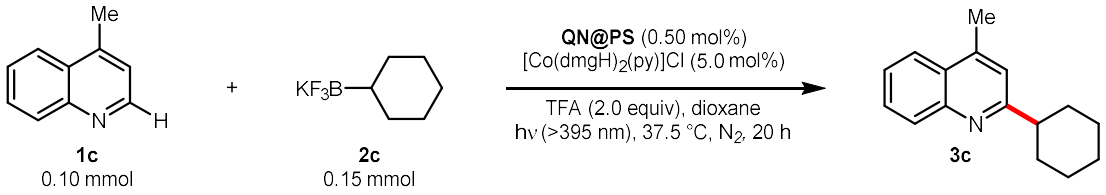

To a 10 mL pyrex microwave tube equipped with a Teflon-coated magnetic stirring bar were added heteroarene (**1a**, 13.3 μL, 0.10 mmol, 1.0 equiv), potassium cyclohexyltrifluoroborate (**2a**, 28.5 mg, 0.15 mmol, 1.5 equiv), polymer **DPQN$^{2,4\text{-di-OR}}$@PS** (6.6 mg, 0.5 μmol, 0.50 mol%) and $[Co(dmgH)_2(py)]Cl$ (2.0 mg, 5.0 μmol, 5.0 mol%). The tube was sealed with a rubber septum, evacuated and backfilled with argon three times before dioxane (1.5 mL) was injected. To the mixture was then added TFA (15.3 μL, 0.20 mmol, 2.0 equiv) in the glovebox, and the tube was sealed again by an aluminum cap with a septum, which was taken out from the glovebox and stirred at room temperature under a 52 W 390 nm Kessil lamp irradiation. After 20 h, to the reaction mixture was added water (~0.50 mL), and the solution was carefully transferred with a glass pipette. The remaining polymer beads were washed with water (~0.50 mL), MeOH (~0.50 mL), acetone (~0.50 mL), and Et_2O (~1.0 mL). The collected solutions were combined, concentrated, basified with sat $NaHCO_3$, extracted with EtOAc, filtered through a short pad of $MgSO_4$, and concentrated again to afford the crude product, which was taken for ^1H NMR analysis.

To be noticed, the 0.50 mol% in our condition is defined by the ratio of immobilized **DPQN$^{2,4\text{-di-OR}}$** relative to the limiting reagent, which is the heteroarene in this case. For 0.50 mol% **DPQN$^{2,4\text{-di-OR}}$@PS** in the recycling test, the quantity used is

$$(0.50\ \text{mol\%} \times 0.10\ \text{mmol}) / 7.6 \cdot 10^{-5}\ \text{mmol/mg} = 6.6\ \text{mg}$$

The resulting polymer beads, along with the reaction tube, were air-dried for 10 min and then dried at 45 °C for 2 h before being used for the next reaction. The ^1H NMR yields

of **3** are shown in Figure S3.

Figure 4.5 Polymer recycling test.

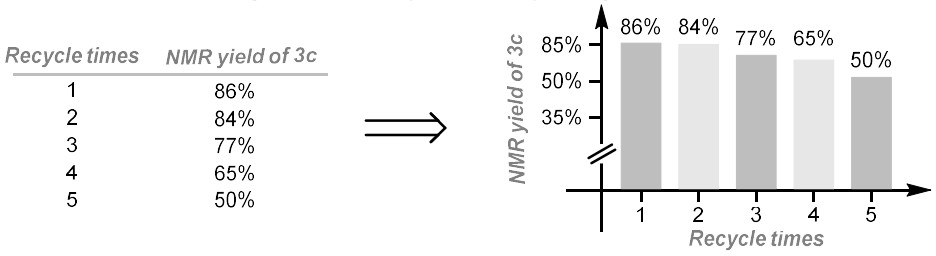

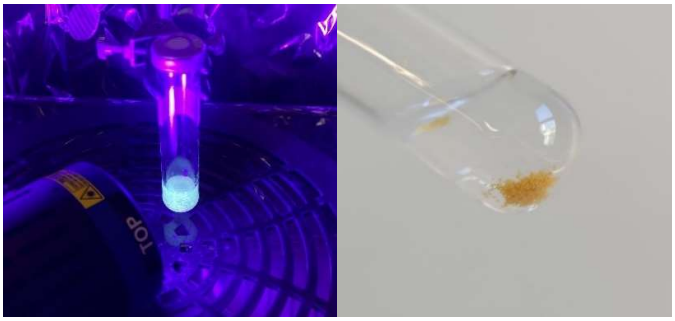

Left: reaction setup. Right: recycled polymer beads.

4.8.2 Electrochemical measurements

The electrochemical experiments were performed with HEKA PG 340 potentiostat with Ag/AgCl as the reference electrode. The working electrode was made of glassy carbon, and a Pt wire was used as the counter electrode to complete the electrochemical setup. Tetrabutylammonium hexafluorophosphate (Bu_4NPF_6) was used as the electrolyte, and degassed CH_3CN was used as the solvent. A scan rate of 20 mV/s was used for all experiments. All the potentials were noted with respect to the Ag/AgCl electrode unless otherwise specified. The reduction potential referenced to the standard calomel electrode (SCE) could be calculated by subtracting 0.039 V from the E(Ag/AgCl). It followed that E(SCE) = E(Ag/AgCl) – 0.039 V.

Potentials were quoted with the following notions: E_p, peak potential; $E_{1/2}$ half-wave potential (for reversible peaks, the average of anodic and cathodic peak potentials); $E_{p/2}$ half peak potential (half-maximum current). The protonated samples were prepared by adding 1.0 equiv trifluoroacetic acid (TFA).

Experimental procedure: the measurement of **DPQN$^{2,4\text{-di-OMe}}$** was used as an example. A 50 mL beaker was charged with **DPQN$^{2,4\text{-di-OMe}}$** (136.8 mg, 0.40 mmol, 0.020 M) and

tetrabutylammonium hexafluorophosphate (Bu_4NPF_6, 774.9 mg, 2.0 mmol, 0.10 M) and 20.0 HPLC-grade CH_3CN (*CH_3CN was used for better solubility instead of dioxane*). TFA (45.6 mg, 0.40 mmol, 30.6 μL, 0.020 M) was added if necessary. After stirring for a while, the homogeneous solution was subjected to the cyclic voltammetric measurement. The spectra are shown in **Figure 4.1**.

4.8.3 Quantum yield measurement

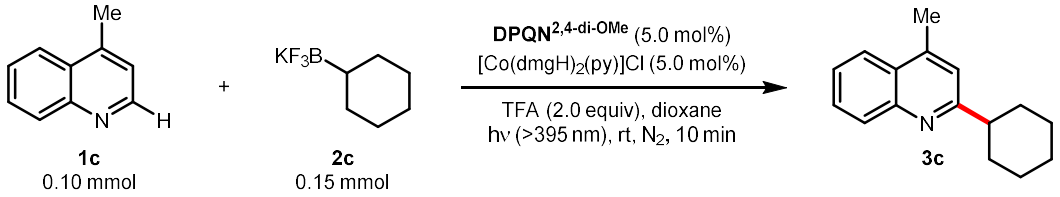

Since the Xe lamp used in the general procedure has a wide wavelength spectrum, a single wavelength 390 nm Kessil lamp (PR160L-390) was used to conduct the experiment. To a cuvette equipped with a Teflon-coated magnetic stirring bar were added heteroarene (**1c**, 13.3 µL, 0.10 mmol, 1.0 equiv), potassium cyclohexyltrifluoroborate (**2c**, 28.5 mg, 0.15 mmol, 1.5 equiv), **DPQN$^{2,4\text{-di-OMe}}$** (1.7 mg, 5.0 mmol, 5.0 mol%), $[Co(dmgH)_2(py)]Cl$ (2.0 mg, 5.0 mmol, 5.0 mol%), TFA (15.3 µL, 0.20 mmol, 2.0 equiv), and dioxane (1.5 mL). The mixture was degassed by purging with argon for 5 min before being capped with a PTFE stopper and stirred at room temperature under a 13 W 390 nm Kessil lamp. After 10 min, the cuvette with the reaction mixture was taken for UV-vis analysis. The absorption spectrum gave a value of 3.34 at 390 nm, implying the fraction of absorbed light (f) is >0.999.

$$\text{incident light} = \text{f} = 1 - 10^{-A(390\,nm)} \approx 1$$

The reaction mixture was then basified with sat $NaHCO_3$ (aq), extracted with EtOAc, and concentrated to afford the crude product, which was taken for ^{1}H NMR analysis using CH_2Br_2 as the internal standard. 33% of the product **3c** was formed without side reactions.

The average light power of the 13 W 390 nm Kessil lamp was determined by an optical parameter to be 127 mW. As a result, the photon flux of the light source was calculated to be $4.14 \cdot 10^{-7}$ einstein $\cdot$ s^{-1}).

$$\text{photon flux} = \frac{P}{N_A \cdot hc/\lambda}$$

$$= \frac{127 \cdot 10^{-3}\ J \cdot s^{-1}}{6.02 \cdot 10^{23}\ mol^{-1} \times 6.63 \cdot 10^{-34}\ J \cdot s\ \times 3 \cdot 10^{8}\ m \cdot s^{-1}\ \div\ (390 \cdot 10^{-9}\ m)}$$

$$= 4.14\ \cdot 10^{-7}\ \text{einstein} \cdot s^{-1}$$

The production of $2.4 \cdot 10^{-5}$ mol **3c** (35%) in 10 min ($6 \cdot 10^{2}$ s) led to the quantum yield (Φ) of 14.5%.

$$\Phi = \frac{\text{mol product}}{\text{photon flux} \cdot t \cdot f} = \frac{3.5 \cdot 10^{-5}\ mol}{4.14\ \times 10^{-7}\text{einstein} \cdot s^{-1} \times\ 6 \cdot 10^{2}\ s\ \times 1} = 14.5\%$$

Since the Φ is far smaller than 1, although we still could not fully exclude the possibility of the radical chain process of this reaction, the quantum yield calculation does not support the radical chain process.

4.9 Characterization data for compounds

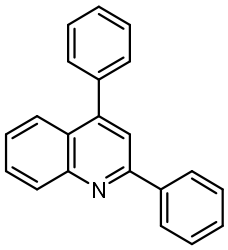

2,4-Diphenylquinoline (DPQN). Pale yellow solid. **^{1}H NMR** (500 MHz, $CDCl_3$) δ 8.28 (d, *J* = 8.8 Hz, 1H), 8.25 – 8.20 (m, 2H), 7.94 (dd, *J* = 8.4, 1.4 Hz, 1H), 7.85 (s, 1H), 7.79 – 7.73 (m, 1H), 7.61 – 7.49 (m, 9H). **^{13}C NMR** (126 MHz, $CDCl_3$) δ 156.9, 149.2, 148.8, 139.7, 138.4, 130.1, 129.6, 129.5, 129.4, 128.9, 128.6, 128.4, 127.6, 126.4, 125.8, 125.7, 119.4. **GC-MS** (EI, m/z) for $C_{21}H_{15}N$ Calcd: 281.1, found: 281.2. Spectra data are consistent with the reported literature.[65]

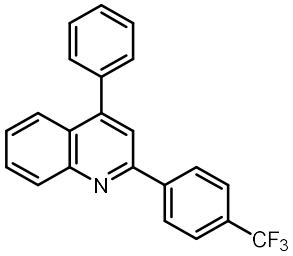

4-Phenyl-2-(4-(trifluoromethyl)phenyl)quinoline (DPQN$^{2\text{-}CF_3}$). Pale yellow solid. **^{1}H NMR** (500 MHz, $CDCl_3$) δ 8.35 (d, *J* = 8.0 Hz, 2H), 8.29 (d, *J* = 8.5 Hz, 1H), 7.96 (dd, *J* = 8.4, 1.4 Hz, 1H), 7.86 (s, 1H), 7.83 – 7.75 (m, 3H), 7.62 – 7.51 (m, 6H). **^{13}C NMR** (126 MHz, $CDCl_3$) δ 155.2, 149.6, 148.8, 143.0, 138.2, 131.1 (q, *J* = 30 Hz), 130.3, 129.9, 129.6, 128.7, 128.6, 127.9, 126.9, 126.1, 125.8 (q, *J* = 4 Hz), 124.2 (q, *J* = 271 Hz), 119.1 (*One aromatic carbon was missing due to overlap*). **^{19}F NMR** (470 MHz, $CDCl_3$) δ -62.55 (s, 3F). **GC-MS** (EI, m/z) for $C_{22}H_{14}F_3N$ Calcd: 349.1, found: 349.1. Spectra data are consistent with the reported literature.[67]

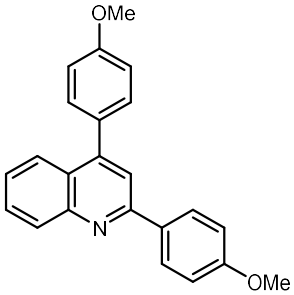

2,4-Bis(4-methoxyphenyl)quinoline (DPQN$^{2,4\text{-}di\text{-}OMe}$). Pale yellow solid. **^{1}H NMR** (500 MHz, $CDCl_3$) δ 8.22 (d, *J* = 8.1 Hz, 1H), 8.19 (d, *J* = 8.9 Hz, 2H), 7.95 (dd, *J* = 8.4, 1.8 Hz, 1H), 7.78 (s, 1H), 7.76 – 7.71 (m, 1H), 7.53 (d, *J* = 8.7 Hz, 2H), 7.49 – 7.44 (m, 1H), 7.11 (d, *J* = 8.9 Hz, 2H), 7.07 (d, *J* = 8.9 Hz, 2H), 3.94 (s, 3H), 3.91 (s, 3H). **^{13}C NMR** (126 MHz, $CDCl_3$) δ 160.8, 159.8, 156.5, 148.9, 148.7, 132.4, 130.8, 130.8, 129.9, 129.4, 128.9, 125.9, 125.7, 125.7, 118.9, 114.2, 114.1, 55.4, 55.4. **GC-MS** (EI, m/z) for $C_{23}H_{19}NO_2$ Calcd: 341.1, found: 341.2. Spectra data are consistent with the reported literature.[68]

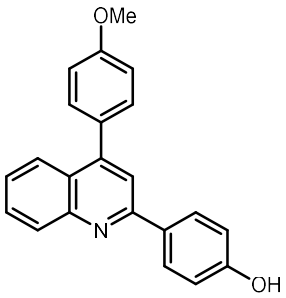

4-(4-(4-Methoxyphenyl)quinolin-2-yl)phenol (DPQN$^{2\text{-OH-4-OMe}}$). Pale yellow solid. **^{1}H NMR** (500 MHz, $CDCl_3$) δ 8.25 (d, *J* = 7.8 Hz, 1H), 8.07 (d, *J* = 8.9 Hz, 2H), 7.95 (dd, *J* = 8.4, 1.2 Hz, 1H), 7.77 – 7.68 (m, 2H), 7.56 – 7.50 (m, 2H), 7.50 – 7.43 (m, 1H), 7.11 (d, *J* = 8.7 Hz, 2H), 6.94 (d, *J* = 8.9 Hz, 2H), 6.45 (br, 1H), 3.94 (s, 3H). **^{13}C NMR** (126 MHz, $CDCl_3$) δ 159.9, 157.4, 156.8, 149.0, 148.7, 132.0, 130.8, 130.7, 129.6, 129.5, 129.3, 126.0, 125.7, 125.7, 119.2, 115.9, 114.1, 55.5. **HRMS** ($M+H^+$) for $C_{22}H_{18}NO_2$ Calcd: 328.1332, found: 328.1331. The compound was unreported.

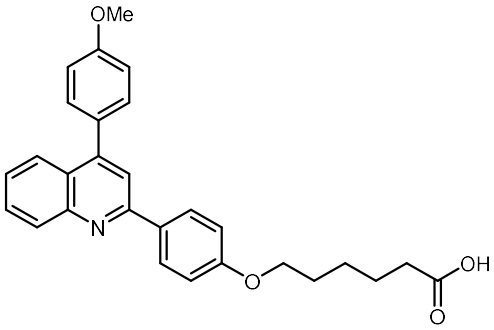

6-(4-(4-(4-Methoxyphenyl)quinolin-2-yl)phenoxy)hexanoic acid (DPQN$^{2\text{-OR-4-OMe}}$). Pale yellow solid. **^{1}H NMR** (500 MHz, $CDCl_3$) δ 8.22 (dd, *J* = 8.2, 0.8 Hz, 1H), 8.16 (d, *J* = 9.0 Hz, 2H), 7.94 (dd, *J* = 8.6, 1.1 Hz, 1H), 7.77 (s, 1H), 7.75 – 7.69 (m, 1H), 7.53 (d, *J* = 8.9 Hz, 2H), 7.50 – 7.44 (m, 1H), 7.11 (d, *J* = 8.9 Hz, 2H), 7.05 (d, *J* = 9.0 Hz, 2H), 4.07 (t, *J* = 6.4 Hz, 2H), 3.94 (s, 3H), 2.44 (t, *J* = 7.4 Hz, 2H), 1.90 – 1.82 (m, 2H), 1.79 – 1.72 (m, 2H), 1.63 – 1.55 (m, 2H) (*One active proton was missing*). **^{13}C NMR** (126 MHz, $CDCl_3$) δ 177.1, 160.3, 159.8, 156.6, 148.8, 148.8, 132.2, 130.8, 129.8, 129.4, 128.9, 125.9, 125.7, 125.7, 119.0, 114.8, 114.1, 67.7, 55.4, 33.5, 29.0, 25.6, 24.5 (*One aromatic carbon was missing due to overlap*). **HRMS** ($M+H^+$) for $C_{28}H_{28}NO_4$ Calcd: 442.2013, found: 442.2013. The compound was unreported.

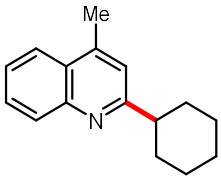

2-Cyclohexyl-4-methylquinoline (3c). Following the general procedure A. Isolated with Hex:EtOAc (10:1) on preparative thin-layer chromatography. Colorless oil (20.5 mg, 91%). **^{1}H NMR** (500 MHz, $CDCl_3$) δ 8.07 (d, *J* = 8.2 Hz, 1H), 7.96 (dd, *J* = 8.3, 1.9 Hz, 1H), 7.72 – 7.63 (m, 1H), 7.56 – 7.47 (m, 1H), 7.19 (s, 1H), 2.90 (tt, *J* = 12.1, 3.4 Hz, 1H), 2.70 (s, 3H), 2.06 – 1.99 (m, 2H), 1.95 – 1.89 (m, 2H), 1.85 – 1.77 (m, 1H), 1.69 – 1.61 (m, 2H), 1.54 – 1.44 (m, 2H), 1.40 – 1.31 (m, 1H). **^{13}C NMR** (126 MHz, $CDCl_3$) δ 166.5, 147.6, 144.2, 129.5, 128.9, 127.1, 125.4, 123.6, 120.3, 47.6, 32.9, 26.6, 26.2, 18.9. **GC-MS** (EI, m/z) for $C_{16}H_{19}N$ Calcd: 225.2, found: 225.1. Spectra data are consistent with the reported literature.[69]

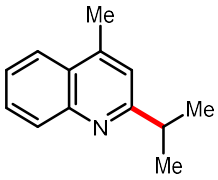

2-Isopropyl-4-methylquinoline (4c). Following the general procedure A. Isolated with Hex:EtOAc (10:1) on preparative thin-layer chromatography. Colorless oil (15.4 mg, 83%). **^{1}H NMR** (500 MHz, $CDCl_3$) δ 8.07 (d, *J* = 8.6 Hz, 1H), 7.97 (dd, *J* = 8.3, 1.4 Hz, 1H), 7.72 – 7.65 (m, 1H), 7.56 – 7.48 (m, 1H), 7.20 (s, 1H), 3.24 (hept, *J* = 7.0 Hz, 1H), 2.71 (s, 3H), 1.41 (d, *J* = 7.0 Hz, 6H). **^{13}C NMR** (126 MHz, $CDCl_3$) δ 167.4, 147.6, 144.3, 129.5, 128.9, 127.0, 125.4, 123.6, 119.8, 37.3, 22.6, 18.9. **GC-MS** (EI, m/z) for $C_{13}H_{15}N$ Calcd: 185.1, found: 185.1. Spectra data are consistent with the reported literature.[69]

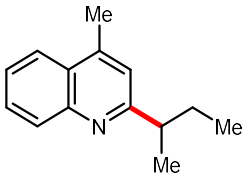

2-(*Sec*-butyl)-4-methylquinoline (5c). Following the general procedure A. Isolated with Hex:EtOAc (10:1) on preparative thin-layer chromatography. Colorless oil (14 mg, 70%). **^{1}H NMR** (500 MHz, $CDCl_3$) δ 8.08 (d, *J* = 8.5 Hz, 1H), 7.97 (dd, *J* = 8.2, 1.5 Hz, 1H), 7.72 – 7.66 (m, 1H), 7.54 – 7.49 (m, 1H), 7.16 (s, 1H), 3.03 – 2.92 (m, 1H), 2.71 (s, 3H), 1.94 – 1.81 (m, 1H), 1.80 – 1.67 (m, 1H), 1.38 (d, *J* = 7.0 Hz, 3H), 0.92 (t, *J* = 7.4 Hz, 3H). **^{13}C NMR**

(126 MHz, $CDCl_3$) δ 166.7, 147.7, 144.2, 129.6, 128.9, 127.1, 125.4, 123.6, 120.2, 44.6, 30.0, 20.4, 18.9, 12.3. **GC-MS** (EI, m/z) for $C_{14}H_{17}N$ Calcd: 199.1, found: 199.0. Spectra data are consistent with the reported literature.[69]

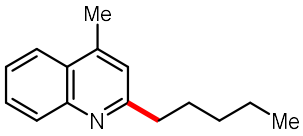

4-Methyl-2-pentylquinoline (6c). Following the general procedure A using EtOAc as the solvent. Isolated with Hex:EtOAc (10:1) on preparative thin-layer chromatography. Colorless oil (6.8 mg, 32%). **^{1}H NMR** (500 MHz, $CDCl_3$) δ 8.07 (d, *J* = 8.4 Hz, 1H), 7.97 (dd, *J* = 8.3, 1.4 Hz, 1H), 7.72 – 7.65 (m, 1H), 7.55 – 7.48 (m, 1H), 7.17 (s, 1H), 2.96 – 2.92 (m, 2H), 2.70 (s, 3H), 1.88 – 1.81 (m, 2H), 1.45 – 1.38 (m, 4H), 0.93 (t, *J* = 7.1 Hz, 3H). **^{13}C NMR** (126 MHz, $CDCl_3$) δ 162.8, 147.8, 144.1, 129.4, 129.0, 126.8, 125.4, 123.6, 122.1, 39.3, 31.8, 29.8, 22.6, 18.7, 14.0. **GC-MS** (EI, m/z) for $C_{15}H_{19}N$ Calcd: 213.2, found: 213.1. Spectra data are consistent with the reported literature.[70]

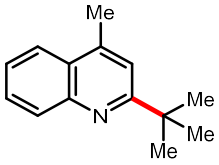

2-(*Tert*-butyl)-4-methylquinoline (7c). Following the general procedure A. Isolated with Hex:EtOAc (10:1) on preparative thin-layer chromatography. Colorless oil (13.9 mg, 70%). **^{1}H NMR** (500 MHz, $CDCl_3$) δ 8.09 (d, *J* = 8.5 Hz, 1H), 7.96 (dd, *J* = 8.4, 1.4 Hz, 1H), 7.71 – 7.64 (m, 1H), 7.55 – 7.48 (m, 1H), 7.38 (s, 1H), 2.72 (s, 3H), 1.49 (s, 9H). **^{13}C NMR** (126 MHz, $CDCl_3$) δ 168.9, 147.3, 143.6, 130.0, 128.7, 126.6, 125.4, 123.4, 118.9, 37.9, 30.1, 19.0. **GC-MS** (EI, m/z) for $C_{14}H_{17}N$ Calcd: 199.1, found: 199.2. Spectra data are consistent with the reported literature.[69]

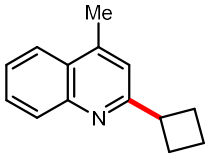

2-Cyclobutyl-4-methylquinoline (8c). Following the general procedure A. Isolated with Hex:EtOAc (10:1) on preparative thin-layer chromatography. Colorless oil (5.4 mg,

27%).**^{1}H NMR** (500 MHz, $CDCl_3$) δ 8.08 (d, *J* = 7.8 Hz, 1H), 7.97 (dd, *J* = 8.1, 1.4 Hz, 1H), 7.71 – 7.66 (m, 1H), 7.54 – 7.48 (m, 1H), 7.22 (s, 1H), 3.85 (quint, *J* = 8.9 Hz, 1H), 2.71 (s, 3H), 2.53 – 2.41 (m, 4H), 2.20 – 2.09 (m, 1H), 2.03 – 1.92 (m, 1H). **^{13}C NMR** (126 MHz, $CDCl_3$) δ 164.7, 147.6, 144.1, 129.6, 128.9, 126.9, 125.4, 123.6, 120.2, 42.7, 28.2, 18.8, 18.4. **GC-MS** (EI, m/z) for $C_{14}H_{15}N$ Calcd: 197.1, found: 197.1. Spectra data are consistent with the reported literature.[70]

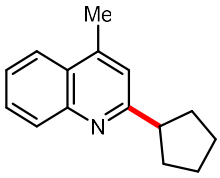

2-Cyclopentyl-4-methylquinoline (9c). Following the general procedure A. Isolated with Hex:EtOAc (10:1) on preparative thin-layer chromatography. Colorless oil (18.2 mg, 86%). **^{1}H NMR** (500 MHz, $CDCl_3$) δ 8.06 (d, *J* = 6.7 Hz, 1H), 7.96 (dd, *J* = 8.2, 1.4 Hz, 1H), 7.70 – 7.65 (m, 1H), 7.54 – 7.48 (m, 1H), 7.20 (s, 1H), 3.41 – 3.30 (m, 1H), 2.70 (s, 3H), 2.23 – 2.14 (m, 2H), 1.95 – 1.87 (m, 4H), 1.82 – 1.73 (m, 2H). **^{13}C NMR** (126 MHz, $CDCl_3$) δ 165.9, 147.5, 144.1, 129.5, 128.9, 127.0, 125.4, 123.5, 120.7, 48.8, 33.6, 26.1, 18.8. **GC-MS** (EI, m/z) for $C_{15}H_{17}N$ Calcd: 211.1, found: 211.2. Spectra data are consistent with the reported literature.[69]

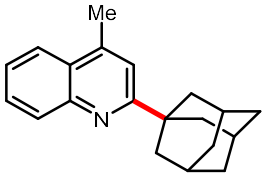

2-(Adamantan-1-yl)-4-methylquinoline (10c). Following the general procedure A. Isolated with Hex:EtOAc (10:1) on preparative thin-layer chromatography. Colorless oil (26 mg, 93%).**^{1}H NMR** (500 MHz, $CDCl_3$) δ 8.09 (d, *J* = 6.9 Hz, 1H), 7.96 (dd, *J* = 8.3, 1.4 Hz, 1H), 7.71 – 7.64 (m, 1H), 7.55 – 7.49 (m, 1H), 7.35 (s, 1H), 2.71 (s, 3H), 2.21 – 2.16 (m, 3H), 2.16 – 2.12 (m, 6H), 1.88 – 1.84 (m, 6H). **^{13}C NMR** (126 MHz, $CDCl_3$) δ 168.7, 147.6, 143.6, 130.0, 128.6, 126.7, 125.3, 123.4, 118.5, 41.8, 39.6, 36.9, 28.9, 19.0. **GC-MS** (EI, m/z) for $C_{20}H_{23}N$ Calcd: 277.2, found: 277.2. Spectra data are consistent with the reported literature.[71]

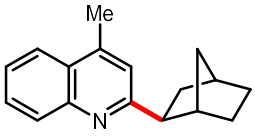

2-(Bicyclo[2.2.1]heptan-2-yl)-4-methylquinoline (11c). Following the general procedure A. Isolated with Hex:EtOAc (10:1) on preparative thin-layer chromatography. Colorless oil (17.1 mg, 72%).**^{1}H NMR** (500 MHz, $CDCl_3$) δ 8.07 (d, *J* = 8.3 Hz, 1H), 7.95 (d, *J* = 8.1 Hz, 1H), 7.72 – 7.62 (m, 1H), 7.54 – 7.47 (m, 1H), 7.20 (d, *J* = 1.1 Hz, 1H), 3.05 – 2.97 (m, 1H), 2.69 (s, 3H), 2.62 – 2.56 (m, 1H), 2.47 – 2.38 (m, 1H), 2.32 – 2.24 (m, 1H), 1.80 – 1.58 (m, 4H), 1.53 – 1.46 (m, 1H), 1.40 – 1.33 (m, 1H), 1.25 – 1.18 (m, 1H). **^{13}C NMR** (126 MHz, $CDCl_3$) δ 165.6, 147.5, 143.7, 129.8, 128.8, 126.8, 125.3, 123.5, 121.6, 50.1, 43.1, 36.8, 36.3, 36.1, 30.6, 29.2, 18.8. **GC-MS** (EI, m/z) for $C_{17}H_{19}N$ Calcd: 237.2, found: 237.1. Spectra data are consistent with the reported literature.[71]

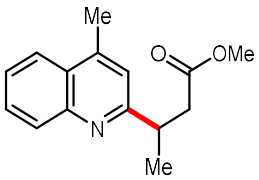

Methyl 3-(4-methylquinolin-2-yl)butanoate (12c). Following the general procedure A. Isolated with Hex:EtOAc (5:2) on preparative thin-layer chromatography. Colorless oil (17 mg, 70%). **^{1}H NMR** (500 MHz, $CDCl_3$) δ 8.05 (d, *J* = 8.4 Hz, 1H), 7.97 (dd, *J* = 8.3, 1.4 Hz, 1H), 7.71 – 7.66 (m, 1H), 7.55 – 7.49 (m, 1H), 7.20 (s, 1H), 3.65 (s, 3H), 3.58 (q, *J* = 7.2 Hz, 1H), 3.09 (dd, *J* = 15.9, 7.5 Hz, 1H), 2.73 – 2.67 (m, 4H), 1.42 (d, *J* = 7.1 Hz, 3H). **^{13}C NMR** (126 MHz, $CDCl_3$) δ 173.3, 164.3, 147.7, 144.3, 129.7, 128.9, 127.1, 125.6, 123.6, 121.1, 51.5, 40.2, 38.6, 20.8, 18.8. **GC-MS** (EI, m/z) for $C_{15}H_{17}NO_2$ Calcd: 243.1, found: 243.2. Spectra data are consistent with the reported literature.[72]

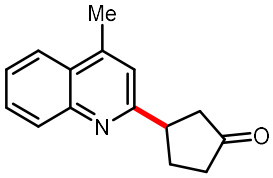

3-(4-Methylquinolin-2-yl)cyclopentan-1-one (13c). Following the general procedure A. Isolated with Hex:EtOAc (5:3) on preparative thin-layer chromatography. Colorless oil (14 mg, 62%).**^{1}H NMR** (500 MHz, $CHCl_3$) δ 8.05 (d, *J* = 8.4 Hz, 1H), 7.99 (dd, *J* = 8.2, 1.5 Hz, 1H), 7.74 – 7.68 (m, 1H), 7.58 – 7.51 (m, 1H), 7.20 (s, 1H), 3.79 – 3.66 (m, 1H), 2.95 – 2.86

(m, 1H), 2.75 – 2.64 (m, 4H), 2.61 – 2.47 (m, 2H), 2.39 – 2.25 (m, 2H). **^{13}C NMR** (126 MHz, $CDCl_3$) δ 218.9, 162.2, 147.7, 144.7, 129.7, 129.2, 127.2, 125.9, 123.6, 121.0, 44.6, 44.1, 38.3, 30.2, 18.8. **HRMS** (M+Na$^+$) for $C_{15}H_{15}NNaO$ Calcd: 248.1046, found: 248.1051. The compound was unreported.

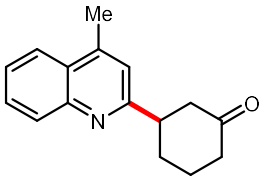

3-(4-Methylquinolin-2-yl)cyclohexan-1-one (14c). Following the general procedure A. Isolated with Hex:EtOAc (5:2) on preparative thin-layer chromatography. Colorless oil (18.2 mg, 76%). **^{1}H NMR** (500 MHz, $CDCl_3$) δ 8.08 – 8.03 (m, 1H), 7.98 (dd, *J* = 8.2, 1.4 Hz, 1H), 7.74 – 7.67 (m, 1H), 7.59 – 7.47 (m, 1H), 7.15 (s, 1H), 3.41 – 3.25 (m, 1H), 3.06 – 2.92 (m, 1H), 2.75 – 2.67 (m, 4H), 2.56 – 2.42 (m, 2H), 2.26 – 2.14 (m, 2H), 2.12 – 2.02 (m, 1H), 1.92 – 1.78 (m, 1H). **^{13}C NMR** (126 MHz, $CDCl_3$) δ 211.4, 162.6, 147.7, 144.8, 129.7, 129.2, 127.1, 125.8, 123.6, 120.8, 46.9, 46.6, 41.3, 31.6, 25.3, 18.8. **GC-MS** (EI, m/z) for $C_{16}H_{17}NO$ Calcd: 239.1, found: 239.2. Spectra data are consistent with the reported literature.[72]

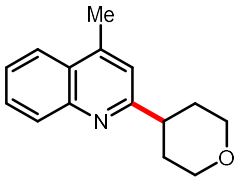

4-Methyl-2-(tetrahydro-2*H*-pyran-4-yl)quinoline (15c). Following the general procedure A. Isolated with Hex:EtOAc (5:3) on preparative thin-layer chromatography. White solid (20.7 mg, 91%). **^{1}H NMR** (500 MHz, $CDCl_3$) δ 8.06 (d, *J* = 8.4 Hz, 1H), 7.98 (dd, *J* = 8.3, 1.4 Hz, 1H), 7.73 – 7.68 (m, 1H), 7.56 – 7.51 (m, 1H), 7.20 (s, 1H), 4.20 – 4.09 (m, 2H), 3.62 (td, *J* = 11.8, 2.2 Hz, 2H), 3.15 (tt, *J* = 12.0, 3.9 Hz, 1H), 2.72 (s, 3H), 2.09 – 1.98 (m, 2H), 1.98 – 1.90 (m, 2H). **^{13}C NMR** (126 MHz, $CDCl_3$) δ 164.3, 147.7, 144.7, 129.6, 129.2, 127.1, 125.7, 123.6, 119.9, 68.2, 44.5, 32.3, 18.9. **GC-MS** (EI, m/z) for $C_{15}H_{17}NO$ Calcd: 227.1, found: 227.2. Spectra data are consistent with the reported literature.[69]

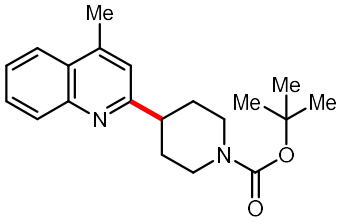

***Tert*-butyl 4-(4-methylquinolin-2-yl)piperidine-1-carboxylate (16c).** Following the general procedure A. Isolated with Hex:EtOAc (5:2) on preparative thin-layer chromatography. Pale yellow oil (19.9 mg, 61%). **^{1}H NMR** (500 MHz, $CDCl_3$) δ 8.05 (d, *J* = 7.9 Hz, 1H), 7.98 (dd, *J* = 8.0, 1.2 Hz, 1H), 7.74 – 7.64 (m, 1H), 7.57 – 7.49 (m, 1H), 7.17 (s, 1H), 4.31 (br, 2H), 3.04 (tt, *J* = 12.0, 3.7 Hz, 1H), 2.90 (br, 2H), 2.71 (s, 3H), 2.05 – 1.95 (m, 2H), 1.93 – 1.79 (m, 2H), 1.51 (s, 9H). **^{13}C NMR** (126 MHz, $CDCl_3$) δ 164.3, 154.9, 147.7, 144.7, 129.5, 129.2, 127.1, 125.7, 123.6, 120.0, 79.4, 45.5, 44.3, 31.6, 28.5, 18.9. **GC-MS** (EI, m/z) for $C_{20}H_{26}N_2O_2$ Calcd: 326.2, found: 326.3. Spectra data are consistent with the reported literature.[73]

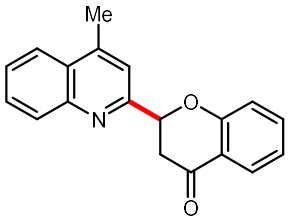

2-(4-Methylquinolin-2-yl)chroman-4-one (17c). Following the general procedure A using 3.0 equiv alkyltrifluoroborate. Isolated with Hex:EtOAc (5:2) on preparative thin-layer chromatography. Colorless solid (15.3 mg, 53%). **^{1}H NMR** (500 MHz, $CDCl_3$) δ 8.11 (d, *J* = 7.8 Hz, 1H), 8.04 (dd, *J* = 8.3, 1.3 Hz, 1H), 7.98 (dd, *J* = 7.9, 1.8 Hz, 1H), 7.79 – 7.72 (m, 1H), 7.65 – 7.59 (m, 2H), 7.57 – 7.53 (m, 1H), 7.14 (dd, *J* = 8.3, 1.1 Hz, 1H), 7.12 – 7.07 (m, 1H), 5.77 (dd, *J* = 12.2, 3.5 Hz, 1H), 3.34 (dd, *J* = 17.0, 12.1 Hz, 1H), 3.23 (dd, *J* = 17.0, 3.5 Hz, 1H), 2.80 (s, 3H). **^{13}C NMR** (126 MHz, $CDCl_3$) δ 191.7, 161.0, 157.4, 147.3, 145.8, 136.1, 130.0, 129.6, 127.8, 127.1, 126.7, 123.7, 121.8, 121.4, 119.1, 118.1, 80.5, 42.7, 19.0. **GC-MS** (EI, m/z) for $C_{19}H_{15}NO_2$ Calcd: 289.1, found: 289.2. Spectra data are consistent with the reported literature.[74]

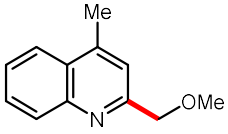

2-(Methoxymethyl)-4-methylquinoline (18c). Following the general procedure A. Isolated with Hex:EtOAc (5:1) on preparative thin-layer chromatography. Pale yellow oil (11.1 mg, 59%). **^{1}H NMR** (500 MHz, $CDCl_3$) δ 8.09 (d, *J* = 6.7 Hz, 1H), 8.01 (dd, *J* = 8.4, 1.4 Hz, 1H), 7.75 – 7.69 (m, 1H), 7.60 – 7.54 (m, 1H), 7.45 (s, 1H), 4.75 (s, 2H), 3.54 (s, 3H), 2.75 (s, 3H). **^{13}C NMR** (126 MHz, $CDCl_3$) δ 158.6, 147.4, 145.0, 129.6, 129.3, 127.6, 126.1, 123.7, 120.0, 76.2, 58.9, 18.8. **GC-MS** (EI, m/z) for $C_{12}H_{13}NO$ Calcd: 187.1, found: 187.1. Spectra data are consistent with the reported literature.[69]

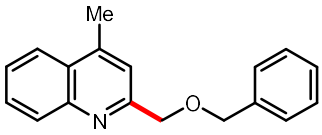

2-((Benzyloxy)methyl)-4-methylquinoline (19c). Following the general procedure A. Isolated with Hex:EtOAc (5:2) on preparative thin-layer chromatography. Colorless oil (15.5 mg, 59%). **^{1}H NMR** (500 MHz, $CDCl_3$) δ 8.08 (d, *J* = 10.4 Hz, 1H), 8.02 (dd, *J* = 8.2, 1.3 Hz, 1H), 7.75 – 7.69 (m, 1H), 7.60 – 7.55 (m, 1H), 7.53 (s, 1H), 7.47 – 7.42 (m, 2H), 7.42 – 7.37 (m, 2H), 7.36 – 7.31 (m, 1H), 4.85 (s, 2H), 4.71 (s, 2H), 2.75 (s, 3H). **^{13}C NMR** (126 MHz, $CDCl_3$) δ 158.7, 147.4, 145.0, 138.0, 129.6, 129.3, 128.5, 127.9, 127.8, 127.6, 126.1, 123.8, 120.1, 73.9, 73.1, 18.9. **GC-MS** (EI, m/z) for $C_{18}H_{17}NO$ Calcd: 263.1, found: 263.0. Spectra data are consistent with the reported literature.[69]

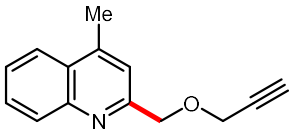

4-Methyl-2-((prop-2-yn-1-yloxy)methyl)quinoline (20c). Following the general procedure A. Isolated with Hex:EtOAc (5:2) on preparative thin-layer chromatography. Yellow oil (11.4 mg, 54%). **^{1}H NMR** (500 MHz, $CDCl_3$) δ 8.09 (d, *J* = 7.3 Hz, 1H), 8.01 (dd, *J* = 8.2, 1.4 Hz, 1H), 7.75 – 7.70 (m, 1H), 7.60 – 7.54 (m, 1H), 7.47 (s, 1H), 4.89 (s, 2H), 4.36 (d, *J* = 2.4 Hz, 2H), 2.75 (s, 3H), 2.52 (t, *J* = 2.4 Hz, 1H). **^{13}C NMR** (126 MHz, $CDCl_3$) δ 157.8, 147.4, 145.1, 129.7, 129.3, 127.6, 126.2, 123.7, 120.2, 79.4, 75.0, 73.3, 58.2, 18.8. **GC-MS** (EI, m/z) for $C_{14}H_{13}NO$ Calcd: 211.1, found: 211.1. Spectra data are consistent with the reported literature.[69]

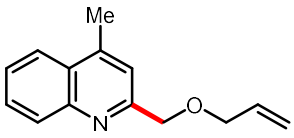

2-((Allyloxy)methyl)-4-methylquinoline (21c). Following the general procedure A. Isolated with Hex:EtOAc (5:2) on preparative thin-layer chromatography. Yellow oil (7.7 mg, 36%). **^{1}H NMR** (500 MHz, $CDCl_3$) δ 8.08 (d, *J* = 8.5 Hz, 1H), 8.01 (dd, *J* = 8.4, 1.4 Hz, 1H), 7.75 – 7.69 (m, 1H), 7.61 – 7.53 (m, 1H), 7.50 (s, 1H), 6.10 – 5.95 (m, 1H), 5.43 – 5.33 (m, 1H), 5.27 (dd, *J* = 10.4, 1.5 Hz, 1H), 4.81 (s, 2H), 4.18 (d, *J* = 5.6 Hz, 2H), 2.75 (s, 3H). **^{13}C NMR** (126 MHz, $CDCl_3$) δ 158.7, 147.4, 145.0, 134.4, 129.6, 129.2, 127.6, 126.0, 123.7, 120.1, 117.6, 73.7, 72.0, 18.9. **GC-MS** (EI, m/z) for $C_{14}H_{15}NO$ Calcd: 213.1, found: 213.1. Spectra data are consistent with the reported literature.[69]

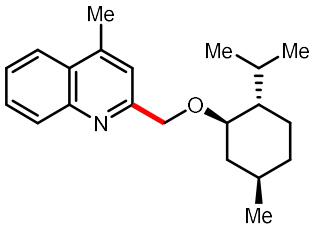

2-((((1*R*,2*S*,5*R*)-2-isopropyl-5-methylcyclohexyl)oxy)methyl)-4-methylquinoline (22c). Following the general procedure A. Isolated with Hex:EtOAc (10:1) on preparative thin-layer chromatography. Colorless oil (17.7 mg, 57%). **^{1}H NMR** (500 MHz, $CDCl_3$) δ 8.06 (d, *J* = 9.9 Hz, 1H), 8.00 (d, *J* = 8.4 Hz, 1H), 7.73 – 7.68 (m, 1H), 7.59 – 7.54 (m, 1H), 7.51 (s, 1H), 4.92 (d, *J* = 13.0 Hz, 1H), 4.72 (d, *J* = 13.1 Hz, 1H), 3.30 (td, *J* = 10.5, 4.1 Hz, 1H), 2.74 (s, 3H), 2.46 – 2.33 (m, 1H), 2.31 – 2.25 (m, 1H), 1.71 – 1.63 (m, 2H), 1.51 – 1.37 (m, 2H), 1.04 – 0.91 (m, 9H), 0.77 (d, *J* = 6.9 Hz, 3H). **^{13}C NMR** (126 MHz, $CDCl_3$) δ 159.7, 147.2, 144.7, 129.5, 129.1, 127.6, 125.9, 123.7, 120.5, 79.5, 72.0, 48.4, 40.3, 34.6, 31.6, 25.7, 23.3, 22.4, 21.1, 18.9, 16.2. **HRMS** ($M+Na^+$) for $C_{21}H_{29}NNaO$ Calcd: 334.2141, found: 334.2144. The compound was unreported.

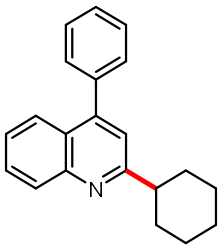

2-Cyclohexyl-4-phenylquinoline (23c). Following the general procedure A. Isolated with Hex:EtOAc (10:1) on preparative thin-layer chromatography. Colorless oil (23 mg, 80%). **^{1}H NMR** (500 MHz, $CDCl_3$) δ 8.14 (d, *J* = 10.2 Hz, 1H), 7.89 (dd, *J* = 8.4, 1.7 Hz, 1H), 7.73 – 7.68 (m, 1H), 7.57 – 7.49 (m, 5H), 7.47 – 7.42 (m, 1H), 7.30 (s, 1H), 2.99 (tt, *J* = 12.1, 3.4 Hz, 1H), 2.14 – 2.06 (m, 2H), 1.98 – 1.90 (m, 2H), 1.87 – 1.79 (m, 1H), 1.73 – 1.63 (m, 2H), 1.57 – 1.45 (m, 2H), 1.41 – 1.31 (m, 1H). **^{13}C NMR** (126 MHz, $CDCl_3$) δ 166.4, 148.6, 148.3, 138.6, 129.6, 129.4, 129.1, 128.5, 128.3, 125.7, 125.6, 125.5, 119.9, 47.7, 32.9, 26.6, 26.1. **GC-MS** (EI, m/z) for $C_{21}H_{21}N$ Calcd: 287.2, found: 287.1. Spectra data are consistent with the reported literature.[72]

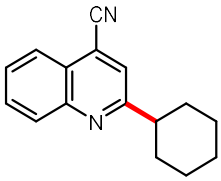

2-Cyclohexylquinoline-4-carbonitrile (24c). Following the general procedure A. Isolated with Hex:EtOAc (5:1) on preparative thin-layer chromatography. Colorless oil (13.2 mg, 56%). **^{1}H NMR** (500 MHz, $CDCl_3$) δ 8.19 – 8.11 (m, 2H), 7.87 – 7.81 (m, 1H), 7.73 – 7.65 (m, 2H), 2.98 (tt, *J* = 12.1, 3.5 Hz, 1H), 2.10 – 2.02 (m, 2H), 1.98 – 1.92 (m, 2H), 1.87 – 1.79 (m, 1H), 1.71 – 1.62 (m, 2H), 1.55 – 1.46 (m, 2H), 1.41 – 1.33 (m, 1H). **^{13}C NMR** (126 MHz, $CDCl_3$) δ 166.2, 147.8, 130.9, 129.9, 128.1, 124.7, 124.4, 124.1, 118.9, 116.0, 47.2, 32.6, 26.4, 25.9. **HRMS** ($M+H^+$) for $C_{16}H_{17}N_2$ Calcd: 237.1386, found: 237.1383. The compound was unreported.

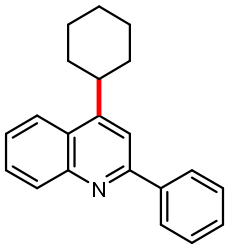

4-Cyclohexyl-2-phenylquinoline (25c). Following the general procedure A. Isolated with Hex:EtOAc (10:1) on preparative thin-layer chromatography. White solid (18.9 mg, 66%). **^{1}H NMR** (500 MHz, $CDCl_3$) δ 8.22 (d, *J* = 8.4 Hz, 1H), 8.20 – 8.15 (m, 2H), 8.14 – 8.08 (m, 1H), 7.79 (s, 1H), 7.75 – 7.69 (m, 1H), 7.59 – 7.52 (m, 3H), 7.52 – 7.45 (m, 1H), 3.46 – 3.34 (m, 1H), 2.17 – 2.08 (m, 2H), 2.02 – 1.94 (m, 2H), 1.95 – 1.87 (m, 1H), 1.70 – 1.53 (m,

4H), 1.47 – 1.35 (m, 1H). **^{13}C NMR** (126 MHz, $CDCl_3$) δ 157.4, 154.0, 148.6, 140.3, 130.7, 129.1, 129.0, 128.8, 127.6, 125.9, 122.9, 115.5, 39.1, 33.7, 27.0, 26.4 (*One aromatic carbon was missing due to overlap*). **GC-MS** (EI, m/z) for $C_{21}H_{21}N$ Calcd: 287.2, found: 287.2. Spectra data are consistent with the reported literature.[21]

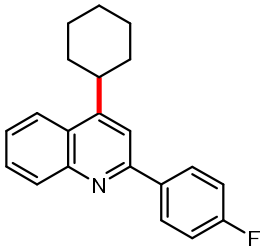

4-Cyclohexyl-2-(4-fluorophenyl)quinoline (26c). Following the general procedure A. Isolated with Hex:EtOAc (10:1) on preparative thin-layer chromatography. White solid (16.2 mg, 53%). **^{1}H NMR** (500 MHz, $CDCl_3$) δ 8.22 – 8.14 (m, 3H), 8.11 (dd, *J* = 8.5, 1.4 Hz, 1H), 7.76 – 7.68 (m, 2H), 7.59 – 7.53 (m, 1H), 7.26 – 7.19 (m, 2H), 3.46 – 3.32 (m, 1H), 2.16 – 2.05 (m, 2H), 2.05 – 1.95 (m, 2H), 1.95 – 1.87 (m, 1H), 1.68 – 1.56 (m, 4H), 1.47 – 1.37 (m, 1H). **^{13}C NMR** (126 MHz, $CDCl_3$) δ 163.7 (d, *J* = 248 Hz) 156.2, 154.1, 148.5, 136.4 (d, *J* = 3 Hz), 130.6, 129.4, 129.3 (q, *J* = 33 Hz), 126.0, 125.8, 122.9, 115.7 (d, *J* = 21 Hz), 115.1, 39.1, 33.7, 27.0, 26.3. **^{19}F NMR** (470 MHz, $CDCl_3$) δ -112.85- -112.94 (m, 1F). **GC-MS** (EI, m/z) for $C_{21}H_{20}FN$ Calcd: 305.2, found: 305.2. Spectra data are consistent with the reported literature.[21]

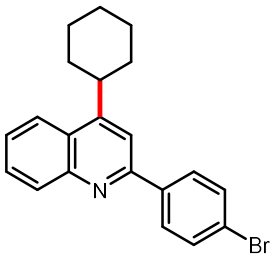

2-(4-Bromophenyl)-4-cyclohexylquinoline (27c). Following the general procedure A. Isolated with Hex:EtOAc (10:1) on preparative thin-layer chromatography. White solid (21.7 mg, 74%). **^{1}H NMR** (500 MHz, $CDCl_3$) δ 8.19 (d, *J* = 9.9 Hz, 1H), 8.11 (d, *J* = 8.5 Hz, 1H), 8.08 – 8.05 (m, 2H), 7.74 – 7.71 (m, 2H), 7.68 – 7.66 (m, 2H), 7.59 – 7.55 (m, 1H), 3.43 – 3.35 (m, 1H), 2.13 – 2.08 (m, 2H), 2.02 – 1.97 (m, 2H), 1.93 – 1.87 (m, 1H), 1.67 – 1.59 (m, 4H), 1.50 – 1.28 (m, 1H). **^{13}C NMR** (126 MHz, $CDCl_3$) δ 156.0, 154.3, 148.6, 139.1, 131.9, 130.7, 129.2, 129.2, 126.1, 126.0, 123.7, 122.9, 115.0, 39.2, 33.7, 27.0, 26.3. **GC-MS** (EI,

m/z) for $C_{21}H_{20}BrN$ Calcd: 365.1, 367.1 found: 365.2, 367.2. Spectra data are consistent with the reported literature.[21]

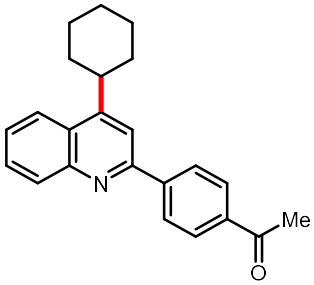

1-(4-(4-Cyclohexylquinolin-2-yl)phenyl)ethan-1-one (28c). Following the general procedure A. Isolated with Hex:DCM:EtOAc (1:1:0.2) on preparative thin-layer chromatography. White solid (14.2 mg, 43%). **^{1}H NMR** (500 MHz, $CDCl_3$) δ 8.31 – 8.26 (m, 2H), 8.24 – 8.20 (m, 1H), 8.16 – 8.11 (m, 3H), 7.81 (s, 1H), 7.78 – 7.72 (m, 1H), 7.63 – 7.57 (m, 1H), 3.47 – 3.37 (m, 1H), 2.70 (s, 3H), 2.16 – 2.08 (m, 2H), 2.03 – 1.97 (m, 2H), 1.95 – 1.88 (m, 1H), 1.69 – 1.59 (m, 4H), 1.48 – 1.36 (m, 1H). **^{13}C NMR** (126 MHz, $CDCl_3$) δ 198.0, 155.9, 154.4, 148.6, 144.5, 137.2, 130.9, 129.3, 128.8, 127.8, 126.4, 126.2, 122.9, 115.4, 39.2, 33.7, 27.0, 26.8, 26.3. **GC-MS** (EI, m/z) for $C_{23}H_{23}NO$ Calcd: 329.2, found: 329.3. Spectra data are consistent with the reported literature.[21]

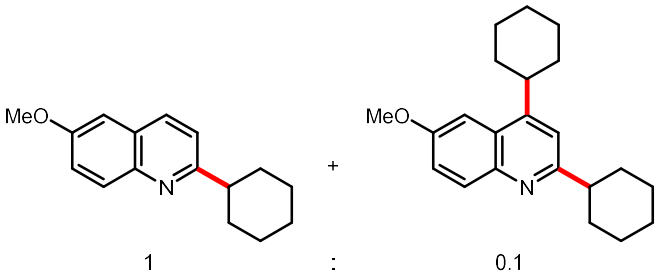

2-Cyclohexyl-6-methoxyquinoline (29c) and 2,4-dicyclohexyl-6-methoxyquinoline (29c'), mono:di=1:0.1. Following the general procedure A using 4.0 equiv alkyltrifluoroborate, EtOAc as the solvent, and run for 40 h. Isolated with Hex:EtOAc (5:1) on preparative thin-layer chromatography. Yellow oil (10.8 mg, 43%). **^{1}H NMR** (500 MHz, $CDCl_3$) δ 8.00 (d, *J* = 8.5 Hz, 1H+0.1H), 7.96 (d, *J* = 9.3 Hz, 1H), 7.35 (dd, *J* = 9.2, 2.7 Hz, 1H+0.1H), 7.31 (d, *J* = 8.5 Hz, 1H+0.1H), 7.18 (s, 0.1 H), 7.06 (d, *J* = 2.9 Hz, 1H), 3.96 (s, 0.3H), 3.94 (s, 3H), 3.26 – 3.15 (m, 0.1H), 2.94 – 2.85 (m, 1H+0.1H), 2.08 – 2.00 (m, 2H+0.4H), 1.95 – 1.86 (m, 2H+0.4H), 1.84 – 1.74 (m, 1H+0.2H), 1.69 – 1.57 (m, 2H+0.4H), 1.56 – 1.44 (m, 2H+0.4H), 1.42 – 1.31 (m, 1H+0.2H). **^{13}C NMR** (126 MHz, $CDCl_3$) δ 164.4,

157.1, 143.8, 135.2, 130.4, 127.8, 126.3, 121.7, 119.8, 115.9, 105.2, 101.9, 55.5, 47.4, 33.4, 33.0, 33.0, 27.0, 26.6, 26.6, 26.4, 26.1 (*Six aromatic and four aliphatic carbons were missing due to overlap*). **HRMS** (M+H$^+$) for $C_{16}H_{20}NO$ Calcd: 242.1539, found: 242.1539; for $C_{22}H_{30}NO$ Calcd: 324.2322, found: 324.2324. The compounds were unreported.

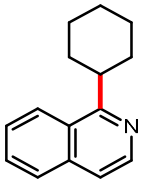

1-Cyclohexylisoquinoline (30c). Following the general procedure A. Isolated with Hex:EtOAc (10:1) on preparative thin-layer chromatography. Colorless oil (13.1 mg, 62%). **^{1}H NMR** (500 MHz, $CDCl_3$) δ 8.50 (d, *J* = 5.6 Hz, 1H), 8.25 (d, *J* = 8.3 Hz, 1H), 7.83 (d, *J* = 9.3 Hz, 1H), 7.70 – 7.64 (m, 1H), 7.64 – 7.57 (m, 1H), 7.50 (dd, *J* = 5.6, 1.0 Hz, 1H), 3.59 (tt, *J* = 11.7, 3.3 Hz, 1H), 2.08 – 1.90 (m, 4H), 1.90 – 1.81 (m, 3H), 1.62 – 1.51 (m, 2H), 1.47 – 1.34 (m, 1H). **^{13}C NMR** (126 MHz, $CDCl_3$) δ 165.7, 142.0, 136.4, 129.5, 127.6, 126.8, 126.3, 124.7, 118.9, 41.5, 32.6, 26.9, 26.3. **GC-MS** (EI, m/z) for $C_{15}H_{17}N$ Calcd: 211.1, found: 211.0. Spectra data are consistent with the reported literature.[75]

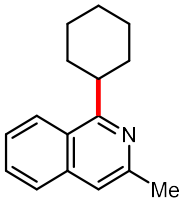

1-Cyclohexyl-3-methylisoquinoline (31c). Following the general procedure A. Isolated with Hex:EtOAc (10:1) on preparative thin-layer chromatography. Colorless oil (15.7 mg, 70%). **^{1}H NMR** (500 MHz, $CDCl_3$) δ 8.19 (d, *J* = 7.5 Hz, 1H), 7.72 (d, *J* = 8.2 Hz, 1H), 7.64 – 7.58 (m, 1H), 7.54 – 7.46 (m, 1H), 7.32 (s, 1H), 3.55 (tt, *J* = 11.4, 3.4 Hz, 1H), 2.68 (s, 3H), 2.01 – 1.81 (m, 7H), 1.60 – 1.49 (m, 2H), 1.47 – 1.39 (m, 1H). **^{13}C NMR** (126 MHz, $CDCl_3$) δ 165.0, 150.5, 137.1, 129.3, 126.9, 125.6, 124.7, 124.3, 116.6, 41.6, 32.5, 26.9, 26.2, 24.6. **GC-MS** (EI, m/z) for $C_{16}H_{19}N$ Calcd: 225.2, found: 225.2. Spectra data are consistent with the reported literature.[21]

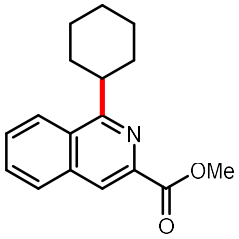

Methyl 1-cyclohexylisoquinoline-3-carboxylate (32c). Following the general procedure A. Isolated with Hex:EtOAc (10:1) on preparative thin-layer chromatography. White solid (17.5 mg, 65%). **^{1}H NMR** (500 MHz, $CDCl_3$) δ 8.42 (s, 1H), 8.32 – 8.27 (m, 1H), 7.99 – 7.92 (m, 1H), 7.77 – 7.69 (m, 2H), 4.05 (s, 3H), 3.59 (tt, *J* = 11.1, 3.8 Hz, 1H), 2.07 – 1.94 (m, 6H), 1.86 – 1.80 (m, 1H), 1.62 – 1.52 (m, 2H), 1.50 – 1.39 (m, 1H). **^{13}C NMR** (126 MHz, $CDCl_3$) δ 166.9, 166.1, 140.7, 136.0, 130.1, 129.1, 129.0, 127.8, 125.0, 122.4, 52.7, 42.1, 32.2, 26.8, 26.1. **GC-MS** (EI, m/z) for $C_{17}H_{19}NO_2$ Calcd: 269.1, found: 269.2. Spectra data are consistent with the reported literature.[76]

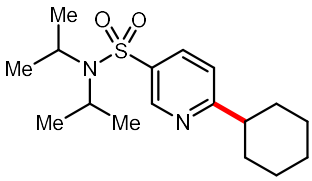

6-Cyclohexyl-*N*,*N*-diisopropylpyridine-3-sulfonamide (33c). Following the general procedure A using 3.0 equiv alkyltrifluoroborate and TFA. Isolated with Hex:EtOAc (5:1) on preparative thin-layer chromatography. White solid (13.3 mg, 41%). **^{1}H NMR** (500 MHz, $CDCl_3$) δ 8.99 (dd, *J* = 2.5, 0.8 Hz, 1H), 8.05 (dd, *J* = 8.3, 2.4 Hz, 1H), 7.27 (d, *J* = 8.2 Hz, 1H), 3.75 (quint, *J* = 6.8 Hz, 2H), 2.79 (tt, *J* = 11.9, 3.4 Hz, 1H), 2.01 – 1.94 (m, 2H), 1.93 – 1.85 (m, 2H), 1.83 – 1.74 (m, 1H), 1.58 – 1.50 (m, 2H), 1.49 – 1.39 (m, 2H), 1.30 (d, *J* = 6.7 Hz, 13H). **^{13}C NMR** (126 MHz, $CDCl_3$) δ 170.2, 147.6, 136.4, 135.1, 120.8, 48.8, 46.6, 32.7, 26.4, 25.9, 22.0. **GC-MS** (EI, m/z) for $C_{17}H_{28}N_2O_2S$ Calcd: 324.2, found: 324.3. Spectra data are consistent with the reported literature.[21]

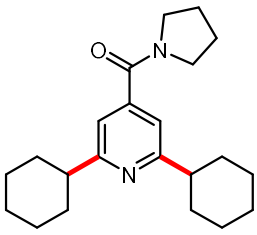

(2,6-Dicyclohexylpyridin-4-yl)(pyrrolidin-1-yl)methanone (34c). Following the

general procedure A using 3.0 equiv alkyltrifluoroborate and TFA. Isolated with Hex:EtOAc (5:2) on preparative thin-layer chromatography. White solid (10.9 mg, 32%). **^{1}H NMR** (500 MHz, $CDCl_3$) δ 7.04 (s, 2H), 3.66 (t, *J* = 7.0 Hz, 2H), 3.37 (t, *J* = 6.6 Hz, 2H), 2.72 (tt, *J* = 11.7, 3.4 Hz, 2H), 2.02 – 1.95 (m, 6H), 1.93 – 1.89 (m, 2H), 1.88 – 1.82 (m, 4H), 1.78 – 1.74 (m, 2H), 1.50 – 1.41 (m, 6H), 1.33 – 1.26 (m, 4H). **^{13}C NMR** (126 MHz, $CDCl_3$) δ 168.6, 166.3, 145.2, 115.2, 49.2, 46.7, 46.1, 33.0, 26.5, 26.3, 26.1, 24.4. **HRMS** ($M+H^+$) for $C_{22}H_{33}N_2O$ Calcd: 341.2587, found: 341.2593. The compound was unreported.

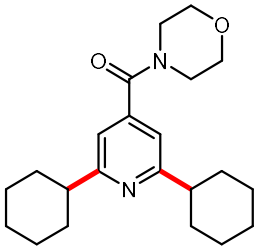

(2,6-Dicyclohexylpyridin-4-yl)(morpholino)methanone (35c). Following the general procedure A using 3.0 equiv alkyltrifluoroborate and TFA. Isolated with Hex:EtOAc (5:2) on preparative thin-layer chromatography. White solid (15 mg, 42%). **^{1}H NMR** (500 MHz, $CDCl_3$) δ 6.94 (s, 2H), 3.81 (br, 4H), 3.64 (br, 2H), 3.39 (br, 2H), 2.77 – 2.67 (m, 2H), 2.01 – 1.94 (m, 4H), 1.89 – 1.82 (m, 4H), 1.79 – 1.74 (m, 2H), 1.54 – 1.39 (m, 8H), 1.31 – 1.27 (m, 2H). **^{13}C NMR** (126 MHz, $CDCl_3$) δ 169.1, 166.6, 143.5, 115.2, 66.8, 47.9, 46.6, 42.3, 32.9, 26.5, 26.1. **GC-MS** (EI, m/z) for $C_{22}H_{32}N_2O_2$ Calcd: 356.2, found: 356.2. Spectra data are consistent with the reported literature.[2]

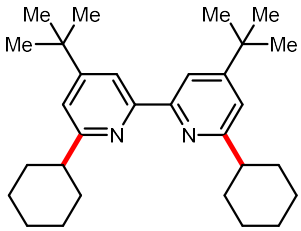

4,4'-Di-*tert*-butyl-6,6'-dicyclohexyl-2,2'-bipyridine (36c). Following the general procedure A using 4.0 equiv alkyltrifluoroborate and 3.0 equiv TFA. Isolated with Hex:EtOAc (30:1) on preparative thin-layer chromatography. White solid (12.1 mg, 28%).**^{1}H NMR** (500 MHz, $CDCl_3$) δ 8.23 (d, *J* = 1.8 Hz, 2H), 7.14 (d, *J* = 1.8 Hz, 2H), 2.83 – 2.74 (m, 2H), 2.07 – 2.02 (m, 4H), 1.93 – 1.88 (m, 4H), 1.82 – 1.76 (m, 2H), 1.68 – 1.59 (m, 4H), 1.53 – 1.49 (m, 24H). **^{13}C NMR** (126 MHz, $CDCl_3$) δ 165.6, 160.6, 156.3, 117.5, 115.8,

46.7, 34.9, 33.1, 30.8, 26.7, 26.3. **GC-MS** (EI, m/z) for $C_{30}H_{44}N_2$ Calcd: 432.4, found: 432.7. Spectra data are consistent with the reported literature.[77]

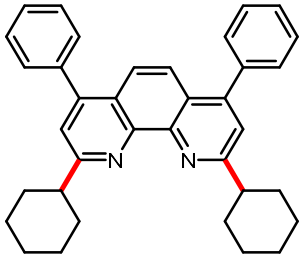

2,9-Dicyclohexyl-4,7-diphenyl-1,10-phenanthroline (37c). Following the general procedure A using 4.0 equiv alkyltrifluoroborate and 3.0 equiv TFA. Isolated with Hex:EtOAc:MeOH (1:1:0.2) on preparative thin-layer chromatography. Yellow oil (NMR yield: 45%). **^{1}H NMR** (500 MHz, $CDCl_3$) δ 7.74 (s, 2H), 7.55 – 7.48 (m, 12H), 3.35 (tt, *J* = 12.1, 3.5 Hz, 2H), 2.29 – 2.20 (m, 4H), 1.98 – 1.92 (m, 4H), 1.89 – 1.82 (m, 2H), 1.74 – 1.68 (m, 4H), 1.61 – 1.53 (m, 4H), 1.44 – 1.37 (m, 2H). **^{13}C NMR** (126 MHz, $CDCl_3$) δ 166.5, 148.6, 146.1, 138.9, 129.7, 128.5, 128.2, 125.2, 123, 120.9, 47.6, 33.3, 26.6, 26.3. **HRMS** ($M+H^+$) for $C_{36}H_{37}N_2$ Calcd: 497.2951, found: 497.2966. The compound was unreported.

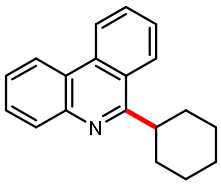

6-Cyclohexylphenanthridine (38c). Following the general procedure A using 4.0 equiv alkyltrifluoroborate and 3.0 equiv TFA. Isolated with Hex:EtOAc (10:1) on preparative thin-layer chromatography. Colorless oil (25 mg, 96%). **^{1}H NMR** (500 MHz, $CDCl_3$) δ 8.68 (dd, *J* = 8.4, 1.2 Hz, 1H), 8.56 (dd, *J* = 8.2, 1.4 Hz, 1H), 8.34 (dd, *J* = 8.2, 1.1 Hz, 1H), 8.17 (dd, *J* = 8.1, 1.3 Hz, 1H), 7.86 – 7.81 (m, 1H), 7.76 – 7.66 (m, 2H), 7.66 – 7.60 (m, 1H), 3.65 (tt, *J* = 11.3, 3.2 Hz, 1H), 2.16 – 2.08 (m, 2H), 2.06 – 1.93 (m, 4H), 1.91 – 1.83 (m, 1H), 1.68 – 1.55 (m, 2H), 1.53 – 1.41 (m, 1H). **^{13}C NMR** (126 MHz, $CDCl_3$) δ 165.3, 143.9, 133.0, 130.0, 129.9, 128.4, 127.1, 126.1, 125.6, 124.8, 123.4, 122.6, 121.8, 42.0, 32.3, 26.9, 26.4. **GC-MS** (EI, m/z) for $C_{19}H_{19}N$ Calcd: 261.2, found: 261.1. Spectra data are consistent with the reported literature.[75]

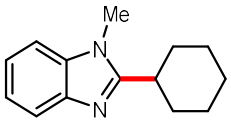

2-Cyclohexyl-1-methyl-1*H*-benzo[*d*]imidazole (39c). Following the general procedure A using 3.0 equiv alkyltrifluoroborate. Isolated with Hex:EtOAc (5:2) on preparative thin-layer chromatography. Colorless oil (12.2 mg, 57%). **^{1}H NMR** (500 MHz, $CDCl_3$) δ 7.79 – 7.74 (m, 1H), 7.33 – 7.30 (m, 1H), 7.28 – 7.22 (m, 2H), 3.77 (s, 3H), 2.93 – 2.83 (m, 1H), 2.06 – 2.00 (m, 2H), 1.98 – 1.91 (m, 2H), 1.88 – 1.79 (m, 3H), 1.49 – 1.36 (m, 3H). **^{13}C NMR** (126 MHz, $CDCl_3$) δ 159.0, 142.5, 135.6, 121.9, 121.7, 119.3, 108.8, 36.4, 31.5, 29.6, 26.4, 25.8. **GC-MS** (EI, m/z) for $C_{14}H_{18}N_2$ Calcd: 214.1, found: 214.1. Spectra data are consistent with the reported literature.[70]

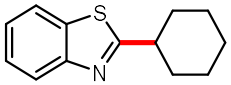

2-Cyclohexylbenzo[*d*]thiazole (40c). Following the general procedure A using 3.0 equiv alkyltrifluoroborate. Isolated with Hex:EtOAc (10:1) on preparative thin-layer chromatography. Colorless oil (13 mg, 60%). **^{1}H NMR** (500 MHz, $CDCl_3$) δ 8.00 (d, *J* = 8.2 Hz, 1H), 7.87 (d, *J* = 7.0 Hz, 1H), 7.49 – 7.43 (m, 1H), 7.39 – 7.33 (m, 1H), 3.13 (tt, *J* = 11.7, 3.6 Hz, 1H), 2.29 – 2.17 (m, 2H), 1.96 – 1.87 (m, 2H), 1.83 – 1.75 (m, 1H), 1.70 – 1.63 (m, 2H), 1.52 – 1.42 (m, 2H), 1.40 – 1.32 (m, 1H). **^{13}C NMR** (126 MHz, $CDCl_3$) δ 177.6, 153.1, 134.6, 125.8, 124.5, 122.6, 121.6, 43.5, 33.5, 26.1, 25.8. **GC-MS** (EI, m/z) for $C_{13}H_{15}NS$ Calcd: 217.1, found: 217.2. Spectra data are consistent with the reported literature.[70]

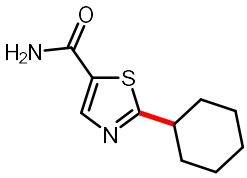

2-Cyclohexylthiazole-5-carboxamide (41c). Following the general procedure A using 3.0 equiv alkyltrifluoroborate. Isolated with Hex:EtOAc:MeOH (1:1:0.5) on preparative thin-layer chromatography. White solid (9.5 mg, 45%). **^{1}H NMR** (500 MHz, $CDCl_3$) δ 8.07 (s, 1H), 5.72 (br, 2H), 3.02 (tt, *J* = 11.4, 3.6 Hz, 1H), 2.21 – 2.14 (m, 2H), 1.92 – 1.84 (m, 2H), 1.81 – 1.74 (m, 1H), 1.60 – 1.51 (m, 2H), 1.49 – 1.39 (m, 2H), 1.36 – 1.26 (m, 1H). **^{13}C NMR** (126 MHz, $CDCl_3$) δ 182.1, 162.3, 143.8, 131.7, 43.0, 33.5, 25.9, 25.7. **HRMS** ($M+Na^+$) for $C_{10}H_{14}N_2NaOS$ Calcd: 233.0719, found: 233.0726. The compound was unreported.

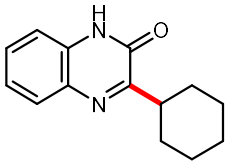

3-Cyclohexylquinoxalin-2(1*H*)-one (42c). Following the general procedure A using 3.0 equiv alkyltrifluoroborate and TFA. Isolated with Hex:EtOAc (5:2) on preparative thin-layer chromatography. White solid (13.2 mg, 58%). **^{1}H NMR** (500 MHz, $CDCl_3$) δ 10.74 (br, 1H), 7.86 (dd, *J* = 8.1, 1.4 Hz, 1H), 7.51 – 7.46 (m, 1H), 7.36 – 7.31 (m, 1H), 7.24 (dd, *J* = 8.1, 1.3 Hz, 1H), 3.37 (tt, *J* = 11.7, 3.4 Hz, 1H), 2.06 – 1.97 (m, 2H), 1.96 – 1.88 (m, 2H), 1.84 – 1.77 (m, 1H), 1.68 – 1.60 (m, 2H), 1.56 – 1.47 (m, 2H), 1.39 – 1.33 (m, 1H). **^{13}C NMR** (126 MHz, $CDCl_3$) δ 165.1, 155.5, 132.9, 130.5, 129.5, 129.0, 123.9, 115.1, 40.2, 30.5, 26.3, 26.1. **GC-MS** (EI, m/z) for $C_{14}H_{16}N_2O$ Calcd: 228.1, found: 228.2. Spectra data are consistent with the reported literature.[78]

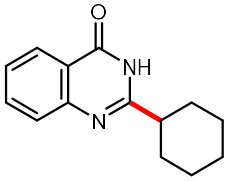

2-Cyclohexylquinazolin-4(3*H*)-one (43c). Following the general procedure A using 3.0 equiv alkyltrifluoroborate. Isolated with Hex:EtOAc (5:2) on preparative thin-layer chromatography. White solid (16.7 mg, 73%). **^{1}H NMR** (500 MHz, $CDCl_3$) δ 10.62 (br, 1H), 8.30 (dd, *J* = 7.9, 1.6 Hz, 1H), 7.83 – 7.76 (m, 1H), 7.72 (dd, *J* = 8.2, 1.4 Hz, 1H), 7.53 – 7.41 (m, 1H), 2.76 – 2.64 (m, 1H), 2.11 – 2.06 (m, 2H), 1.98 – 1.93 (m, 2H), 1.85 – 1.79 (m, 1H), 1.76 – 1.67 (m, 2H), 1.52 – 1.34 (m, 3H). **^{13}C NMR** (126 MHz, $CDCl_3$) δ 163.5, 159.7, 149.4, 134.7, 127.4, 126.3, 126.3, 120.9, 44.8, 30.6, 26.0, 25.7. **GC-MS** (EI, m/z) for $C_{14}H_{16}N_2O$ Calcd: 228.1, found: 228.2. Spectra data are consistent with the reported literature.[70]

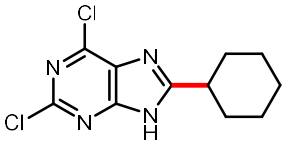

2,6-Dichloro-8-cyclohexyl-9*H*-purine (44c). Following the general procedure A using 3.0 equiv alkyltrifluoroborate and TFA. Isolated with Hex:EtOAc (2:1) on preparative thin-layer chromatography. White solid (17.4 mg, 64%). **^{1}H NMR** (500 MHz, $CDCl_3$) δ 11.48 (br,

1H), 3.16 – 3.04 (m, 1H), 2.24 – 2.14 (m, 2H), 2.00 – 1.91 (m, 2H), 1.87 – 1.71 (m, 3H), 1.53 – 1.41 (m, 2H), 1.41 – 1.32 (m, 1H). **^{13}C NMR** (126 MHz, $CDCl_3$) δ 163.1, 154.4, 151.3, 150.2, 131.2, 38.9, 31.3, 25.7, 25.4. **HRMS** (M+Na^+) for $C_{11}H_{12}Cl_2N_4Na$ Calcd: 293.0331, found: 293.0329. The compound was unreported.

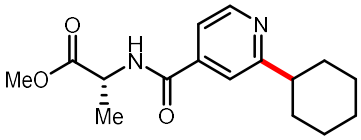

Methyl (2-cyclohexylisonicotinoyl)-*D*-alaninate (45c). Following the general procedure A using 3.0 equiv TFA. Isolated with Hex:EtOAc (5:2) on preparative thin-layer chromatography. Colorless oil (6.1 mg, 21%). **^{1}H NMR** (500 MHz, $CDCl_3$) δ 8.67 (d, *J* = 4.2 Hz, 1H), 7.57 – 7.48 (m, 1H), 7.43 (dd, *J* = 5.1, 1.7 Hz, 1H), 6.81 (br, 1H), 4.82 (quint, *J* = 7.1 Hz, 1H), 3.84 (s, 3H), 2.80 (tt, *J* = 12.0, 3.4 Hz, 1H), 2.03 – 1.94 (m, 2H), 1.93 – 1.85 (m, 2H), 1.81 – 1.75 (m, 1H), 1.63 – 1.52 (m, 5H), 1.51 – 1.38 (m, 2H), 1.38 – 1.29 (m, 1H). **^{13}C NMR** (126 MHz, $CDCl_3$) δ 173.4, 167.9, 165.4, 149.9, 141.4, 118.5, 118.1, 52.8, 48.6, 46.7, 32.8, 26.5, 26.0, 18.6. **GC-MS** (EI, m/z) for $C_{16}H_{22}N_2O_3$ Calcd: 290.2, found: 290.3. Spectra data are consistent with the reported literature.[76]

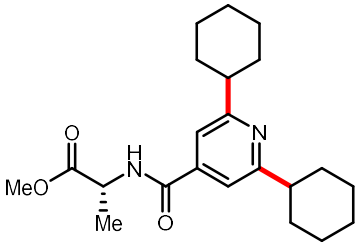

Methyl (2,6-dicyclohexylisonicotinoyl)-*D*-alaninate (45c'). Following the general procedure A using 3.0 equiv TFA. Isolated with Hex:EtOAc (5:2) on preparative thin-layer chromatography. White solid (7.1 mg, 19%). **^{1}H NMR** (500 MHz, $CDCl_3$) δ 7.28 (s, 2H), 6.77 (br, 1H), 4.82 (quint, *J* = 7.2 Hz, 1H), 3.83 (s, 3H), 2.76 (tt, *J* = 11.9, 3.4 Hz, 2H), 2.00 – 1.95 (m, 4H), 1.89 – 1.85 (m, 4H), 1.79 – 1.75 (m, 2H), 1.57 – 1.42 (m, 11H), 1.34 – 1.28 (m, 2H). **^{13}C NMR** (126 MHz, $CDCl_3$) δ 173.5, 166.9, 166.1, 141.8, 115.1, 52.7, 48.5, 46.7, 33.0, 26.5, 26.1, 18.6. **GC-MS** (EI, m/z) for $C_{22}H_{32}N_2O_3$ Calcd: 372.2, found: 372.4. Spectra data are consistent with the reported literature.[77]

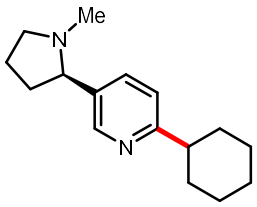

(*R*)-2-cyclohexyl-5-(1-methylpyrrolidin-2-yl)pyridine (46c). Following the general procedure A using 3.0 equiv alkyltrifluoroborate. Isolated with Hex:EtOAc:MeOH (2:1:0.5) on preparative thin-layer chromatography. Yellow oil (10.8 mg, 44%). **^{1}H NMR** (500 MHz, $CDCl_3$) δ 8.43 (d, *J* = 2.3 Hz, 1H), 7.64 (dd, *J* = 8.1, 2.3 Hz, 1H), 7.14 (d, *J* = 8.0 Hz, 1H), 3.30 – 3.22 (m, 1H), 3.07 (t, *J* = 8.3 Hz, 1H), 2.71 (tt, *J* = 12.0, 3.4 Hz, 1H), 2.31 (q, *J* = 9.2 Hz, 1H), 2.23 – 2.13 (m, 4H), 2.00 – 1.96 (m, 2H), 1.90 – 1.74 (m, 5H), 1.59 – 1.24 (m, 6H). **^{13}C NMR** (126 MHz, $CDCl_3$) δ 165.5, 148.8, 135.2, 120.9, 68.7, 57.0, 46.3, 40.4, 35.0, 33.0, 33.0, 26.6, 26.1, 22.5. **GC-MS** (EI, m/z) for $C_{16}H_{24}N_2$ Calcd: 244.2, found: 244.1. Spectra data are consistent with the reported literature.[77]

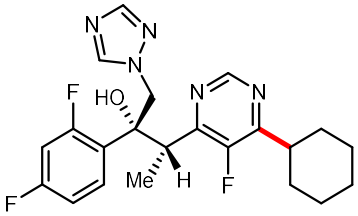

(2*R*,3*S*)-3-(6-cyclohexyl-5-fluoropyrimidin-4-yl)-2-(2,4-difluorophenyl)-1-(1*H*-1,2,4-triazol-1-yl)butan-2-ol (47c). Following the general procedure A using 3.0 equiv alkyltrifluoroborate and TFA. Isolated with Hex:EtOAc (1:1) on preparative thin-layer chromatography. Yellow oil (16.8 mg, 39%). **^{1}H NMR** (500 MHz, $CDCl_3$) δ 8.82 (d, *J* = 1.8 Hz, 1H), 7.99 (s, 1H), 7.66 – 7.58 (m, 1H), 7.54 (s, 1H), 6.89 – 6.80 (m, 2H), 6.77 (br, 1H), 4.72 (d, *J* = 14.5 Hz, 1H), 4.31 (d, *J* = 14.3 Hz, 1H), 4.13 (qd, *J* = 7.0, 1.3 Hz, 1H), 3.15 – 3.04 (m, 1H), 1.96 – 1.80 (m, 5H), 1.73 – 1.62 (m, 2H), 1.51 – 1.33 (m, 3H), 1.09 (d, *J* = 7.0 Hz, 3H). **^{13}C NMR** (126 MHz, $CDCl_3$) δ 163.8, 163.7, 163.0, 162.9, 161.8, 161.7, 159.6, 159.5, 157.8, 157.7, 157.6, 157.5, 154.4, 152.8, 152.7, 152.3, 150.8, 144.0, 130.7, 130.7, 130.7, 130.6, 123.7, 123.7, 123.6, 123.6, 111.6, 111.6, 111.5, 111.4, 104.3, 104.1, 104.0, 103.8, 57.6, 57.5, 39.2, 39.1, 36.4, 36.3, 30.7, 30.5, 26.1, 26.1, 26.1, 25.7, 16.2. **^{19}F NMR** (470 MHz, $CDCl_3$) δ -109.08 (q, *J* = 9.8 Hz, 1F), -110.52 (quint, *J* = 7.6 Hz, 1F), -139.55 (s, 1F). **HRMS** ($M+Na^+$) for $C_{22}H_{24}F_3N_5NaO$ Calcd: 454.1825, found: 454.1820. Spectra data are consistent with the reported literature.[71]

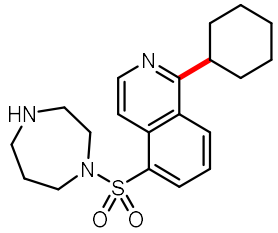

5-((1,4-Diazepan-1-yl)sulfonyl)-1-cyclohexylisoquinoline (48c). Following the general procedure A using 3.0 equiv alkyltrifluoroborate and TFA. Isolated with Hex:EtOAc:MeOH (1:1:2) on preparative thin-layer chromatography. White solid (24.3 mg, 65%). **^{1}H NMR** (500 MHz, $CDCl_3$) δ 8.64 (d, *J* = 6.1 Hz, 1H), 8.49 (d, *J* = 8.1 Hz, 1H), 8.33 (dd, *J* = 7.4, 1.1 Hz, 1H), 8.30 (dd, *J* = 6.1, 1.0 Hz, 1H), 7.68 – 7.64 (m, 1H), 3.62 – 3.55 (m, 1H), 3.55 – 3.39 (m, 4H), 3.02 – 2.91 (m, 4H), 2.04 – 1.93 (m, 4H), 1.90 – 1.82 (m, 5H), 1.72 (br, 1H), 1.60 – 1.51 (m, 2H), 1.46 – 1.37 (m, 1H). **^{13}C NMR** (126 MHz, $CDCl_3$) δ 166.6, 143.8, 135.3, 132.3, 132.2, 130.2, 126.9, 125.1, 115.5, 51.4, 50.4, 47.8, 47.5, 42.1, 32.7, 31.4, 26.8, 26.1. **GC-MS** (EI, m/z) for $C_{20}H_{27}N_3O_2S$ Calcd: 373.2, found: 373.3. Spectra data are consistent with the reported literature.[79]

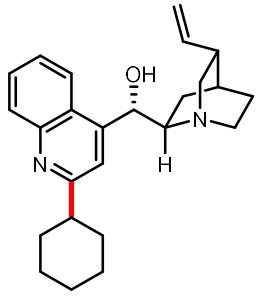

(*S*)-(2-cyclohexylquinolin-4-yl)((1*S*,2*S*,4*S*,5*R*)-5-vinylquinuclidin-2-yl)methanol (49c). Following the general procedure A. Isolated with Hex:EtOAc:MeOH (1:1:0.5) on preparative thin-layer chromatography. White solid (16.6 mg, 44%). **^{1}H NMR** (500 MHz, $CDCl_3$) δ 8.07 (d, *J* = 7.2 Hz, 1H), 7.88 (d, *J* = 7.9 Hz, 1H), 7.67 – 7.61 (m, 1H), 7.59 (s, 1H), 7.43 – 7.34 (m, 1H), 6.08 – 5.96 (m, 1H), 5.82 (br, 1H), 5.11 – 4.94 (m, 2H), 3.52 – 3.39 (m, 1H), 3.14 – 3.03 (m, 1H), 3.00 – 2.86 (m, 3H), 2.84 – 2.71 (m, 1H), 2.34 – 2.22 (m, 1H), 2.09 – 1.97 (m, 3H), 1.95 – 1.84 (m, 2H), 1.84 – 1.76 (m, 2H), 1.72 – 1.27 (m, 8H), 1.17 – 1.07 (m, 1H). ^{13}C NMR (126 MHz, $CDCl_3$) δ 166.5, 148.6, 147.9, 140.1, 129.9, 128.8, 125.7, 124.4, 122.6, 116.7, 114.9, 71.3, 60.0, 50.0, 49.5, 47.8, 39.9, 32.8, 32.8, 28.3, 26.5, 26.1, 20.6. **HRMS** ($M+H^+$) for $C_{25}H_{33}N_2O$ Calcd: 377.2587, found: 377.2589. The compound was

unreported.

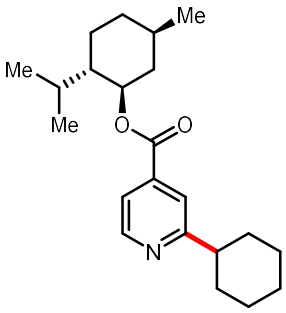

(1*R*,2*S*,5*R*)-2-isopropyl-5-methylcyclohexyl 2-cyclohexylisonicotinate (50c). Following the general procedure A using 3.0 equiv TFA. Isolated with Hex:EtOAc (10:1) on preparative thin-layer chromatography. Colorless oil (8.6 mg, 25%). **^{1}H NMR** (500 MHz, $CDCl_3$) δ 8.68 (dd, *J* = 5.0, 0.9 Hz, 1H), 7.72 (s, 1H), 7.66 (dd, *J* = 5.0, 1.6 Hz, 1H), 4.98 (td, *J* = 10.9, 4.4 Hz, 1H), 2.81 (tt, *J* = 11.9, 3.4 Hz, 1H), 2.18 – 2.09 (m, 1H), 2.03 – 1.86 (m, 5H), 1.84 – 1.72 (m, 3H), 1.65 – 1.54 (m, 5H), 1.51 – 1.39 (m, 2H), 1.38 – 1.27 (m, 1H), 1.22 – 1.09 (m, 2H), 0.95 (t, *J* = 6.6 Hz, 6H), 0.82 (d, *J* = 7.0 Hz, 3H). **^{13}C NMR** (126 MHz, $CDCl_3$) δ 167.7, 165.1, 149.8, 138.4, 120.4, 120.2, 75.7, 47.2, 46.6, 40.8, 34.2, 32.8, 32.8, 31.5, 26.6, 26.5, 26.0, 23.6, 22.0, 20.7, 16.5. **GC-MS** (EI, m/z) for $C_{22}H_{33}NO_2$ Calcd: 343.3, found: 343.4. Spectra data are consistent with the reported literature.[21]

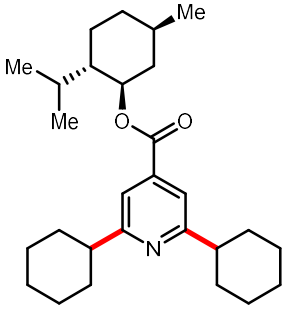

(1*R*,2*S*,5*R*)-2-isopropyl-5-methylcyclohexyl 2,6-dicyclohexylisonicotinate (50c'). Following the general procedure A using 3.0 equiv TFA. Isolated with Hex:EtOAc (10:1) on preparative thin-layer chromatography. White solid (10.6 mg, 25%). **^{1}H NMR** (500 MHz, $CDCl_3$) δ 7.51 (s, 2H), 4.98 (td, *J* = 10.9, 4.4 Hz, 1H), 2.77 (tt, *J* = 11.9, 3.4 Hz, 2H), 2.11 (d, *J* = 12.0 Hz, 1H), 2.03 – 1.83 (m, 9H), 1.81 – 1.71 (m, 4H), 1.63 – 1.52 (m, 6H), 1.50 – 1.40 (m, 4H), 1.37 – 1.27 (m, 2H), 1.22 – 1.11 (m, 2H), 0.98 – 0.90 (m, 7H), 0.82 (d, *J* = 7.0 Hz, 3H). **^{13}C NMR** (126 MHz, $CDCl_3$) δ 166.7, 165.6, 138.6, 117.2, 75.4, 47.1, 46.6, 40.9,

34.3, 32.9, 31.5, 26.6, 26.5, 26.1, 23.7, 22.0, 20.7, 16.6. **GC-MS** (EI, m/z) for $C_{28}H_{43}NO_2$ Calcd: 425.3, found: 425.1. Spectra data are consistent with the reported literature.[77]

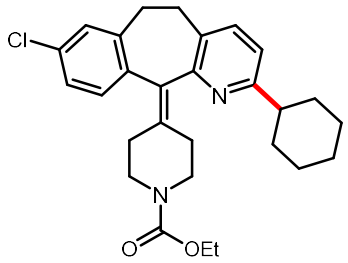

Ethyl 4-(8-chloro-2-cyclohexyl-5,6-dihydro-11*H*-benzo[5,6]cyclohepta[1,2-*b*]pyridin-11-ylidene)piperidine-1-carboxylate (51c). Following the general procedure A using 3.0 equiv alkyltrifluoroborate and TFA. Isolated with Hex:EtOAc (5:1) on preparative thin-layer chromatography. White solid (21.4 mg, 46%). **^{1}H NMR** (500 MHz, $CDCl_3$) δ 7.36 (d, *J* = 7.9 Hz, 1H), 7.21 – 7.14 (m, 3H), 6.98 (d, *J* = 7.9 Hz, 1H), 4.19 – 4.13 (m, 2H), 3.86 (br, 2H), 3.44 – 3.35 (m, 1H), 3.35 – 3.26 (m, 1H), 3.16 – 3.09 (m, 2H), 2.89 – 2.76 (m, 2H), 2.76 – 2.67 (m, 1H), 2.57 – 2.45 (m, 1H), 2.41 – 2.28 (m, 3H), 2.00 – 1.94 (m, 1H), 1.93 – 1.89 (m, 1H), 1.87 – 1.82 (m, 2H), 1.77 – 1.71 (m, 1H), 1.55 – 1.40 (m, 4H), 1.28 (t, *J* = 7.1 Hz, 4H). **^{13}C NMR** (126 MHz, $CDCl_3$) δ 163.6, 155.7, 155.5, 139.9, 138.2, 138.0, 137.3, 134.6, 132.7, 130.5, 130.2, 128.8, 126.0, 118.8, 61.3, 46.1, 44.9, 33.9, 32.4, 31.8, 31.4, 31.0, 30.6, 26.6, 26.4, 26.1, 14.7. **HRMS** ($M+Na^+$) for $C_{28}H_{33}ClN_2NaO_2$ Calcd: 487.2123, found: 487.2126. Spectra data are consistent with the reported literature.[80]

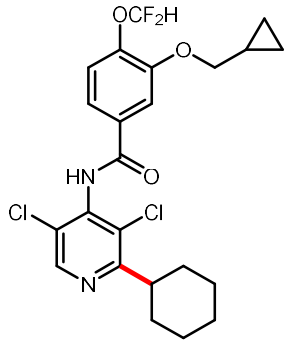

3-(Cyclopropylmethoxy)-*N*-(3,5-dichloro-2-cyclohexylpyridin-4-yl)-4-(difluoromethoxy)benzamide (52c). Following the general procedure A using 3.0 equiv alkyltrifluoroborate and TFA. Isolated with Hex:EtOAc:MeOH (1:1:0.5) on preparative thin-layer chromatography. White solid (27.7 mg, 57%). **^{1}H NMR** (500 MHz, $CDCl_3$) δ 8.54 (s, 1H), 7.69 (s, 1H), 7.61 (d, *J* = 2.0 Hz, 1H), 7.49 (dd, *J* = 8.3, 2.1 Hz, 1H), 7.30 (d, *J* = 8.3

Hz, 1H), 6.76 (t, *J* = 74.9 Hz, 1H), 3.98 (d, *J* = 6.9 Hz, 2H), 3.28 – 3.16 (m, 1H), 1.92 – 1.83 (m, 4H), 1.82 – 1.74 (m, 1H), 1.68 – 1.60 (m, 2H), 1.49 – 1.31 (m, 4H), 0.74 – 0.66 (m, 2H), 0.43 – 0.36 (m, 2H). **^{13}C NMR** (126 MHz, $CDCl_3$) δ 163.8, 162.6, 150.9, 147.1, 143.8, 139.3, 131.2, 127.2, 126.9, 126.3, 122.3, 119.8, 115.7 (t, *J* = 261 Hz), 114.2, 74.2, 42.4, 31.3, 26.4, 25.9, 10.0, 3.3. **^{19}F NMR** (470 MHz, $CDCl_3$) δ -82.03 (d, *J* = 74.6 Hz, 2F). **HRMS** ($M+Na^+$) for $C_{23}H_{24}Cl_2F_2N_2NaO_3$ Calcd: 507.1024, found: 507.1036. The compound was unreported.

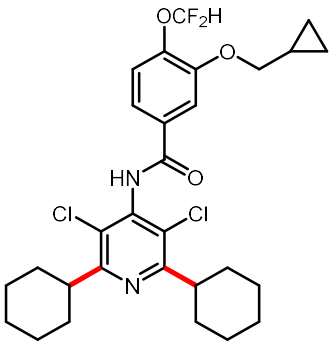

3-(Cyclopropylmethoxy)-*N*-(3,5-dichloro-2,6-dicyclohexylpyridin-4-yl)-4-(difluoromethoxy)benzamide (52c'). Following the general procedure A using 3.0 equiv alkyltrifluoroborate and TFA. Isolated with Hex:EtOAc:MeOH (1:1:0.5) on preparative thin-layer chromatography. White solid (16.4 mg, 29%). **^{1}H NMR** (500 MHz, $CDCl_3$) δ 7.62 (d, *J* = 2.1 Hz, 1H), 7.60 (s, 1H), 7.48 (dd, *J* = 8.3, 2.0 Hz, 1H), 7.30 (d, *J* = 8.2 Hz, 1H), 6.76 (t, *J* = 75.0 Hz, 1H), 3.99 (d, *J* = 7.0 Hz, 2H), 3.17 (tt, *J* = 11.4, 3.3 Hz, 2H), 1.92 – 1.81 (m, 8H), 1.80 – 1.75 (m, 2H), 1.70 – 1.62 (m, 4H), 1.50 – 1.29 (m, 7H), 0.72 – 0.66 (m, 2H), 0.42 – 0.37 (m, 2H). **^{13}C NMR** (126 MHz, $CDCl_3$) δ 164.0, 160.7, 150.9, 143.6, 138.6, 131.5, 124.4, 122.4, 119.7, 115.7 (t, *J* = 261 Hz), 114.2, 74.2, 42.4, 31.3, 26.4, 26.0, 10.0, 3.3. **^{19}F NMR** (470 MHz, $CDCl_3$) δ -82.00 (d, *J* = 75.8 Hz, 2F). **HRMS** ($M+Na^+$) for $C_{29}H_{34}Cl_2F_2N_2NaO_3$ Calcd: 589.1807, found: 589.1811. Spectra data are consistent with the reported literature.[71]

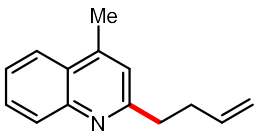

2-(But-3-en-1-yl)-4-methylquinoline (53c). Following the general procedure A using 3.0 equiv alkyltrifluoroborate and TFA. Isolated with Hex:EtOAc (10:1) on preparative thin-layer chromatography. Colorless oil (3.6 mg, 18%). **^{1}H NMR** (500 MHz, $CDCl_3$) δ 8.07

(d, *J* = 8.5 Hz, 1H), 7.98 (dd, *J* = 8.4, 1.8 Hz, 1H), 7.74 – 7.63 (m, 1H), 7.61 – 7.49 (m, 1H), 7.17 (s, 1H), 5.96 (ddt, *J* = 16.8, 10.2, 6.6 Hz, 1H), 5.12 (dd, *J* = 17.1, 1.8 Hz, 1H), 5.02 (dd, *J* = 10.1, 1.9 Hz, 1H), 3.07 – 3.02 (m, 2H), 2.71 (d, *J* = 1.1 Hz, 3H), 2.64 – 2.57 (m, 2H). **^{13}C NMR** (126 MHz, $CDCl_3$) δ 161.7, 147.8, 144.3, 137.8, 129.4, 129.1, 126.9, 125.5, 123.6, 122.1, 115.1, 38.5, 33.8, 18.7. **GC-MS** (EI, m/z) for $C_{14}H_{15}N$ Calcd: 197.1, found: 197.1. Spectra data are consistent with the reported literature.[80]

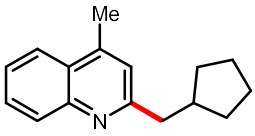

2-(Cyclopentylmethyl)-4-methylquinoline (54c). Following the general procedure A using 3.0 equiv alkyltrifluoroborate and TFA. Isolated with Hex:EtOAc (10:1) on preparative thin-layer chromatography. Colorless oil (3.2 mg, 14%). **^{1}H NMR** (500 MHz, $CDCl_3$) δ 8.07 (d, *J* = 8.4 Hz, 1H), 7.97 (dd, *J* = 8.4, 1.8 Hz, 1H), 7.72 – 7.67 (m, 1H), 7.54 – 7.49 (m, 1H), 7.16 (s, 1H), 2.95 (d, *J* = 7.5 Hz, 2H), 2.70 (d, *J* = 1.1 Hz, 3H), 2.47-2.33 (m, 1H), 1.81 – 1.65 (m, 4H), 1.62 – 1.50 (m, 2H), 1.37 – 1.25 (m, 2H). **^{13}C NMR** (126 MHz, $CDCl_3$) δ 162.3, 147.8, 143.9, 129.4, 129.0, 126.8, 125.4, 123.6, 122.5, 45.2, 40.8, 32.6, 25.0, 18.7. **GC-MS** (EI, m/z) for $C_{16}H_{19}N$ Calcd: 225.2, found: 225.2. Spectra data are consistent with the reported literature.[80]

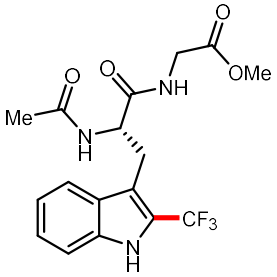

Methyl (*S*)-(2-acetamido-3-(2-(trifluoromethyl)-1*H*-indol-3-yl)propanoyl)glycinate (55c). Following the general procedure C. Isolated with DCM:MeOH (30:1) on preparative thin-layer chromatography. White solid (17.3 mg, 45%). **^{1}H NMR** (500 MHz, CD_3OD) δ 7.69 (d, *J* = 8.1 Hz, 1H), 7.43 (d, *J* = 7.3 Hz, 1H), 7.31 – 7.27 (m, 1H), 7.19 – 7.14 (m, 1H), 4.76 (t, *J* = 7.3 Hz, 1H), 3.89 – 3.74 (m, 2H), 3.59 (s, 3H), 3.48 – 3.42 (m, 1H), 3.36 – 3.30 (m, 1H), 1.97 (s, 3H). **^{13}C NMR** (126 MHz, CD_3OD) δ 172.3, 171.8, 169.9, 136.0, 127.1, 124.1, 122.4 (q, *J* = 256 Hz), 122.4 (q, *J* = 37 Hz), 120.0, 119.4, 111.8, 111.5 (q, *J* = 3 Hz), 53.4, 51.3, 41.9, 26.1, 21.0. **^{19}F NMR** (470 MHz, CD_3OD) δ -59.25

(s, 3F). **GC-MS** (EI, m/z) for $C_{17}H_{18}F_3N_3O_4$ Calcd: 385.1, found: 385.3. Spectra data are consistent with the reported literature.[81]

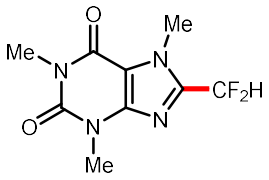

8-(Difluoromethyl)-1,3,7-trimethyl-3,7-dihydro-1*H*-purine-2,6-dione (56c). Following the general procedure C using 10 equiv TFA. Isolated with Hex:EtOAc (1:1) on preparative thin-layer chromatography. White solid (10.2 mg, 42%). **^{1}H NMR** (500 MHz, $CDCl_3$) δ 6.77 (t, *J* = 52.3 Hz, 1H), 4.18 (s, 3H), 3.60 (s, 3H), 3.44 (s, 3H). **^{13}C NMR** (126 MHz, $CDCl_3$) δ 155.6, 151.5, 146.9, 142.8 (t, *J* = 27 Hz), 109.8 (t, *J* = 238 Hz), 109.5, 32.9, 32.9, 29.8, 28.1. **^{19}F NMR** (470 MHz, $CDCl_3$) δ -114.97 (d, *J* = 52.3 Hz, 2F). **GC-MS** (EI, m/z) for $C_9H_{10}F_2N_4O_2$ Calcd: 244.1, found: 244.2. Spectra data are consistent with the reported literature.[82]

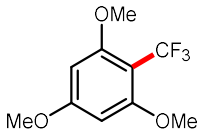

1,3,5-Trimethoxy-2-(trifluoromethyl)benzene (57cc). Following the general procedure D. Isolated with Hex:EtOAc (10:1) on preparative thin-layer chromatography. White solid (14.2 mg, 60%). **^{1}H NMR** (500 MHz, $CDCl_3$) δ 6.15 (s, 2H), 3.86 (s, 9H). **^{13}C NMR** (126 MHz, $CDCl_3$) δ 163.5, 160.4, 124.3 (q, *J* = 273 Hz), 100.4 (q, *J* = 30 Hz), 91.2, 56.3, 55.4. **^{19}F NMR** (470 MHz, $CDCl_3$) δ -54.15 (s, 3F). **GC-MS** (EI, m/z) for $C_{10}H_{11}F_3O_3$ Calcd: 236.1, found: 236.1. Spectra data are consistent with the reported literature.[81]

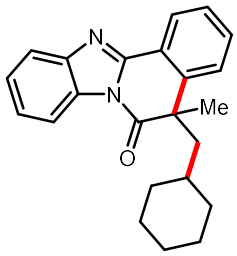

5-(Cyclohexylmethyl)-5-methylbenzo[4,5]imidazo[2,1-*a*]isoquinolin-6(5*H*)-one (58c). Following the general procedure I. Isolated with Hex:EtOAc (10:1) on preparative

thin-layer chromatography. White solid (23.4 mg, 68%). **^{1}H NMR** (500 MHz, $CDCl_3$) δ 8.54 – 8.48 (m, 1H), 8.43 – 8.38 (m, 1H), 7.88 – 7.80 (m, 1H), 7.62 – 7.57 (m, 1H), 7.52 – 7.42 (m, 4H), 2.51 (dd, *J* = 14.3, 8.0 Hz, 1H), 2.08 (dd, *J* = 14.3, 5.0 Hz, 1H), 1.69 (s, 3H), 1.51 – 1.36 (m, 3H), 1.32 – 1.26 (m, 1H), 1.22 – 1.15 (m, 1H), 1.07 – 0.92 (m, 3H), 0.88 – 0.74 (m, 3H). **^{13}C NMR** (126 MHz, $CDCl_3$) δ 173.5, 149.9, 144.1, 141.9, 131.6, 131.5, 127.6, 126.6, 126.0, 125.8, 125.5, 122.6, 119.7, 115.8, 48.8, 48.3, 34.9, 34.3, 32.9, 31.8, 26.0, 25.9, 25.9. **GC-MS** (EI, m/z) for $C_{23}H_{24}N_2O$ Calcd: 344.2, found: 344.3. Spectra data are consistent with the reported literature.[83]

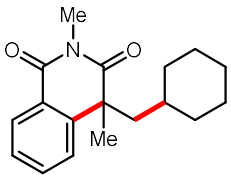

4-(Cyclohexylmethyl)-2,4-dimethylisoquinoline-1,3(2*H*,4*H*)-dione (59c). Following the general procedure J. Isolated with Hex:EtOAc (10:1) on preparative thin-layer chromatography. Colorless oil (16.8 mg, 59%). **^{1}H NMR** (500 MHz, $CDCl_3$) δ 8.28 (dd, *J* = 7.9, 1.6 Hz, 1H), 7.69 – 7.62 (m, 1H), 7.48 – 7.40 (m, 2H), 3.41 (s, 3H), 2.35 (dd, *J* = 14.1, 7.4 Hz, 1H), 1.92 (dd, *J* = 14.0, 4.7 Hz, 1H), 1.59 (s, 3H), 1.55 – 1.43 (m, 3H), 1.31 – 1.26 (m, 1H), 1.21 – 1.13 (m, 1H), 1.03 – 0.74 (m, 6H). **^{13}C NMR** (126 MHz, $CDCl_3$) δ 176.9, 164.6, 143.9, 133.8, 128.9, 127.2, 125.8, 124.6, 49.6, 46.7, 34.9, 34.3, 33.0, 31.7, 27.2, 26.0, 26.0, 26.0. **GC-MS** (EI, m/z) for $C_{18}H_{23}N_2O$ Calcd: 285.2, found: 285.2. Spectra data are consistent with the reported literature.[84]

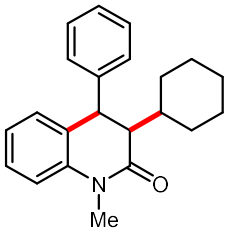

***Trans*-3-cyclohexyl-1-methyl-4-phenyl-3,4-dihydroquinolin-2(1*H*)-one (60c).** Following the general procedure K. Isolated with Hex:EtOAc (5:1) on preparative thin-layer chromatography. Colorless oil (15.6 mg, 49%). **^{1}H NMR** (500 MHz, $CDCl_3$) δ 7.38 – 7.32 (m, 1H), 7.26 – 7.14 (m, 4H), 7.11 – 7.05 (m, 2H), 7.00 – 6.96 (m, 2H), 4.23 (s, 1H), 3.28 (s, 3H), 2.70 (dd, *J* = 8.8, 1.8 Hz, 1H), 1.99 – 1.90 (m, 1H), 1.78 – 1.67 (m, 2H), 1.65 –

1.56 (m, 2H), 1.44 – 1.35 (m, 1H), 1.33 – 1.21 (m, 1H), 1.21 – 1.04 (m, 4H). **^{13}C NMR** (126 MHz, $CDCl_3$) δ 170.5, 142.4, 140.1, 129.6, 128.7, 128.0, 127.1, 126.7, 126.7, 123.2, 114.8, 55.6, 44.5, 37.8, 31.4, 31.1, 29.5, 26.2, 26.2, 26.0. **GC-MS** (EI, m/z) for $C_{22}H_{25}NO$ Calcd: 319.2, found: 319.2. data are consistent with the reported literature.[85]

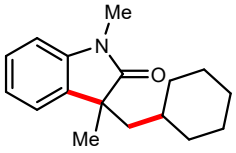

3-(Cyclohexylmethyl)-1,3-dimethylindolin-2-one (61c). Following the general procedure L. Isolated with Hex:EtOAc (5:1) on preparative thin-layer chromatography. White solid (13.9 mg, 54%). **^{1}H NMR** (500 MHz, $CDCl_3$) δ 7.30 – 7.27 (m, 1H), 7.19 – 7.17 (m, 1H), 7.10 – 7.06 (m, 1H), 6.86 (d, *J* = 7.8 Hz, 1H), 3.24 (s, 3H), 1.95 (dd, *J* = 14.1, 6.9 Hz, 1H), 1.75 (dd, *J* = 14.0, 5.3 Hz, 1H), 1.56 – 1.47 (m, 3H), 1.38 – 1.32 (m, 4H), 1.24 – 1.19 (m, 1H), 1.03 – 0.92 (m, 4H), 0.88 – 0.75 (m, 2H). **^{13}C NMR** (126 MHz, $CDCl_3$) δ 181.2, 143.1, 134.4, 127.5, 122.7, 122.3, 108.0, 47.9, 45.4, 34.7, 34.5, 33.5, 26.2, 26.2, 26.1, 26.0 (*One aliphatic carbon was missing due to overlap*). **GC-MS** (EI, m/z) for $C_{17}H_{23}NO$ Calcd: 257.2, found: 257.3. Spectra data are consistent with the reported literature.[21]

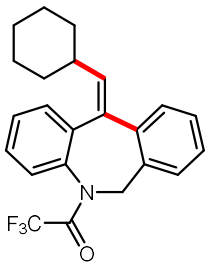

(*Z*)-1-(11-(cyclohexylmethylene)-6,11-dihydro-5*H*-dibenzo[*b*,*e*]azepin-5-yl)-2,2,2-trifluoroethan-1-one (62c). Following the general procedure M. Isolated with Hex:EtOAc (10:1) on preparative thin-layer chromatography. Pale yellow oil (NMR yield: 48%, pure spectra could not be obtained due to irremovable impurity). **^{1}H NMR** (500 MHz, $CDCl_3$) δ 7.46 – 7.34 (m, 4H), 7.33 – 7.29 (m, 1H), 7.27 – 7.21 (m, 2H), 7.11 – 7.06 (m, 1H), 5.92 (d, *J* = 16.6 Hz, 1H), 5.88 (d, *J* = 10.5 Hz, 1H), 4.35 (d, *J* = 16.8 Hz, 1H), 2.09 – 1.98 (m, 1H), 1.87 – 1.75 (m, 2H), 1.70 – 1.61 (m, 2H), 1.39 – 1.08 (m, 6H). **^{19}F NMR** (470 MHz, $CDCl_3$) δ -67.72 (s, 3F). **HRMS** ($M+Na^+$) for $C_{23}H_{22}F_3NNaO$ Calcd: 408.1546, found: 408.1550. The compound was unreported.

4.10 References

1. J. Li, C.-Y. Huang, J.-T. Han & C.-J. Li. Development of a Quinolinium/Cobaloxime Dual Photocatalytic System for Oxidative C-C Cross-Couplings via H_2 Release. *ACS Catal.* **2021**, *11*, 14148-14158.

2. W. Liu, J. Li, C.-Y. Huang & C.-J. Li. Aromatic Chemistry in the Excited State: Facilitating Metal-Free Substitutions and Cross-Couplings. *Angew. Chem. Int. Ed.* **2020**, *59*, 1786-1796.

3. J. M. R. Narayanam & C. R. J. Stephenson. Visible Light Photoredox Catalysis: Applications in Organic Synthesis. *Chem. Soc. Rev.* **2011**, *40*, 102-113.

4. C. K. Prier, D. A. Rankic & D. W. C. MacMillan. Visible Light Photoredox Catalysis with Transition Metal Complexes: Applications in Organic Synthesis. *Chem. Rev.* **2013**, *113*, 5322-5363.

5. D. M. Schultz & T. P. Yoon. Solar Synthesis: Prospects in Visible Light Photocatalysis. *Science* **2014**, *343*, 1239176.

6. M. H. Shaw, J. Twilton & D. W. C. MacMillan. Photoredox Catalysis in Organic Chemistry. *J. Org. Chem.* **2016**, *81*, 6898-6926.

7. K. L. Skubi, T. R. Blum & T. P. Yoon. Dual Catalysis Strategies in Photochemical Synthesis. *Chem. Rev.* **2016**, *116*, 10035-10074.

8. J. Twilton *et al.* The Merger of Transition Metal and Photocatalysis. *Nat. Rev. Chem.* **2017**, *1*, 1-19.

9. G. E. M. Crisenza, D. Mazzarella & P. Melchiorre. Synthetic Methods Driven by the Photoactivity of Electron Donor-Acceptor Complexes. *J. Am. Chem. Soc.* **2020**, *142*, 5461-5476.

10. M. N. Hopkinson, A. Tlahuext-Aca & F. Glorius. Merging Visible Light Photoredox and Gold Catalysis. *Acc. Chem. Res.* **2016**, *49*, 2261-2272.

11. K. A. Margrey & D. A. Nicewicz. A General Approach to Catalytic Alkene Anti-Markovnikov Hydrofunctionalization Reactions via Acridinium Photoredox Catalysis. *Acc. Chem. Res.* **2016**, *49*, 1997-2006.

12. J. K. Matsui, S. B. Lang, D. R. Heitz & G. A. Molander. Photoredox-Mediated Routes to Radicals: The Value of Catalytic Radical Generation in Synthetic Methods Development. *ACS Catal.* **2017**, *7*, 2563-2575.

13. D. A. Nicewicz & T. M. Nguyen. Recent Applications of Organic Dyes as Photoredox Catalysts in Organic Synthesis. *ACS Catal.* **2014**, *4*, 355-360.

14. N. A. Romero & D. A. Nicewicz. Organic Photoredox Catalysis. *Chem. Rev.* **2016**, *116*, 10075-10166.

15. D. Staveness, I. Bosque & C. R. J. Stephenson. Free Radical Chemistry Enabled by Visible Light-Induced Electron Transfer. *Acc. Chem. Res.* **2016**, *49*, 2295-2306.

16. J. C. Tellis *et al.* Single-Electron Transmetalation via Photoredox/Nickel Dual Catalysis: Unlocking a New Paradigm for sp^3-sp^2 Cross-Coupling. *Acc. Chem. Res.* **2016**, *49*, 1429-1439.

17. J. Xuan & W.-J. Xiao. Visible-Light Photoredox Catalysis. *Angew. Chem. Int. Ed.* **2012**, *51*, 6828-6838.

18. A. Joshi-Pangu *et al.* Acridinium-Based Photocatalysts: A Sustainable Option in Photoredox Catalysis. *J. Org. Chem.* **2016**, *81*, 7244-7249.

19. L. K. G. Ackerman, J. I. Martinez Alvarado & A. G. Doyle. Direct C-C Bond Formation from Alkanes Using Ni-Photoredox Catalysis. *J. Am. Chem. Soc.* **2018**, *140*, 14059-14063.

20. X. Cai, M. Sakamoto, M. Fujitsuka & T. Majima. One-Electron Oxidation of Alcohols by the 1,3,5-Trimethoxybenzene Radical Cation in the Excited State During Two-Color Two-Laser Flash Photolysis. *J. Phys. Chem. A* **2007**, *111*, 1788-1791.

21. C.-Y. Huang, J. Li & C.-J. Li. A Cross-Dehydrogenative C(sp^3)-H Heteroarylation via Photo-Induced Catalytic Chlorine Radical Generation. *Nat. Commun.* **2021**, *12*, 4010-4018.

22. W. Liu, X. Yang, Z.-Z. Zhou & C.-J. Li. Simple and Clean Photo-Induced Methylation of Heteroarenes with MeOH. *Chem* **2017**, *2*, 688-702.

23. A. O. Adeloye & M. J. Mphahlele. 2,4-Diarylquinolines: Synthesis, Absorption and Emission Properties. *J. Chem. Res.* **2014**, *38*, 254-259.

24. M. El Khatib, R. A. M. Serafim & G. A. Molander. α-Arylation/Heteroarylation of Chiral α-Aminomethyltrifluoroborates by Synergistic Iridium Photoredox/Nickel Cross-Coupling Catalysis. *Angew. Chem. Int. Ed.* **2016**, *55*, 254-258.

25. J. K. Matsui & G. A. Molander. Organocatalyzed, Photoredox Heteroarylation of 2-Trifluoroboratochromanones via C-H Functionalization. *Org. Lett.* **2017**, *19*, 950-953.

26. J. K. Matsui, D. N. Primer & G. A. Molander. Metal-Free C-H Alkylation of Heteroarenes with Alkyltrifluoroborates: A General Protocol for 1°, 2° and 3° Alkylation. *Chem. Sci.* **2017**, *8*, 3512-3522.

27. G. A. Molander, V. Colombel & V. A. Braz. Direct Alkylation of Heteroaryls Using Potassium Alkyl- and Alkoxymethyltrifluoroborates. *Org. Lett.* **2011**, *13*, 1852-1855.

28. G. A. Molander & N. Ellis. Organotrifluoroborates: Protected Boronic Acids That Expand the Versatility of the Suzuki Coupling Reaction. *Acc. Chem. Res.* **2007**, *40*, 275-286.
29. M. Presset *et al.* Synthesis and Minisci Reactions of Organotrifluoroborato Building Blocks. *J. Org. Chem.* **2013**, *78*, 4615-4619.
30. D. N. Primer, I. Karakaya, J. C. Tellis & G. A. Molander. Single-Electron Transmetalation: An Enabling Technology for Secondary Alkylboron Cross-Coupling. *J. Am. Chem. Soc.* **2015**, *137*, 2195-2198.
31. D. N. Primer & G. A. Molander. Enabling the Cross-Coupling of Tertiary Organoboron Nucleophiles through Radical-Mediated Alkyl Transfer. *J. Am. Chem. Soc.* **2017**, *139*, 9847-9850.
32. J. C. Tellis, D. N. Primer & G. A. Molander. Single-Electron Transmetalation in Organoboron Cross-Coupling by Photoredox/Nickel Dual Catalysis. *Science* **2014**, *345*, 433-436.
33. Y. Yamashita, J. C. Tellis & G. A. Molander. Protecting Group-Free, Selective Cross-Coupling of Alkyltrifluoroborates with Borylated Aryl Bromides via Photoredox/Nickel Dual Catalysis. *Proc. Natl. Acad. Sci. U.S.A.* **2015**, *112*, 12026-12029.
34. W. Liu, J. Li, P. Querard & C.-J. Li. Transition-Metal-Free C-C, C-O, and C-N Cross-Couplings Enabled by Light. *J. Am. Chem. Soc.* **2019**, *141*, 6755-6764.
35. W. Liu, P. Liu, L. Lv & C.-J. Li. Metal-Free and Redox-Neutral Conversion of Organotrifluoroborates into Radicals Enabled by Visible Light. *Angew. Chem. Int. Ed.* **2018**, *57*, 13499-13503.
36. P. S. Mariano. Electron-Transfer Mechanisms in Photochemical Transformations of Iminium Salts. *Acc. Chem. Res.* **1983**, *16*, 130-137.
37. T. McCallum *et al.* The Photochemical Alkylation and Reduction of Heteroarenes. *Chem. Sci.* **2017**, *8*, 7412-7418.
38. J. J. Devery Iii *et al.* Ligand Functionalization as a Deactivation Pathway in a *fac*-$Ir(ppy)_3$-Mediated Radical Addition. *Chem. Sci.* **2015**, *6*, 537-541.
39. N. A. Romero, K. A. Margrey, N. E. Tay & D. A. Nicewicz. Site-Selective Arene C-H Amination via Photoredox Catalysis. *Science* **2015**, *349*, 1326-1330.
40. L. Buzzetti, G. E. M. Crisenza & P. Melchiorre. Mechanistic Studies in Photocatalysis. *Angew. Chem. Int. Ed.* **2019**, *58*, 3730-3747.
41. B. Bieszczad, L. A. Perego & P. Melchiorre. Photochemical C-H Hydroxyalkylation of Quinolines and Isoquinolines. *Angew. Chem. Int. Ed.* **2019**, *58*, 16878-16883.

42. F. Le Vaillant *et al.* Fine-Tuned Organic Photoredox Catalysts for Fragmentation-Alkynylation Cascades of Cyclic Oxime Ethers. *Chem. Sci.* **2018**, *9*, 5883-5889.

43. L. Zhang & L. Jiao. Visible-Light-Induced Organocatalytic Borylation of Aryl Chlorides. *J. Am. Chem. Soc.* **2019**, *141*, 9124-9128.

44. N. A. Romero & D. A. Nicewicz. Organic Photoredox Catalysis. *Chem. Rev.* **2016**, *116*, 10075–10166.

45. N. A. Romero & D. A. Nicewicz. Mechanistic Insight into the Photoredox Catalysis of Anti-Markovnikov Alkene Hydrofunctionalization Reactions. *J. Am. Chem. Soc.* **2014**, *136*, 17024-17035.

46. Y. H. Hong, Y.-M. Lee, W. Nam & S. Fukuzumi. Photocatalytic Hydrogen Evolution from Plastoquinol Analogues as a Potential Functional Model of Photosystem I. *Inorg. Chem.* **2020**, *59*, 14838-14846.

47. Á. Gutiérrez-Bonet, C. Remeur, J. K. Matsui & G. A. Molander. Late-Stage C-H Alkylation of Heterocycles and 1,4-Quinones via Oxidative Homolysis of 1,4-Dihydropyridines. *J. Am. Chem. Soc.* **2017**, *139*, 12251-12258.

48. T. Brückl, R. D. Baxter, Y. Ishihara & P. S. Baran. Innate and Guided C-H Functionalization Logic. *Acc. Chem. Res.* **2012**, *45*, 826-839.

49. Y. Fujiwara *et al.* Practical and Innate Carbon-Hydrogen Functionalization of Heterocycles. *Nature* **2012**, *492*, 95-99.

50. Y. Fujiwara *et al.* A New Reagent for Direct Difluoromethylation. *J. Am. Chem. Soc.* **2012**, *134*, 1494-1497.

51. R. Gianatassio *et al.* Simple Sulfinate Synthesis Enables C-H Trifluoromethylcyclopropanation. *Angew. Chem. Int. Ed.* **2014**, *53*, 9851-9855.

52. Y. Ji *et al.* Innate C-H Trifluoromethylation of Heterocycles. *Proc. Natl. Acad. Sci. U.S.A.* **2011**, *108*, 14411-14415.

53. B. R. Langlois, E. Laurent & N. Roidot. Trifluoromethylation of Aromatic Compounds with Sodium Trifluoromethanesulfinate under Oxidative Conditions. *Tetrahedron Lett.* **1991**, *32*, 7525-7528.

54. L. Li *et al.* Simple and Clean Photoinduced Aromatic Trifluoromethylation Reaction. *J. Am. Chem. Soc.* **2016**, *138*, 5809-5812.

55. P. Liu, W. Liu & C.-J. Li. Catalyst-Free and Redox-Neutral Innate Trifluoromethylation and Alkylation of Aromatics Enabled by Light. *J. Am. Chem. Soc.* **2017**, *139*, 14315-14321.

56. A. G. O'Brien *et al.* Radical C-H Functionalization of Heteroarenes under Electrochemical Control. *Angew. Chem. Int. Ed.* **2014**, *53*, 11868-11871.
57. Y. Qiu, A. Scheremetjew, L. H. Finger & L. Ackermann. Electrophotocatalytic Undirected C-H Trifluoromethylations of (Het)arenes. *Chem. Eur. J.* **2020**, *26*, 3241-3246.
58. Q. Zhou *et al.* Direct Synthesis of Fluorinated Heteroarylether Bioisosteres. *Angew. Chem. Int. Ed.* **2013**, *52*, 3949-3952.
59. J. Lin *et al.* Photo-Driven Redox-Neutral Decarboxylative Carbon-Hydrogen Trifluoromethylation of (Hetero)arenes with Trifluoroacetic Acid. *Nat. Commun.* **2017**, *8*, 14353-14359.
60. P. Xiong, H. H. Xu, J. Song & H. C. Xu. Electrochemical Difluoromethylarylation of Alkynes. *J. Am. Chem. Soc.* **2018**, *140*, 2460-2464.
61. T. Uchikura *et al.* Benzothiazolines as Radical Transfer Reagents: Hydroalkylation and Hydroacylation of Alkenes by Radical Generation under Photoirradiation Conditions. *Chem. Commun.* **2019**, *55*, 11171-11174.
62. B. Wu, J. Wang, X. Liu & R. Zhu. Bicyclo[2.2.0]hexene Derivatives as a Proaromatic Platform for Group Transfer and Chemical Sensing. *Nat. Commun.* **2021**, *12*, 3680-3687.
63. C. R. Jamison & L. E. Overman. Fragment Coupling with Tertiary Radicals Generated by Visible-Light Photocatalysis. *Acc. Chem. Res.* **2016**, *49*, 1578-1586.
64. C. C. Nawrat *et al.* Oxalates as Activating Groups for Alcohols in Visible Light Photoredox Catalysis: Formation of Quaternary Centers by Redox-Neutral Fragment Coupling. *J. Am. Chem. Soc.* **2015**, *137*, 11270-11273.
65. J. Yang *et al.* Acid-Promoted Iron-Catalysed Dehydrogenative [4 + 2] Cycloaddition for the Synthesis of Quinolines under Air. *Rsc Adv* **2018**, *8*, 31603-31607.
66. J. Ma *et al.* Direct Dearomatization of Pyridines via an Energy-Transfer-Catalyzed Intramolecular [4+2] Cycloaddition. *Chem* **2019**, *5*, 2854-2864.
67. R. Martínez, D. J. Ramón & M. Yus. $RuCl_2(DMSO)_4$ Catalyzes the Solvent-Free Indirect Friedländer Synthesis of Polysubstituted Quinolines from Alcohols. *Eur. J. Org. Chem.* **2007**, *2007*, 1599-1605.
68. F. Jin *et al.* TMSBr-Promoted Cascade Cyclization of *ortho*-Propynol Phenyl Azides for the Synthesis of 4-Bromo Quinolines and Its Applications. *Molecules* **2019**, *24*, 3999-4013.
69. G. A. Molander, V. Colombel & V. A. Braz. Direct Alkylation of Heteroaryls Using Potassium Alkyl- and Alkoxymethyltrifluoroborates. *Org. Lett.* **2011**, *13*, 1852-1855.

70. L. Zhang & Z.-Q. Liu. Molecular Oxygen-Mediated Minisci-Type Radical Alkylation of Heteroarenes with Boronic Acids. *Org. Lett.* **2017**, *19*, 6594-6597.

71. H. Zhao, Z. Li & J. Jin. Green Oxidant H_2O_2 as a Hydrogen Atom Transfer Reagent for Visible Light-Mediated Minisci Reaction. *New J. Chem.* **2019**, *43*, 12533-12537.

72. H. Zhao & J. Jin. Visible Light-Promoted Aliphatic C-H Arylation Using Selectfluor as a Hydrogen Atom Transfer Reagent. *Org. Lett.* **2019**, *21*, 6179-6184.

73. M. Presset *et al.* Synthesis and Minisci Reactions of Organotrifluoroborato Building Blocks. *J. Org. Chem.* **2013**, *78*, 4615-4619.

74. J. K. Matsui & G. A. Molander. Organocatalyzed, Photoredox Heteroarylation of 2-Trifluoroboratochromanones via C-H Functionalization. *Org. Lett.* **2017**, *19*, 950-953.

75. J. Dong *et al.* Visible-Light-Mediated Photoredox Minisci C-H Alkylation with Alkyl Boronic Acids Using Molecular Oxygen as an Oxidant. *Chem. Commun.* **2020**, *56*, 12652-12655.

76. W. Zhang *et al.* Redox-Active Benzimidazolium Sulfonamides as Cationic Thiolating Reagents for Reductive Cross-Coupling of Organic Halides. *Chem. Sci.* **2020**, *12*, 2509-2514.

77. C.-Y. Huang, J. Li, W. Liu & C.-J. Li. Diacetyl as a "Traceless" Visible Light Photosensitizer in Metal-Free Cross-Dehydrogenative Coupling Reactions. *Chem. Sci.* **2019**, *10*, 5018-5024.

78. Y. Gao *et al.* Alkyl Carbazates for Electrochemical Deoxygenative Functionalization of Heteroarenes. *Angew. Chem. Int. Ed.* **2020**, *59*, 10859-10863.

79. H. Tian *et al.* Cross-Dehydrogenative Coupling of Strong C(sp^3)-H with *N*-Heteroarenes through Visible-Light-Induced Energy Transfer. *Org. Lett.* **2020**, *22*, 7709-7715.

80. J. Dong *et al.* Visible-Light-Mediated Minisci C-H Alkylation of Heteroarenes with Unactivated Alkyl Halides Using O_2 as an Oxidant. *Chem. Sci.* **2019**, *10*, 976-982.

81. P. Liu, W. Liu & C.-J. Li. Catalyst-Free and Redox-Neutral Innate Trifluoromethylation and Alkylation of Aromatics Enabled by Light. *J. Am. Chem. Soc.* **2017**, *139*, 14315-14321.

82. V. Bacauanu *et al.* Metallaphotoredox Difluoromethylation of Aryl Bromides. *Angew. Chem. Int. Ed.* **2018**, *57*, 12543-12548.

83. Y. Yuan *et al.* Mn-Catalyzed Electrochemical Radical Cascade Cyclization toward the Synthesis of Benzo[4,5]imidazo[2,1-α]isoquinolin-6(5*H*)-one Derivatives. *ACS Catal.* **2020**, *10*, 6676-6681.

84. P. Qian *et al.* Cascade Alkylarylation of Substituted *N*-Allylbenzamides for the Construction of Dihydroisoquinolin-1(2*H*)-ones and Isoquinoline-1,3(2*H*,4*H*)-diones. *Beilstein J. Org. Chem.* **2016**, *12*, 301-308.

85. R.-X. Gao *et al.* Fe-Catalyzed Decarbonylative Cascade Reaction of *N*-Aryl Cinnamamides with Aliphatic Aldehydes to Construct 3,4-Dihydroquinolin-2(1*H*)-ones. *Org. Biomol. Chem.* **2019**, *17*, 5262-5268.

Chapter 5 Future perspective for the methodologies developed in this thesis

In chapter 2, diacetyl was explored as a photosensitizable HAT agent for ethereal C(sp^3)-H bonds activation, which also served as a terminal oxidant for cross-dehydrogenative Minisci alkylation under visible light irradiation. While it is considered a clean and simple protocol, there is still room for improvement, and it also shows some interesting research directions.

(1) Large excess of diacetyl and C(sp^3)-H substrates were required, making the protocol less attractive. The main issue was the inefficient activation toward strong C(sp^3)-H bonds, in which a stronger oxidant would sometimes be required to mediate the HAT process. Other than diacetyl, there are other ketone candidates with visible light absorption, longer triplet state lifetime, and stronger HAT ability; balancing these properties and finding a suitable ketone could be a great advancement of the current protocol.

(2) A stoichiometric amount of ketone was required in the protocol due to the net oxidative process. If a green and sustainable oxidant (i.e., molecular oxygen) or electrochemistry could be introduced for efficient ketone turnover, the reaction becomes catalytic. However, in the case of diacetyl, oxygen deteriorated the reaction, presumably due to side reactions with labile photoexcited diacetyl; therefore, seeking a more stable ketone catalyst would be the priority.

(3) Our lab has developed three types of diacetyl photochemistry, and all of them were transition metal-free. It would be promising if future endeavors could merge diacetyl into metallaphotoredox catalysis as a traceless reagent, such as a HAT agent for transition metal-catalyzed ether/aryl halide coupling.

In chapter 3, a chemical oxidant-free photoinduced cross-dehydrogenative Minisci alkylation was developed with catalytic chloride and cobaloxime, in which chlorine radical served as a strong HAT agent through SET between the photoexcited heteroarene and chloride. There are some thoughts regarding this challenging and novel protocol.

(1) The protocol required >280 nm light source to activate various heteroarenes and was not friendly to ultraviolet light-sensitive substrates. In this regard, our preliminary attempt conceived visible light-induced chloride oxidation with a quinoline-based photocatalyst. Although the current quinoline-catalyzed protocol still shows lower chloride-to-chlorine radical efficiency, a more powerful photocatalyst for this awarding transformation is worth exploring.

(2) In this CDC protocol, bromide salt failed to activate inert alkanes due to its low HAT ability. However, it might be useful in generating bromine radical for regioselective activation of benzylic, ethereal, and amido C(sp^3)-H bonds under milder reaction conditions.

(3) Besides CDC, using halide salt for halogenation is also intriguing. Other Minisci-type reactions such as halide-alkene-heteroarene coupling would be an interesting route to afford synthetically valuable halogenalkylated heteroarenes under a similar mechanistic scenario.

In chapter 4, a quinolinium photoredox catalyst has been explored for oxidative coupling between alkyl trifluoroborates and heteroarenes. As an advanced protocol to the previous work, it has solved two major concerns, high-energy photon requirement and regioselective problem. We also have some thoughts on the current protocol.

(1) While protonation was a feature in our photocatalyst activation mode, it implied the necessity of acidic reaction conditions, limiting its applications to acid-sensitive reactions. More protocols would be extended once the basic DPQN is modified to have similar redox potential under visible light excitation.

(2) The catalytic efficiency of polymer-supported DPQN dropped after each recycling due to the catalyst depletion from the amide linker under acidic conditions. Immobilizing DPQN on other materials or switching to other linkers might extend the heterogeneous catalyst's lifetime.

Chapter 6 Conrtibutions to fundamental knowledge

Merging photochemistry with organic synthesis is a trend in modern chemistry. Following our laboratory's endeavor in sustainable chemistry, in this thesis, we aimed to advance photoinduced alkyl radical generations with accessible precursors such as alkanes and trifluoroborate salts. Furthermore, to evaluate the applicability of our alkyl radical generation methods, Minisci alkylation was employed for practical heteroarene functionalizations under oxidative environments.

Chapter 2 employed diacetyl as a novel HAT agent to couple ethereal C(sp^3)-H bonds and heteroaryl C(sp^2)-H under visible light irradiation. As a non-hazardous and accessible reagent, diacetyl could be removed simply by aqueous workup during product isolation, so as its byproducts.

Using ketone for photoinduced CDC reactions was unprecedented. We were optimistic that this work would inspire future endeavors on ketone photochemistry and its applications in oxidative couplings and metal-free reactions.

In chapter 3, chlorine radical was generated in situ from chloride anion for C(sp^3)-H abstraction under ultraviolet light irradiation, in which the formed alkyl radical was used for cross-dehydrogenative Minisci alkylation. A cobalt catalyst was used for hydrogen evolution; therefore, the protocol did not require a chemical oxidant.

Using chlorine radical as a potent and sustainable oxy radical surrogate has received attention from synthetic chemists, yet, this transformation and the following applications in organic chemistry were rarely documented. In this work, we have demonstrated that various photoexcited heteroarenes could efficiently oxidize chloride, which bypassed the developed Iridium polypyridine-enabled SET and LMCT, or photoelectrochemistry. Furthermore, the 2,4-diphenylquinoline was shown to catalytically oxidize chloride under visible light excitation, which shed light on organophotocatalyzed chlorine radical generation. Notably, this work demonstrated that cobaloxime catalyst is compatible with not only arenes but also heteroarenes in acceptorless CDC reactions.

Next, chapter 4 explored a quinolinium photoredox catalyst for oxidative coupling between alkyl trifluoroborates and heteroarenes. An extensive study of the photocatalyst showed that 2,4-bis(4-methoxyphenyl)quinoline is visible light-excitable upon protonation, which has a comparable redox window with well-developed iridium and

acridinium photoredox catalysts.

The protocol could be conducted under visible light irradiation; therefore, the functional group tolerance was improved. Of equal importance, this SET-induced alkyl radical generation allowed efficient and regioselective alkyl radical formation. As extensions, we also showcased the Minisci alkylation with other alkyl radical sources and demonstrated the potential application of this dual catalytic system in different oxidative coupling settings and heterogeneous photocatalysis.

Undoubtablely, these protocols have provided some instructions for future endeavors of photochemistry, oxidative coupling, and many other relevant transformations in a sustainable way.

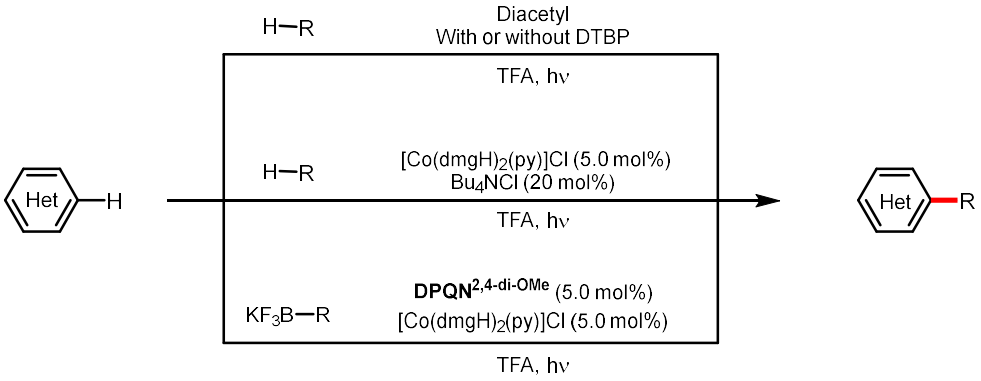

Appendix

Appendix 1: NMR spectra for new compounds in chapter 2

^{1}H NMR (500 MHz, $CDCl_3$) of 2-phenyl-4-(heptadeuterotetrafuran-2-yl)quinoline (3a-d_7)

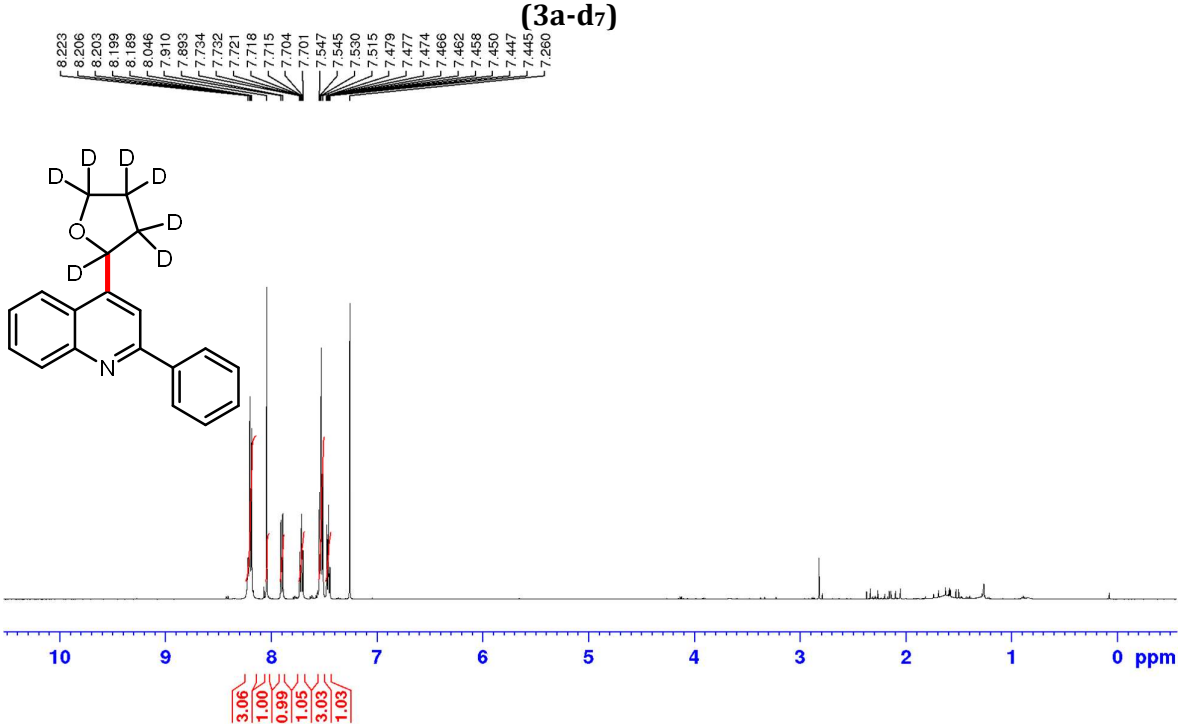

^{13}C NMR (126 MHz, $CDCl_3$) of 2-phenyl-4-(heptadeuterotetrafuran-2-yl)quinoline (3a-d_7)

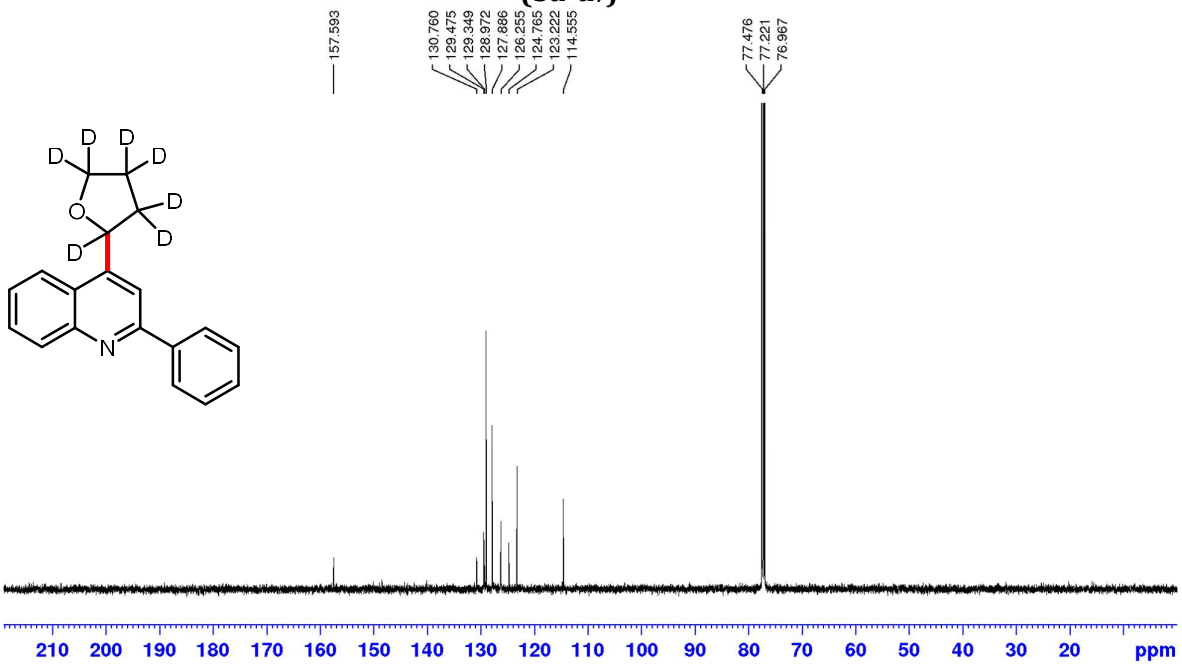

^{1}H NMR (500 MHz, $CDCl_3$) of 2-(4-fluorophenyl)-4-(tetrahydrofuran-2-yl)quinoline (4a)

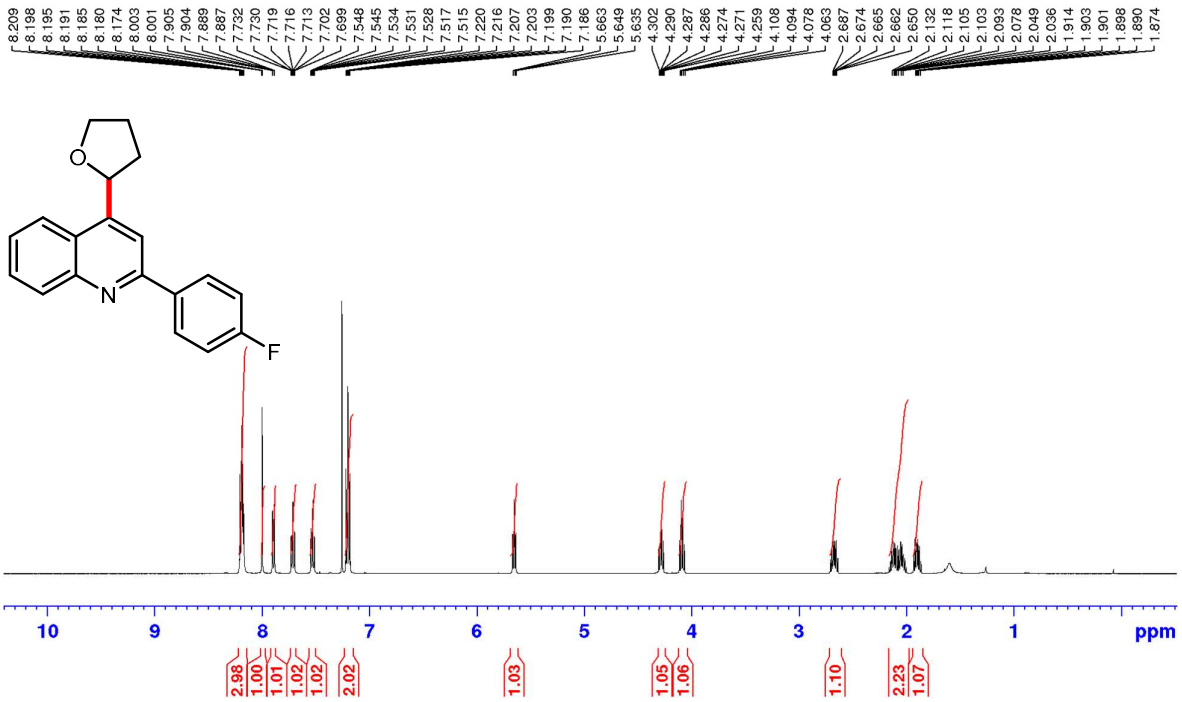

^{13}C NMR (126 MHz, $CDCl_3$) of 2-(4-fluorophenyl)-4-(tetrahydrofuran-2-yl)quinoline (4a)

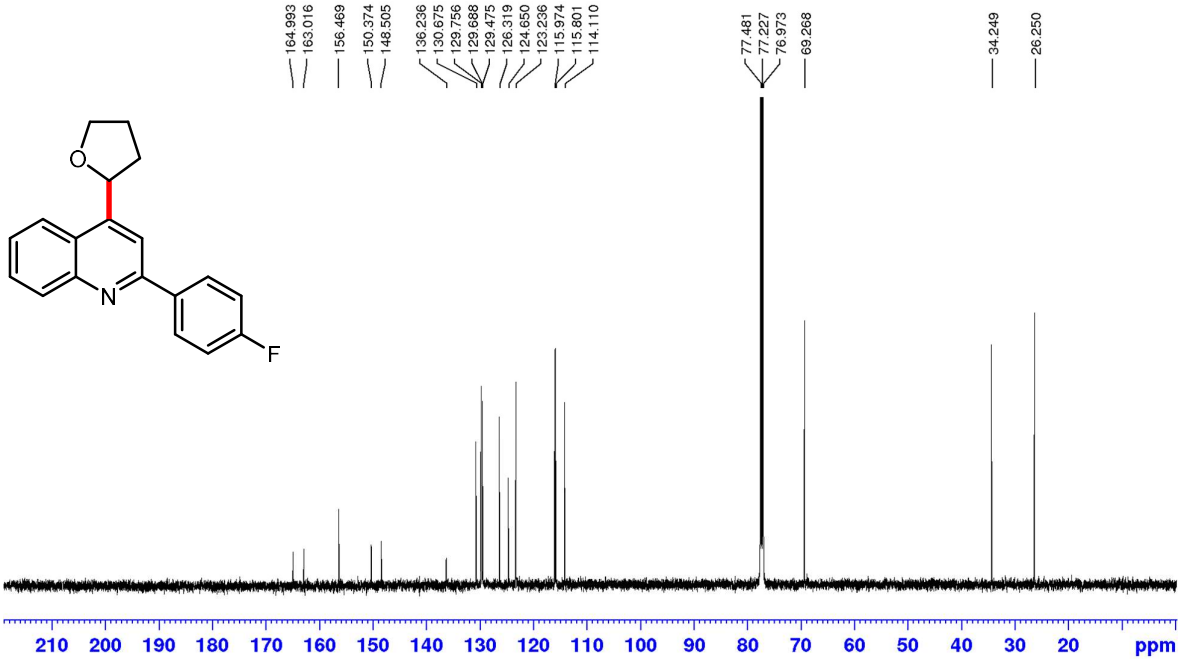

^{1}H NMR (500 MHz, $CDCl_3$) of 2-(4-chlorophenyl)-4-(tetrahydrofuran-2-yl)quinoline (5a)

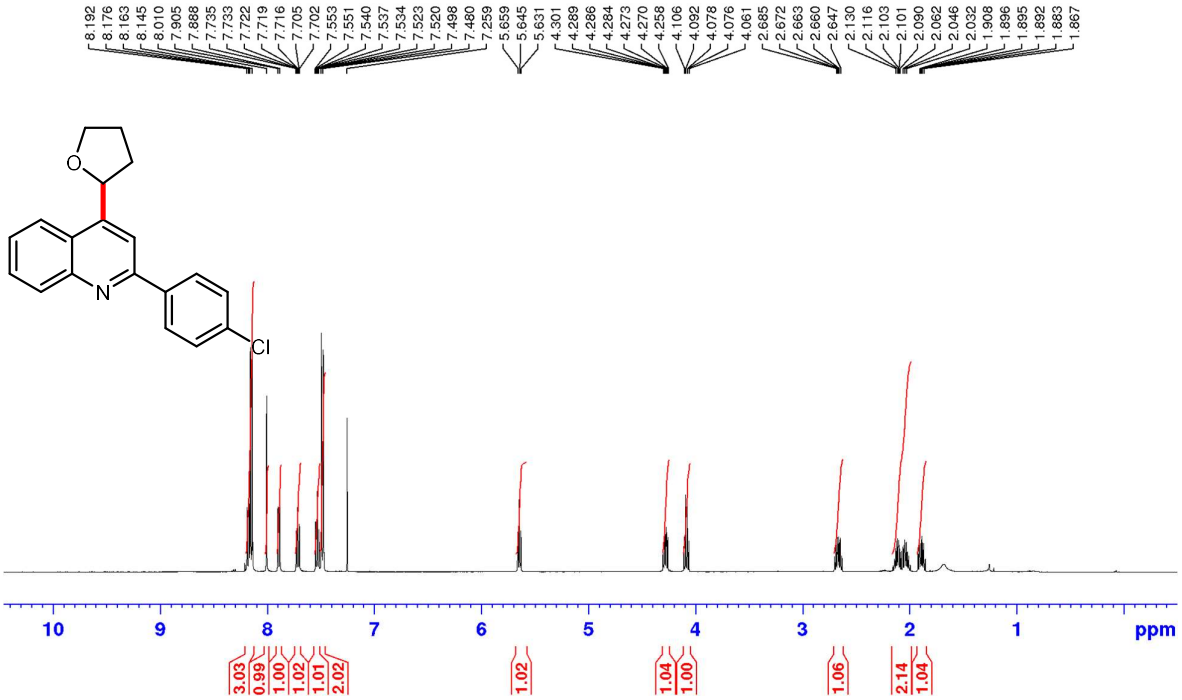

^{13}C NMR (126 MHz, $CDCl_3$) of 2-(4-chlorophenyl)-4-(tetrahydrofuran-2-yl)quinoline (5a)

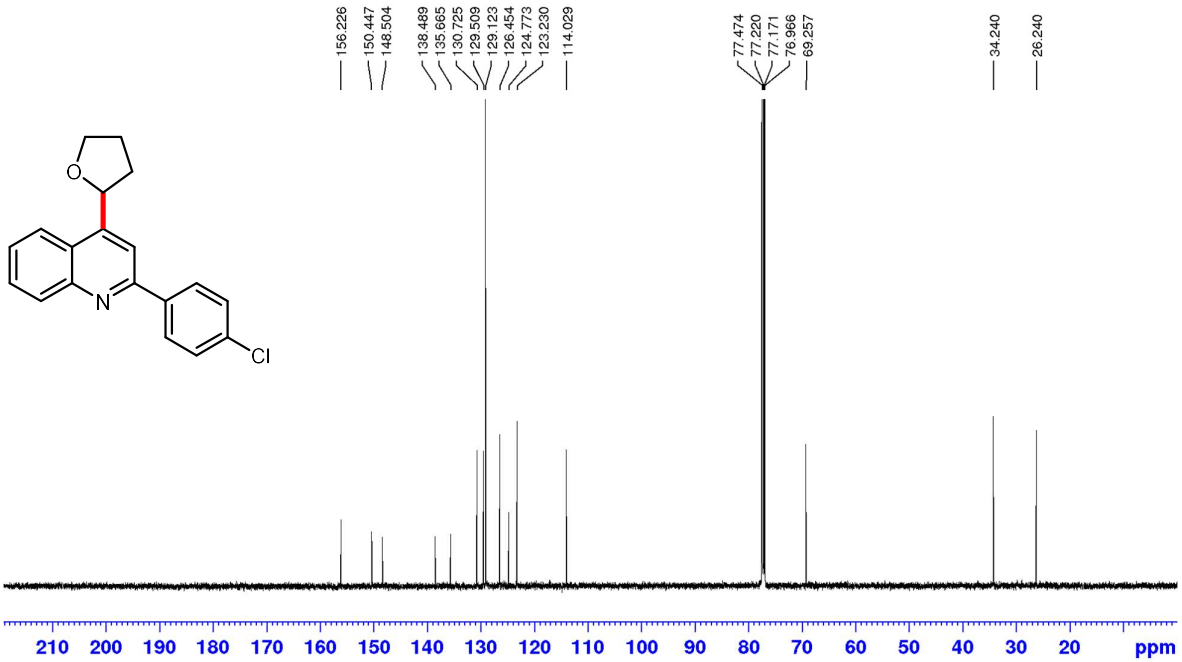

^{1}H NMR (500 MHz, $CDCl_3$) of 2-(4-bromophenyl)-4-(tetrahydrofuran-2-yl)quinoline (6a)

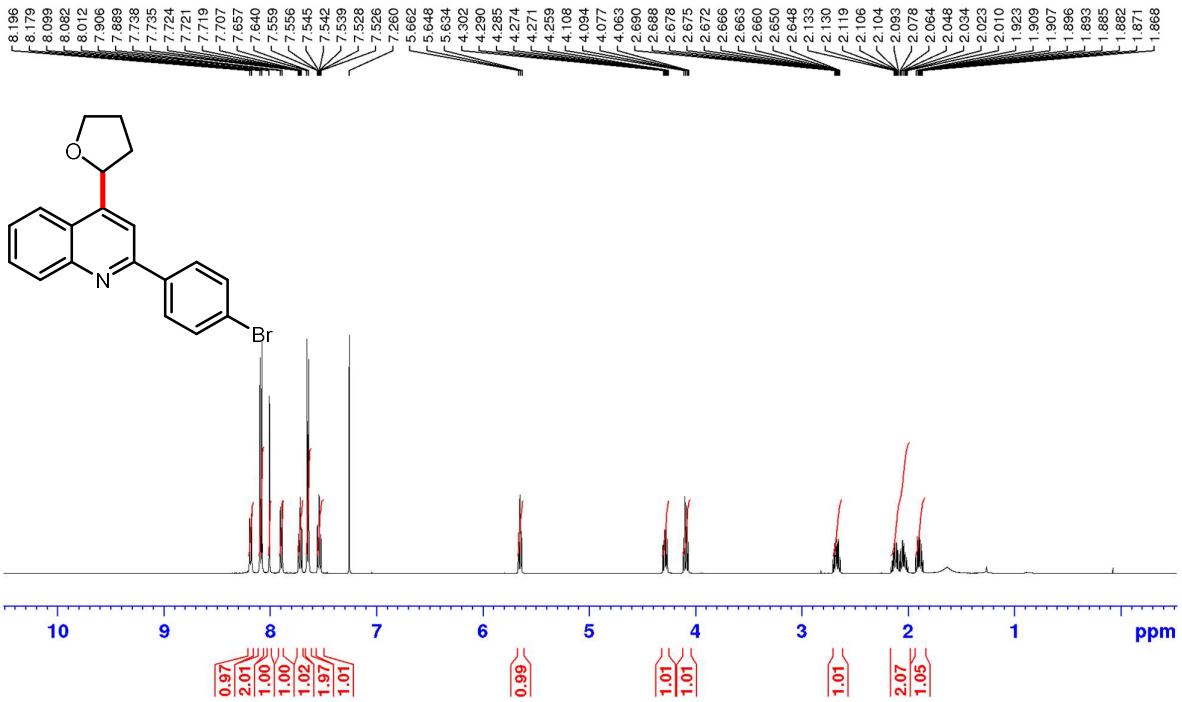

^{13}C NMR (126 MHz, $CDCl_3$) of 2-(4-bromophenyl)-4-(tetrahydrofuran-2-yl)quinoline (6a)

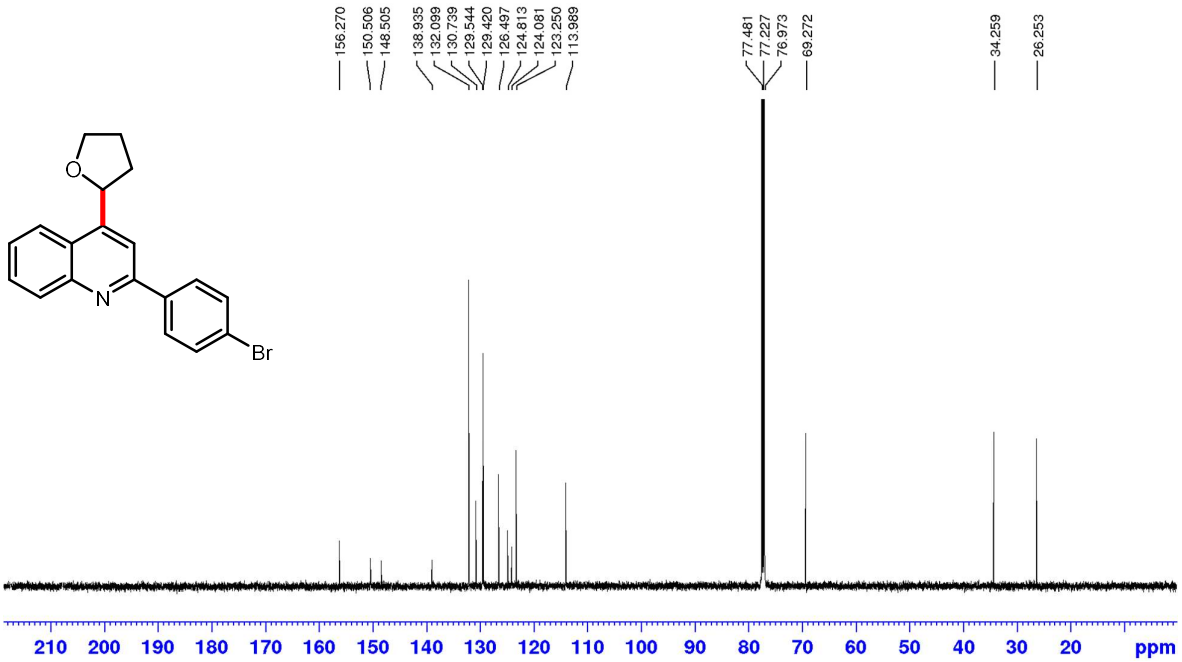

^{1}H NMR (500 MHz, $CDCl_3$) of 4-(4-(tetrahydrofuran-2-yl)quinolin-2-yl)benzonitrile (7a)

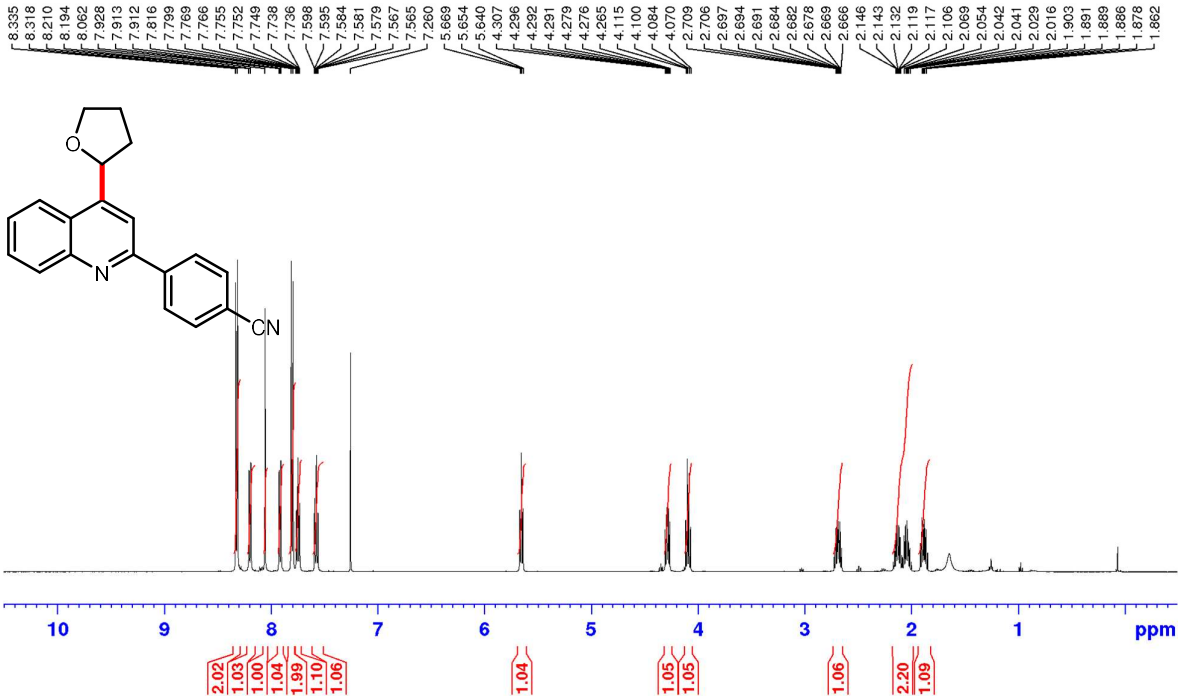

^{13}C NMR (126 MHz, $CDCl_3$) of 4-(4-(tetrahydrofuran-2-yl)quinolin-2-yl)benzonitrile (7a)

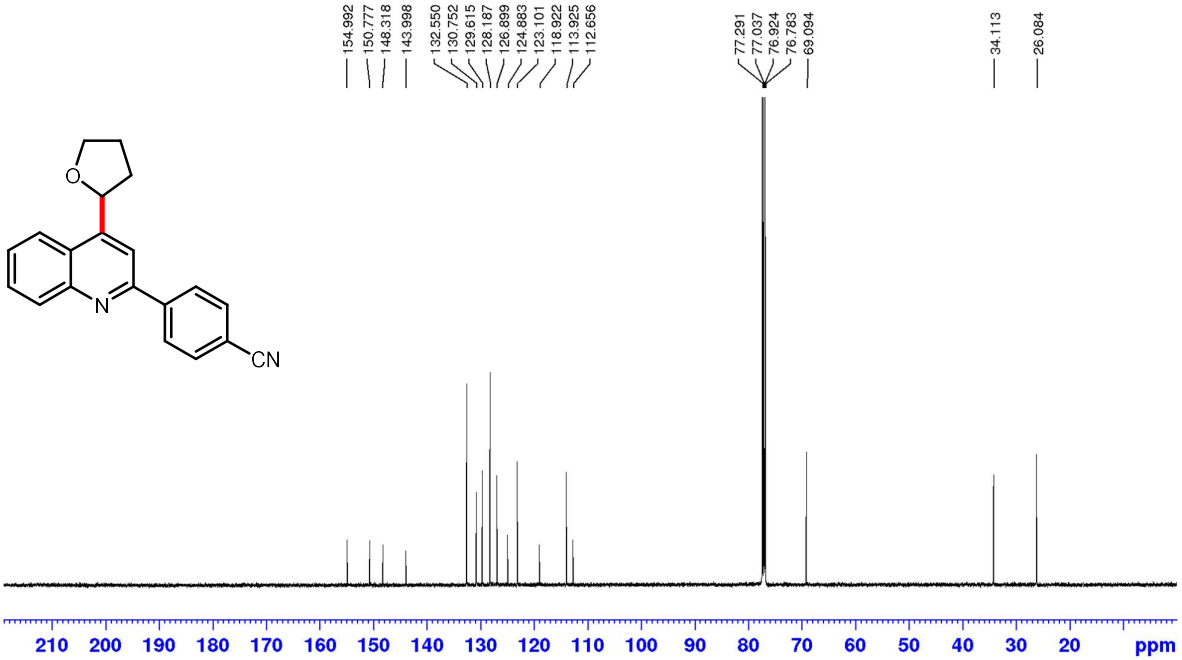

^{1}H NMR (500 MHz, $CDCl_3$) of 4-(tetrahydrofuran-2-yl)-2-(3-(trifluoromethyl)phenyl)quinoline (8a)

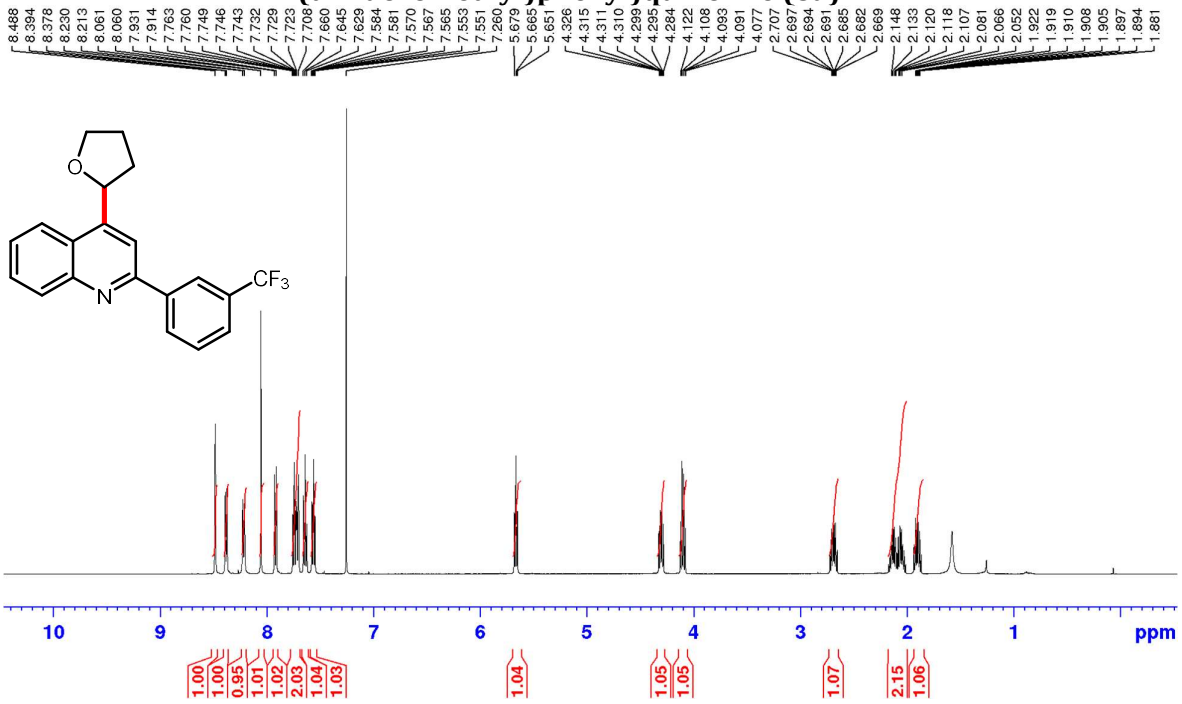

^{13}C NMR (126 MHz, $CDCl_3$) of 4-(tetrahydrofuran-2-yl)-2-(3-(trifluoromethyl)phenyl)quinoline (8a)

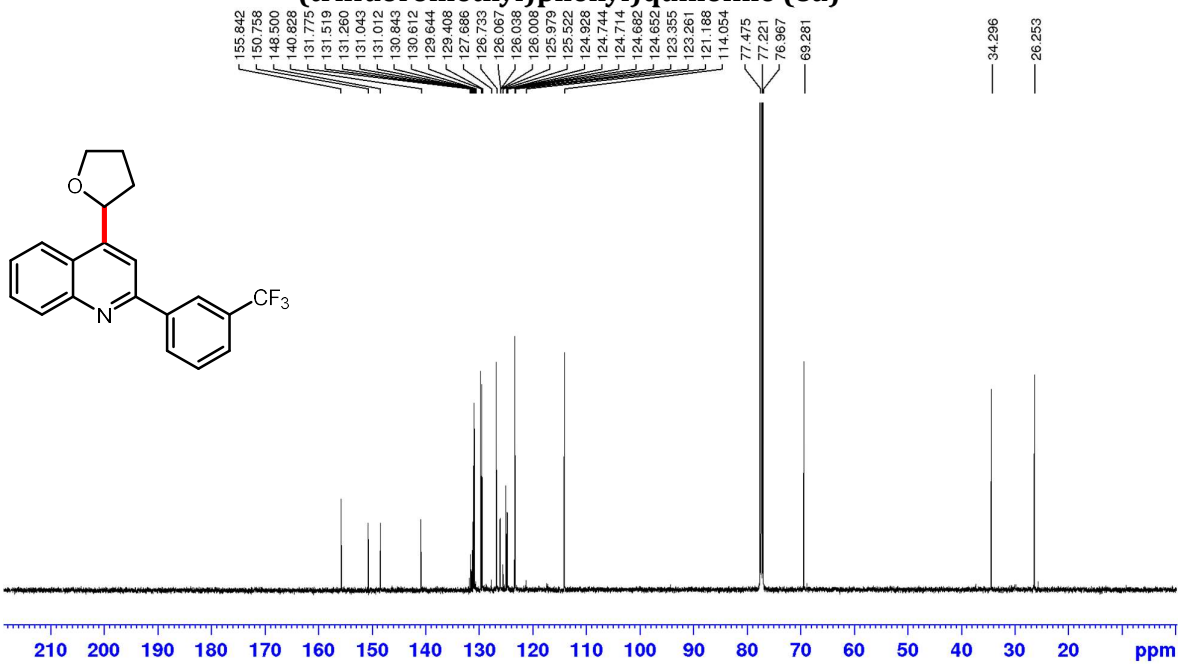

^{1}H NMR (500 MHz, $CDCl_3$) of 1-(4-(4-(tetrahydrofuran-2-yl)quinolin-2-yl)phenyl)ethanone (9a)

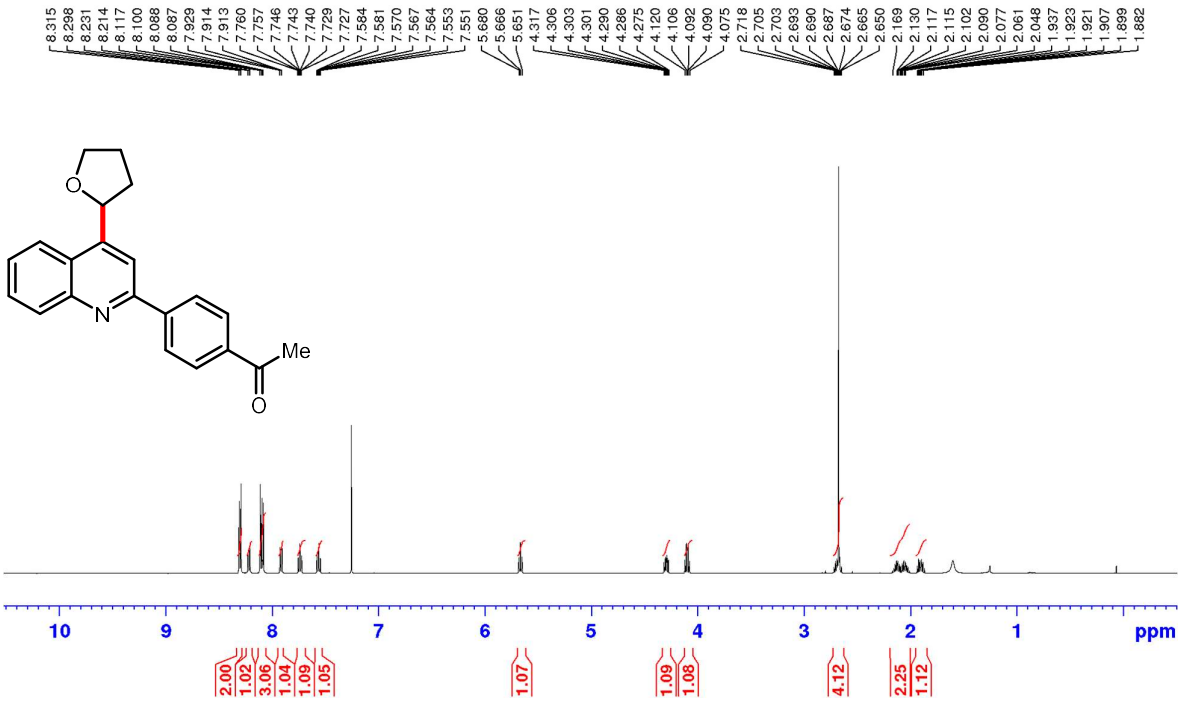

^{13}C NMR (126 MHz, $CDCl_3$) of 1-(4-(4-(tetrahydrofuran-2-yl)quinolin-2-yl)phenyl)ethanone (9a)

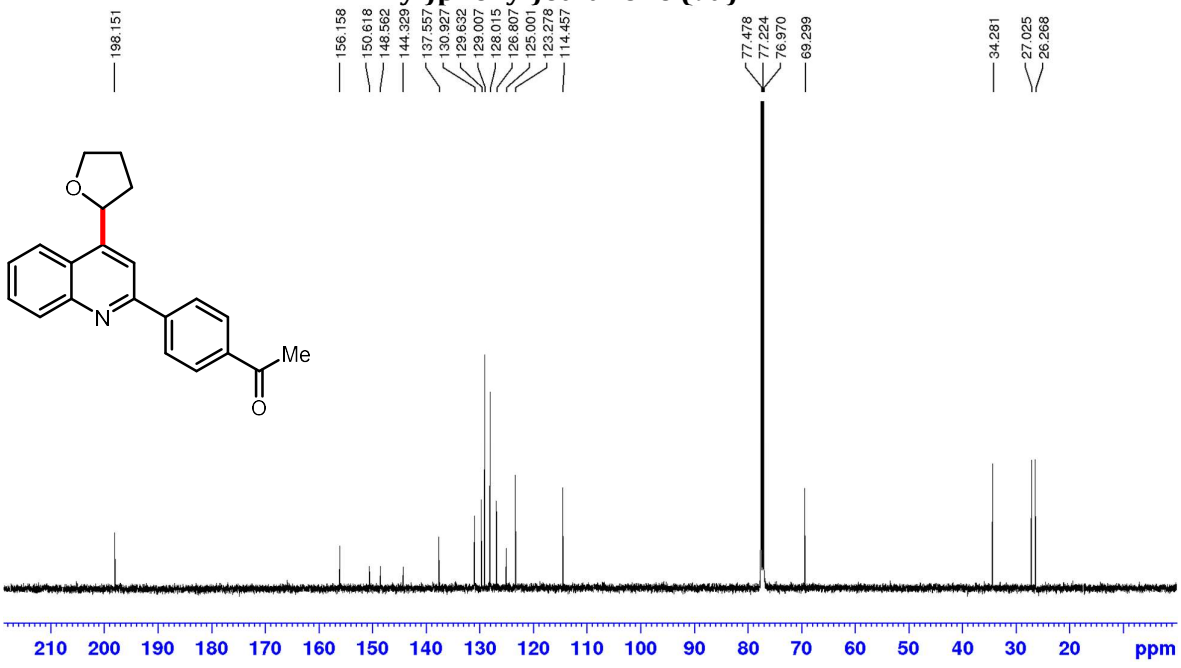

^{1}H NMR (500 MHz, $CDCl_3$) of 4-(tetrahydrofuran-2-yl)-2-(*p*-tolyl)quinoline (10a)

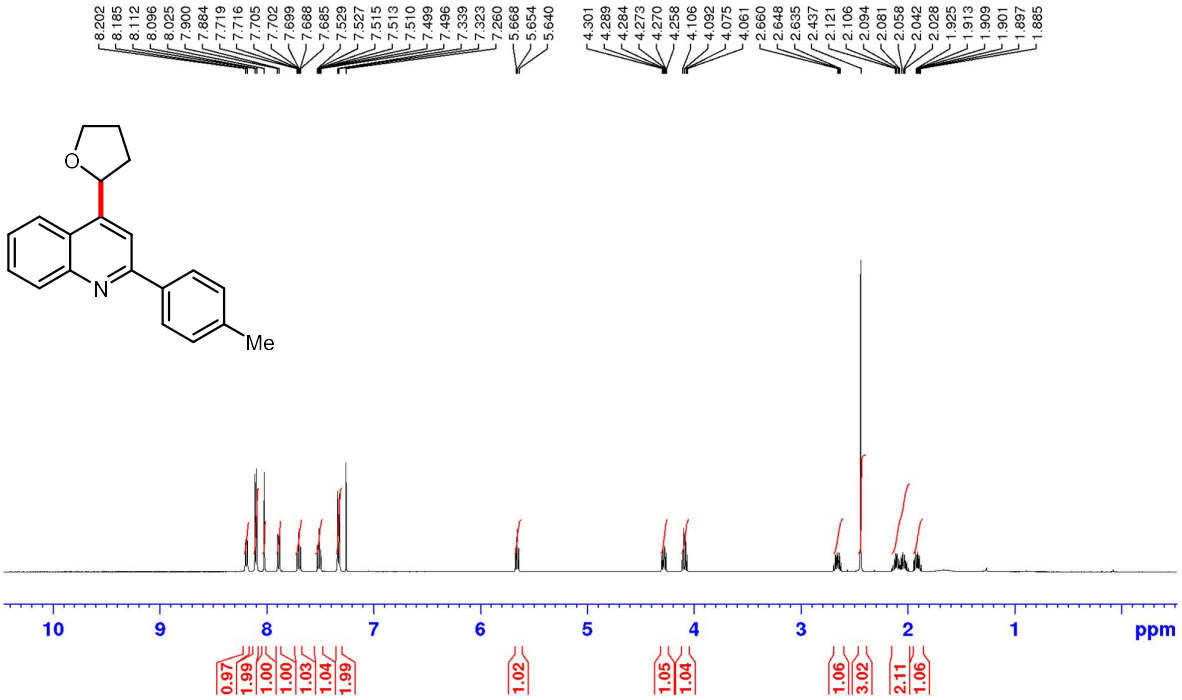

^{13}C NMR (126 MHz, $CDCl_3$) of 4-(tetrahydrofuran-2-yl)-2-(*p*-tolyl)quinoline (10a)

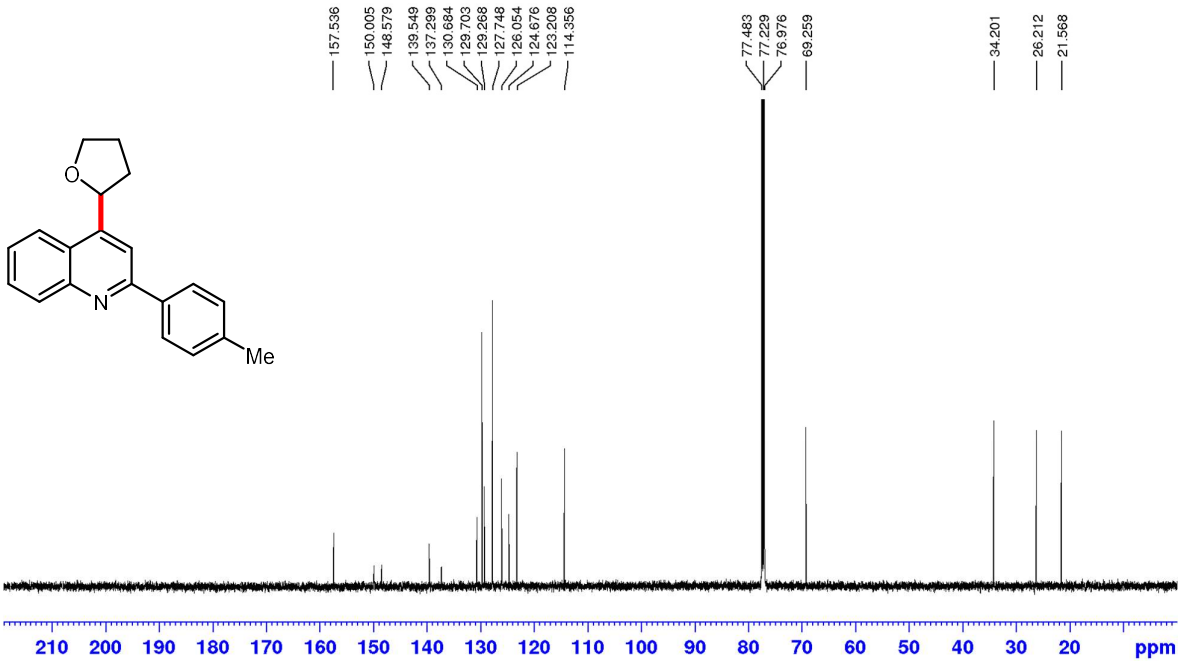

^{1}H NMR (500 MHz, $CDCl_3$) of 2-(4-methoxyphenyl)-4-(tetrahydrofuran-2-yl)quinoline (11a)

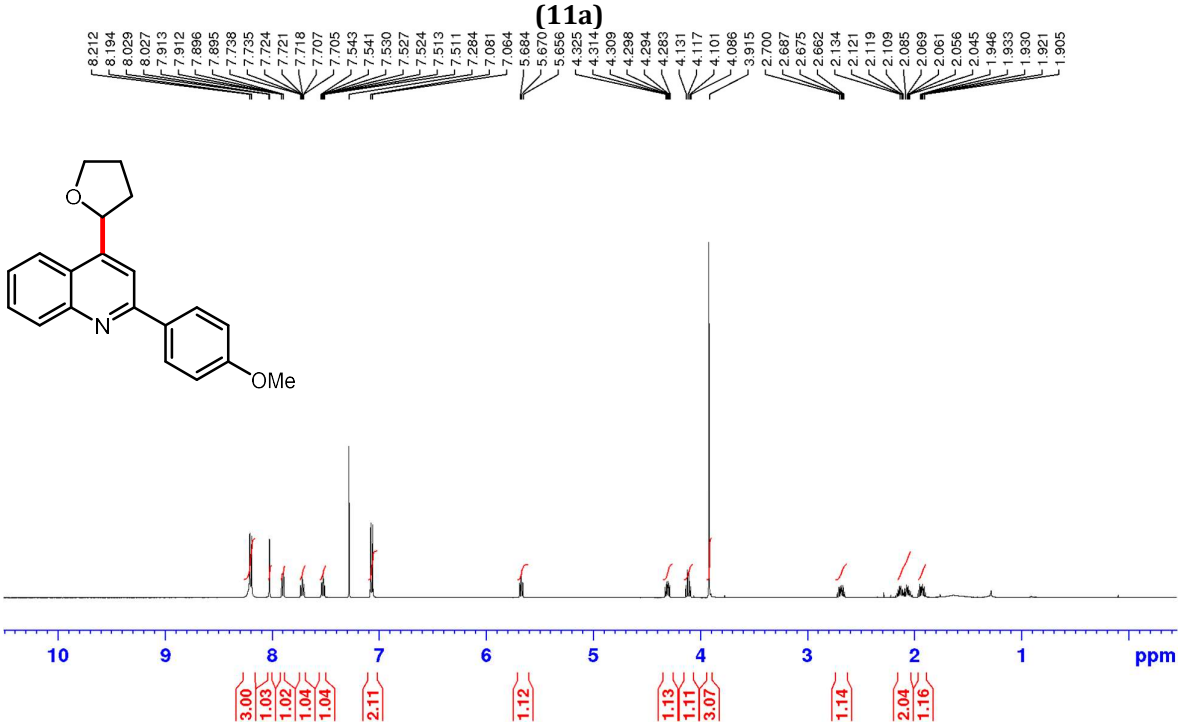

^{13}C NMR (126 MHz, $CDCl_3$) of 2-(4-methoxyphenyl)-4-(tetrahydrofuran-2-yl)quinoline (11a)

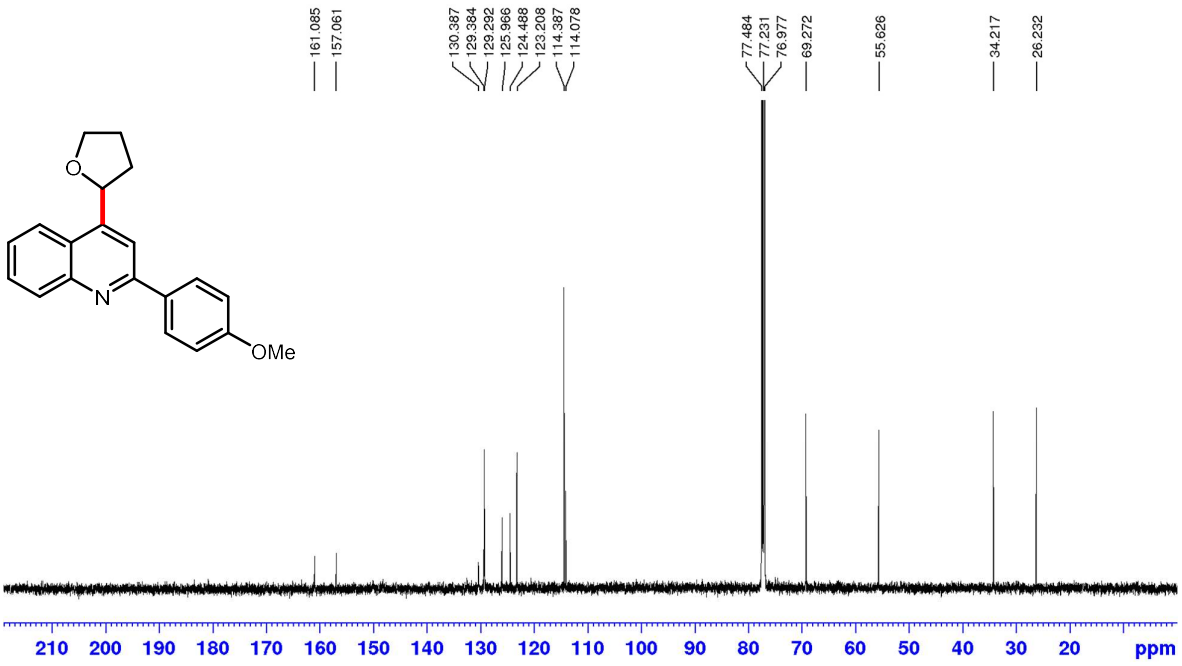

^{1}H NMR (500 MHz, $CDCl_3$) of 2-([1,1'-biphenyl]-4-yl)-4-(tetrahydrofuran-2-yl)quinoline (12a)

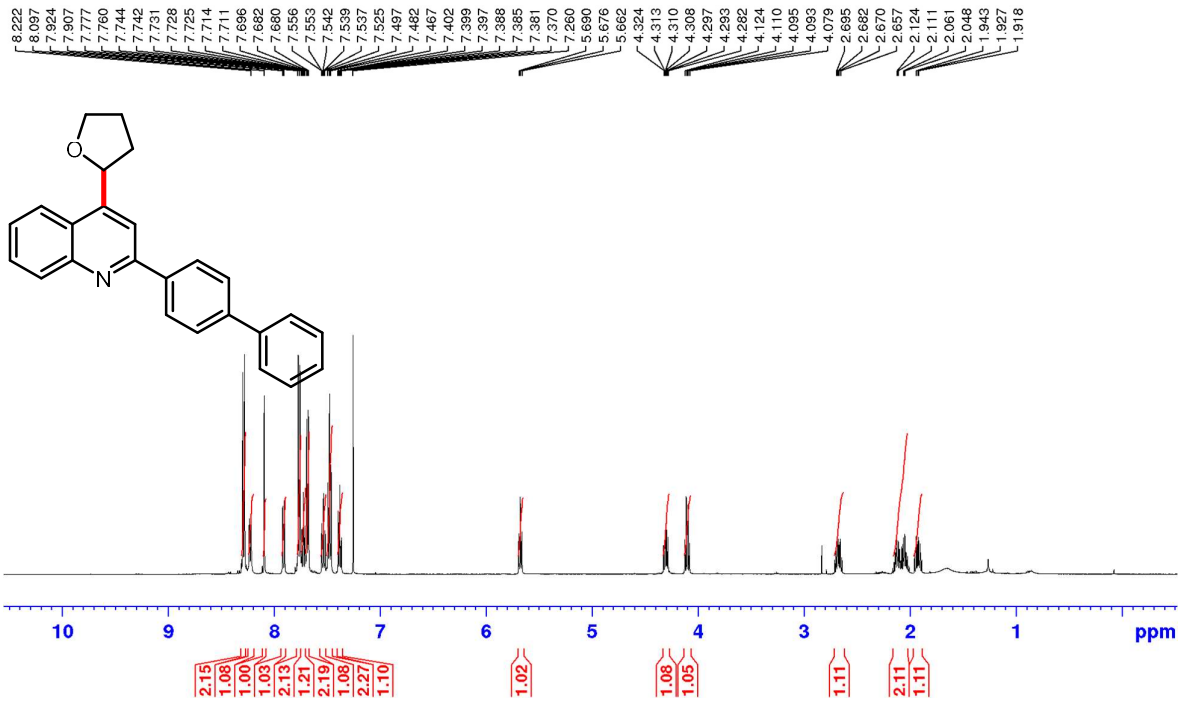

^{13}C NMR (126 MHz, $CDCl_3$) of 2-([1,1'-biphenyl]-4-yl)-4-(tetrahydrofuran-2-yl)quinoline (12a)

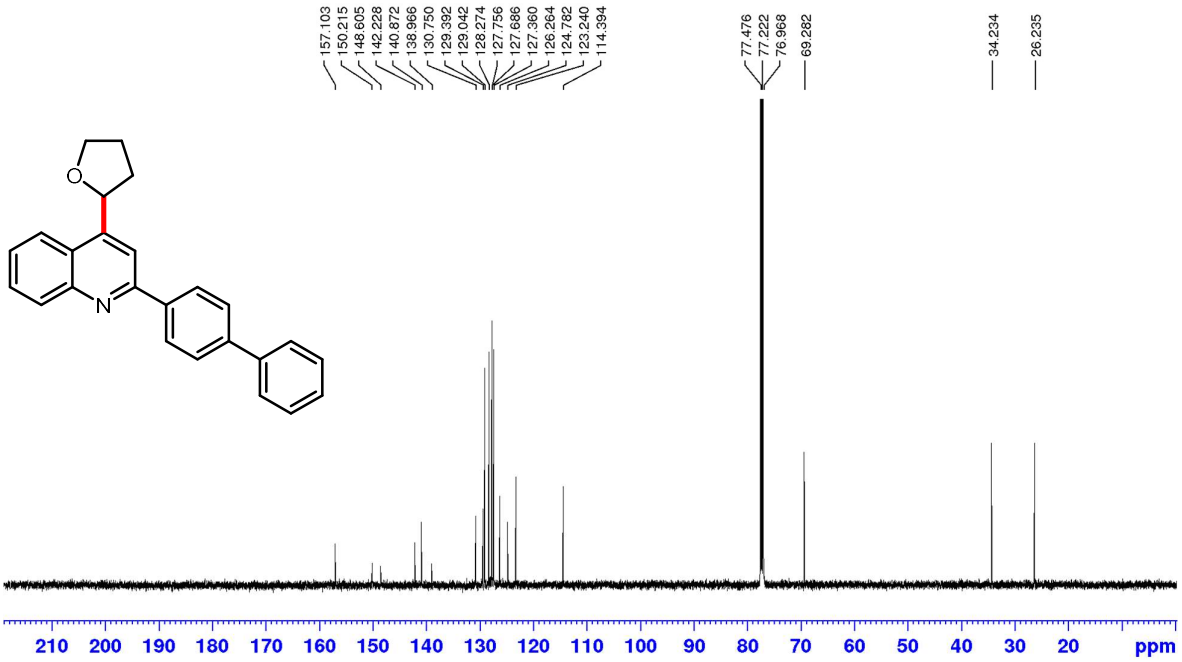

^{1}H NMR (500 MHz, $CDCl_3$) of 2-phenethyl-4-(tetrahydrofuran-2-yl)quinoline (13a)

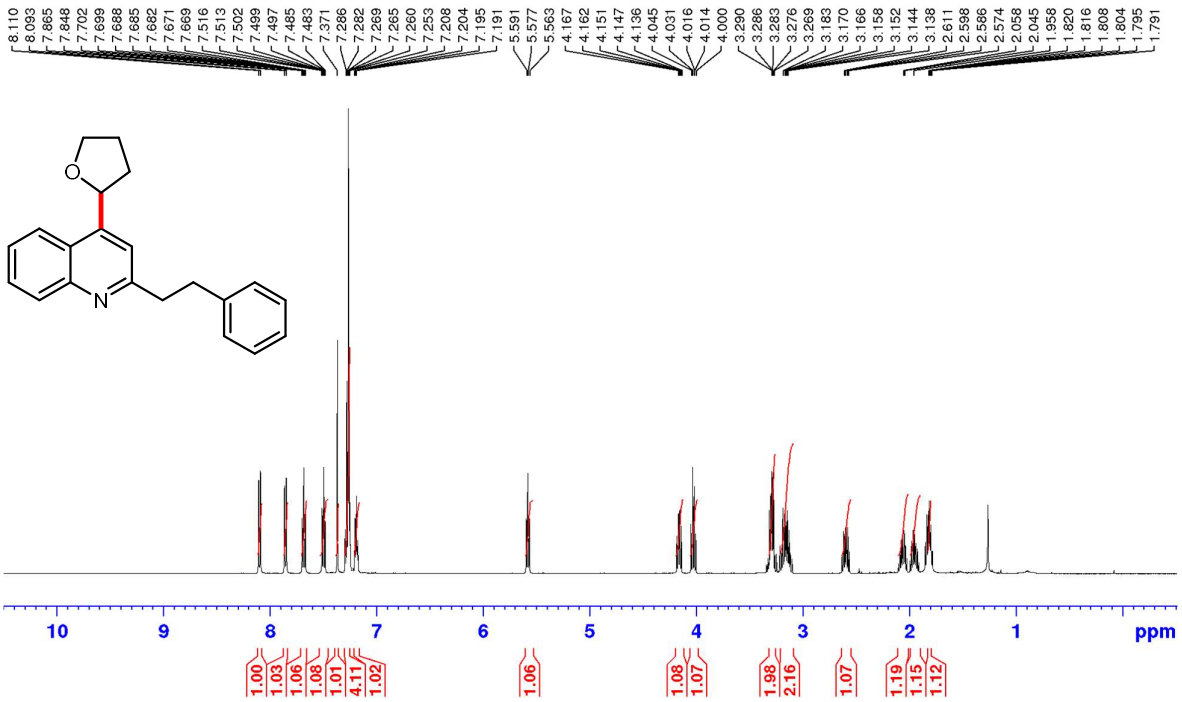

^{13}C NMR (126 MHz, $CDCl_3$) of 2-phenethyl-4-(tetrahydrofuran-2-yl)quinoline (13a)

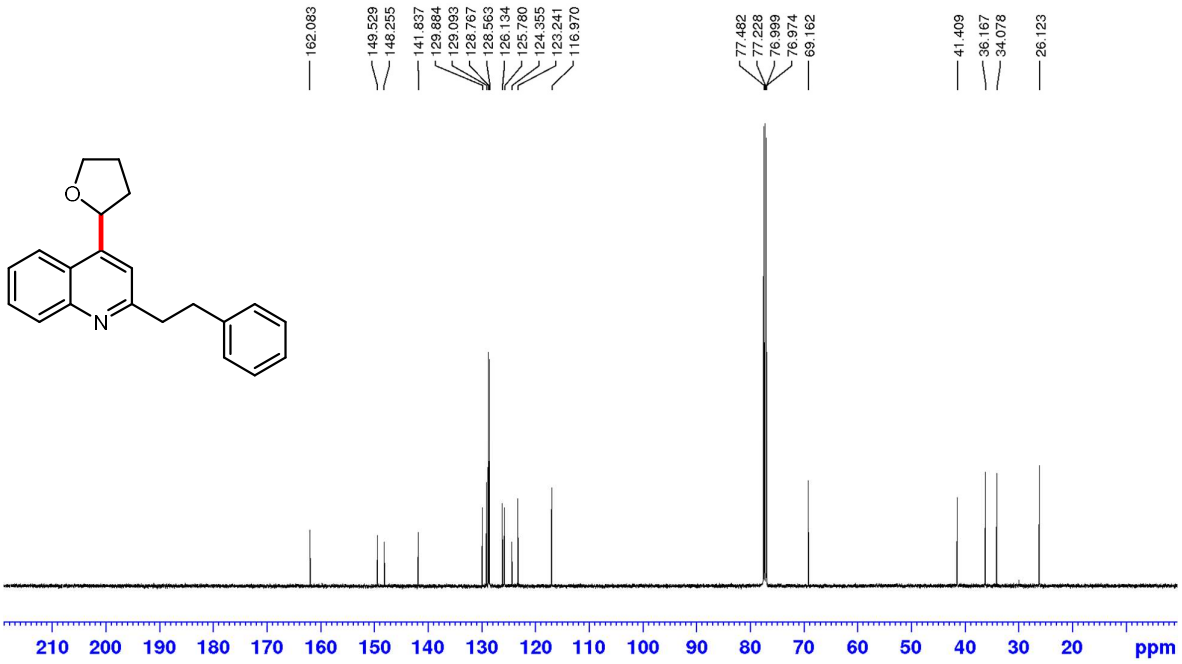

^{1}H NMR (500 MHz, $CDCl_3$) of 2-(2-bromo-5-methoxyphenethyl)-4-(tetrahydrofuran-2-yl)quinoline (14a)

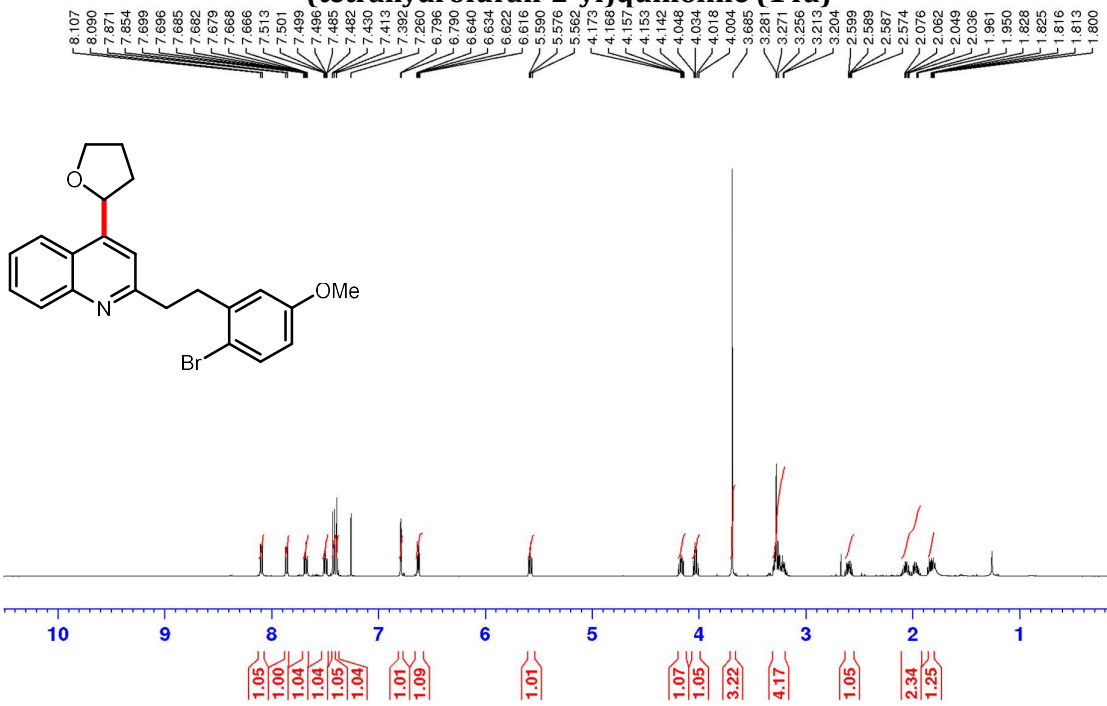

^{13}C NMR (126 MHz, $CDCl_3$) of 2-(2-bromo-5-methoxyphenethyl)-4-(tetrahydrofuran-2-yl)quinoline (14a)

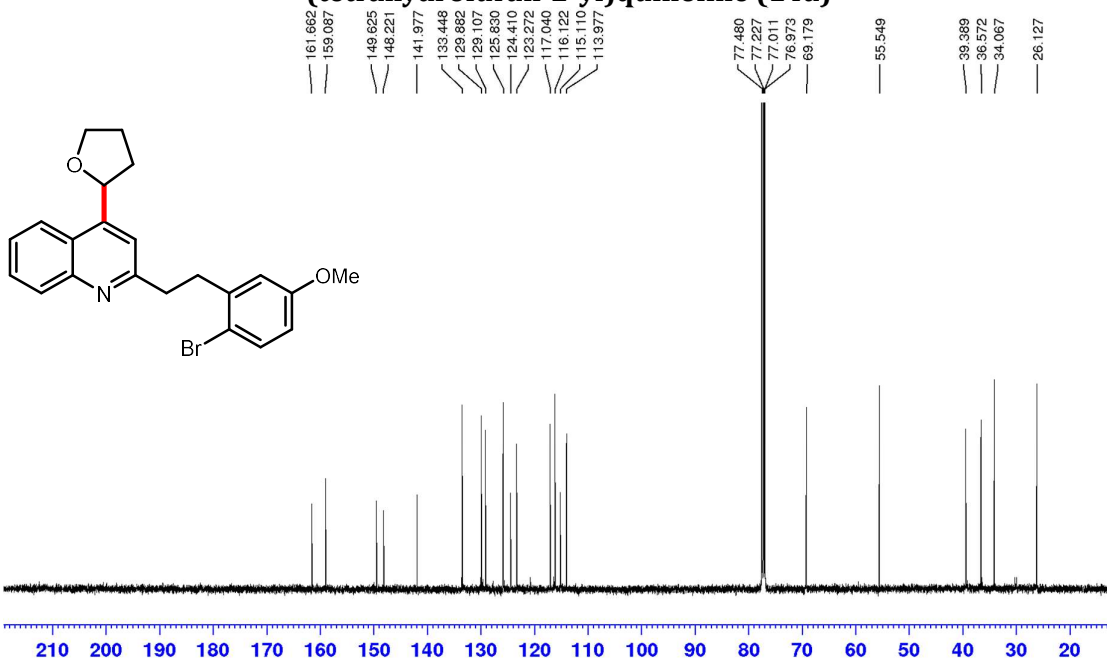

^{1}H NMR (500 MHz, $CDCl_3$) of 4-(tetrahydrofuran-2-yl)quinoline-3-carbonitrile (17a)

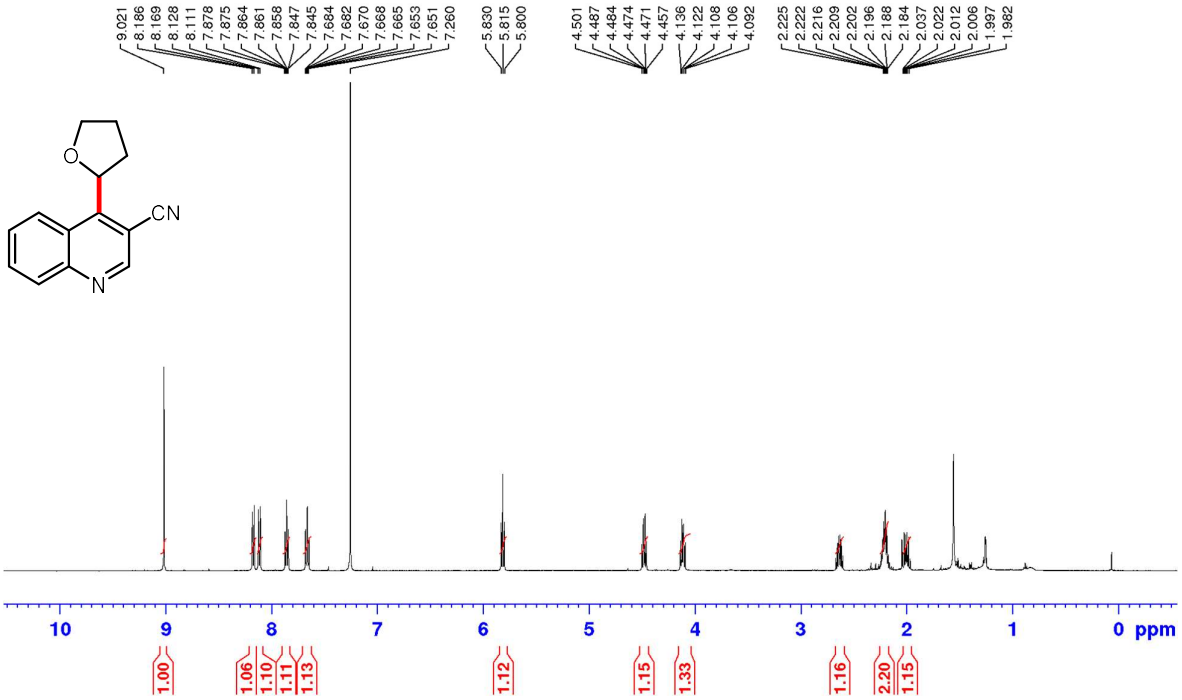

^{13}C NMR (126 MHz, $CDCl_3$) of 4-(tetrahydrofuran-2-yl)quinoline-3-carbonitrile (17a)

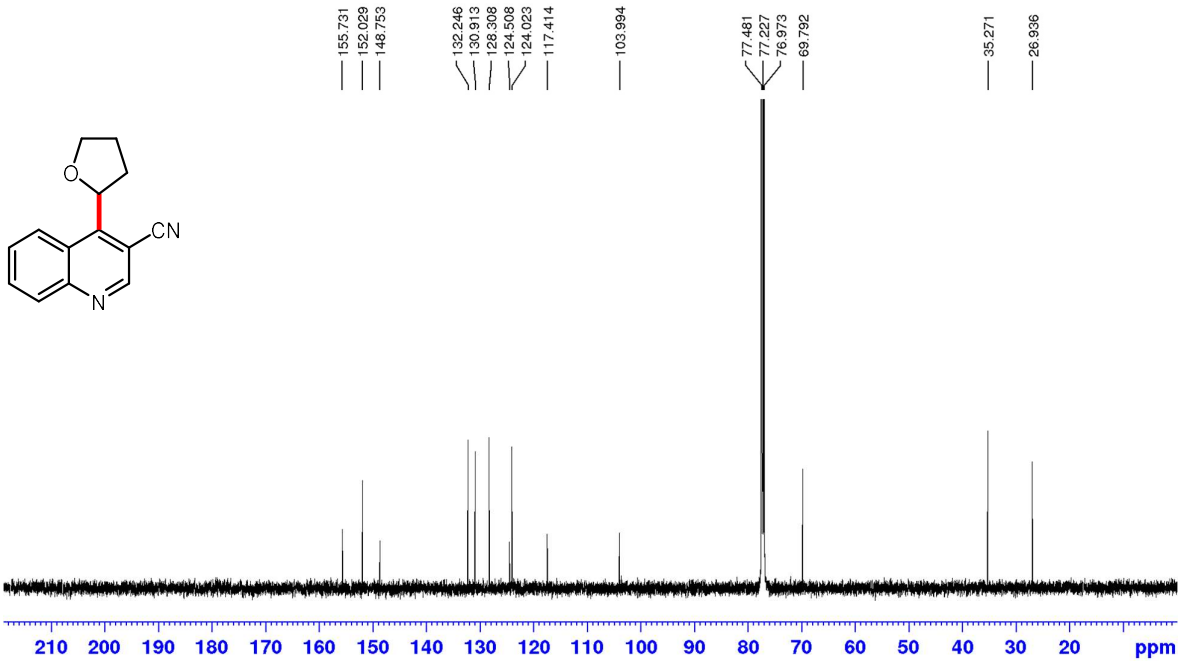

^{1}H NMR (500 MHz, $CDCl_3$) of 4-phenyl-2-(tetrahydrofuran-2-yl)quinoline (18a)

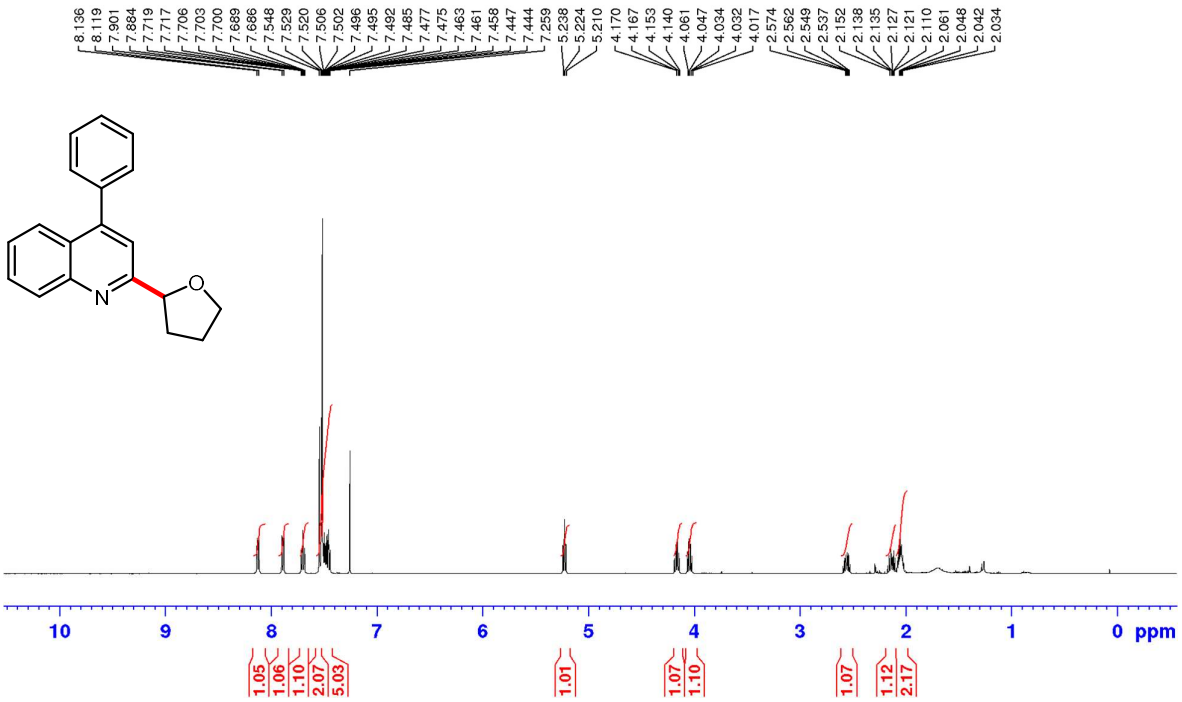

^{13}C NMR (126 MHz, $CDCl_3$) of 4-phenyl-2-(tetrahydrofuran-2-yl)quinoline (18a)

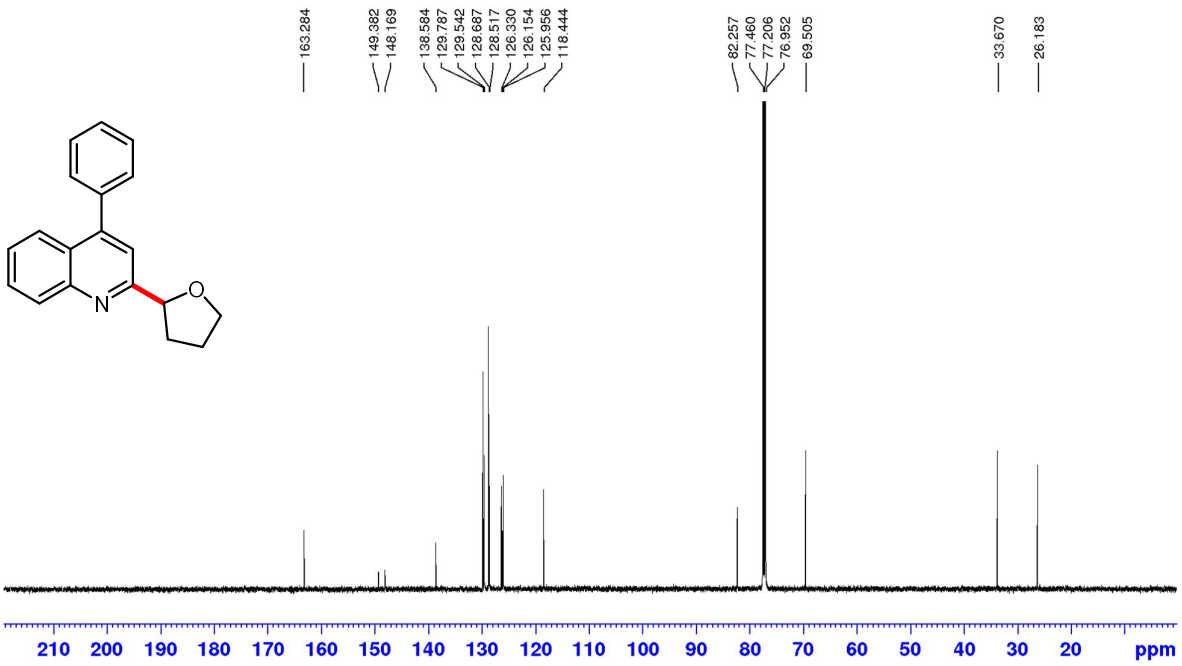

^{1}H NMR (500 MHz, $CDCl_3$) of 3-methyl-4-phenyl-2-(tetrahydrofuran-2-yl)quinoline (19a)

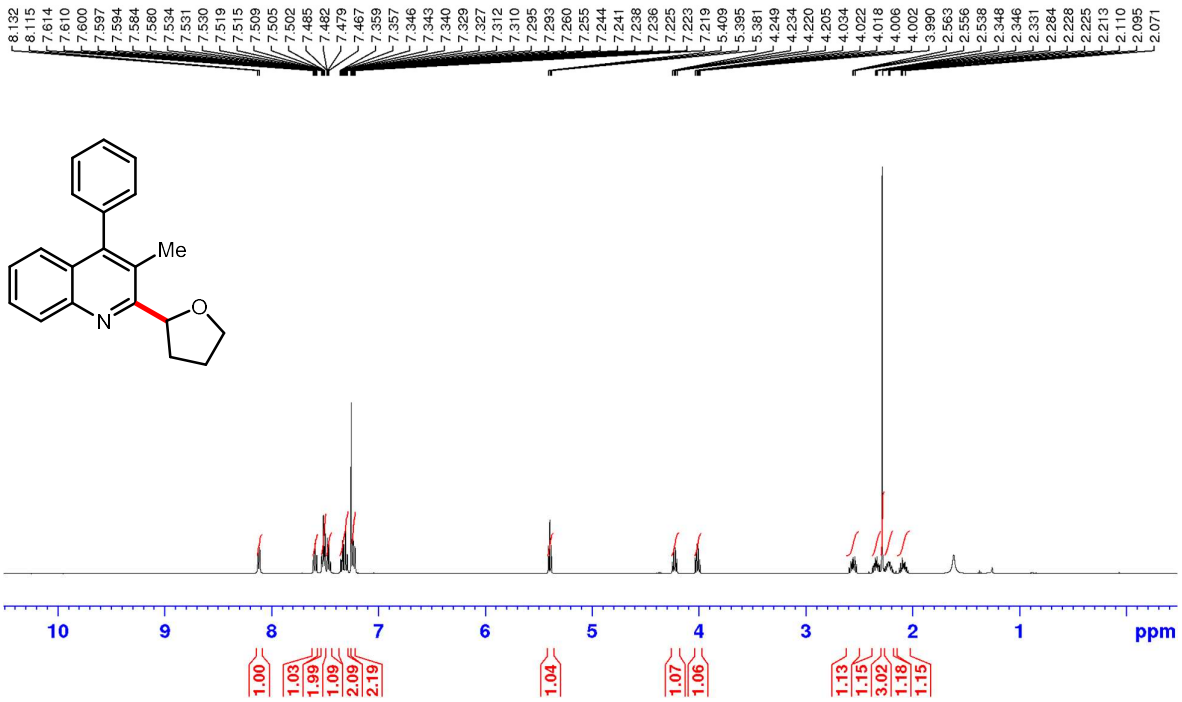

^{13}C NMR (126 MHz, $CDCl_3$) of 3-methyl-4-phenyl-2-(tetrahydrofuran-2-yl)quinoline (19a)

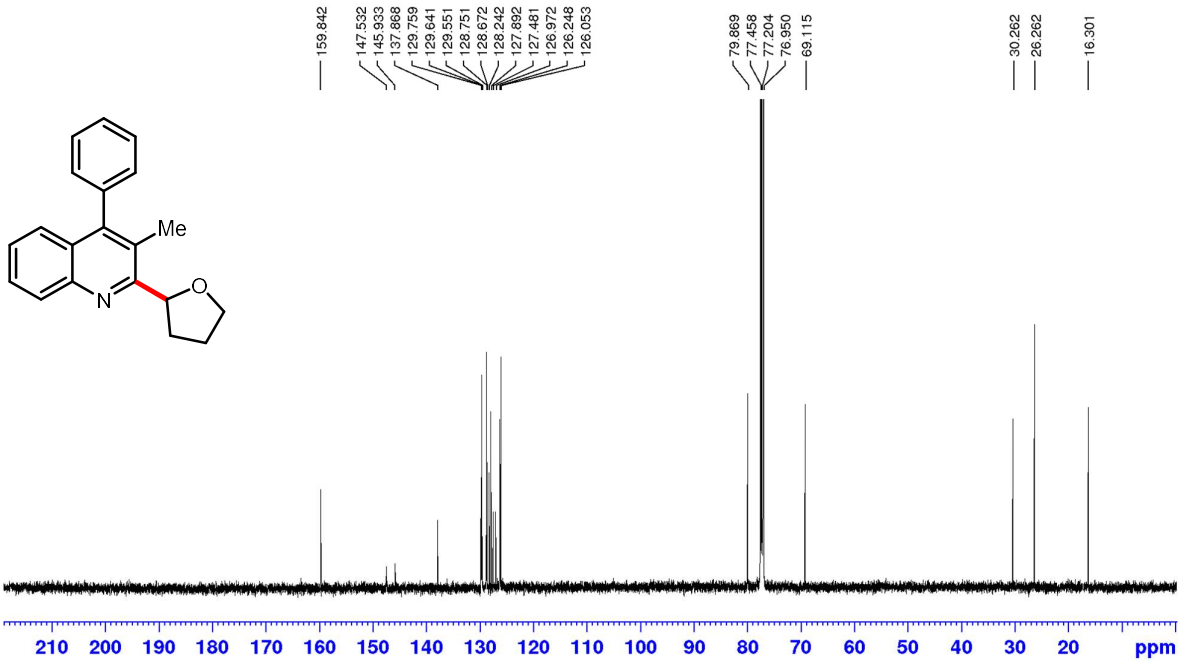

^{1}H NMR (500 MHz, $CDCl_3$) of 2-(tetrahydrofuran-2-yl)-4-(trifluoromethyl)pyridine (24a) and 2-(tetrahydrofuran-2-yl)-6-(tetrahydrofuran-2-yl)-4-(trifluoromethyl)pyridine (24a')

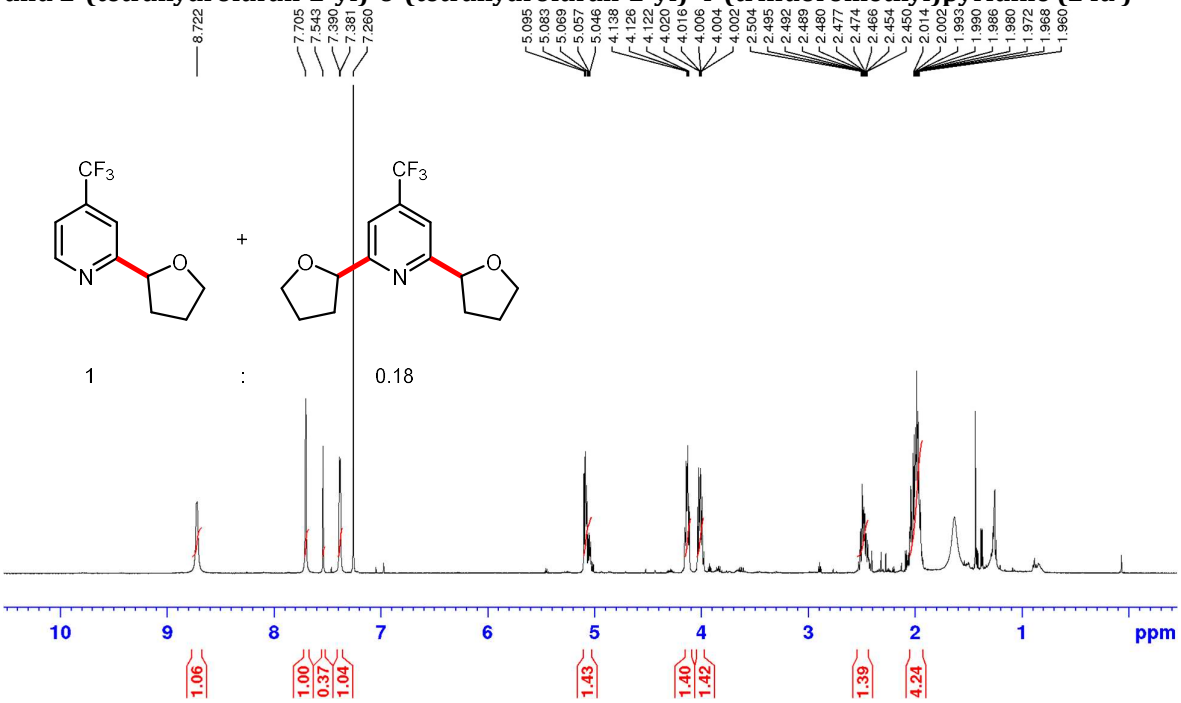

^{13}C NMR (126 MHz, $CDCl_3$) of 2-(tetrahydrofuran-2-yl)-4-(trifluoromethyl)pyridine (24a) and 2-(tetrahydrofuran-2-yl)-6-(tetrahydrofuran-2-yl)-4-(trifluoromethyl)pyridine (24a')

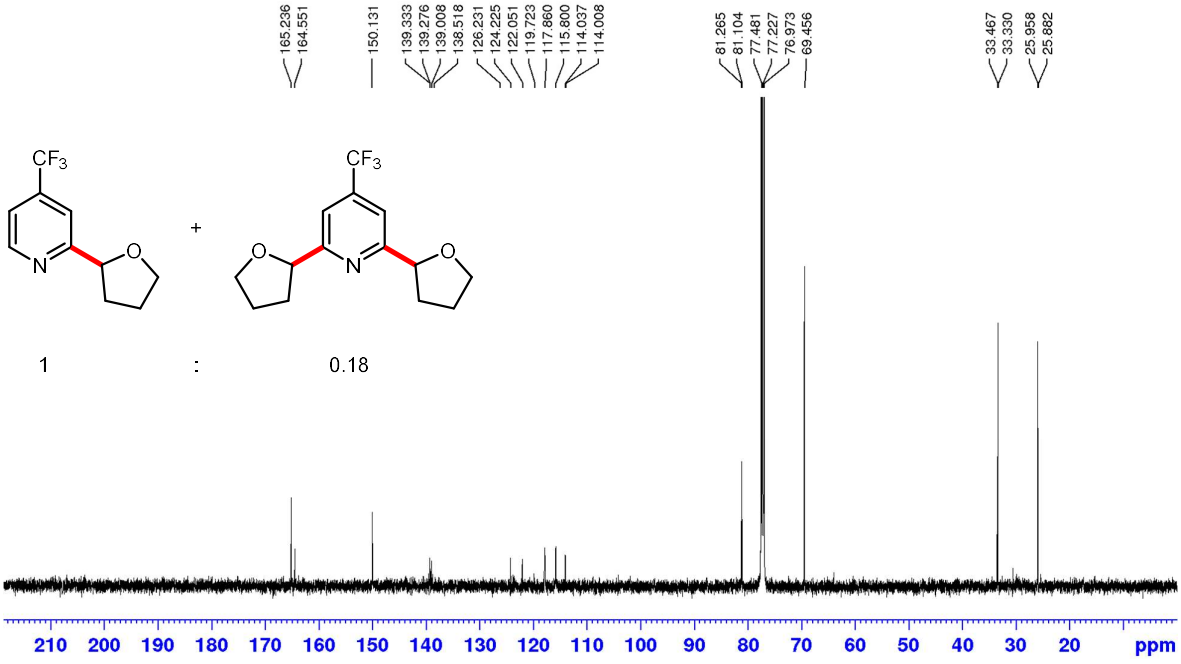

^{1}H NMR (500 MHz, $CDCl_3$) of 2,5-dimethyl-3-(tetrahydrofuran-2-yl)pyrazine (25a)

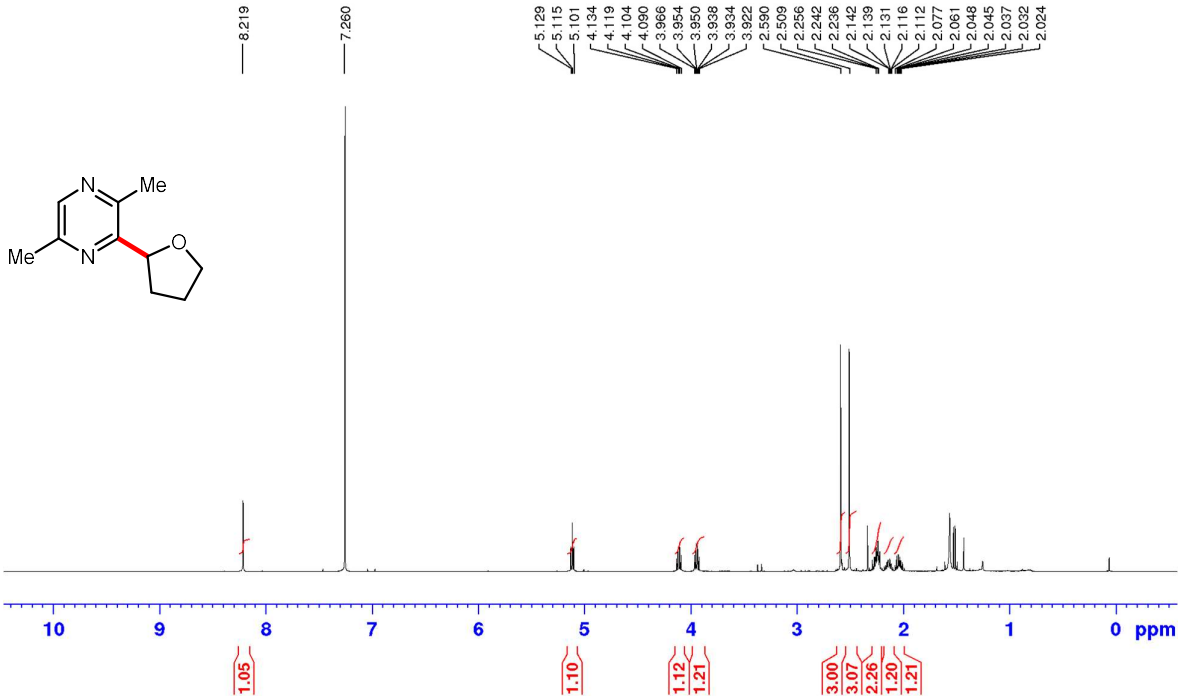

^{13}C NMR (126 MHz, $CDCl_3$) of 2,5-dimethyl-3-(tetrahydrofuran-2-yl)pyrazine (25a)

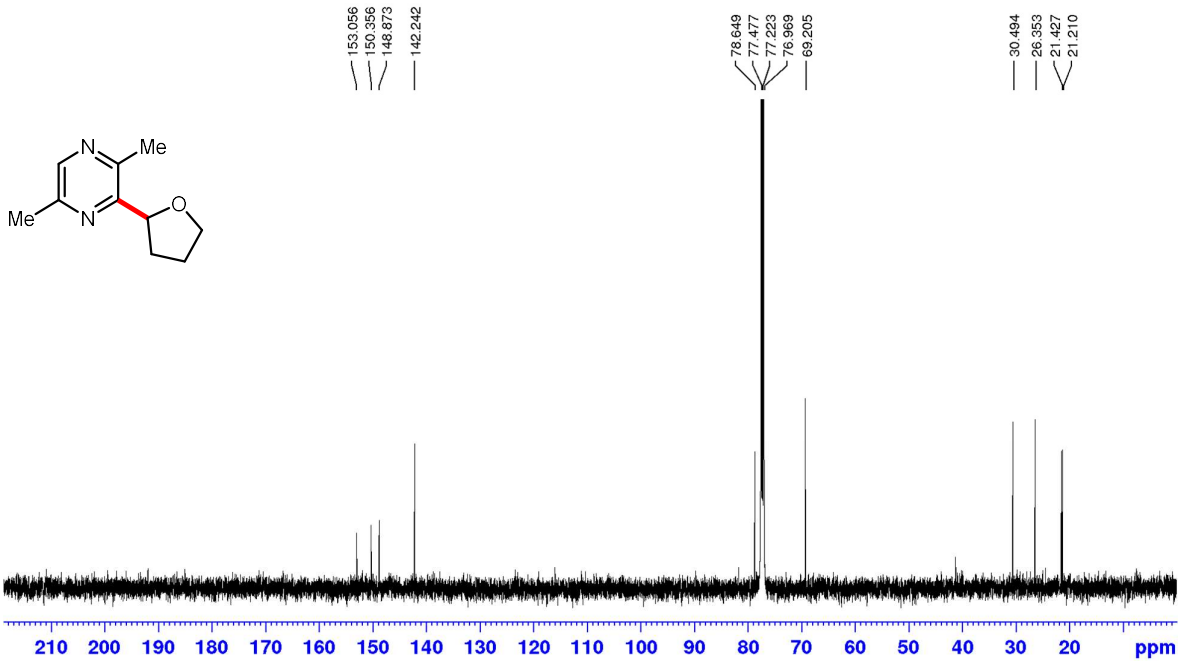

^{1}H NMR (500 MHz, $CDCl_3$) of (1*R*)-(6-methoxy-2-(tetrahydrofuran-2-yl)quinolin-4-yl)((2*S*,4*S*,5*R*)-5-vinylquinuclidin-2-yl)methanol (26a)

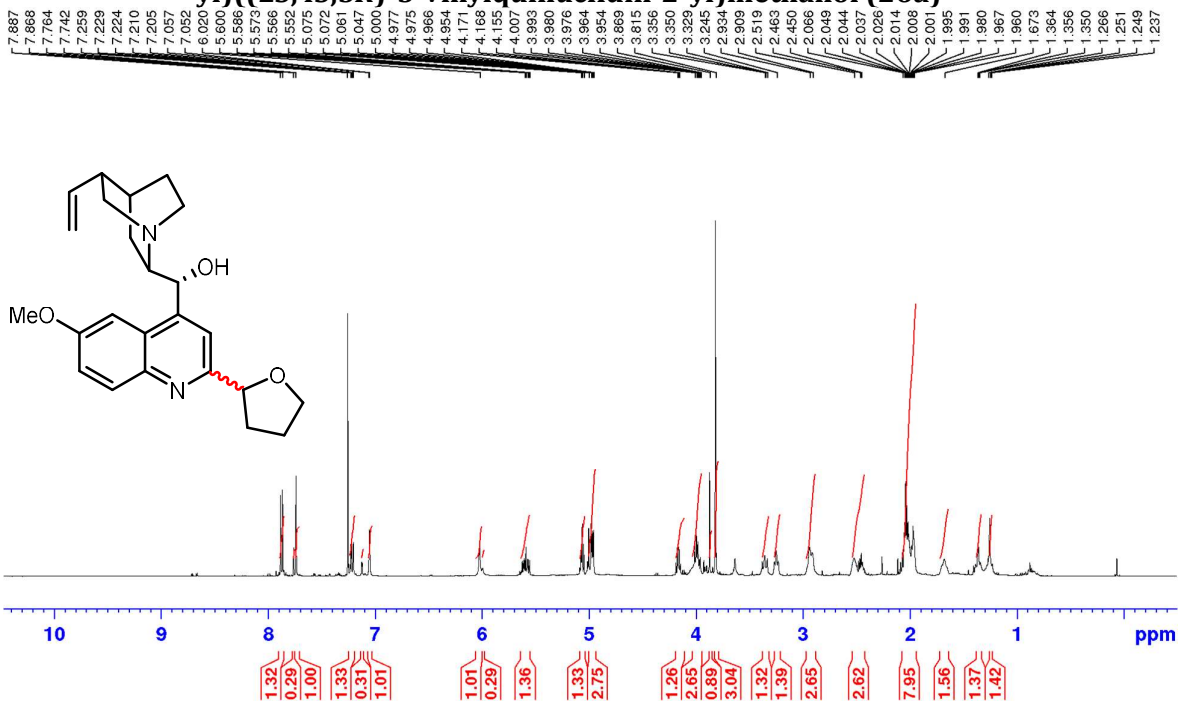

^{13}C NMR (126 MHz, $CDCl_3$) of (1*R*)-(6-methoxy-2-(tetrahydrofuran-2-yl)quinolin-4-yl)((2*S*,4*S*,5*R*)-5-vinylquinuclidin-2-yl)methanol (26a)

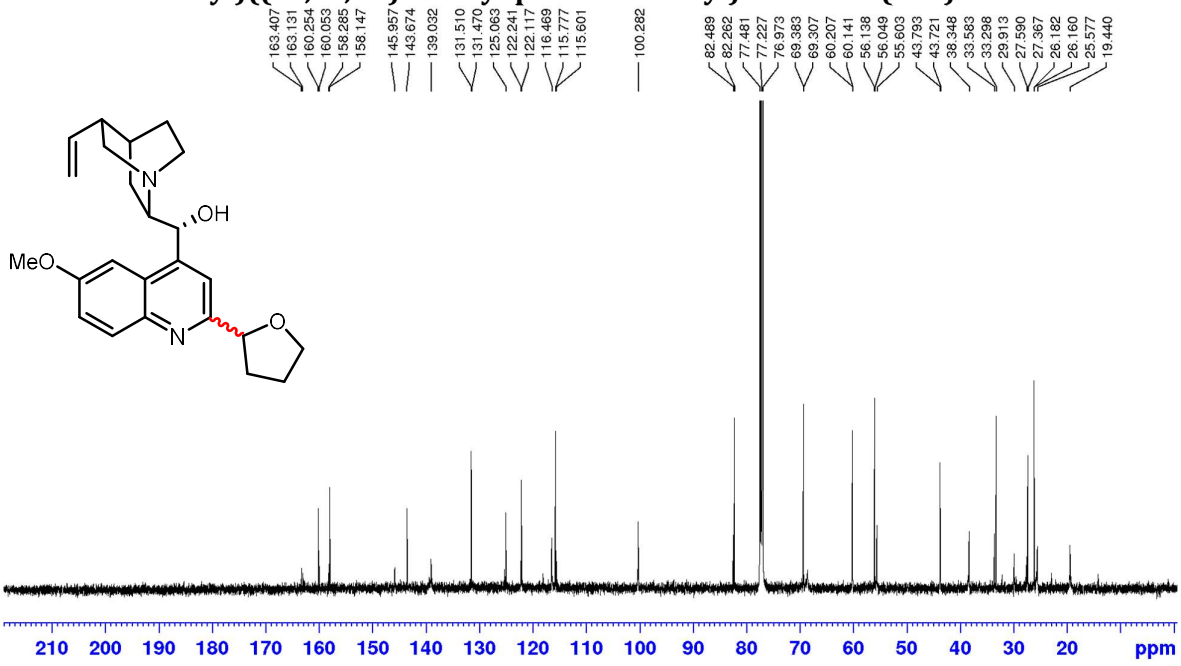

^{1}H NMR (500 MHz, $CDCl_3$) of 2,2-dimethyl-1-(4-((1-(tetrahydrofuran-2-yl)isoquinolin-5-yl)sulfonyl)azepan-1-yl)propan-1-one (27a)

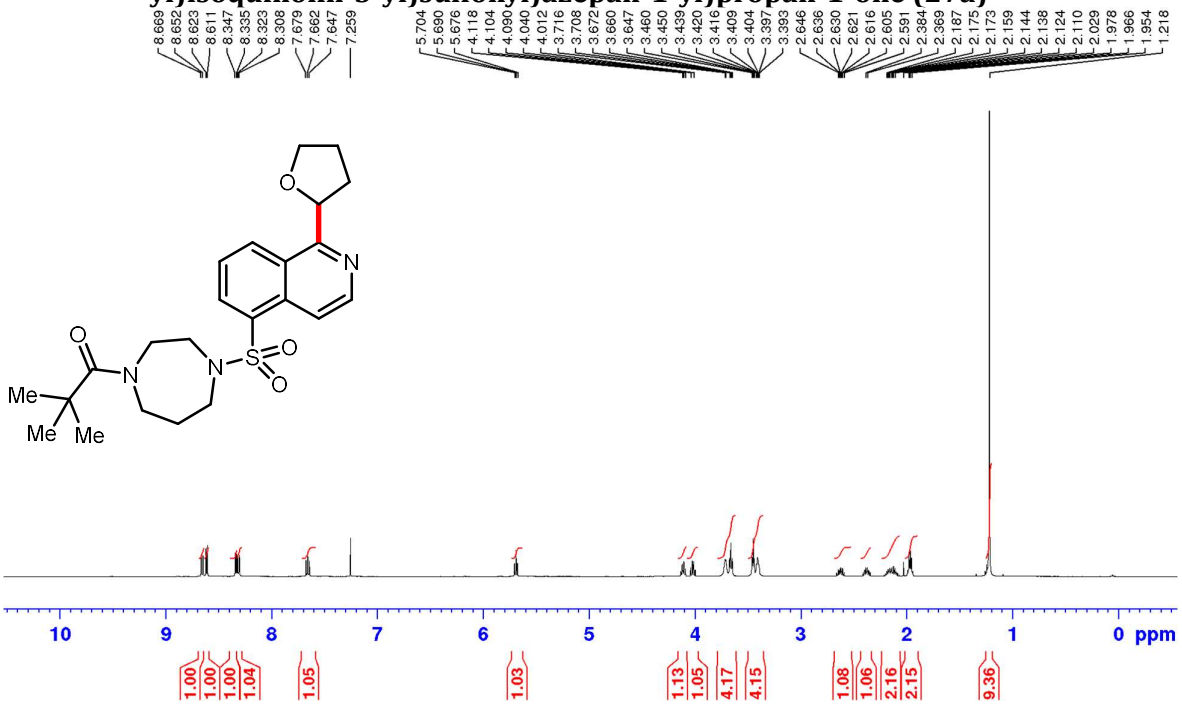

^{13}C NMR (126 MHz, $CDCl_3$) of 2,2-dimethyl-1-(4-((1-(tetrahydrofuran-2-yl)isoquinolin-5-yl)sulfonyl)azepan-1-yl)propan-1-one (27a)

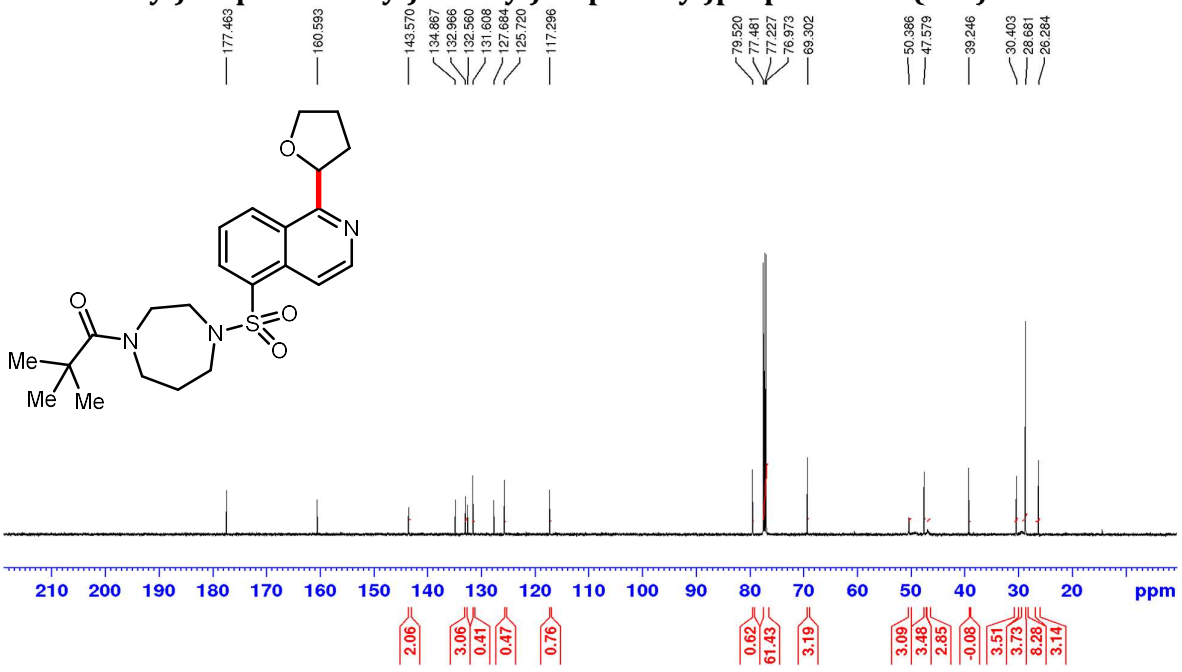

^{1}H NMR (500 MHz, $CDCl_3$) of (1*R*,2*S*,5*R*)-2-isopropyl-5-methylcyclohexyl-2-(tetrahydrofuran-2-yl)isonicotinate (28a)

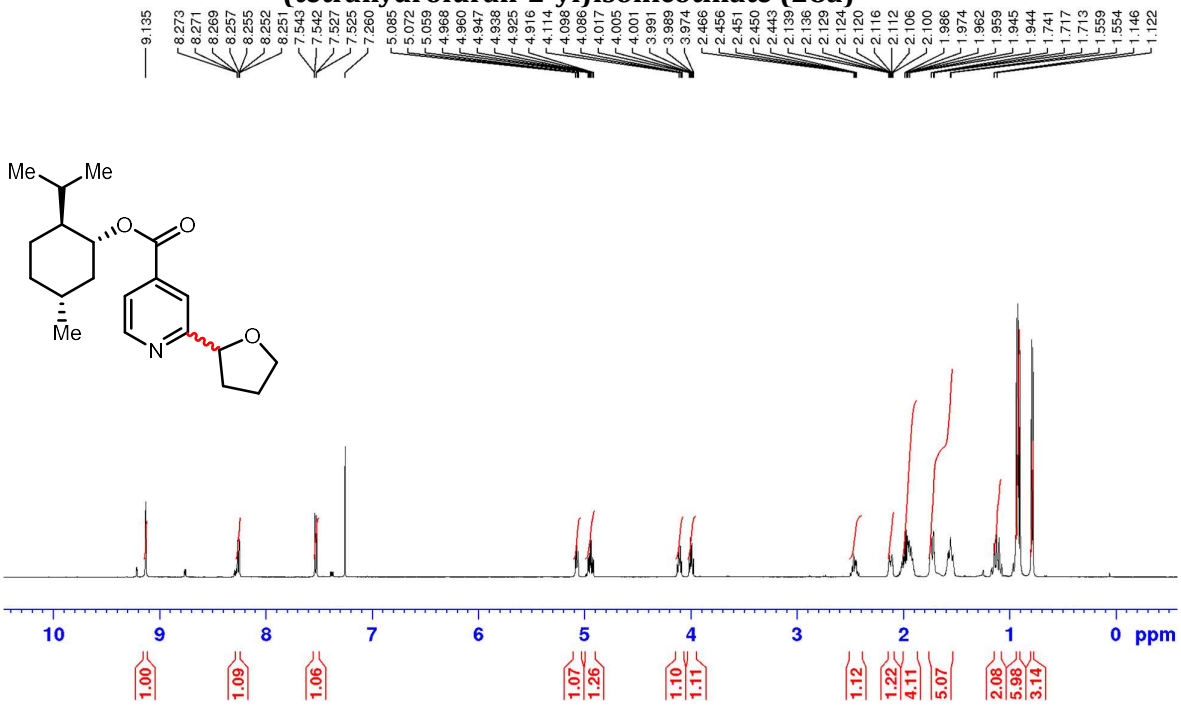

^{13}C NMR (126 MHz, $CDCl_3$) of (1*R*,2*S*,5*R*)-2-isopropyl-5-methylcyclohexyl-2-(tetrahydrofuran-2-yl)isonicotinate (28a)

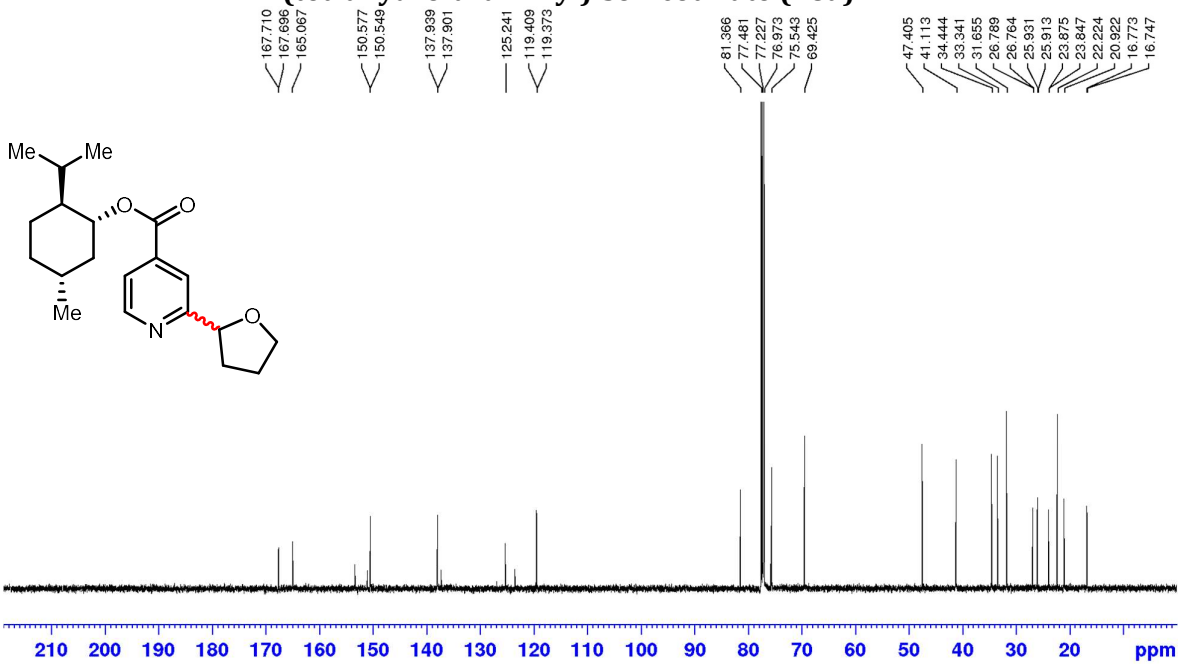

^{1}H NMR (500 MHz, $CDCl_3$) of (*R*)-methyl-2-(2-(tetrahydrofuran-2-yl)isonicotinamido)propanoate (29a)

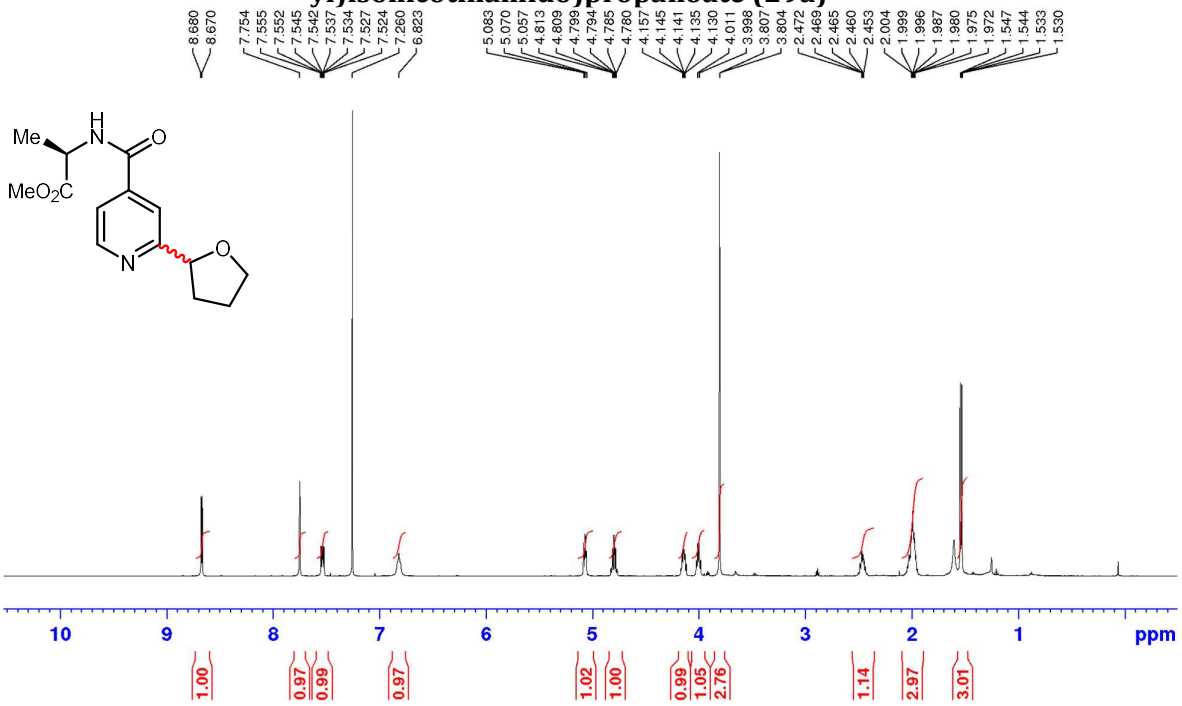

^{13}C NMR (126 MHz, $CDCl_3$) of (*R*)-methyl-2-(2-(tetrahydrofuran-2-yl)isonicotinamido)propanoate (29a)

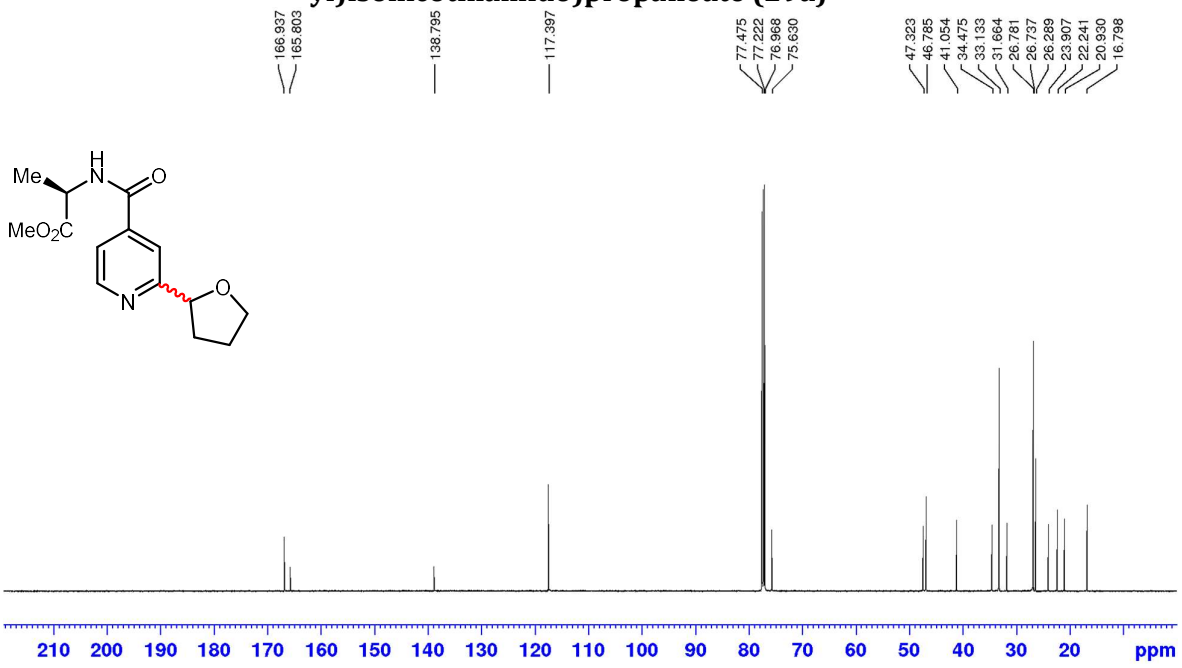

^{1}H NMR (500 MHz, $CDCl_3$) of 4-(5-methyltetrahydrofuran-2-yl)-2-phenylquinoline (31a)

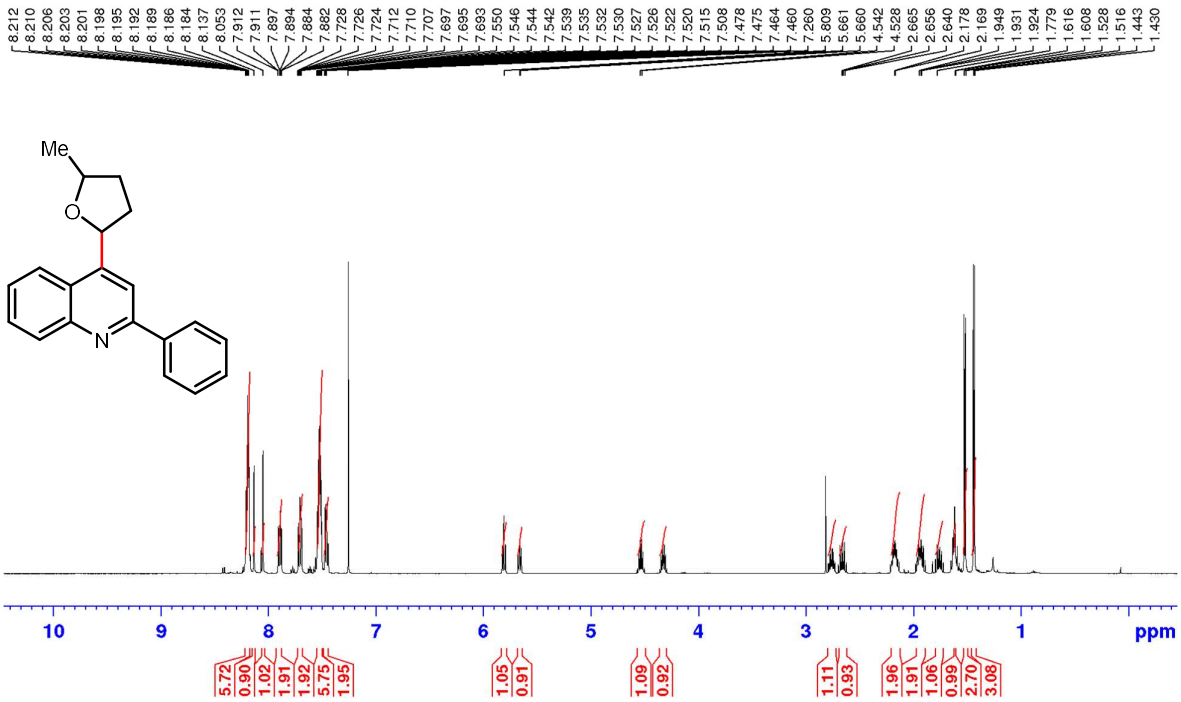

^{13}C NMR (126 MHz, $CDCl_3$) of 4-(5-methyltetrahydrofuran-2-yl)-2-phenylquinoline (31a)

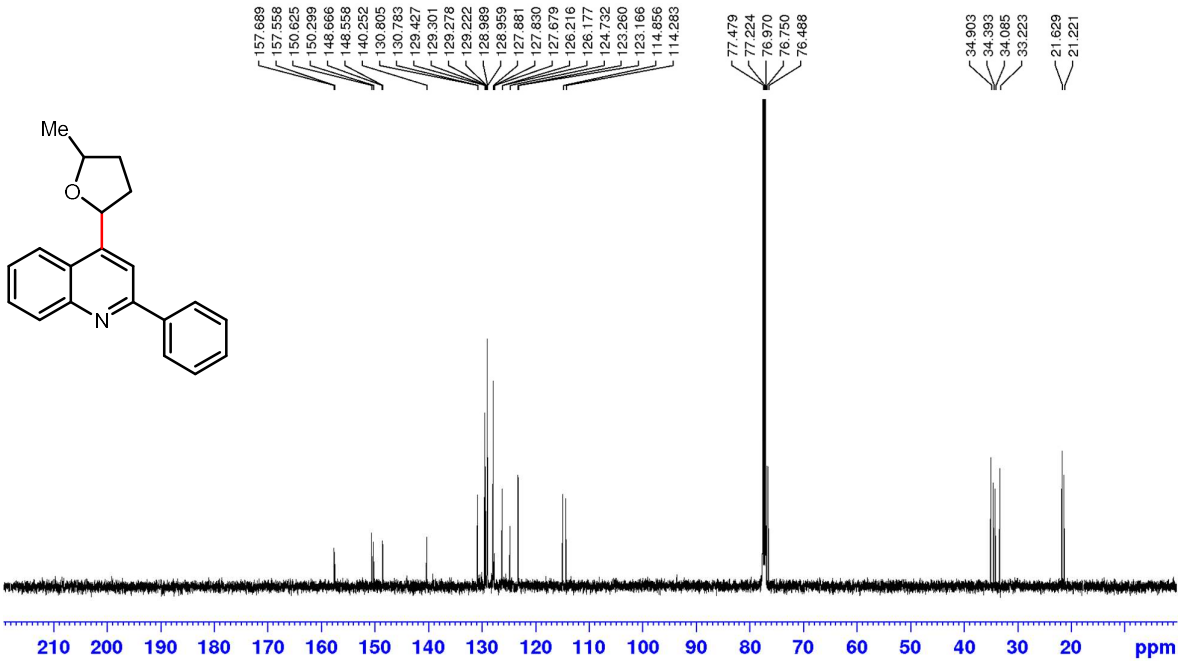

^{1}H NMR (500 MHz, $CDCl_3$) of 4-(1-(benzyloxy)ethyl)-2-phenylquinoline (32a)

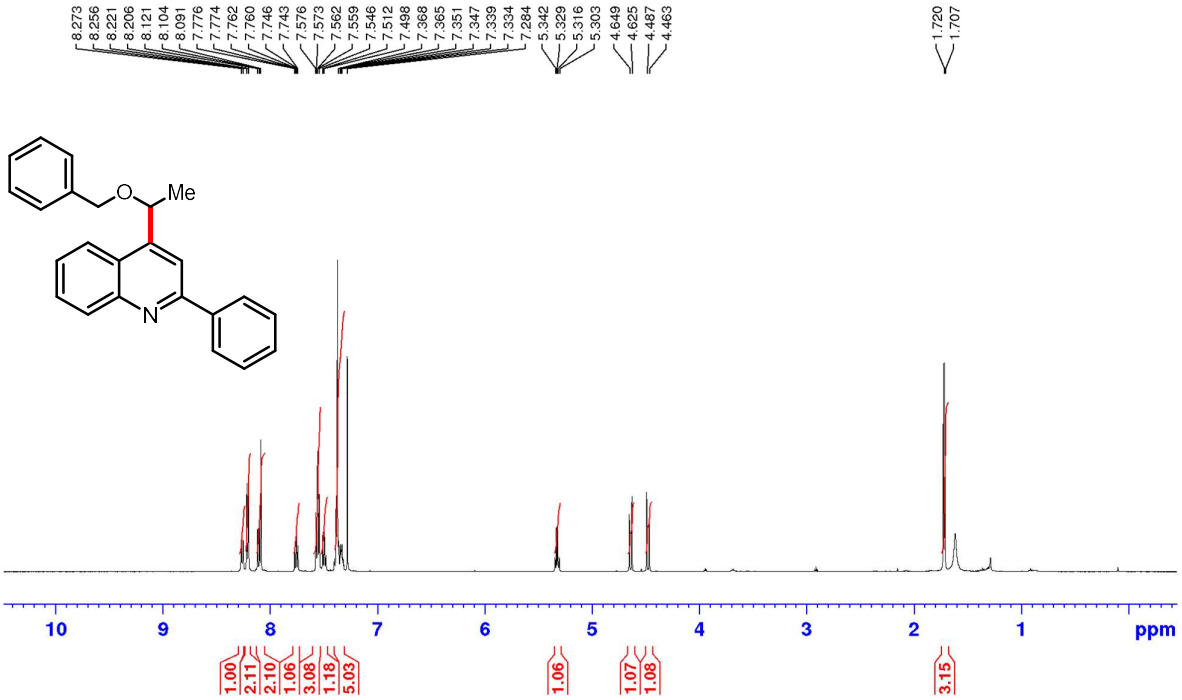

^{13}C NMR (126 MHz, $CDCl_3$) of 4-(1-(benzyloxy)ethyl)-2-phenylquinoline (32a)

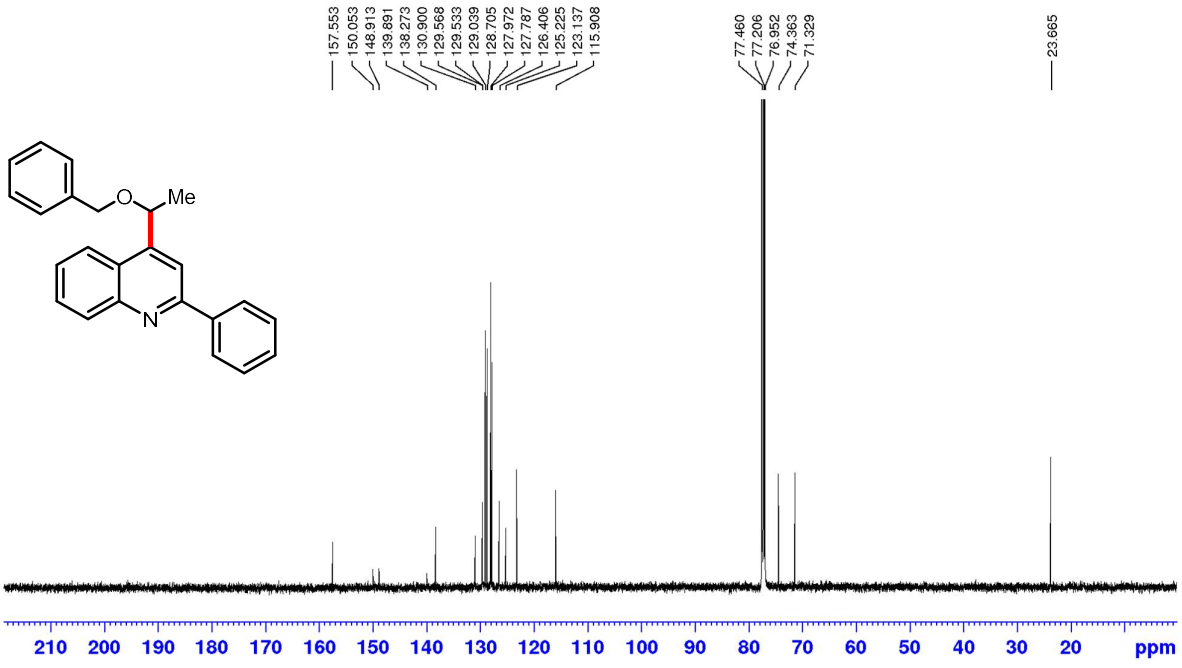

^{1}H NMR (500 MHz, $CDCl_3$) of 4-(1,2-dimethoxyethyl)-2-phenylquinoline (33a)

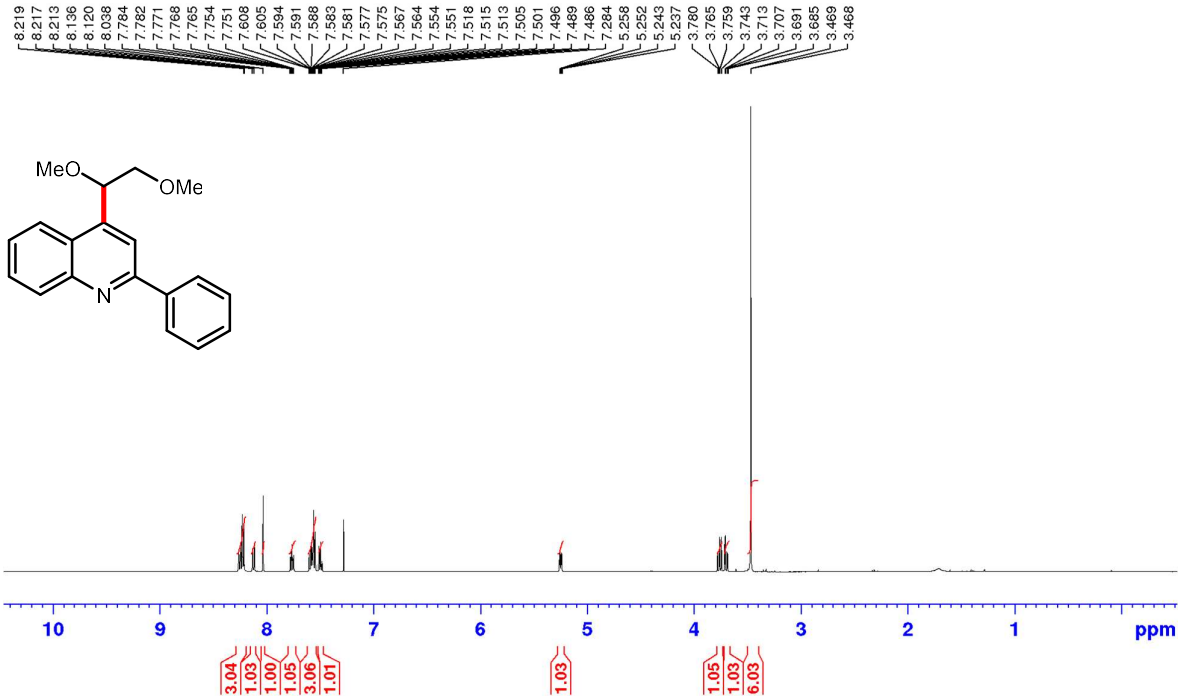

^{13}C NMR (126 MHz, $CDCl_3$) of 4-(1,2-dimethoxyethyl)-2-phenylquinoline (33a)

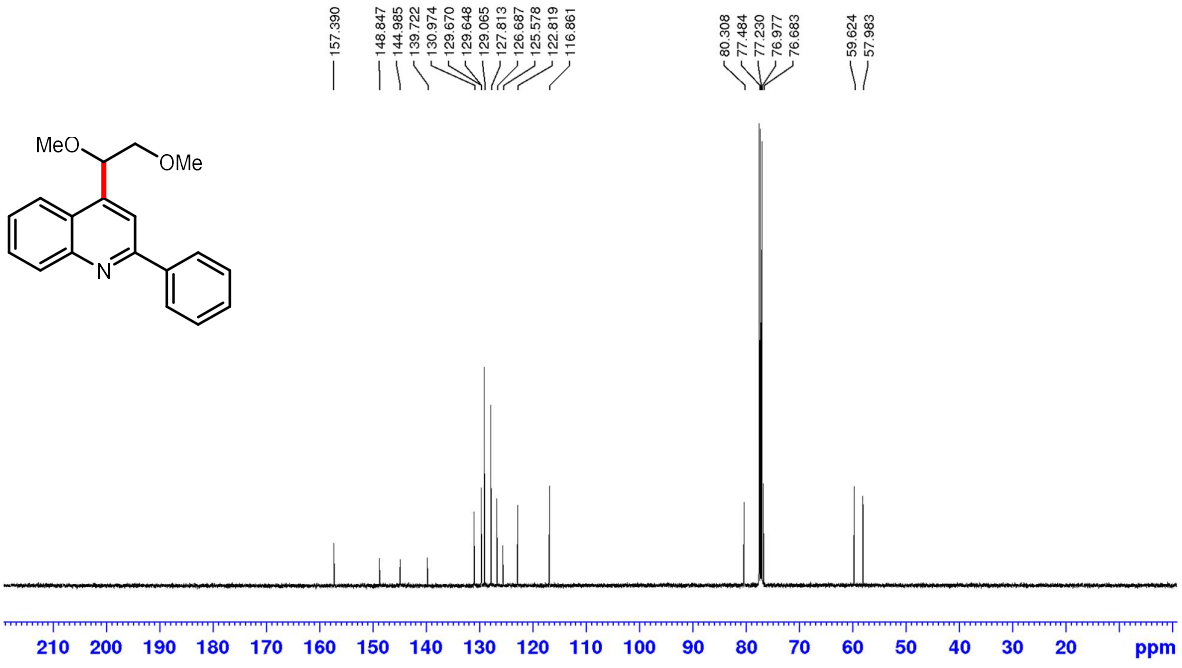

^{1}H NMR (500 MHz, $CDCl_3$) of 4-cyclohexyl-2-phenethylquinoline (39a)

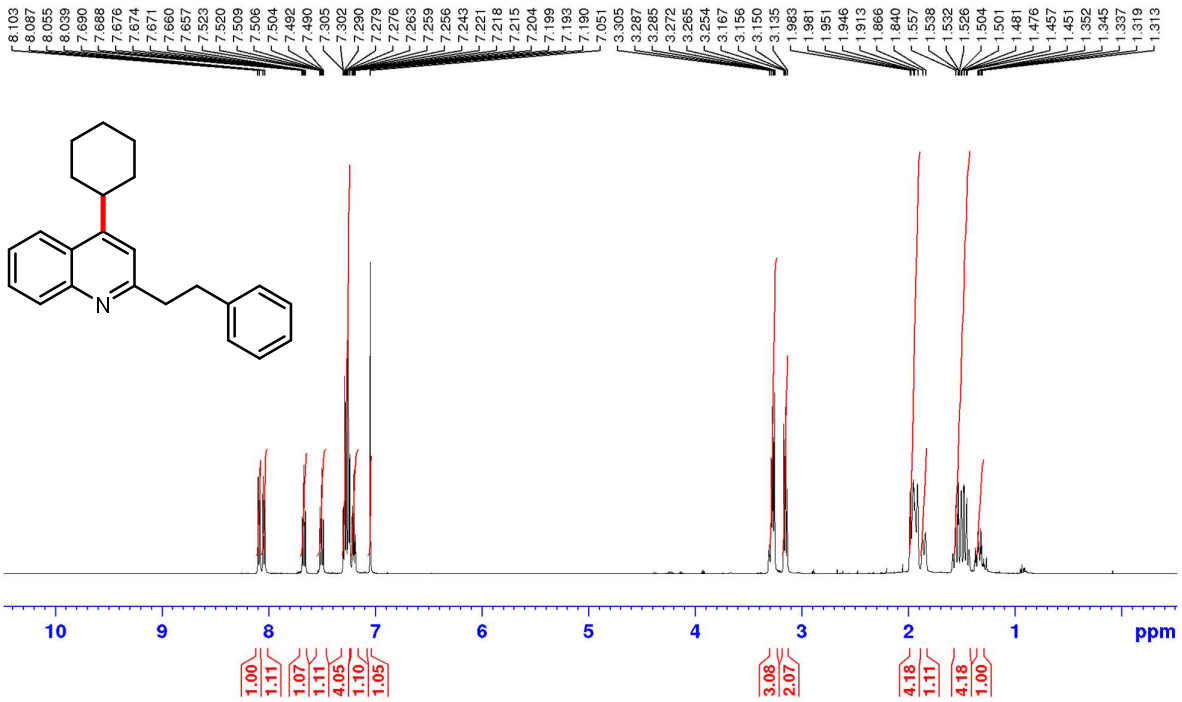

^{13}C NMR (126 MHz, $CDCl_3$) of 4-cyclohexyl-2-phenethylquinoline (39a)

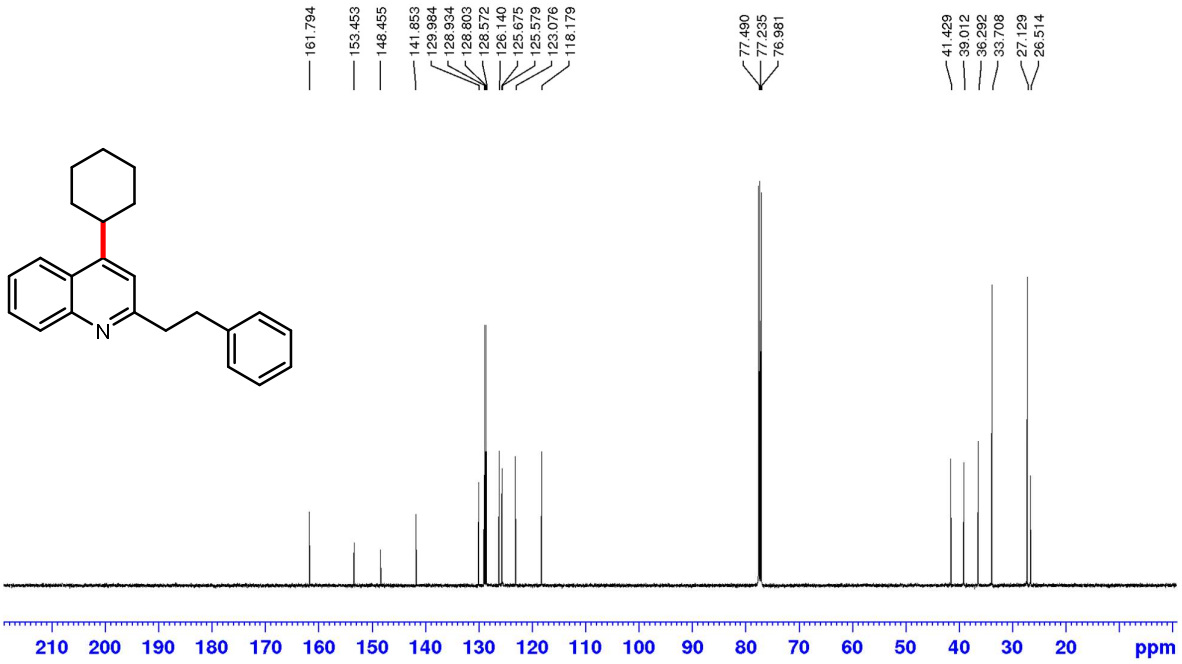

^{1}H NMR (500 MHz, $CDCl_3$) of 4,6-dichloro-2-cyclohexylpyrimidine (44a)

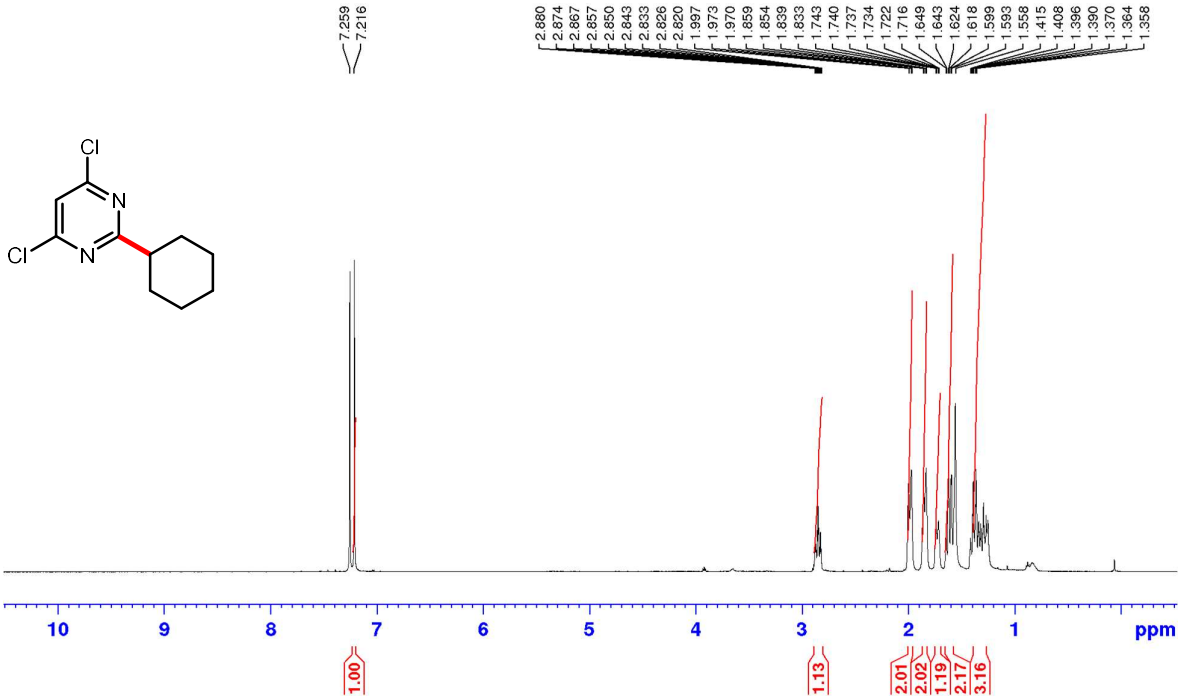

^{13}C NMR (126 MHz, $CDCl_3$) of 4,6-dichloro-2-cyclohexylpyrimidine (44a)

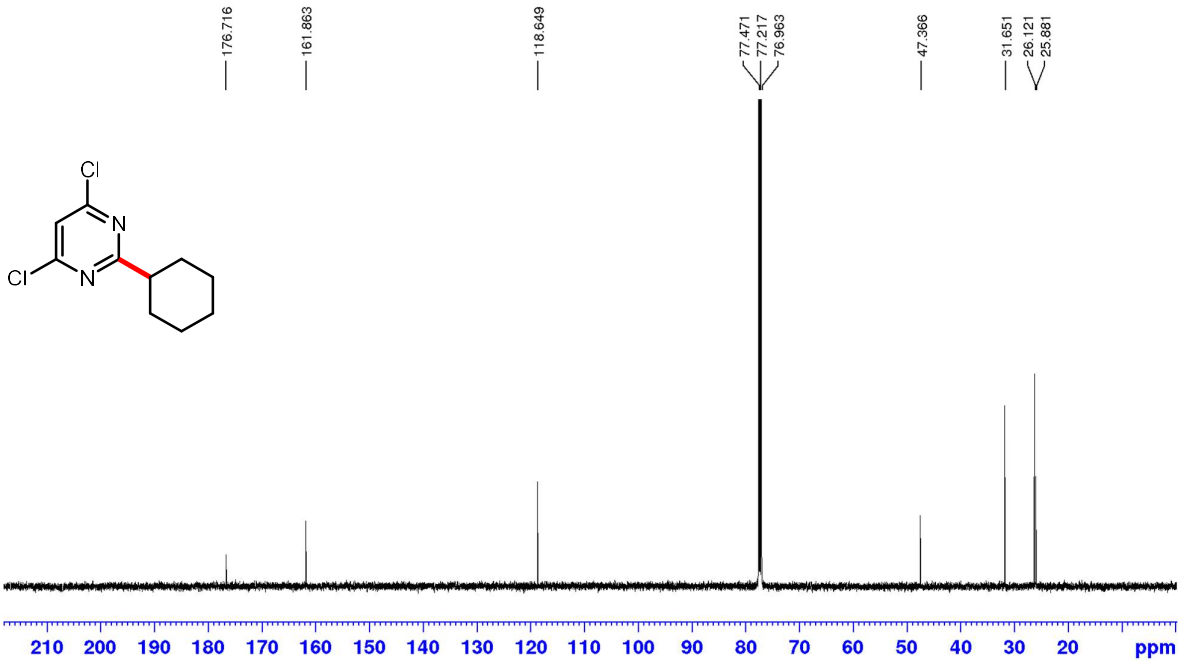

^{1}H NMR (500 MHz, $CDCl_3$) of ethyl 2-cyclohexylisonicotinate (45a)

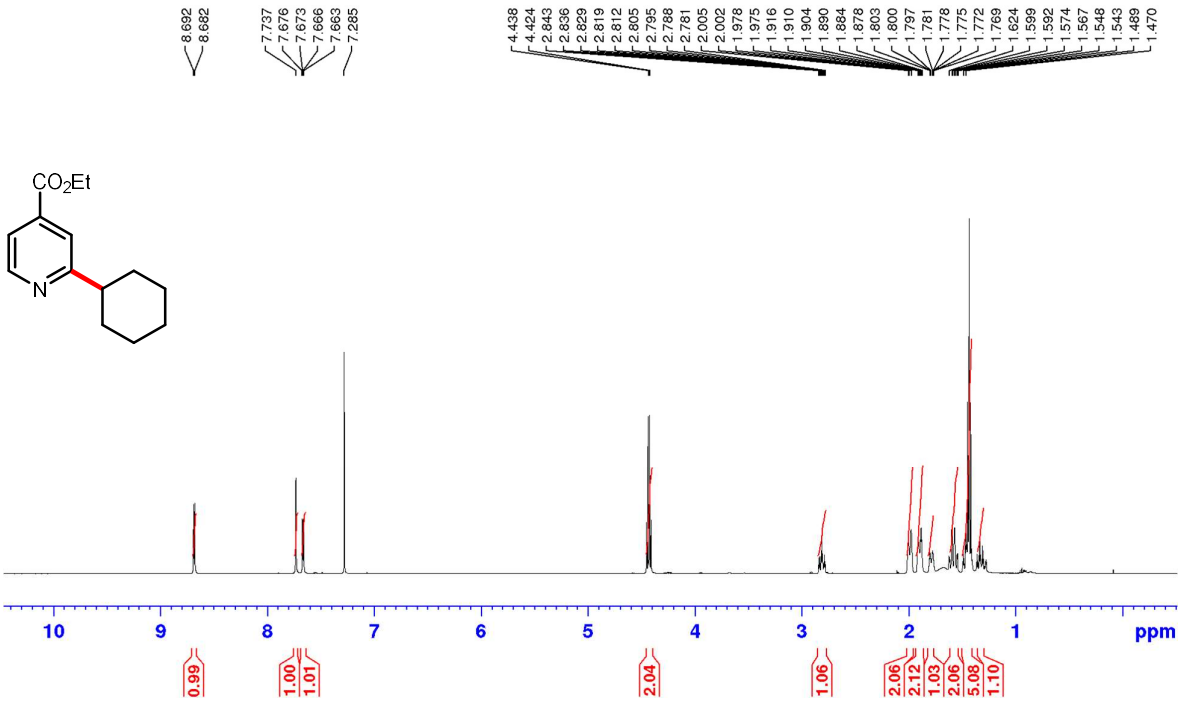

^{13}C NMR (126 MHz, $CDCl_3$) of ethyl 2-cyclohexylisonicotinate (45a)

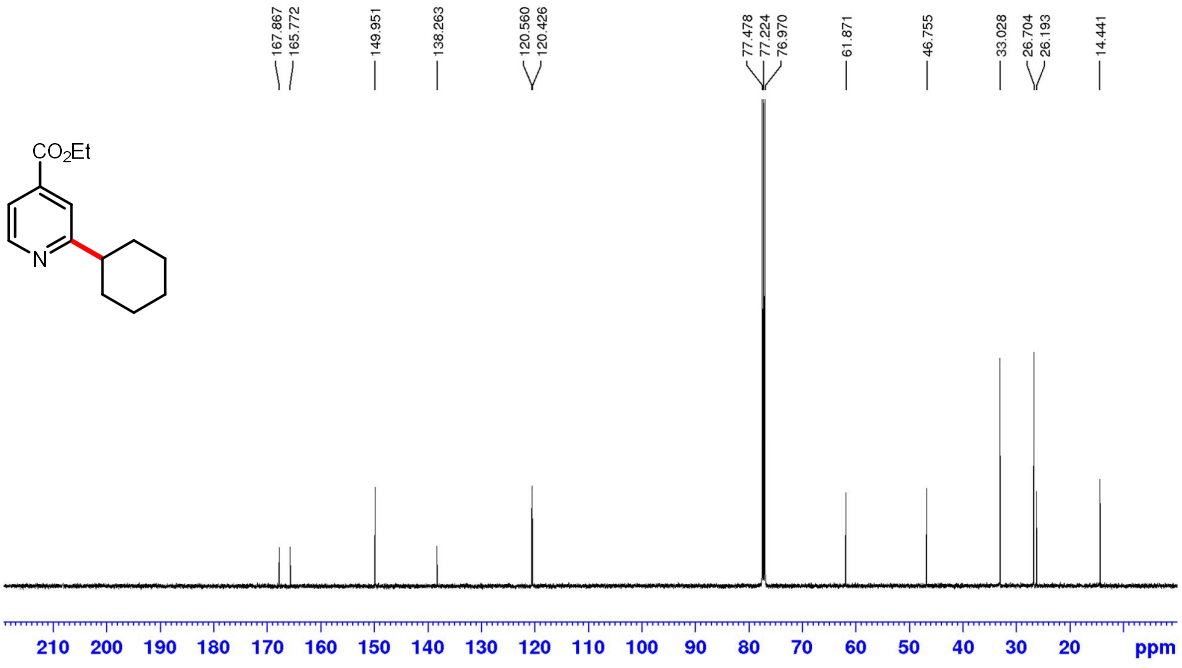

^{1}H NMR (500 MHz, $CDCl_3$) of ethyl 2-cyclohexylpyridine-4-carbothioate (46a)

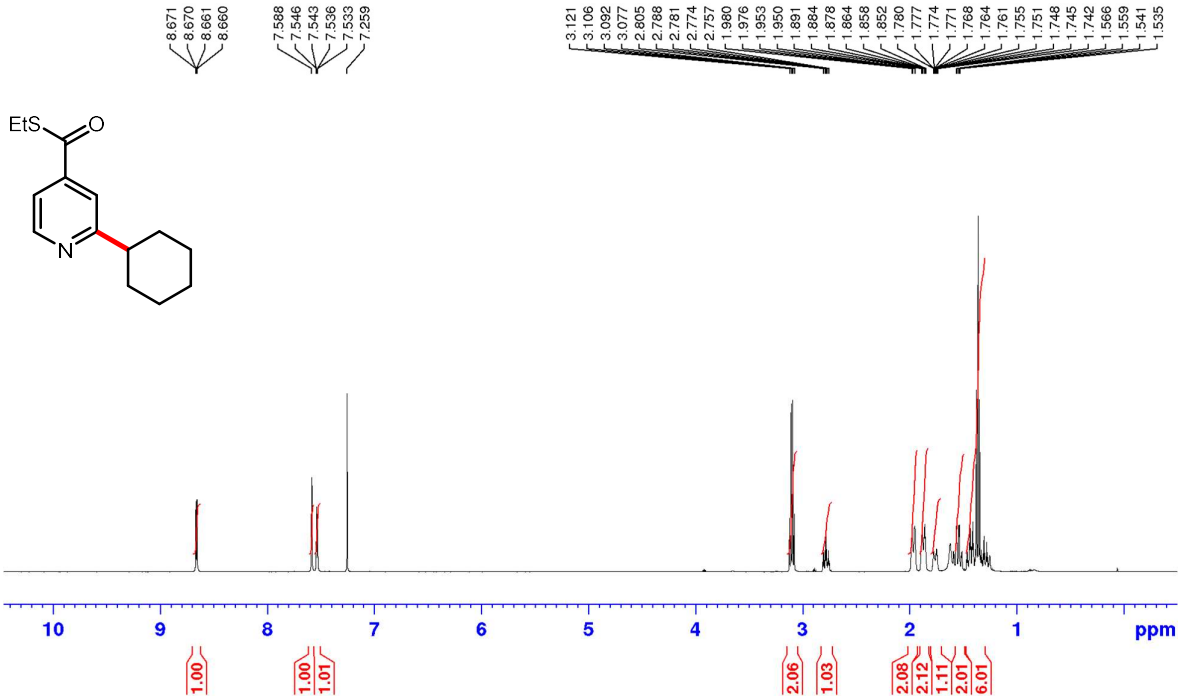

^{13}C NMR (126 MHz, $CDCl_3$) of ethyl 2-cyclohexylpyridine-4-carbothioate (46a)

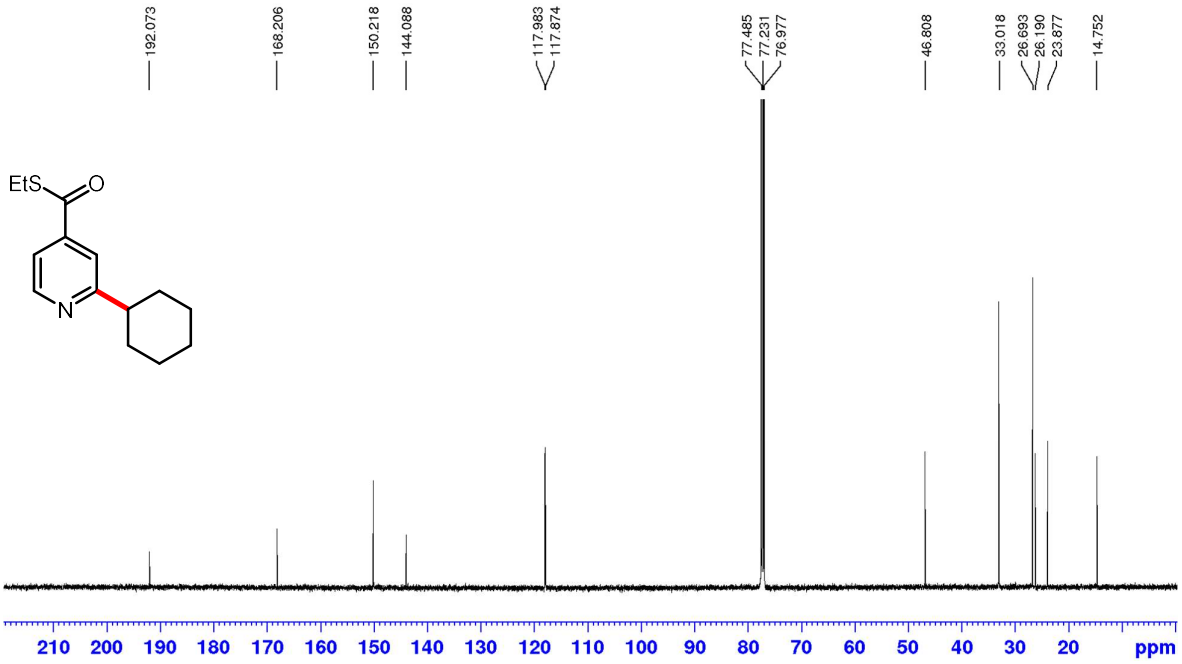

^{1}H NMR (500 MHz, $CDCl_3$) of (2,6-dicyclohexylpyridin-4-yl)(morpholino)methanone (47a)

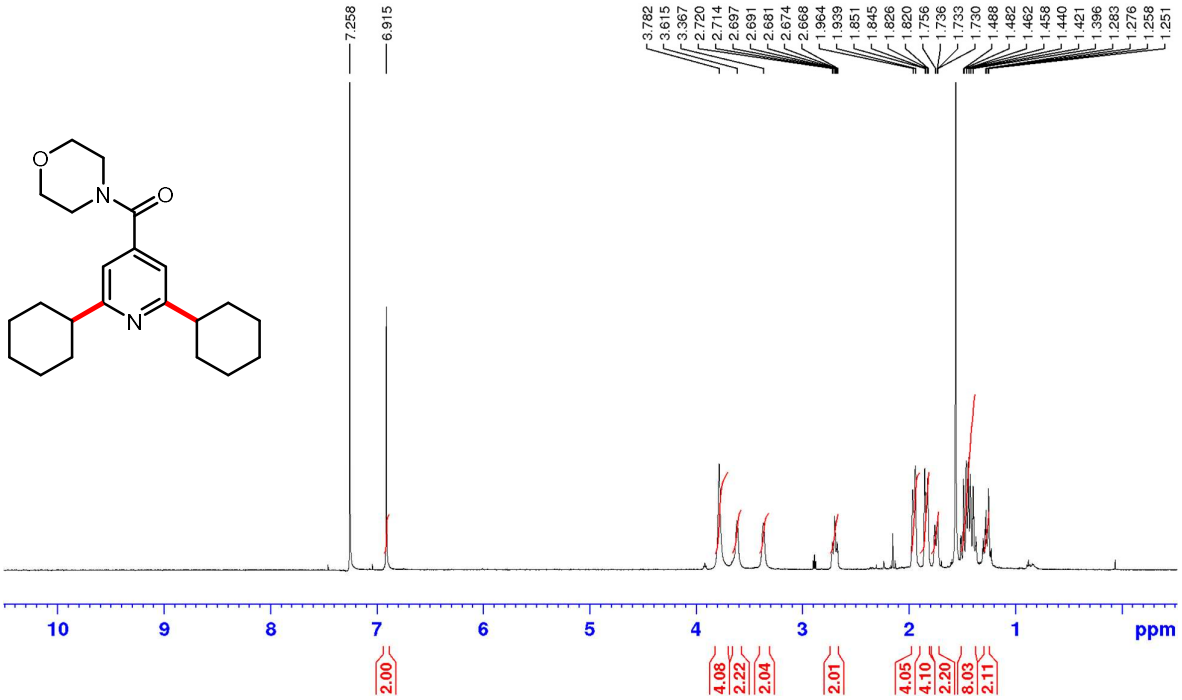

^{13}C NMR (126 MHz, $CDCl_3$) of (2,6-dicyclohexylpyridin-4-yl)(morpholino)methanone (47a)

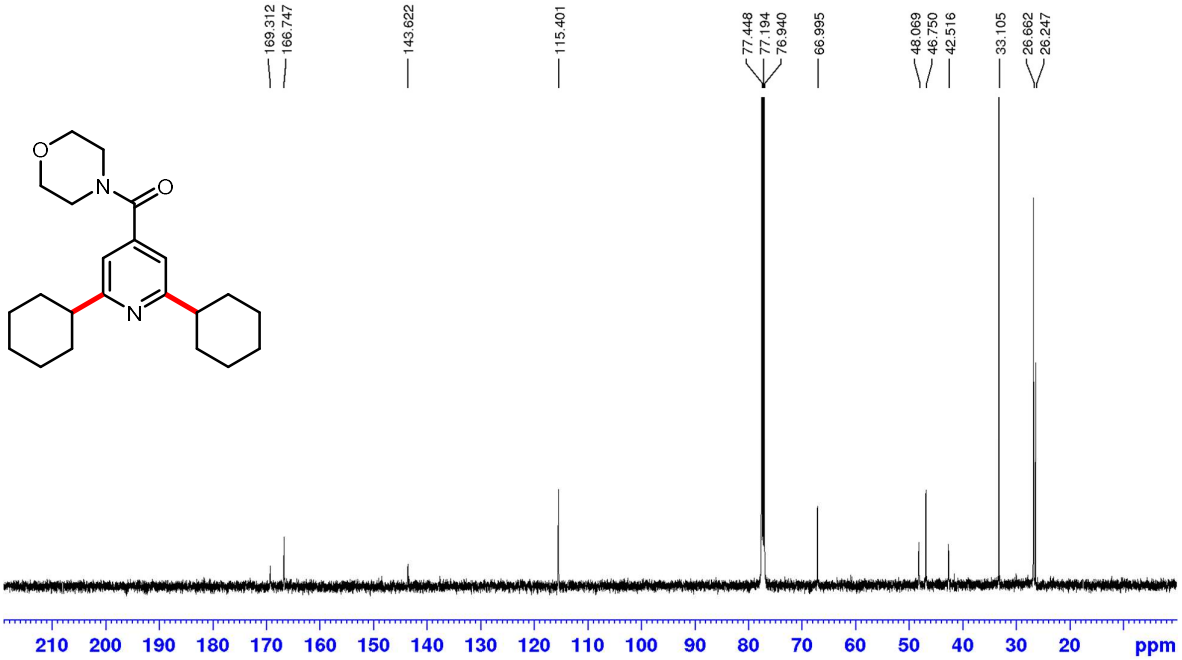

^{1}H NMR (500 MHz, $CDCl_3$) of 4-cyclopentyl-2-phenylquinoline (49a)

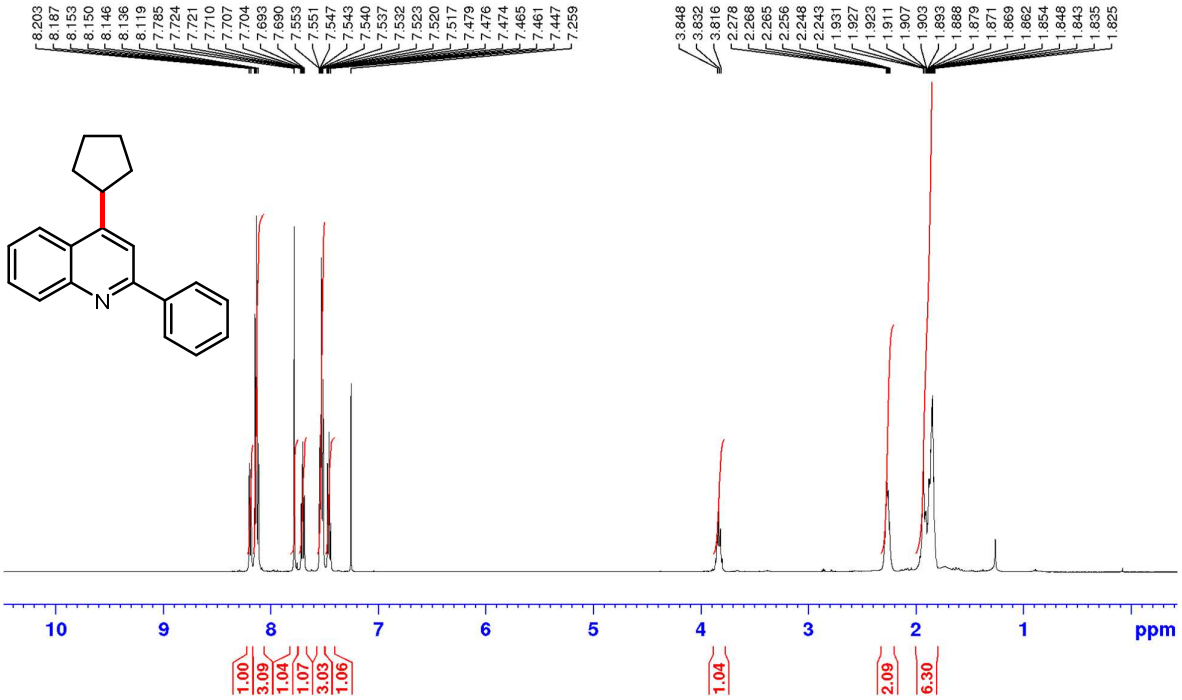

^{13}C NMR (126 MHz, $CDCl_3$) of 4-cyclopentyl-2-phenylquinoline (49a)

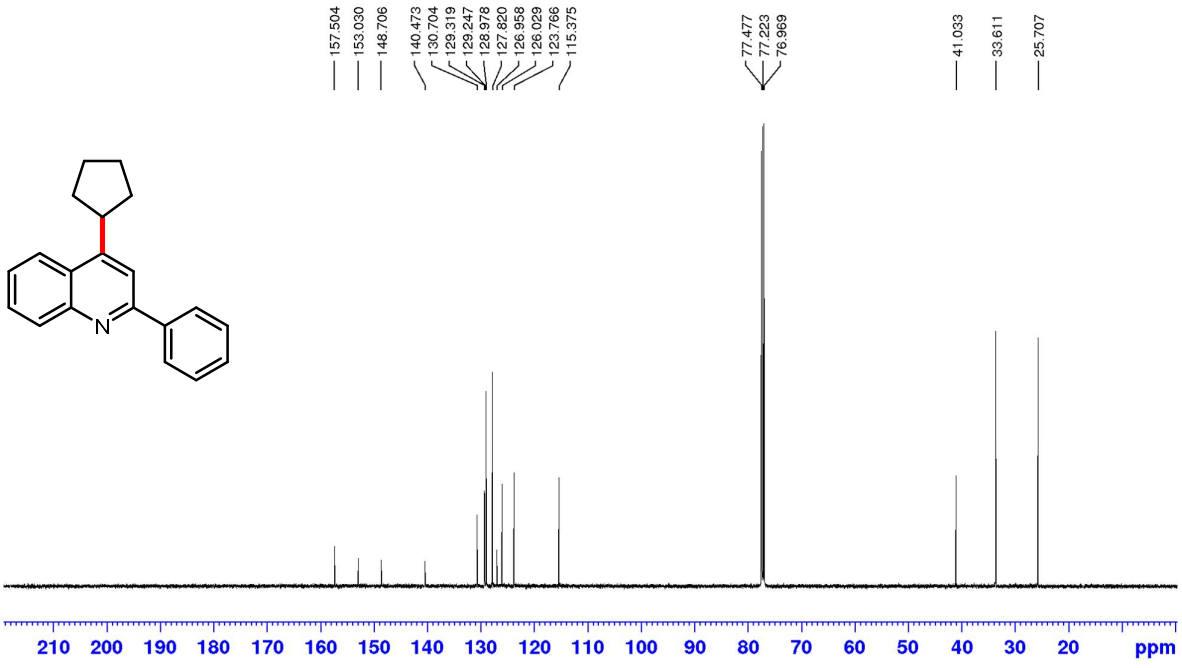

^{1}H NMR (500 MHz, $CDCl_3$) of 4-cyclooctyl-2-phenylquinoline (50a)

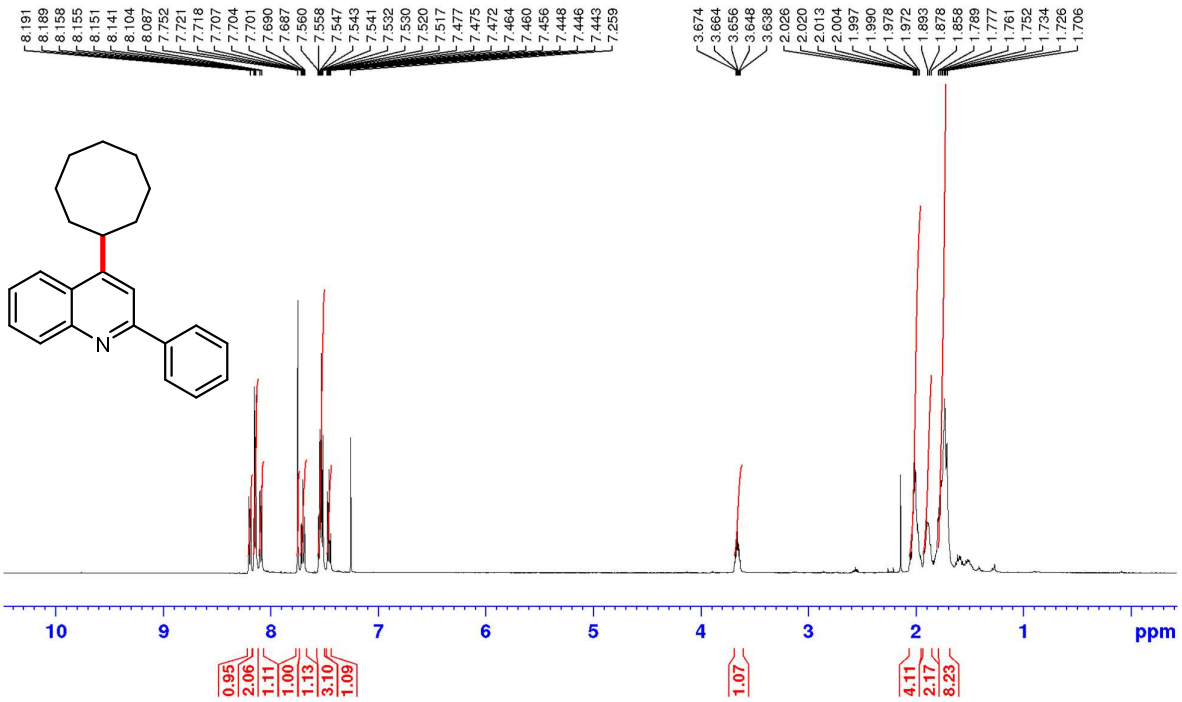

^{13}C NMR (126 MHz, $CDCl_3$) of 4-cyclooctyl-2-phenylquinoline (50a)

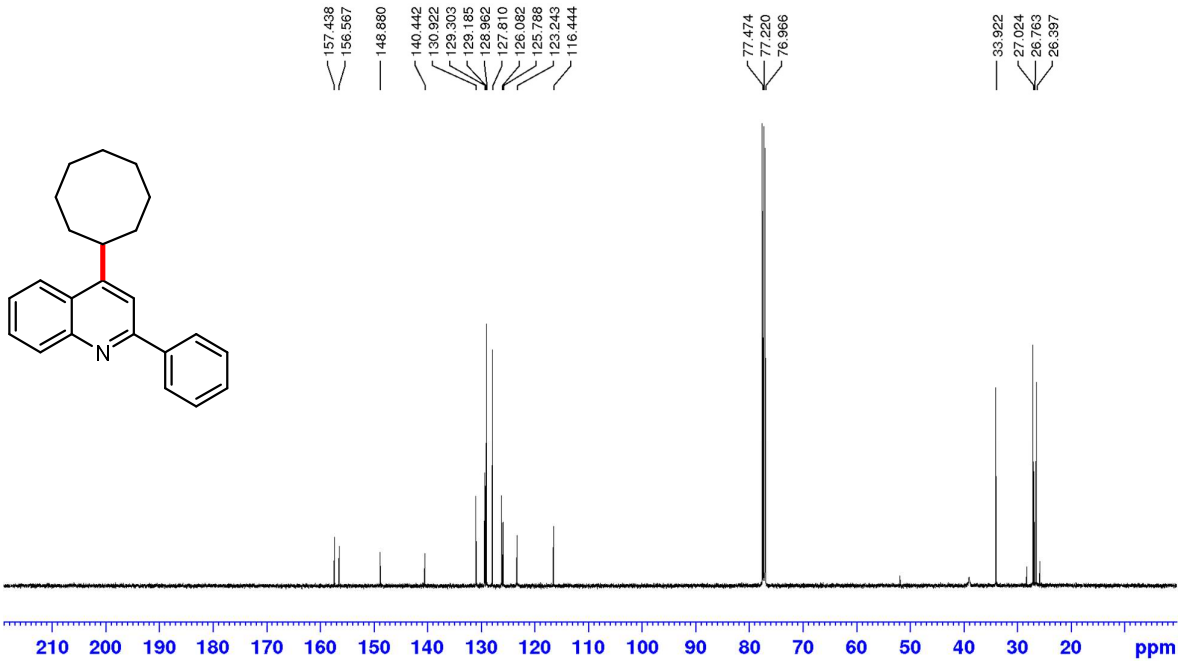

^{1}H NMR (500 MHz, $CDCl_3$) of 4-(bicyclo[2.2.1]heptan-2-yl)-2-phenylquinoline (51a)

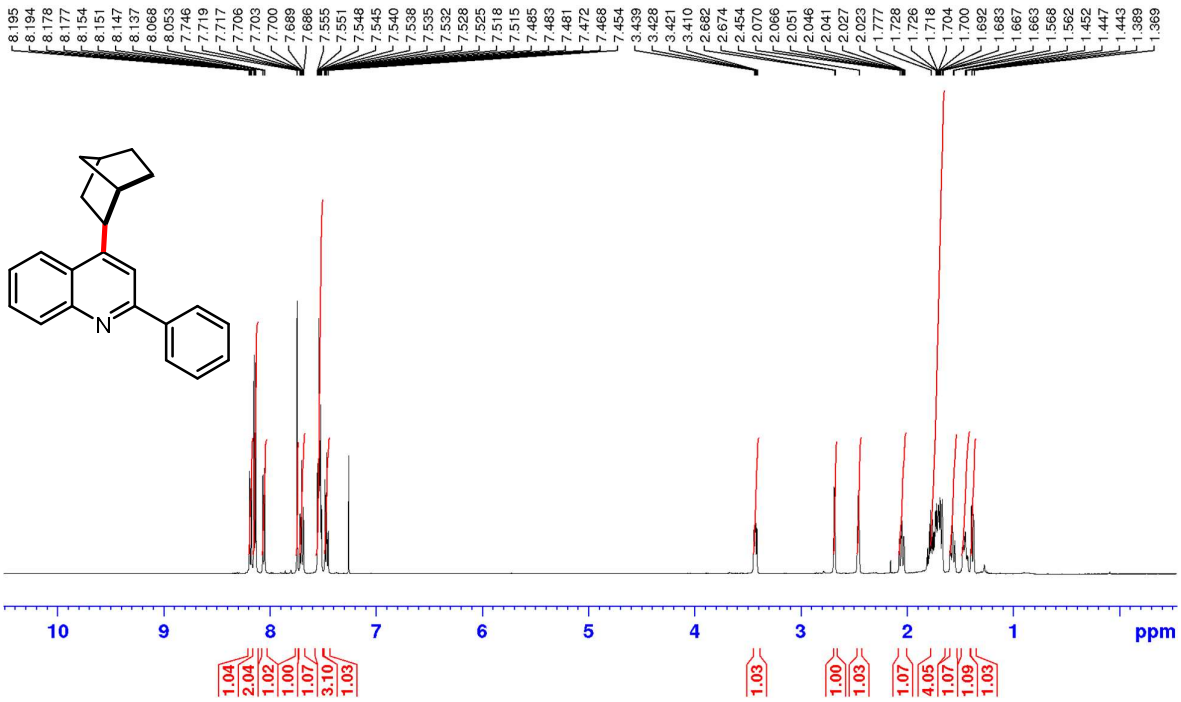

^{13}C NMR (126 MHz, $CDCl_3$) of 4-(bicyclo[2.2.1]heptan-2-yl)-2-phenylquinoline (51a)

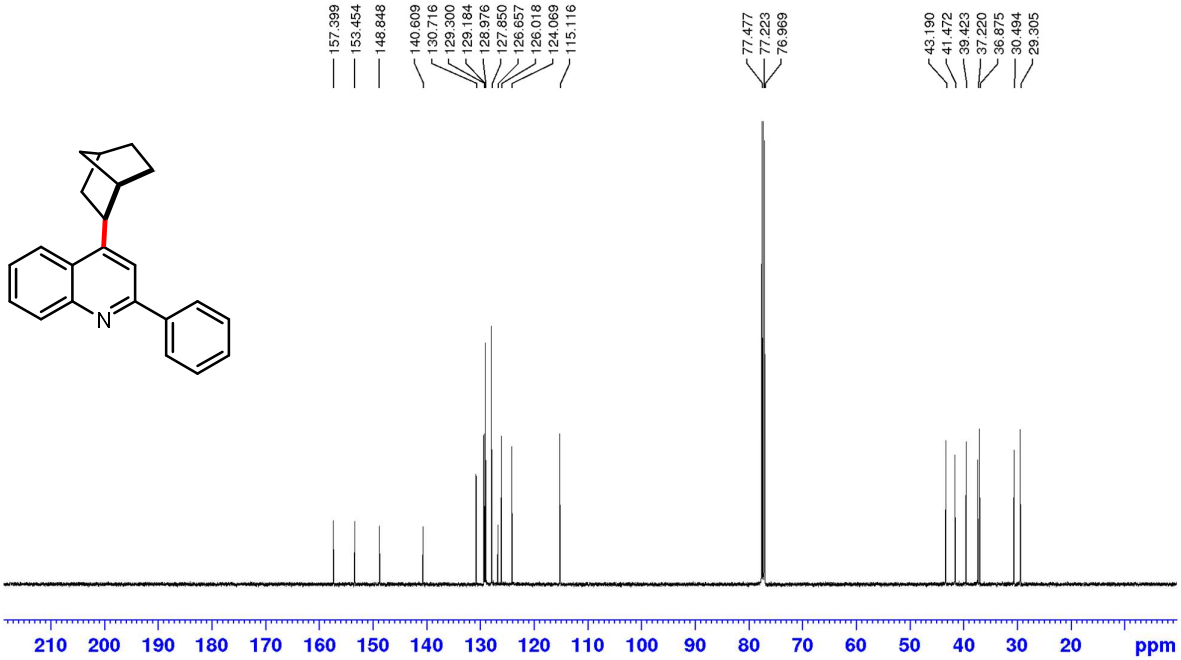

^{1}H NMR (500 MHz, $CDCl_3$) of 3-(2-phenylquinolin-4-yl)cyclopentanone (52a)

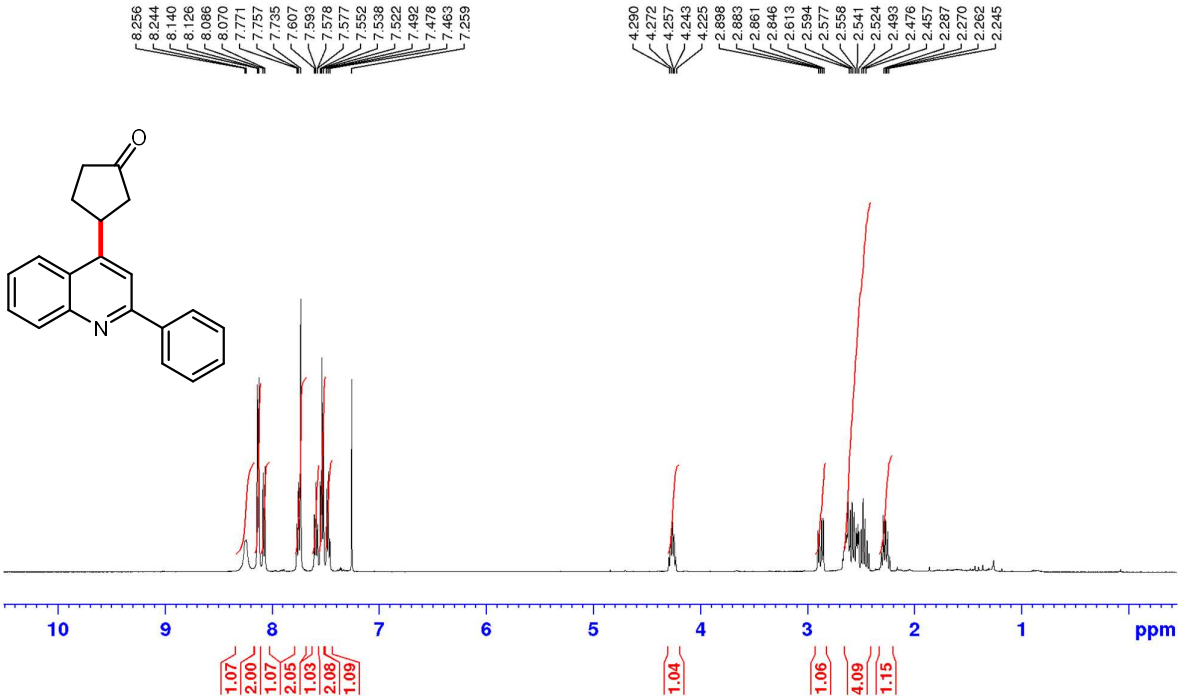

^{13}C NMR (126 MHz, $CDCl_3$) of 3-(2-phenylquinolin-4-yl)cyclopentanone (52a)

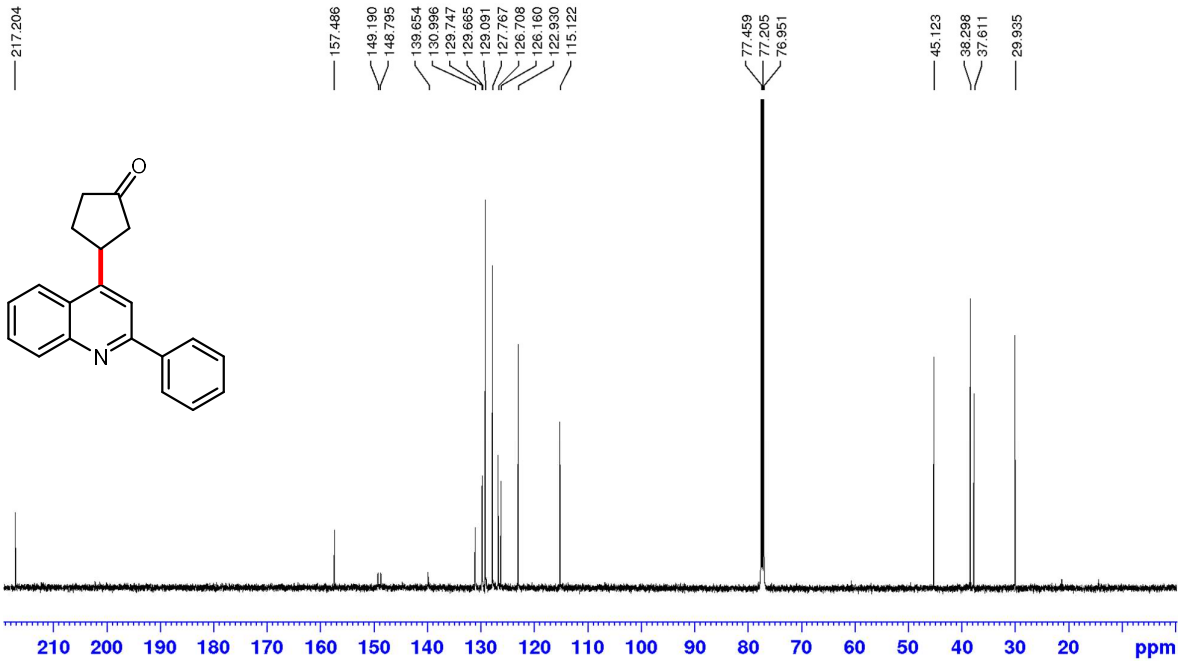

^{1}H NMR (500 MHz, $CDCl_3$) of 4-(7-oxabicyclo[2.2.1]heptan-2-yl)-2-phenylquinoline (53a)

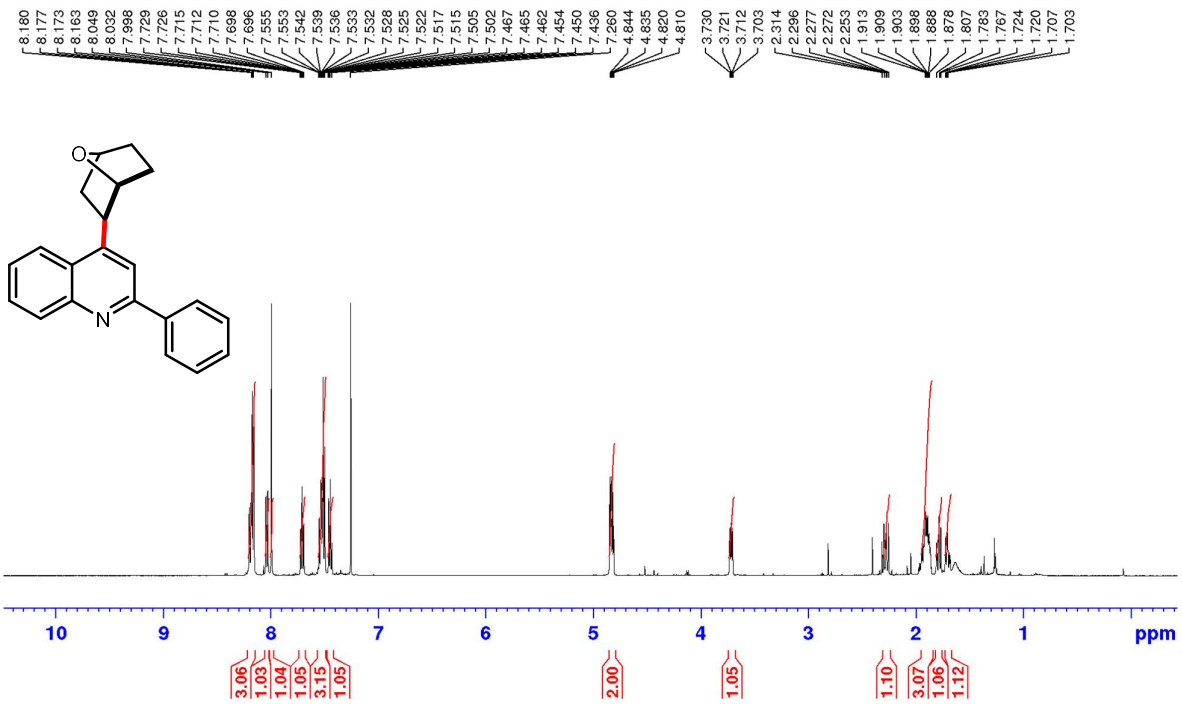

^{13}C NMR (126 MHz, $CDCl_3$) of 4-(7-oxabicyclo[2.2.1]heptan-2-yl)-2-phenylquinoline (53a)

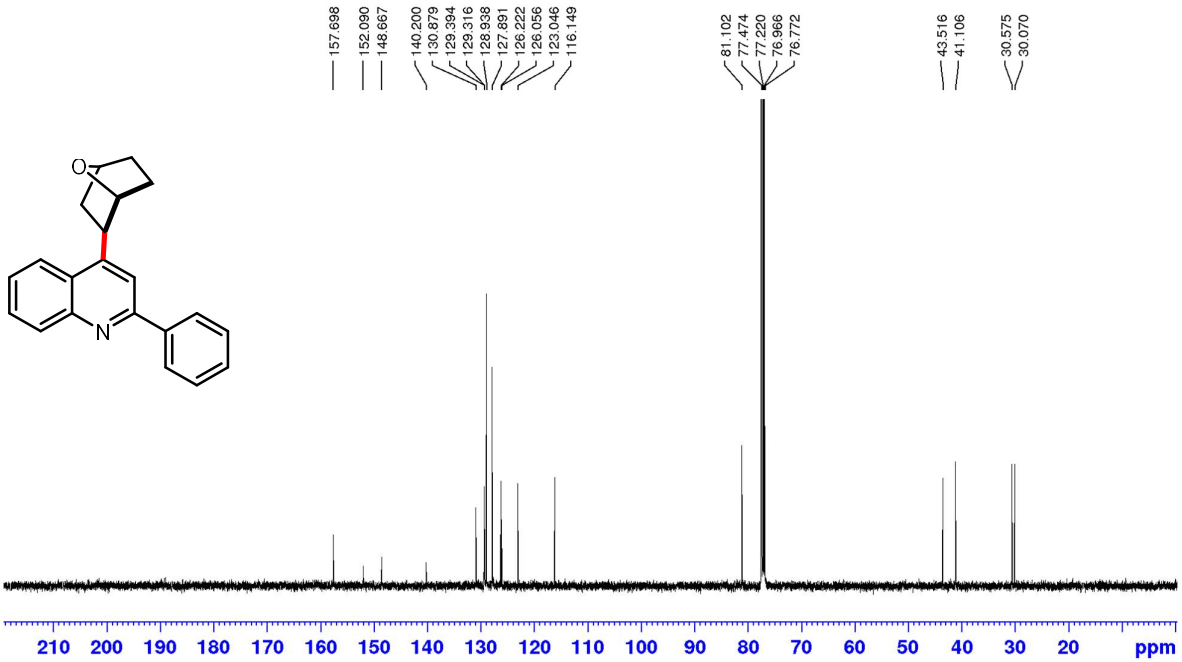

^{1}H NMR (500 MHz, $CDCl_3$) of 4-benzyl-2-phenylquinoline (54a)

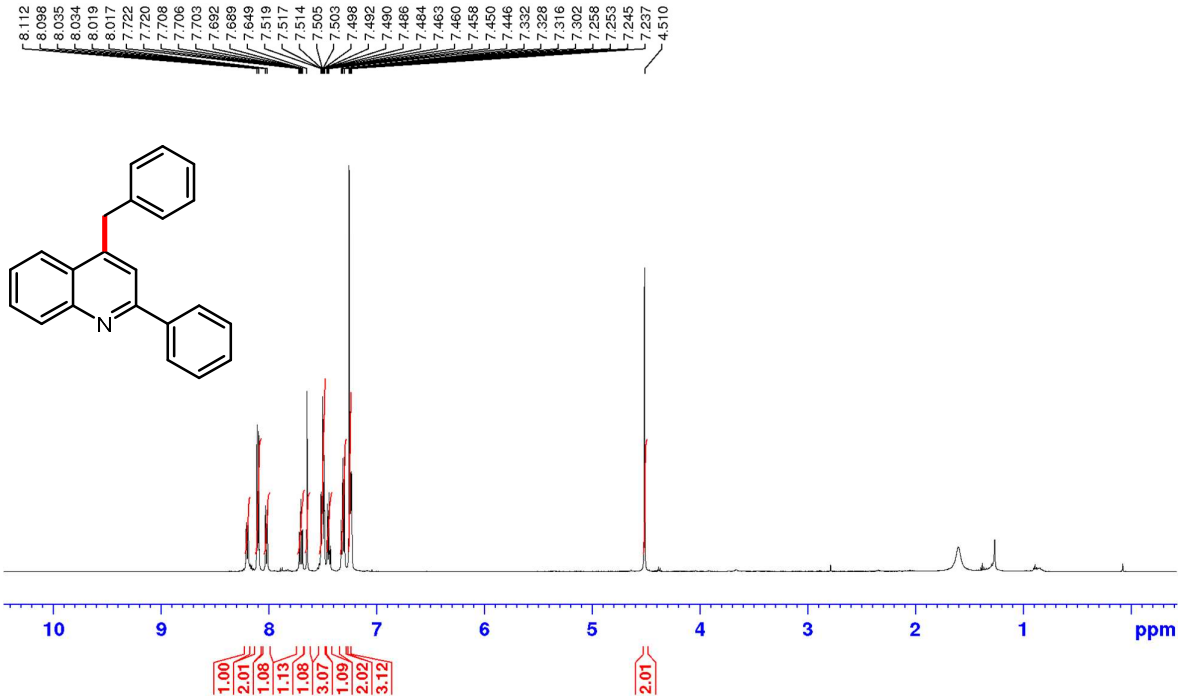

^{13}C NMR (126 MHz, $CDCl_3$) of 4-benzyl-2-phenylquinoline (54a)

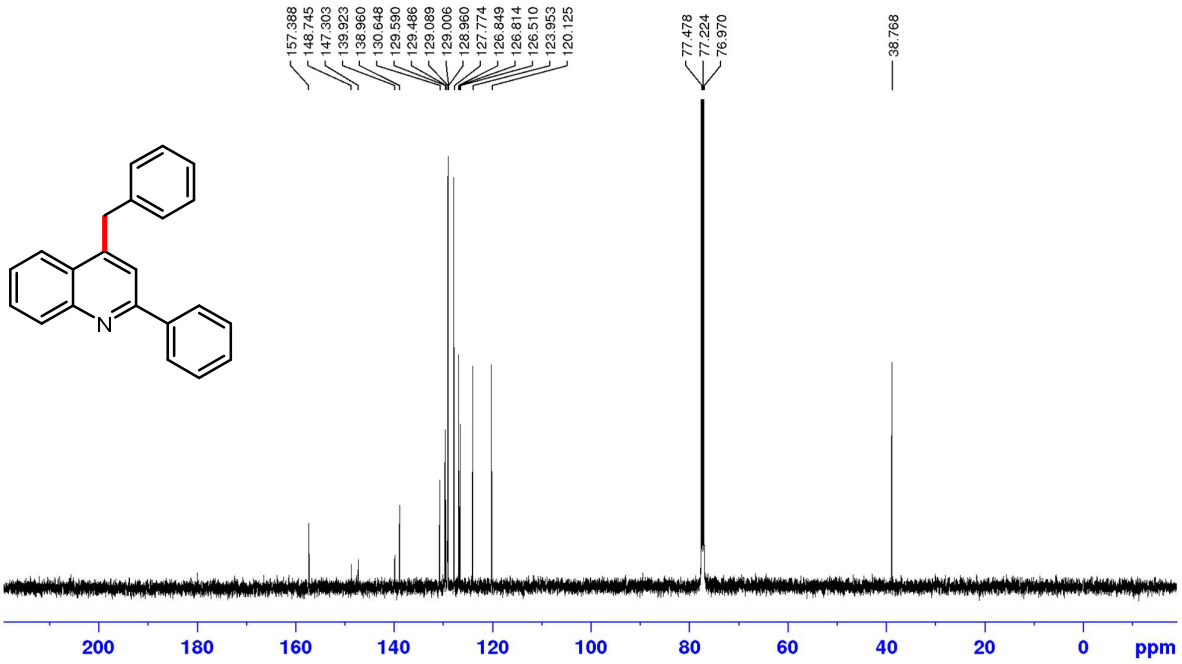

^{1}H NMR (500 MHz, $CDCl_3$) of (1*R*)-(2-cyclohexyl-6-methoxyquinolin-4-yl)((2*S*,4*S*,5*R*)-5-vinylquinuclidin-2-yl)methanol (55a)

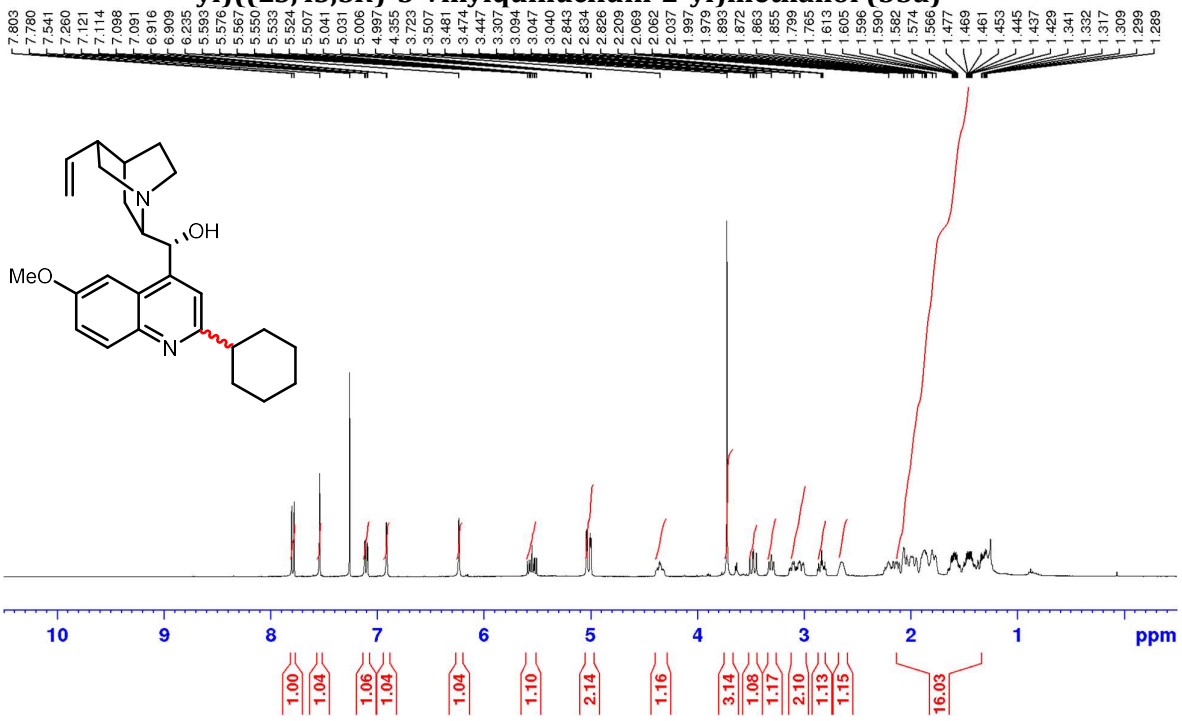

^{13}C NMR (126 MHz, $CDCl_3$) of (1*R*)-(2-cyclohexyl-6-methoxyquinolin-4-yl)((2*S*,4*S*,5*R*)-5-vinylquinuclidin-2-yl)methanol (55a)

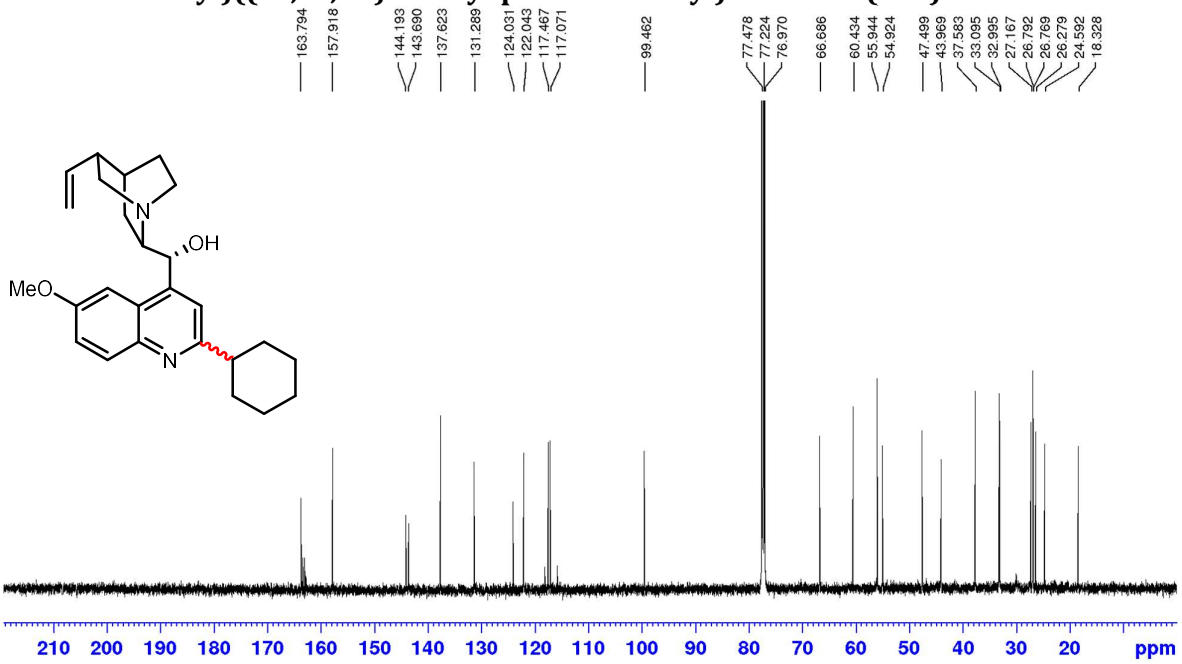

^{1}H NMR (500 MHz, $CDCl_3$) of (1*R*,2*S*,5*R*)-2-isopropyl-5-methylcyclohexyl-2,6-dicyclohexylisonicotinate (57a)

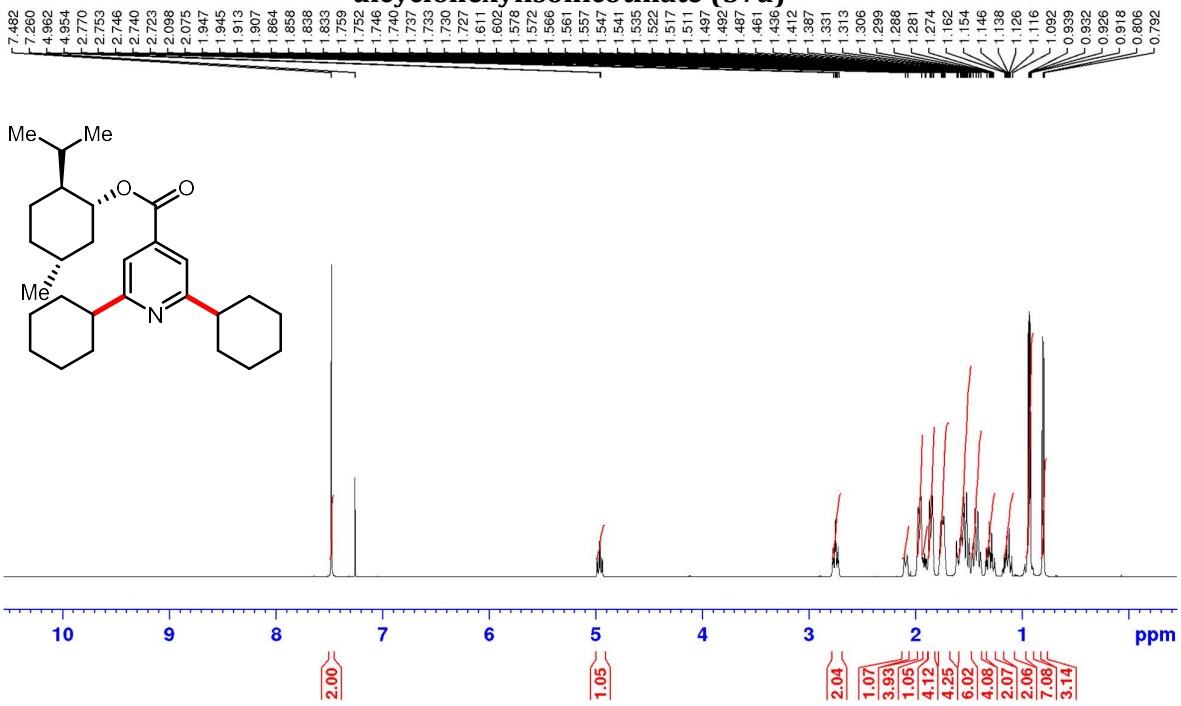

^{13}C NMR (126 MHz, $CDCl_3$) of (1*R*,2*S*,5*R*)-2-isopropyl-5-methylcyclohexyl-2,6-dicyclohexylisonicotinate (57a)

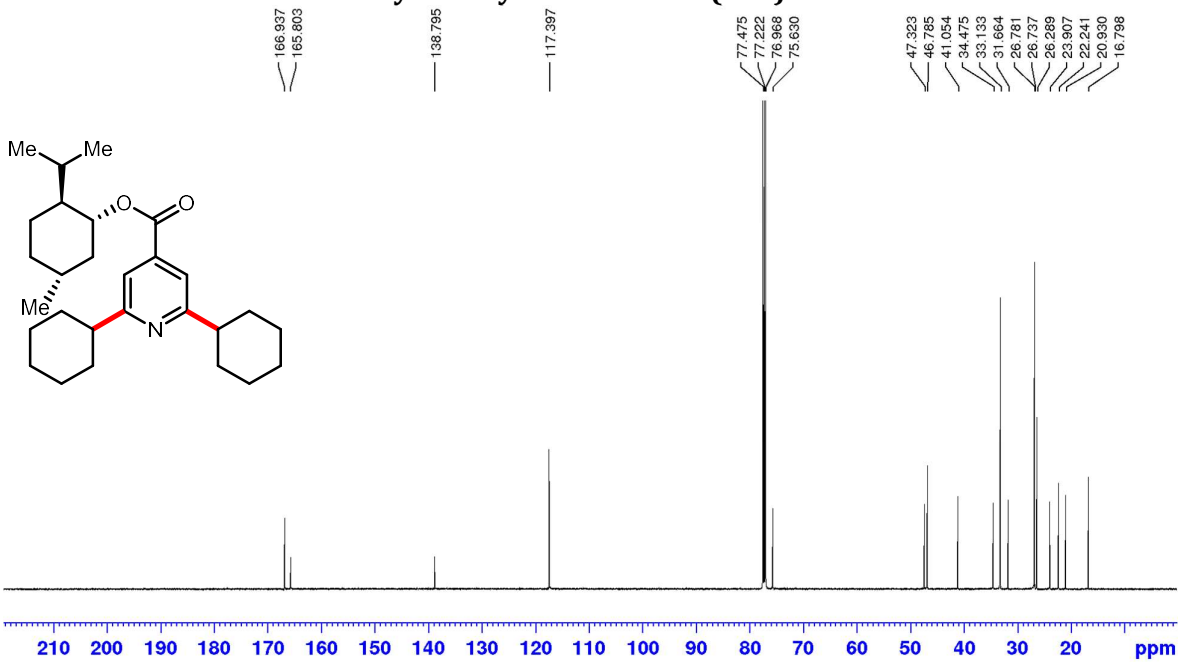

^{1}H NMR (500 MHz, $CDCl_3$) of (*R*)-methyl-2-(2,6-dicyclohexylisonicotinamido)propanoate (58a)

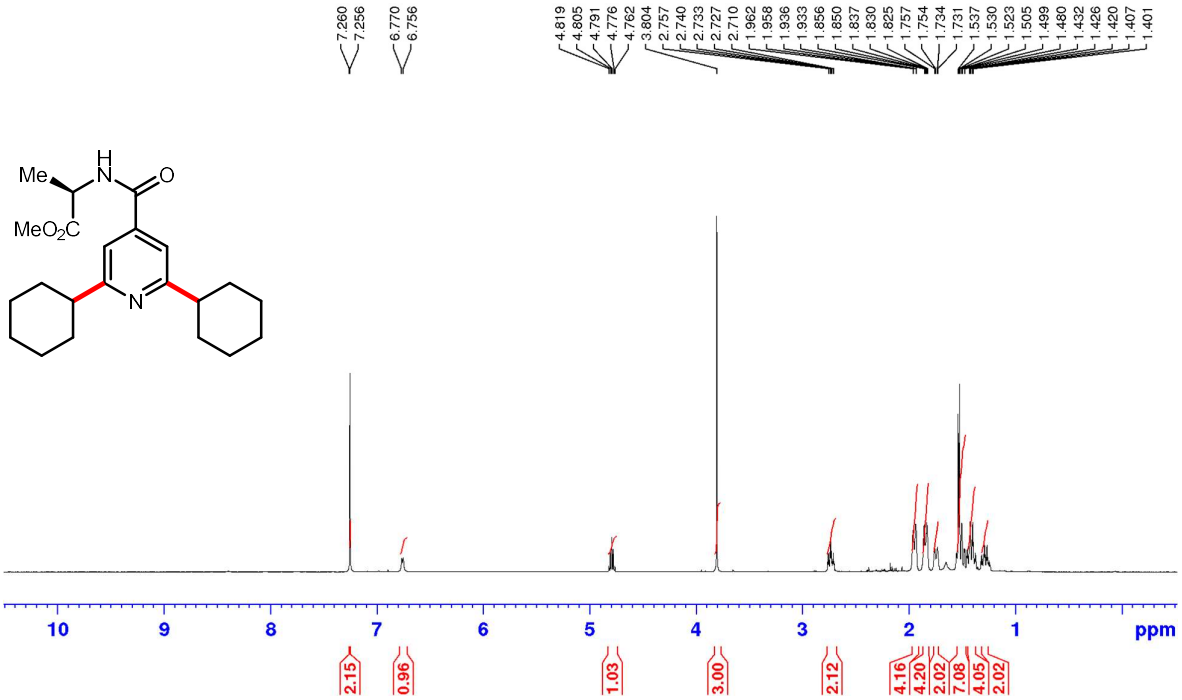

^{13}C NMR (126 MHz, $CDCl_3$) of (*R*)-methyl-2-(2,6-dicyclohexylisonicotinamido)propanoate (58a)

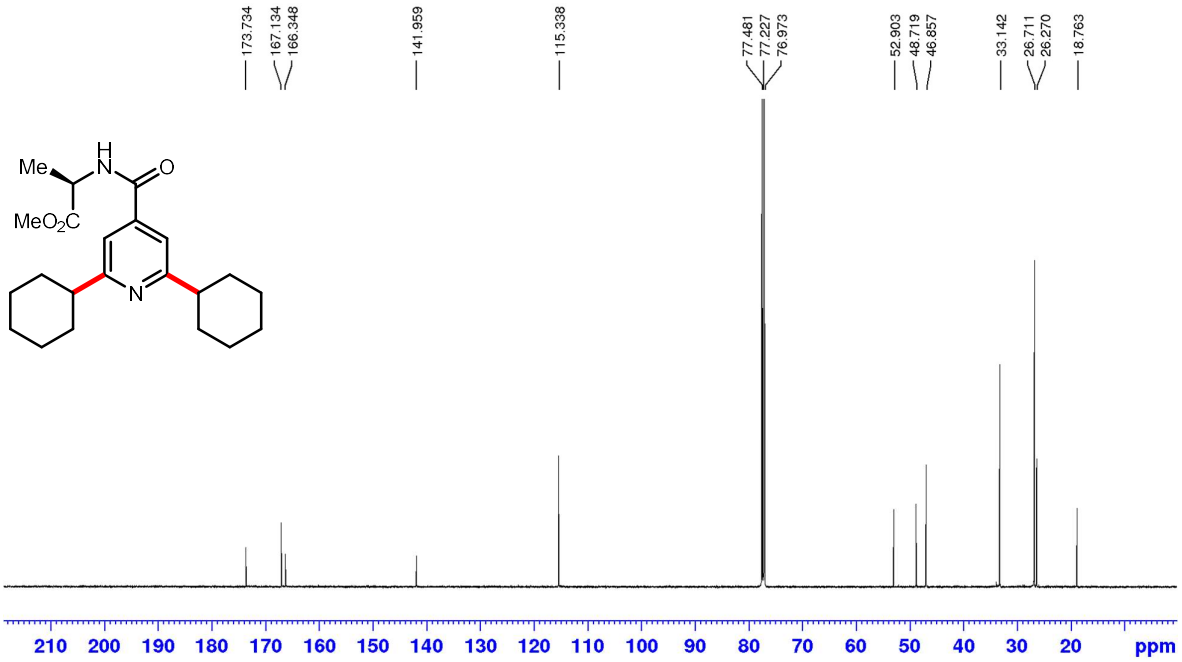

^{1}H NMR (500 MHz, $CDCl_3$) of 4,4'-di-tert-butyl-6,6'-dicyclohexyl-2,2'-bipyridine (59a)

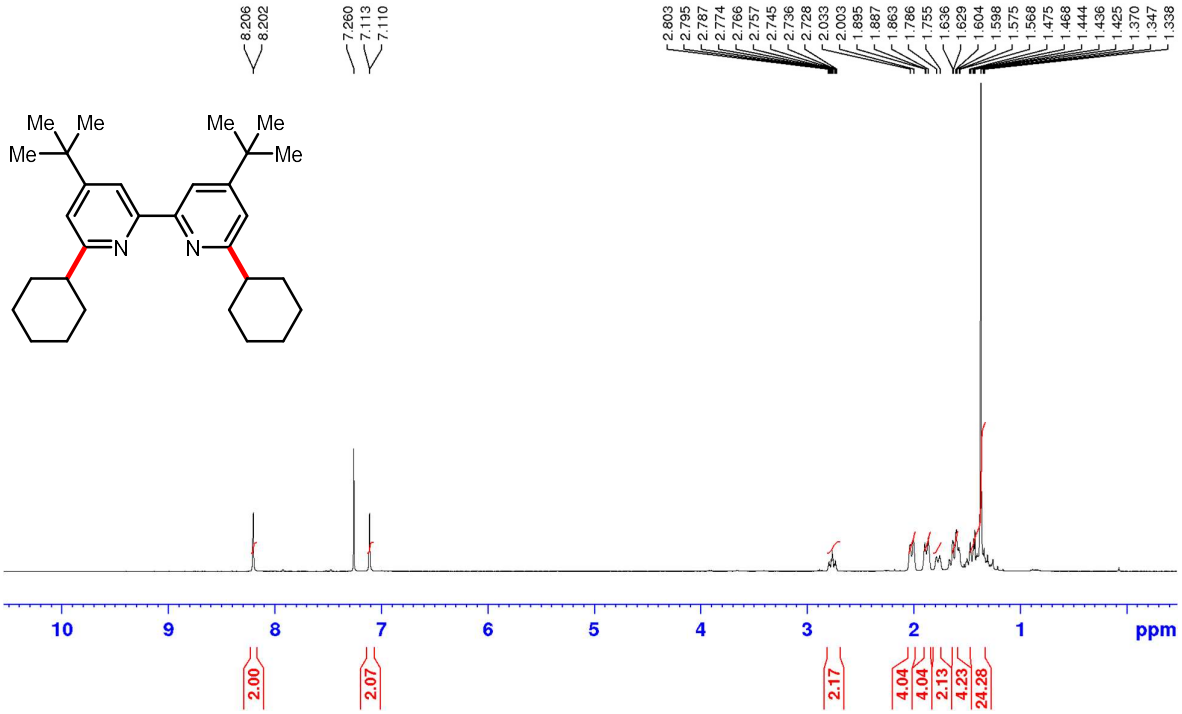

^{13}C NMR (126 MHz, $CDCl_3$) of 4,4'-di-tert-butyl-6,6'-dicyclohexyl-2,2'-bipyridine (59a)

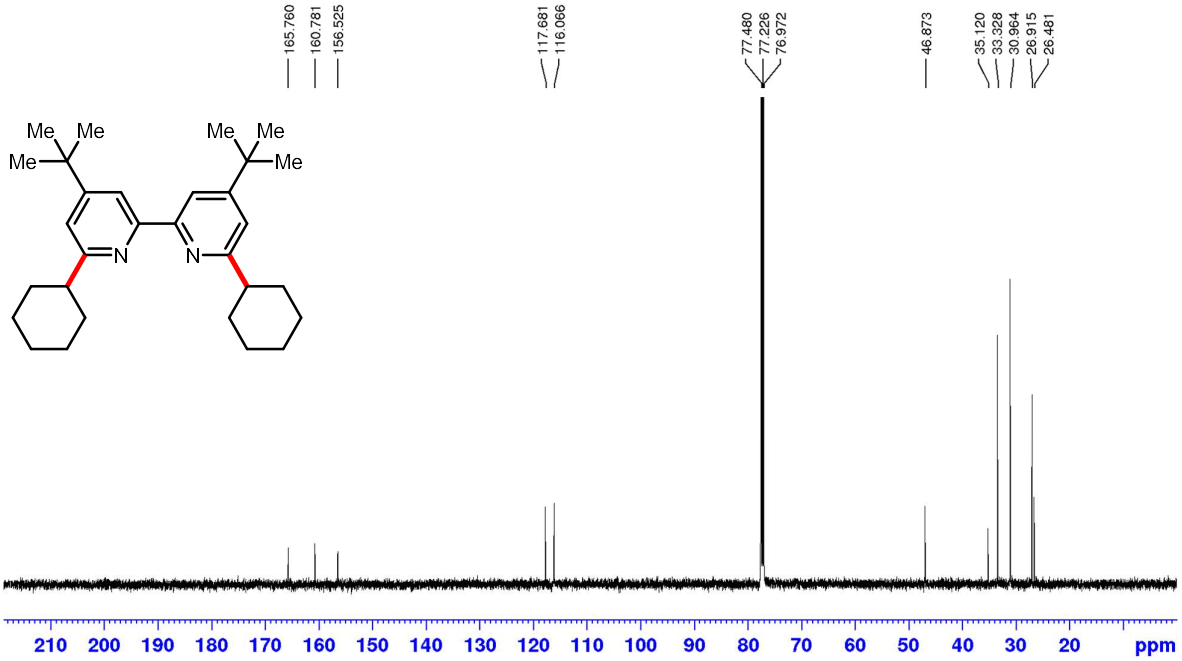

^{1}H NMR (500 MHz, $CDCl_3$) of 2-((3,4-dihydronaphthalen-1-yl)methyl)tetrahydrofuran (61a)

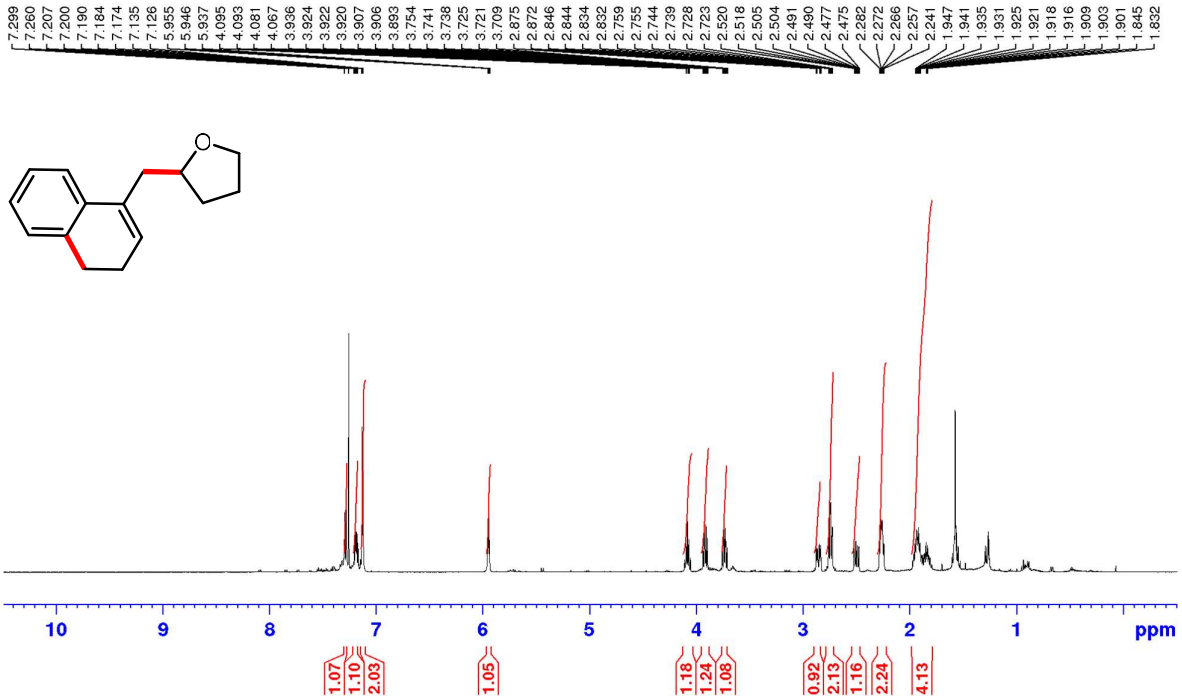

^{13}C NMR (126 MHz, $CDCl_3$) of 2-((3,4-dihydronaphthalen-1-yl)methyl)tetrahydrofuran (61a)

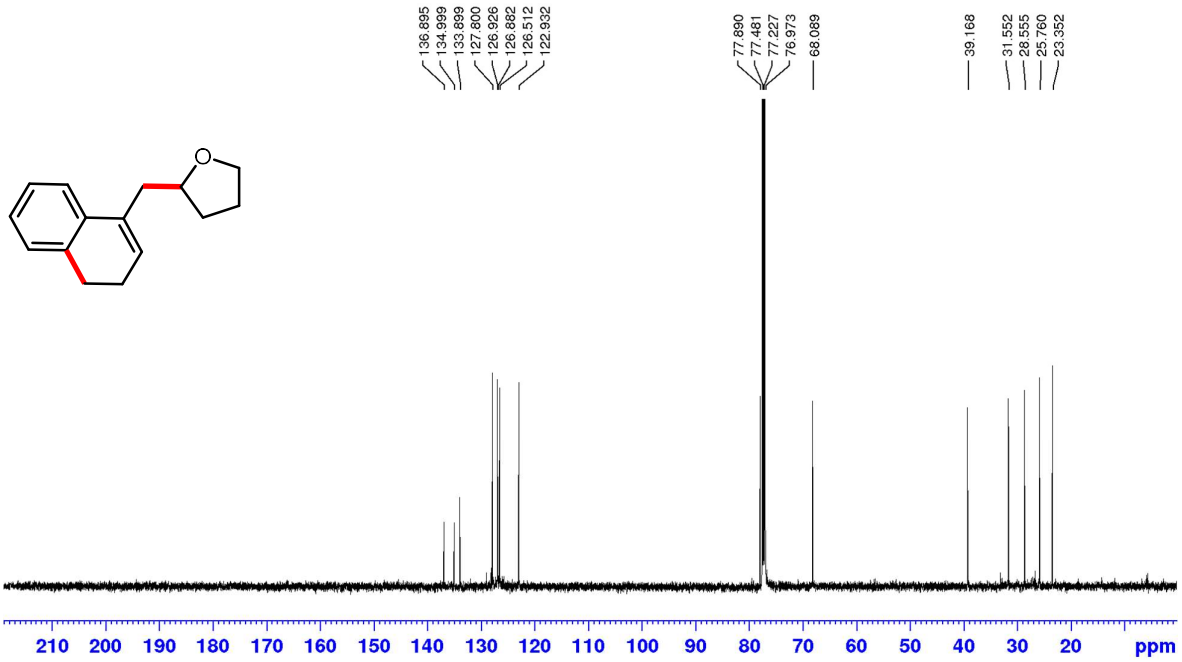

Appendix 2: NMR spectra for new compounds in chapter 3

^{1}H NMR (500 MHz, $CDCl_3$) of (4-adamantan-1-yl)-2-phenylquinoline (9b) and 4-adamantan-2-yl)-2-phenylquinoline (9b'), 1:0.9 congeners

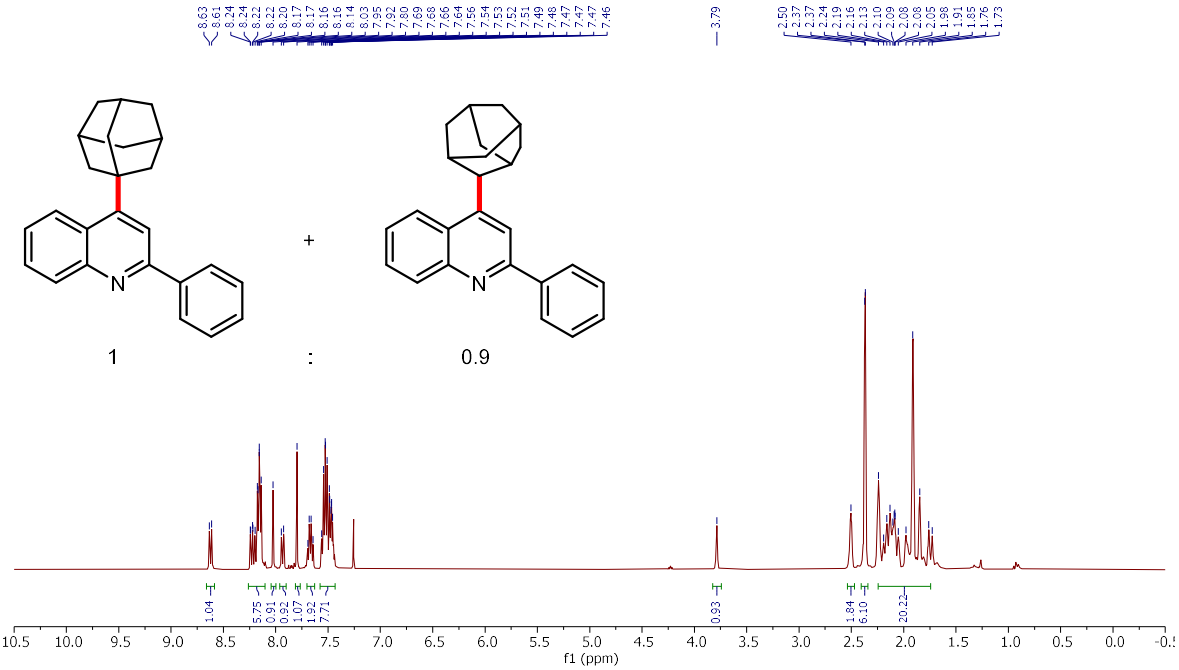

^{13}C NMR (125 MHz, $CDCl_3$) of (4-adamantan-1-yl)-2-phenylquinoline (9b) and 4-adamantan-2-yl)-2-phenylquinoline (9b'), 1:0.9 congeners

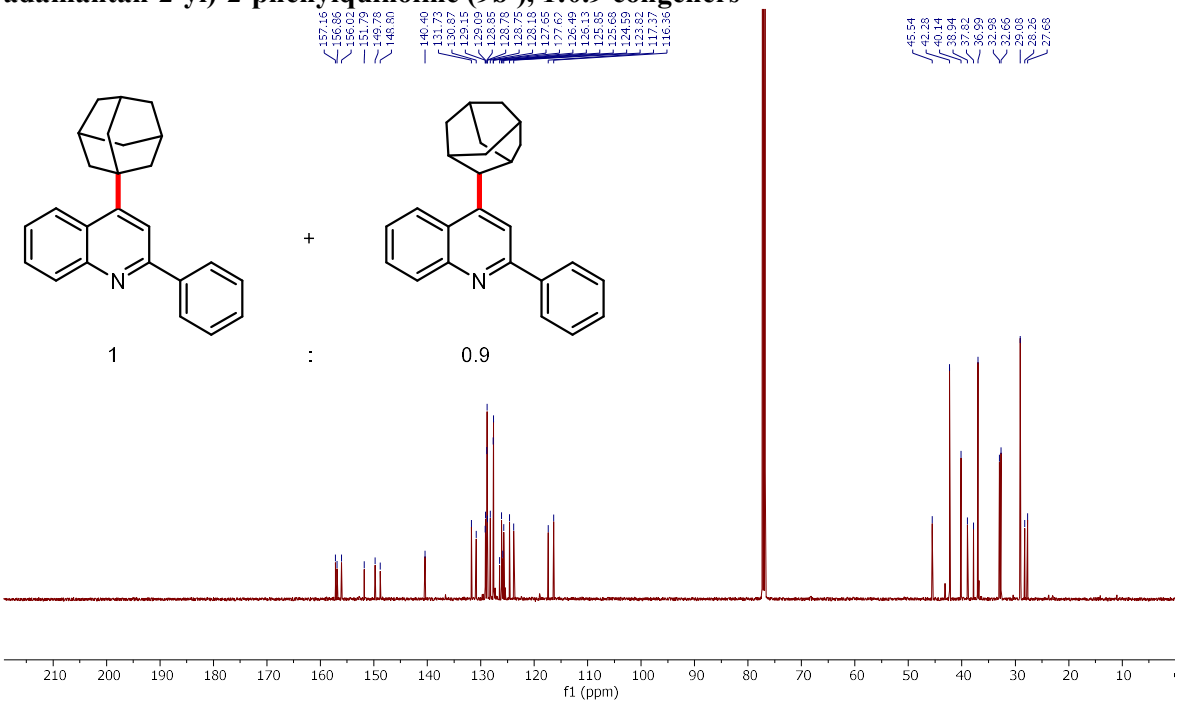

^{1}H NMR (500 MHz, $CDCl_3$) of 4-(4-methoxylbenzyl)-2-phenylquinoline (13b)

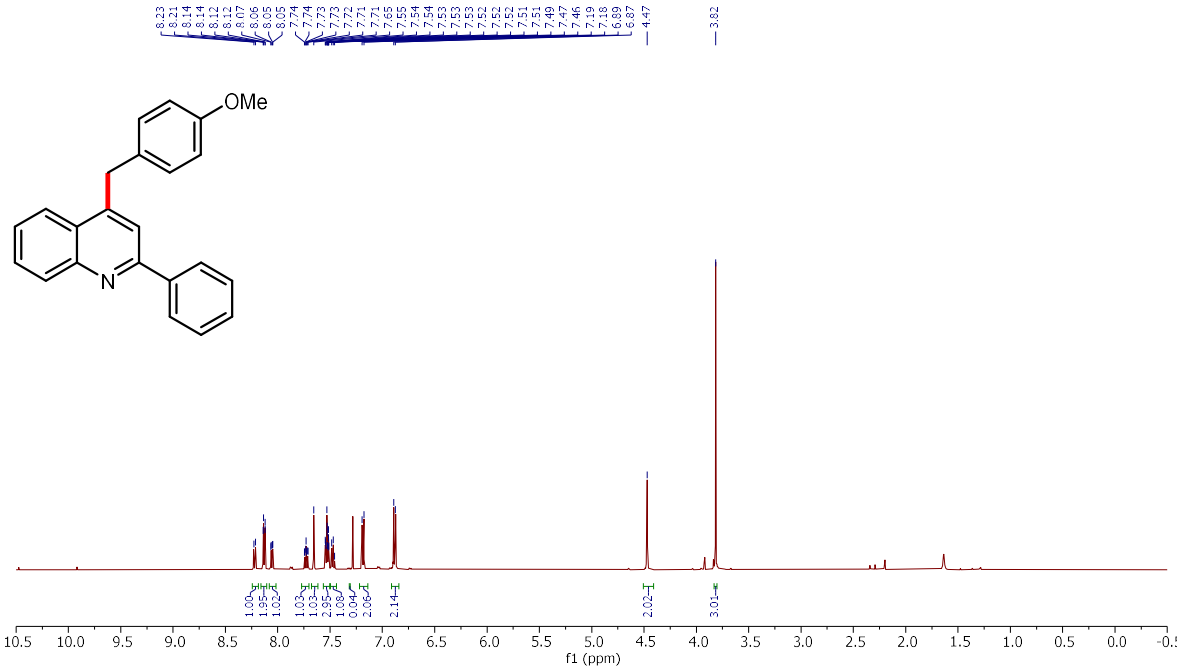

^{13}C NMR (125 MHz, $CDCl_3$) of 4-(4-methoxylbenzyl)-2-phenylquinoline (13b)

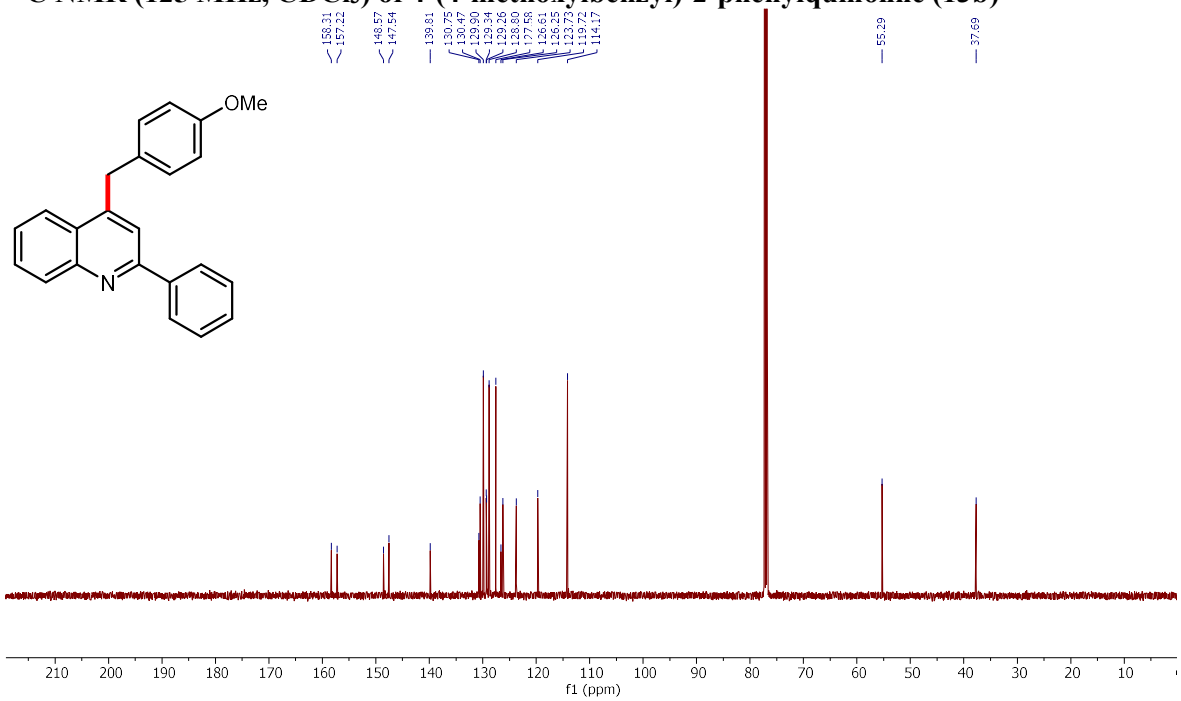

^{1}H NMR (500 MHz, $CDCl_3$) of 4-([1,1'-biphenyl]-4-ylmethyl)-2-phenylquinoline (14b)

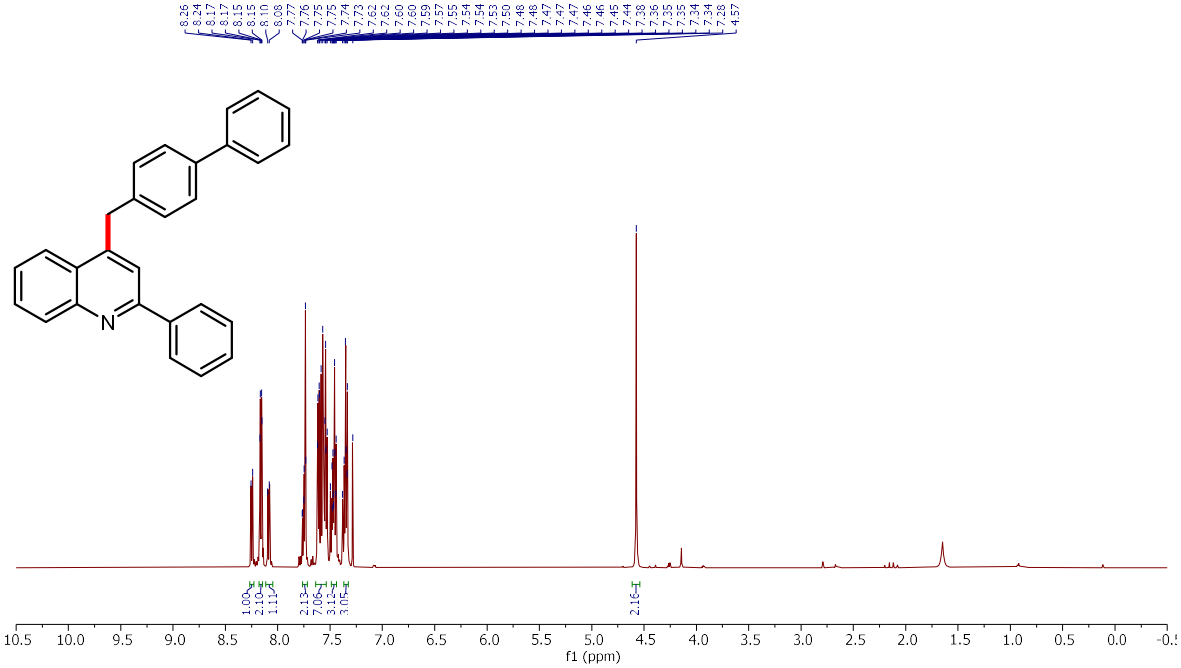

^{13}C NMR (125 MHz, $CDCl_3$) of 4-([1,1'-biphenyl]-4-ylmethyl)-2-phenylquinoline (14b)

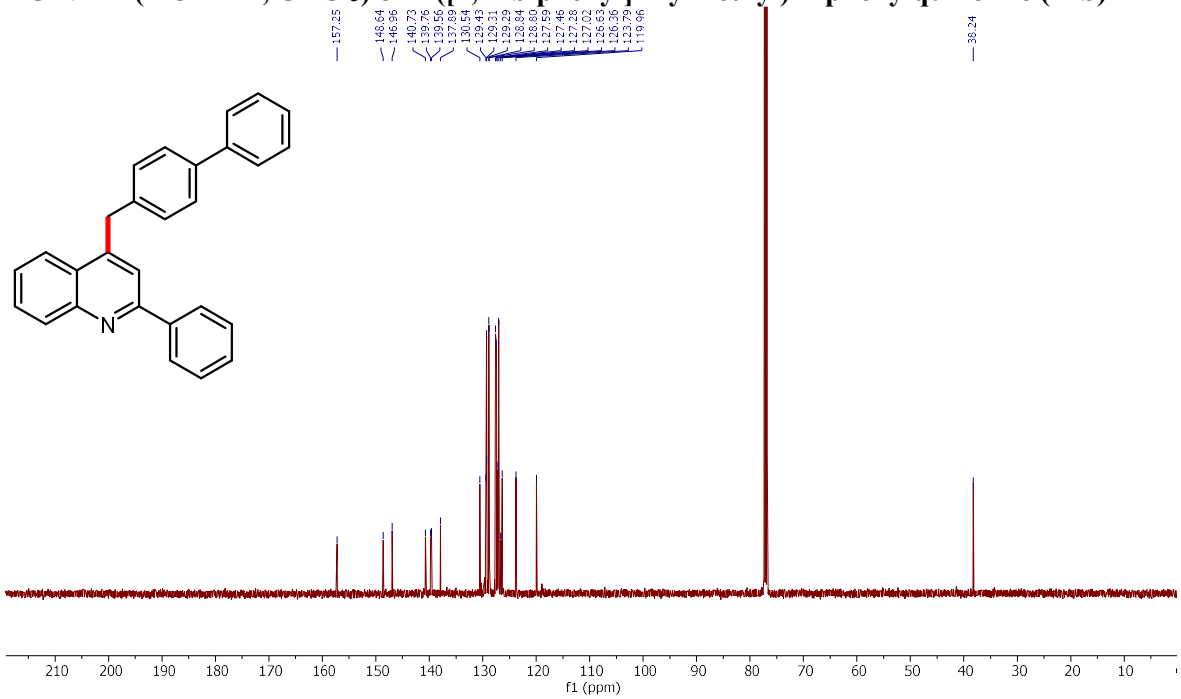

^{1}H NMR (500 MHz, $CDCl_3$) of 4-(2-methoxyethyl)-2-phenylquinoline (16b)

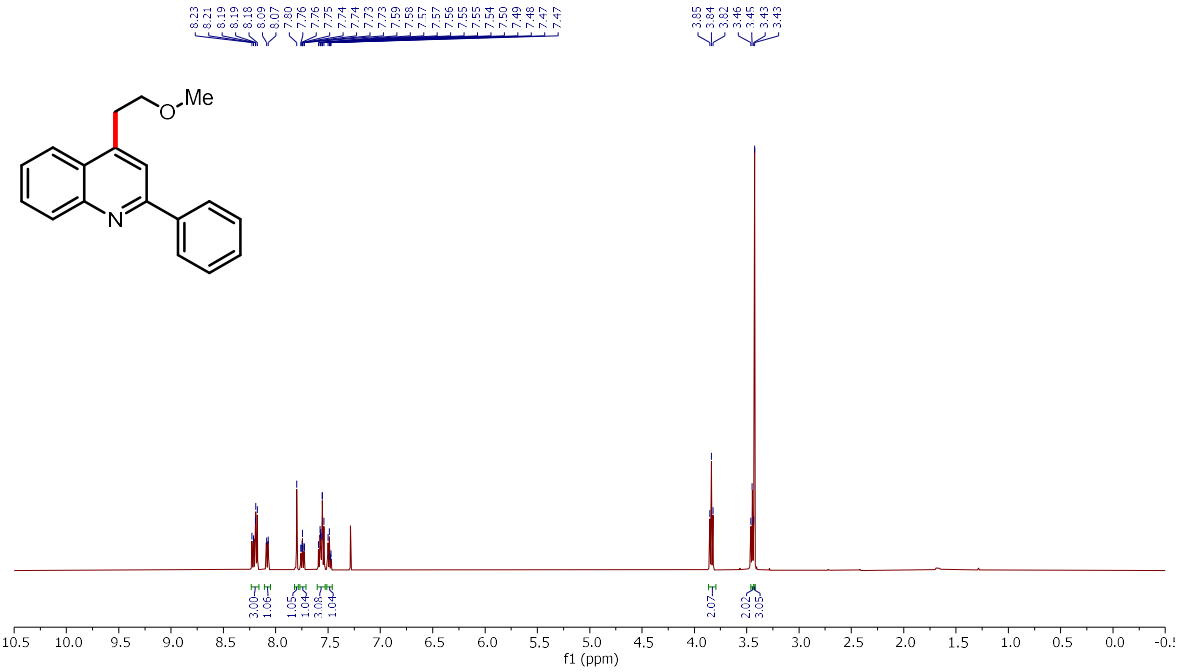

^{13}C NMR (125 MHz, $CDCl_3$) of 4-(2-methoxyethyl)-2-phenylquinoline (16b)

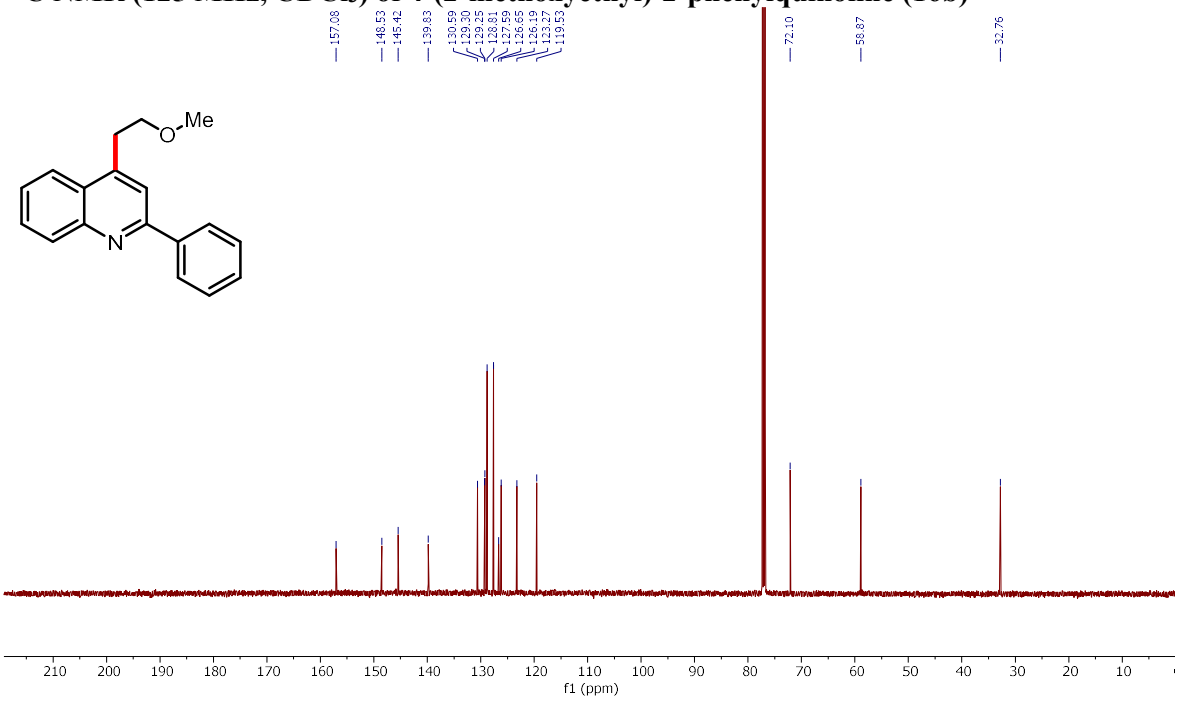

^{1}H NMR (500 MHz, $CDCl_3$) of 5-(2-phenylquinolin-4-yl)pentan-2-ol (20b)

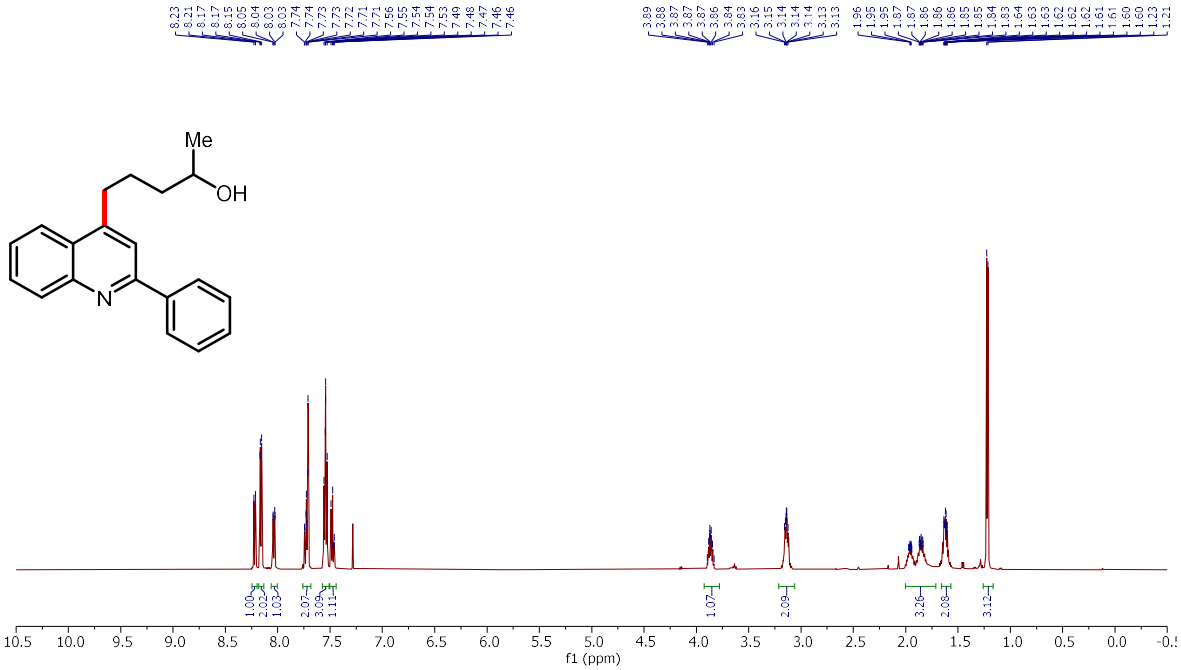

^{13}C NMR (125 MHz, $CDCl_3$) of 5-(2-phenylquinolin-4-yl)pentan-2-ol (20b)

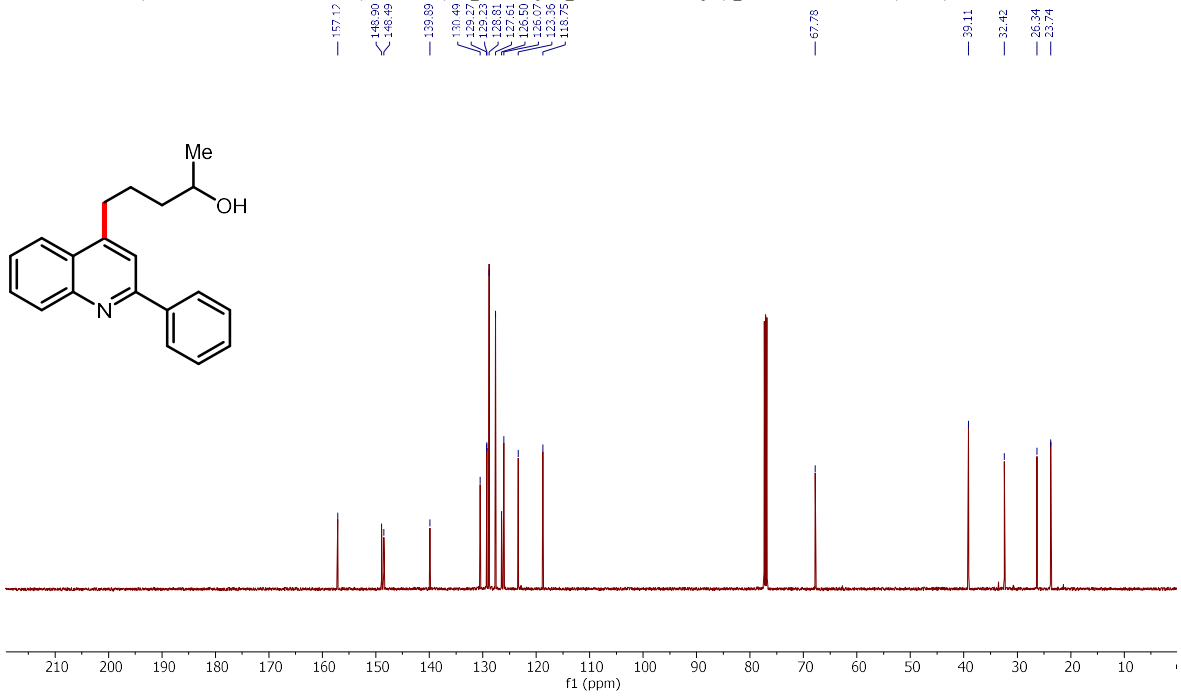

^{1}H NMR (500 MHz, $CDCl_3$) of 4-(methyl-d3)-2-phenylquinoline (22b)

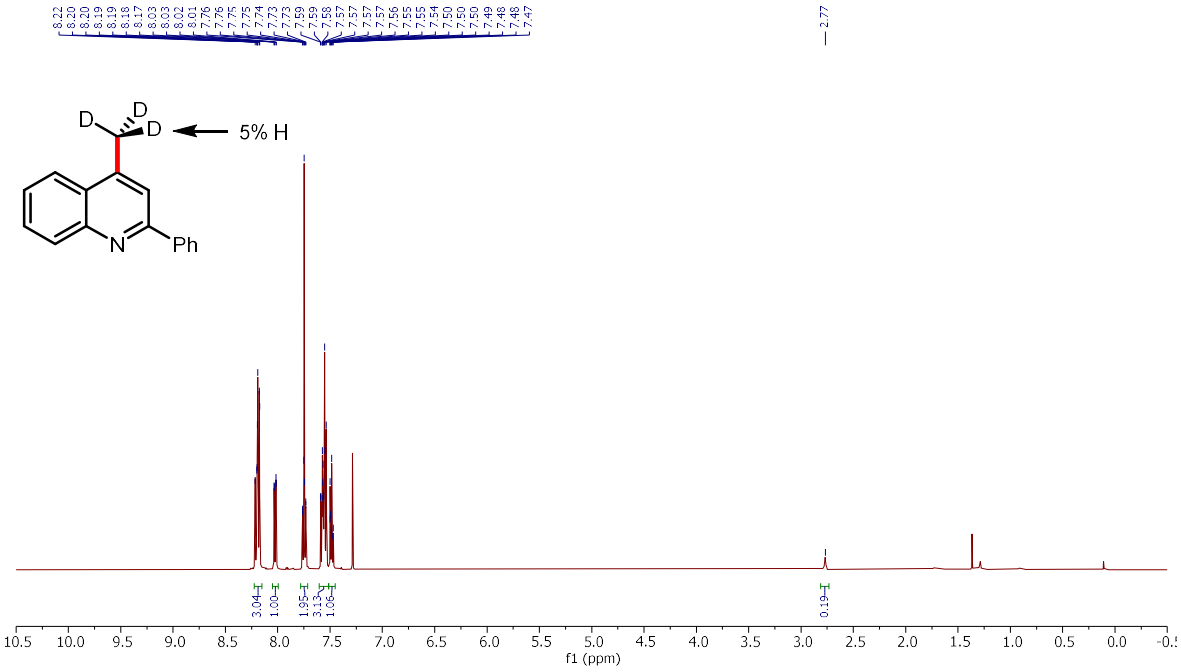

^{13}C NMR (125 MHz, $CDCl_3$) of 4-(methyl-d3)-2-phenylquinoline (22b)

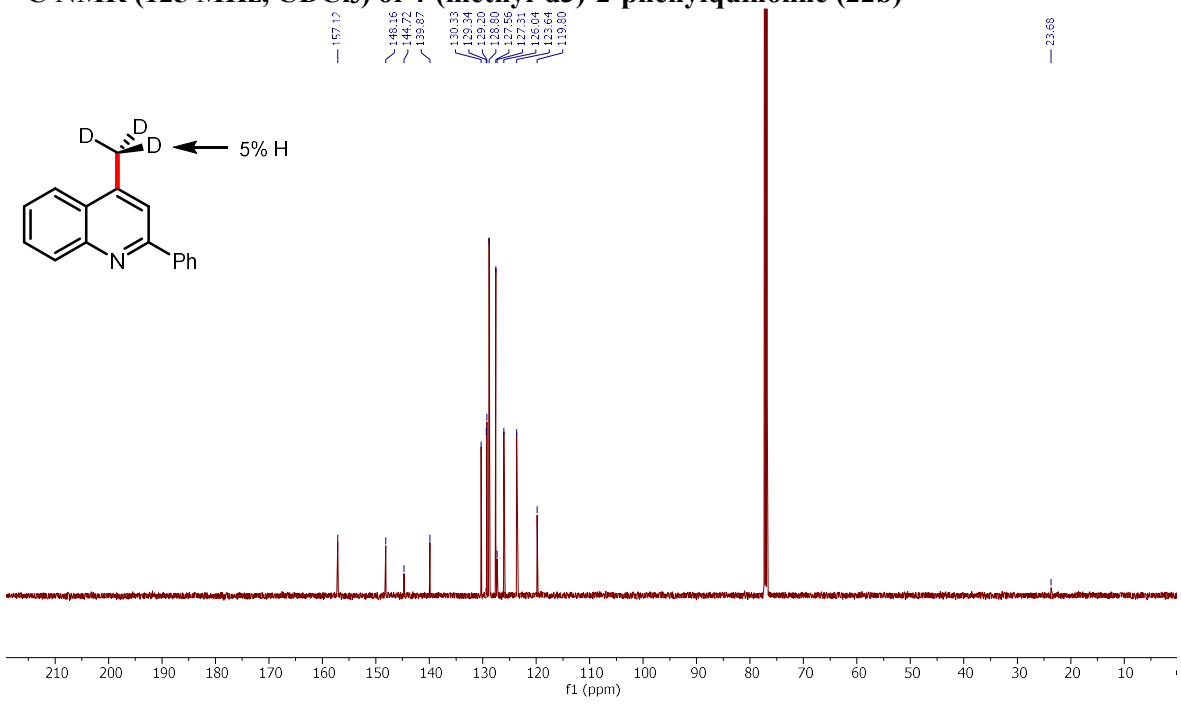

^{2}H NMR (77 MHz, $CDCl_3$) of 4-(methyl-d3)-2-phenylquinoline (22b)

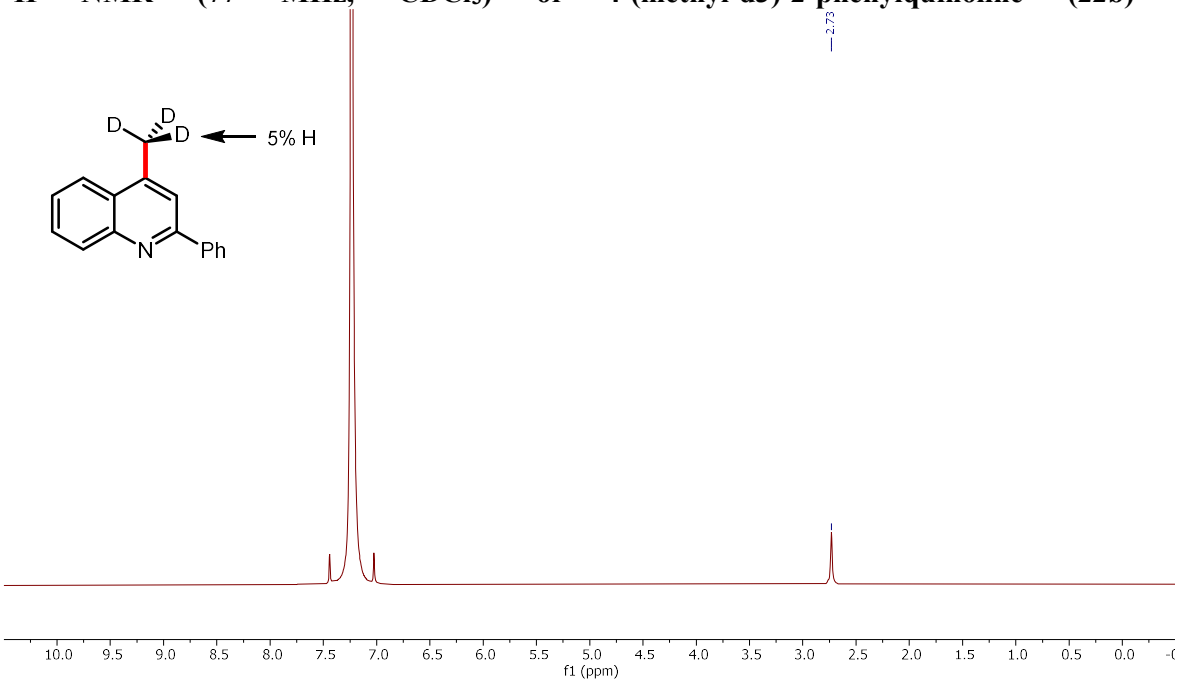

^{1}H NMR (500 MHz, $CDCl_3$) of 2-(2-phenylquinolin-4-yl)tetrahydro-4*H*-pyran-4-one (26b)

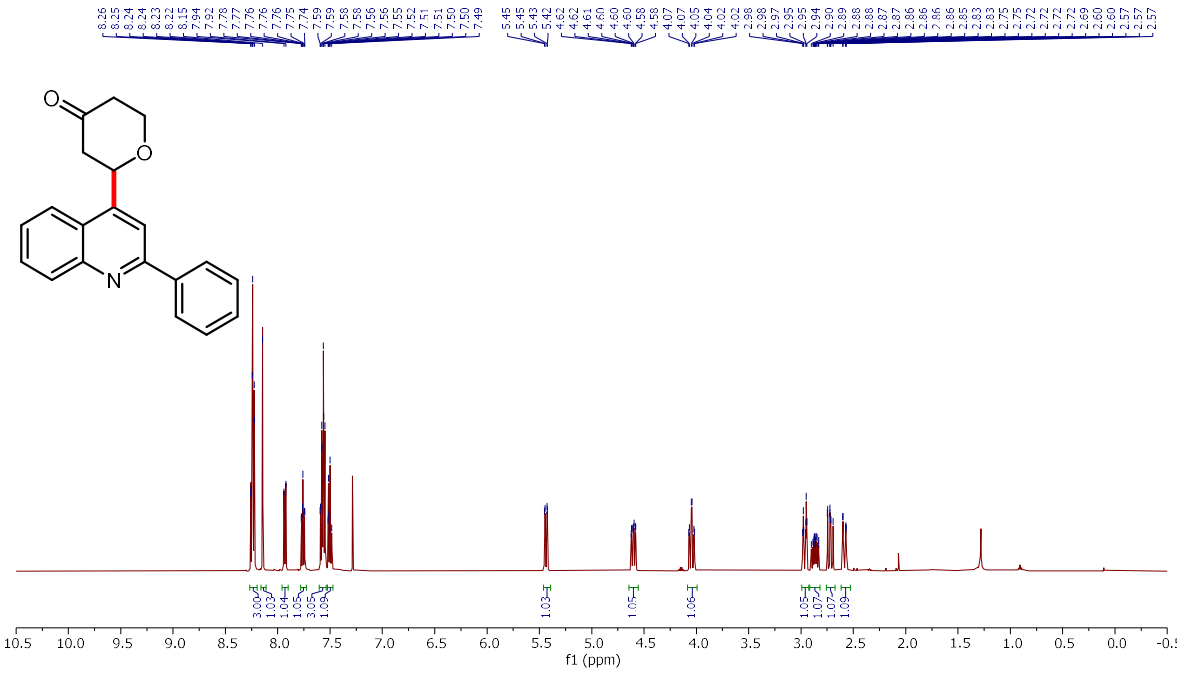

^{13}C NMR (125 MHz, $CDCl_3$) of 2-(2-phenylquinolin-4-yl)tetrahydro-4*H*-pyran-4-one (26b)

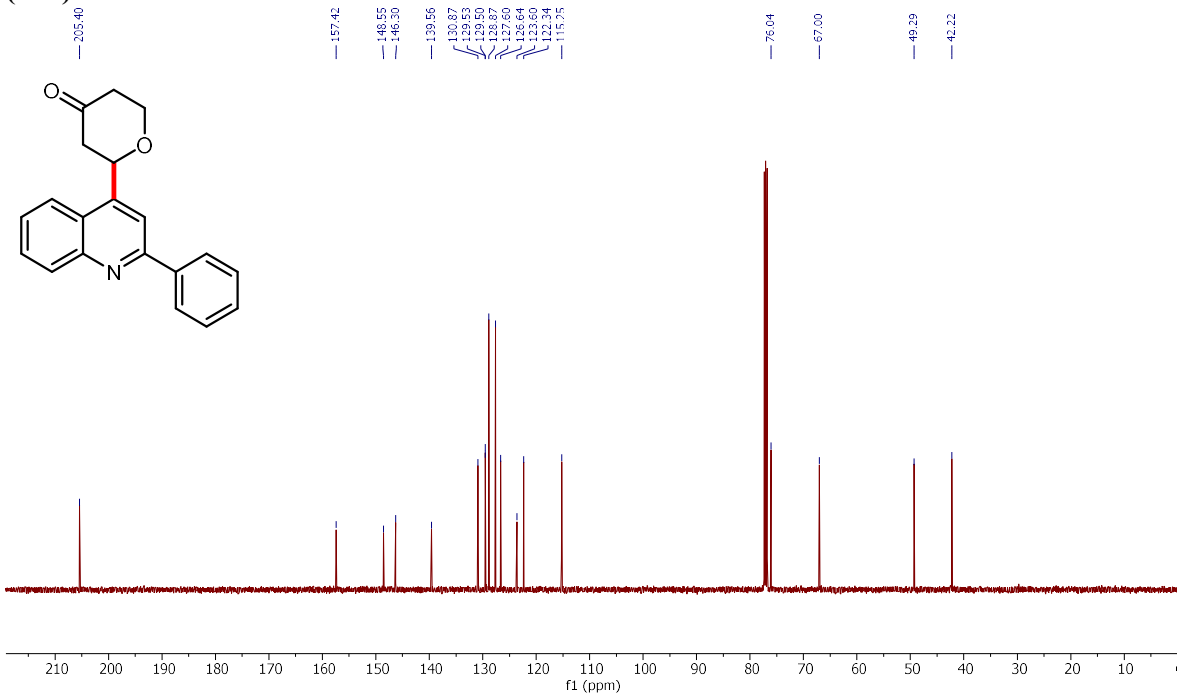

^{1}H NMR (500 MHz, $CDCl_3$) of 5-(2-phenylquinolin-4-yl)pyrrolidin-2-one (28b)

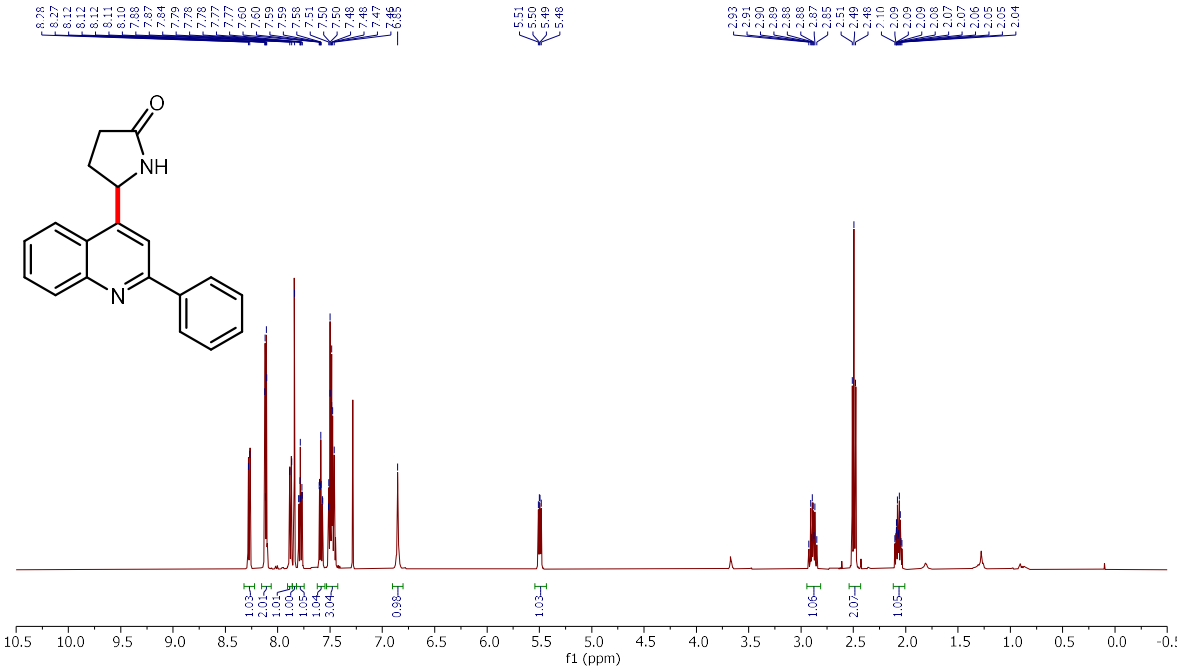

^{13}C NMR (125 MHz, $CDCl_3$) of 5-(2-phenylquinolin-4-yl)pyrrolidin-2-one (28b)

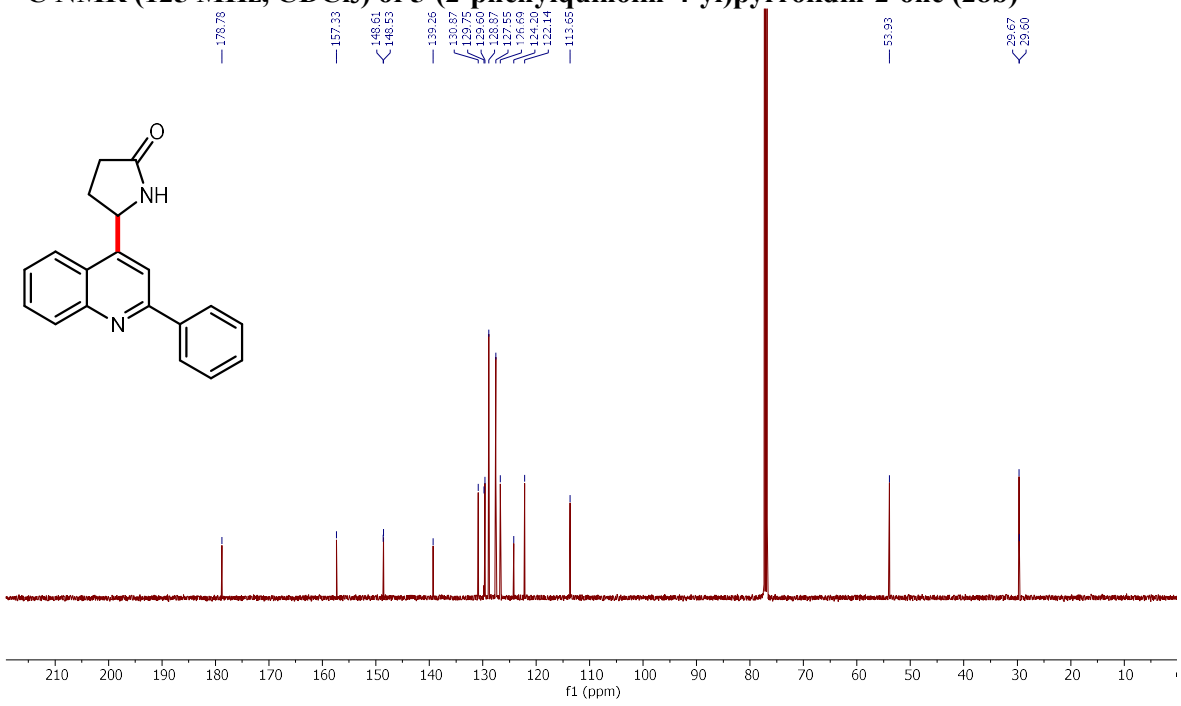

^{1}H NMR (500 MHz, $CDCl_3$) of *N*-methyl-*N*-((2-phenylquinolin-4-yl)methyl)formamide, 1:0.5 rotamers (29b)

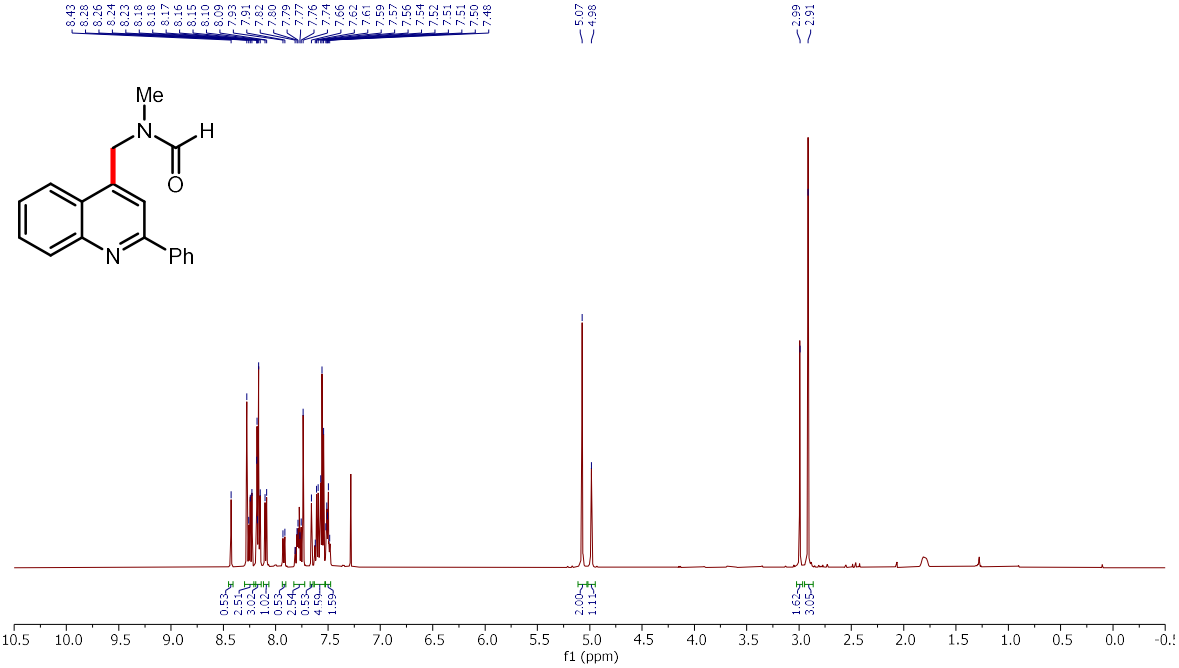

^{13}C NMR (125 MHz, $CDCl_3$) of *N*-methyl-*N*-((2-phenylquinolin-4-yl)methyl)formamide 1:0.5 rotamers (29b)

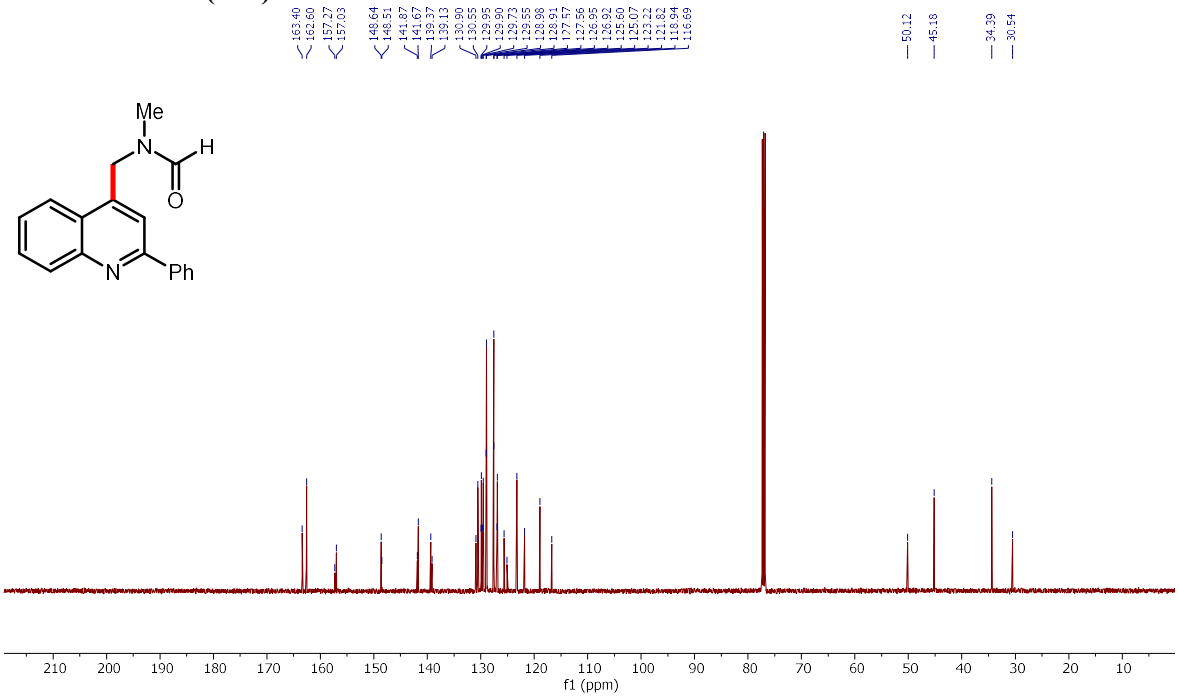

^{1}H NMR (500 MHz, $CDCl_3$) of *N*-methyl-*N*-((2-phenylquinolin-4-yl)methyl)acetamide, 1:0.5 rotamers (30b)

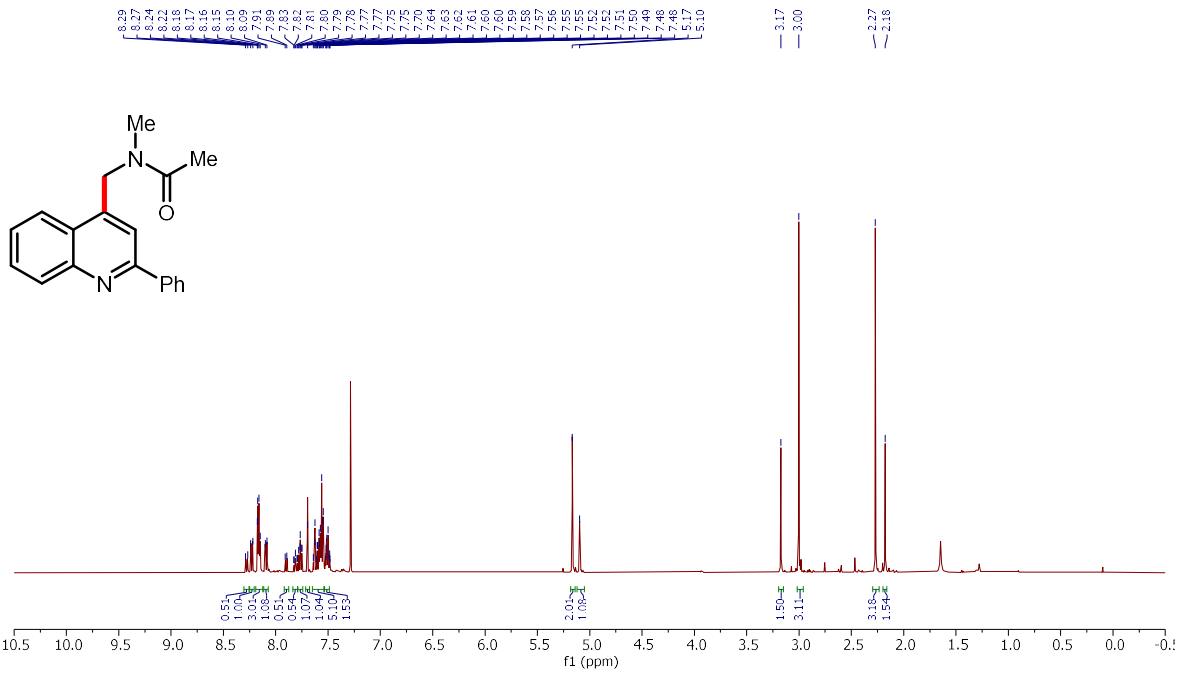

^{13}C NMR (125 MHz, $CDCl_3$) of *N*-methyl-*N*-((2-phenylquinolin-4-yl)methyl)acetamide, 1:0.5 rotamers (30b)

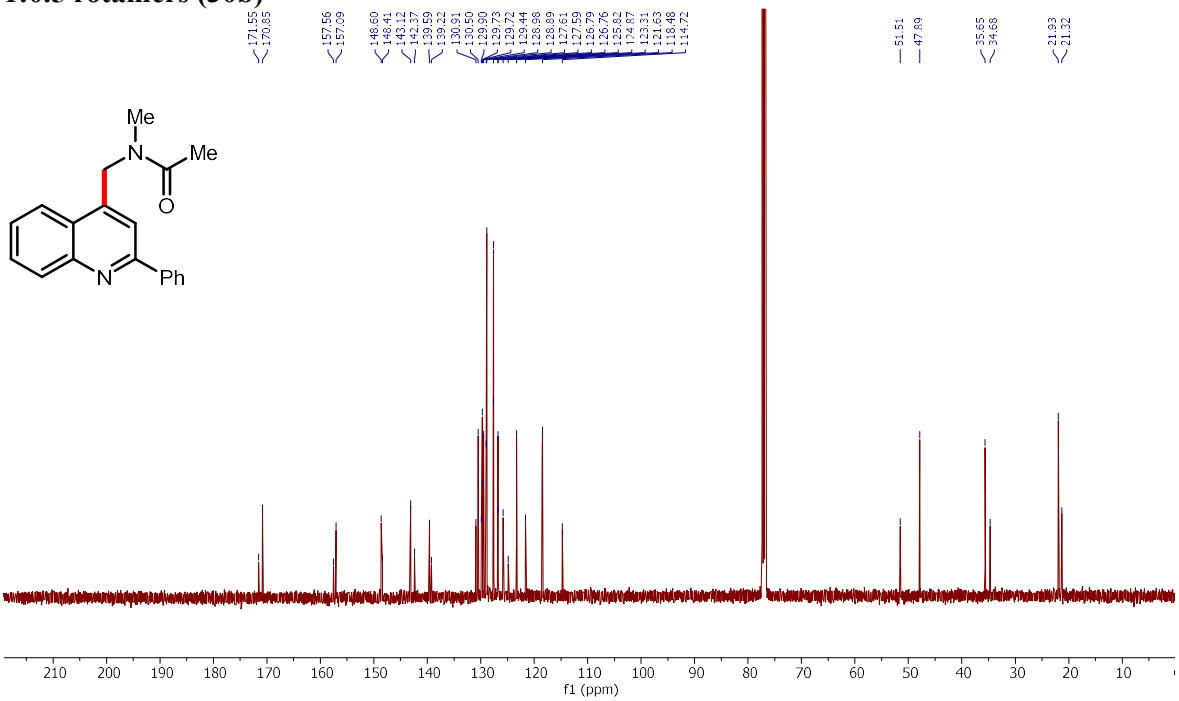

^{1}H NMR (500 MHz, $CDCl_3$) of 1-methyl-5-(2-phenylquinolin-4-yl)pyrrolidin-2-one (31b) and 1-((2-phenylquinolin-4-yl)methyl)pyrrolidin-2-one (31b'), 1:0.26 congeners (better purity could not be obtained)

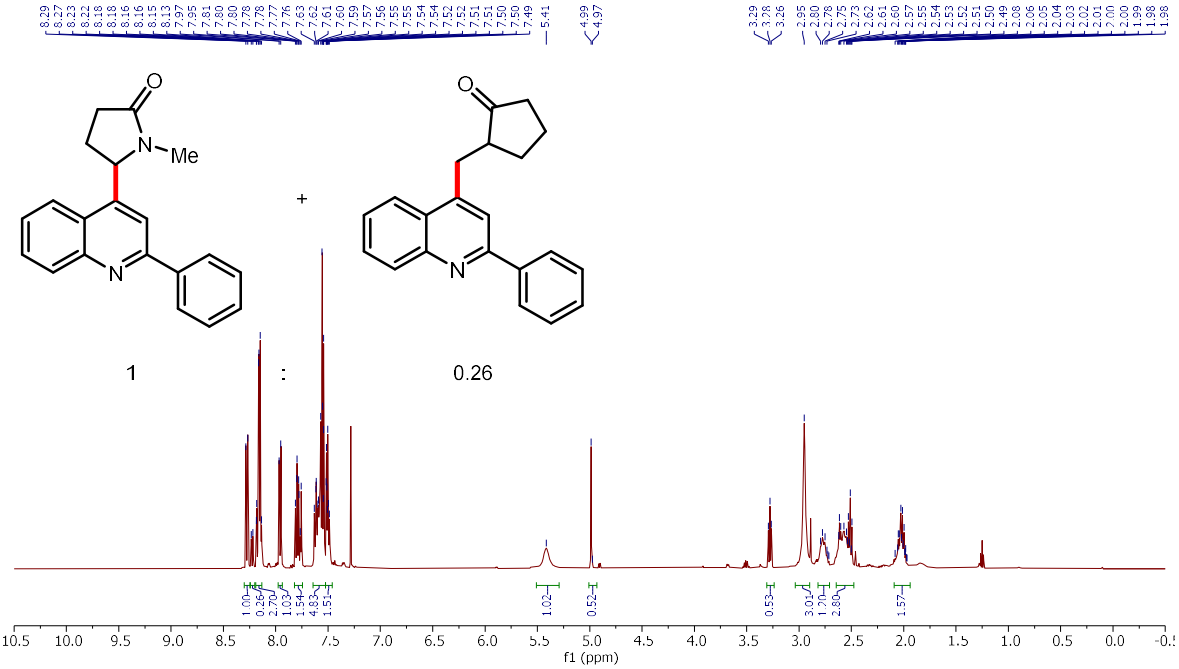

^{13}C NMR (125 MHz, $CDCl_3$) of 1-methyl-5-(2-phenylquinolin-4-yl)pyrrolidin-2-one (31b) and 1-((2-phenylquinolin-4-yl)methyl)pyrrolidin-2-one (31b'), 1:0.26 congeners (better purity could not be obtained)

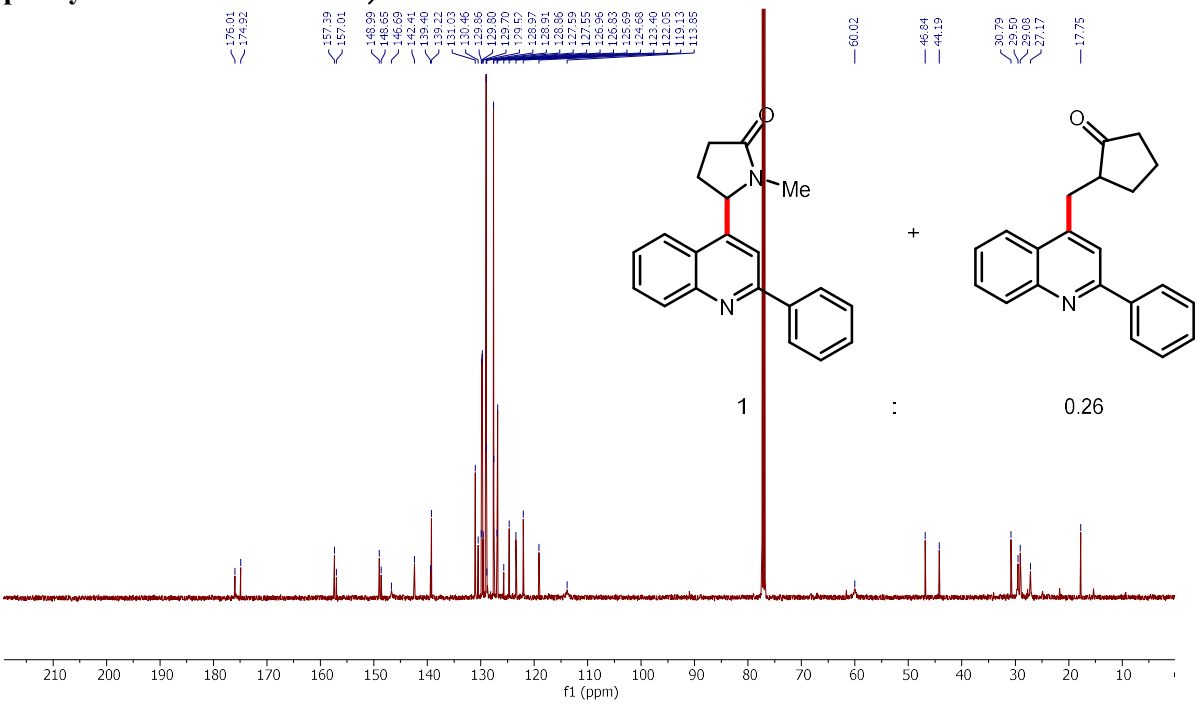

^{1}H NMR (500 MHz, $CDCl_3$) of 4-cyclohexyl-2-(4-fluorophenyl)quinoline (35b)

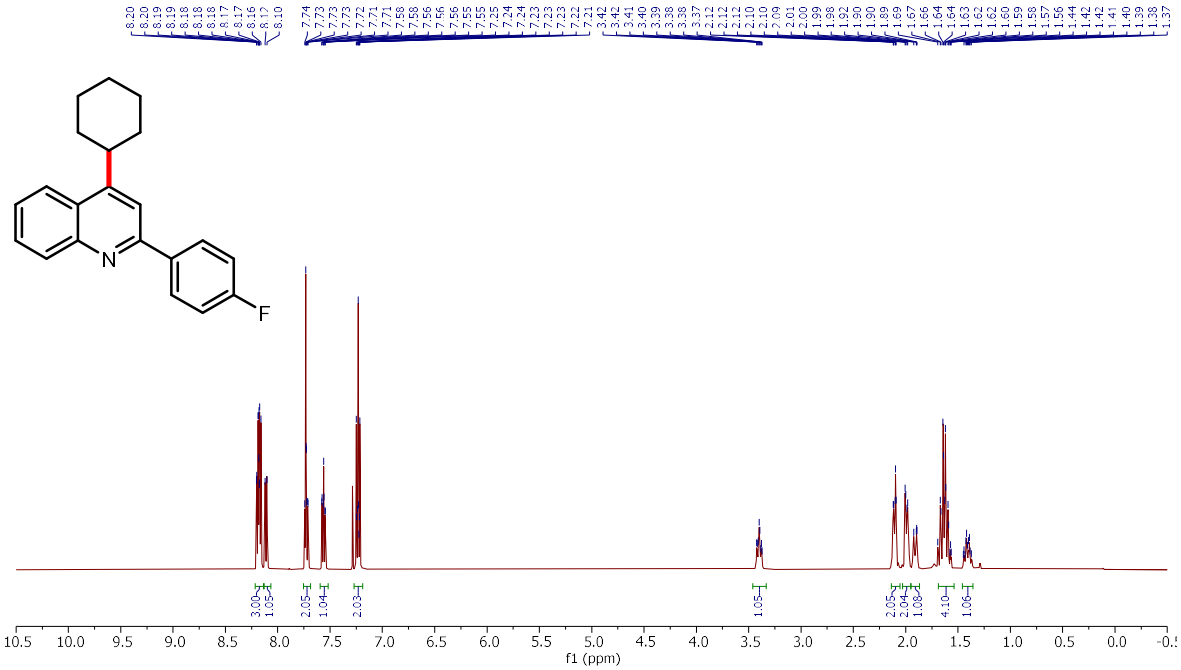

^{13}C NMR (125 MHz, $CDCl_3$) of 4-cyclohexyl-2-(4-fluorophenyl)quinoline (35b)

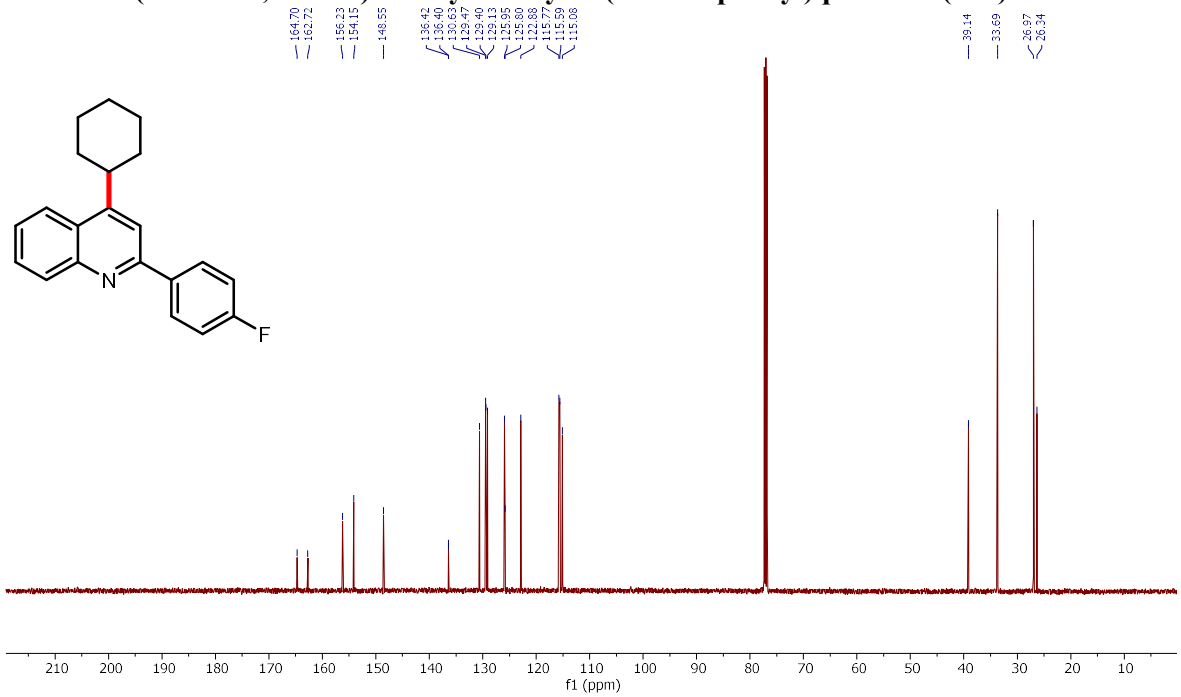

^{19}F NMR (470 MHz, $CDCl_3$) of 4-cyclohexyl-2-(4-fluorophenyl)quinoline (35b)

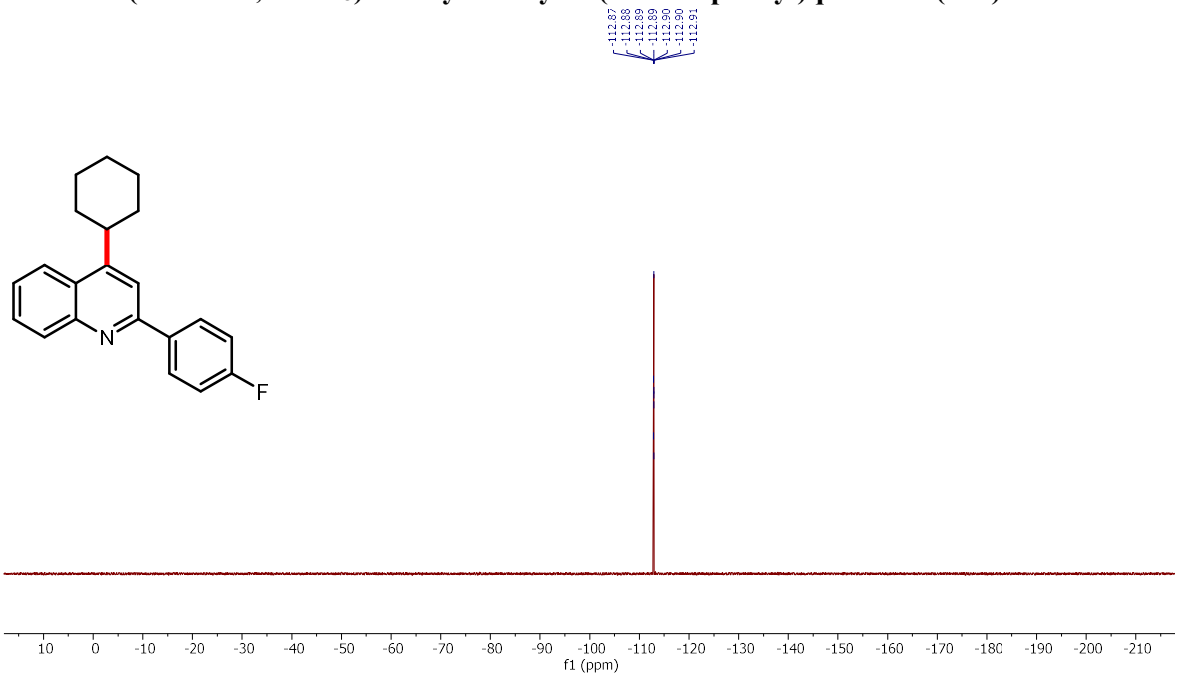

^{1}H NMR (500 MHz, $CDCl_3$) of 2-(4-chlorophenyl)-4-cyclohexylquinoline (36b)

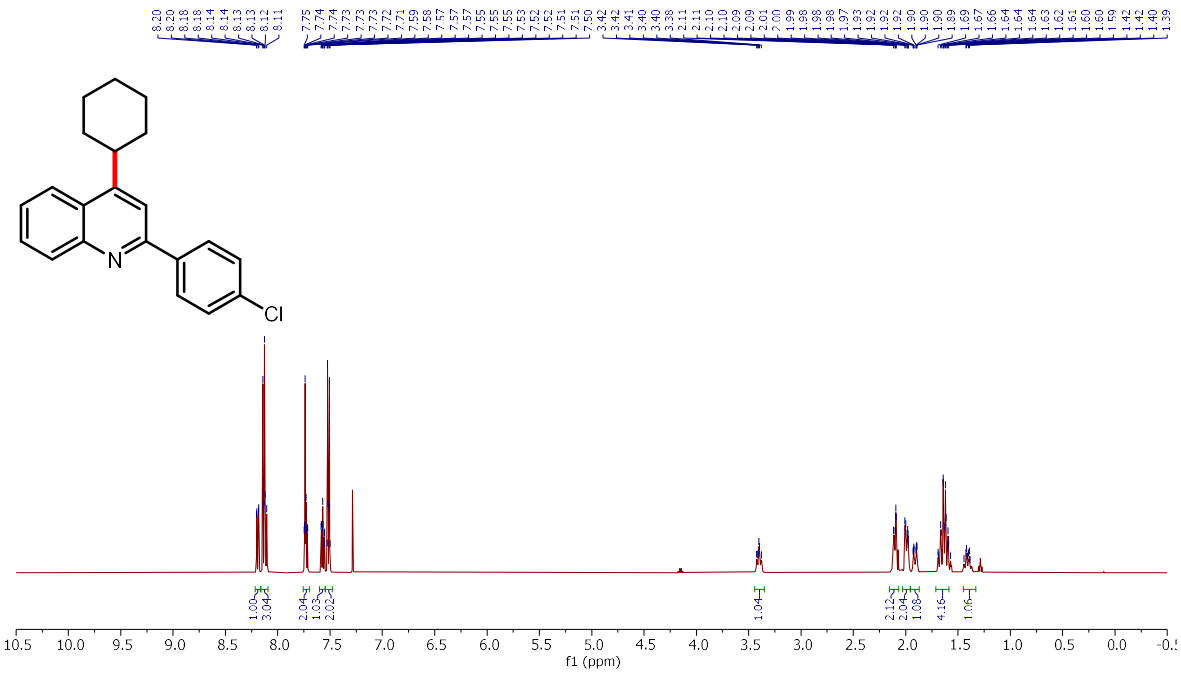

^{13}C NMR (125 MHz, $CDCl_3$) of 2-(4-chlorophenyl)-4-cyclohexylquinoline (36b)

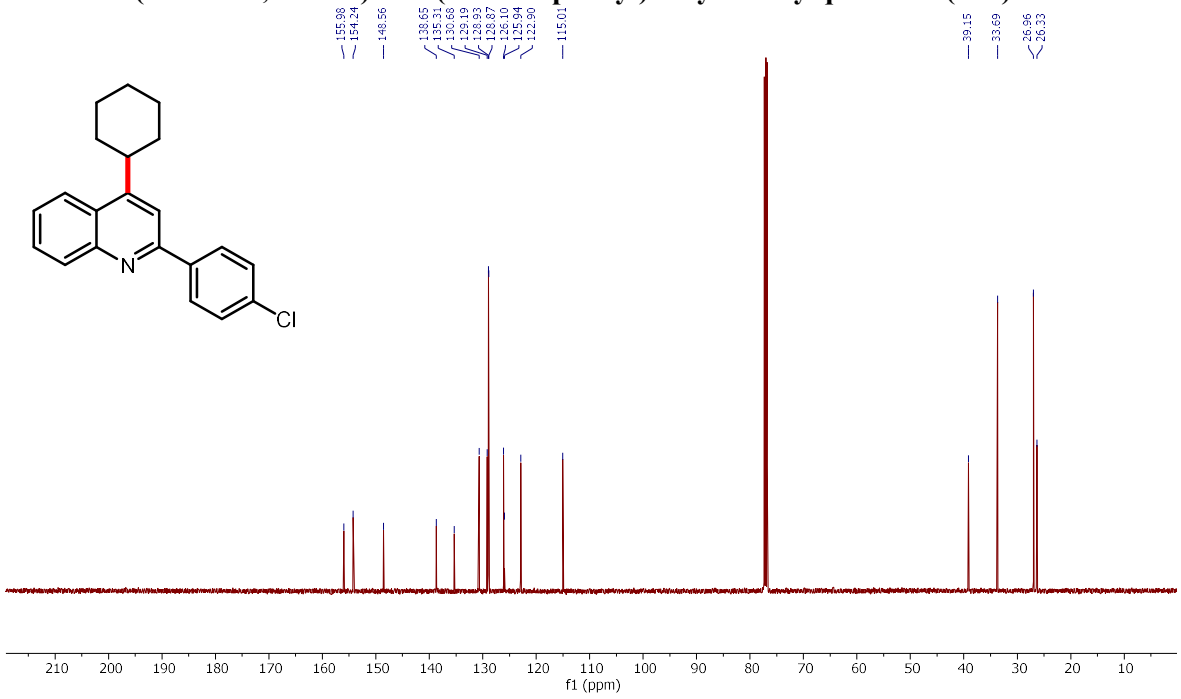

^{1}H NMR (500 MHz, $CDCl_3$) of 2-(4-bromophenyl)-4-cyclohexylquinoline (37b)

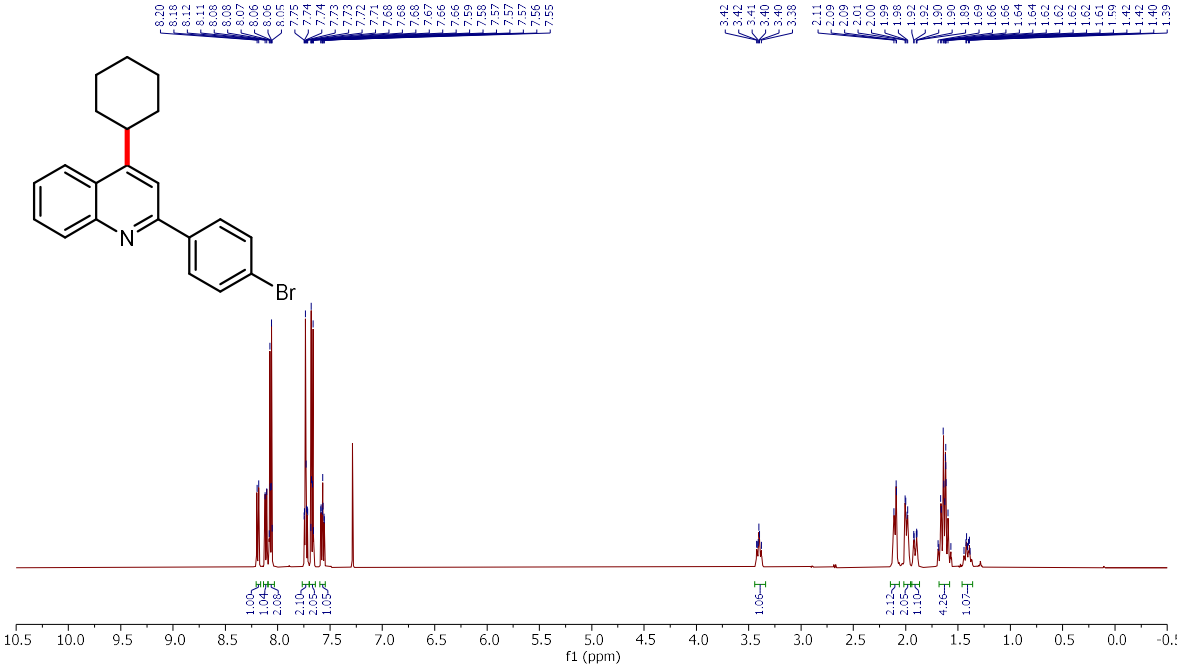

^{13}C NMR (125 MHz, $CDCl_3$) of 2-(4-bromophenyl)-4-cyclohexylquinoline (37b)

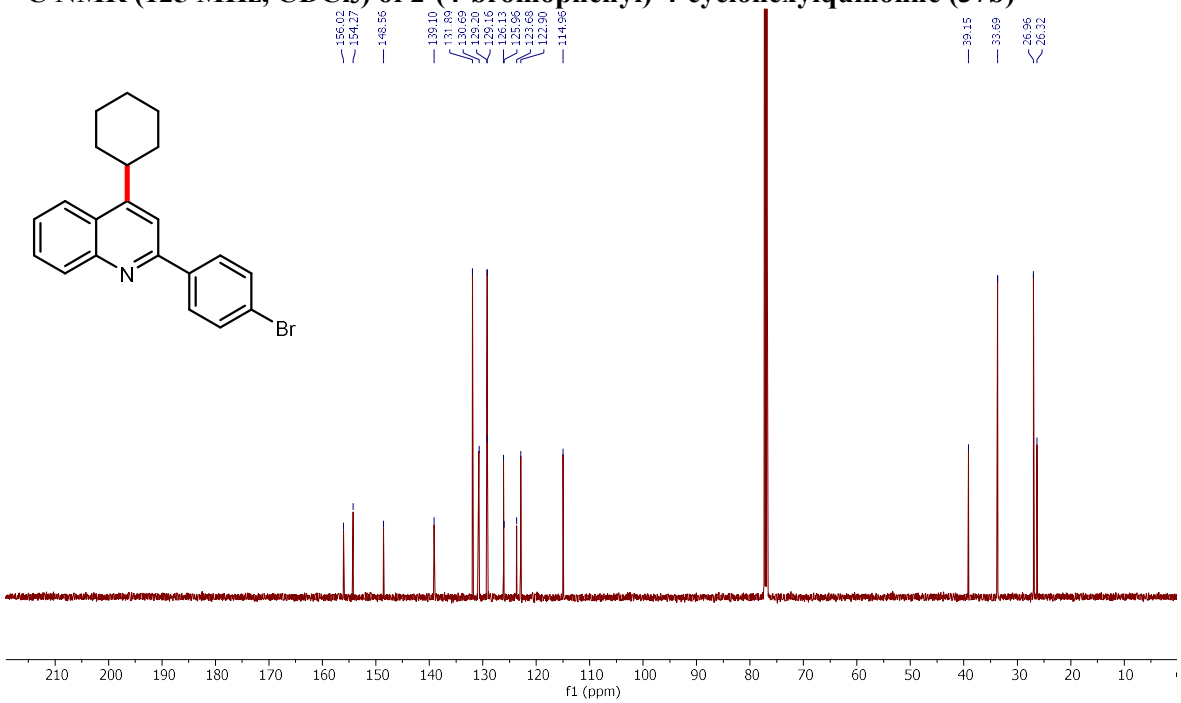

^{1}H NMR (500 MHz, $CDCl_3$) of 4-(4-cyclohexylquinolin-2-yl)benzonitrile (38b)

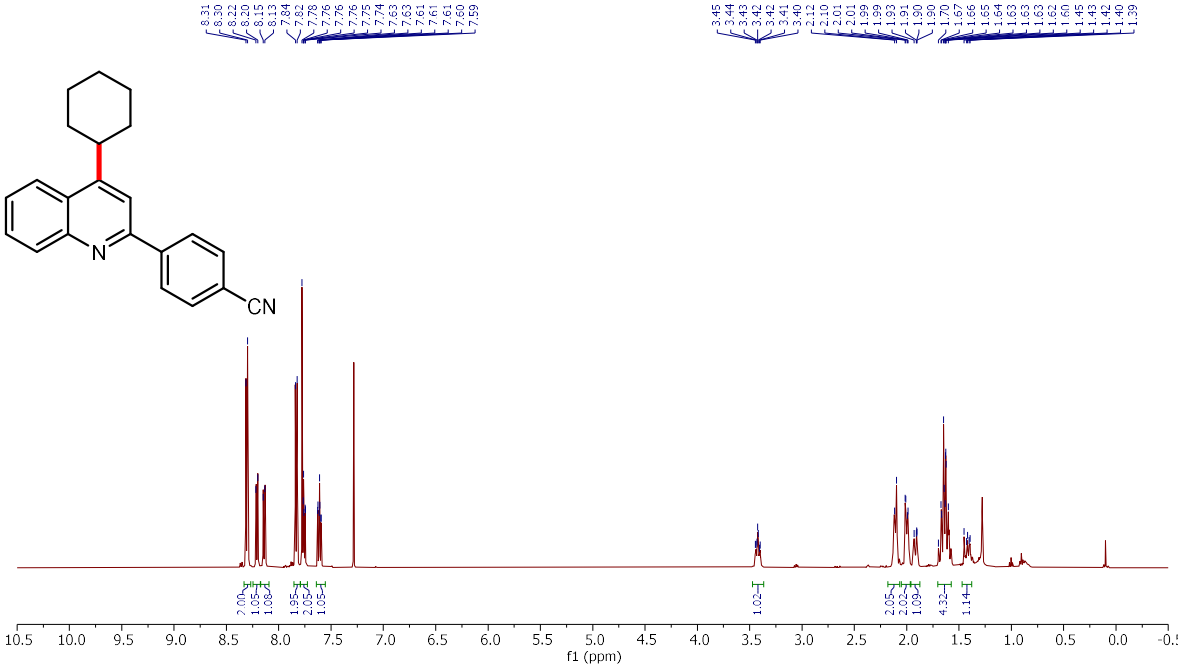

^{13}C NMR (125 MHz, $CDCl_3$) of 4-(4-cyclohexylquinolin-2-yl)benzonitrile (38b)

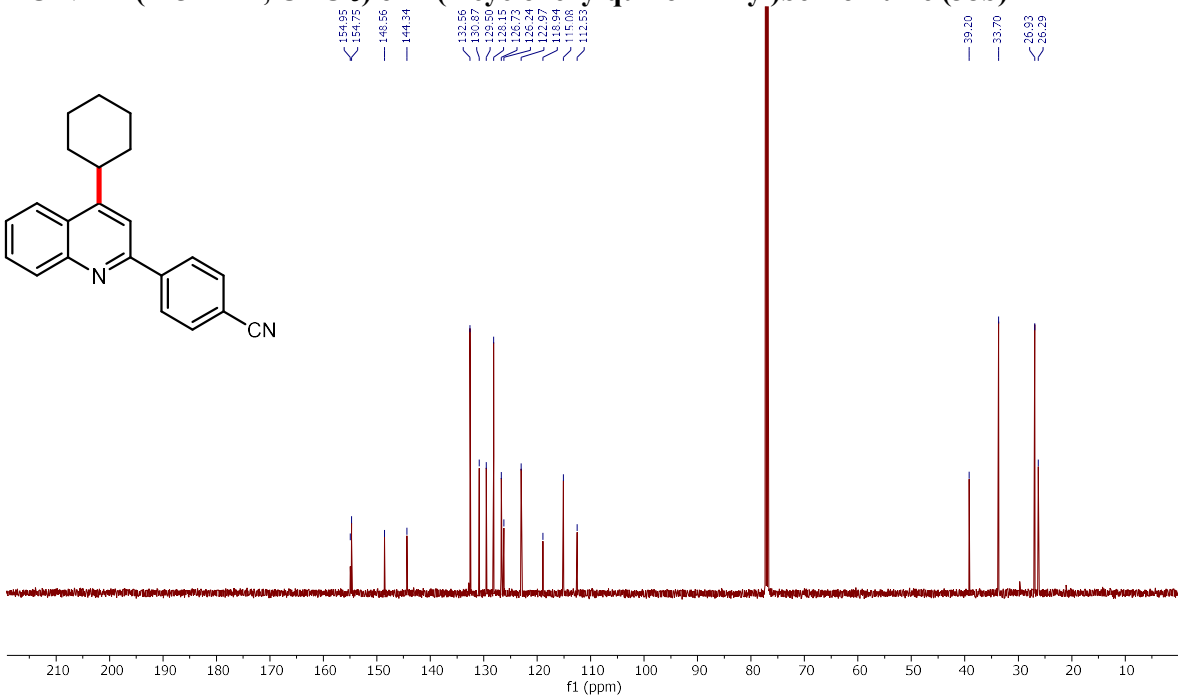

^{1}H NMR (500 MHz, $CDCl_3$) of 1-(4-(4-cyclohexylquinolin-2-yl)phenyl)ethan-1-one (39b)

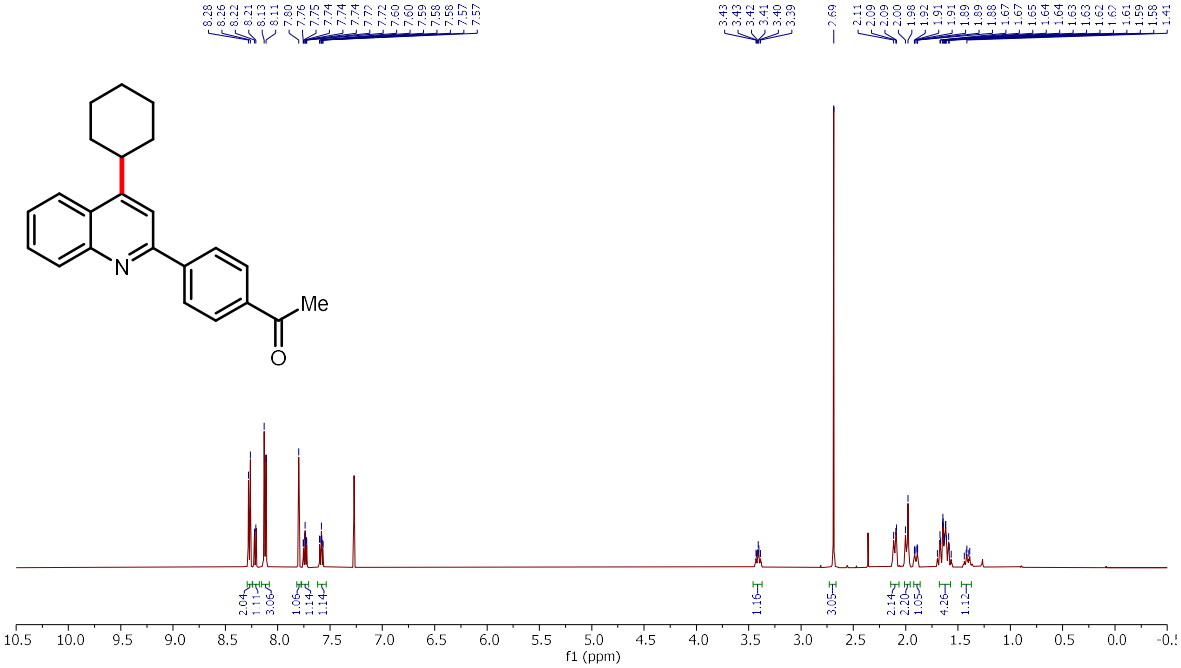

^{13}C NMR (125 MHz, $CDCl_3$) of 1-(4-(4-cyclohexylquinolin-2-yl)phenyl)ethan-1-one (39b)

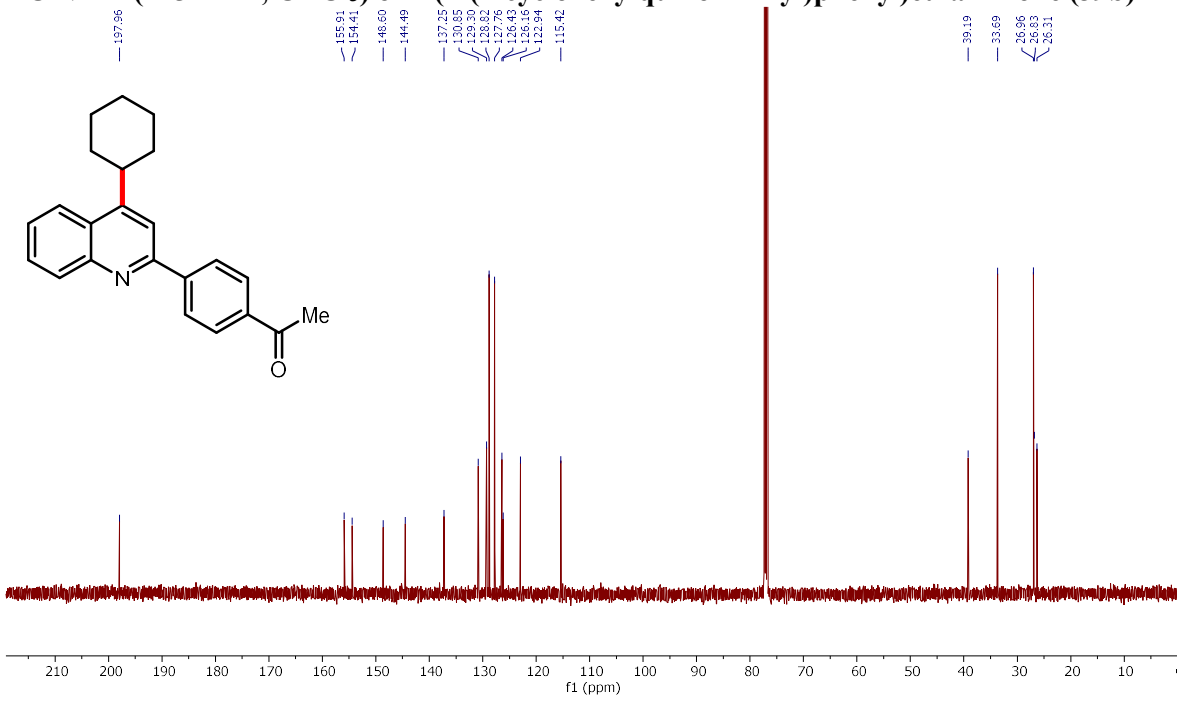

^{1}H NMR (500 MHz, $CDCl_3$) of 4-cyclohexyl-2-(p-tolyl)quinoline (40b)

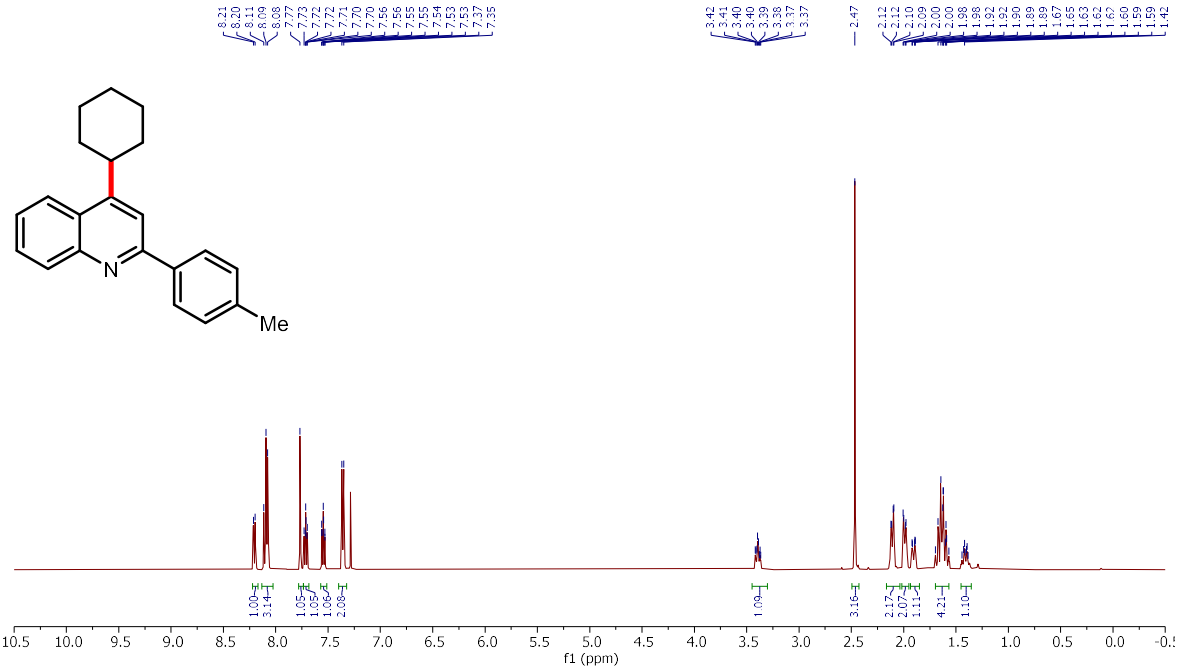

^{13}C NMR (125 MHz, $CDCl_3$) of 4-cyclohexyl-2-(p-tolyl)quinoline (40b)

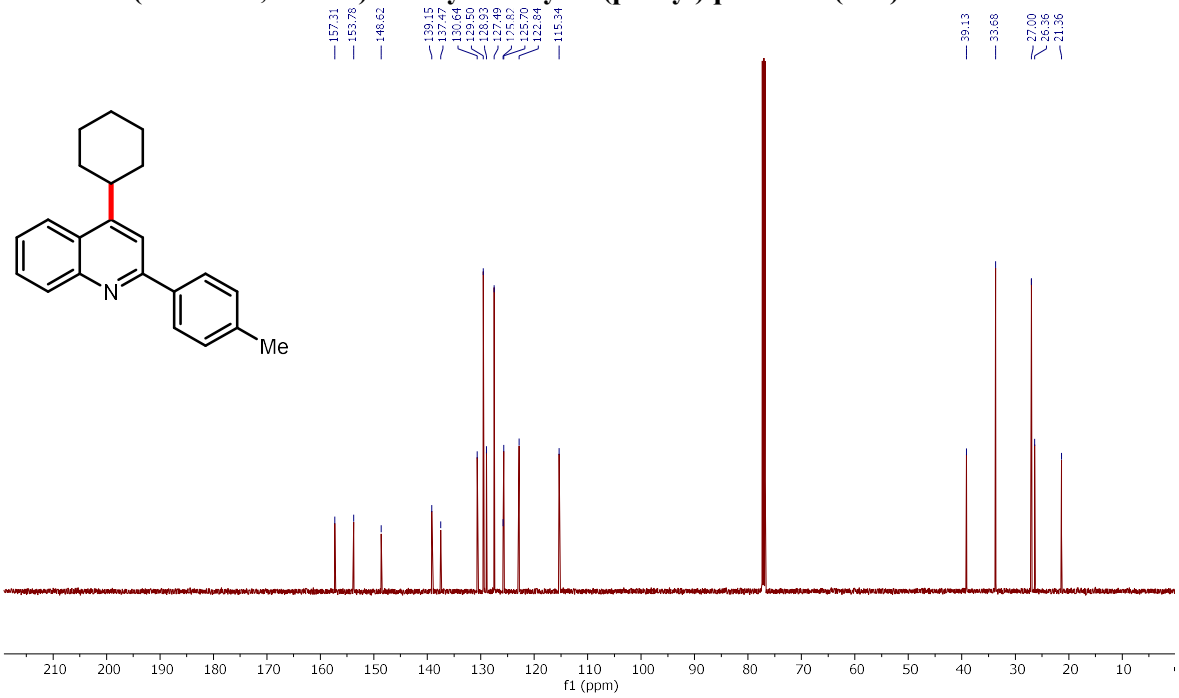

^{1}H NMR (500 MHz, $CDCl_3$) of 2-([1,1'-biphenyl]-4-yl)-4-cyclohexylquinoline (41b)

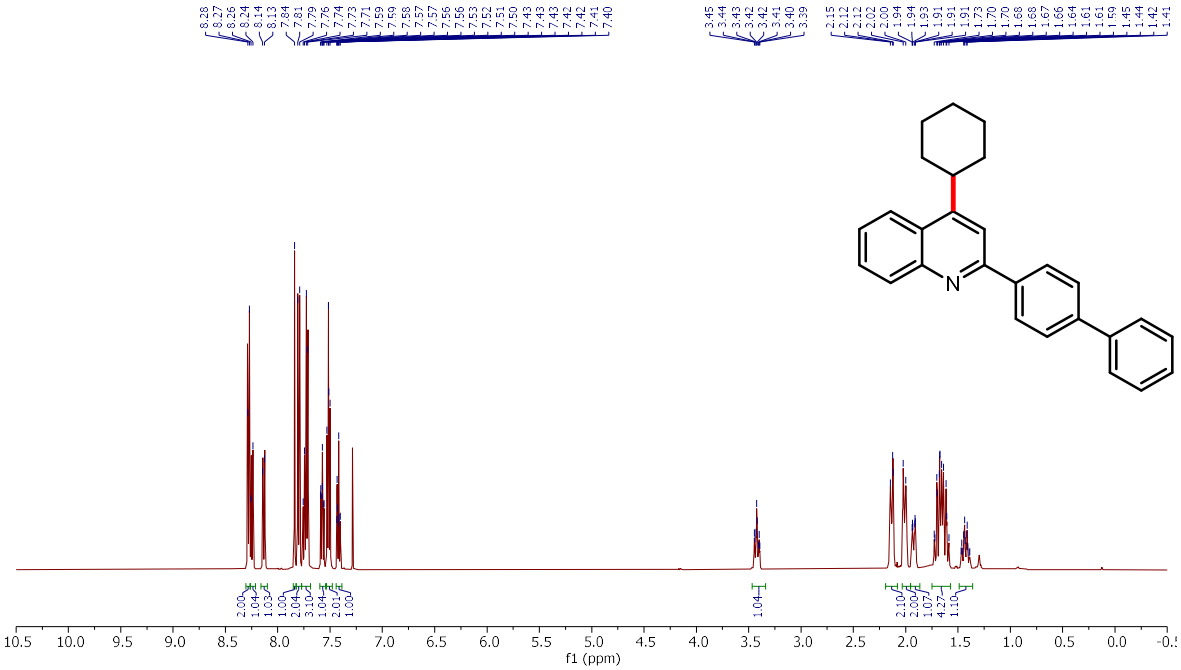

^{13}C NMR (125 MHz, $CDCl_3$) of 2-([1,1'-biphenyl]-4-yl)-4-cyclohexylquinoline (41b)

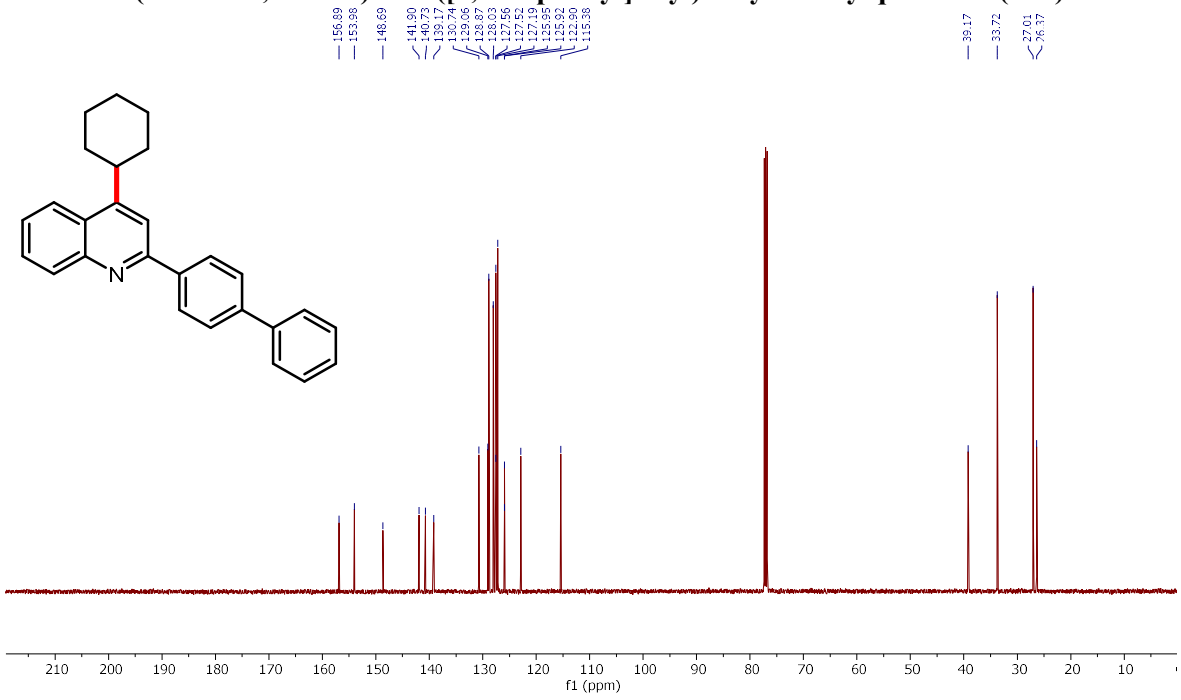

^{1}H NMR (500 MHz, $CDCl_3$) of 4-cyclohexyl-2-(4-methoxyphenyl)quinoline (42b)

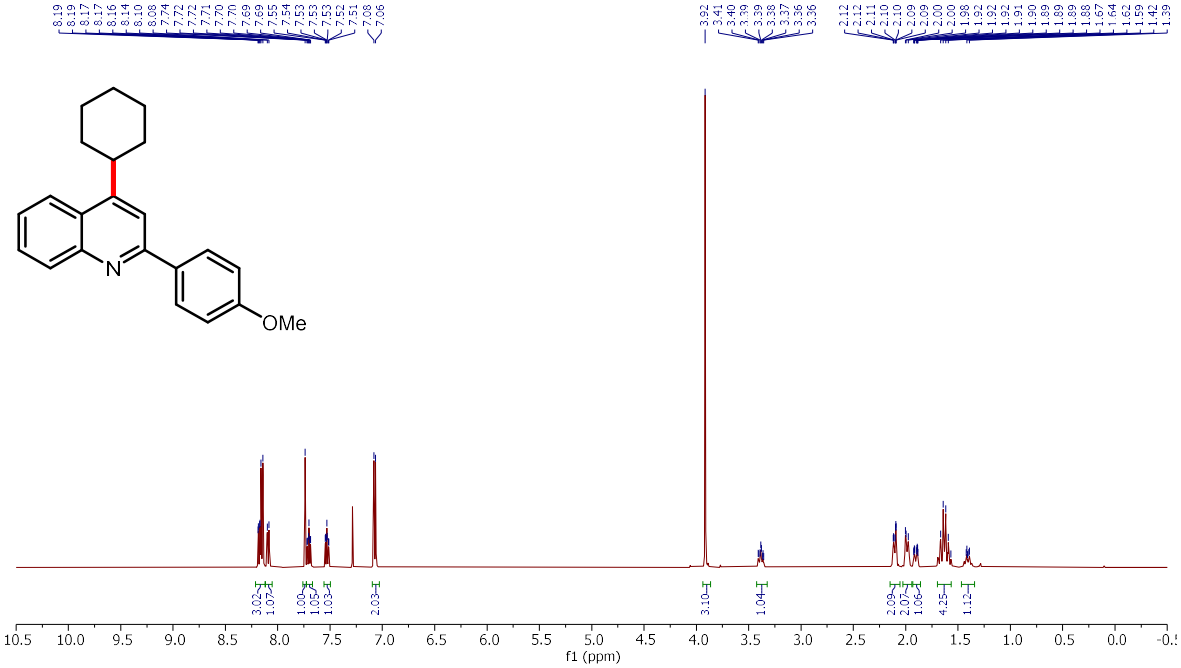

^{13}C NMR (125 MHz, $CDCl_3$) of 4-cyclohexyl-2-(4-methoxyphenyl)quinoline (42b)

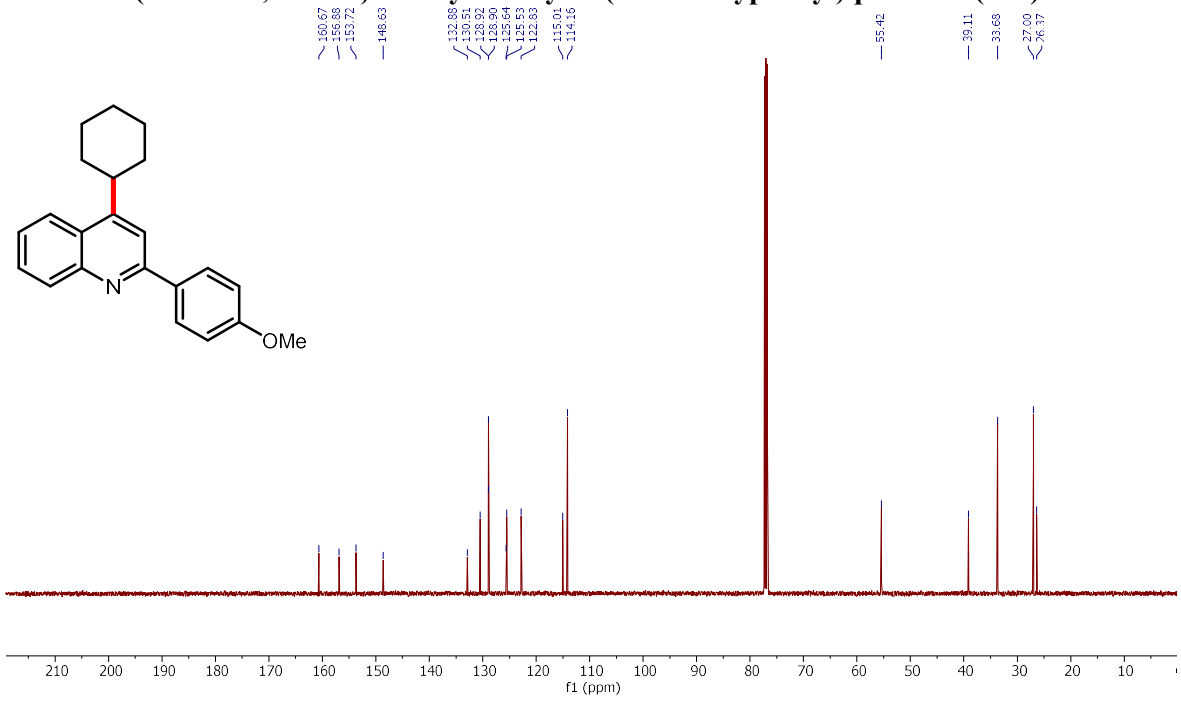

^{1}H NMR (500 MHz, $CDCl_3$) of 4-cyclohexyl-2-phenethylquinoline (46b)

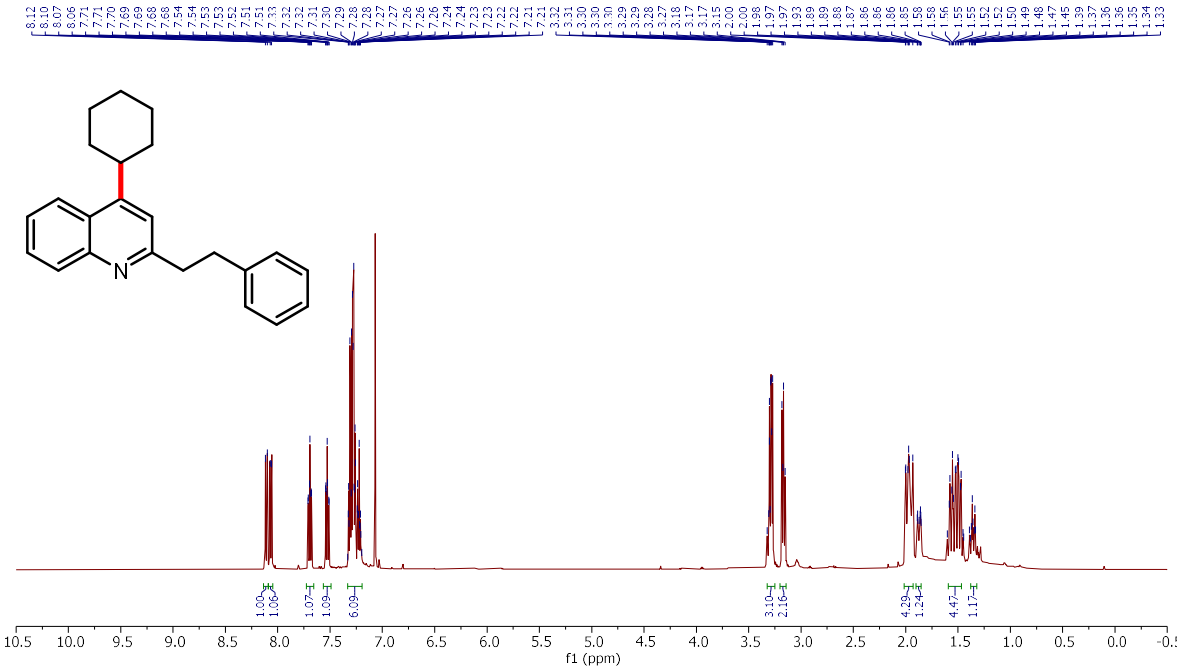

^{13}C NMR (125 MHz, $CDCl_3$) of 4-cyclohexyl-2-phenethylquinoline (46b)

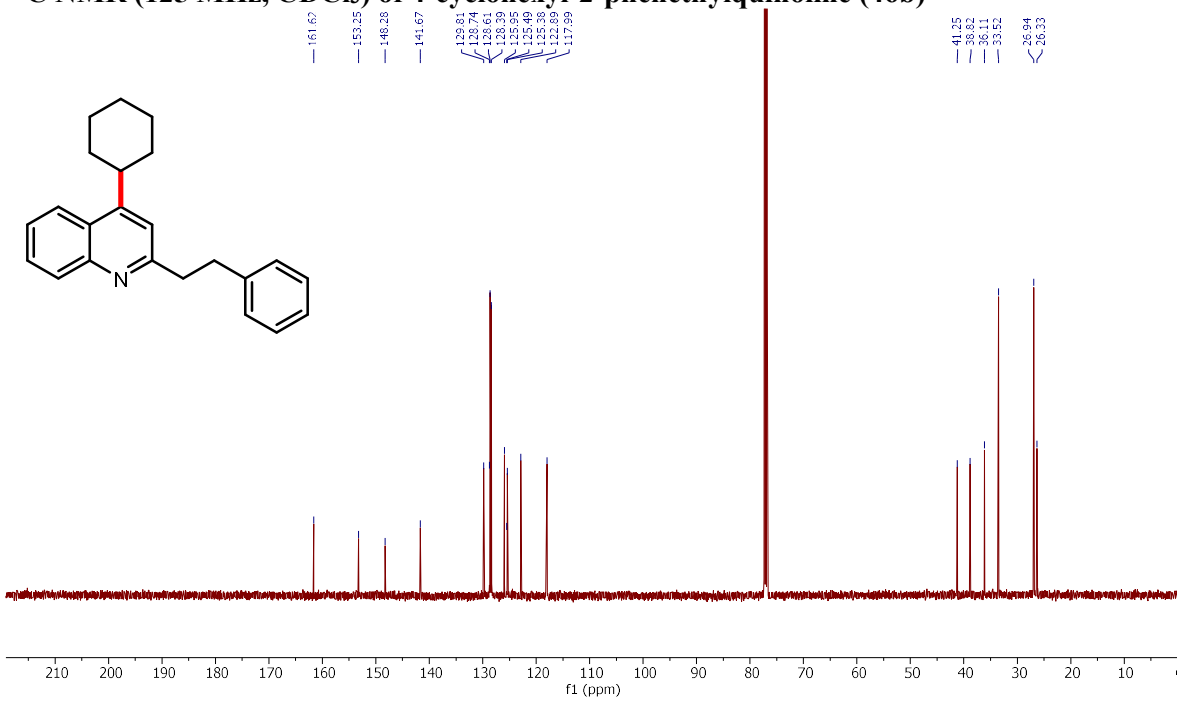

^{1}H NMR (500 MHz, $CDCl_3$) of 6-cyclohexylpyridine-2,4-dicarbonitrile (49b)

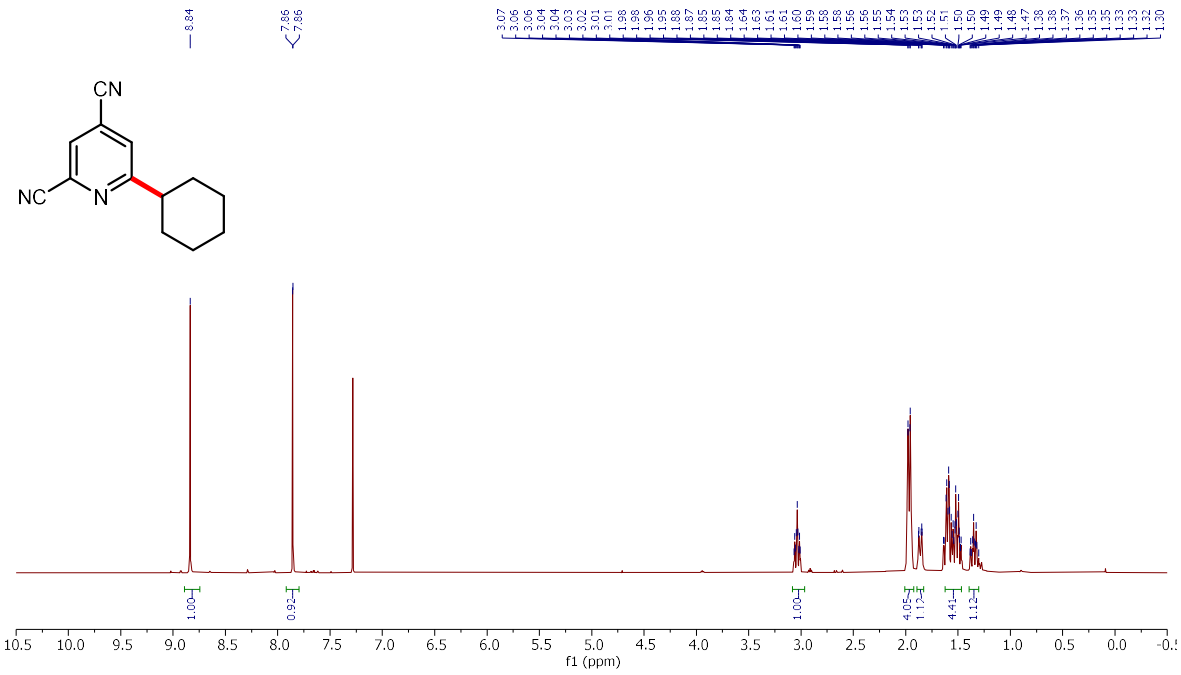

^{13}C NMR (125 MHz, $CDCl_3$) of 6-cyclohexylpyridine-2,4-dicarbonitrile (49b)

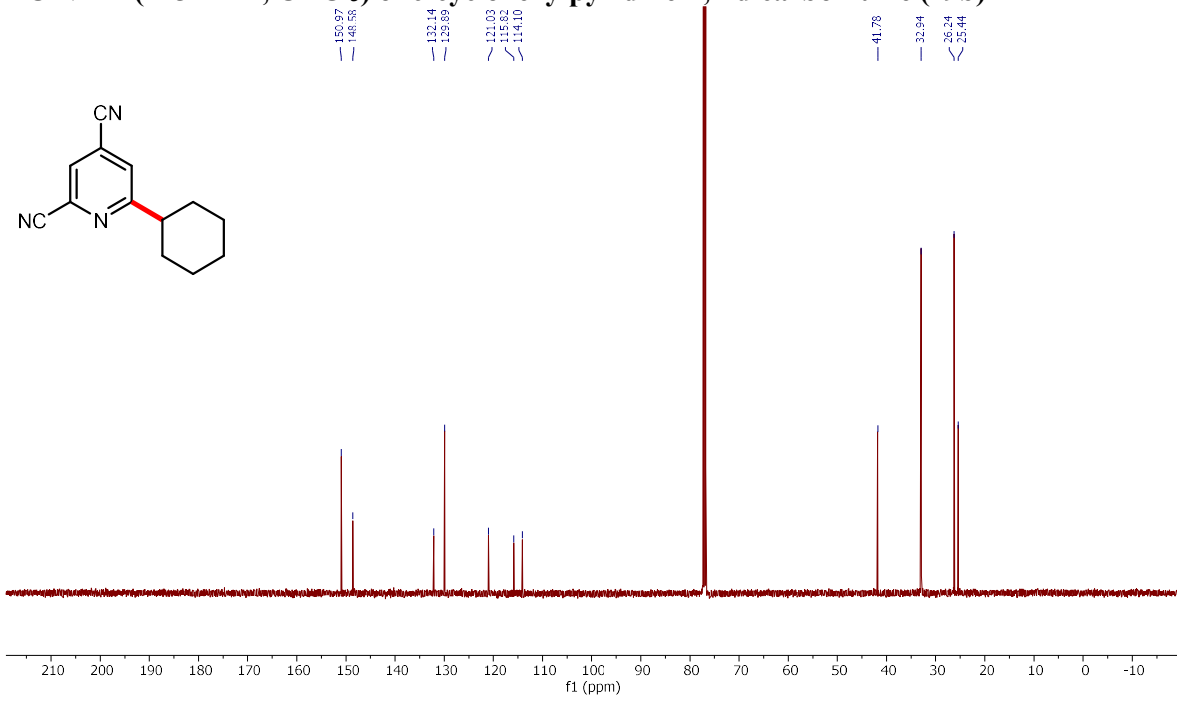

^{1}H NMR (500 MHz, $CDCl_3$) of 6-cyclohexyl-*N*,*N*-diisopropylpyridine-3-sulfonamide (51b)

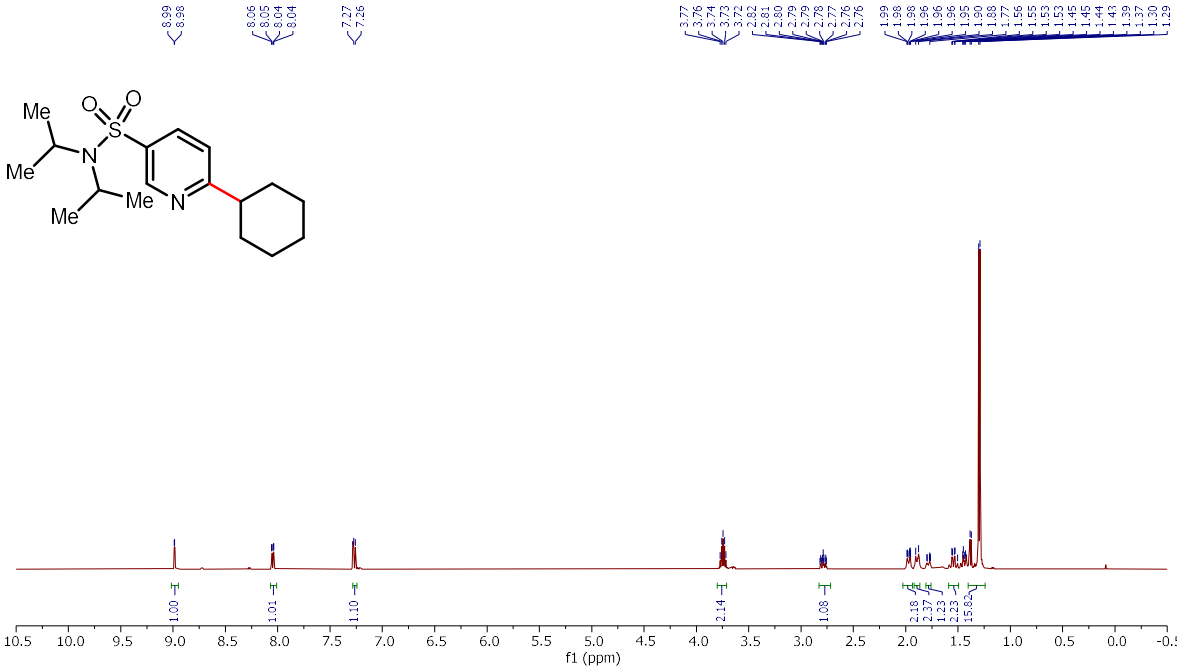

^{13}C NMR (125 MHz, $CDCl_3$) of 6-cyclohexyl-*N*,*N*-diisopropylpyridine-3-sulfonamide (51b)

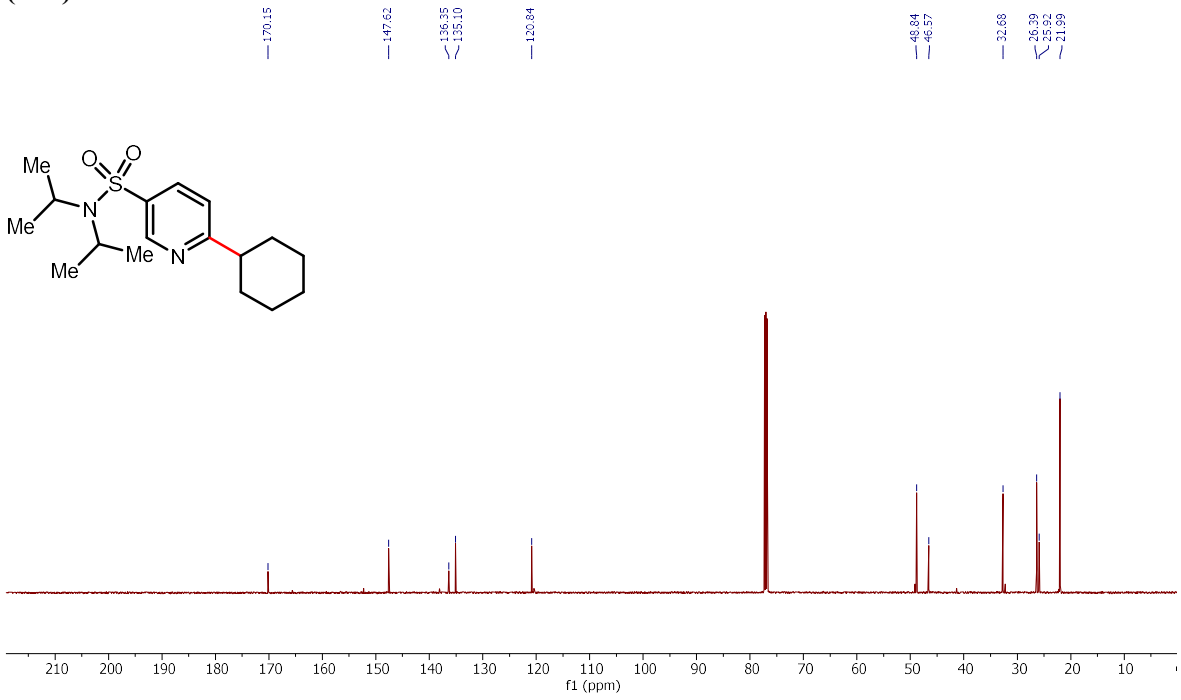

^{1}H NMR (500 MHz, $CDCl_3$) of 5-cyclohexylpyrazine-2,3-dicarbonitrile (59b)

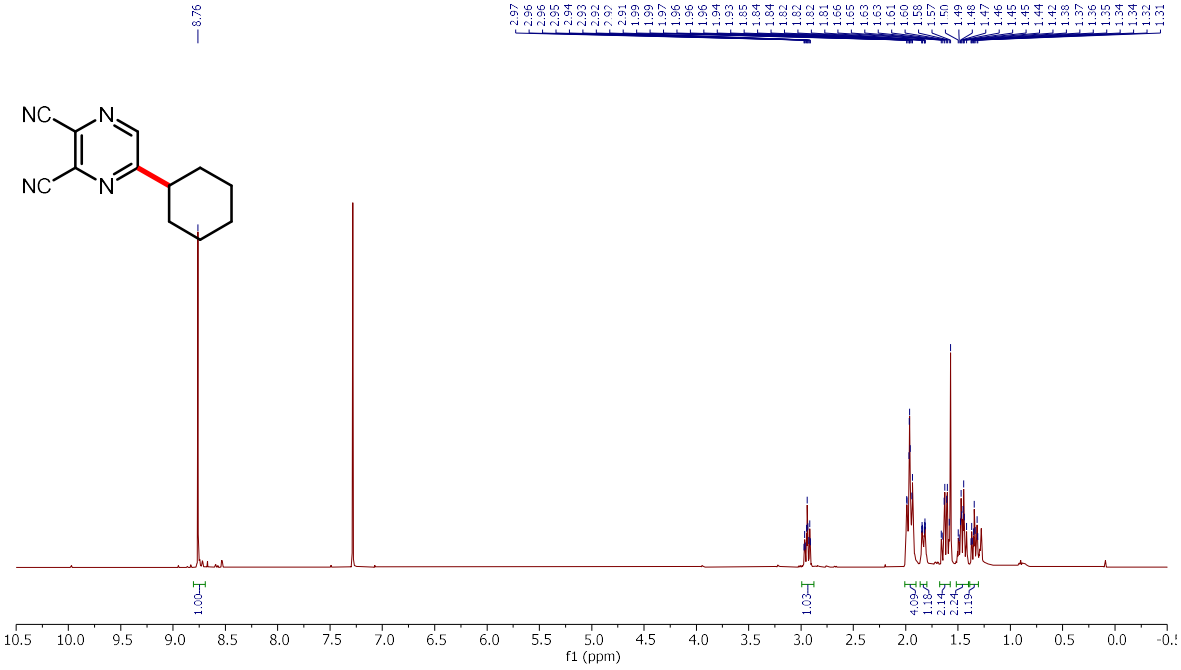

^{13}C NMR (125 MHz, $CDCl_3$) of 5-cyclohexylpyrazine-2,3-dicarbonitrile (59b)

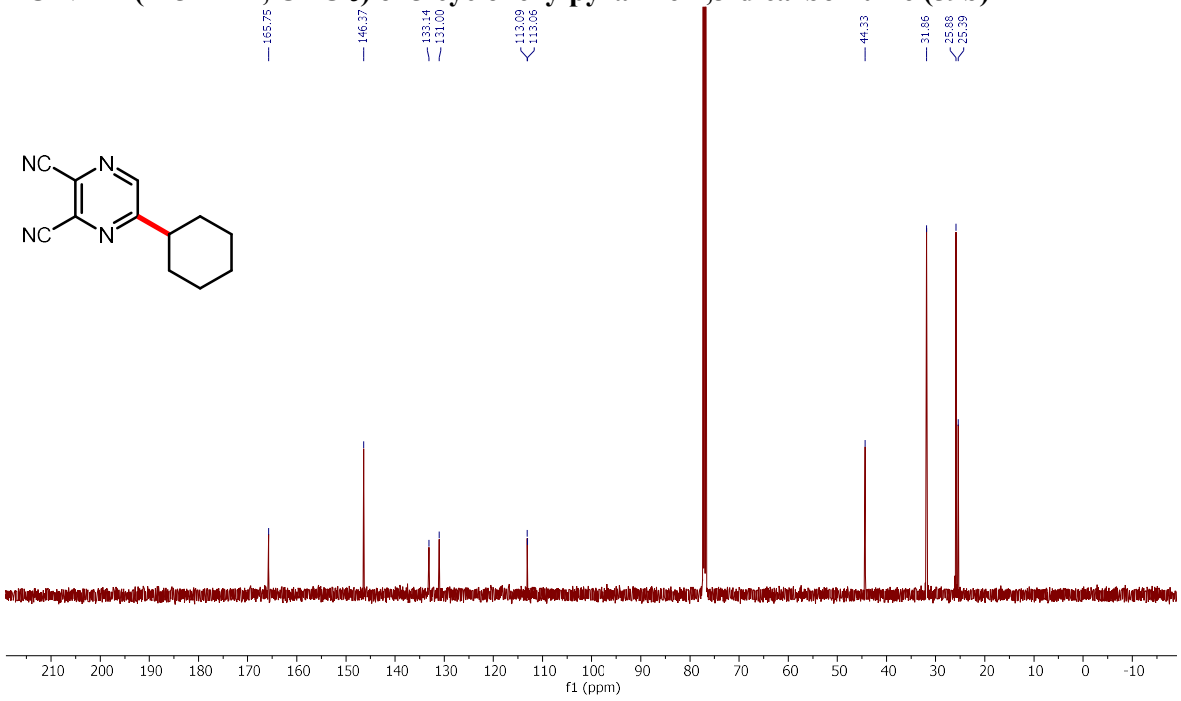

^{1}H NMR (500 MHz, $CDCl_3$) of 8-cyclohexyl-7-methyl-1-(4-oxopentyl)-3,7-dihydro-1*H*-purine-2,6-dione (62b)

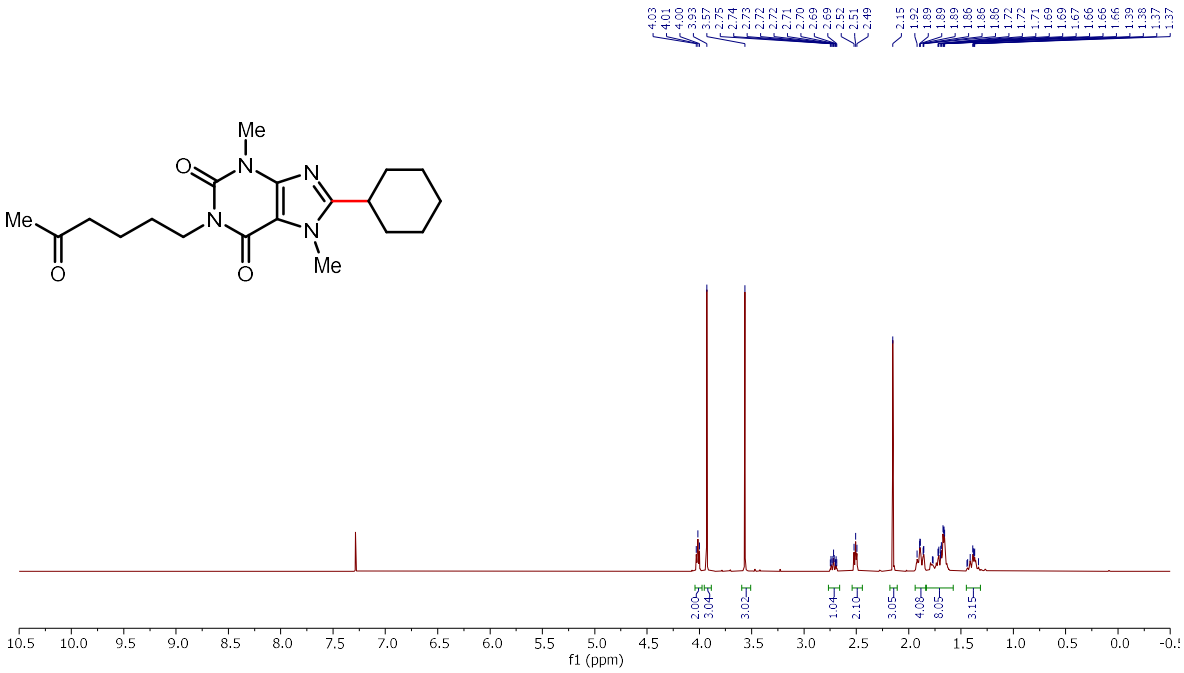

^{13}C NMR (125 MHz, $CDCl_3$) of 8-cyclohexyl-7-methyl-1-(4-oxopentyl)-3,7-dihydro-1*H*-purine-2,6-dione (62b)

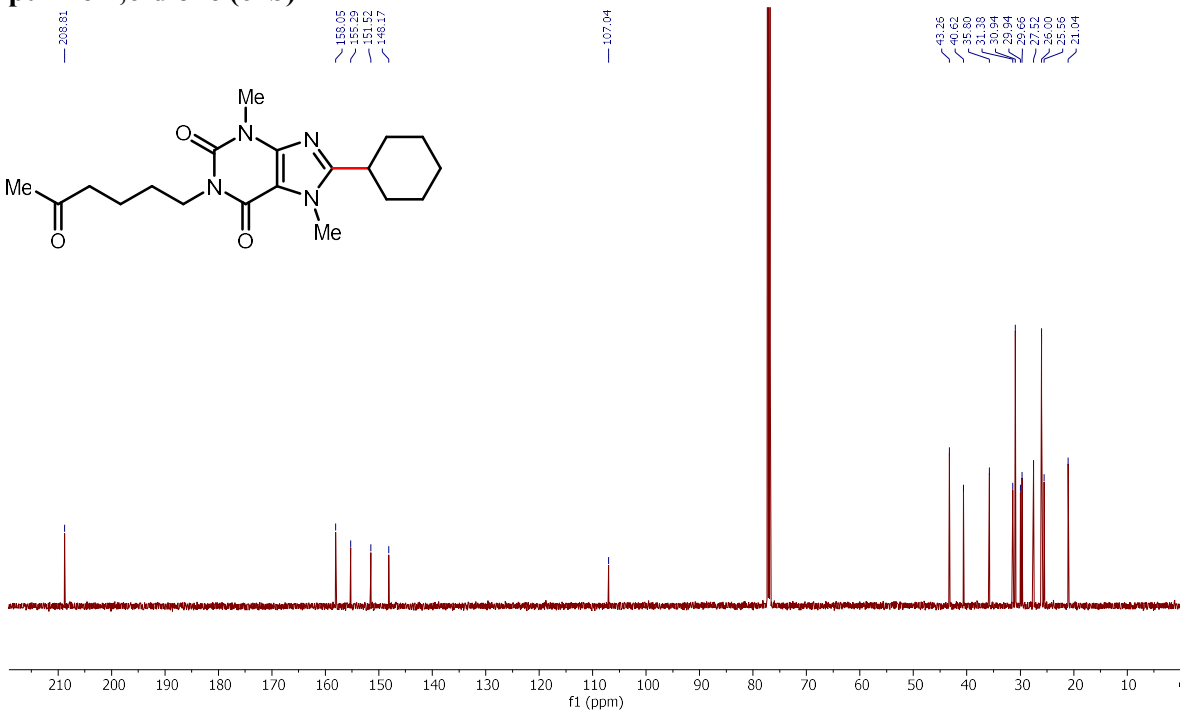

^{1}H NMR (500 MHz, $CDCl_3$) of (*R*)-methyl-2-(2-cyclohexylisonicotinamido)propanoate (64b)

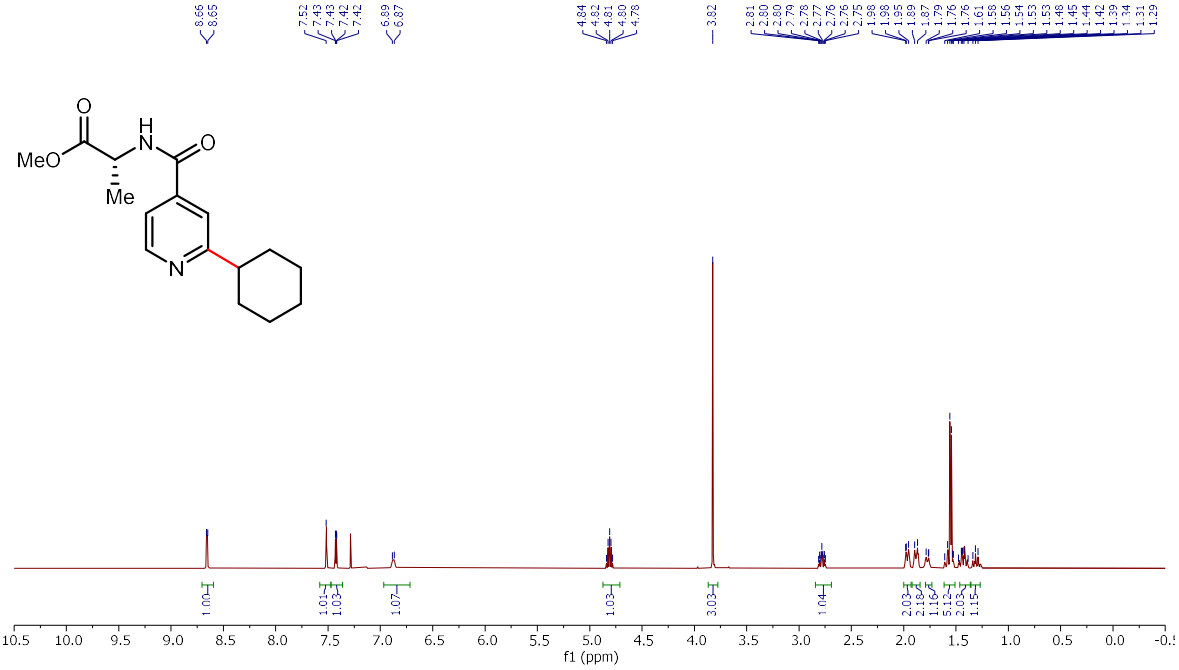

^{13}C NMR (125 MHz, $CDCl_3$) of (*R*)-methyl-2-(2-cyclohexylisonicotinamido)propanoate (64b)

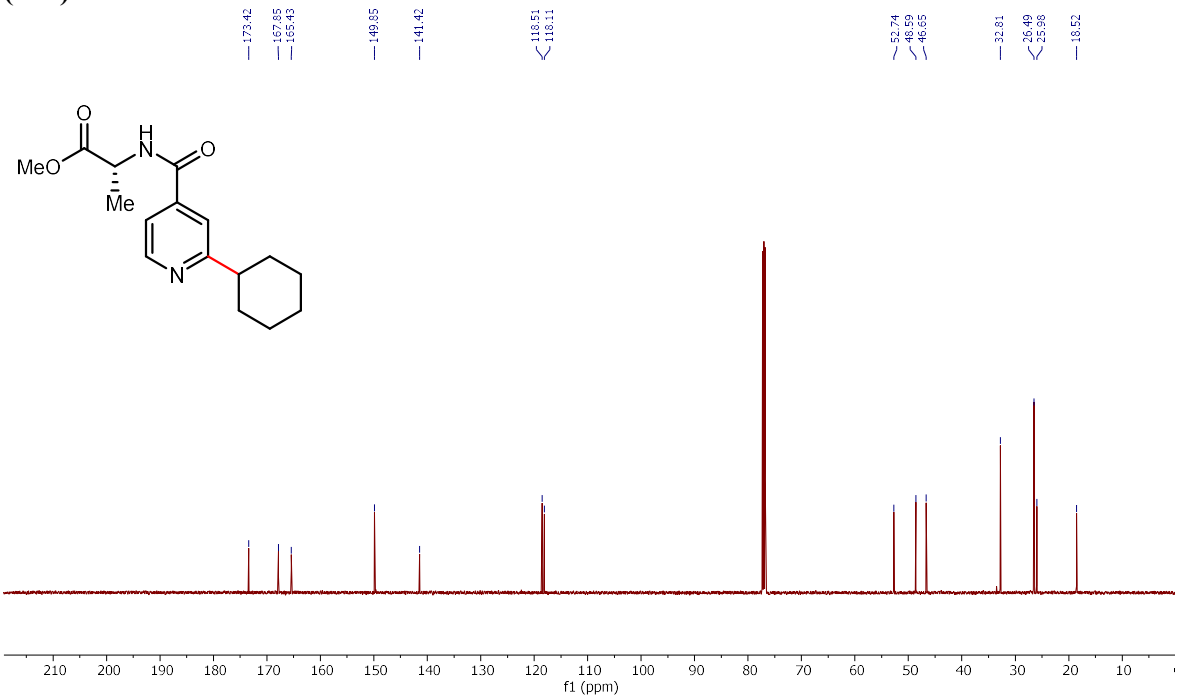

^{1}H NMR (500 MHz, $CDCl_3$) of (*1R*,*2S*,*5R*)-2-isopropyl-5-methylcyclohexyl 2-cyclohexylisonicotinate (65b)

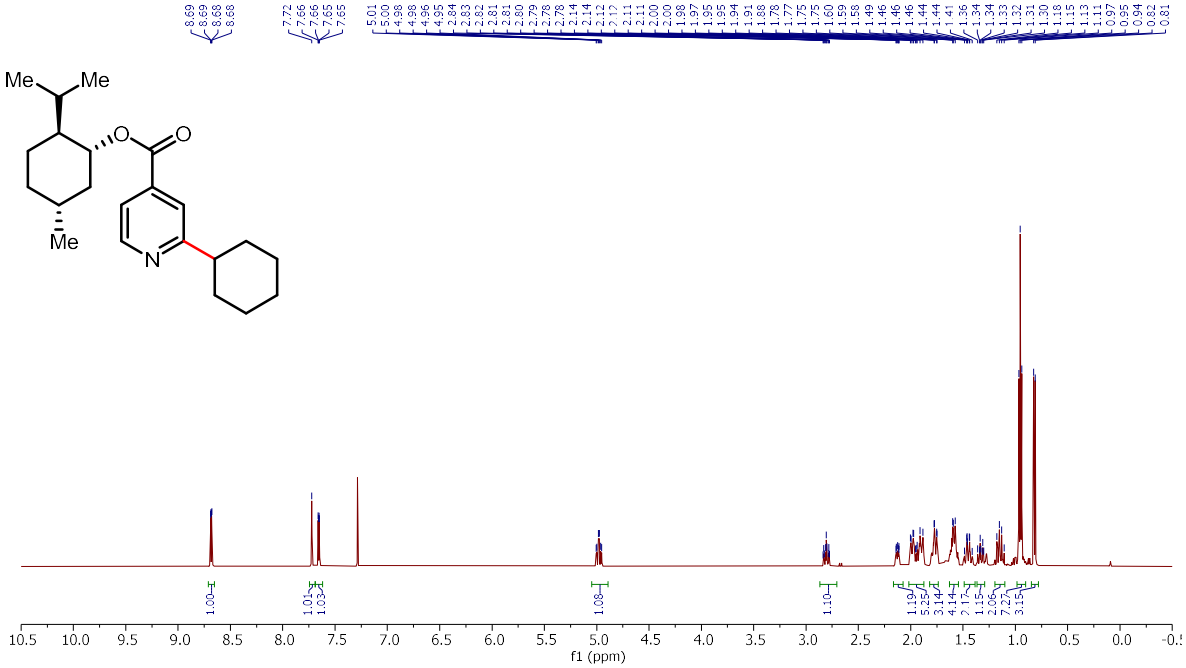

^{13}C NMR (125 MHz, $CDCl_3$) of (*1R*,*2S*,*5R*)-2-isopropyl-5-methylcyclohexyl 2-cyclohexylisonicotinate (65b)

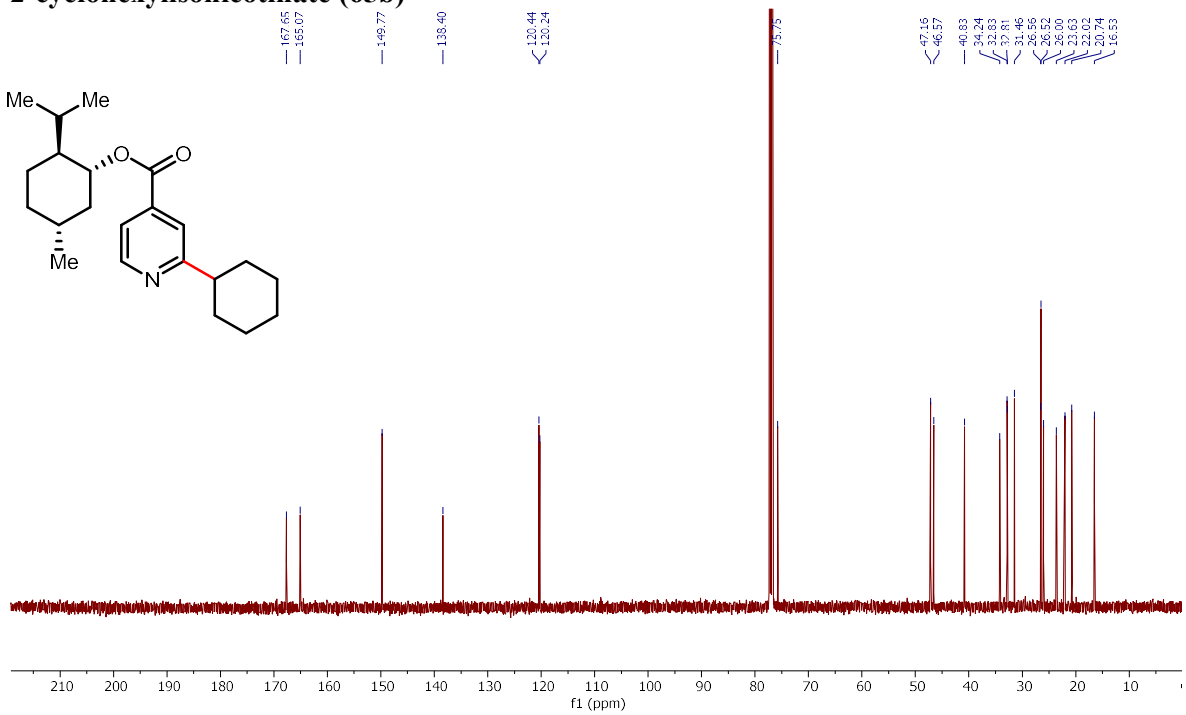

^{1}H NMR (500 MHz, $CDCl_3$) of (*S*)-(2-cyclohexylquinolin-4-yl)((1*S*,2*S*,4*S*,5*R*)-5-ethylquinuclidin-2-yl)methanol (67b)

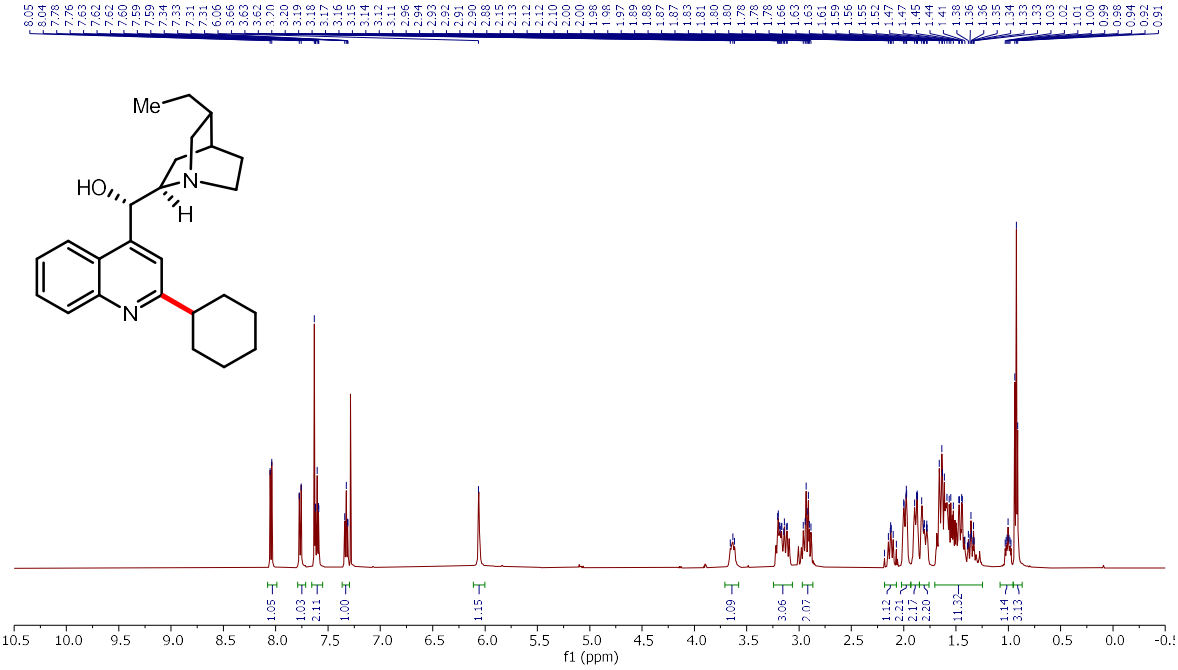

^{13}C NMR (125 MHz, $CDCl_3$) of (*S*)-(2-cyclohexylquinolin-4-yl)((1*S*,2*S*,4*S*,5*R*)-5-ethylquinuclidin-2-yl)methanol (67b)

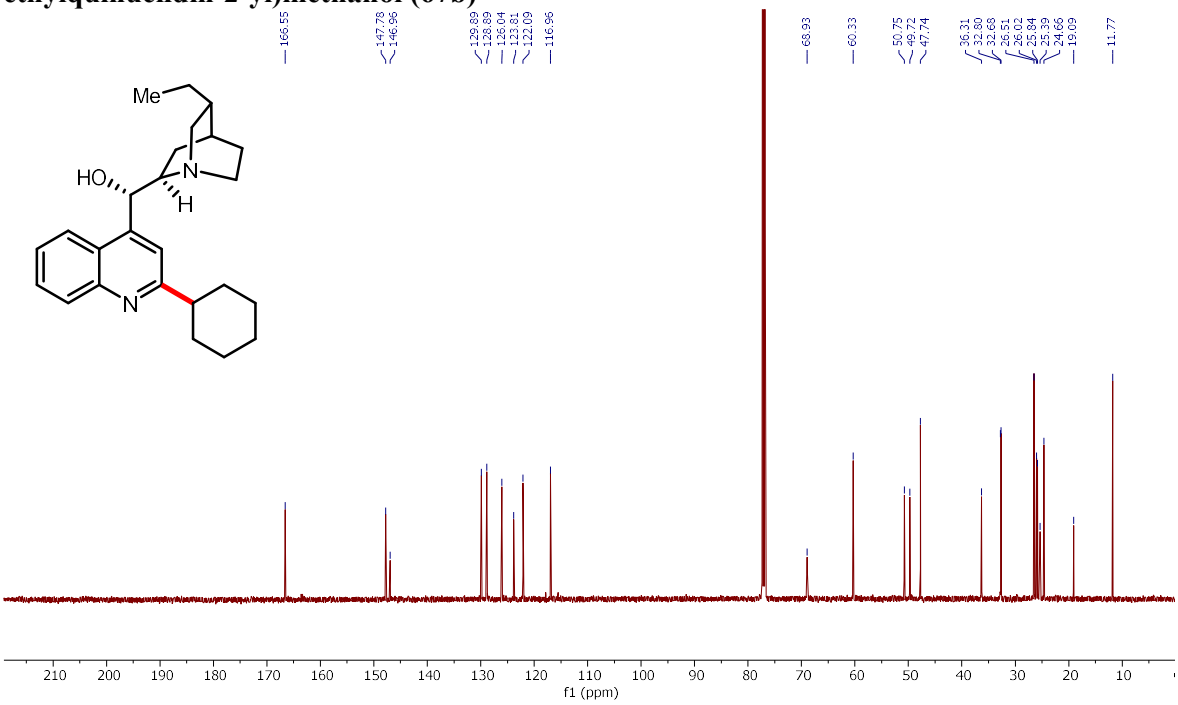

^{1}H NMR (500 MHz, $CDCl_3$) of 4-(cyclohexyl-d_{11})-2-phenylquinoline (3b-d_{11})

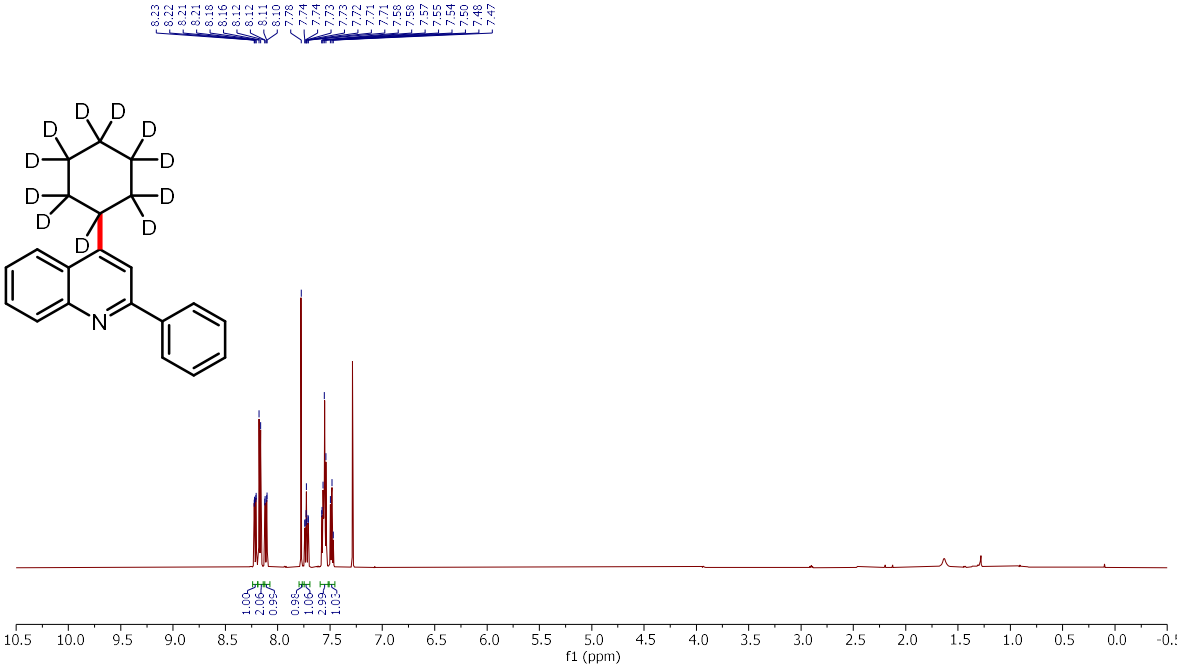

^{13}C NMR (125 MHz, $CDCl_3$) of 4-(cyclohexyl-d_{11})-2-phenylquinoline (3b-d_{11})

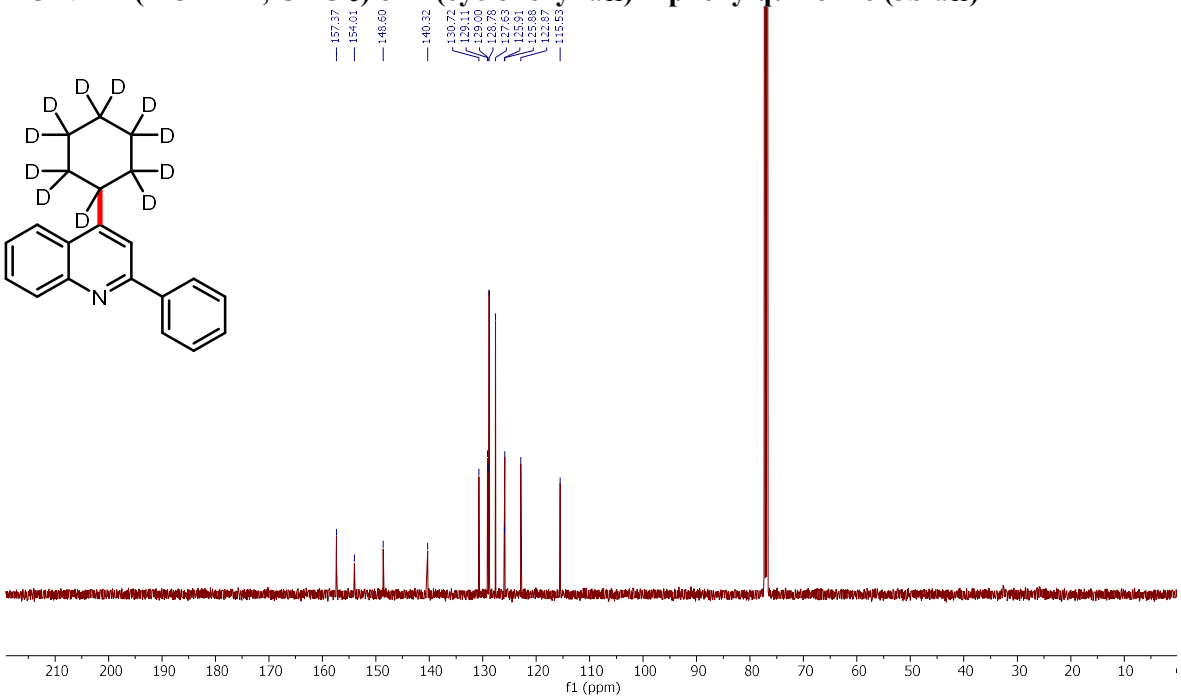

^{2}H NMR (77 MHz, $CDCl_3$) of 4-(cyclohexyl-d_{11})-2-phenylquinoline (3b-d_{11})

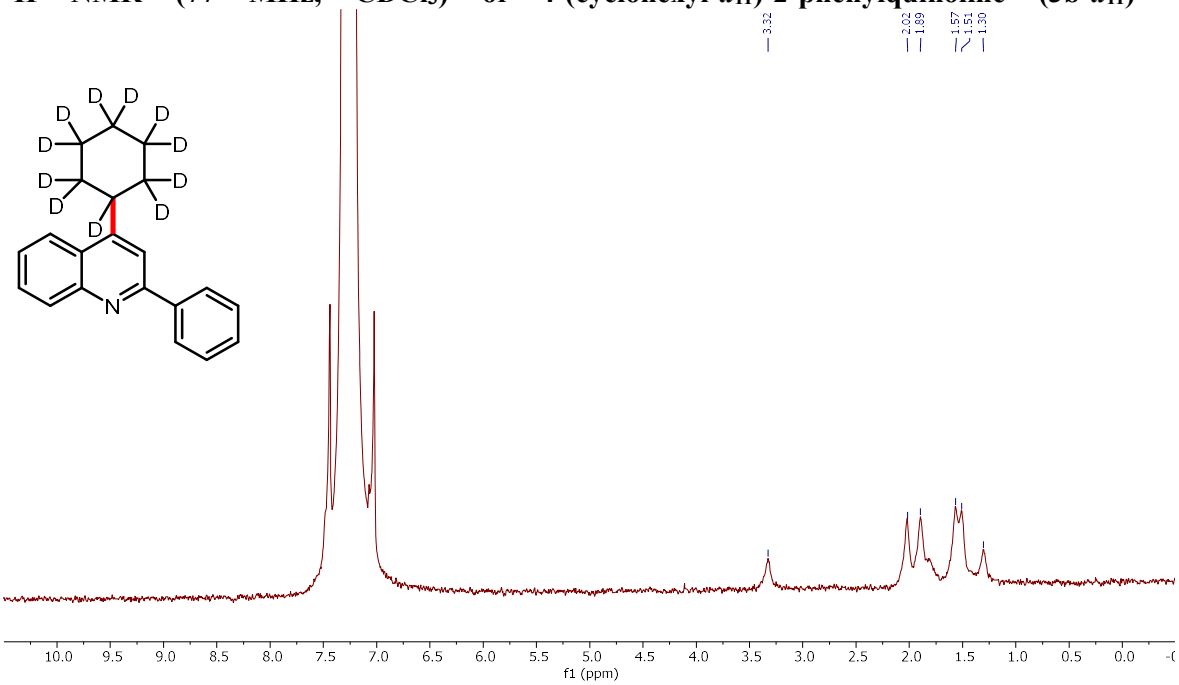

Appendix 3: NMR spectra for new compounds in chapter 4

^{1}H NMR (500 MHz, $CDCl_3$) of 4-(4-(4-methoxyphenyl)quinolin-2-yl)phenol ($DPQN^{2\text{-}OH\text{-}4\text{-}OMe}$)

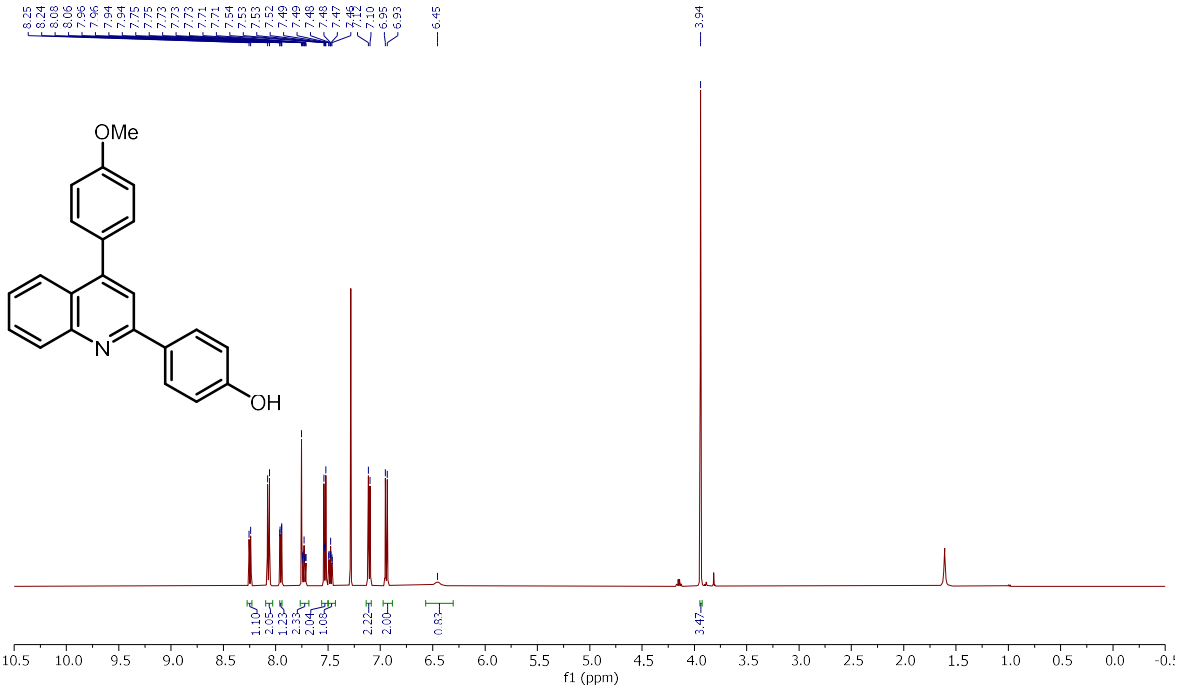

^{13}C NMR (126 MHz, $CDCl_3$) of 4-(4-(4-methoxyphenyl)quinolin-2-yl)phenol ($DPQN^{2\text{-}OH\text{-}4\text{-}OMe}$)

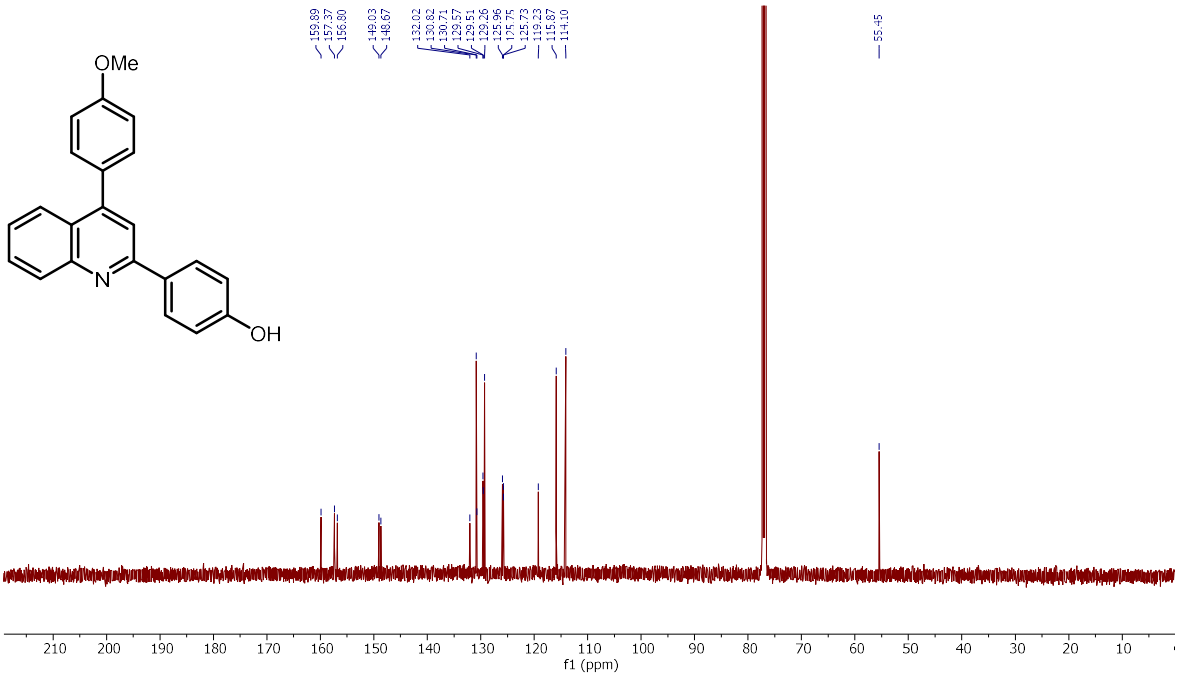

^{1}H NMR (500 MHz, $CDCl_3$) of 4-(4-(4-methoxyphenyl)quinolin-2-yl)phenol (DPQN^{2}-OH-4-eOMe)

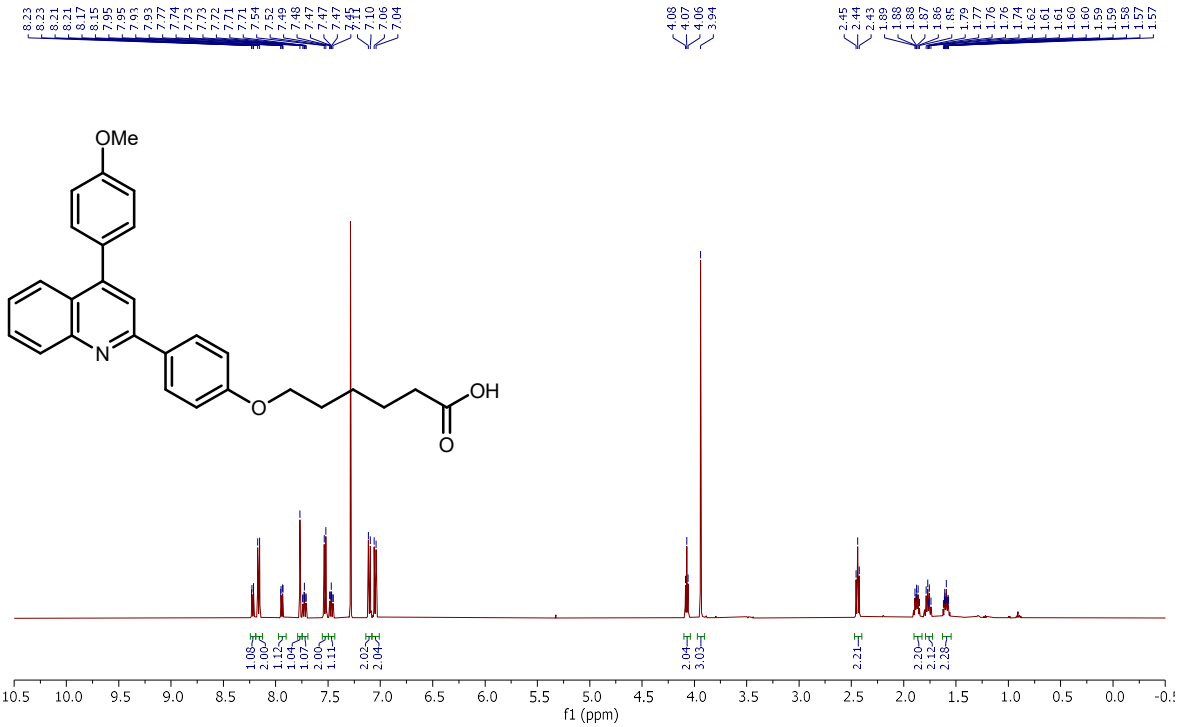

^{13}C NMR (126 MHz, $CDCl_3$) of 4-(4-(4-methoxyphenyl)quinolin-2-yl)phenol (DPQN^{2}-OH-4-OMe)

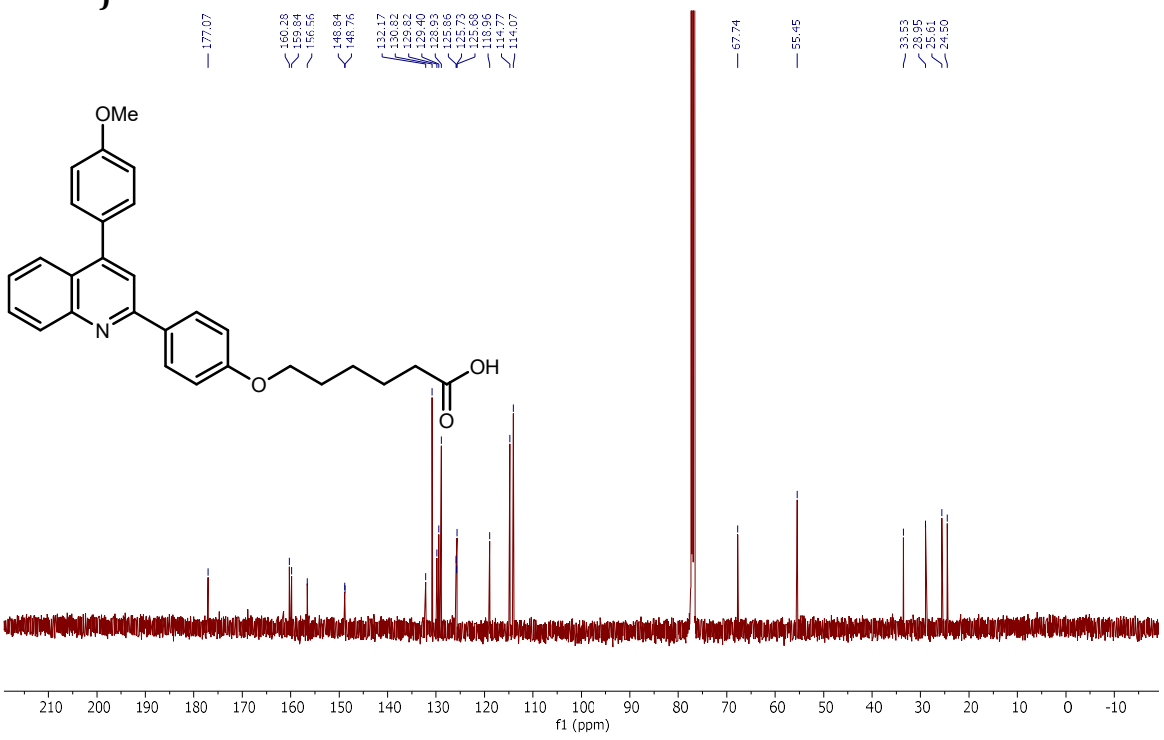

^{1}H NMR (500 MHz, $CDCl_3$) of 3-(4-methylquinolin-2-yl)cyclopentan-1-one (13c)

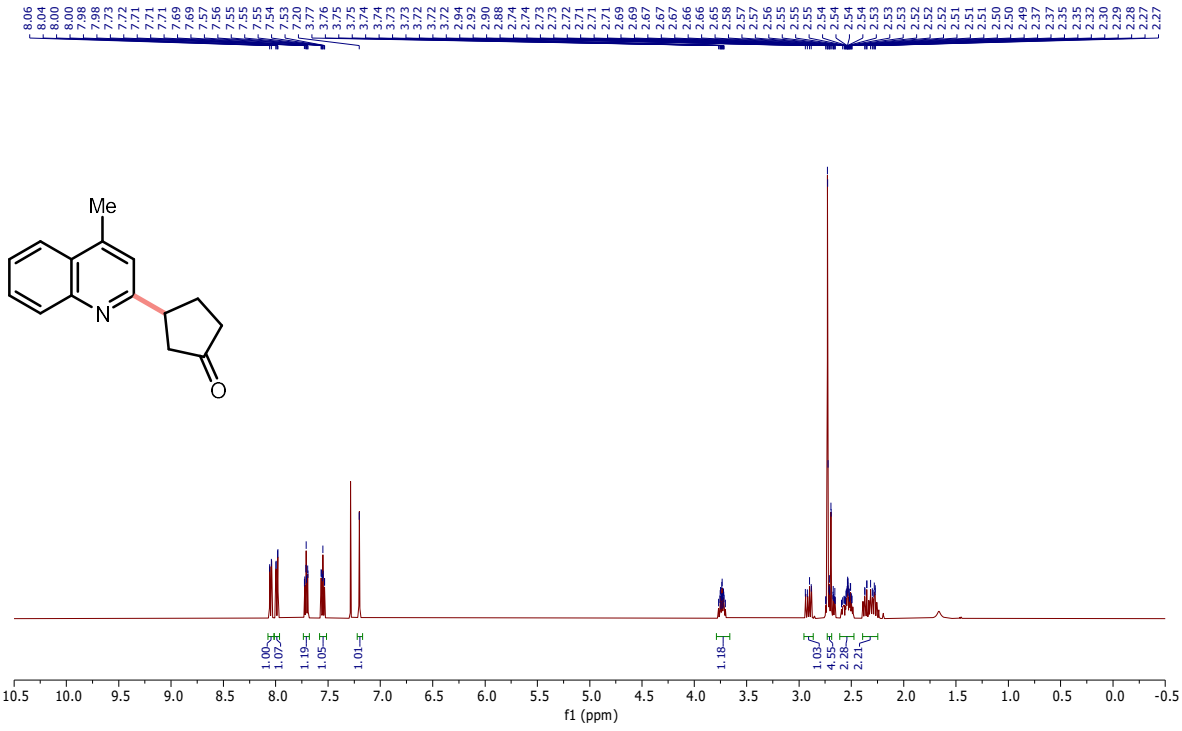

^{13}C NMR (126 MHz, $CDCl_3$) of 3-(4-methylquinolin-2-yl)cyclopentan-1-one (13c)

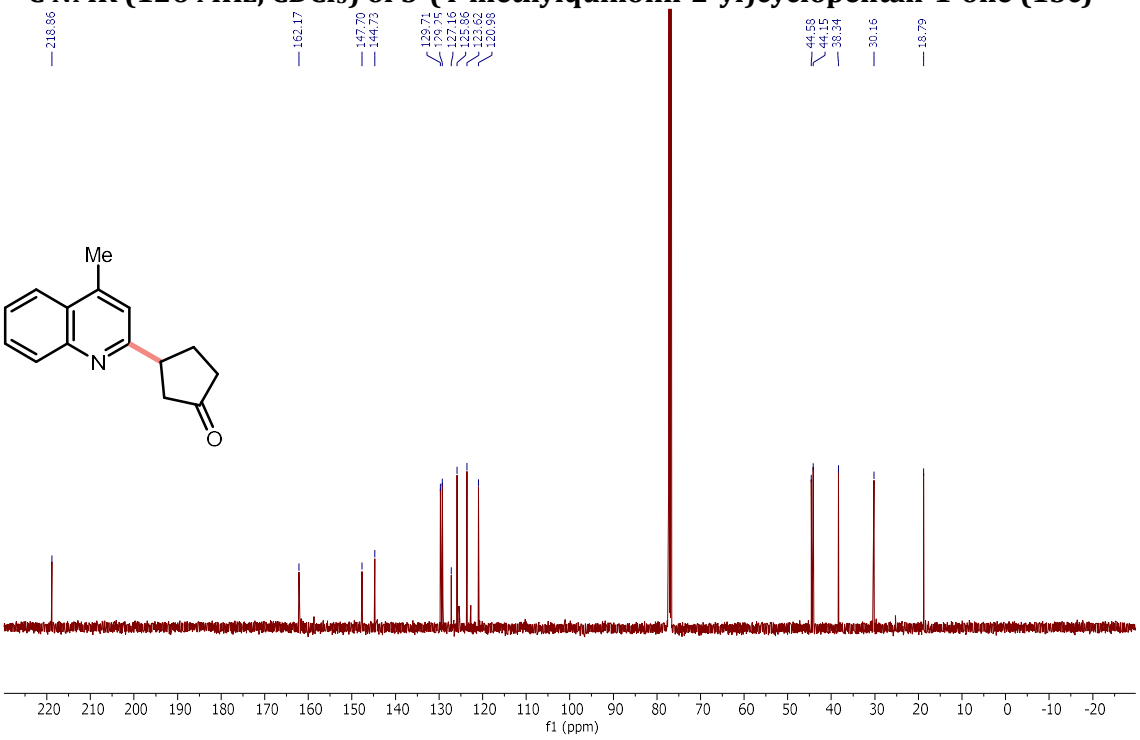

^{1}H NMR (500 MHz, $CDCl_3$) of 2-((((1*R*,2*S*,5*R*)-2-isopropyl-5-methylcyclohexyl)oxy)methyl)-4-methylquinoline (22b)

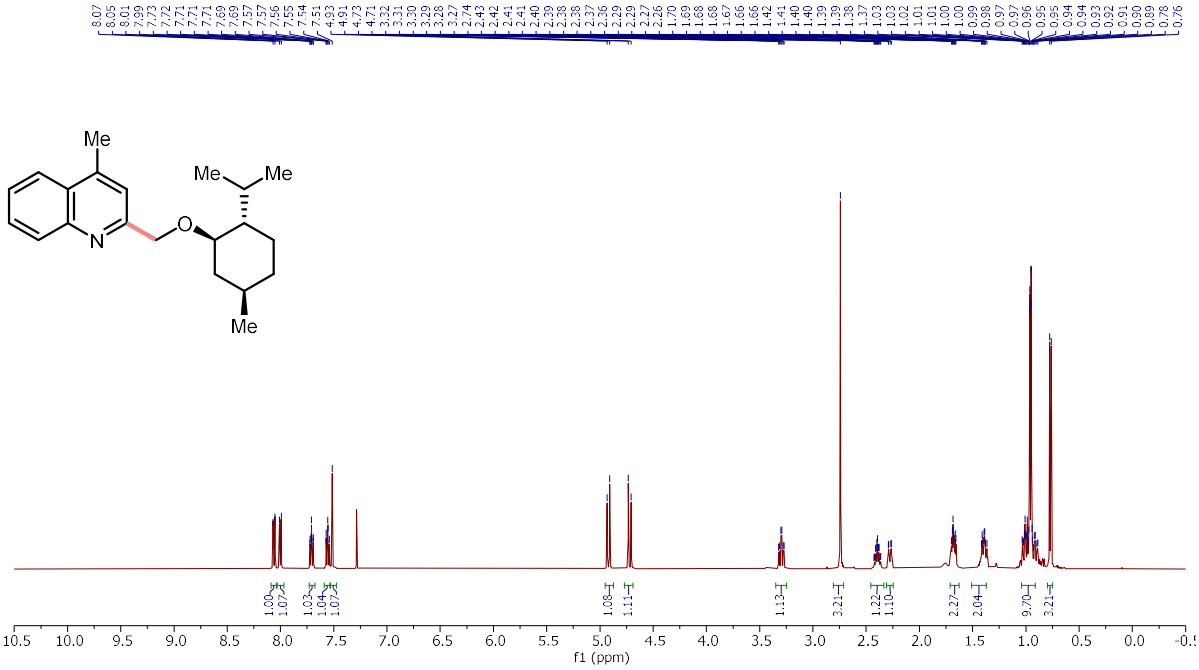

^{13}C NMR (126 MHz, $CDCl_3$) of 2-((((1*R*,2*S*,5*R*)-2-isopropyl-5-methylcyclohexyl)oxy)methyl)-4-methylquinoline (22b)

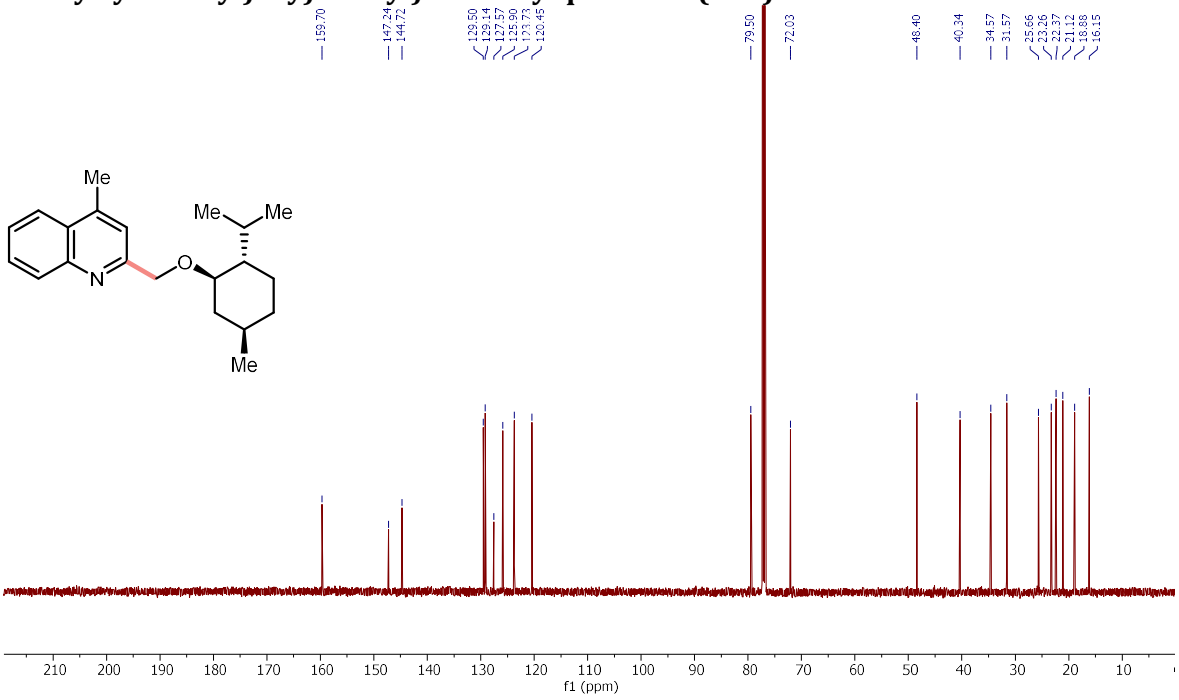

^{1}H NMR (500 MHz, $CDCl_3$) of 2-cyclohexylquinoline-4-carbonitrile (24b)

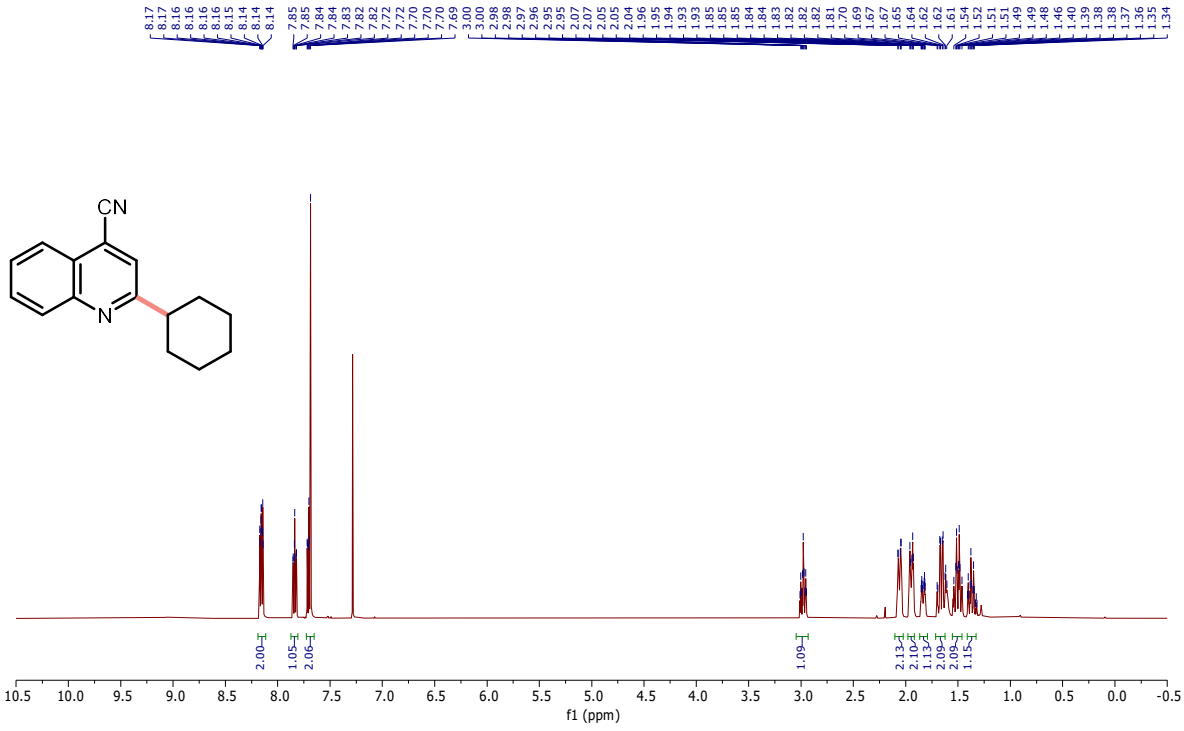

^{13}C NMR (126 MHz, $CDCl_3$) of 2-cyclohexylquinoline-4-carbonitrile (24b)

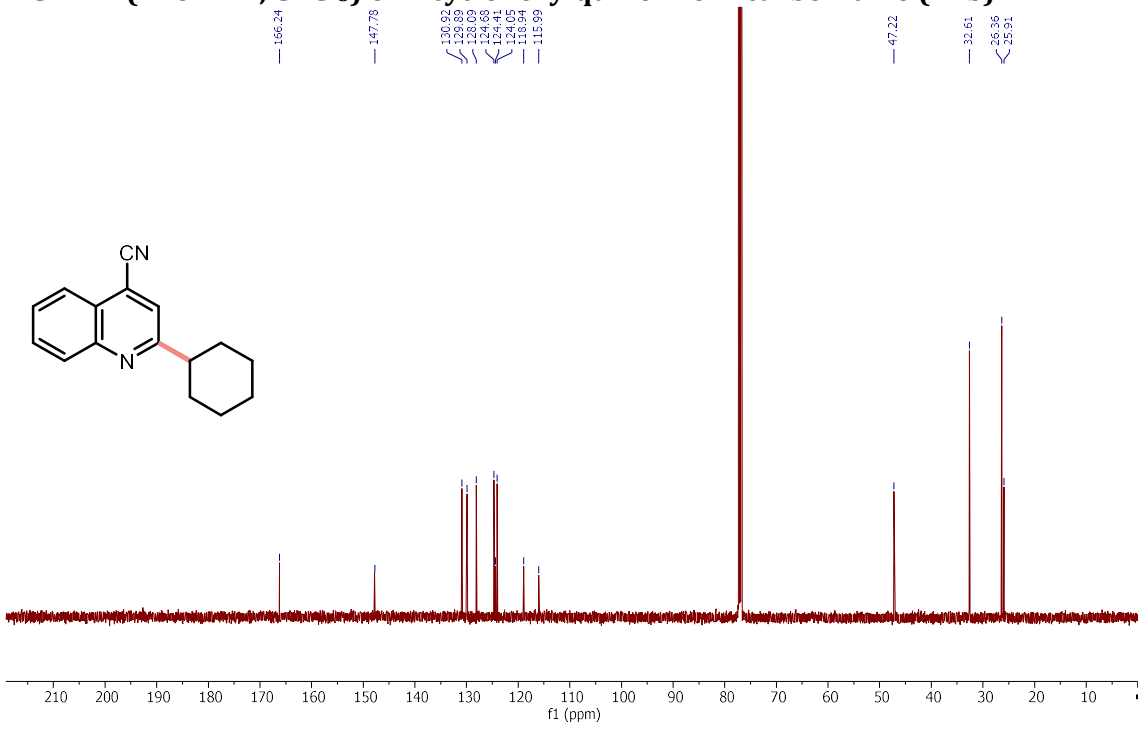

^{1}H NMR (500 MHz, $CDCl_3$) of 2-cyclohexyl-6-methoxyquinoline (29c) and 2,4-dicyclohexyl-6-methoxyquinoline (29c'), mono:di=1:0.1

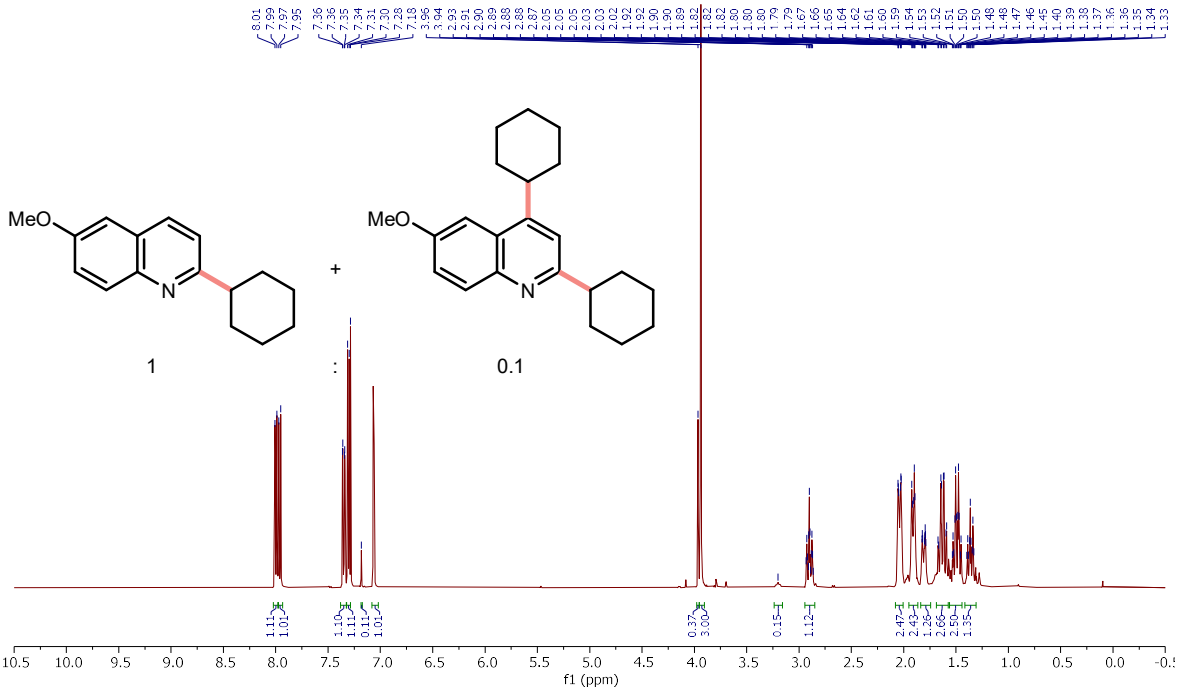

^{13}C NMR (126 MHz, $CDCl_3$) of 2-cyclohexyl-6-methoxyquinoline (29c) and 2,4-dicyclohexyl-6-methoxyquinoline (29c'), mono:di=1:0.1

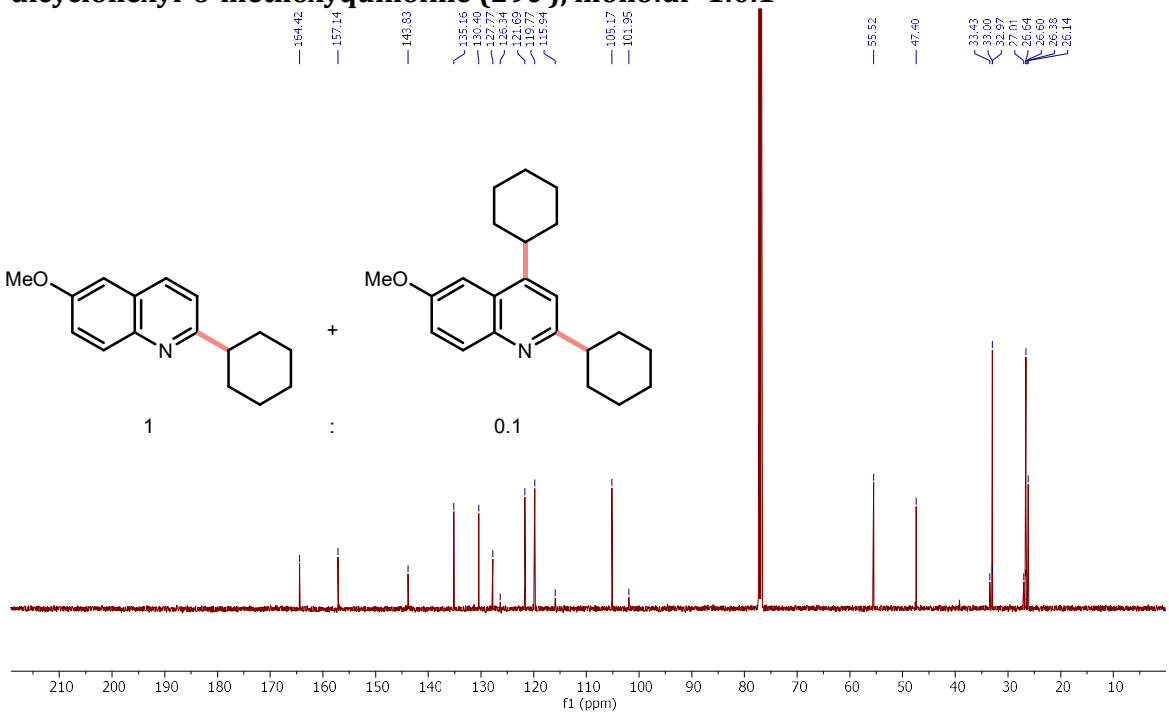

^{1}H NMR (500 MHz, $CDCl_3$) of (2,6-dicyclohexylpyridin-4-yl)(pyrrolidin-1-yl)methanone (34c)

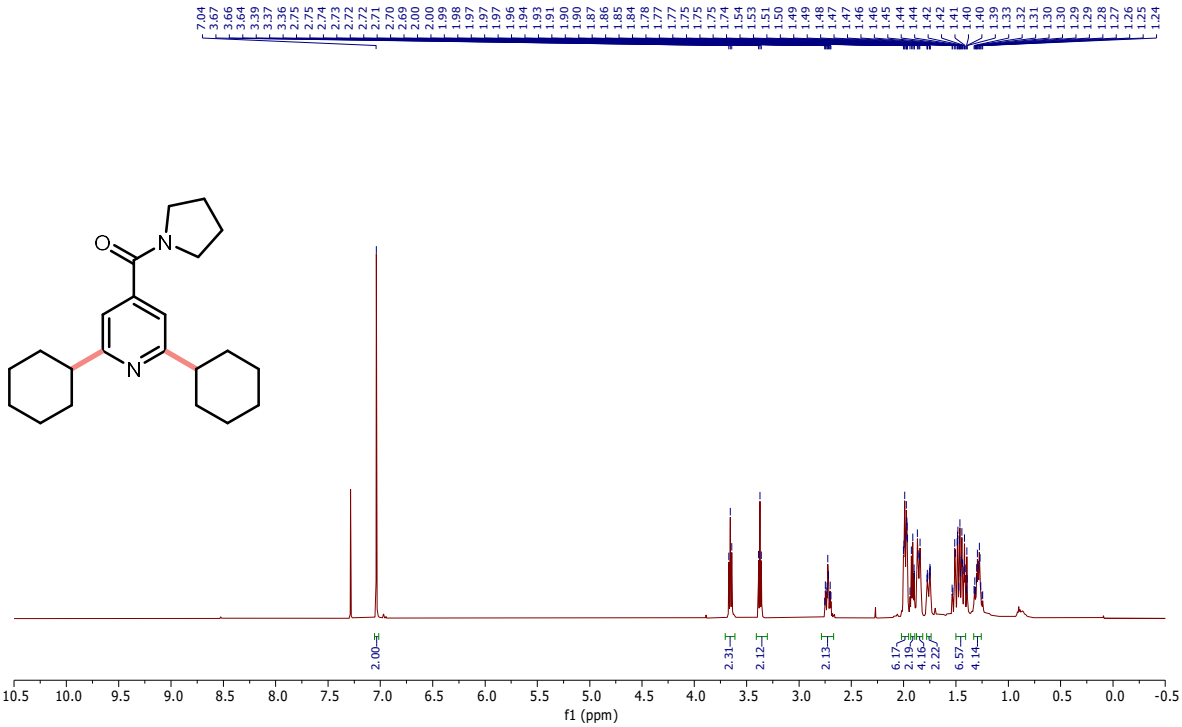

^{13}C NMR (126 MHz, $CDCl_3$) of (2,6-dicyclohexylpyridin-4-yl)(pyrrolidin-1-yl)methanone (34c)

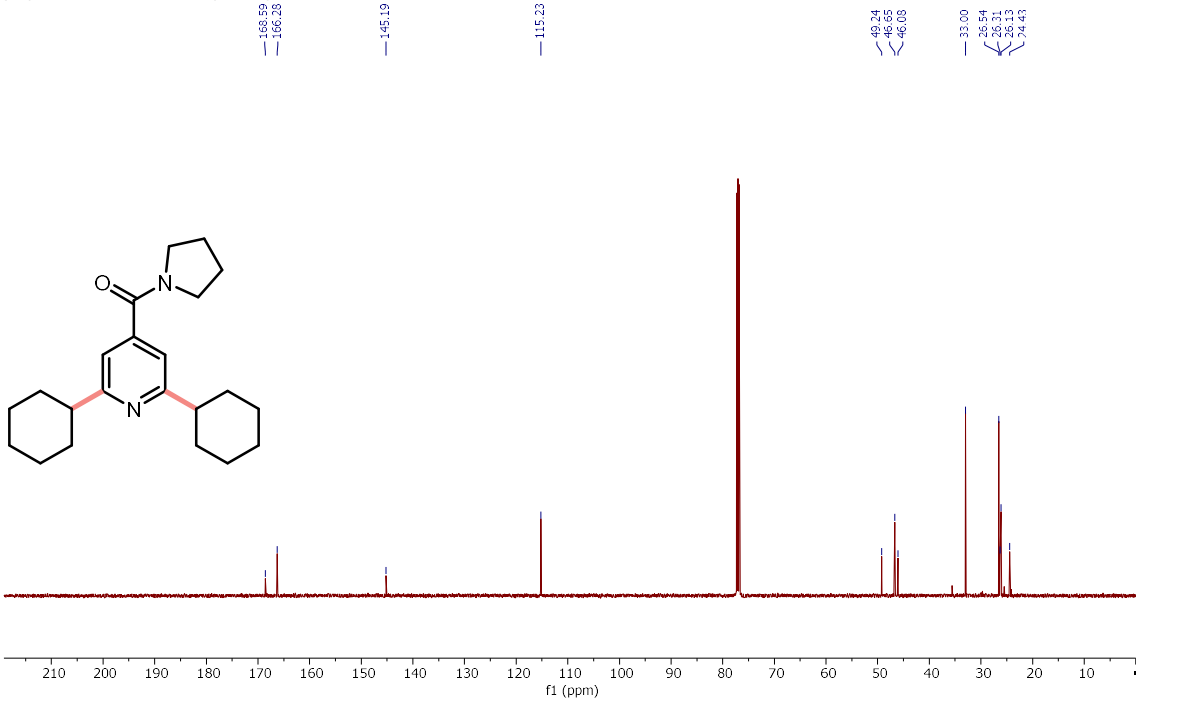

^{1}H NMR (500 MHz, $CDCl_3$) of 2,9-dicyclohexyl-4,7-diphenyl-1,10-phenanthroline (37c) (better purity could not be obtained)

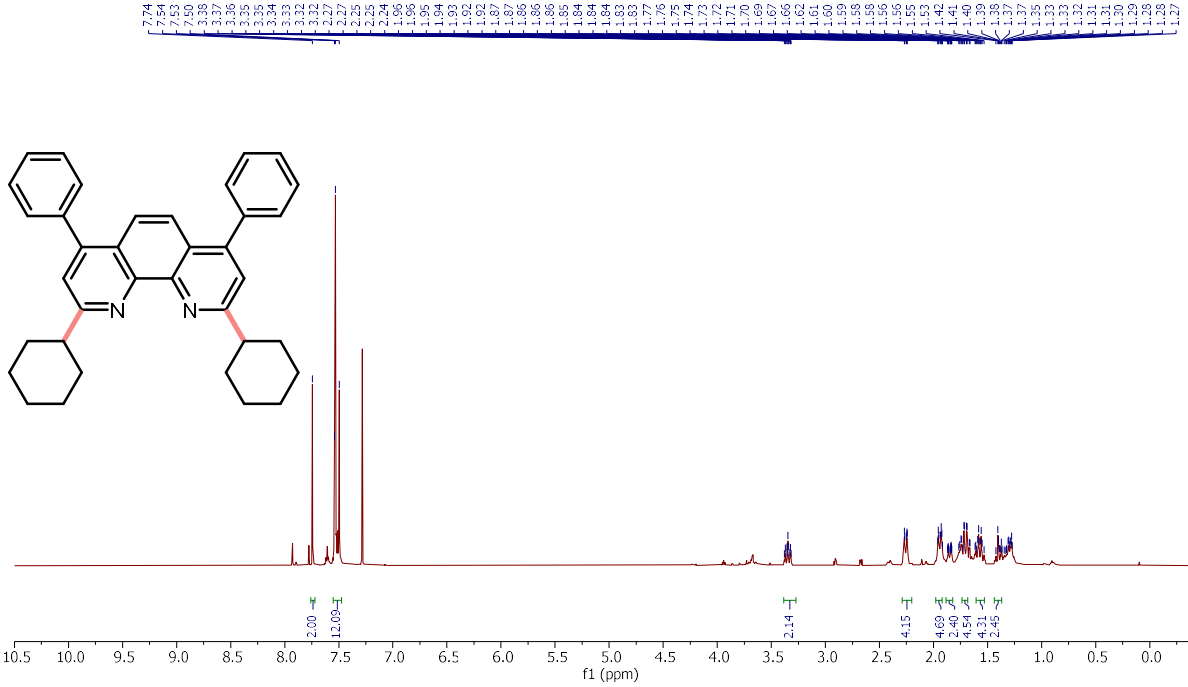

^{13}C NMR (126 MHz, $CDCl_3$) of 2,9-dicyclohexyl-4,7-diphenyl-1,10-phenanthroline (37c) (better purity could not be obtained)

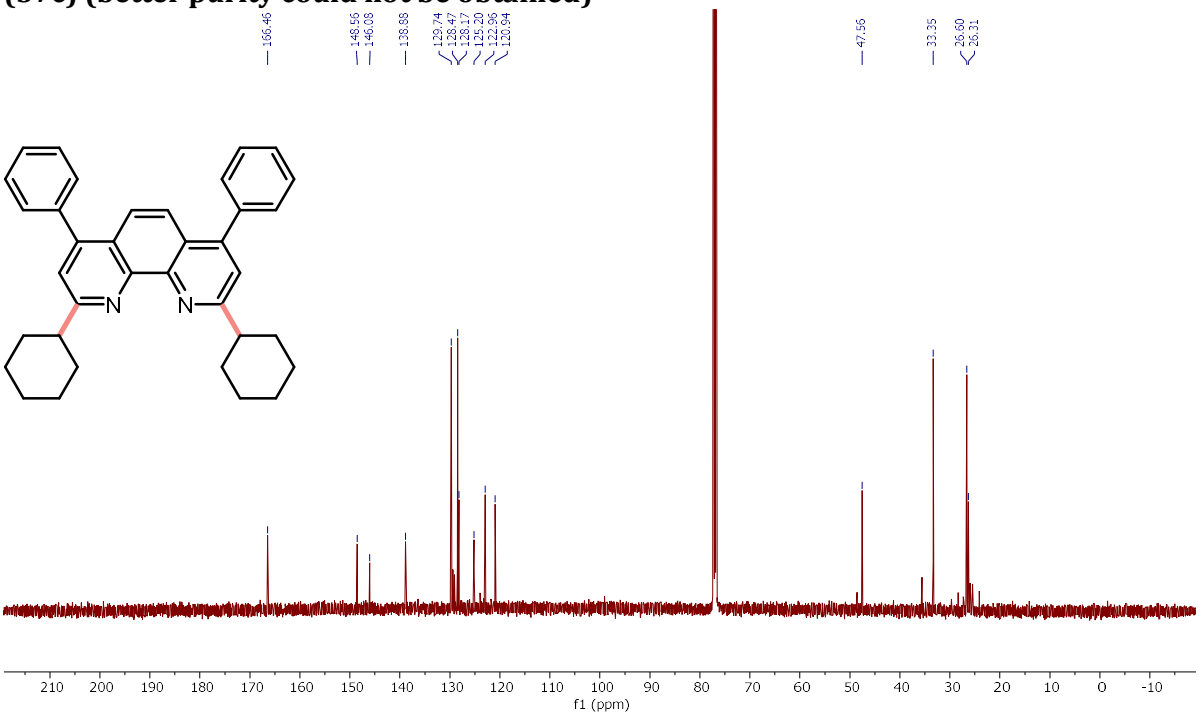

^{1}H NMR (500 MHz, $CDCl_3$) of 2-cyclohexylthiazole-5-carboxamide (41c)

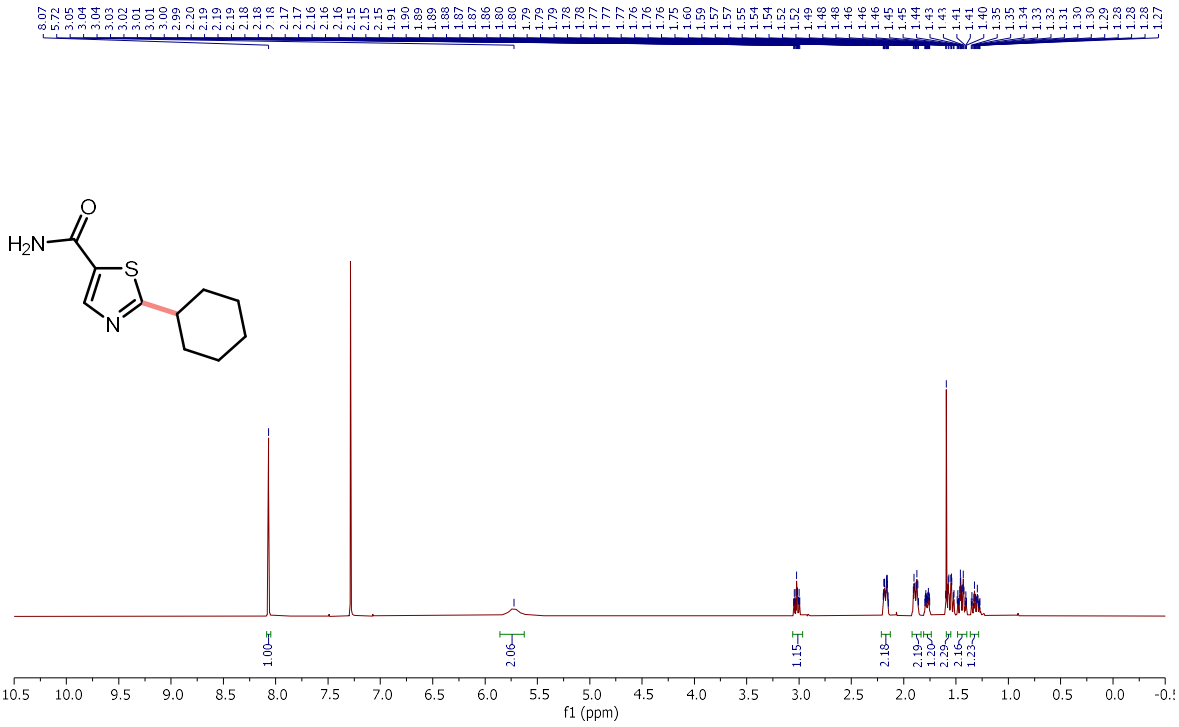

^{13}C NMR (126 MHz, $CDCl_3$) of 2-cyclohexylthiazole-5-carboxamide (41c)

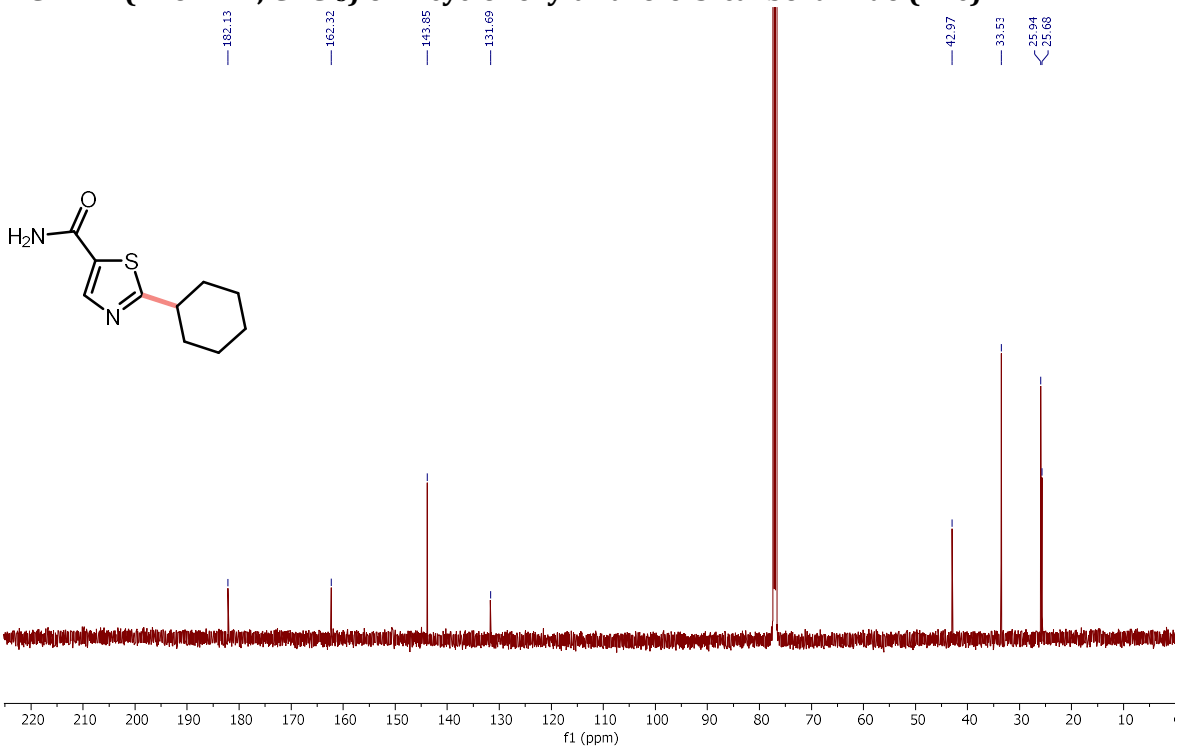

^{1}H NMR (500 MHz, $CDCl_3$) of 2,6-dichloro-8-cyclohexyl-9*H*-purine (44c)

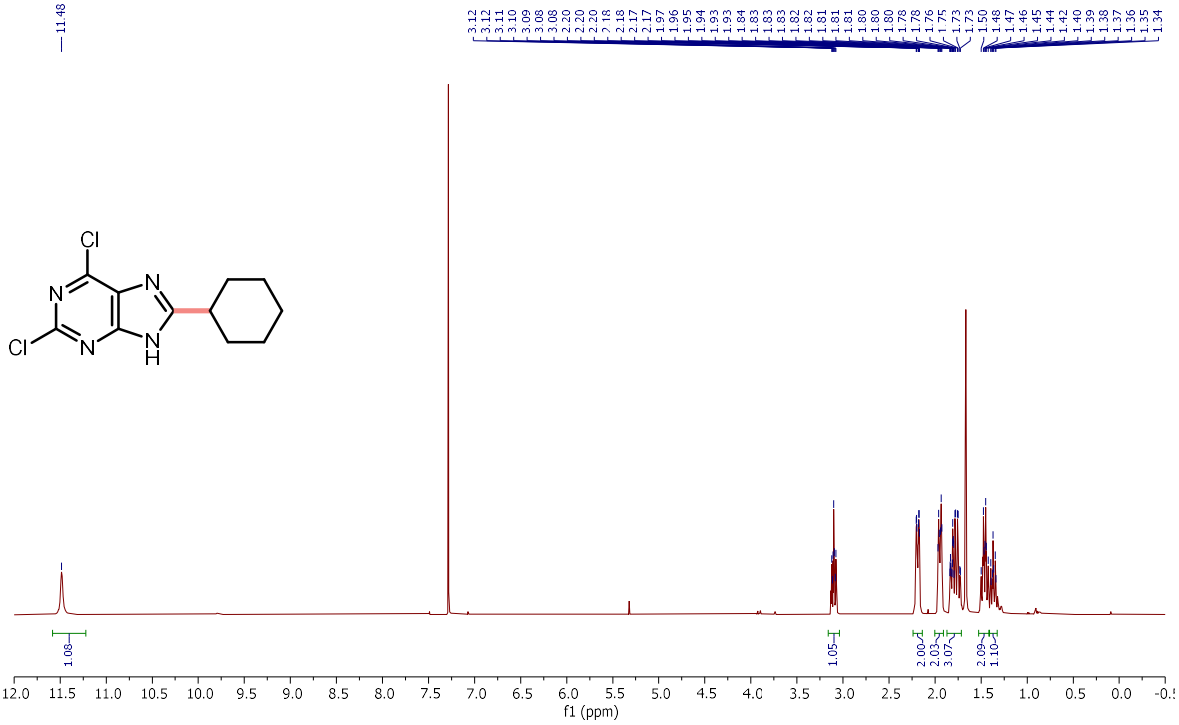

^{13}C NMR (126 MHz, $CDCl_3$) of 2,6-dichloro-8-cyclohexyl-9*H*-purine (44c)

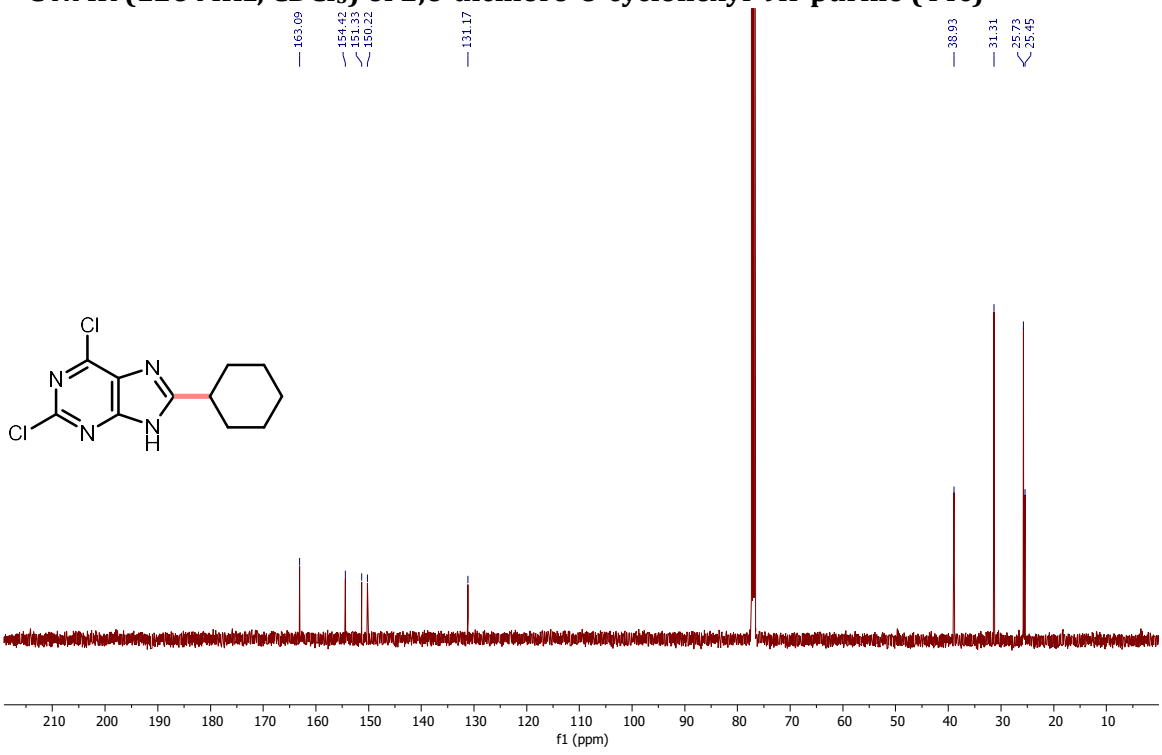

^{1}H NMR (500 MHz, $CDCl_3$) of (*S*)-(2-cyclohexylquinolin-4-yl)((1*S*,2*R*,4*S*,5*R*)-5-vinylquinuclidin-2-yl)methanol (49c)

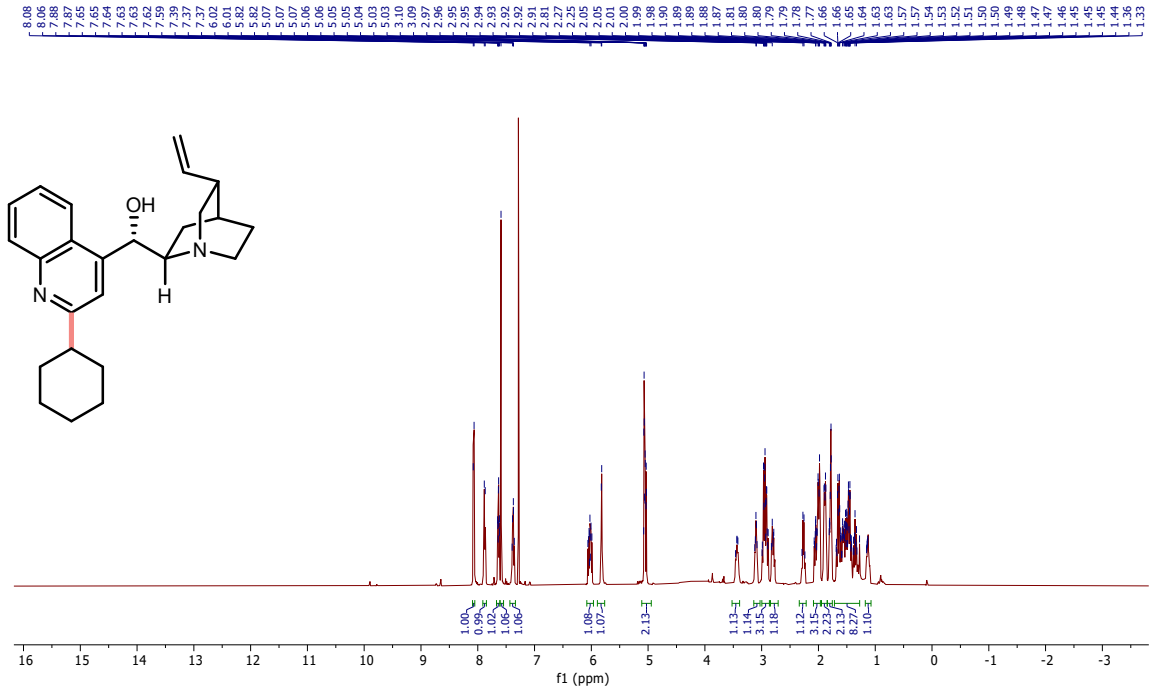

^{13}C NMR (126 MHz, $CDCl_3$) of (*S*)-(2-cyclohexylquinolin-4-yl)((1*S*,2*R*,4*S*,5*R*)-5-vinylquinuclidin-2-yl)methanol (49c)

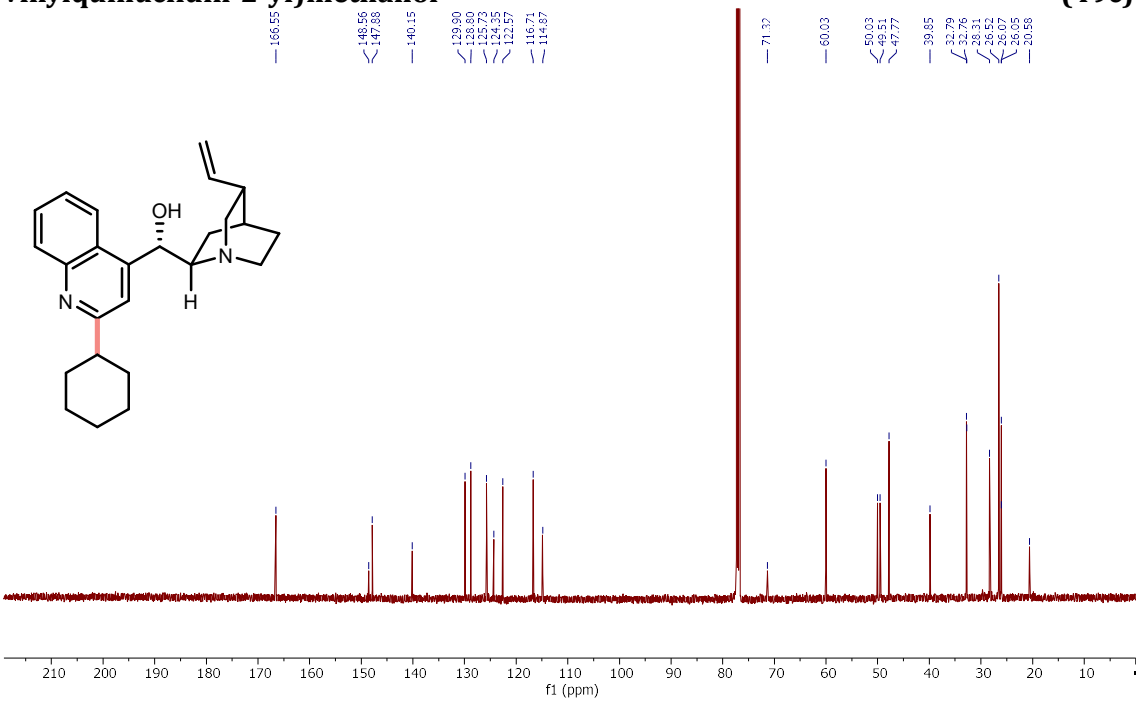

^{1}H NMR (500 MHz, $CDCl_3$) of 3-(cyclopropylmethoxy)-N-(3,5-dichloro-2-cyclohexylpyridin-4-yl)-4-(difluoromethoxy)benzamide (52c)

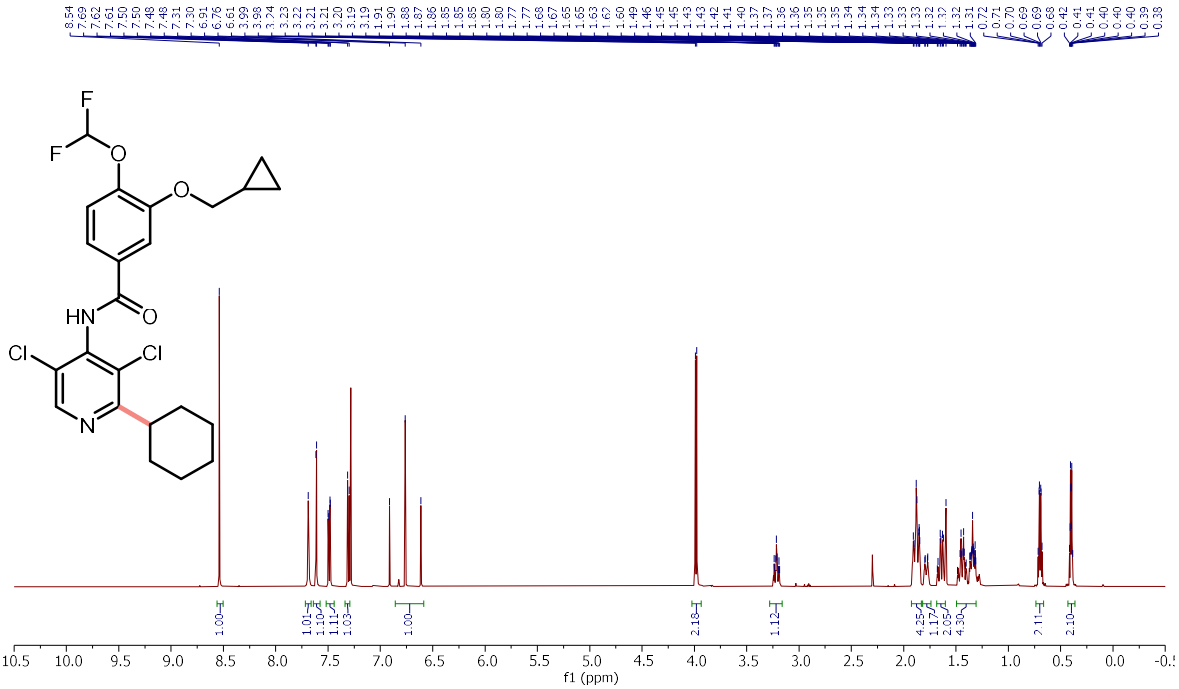

^{13}C NMR (126 MHz, $CDCl_3$) of 3-(cyclopropylmethoxy)-N-(3,5-dichloro-2-cyclohexylpyridin-4-yl)-4-(difluoromethoxy)benzamide (52c)

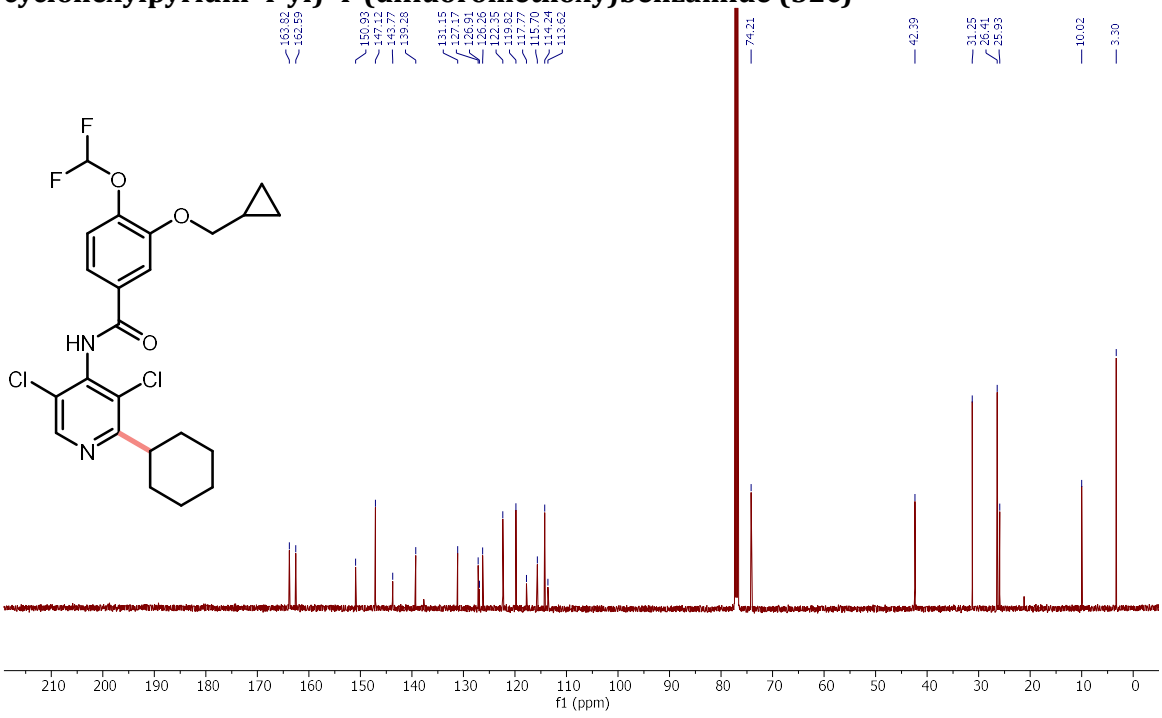

^{19}F NMR (470 MHz, $CDCl_3$) of 3-(cyclopropylmethoxy)-*N*-(3,5-dichloro-2-cyclohexylpyridin-4-yl)-4-(difluoromethoxy)benzamide (52c)

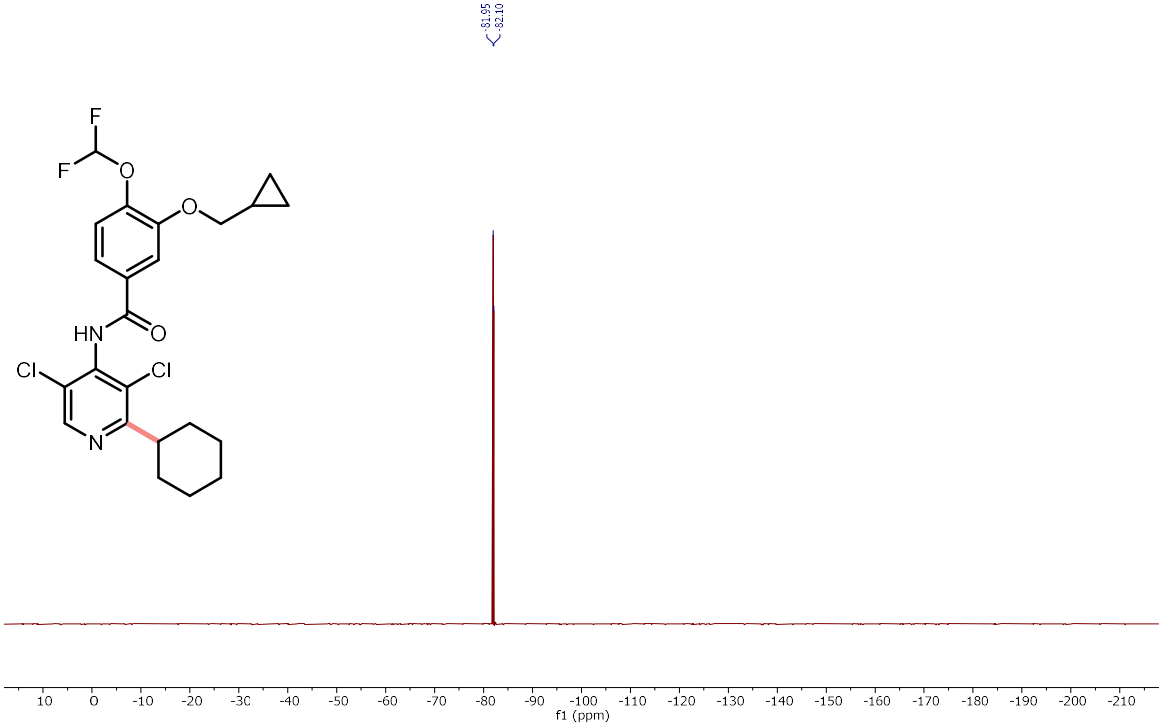

^{1}H NMR (500 MHz, $CDCl_3$) of (*Z*)-1-(11-(cyclohexylmethylene)-6,11-dihydro-5*H*-dibenzo[*b*,*e*]azepin-5-yl)-2,2,2-trifluoroethan-1-one (62c) (Higher purity could not be obtained.)

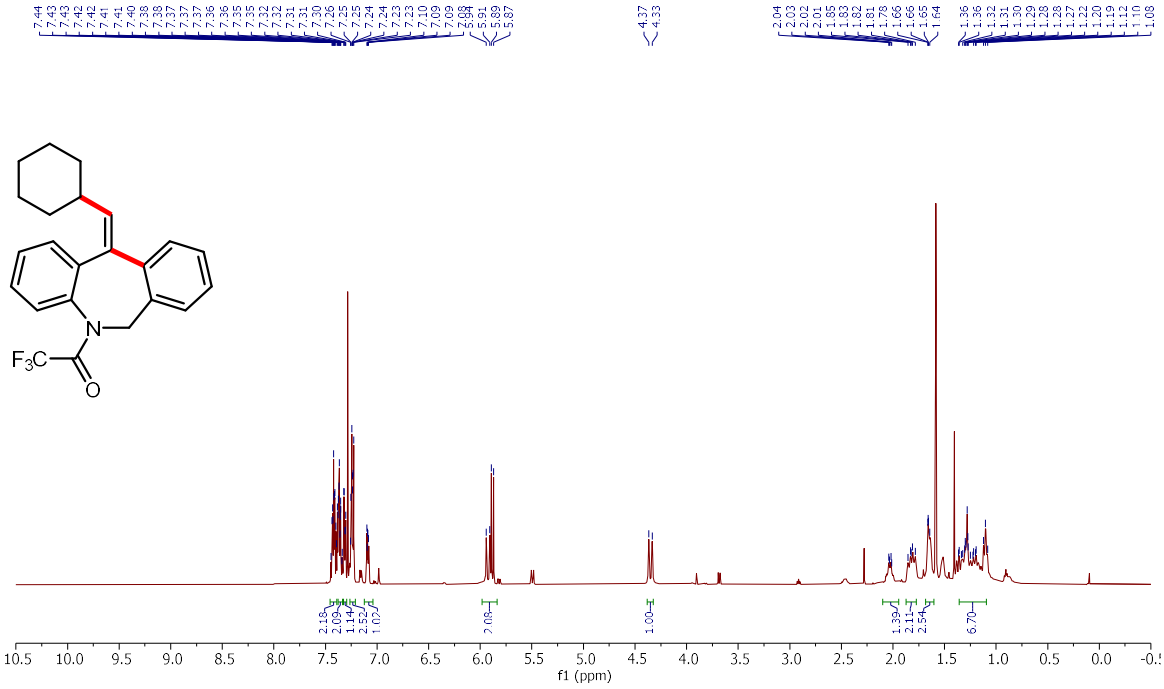

^{19}F NMR (470 MHz, $CDCl_3$) of (*Z*)-1-(11-(cyclohexylmethylene)-6,11-dihydro-5*H*-dibenzo[*b*,*e*]azepin-5-yl)-2,2,2-trifluoroethan-1-one (62c) (Higher purity could not be obtained)